UNIVERSITAT DE BARCELONA

Design and Synthesis of Bifunctional Compounds for Targeted Protein Degradation and Phosphorylation

Guillem Loren Parrondo

Memòria presentada per Guillem Loren Parrondo per a optar al grau de Doctor en Química Orgànica per la Universitat de Barcelona

Guillem Loren Parrondo

El Prof. Antoni Riera Escalé, catedràtic del departament de Química Inorgànica i Orgànica, Secció de Química Orgànica, de la Facultat de Química de la Universitat de Barcelona,

CERTIFICA: que la present tesi doctoral titulada “Design and Synthesis of Bifunctional Compounds for Targeted Protein Degradation and Phosphorylation” presentada per Guillem Loren Parrondo per optar al títol de doctor per la Universitat de Barcelona, ha estat realitzada sota la seva direcció.

Prof. Antoni Riera Escalé

Barcelona, Juliol 2023

Design and Synthesis of Bifunctional Compounds for Targeted Protein Degradation and Phosphorylation

Guillem Loren Parrondo

Doctoral programme: Química Orgànica

Thesis director: **Prof. Antoni Riera Escalé**

Facultat de Química

Departament de Química Inorgànica i Orgànica

Secció de Química Orgànica

Universitat de Barcelona

UNIVERSITAT DE BARCELONA

Memòria presentada per Guillem Loren Parrondo per a optar al grau de Doctor en Química Orgànica per la Universitat de Barcelona

Guillem Loren Parrondo

El Prof. Antoni Riera Escalé, catedràtic del departament de Química Inorgànica i Orgànica, Secció de Química Orgànica, de la Facultat de Química de la Universitat de Barcelona,

CERTIFICA: que la present tesi doctoral titulada “Design and Synthesis of Bifunctional Compounds for Targeted Protein Degradation and Phosphorylation” presentada per Guillem Loren Parrondo per optar al títol de doctor per la Universitat de Barcelona, ha estat realitzada sota la seva direcció.

Prof. Antoni Riera Escalé

Barcelona, Juliol 2023

La present memòria recull el treball realitzat des del juny de 2019 fins al juny de 2023, amb el suport econòmic del *Ministerio de Ciencia, Innovación y Universidades* (beca FPI Severo Ochoa, SEV-2015-0500-18-3). La investigació s'ha finançat amb projectes de recerca del *Ministerio de Ciencia e Innovación* (*Nuevas herramientas para catálisis asimétrica y química biológica*, PID2020-115074GB-100) i el *Ministerio de Economía, Industria y Competitividad* (*Desarrollo de nueva metodología sintètica y apicación a la síntesis de compuestos con actividad biológica*, CTQ2017-87840-P).

El treball experimental s'ha dut a terme a la Unitat de Recerca en Síntesi Asimètrica (URSA), laboratori sota la direcció del professor Antoni Riera Escalé a l'Institut de Recerca Biomèdica de Barcelona (IRB Barcelona).

La investigació descrita en la present memòria s'ha dut a terme en col·laboració amb altres grups d'investigació del camp de l'oncologia i la biologia molecular, ubicats també a l'IRB Barcelona. L'avaluació biològica dels compostos sintetitzats, incloent-hi el tractament a cèl·lules, l'anàlisi per *Western blotting* i l'administració *in vivo*, ha sigut realitzada per les parts col·laboradores.

L'avaluació biològica dels compostos descrits al capítol 3, els degradadors de receptor d'estrogen, s'ha dut a terme al *Growth Control and Cancer Metastasis Laboratory*, sota la direcció d'en Prof. Roger Gomis. Els experiments han estat realitzats per la Dra. Alícia Llorente i la Irene Espuny.

L'avaluació biològica dels compostos descrits al capítol 4 s'ha dut a terme al laboratori d'en Prof. Travis Stracker, qui inicialment estava ubicat a l'IRB Barcelona i al 2020 es va traslladar al *National Cancer Institute's Centre for Cancer Research*, a Nova York. Els experiments han estat realitzats per la Dra. Marina Villamor i en Prof. Travis Stracker.

L'avaluació biològica dels compostos descrits al capítol 5, els degradadors de p38, s'ha dut a terme al *Signalling and Cell Cycle Laboratory*, sota la direcció del Prof. Angel Nebreda. Els experiments cel·lulars i en ratolins han estat realitzats per la Dra. Monica Cubillos-Rojas.

L'avaluació biològica dels compostos descrits al capítol 6, els inductors de fosforilació, s'ha dut a terme al *Targeted Protein Degradation and Drug Discovery Laboratory*, sota la direcció de la Prof. Cristina Mayor-Ruiz. Els experiments han estat realitzat per la Dra. Ana Domostegui.

Chapter 1.

Introduction and Objectives

1. Introduction and Objectives

1.1. Targeted Protein Degradation

The traditional mode of action of most small-molecule drugs is based on the binding to an active site on the surface of the protein of interest (POI). This binding site is usually a well-defined, hydrophobic hole where the molecule fits with high affinity, producing a change in protein activity.[1]

Targeted protein degradation (TPD), in contrast, exploits the cell's own mechanisms for protein homeostasis to induce degradation of a POI. In most cases, the drug interacts with the POI and induces the formation of protein-protein interactions (PPIs) between the POI and a member of the ubiquitin-proteasome system (UPS), typically an E3 ubiquitin ligase.[2,3] The UPS is a regulatory system native to eukaryotic cells that is responsible for protein homeostasis. A favourable interaction between the target protein, degrader and the E3 ligase leads to the formation of a ternary complex, ubiquitination of the POI, recognition by the proteasome and degradation of the POI.[4]

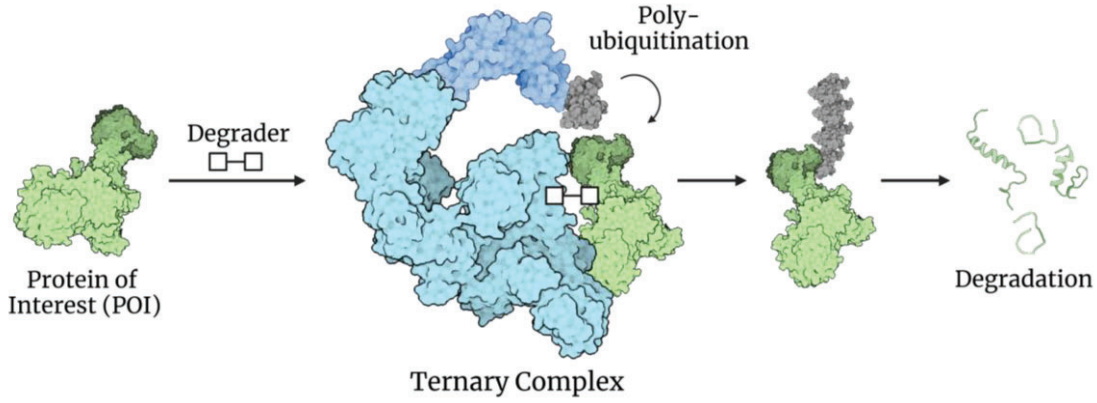

Figure 1.1. Schematic representation of the TPD mode of action. A degrader induces proximity between a target protein and an E3 ubiquitin ligase, followed by polyubiquitination and degradation.

Although the outcome is very similar in both cases –downregulation of a target protein- the two modalities have mechanistic implications that differentiate them. Traditional occupancy-driven pharmacology requires compounds with very high affinity for the target protein. Because occupation is a dynamic equilibrium, the drug must exhibit a high affinity constant to have a prolonged effect. This need can be circumvented by ensuring a high concentration of the inhibitor, or by analogues with a covalent irreversible binding. Other drawbacks, however, cannot be addressed with this mode of action. Arround 85% of the human proteome is considered undruggable by occupancy-based pharmacology, due to the lack of known well-defined hydrophobic pockets at the protein's surface.[5] Some of these "undruggable" targets have key roles in cancer, neurodegenerative disorders and other complex diseases.[6,7]

Because TPD is event driven, meaning that degradation takes place after a transient interaction between the drug, the target protein and the E3 ubiquitin ligase, a potential drug does not need such a high affinity to have a potent effect.[8] Lowering the affinity threshold needed to have a significant pharmacological effect allows targeting proteins previously considered undruggable.[9] Even when a compound is unable to bind strongly enough to a protein to have an inhibitory effect, if it can trigger the transfer of ubiquitination before dissociation takes place it can become a potential degrader. Thus, drugs acting by TPD can potentially circumvent two of the major drawbacks of traditional inhibitors: the need for strong binders and the impossibility to tackle undruggable proteins.

1.2. PROTACs

PROTACs (proteolysis targeting chimaeras), more generally called "bifunctional protein degraders", are a major class of molecules that act through a TPD mode of action.[10] These molecules are comprised of two ligands (warheads) united by a linker. A PROTAC binds to two proteins simultaneously: the protein of interest (POI) and an E3 ubiquitin ligase. This interaction induces the transfer of ubiquitin to the POI and its subsequent degradation by the proteasome. This pharmacology is event driven, meaning that the effect comes after the simultaneous interaction between PROTAC, POI and E3 ligase. This means that after the ternary complex is dismantled the drug is recycled, acting on another unit of the POI in a catalytic manner.

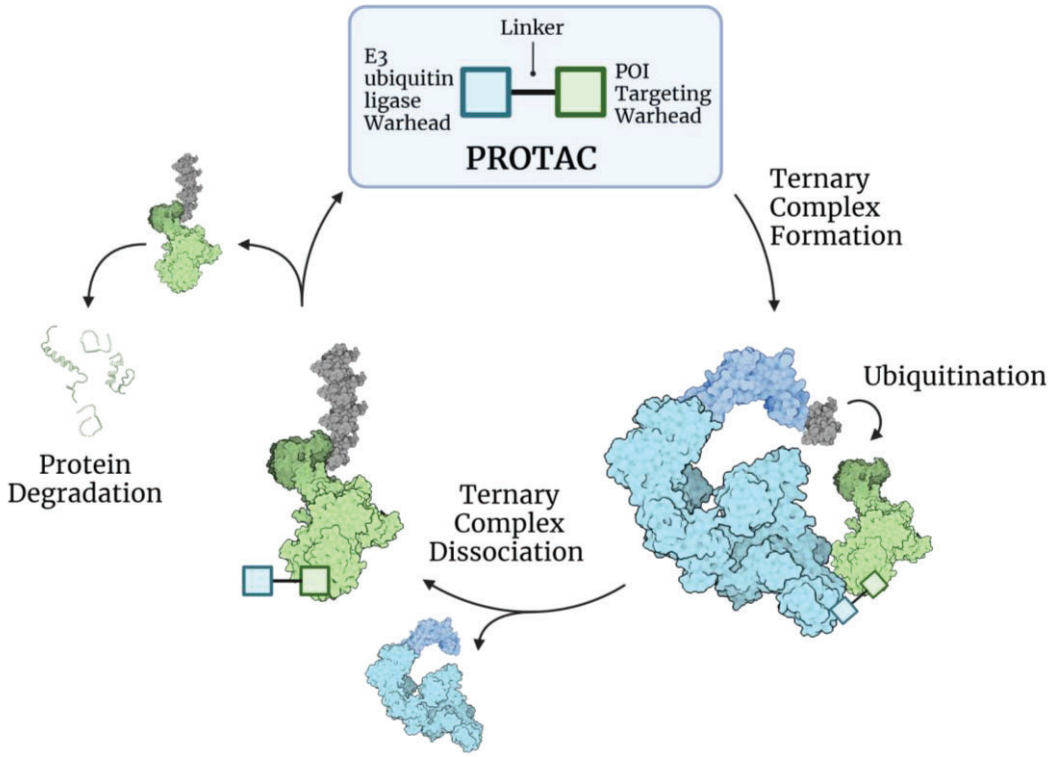

Figure 1.2. Schematic representation of a PROTAC. **b)** Catalytic mechanism of action of a PROTAC.

The first proof of concept for a synthetic PROTAC was published in 2001. Sakamoto *et. al.* reported a compound able to bring into proximity METAP2 (methionyl aminopeptidase 2) and β-TRCP (β-transducin repeat –containing E3 ligase), inducing the degradation of METAP2.[11] The compound consisted on a warhead based on ovalicin, which recruited the target protein, and a peptidic sequence recognized by the E3 ligase. This example was followed by other peptide-based PROTACs, but it was not until 2012 that fully small-molecule based PROTACs were developed. The discovery of a small molecule mimicking the HIF1α interaction with the von Hippel-Lindau tumour suppressor (VHL), opened the door to the synthesis of PROTACs targeting this E3 ligase.[12] Parallel to these discoveries, cereblon (CRBN), the substrate receptor of the $Cul4^{CRBN}$ E3 ligase, was identified as the target of thalidomide and its analogues, commonly referred to as immunomodulatory drugs (IMiDs) in the context of cancer therapy.[13]

These discoveries were followed by an exponential growth in publications reporting new protein degraders from 2016 and onwards,[14] thanks to the modular structure of PROTACs, which allowed an easy exploration of diverse targets. Thanks to the availability of small-molecule ligands, the E3 ligases CRBN and VHL have been the most targeted in PROTAC design. The possibility to use any inhibitor or ligand of a target protein as a warhead has led to the targeting of both druggable and undruggable proteins, including kinases,[8,15,16] transcription factors,[17,18] membrane receptors[19] and other proteins involved in complex diseases.[20,21]

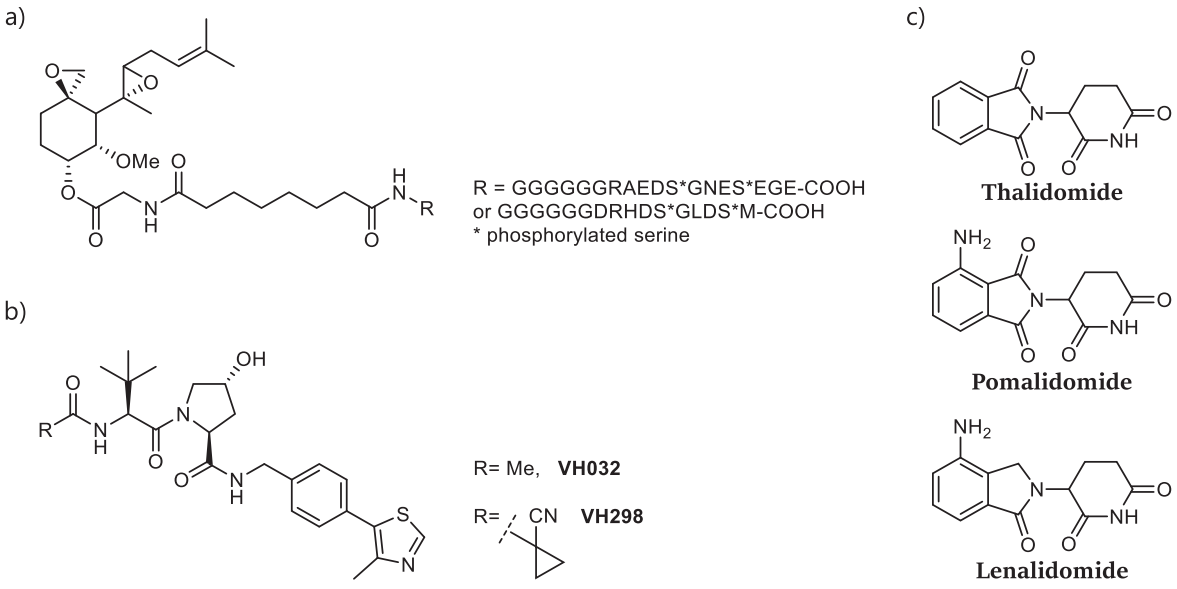

Figure 1.3. Structures of **a)** Protac-1, **b)** small-molecule VHL ligands, **c)** thalidomide and other IMiDs.

1.3. p38 PROTACs

Our research group also took part in the PROTAC gold rush. During his doctoral thesis, Dr. Donoghue developed the synthesis of PROTACs targeting p38, a group of kinases involved in the mitogen-activated protein kinase (MAPK) pathway, responsible of directing cellular responses to stress and other external stimuli.[22] His work led to the discovery of **NR-7h**, a PROTAC recruiting CRBN through a thalidomide derivative and using **PH-797804**, a p38 inhibitor, as a warhead.[23] Although the compound achieved good potency degrading p38 in cells, it could not be administered in mice due to its poor water solubility. **The first objective of this doctoral thesis was to optimize the design of NR-7h, in order to synthesize compounds with higher water solubility, which could be administered and studied in-vivo.** The synthesis of p38 degrader analogues and their biological evaluation is described in chapter 5 of this doctoral thesis.

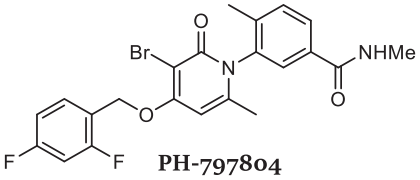

PH-797804

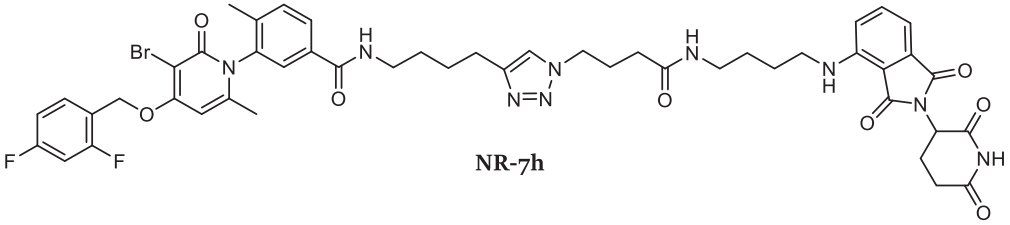

NR-7h

Figure 1.4. Structures of **PH-797804** and **NR-7h**.

1.4. ER and TLK PROTACs

Following the successful preparation of p38 PROTACs and parallel to their optimization, we underwent a search for other targets to degrade. While motivation on the choice of the target relied mainly on our collaborations with other research groups that focused on the study of those proteins, we also considered the synthetic feasibility of the warhead and the ease of derivatization into a bifunctional molecule. Our general workflow consisted in finding a suitable ligand and identifying a proper functionalization spot, afterwards we proceeded to attach part of the linker and the E3 ligase recruiter.

A central aspect in our synthetic strategy was the use of a copper(I)- that allow the connection of two molecular blocks in a selective, high yielding manner under mild conditions and with few or no by-products.[24] The use of a CuAAC at the last step of the synthesis allowed us to couple in a reliable

way and in good yields two advanced intermediates, one bearing a terminal azide or alkyne and the other the complimentary functionality.

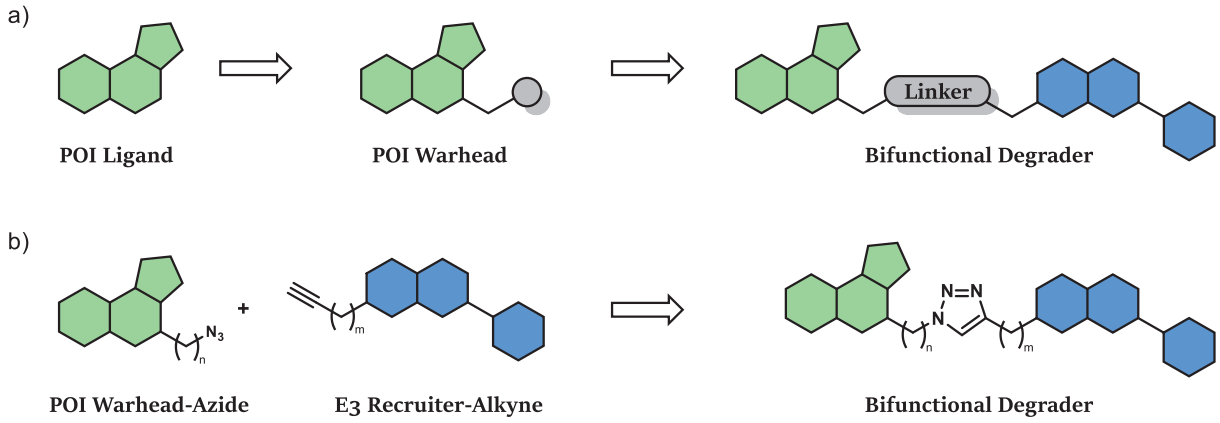

Figure 1.5. Workflow scheme. a) A know ligand for a protein of interest (POI) is turned into a warhead that permits attachment of the linker and E3 ligase recruiter. **b)** POI and E3 ligase ligands are functionalized into azide/alkyne fragments, then coupled via CuAAC.

In this fashion, we envisioned the construction of Oestrogen Receptor (ER) PROTACs based on 4-hydroxitamoxifen (4OHT), a well-known ligand of ER. We adapted the synthesis developed in our laboratory by Dr. Byrom and Dr. Donoghue in order to incorporate a terminal alkyne that could be further functionalized into a protein degrader. **The second objective of this doctoral thesis was to design a warhead derived from 4OHT, and then synthesize and identify protein degraders targeting the ER.** The synthesis and evaluation of ER PROTACs is described in chapter 3 of this doctoral thesis.

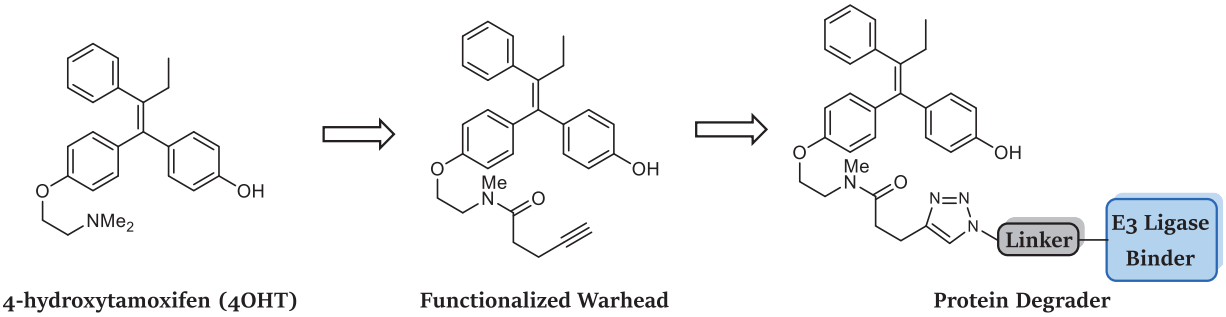

Figure 6. Synthetic outline of protein degraders derived from **4OHT**.

The third type of proteins that we targeted for degradation are the tousled-like kinases (TLKs), a

group of kinases involved in histone activity and stability. TLKs play an important role in DNA repair, DNA replication, transcription and mitosis,[25] and a PROTAC targeting these kinases selectively could be used as a powerful tool to study their biology. The starting point for this project was a collaboration with Prof. Travis Stracker and co-workers, who reported a panel of kinase inhibitors with varying degrees of selectivity towards TLK. From the most selective compounds, we selected the bisindolylmaleimide scaffold to pursue the design of TLK-binding warheads that could be amenable to synthesizing protein degraders. **The third objective of this doctoral thesis was to synthesize and derivatize the kinase inhibitors into TLK-targeting warheads, and explore different attachment points and linker compositions to construct potential protein degraders for the degradation of TLK.** This is described in chapter 4 of this doctoral thesis.

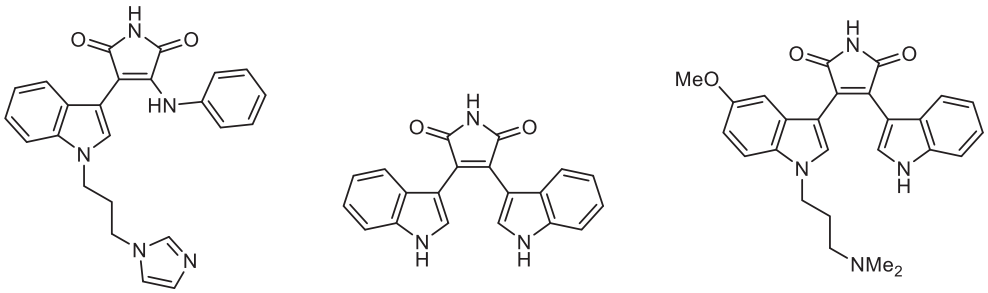

Figure 7: Bisindolylmaleimide-based drugs with affinity for TLK2.

1.5. Phosphorylation Inducers

As the field of proximity-inducing bifunctional molecules evolved towards a more general applicability, which was not exclusively confined in the use of an E3 ligase as an effector, we looked to move away from degradation and explore other post-translational modifications that could be induced by hetero-bifunctional molecules.[26] Phosphorylation-inducing chimeric Small Molecules (PHICS) are heterobifunctional compounds that induce proximity between a protein of interest and a kinase, resulting in the phosphorylation of the POI. A few examples of PHICS have been reported in the literature,[27,28] and we wanted to investigate a general application of this technology.

To do so, we gained inspiration in the dTAG system, a chemogenetic strategy that allows the degradation of a POI without the need of having a good ligand for that protein. The system is based on the construction of a fusion protein between the POI and the mutant $FKBP12^{F36V}$. This mutant is targeted by a specific ligand, incorporated in a protein degrader that targets $FKBP12^{F36V}$with high affinity and selectivity. Treatment with the bifunctional drug induces degradation of $FKBP12^{F36V}$, together with the fused POI. The advantages of this technology as a chemical biology tool over traditional target-specific PROTACs are obvious, eliminating all the medicinal chemistry effort usually required to find an active compound and targeting proteins for which there are no known

ligands.

The aim of this project was to merge the PHICS and the dTAG technologies into an inducible system that would be activated by a bifunctional molecule, able to induce phosphorylation of any protein of interest that was expressed in-frame with the FKBP12 mutant. **The fourth objective of this doctoral thesis was to design and synthesize potential phosphorylation inducers.**

First, we investigated the use of a potential allosteric binder of p38 as a kinase-recruiting warhead. **We planned to derivatize a novel p38 binder in order to be used in the synthesis of PHICS, and to synthesize bifunctional molecules recruiting p38 as either POI or effector.** We then moved to the use of a protein kinase C (PKC) activator to recruit PKC, paired with the ligands for the dTAG and the aTAG systems. **We synthesized bifunctional molecules that could recruit simultaneously PKC and the a or dTAG, in order to induce phosphorylation to a POI expressed in-frame with the tag.** The synthesis and evaluation of phosphorylation inducers is described in chapter 6 of this doctoral thesis.

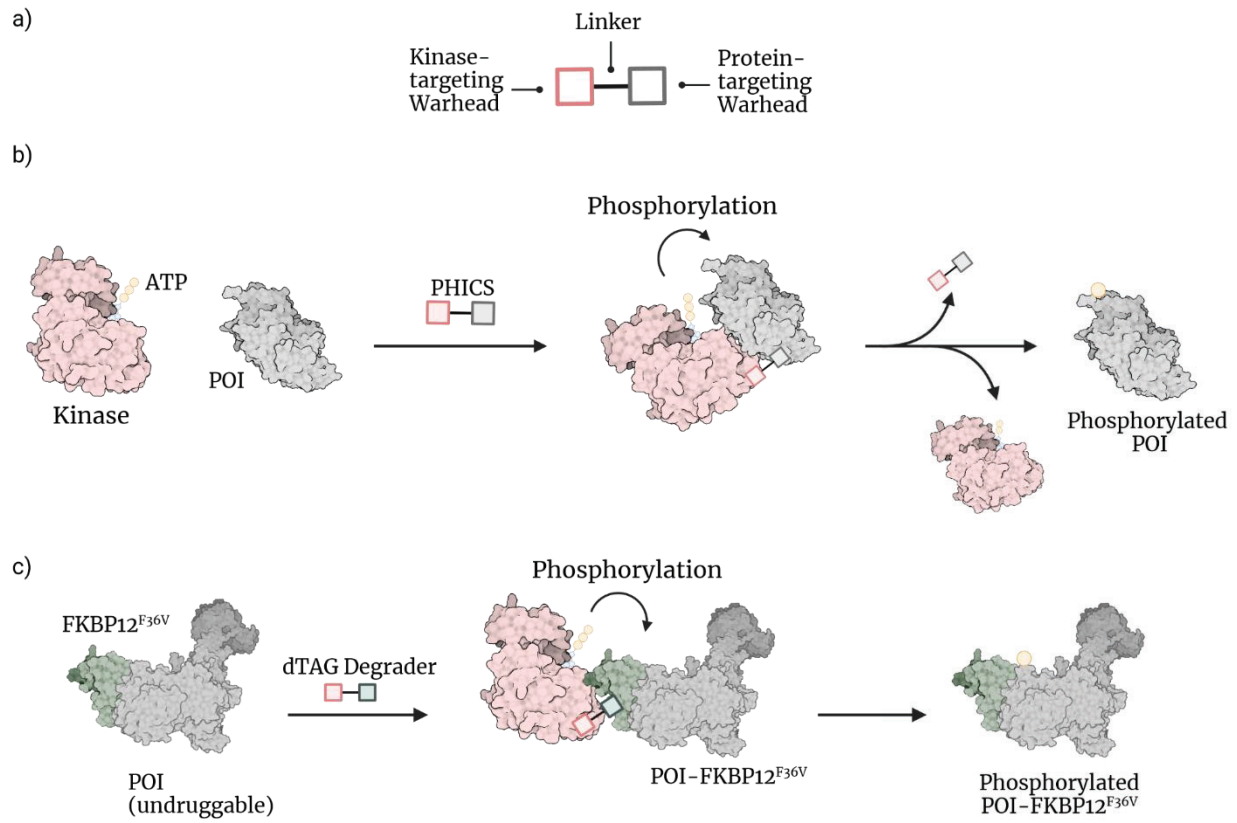

Figure 1.8. Phosphorylation-inducing small molecules (PHICS). a) Schematic representation of a PHICS. **b)** Mechanism of action of PHICS. **c)** Schematic representation of a dTAG-based PHICS.

To summarize, the main objectives of this doctoral thesis are:

1. The optimization of **NR-7h**. The synthesis of p38 degraders with higher solubility in water, followed by a structure-activity relationship study on the linker.

2. The synthesis of ER degraders based on **4OHT**.

3. The synthesis of TLK degraders based on kinase inhibitors.

4. The synthesis of novel phosphorylation inducers.

References

[1] Stank, A., Kokh, D. B., Fuller, J. C. & Wade, R. C. Protein Binding Pocket Dynamics. *Acc. Chem. Res.* **2016**, *49*, 809–815.

[2] Lai, A. C., Crews, C. M. & Haven, N. Induced protein degradation. *Nat. Rev. Drug Discov.* **2017**, *16*, 101–114.

[3] Zhao, L., Zhao, J., Zhong, K., Tong, A. & Jia, D. Targeted protein degradation: mechanisms, strategies and application. *Signal Transduct. Target. Ther.* **2022**, *7*.

[4] Paiva, S. L., Da Silva, S. R., De Araujo, E. D. & Gunning, P. T. Regulating the Master Regulator: Controlling Ubiquitination by Thinking Outside the Active Site. *J. Med. Chem.* **2018**, *61*, 405–421.

[5] Hopkins, A. L. & Groom, C. R. The druggable genome. *Nat. Rev. Drug Discov.* **2002**, *1*, 727–730.

[6] Lazo, J. S. & Sharlow, E. R. Drugging Undruggable Molecular Cancer Targets. *Annu. Rev. Pharmacol. Toxicol.* **2016**, *56*, 23–40.

[7] Henley, M. J. & Koehler, A. N. Advances in targeting 'undruggable' transcription factors with small molecules. *Nat. Rev. Drug Discov.* **2021**, *20*, 669–688.

[8] Han, X. *et al.* Discovery of Highly Potent and Efficient PROTAC Degraders of Androgen Receptor (AR) by Employing Weak Binding Affinity VHL E3 Ligase Ligands. *J. Med. Chem.* **2019**, *62*, 11218–11231.

[9] Bond, M. J., Chu, L., Nalawansha, D. A., Li, K. & Crews, C. M. Targeted Degradation of Oncogenic KRASG12Cby VHL-Recruiting PROTACs. *ACS Cent. Sci.* **2020**, *6*, 1367–1375.

[10] Hu, Z. & Crews, C. M. Recent Developments in PROTAC-Mediated Protein Degradation: From Bench to Clinic. *ChemBioChem* **2022**, *23*, e202100270.

[11]Sakamoto, K. M.; Kim, K. B.; Kumagai, A.; Mercurio, F.; Crews, C. M.; Deshaies, R. J. Protacs: Chimeric Molecules That Target Proteins to the Skp1-Cullin-F Box Complex for Ubiquitination and Degradation. *Proc. Natl. Acad. Sci. U. S. A.* **2001**, *98*, 8554–8559.

[12] Buckley, D. L. *et al.* Small-molecule inhibitors of the interaction between the E3 ligase VHL and HIF1α. *Angew. Chemie - Int. Ed.* **2012**, *51*, 11463–11467.

[13] Ito, T. *et al.* Identification of a primary target of thalidomide teratogenicity. *Science (80-.).* **2010**, *327*, 1345–1350.

[14] Li, D., Yu, D., Li, Y. & Yang, R. A bibliometric analysis of PROTAC from 2001 to 2021. *Eur. J. Med. Chem.* **2022**, *244*, 114838.

[15] Nunes, J. *et al.* Targeting IRAK4 for Degradation with PROTACs. *ACS Med. Chem. Lett.* **2019**, *10*, 1081–1085.

[16] Cromm, P. M., Samarasinghe, K. T. G., Hines, J. & Crews, C. M. Addressing Kinase-Independent Functions of Fak via PROTAC-Mediated Degradation. *J. Am. Chem. Soc.* **2018**, *140*, 17019–17026.

[17] Han, X. *et al.* Discovery of Highly Potent and Efficient PROTAC Degraders of Androgen Receptor (AR) by Employing Weak Binding Affinity VHL E3 Ligase Ligands. *J. Med. Chem.* **2019**, *62*, 11218–11231.

[18] Hazen, G. *et al.* Targeting steroid hormone receptors for ubiquitination and degradation in breast and prostate cancer. *Oncogene* **2017**, *27*, 7201–7211.

[19] Hong, D. *et al.* Recent advances in the development of EGFR degraders: PROTACs and LYTACs. *Eur. J. Med. Chem.* **2022**, *239*, 114533.

[20] Silva, M. C. *et al.* Targeted degradation of aberrant tau in frontotemporal dementia patient-derived neuronal cell models. *Elife* **2019**, *8*, 1–31.

[21] Lv, D. *et al.* Development of a BCL-xL and BCL-2 dual degrader with improved anti-leukemic activity. *Nat. Commun.* **2021**, *12*, 1–14.

[22] Canovas, B. & Nebreda, A. R. Diversity and versatility of p38 kinase signalling in health and disease. *Nat. Rev. Mol. Cell Biol.* **2021**, *22*, 346–366.

[23] Donoghue, C., Cubillos-Rojas, M., Gutierrez-Prat, N., Sanchez-Zarzalejo, C., Verdaguer, X., Riera, A., Nebreda, A.R.. Optimal linker length for small molecule PROTACs that selectively target p38α and p38β for degradation. *Eur. J. Med. Chem.* **2020**, *201*, 112451.

[24] Kolb, H. C., Finn, M. G. & Sharpless, K. B. Click Chemistry: Diverse Chemical Function from a Few Good Reactions. *Angew. Chemie - Int. Ed.* **2001**, *40*, 2004–2021.

[25] Mortuza, G. B. *et al.* Molecular basis of Tousled-Like Kinase 2 activation. *Nat. Commun.* **2018**, *9*,.

[26] Hua, L. *et al.* Beyond Proteolysis-Targeting Chimeric Molecules: Designing Heterobifunctional Molecules Based on Functional Effectors. *J. Med. Chem.* **2022**, *65*, 8091–8112.

[27] Siriwardena, S. U. *et al.* Phosphorylation-Inducing Chimeric Small Molecules. *J. Am. Chem. Soc.* **2020**, *142*, 14052–14057.

[28] Shoba, V. M. *et al.* Synthetic Reprogramming of Kinases Expands Cellular Activities of Proteins. *Angew. Chemie - Int. Ed.* **2022**, *61*, 6–11.

Chapter 2.

Precedents

2. Precedents

2.1. The Role of Proximity in Biological Processes

All aspects of cellular biology are governed by protein activity. They are responsible for nearly every task of cellular function, from the organization of the internal structure to controlling biochemical processes necessary for the cell to grow and maintain itself, its management of cellular waste and communication with the exterior.[1]

Protein function is highly regulated by an intricate net of protein-protein interactions (PPIs).[2] Usually, multi-protein complexes composed of auxiliary proteins are formed surrounding a central enzyme, controlling and regulating many aspects of its activity, specificity, and cellular location. The formation of multi-protein complexes affects cellular processes pivotal for its growth and survival, including protein homeostasis, cell division or gene expression.[3] PPIs allow the assembly of these complexes, creating unique interactions that allow an exquisite degree of sophistication to protein function and regulation.

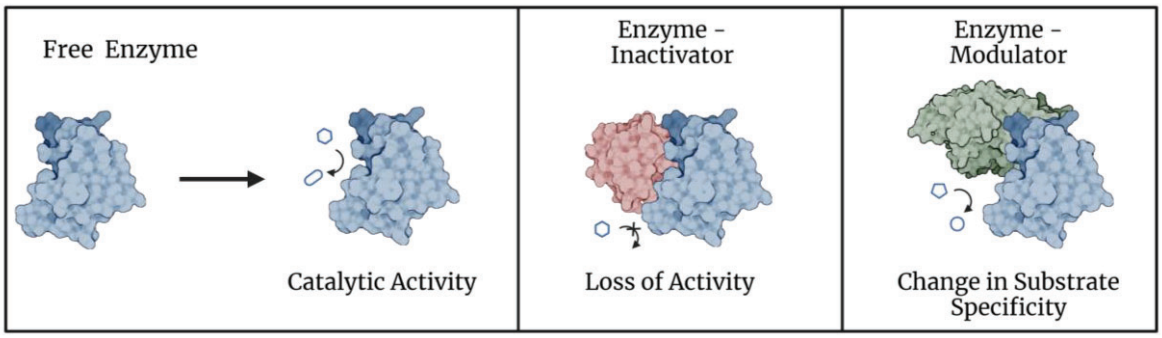

Figure 2.1. Schematic representation of protein-protein interactions modulating the activity of an enzyme.

Proximity, or physical closeness between the proteins is ultimately responsible for the formation of such interactions. Unlike most ligand-protein interactions, where a molecule with affinity for the protein binds in a well-defined "pocket" on the protein surface, PPIs involve interaction between relatively flat protein surfaces.[4] Following proximity between the two proteins, a series of interactions, mostly hydrophobic, are formed. These regions are mostly populated with aromatic residues, and usually display a planar landscape, although globular examples have been reported too.[5]

In addition to the formation of multi-protein complexes that fine-tune enzyme activity, closeness between proteins also plays an important role in enzyme activity when it targets a protein substrate. Post-translational modifications (PTMs) are chemical modifications, covalent and often

reversible, on proteins posterior to translation and folding.[6] PTMs are important in a wide range of cellular processes, such as promoting degradation of proteins to maintain cellular homeostasis, methylation and acetylation of histones to regulate gene expression, or phosphorylation across a signalling pathway. In such processes, recognition of the target protein by the enzymatic complex responsible for the PTM has to be precise, and it usually involves the formation of unique PPIs between the substrate protein and the enzyme, allowing high levels of complexity and specificity.

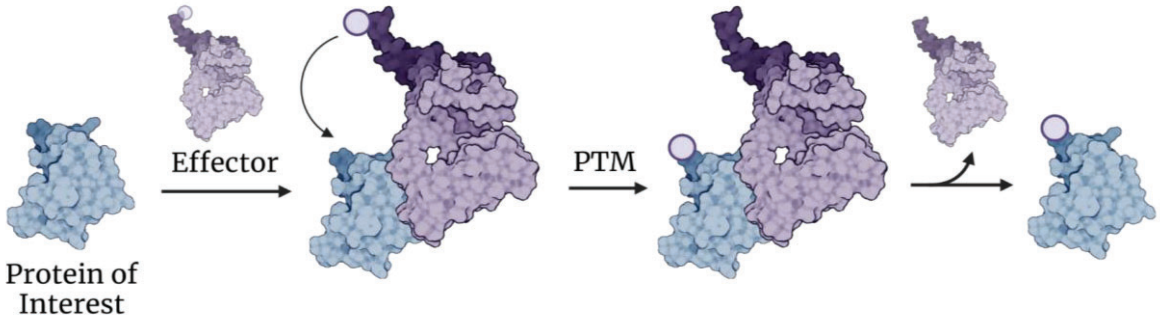

Figure 2.2. Schematic representation of a post-translational modification of a protein substrate.

2.2. PPI Inhibitors and Molecular Glues

Due to the pivotal role multi-protein complexes play in almost any cellular function, their dysfunction, hyperactivation or disruption are associated with many diseases, including autoimmune disorders, neurodegenerative diseases or cancer.[3] Despite their relevance, targeting PPI with small molecules has been extremely challenging, and examples of PPI inhibitors have only appeared during the last 20 years.

Traditionally, approaches in chemical biology and drug discovery have relied on the existence of well-defined binding pockets, hydrophobic “holes” found on the protein surface that can accommodate a small-molecule ligand. Traditional inhibitors bind to such binding sites, blocking protein activity by preventing the natural substrate from entering the active site of the protein (antagonism) or promoting changes in protein structure that turn it inactive (allosterism). Proteins lacking such well-defined binding pockets have been deemed “undruggable” until the last twenty years, when small-molecule inhibitors able to target the interfaces involved in PPIs have started emerging in the literature and the clinic.[7] Examples of molecules acting on this fashion are inhibitors of the p53-MDM2 interaction[8] and of the Bcl protein family.[9] Such inhibitors mimic the effect of the partner protein, fitting in a hydrophobic region on the protein surface that has affinity for a peptidic sequence of the PPI partner.[10] PPIs can also be robustly inhibited by molecules acting through an allosteric mechanism. Examples of this mechanism of action are the disruption

of the CBFβ-Runx1 complex by a class of 2-aminothiazoles that bind allosterically to CBFβ,[11] or the inhibition of the RGS4-Gα interaction by an irreversible allosteric inhibitor.[12]

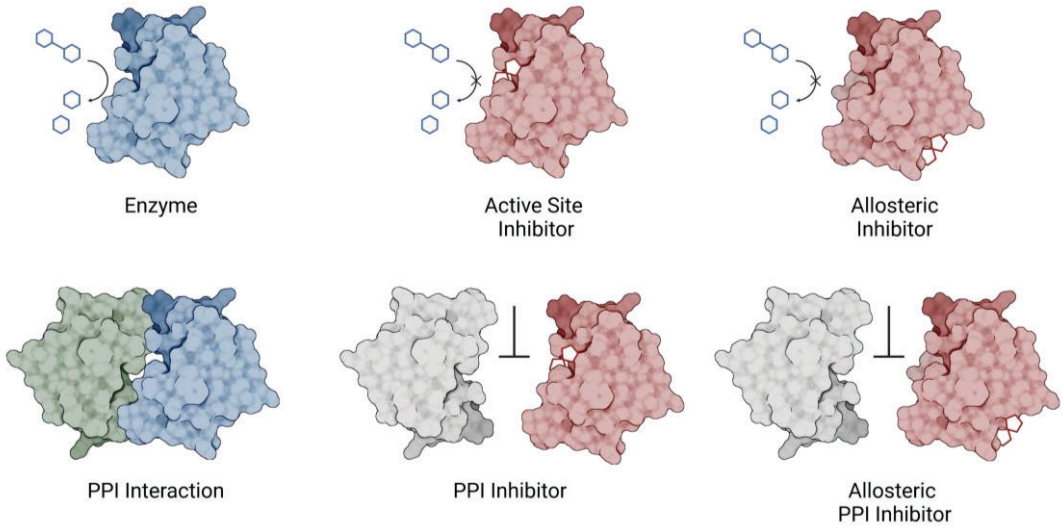

Figure 2.3. Mechanism of small molecule inhibitors. An enzyme-catalysed reaction (a) inhibited by an orthosteric (b) and an allosteric inhibitor (c). A protein-protein interaction (d) inhibited by an orthosteric inhibitor (e) and an allosteric inhibitor (f).

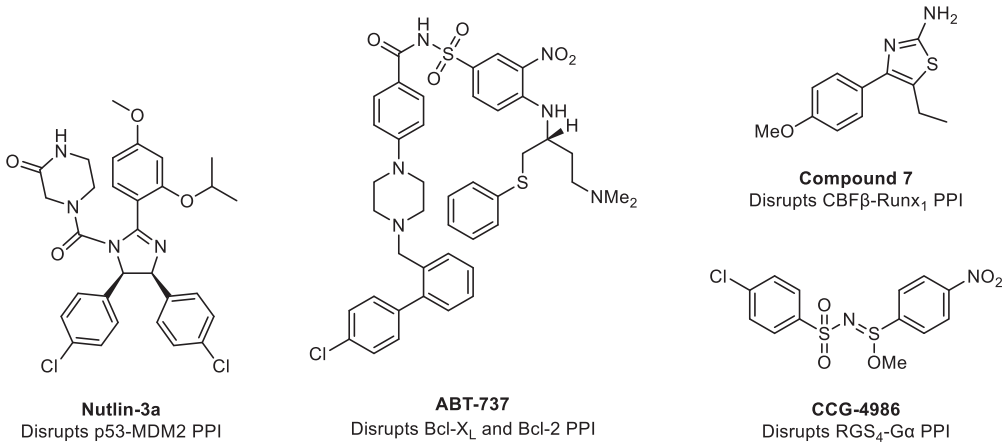

Figure 2.4. Structures of PPI inhibitors.

Small molecules have also been found to stabilize PPI. Nature has produced macrocyclic compounds able to "glue" together two proteins, forming a tertiary complex that inhibits their activity by blocking the access to the active site of the enzyme. Some of these natural products, initially isolated from soil bacteria and fungi, illustrate an early example on how targeting PPI is therapeutically beneficial, as they display immunosuppressant activity in humans and have been

widely used in the clinic to prevent immune responses during organ transplant and in cancer therapy.[13] Cyclosporin A inhibits the activity of calcineurin by promoting its dimerization with cyclophilin A, a prolyl isomerase. FK506 is another natural macrocycle that targets a prolyl isomerase, FKBP12, promoting its dimerization with calcineurin. Perhaps the most important compound of this family is Rapamycin, which binds also to FKBP12 but induces its dimerization with another protein, the mammalian target of rapamycin (mTOR). Rapamycin has been studied for its antifungal and immunosuppressant activity, and the discovery of its target protein, mTOR, triggered basic research on the function of this protein and its role in aging and cancer.[14] Several second-generation analogues, colloquially referred as "rapalogs", have been developed and approved as antitumor agents.[15]

Nature also uses endogenous molecules that stabilize native PPI within an organism. These monovalent and surprisingly simple compounds form *de novo* PPIs that have important physiological consequences in plants. Hormones such as jasmonate and auxin bind to E3 ligases, a type of proteins responsible to induce ubiquitination and degradation of other proteins, promoting recruitment and degradation of neo-substrates that are not targeted in the absence of the ligands.[16] This same mechanism of action is responsible too for the anti-cancer and immunosuppressant activity of immunomodulatory drugs (ImIDs), namely thalidomide and its derivatives, which bind to cereblon (CRBN), the substrate-recognition subunit of the $CRL4A^{CRBN}$ E3 ligase complex[17] and promote degradation of neo-substrates, including transcription factors Ikaros (IKZF1) and Aiolos (IKZF3), CK1alpha and GSPT1. More recently, SALL4 has been identified as the neo-substrate responsible for the infamous teratogenicity of thalidomide.[18] Another synthetic molecule that modulates E3 ligase specificity is Indisulam. This anticancer drug was shown to bind the DCAF15 E3 ligase substrate receptor, increasing the E3 ligase affinity for RBM39, an essential mRNA splicing factor.[19]

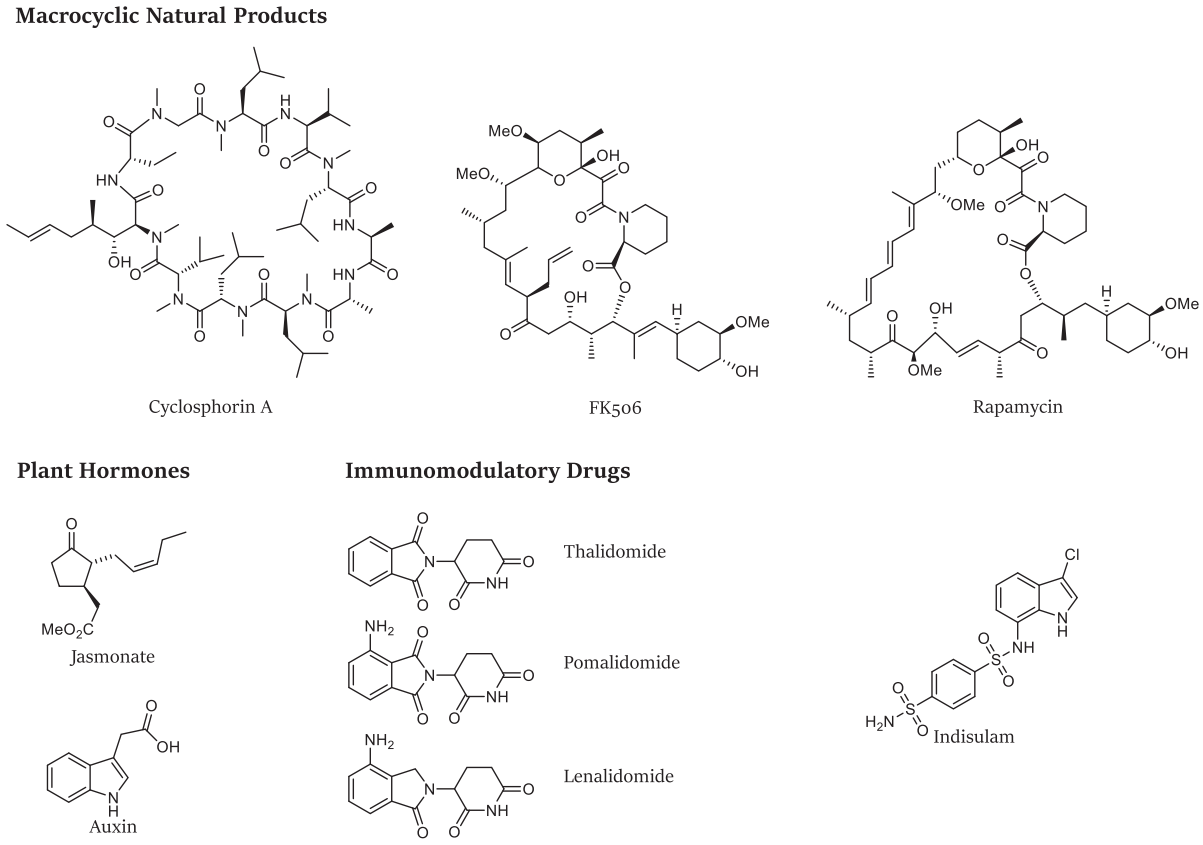

Figure 2.5. Structures of molecular glues.

Following these discoveries, the term "molecular glue" (MG) was coined to describe molecules that upon binding a protein induce the formation of novel PPI with another protein, that would not interact with in the absence of the binder. Although the specifics of the mechanism vary depending on the molecule, the role of the ternary complex (protein-MG-protein) is prominent; the MG either binds preferentially to only one of the two proteins and later forms the ternary complex, or it binds weakly to each individual component and shows measurable binding affinity only as a part of the fully formed complex. This feature has implications in the process of finding new MGs; even when the first protein-ligand interaction is identified, there is no control on the second target recruited.[2] This makes it very challenging to design MGs rationally, as the structure of the ligand is not directly responsible for the second protein recruited. MG identification has been traditionally due to serendipity (as the case of thalidomide derivatives and indisulam) and more recently to rational discovery enabled by technologies such as high-throughput screening, multicovalent chemoproteomic profiling, scalable chemical profiling, systemic data mining, and chemical genetics.[20] These methods, however, depend on intensive screenings and their results have to be subjected to extensive mechanistic validations.

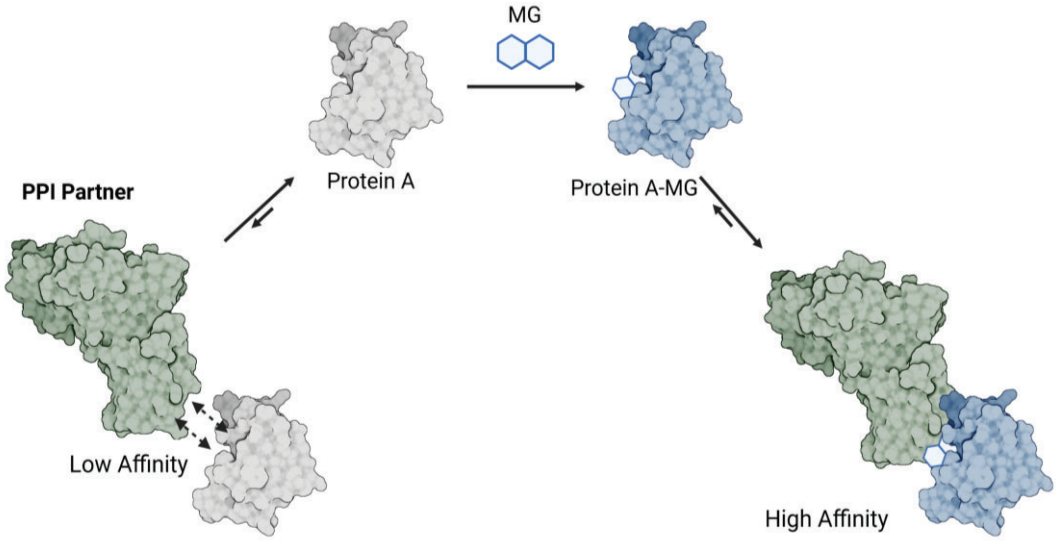

Figure 2.6. Mechanism of action of a molecular glue. Protein A and its PPI partner do not form a stable complex. However, upon binding of the MG to Protein A, the interaction is much more favoured.

2.3. Bifunctional Binders

To gain control over the second dimerization partner in a PPI event, chemists have designed bivalent molecules that act as MGs. Bivalent inhibitors are composed of two regions responsible for binding simultaneously to two molecules of the target protein. A notable example of this strategy are bivalent inhibitors of the bromo and extraterminal domain (BET) proteins, MT1[21] and biBETs.[22] In MT1 two molecules of JQ1, a known BET inhibitor, are linked together by a polyethylene glycol (PEG) based linker, resulting in a compound 100-fold more potent than the parent inhibitor. Similarly, biBETs were shown to bind to two bromodomains of a single BET protein, enhancing antriproliferative effects on cells in a manner consistent with sensitivity to BET inhibition. In both cases, the dimerization between two bromodomains (both in a single BET protein) was evidenced by co-crystal structures and biophysical studies; the dimerization mechanism would also explain the enhancement in potency, consistent with strong avidity effects.[21]

Another example of this mode of action is the dimerizer FK1012, a dimer of FK506, a molecular glue targeting the interaction between FKBP12 and calcineurin.[23] FK1012 binds simultaneously to two FKBP12 units, promoting its dimerization, and this has been used to induce proximity between fusion proteins equipped with immunophilin domains to mimic and study transmembrane signalling by the T cell receptor (TCR).[24] The consequences of those experiments were remarkable; a simple effect of proximity between two proteins was enough to promote qualitative cellular changes in a causative manner. Moreover, it showed that drug-like small molecules were capable of triggering a complex biological cascade signalling, mimicking the outcome of natural biological inputs. FK1012 was the first example of a chemical inducer of proximity (CIP).

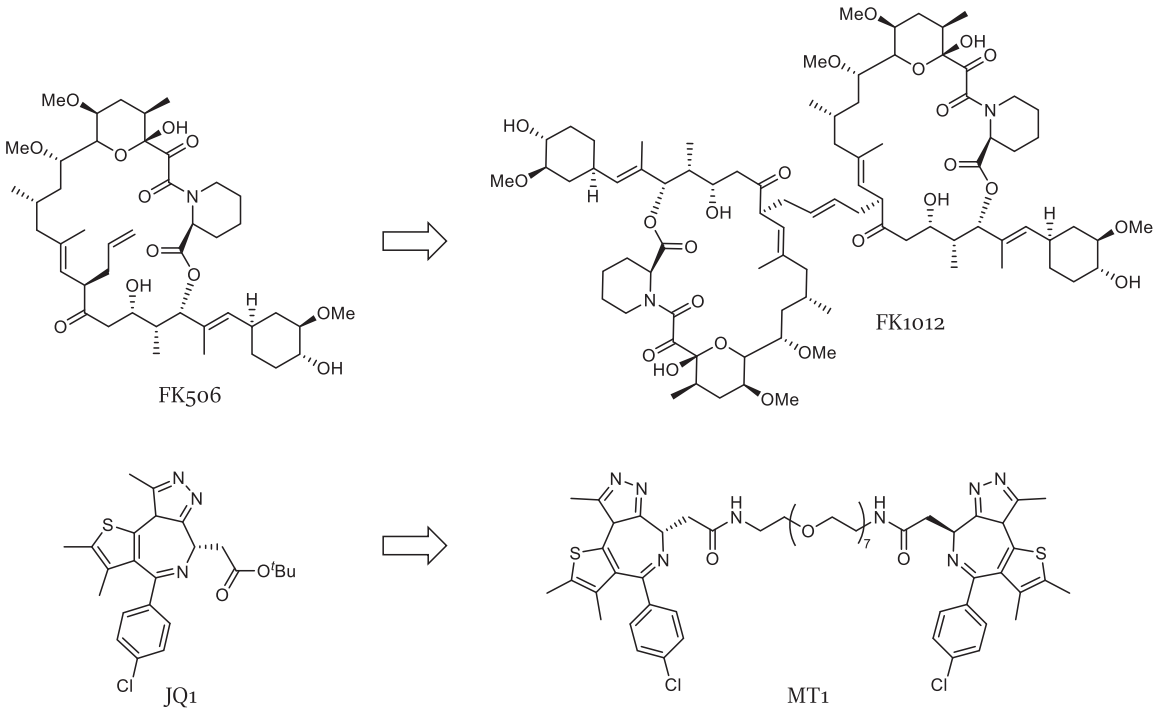

Figure 2.7. Examples of bifunctional inhibitors, derivatized from the corresponding monovalent compound.

Combining the dimerizing effect of a CIP with expression of biological fusion constructs has created very sophisticated tools for the study of biological processes, contributing heavily on the field of chemical biology during the last 20 years. These systems can initiate and track the consequences of biochemical processes in living cells, allowing biologic mimicry of processes that occur naturally. It has fuelled conceptual advances in signal transduction and transcription,[25,26,27] protein folding and localization,[28,29,30,31] chromatin regulation[32] and protein degradation,[33,34] among others. CIP-based strategies have also been used in biocomputing, where a combination of CIP systems can be used to create Boolean logic gates in living cells,[35] showing the applicability of these chemical tools in biology research as well as in the development of new biotechnologies.

Application of such technologies in medicine is challenging, as it requires that proteins must be tagged with dimerizing peptides. In order to treat diseases in living organisms, a CIP needs to target endogenous, unmodified proteins. Potential therapeutics that bind both to FKBP and the β-amyloid peptide have been designed to treat Alzheimer's disease,[36] and a similar approach has targeted to extend the half-life of an HIV protease inhibitor.[37] Although neither of those molecules had good pharmacologic characteristics, this conceptual advance motivated efforts to extend proximity-inducing molecules to meet other medical needs.

Perhaps the most successful application of CIPs outside a system employing fusion constructs has been that of protein degraders. This type of bifunctional compounds induce degradation of a

protein of interest by hijacking the cell's own machinery responsible for protein degradation. This technology has evolved from the first prototypes devised as chemical biology tools to drug-like compounds, some of which are in clinical trials. The field has produced during the last two decades hundreds of examples, targeting a plethora of proteins with therapeutic applications on oncology, neurodegeneration and other complex diseases.[38]

2.4. Protein Degraders

Initially however, protein degraders were not conceived as bifunctional molecules, nor as part of the CIP toolkit. This discovery process began with technologies applied to protein degradation that employed large biomolecules, containing peptide fragments, hydrophobic tags or incorporated the use of fusion proteins. What these strategies had in common was the objective to promote protein degradation by hijacking molecular mechanisms native to living cells.

The two responsible pathways to maintain protein homeostasis in the cell are autophagy by the endosomal-lysosomal system and the ubiquitin-proteasome system (UPS). The endosomal-lysosomal system consists on a set of intracellular membranous compartments that internalize, traffic and degrade proteins.[39] Autophagy mostly aims at long-lived proteins, insoluble aggregates and bigger structures such as whole organelles or intracellular pathogens.[40] The UPS targets short-lived proteins and soluble misfolded proteins, and relies on the proteasome, a protein complex that degrades proteins tagged with ubiquitin chains via proteolysis. Ubiquitin is a small protein (8.5 kDa) that is transferred to protein substrates via a multistep process mediated by E1 ubiquitin-activating enzymes, E2 ubiquitin-conjugating enzymes and E3 ubiquitin ligases. Ubiquitin conjugates initially to an E1 enzyme via covalent thioesther conjugate, followed by transfer to a cysteine residue of the E2 enzyme. The transfer of ubiquitin from E2 to a lysine of the substrate protein is mediated by E3 ligases, a large family of adaptor proteins responsible of recruiting the protein substrate. In the human proteome, there are 8 known E1s, over 40 E2s and around 600 E3 ligases.[41] Depending on their characteristic domains and the mechanism of ubiquitin transfer, E3 ligases are classified in RING E3s, HECT E3s and RBR E3s. RING E3s are the most abundant type of E3 ligases, they are characterized by the presence of a RING (Really Interesting New Gene) or a U-box domain. They mediate a direct ubiquitin transfer by functioning as a scaffold to orient the E2 respect to the substrate protein. Some RING E3s are composed by other subunits, such as the cullin-RING ligases (CRLs), which assemble around a cullin scaffold and incorporate a RING-box protein, an adaptor protein and a substrate receptor protein, responsible for the substrate recognition.[42]

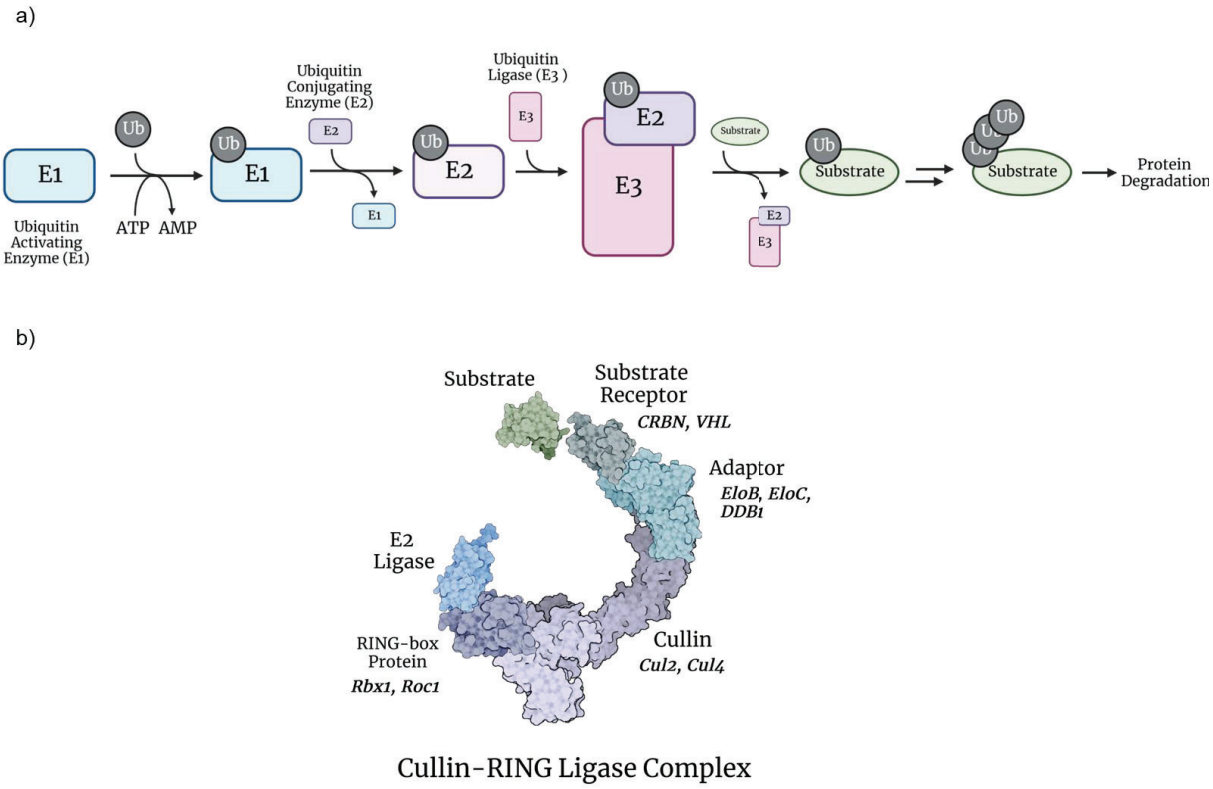

Figure 2.8. (a) The Ubiquitin-Proteasome System. (b) General structure and components of a Cullin-RING E3 ligase complex.

Regulating protein homeostasis is indispensable for the cell's maintenance and survival, as misfolded proteins cannot perform their function and are prone to aggregation.[43] Missfolding and dysregulation of protein levels has been linked to neurodegenerative diseases and cancer, among other diseases.[44] Over the years, technologies that down-regulate expression or knock-down protein levels have been developed and used as means to study the role of proteins and to better understand disease. Small interfering RNA (siRNA) and CRISPR-Cas9 are examples of such technologies, which have become of standard use in biology research. However, they show some limitations; CRISPR-Cas9 shows off-target effects and low efficiency, limiting its application *in vivo*,[45] while siRNA suffers from inefficient delivery and non-specific immune responses which hamper its clinical applications.[46] In this context, small-molecule protein degraders emerged as an alternative to such technologies.

An early example of a technology that attempted to achieve protein degradation using bifunctional small-molecules was hydrophobic tagging (HyT). A HyT molecule consists of two fragments; one based on a ligand with affinity for the protein of interest (POI) and a hydrophobic fragment, spaced by a linker. The HyT binds to the protein surface and mimics a partially unfolded protein state, triggering the cytosolic unfolded protein response to degrade the target.[47] In 2014, this technology was used to degrade erythroblastosis oncogene B3 (HER3), a pseudokinase considered undruggable by a traditional inhibitory approach, using an adamantane fragment coupled to a

HER ligand to induce missfolding recognition.[48] Apart from other tags containing lipophilic organic moieties, the amino acid fragment *tert*-butyl carbamate-protected arginine (Boc_3-Arg) has also been used as a hydrophobic tag. Chemically linked to covalent and non-covalent inhibitors, it has induced degradation of gluthatione-S-transferase (GST) and dihydrofolate reductase.[49]

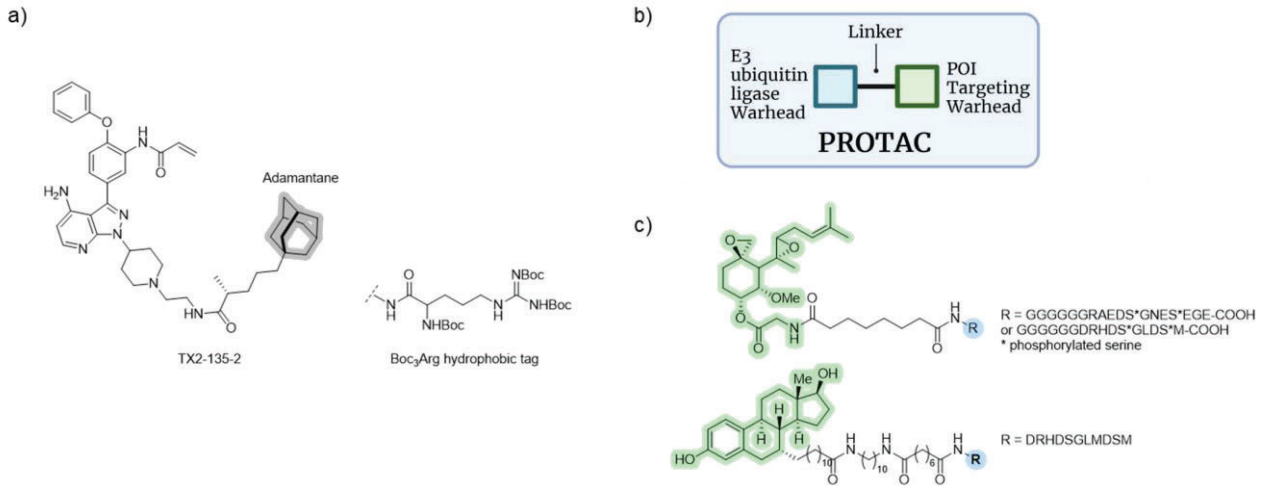

Figure 2.9. a) example of a HyT degrader and the hydrophobic Boc_3Arg tag. **b)** Schematic representation of a PROTAC. **c)** Examples of peptide-based PROTACs.

It is after those precedents that the first proof-of-concept of a PROTAC (Proteolysis Targeting Chimaera) emerged in the literature. PROTACs are bifunctional molecules composed of two warheads, one with affinity for the POI and the other for an E3 ligase. Both warheads are connected by a linker, which can vary in composition and length. (**Figure 2.9**). While HyT degradation relied on inducing a misfolded recognition leading to ubiquitination of the POI mediated by a chaperone, PROTACs directly recruit–an E3 ligase, responsible for the ubiquitin transfer. Simultaneous binding to the POI and the E3 ligase leads to induced proximity, ternary complex formation, ubiquitination and subsequent degradation of the protein.

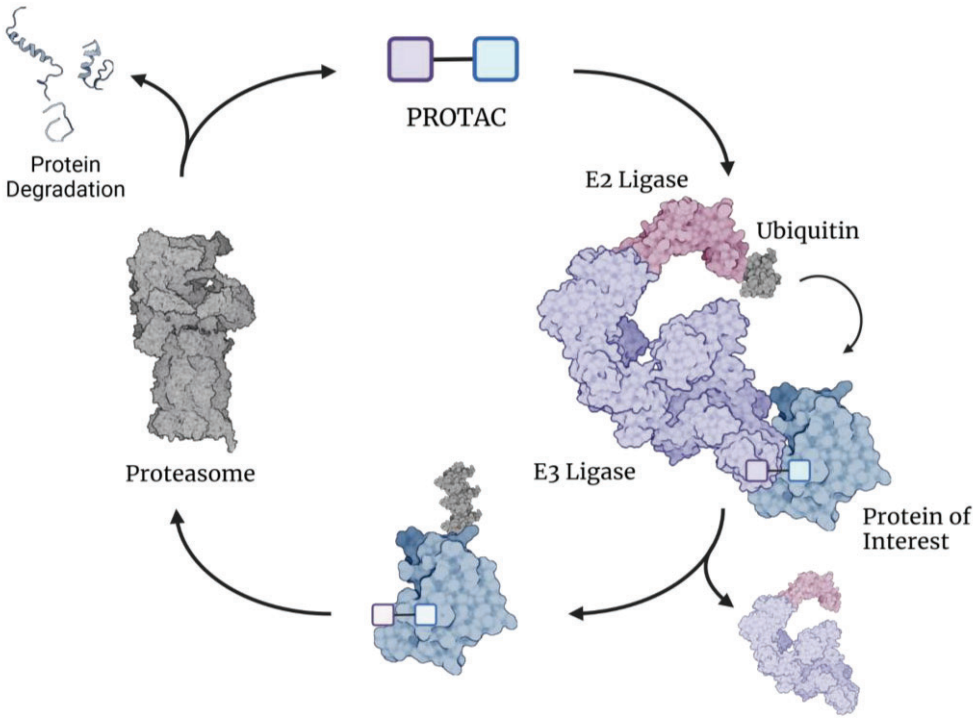

Figure 2.10. Catalytic mechanism of action of a PROTAC.

The first example of a PROTAC, reported in 2001, was composed of a phosphopeptide targeting the F-box protein β-transductin repeat-containing protein (βTRCP), a component of the E3 ligase complex $SCF^{\beta TRCP}$, and ovalicin, a small-molecule that covalently binds to methionine aminopeptidase 2 (MetAP2), the target protein.[50] βTRCP was also targeted in the design of molecules for the androgen receptor (AR) degradation,[51] using dihydrotestosterone (DHT) as the AR-recruiting warhead. The von Hippel-Lindau (VHL) is another E3 ligase that can also be targeted with a peptidic fragment. It recognizes a seven-amino-acid sequence of hypoxia-inducible factor 1α (HIF1α), characterized by a core hydroxylated proline.[52] This peptidic VHL-recruiting fragment was used to develop AR,[53] oestrogen receptor (ER),[54] protein kinase AKT[55] and Tau[56] degraders. The potency of these PROTACs remained typically on the micromolar range, probably due to their poor cell penetration associated with their peptidic composition. In order to overcome the pharmacokinetic difficulties that peptidic PROTACs might present, research turned to the development of small-molecule based PROTACs. The search began by finding small-molecule ligands that could engage with E3 ligases.

Nutlins are a class of MDM2 inhibitors that inhibit its interaction with p53. In 2008, nutlin-3a was used as a ligand to target the E3 ligase mouse double minute 2 homologue (MDM2), producing PROTACs of moderate potencies.[57] Another attempt to target an E3 ligase with a small molecule was using bestatin to target the E3 ligase cellular inhibitor of apoptosis protein 1 (cIAP1). The degraders, named SNIPER (specific and non-genetic IAP dependent protein eraser), were reported

on 2010. SNIPERs targeted the cellular retinoic acid binding protein 1 (CRABP1) and CRABP2, using *trans*-retinoic acid as the target ligand. However, bestatin is not a specific ligand of cIAP1, and the compounds had off-target activity as well as autoubiquitination and degradation of the E3 ligase cIAP1, limiting their potency.[58]

Subsequent efforts aimed at identifying a small-molecule replacement for the VHL-targeting HIF1α fragment. In 2012, a combined effort of *in silico* and fragment-based screening identified the first small-molecule ligand for this protein,[59] which was optimized via structure-activity relationship campaigns.[60] The utility of this ligand was demonstrated with the synthesis of an oestrogen-related receptor α (ERRα) degrader with nanomolar activity, achieving 40% of protein knockdown *in vivo*.[61] That milestone demonstrated that small-molecule based PROTACs could be more effective than their peptide-based precedents, and despite their high molecular weight they could show activity in mouse models.

Parallel to the establishment of VHL-based PROTACs, a different system utilizing a fourth small-molecule E3 ligase ligand was developed in 2010. Following the discovery of immunomodulatory drugs (ImIDs) and their molecular glue mechanism of action, it was sought to use them as E3 ligase recruiters. ImIDs bind to cereblon (CRBN), the substrate recognition unit of the $CRL4^{CRBN}$ubiquitin ligase, and induce the degradation of neosubstrates by the E3 ligase. Conjugating the ImID to a ligand of the target protein meant that the phthalimide would not simply act as a molecular glue, but that neosubstrate recognition could be fine-tuned by the ligand choice. Conjugation of a BRD4 ligand to pomalidomide yielded a PROTAC with picomolar potency.[62] In a parallel study, another thalidomide-based PROTAC targeting BRD4 was synthesized using JQ1 as the POI-targeting warhead.[63] Bromodomains have been traditional targets in heterobifunctional molecule design, and more examples of BDR-targeting PROTACs incorporating the VHL-binding fragment emerged, including a pan-BET-degrader[64] and JQ1-based VHL PROTACs.[65]

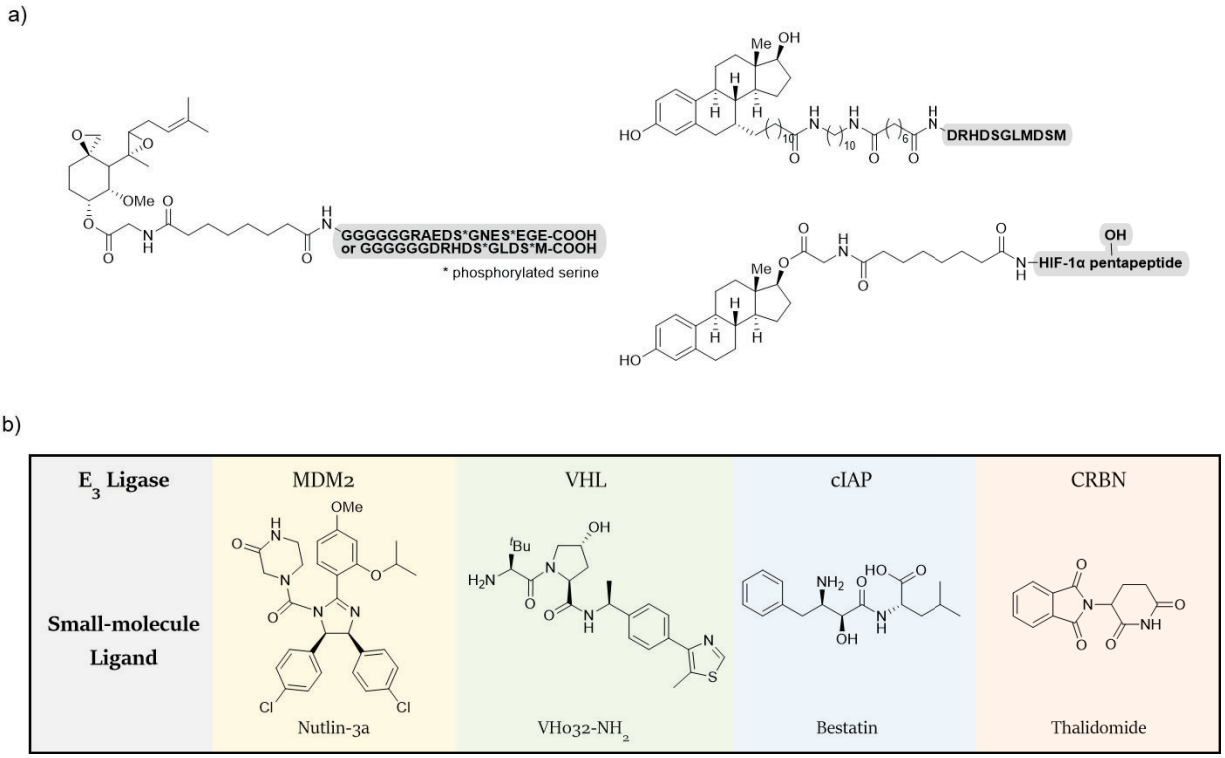

Figure 2.11. a) Examples of peptide-based PROTACs. **b)** E3 ligases most commonly used in PROTAC design, and their small-molecule ligands.

The field of targeted protein degradation has been highly prolific in the past 20 years, producing examples of PROTACs targeting BCR-ABL,[66] EGFR,[67] p38,[68] FAK,[69] IRAK4,[70] SMARCA2-4,[71] KRAS,[72] PCAF/GCN5,[73] CDK4/6,[74] BCL2 and CBL-xL,[75] BDR7/9,[76] Tau,[77] MDM2,[78] BTK[79] and ALK,[80] among many others. Most of these examples employ a VHL or CRBN recruiter. Although the number of E3 ligases in the human proteome is over 600, these two E3 ligases are the most commonly used in PROTAC design, due to the existence of small-molecule binders, with accessible and relatively easy syntheses and reliable activity.

There is a big potential in targeting other E3 ligases, as studies have evaluated their applicability to be employed in targeted protein degradation.[81] However, to be incorporated into mainstream PROTAC design, small-molecule ligands for those proteins need to be discovered. There is work in progress. Indisulam, which is also a molecular glue acting on the E3 ligase DCAF15, has been proposed as a DCAF15 binder.[82] DCAF16 is another E3 ligase that can be targeted using a covalent binder, identified through a chemoproteomic screen.[83] Other screening techniques have been used to find ligands for the E3 ligases RNF114[84] and RNF4.[85] However, PROTACs bearing ligands targeting those E3 ligases are underrepresented in the literature, and the biology of those E3 ligases is not fully understood.

PROTACs have been very useful as chemical biology tools to interrogate biological systems. It was not clear, however, if they could be able to make their way to the clinic. Primarily due to its high

molecular weight, PROTACs do not usually adjust to the "Lipinski's rule of 5", a set of molecular descriptors associated to drug activity and pharmacokinetics.[86] Showing molecular weights in the range of 900-1100 Da and a number of rotatable bonds between 20 and 25, most PROTACs exceed the limits proposed by the rules.[87] These facts, however, did not prevent PROTACs from attracting the attention of the pharmaceutical industry, with few companies being created around developing this technology and making it amenable for therapeutic use. In 2019, two PROTACs targeting the AR and the ER entered clinical trials for the treatment of prostate and breast cancer, respectively. Both degraders have advanced to phase II clinical trials, and have been followed by other compounds targeting neoplastic and degenerative pathologies.[38] Although the transfer of PROTAC technology from the bench to the clinic is fairly recent, there are already fifteen PROTACs that entered some stage of clinical development in the last three years.[38]

2.5. Protein Degradation – Advantages and Challenges

Traditional small-molecule inhibitors act by occupancy-driven mechanisms; by binding to the active site of the protein or to an allosteric site which induces inhibition of protein activity. Historically, pharmacological intervention has been focused on targeting these well-defined pockets. Traditionally stablished methods of drug development focus on this paradigm and, although drugs with alternative modes of action such as biologics already account for an important part of marketed drugs, most approved compounds primarily operate *via* occupancy-driven pharmacology.[88] Although successful, this mechanism of action has its drawbacks. Not all proteins can be inhibited by small-molecule inhibitors, especially those lacking enzymatic activity, such as scaffolding proteins or proteins that exert their function mainly through PPIs.[89] Occupancy is a dynamic equilibrium and in order to achieve high potencies, a systemic high drug exposure is necessary.[90] High concentrations are difficult to maintain in *in vivo* settings and will usually require higher doses of drug administration. Moreover, high levels of compound may induce unwanted off-target effects. Protein degradation, and in particular PROTAC technology, seeks to overcome these difficulties posed by traditional inhibitors.

PROTACs have an event-driven mechanism of action, they require only a temporary binding to induce their pharmacological effect, based on the proximity between E3 ligase and POI. This confers a catalytic mechanism to PROTACs based on reversible binders; a single molecule is able to promote more degradation events after dissociation from the target protein. Another advantage of PROTACs is that they do not need binders with great affinities towards the target protein, since high occupancy is not a requirement for activity. The term "undruggable" was coined to describe proteins for which no known strong ligands were known, or whose surface lacked binding cavities that could be targeted strongly by small molecules.[91] PROTACs promise degradation of even such proteins, for which potent small-molecule inhibitors are not known.

The critical aspect of PROTAC's pharmacodynamics is the formation of a sufficiently stable tertiary complex between E3 ligase, PROTAC and POI, allowing the ubiquitination of the POI to take place. The formation of such ternary complex is directly associated with degradation efficiency,[92] making cooperative interactions between E3 ligase, PROTAC and POI play in favour of the compound's efficiency. A PROTAC's efficiency is not, however, linearly related to the compound's concentration; as the formation of unproductive binary complexes (E3 ligase-PROTAC and POI-PROTAC) increases with PROTAC concentration, resulting in a bell-shaped concentration-effect curve, commonly referred to as the hook effect. (**Figure 2.12b**)[93]

The cooperative effect due to the formation of a ternary complex has been studied and parametrized for BET degraders.[94] A K_d^{binary} is defined for the binary complex between PROTAC and POI and a $K_d^{ternary}$ for the formation of the ternary complex POI-PROTAC-E3 ligase. A cooperative interaction exists when $K_d^{ternary}$ is greater than K_d^{binary}, indicating a positive contribution of the PPIs towards the formation of the ternary complex. This supports the idea that favourable PPIs play in favour of PROTAC efficiency, and can compensate for the low affinity of the PROTAC towards the POI.

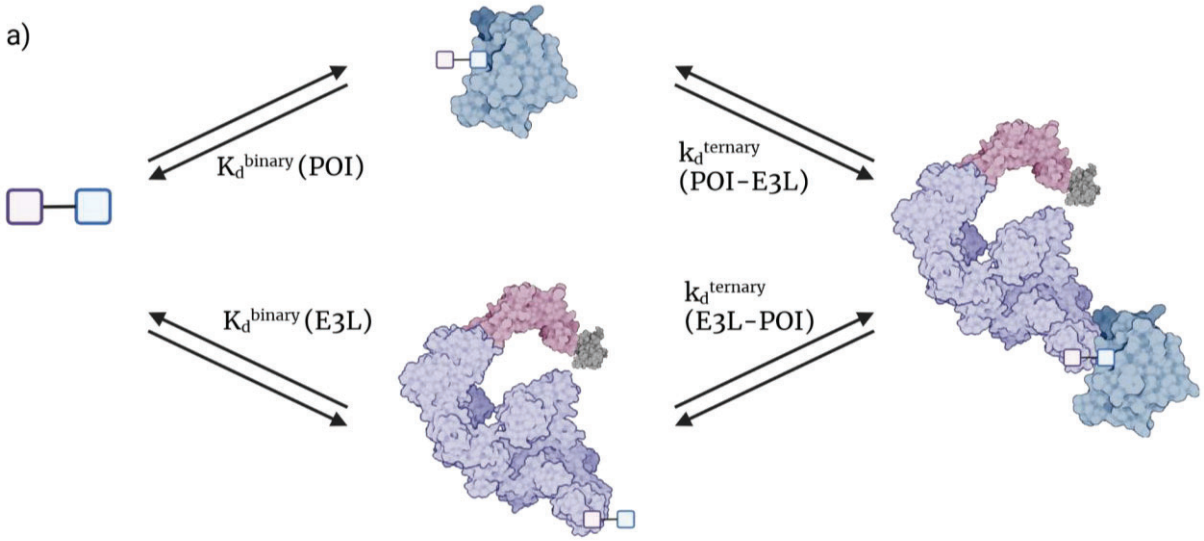

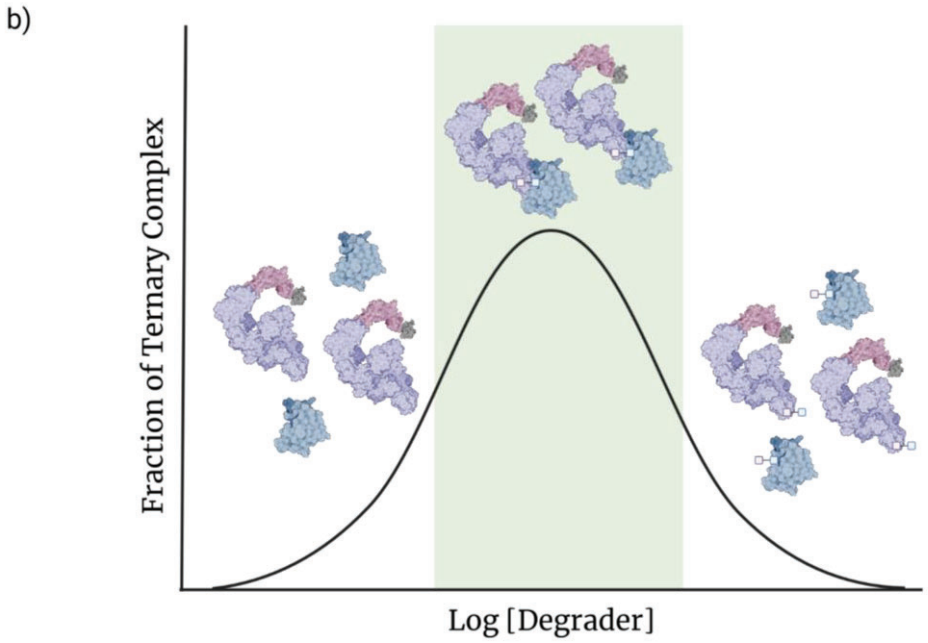

Figure 2.12. a) Ternary complex equilibria. **b)** Representation of the hook effect.

In spite of these advantages, PROTAC technology also has challenges to overcome. Most PROTACs are not considered drug-like; they exceed in molecular weight, lack ideal rigidity and show poor water solubility and oral absorption, as well as poor transmembrane properties. Rational optimization of PROTACs is costly and usually limited in linker length and composition, as the two warhead regions cannot be heavily modified without function loss. Achieving a good pharmacokinetic profile, good oral absorption and cell permeability are the main obstacles in converting PROTAC into good drug candidates, and structural optimization mainly focuses on the evaluation of SAR for various linkers. In spite of that, medicinal chemistry efforts have partially circumvented those challenges, as demonstrates the growth of the field and the increasing examples of protein degraders found in the literature. Either as chemical biology tools or therapeutic agents, protein degraders pose a new paradigm of pharmacology that has already consolidated, and may be instrumental in solving current challenges in the fields of biology and medicine.

References

[1] https://www.nature.com/scitable/topicpage/protein-function-14123348/

[2] Maniaci, C. & Ciulli, A. Bifunctional chemical probes inducing protein–protein interactions. *Curr. Opin. Chem. Biol.* **2019**, *52*, 145–156.

[3]Cesa, L. C., Mapp, A. K. & Gestwicki, J. E. Direct and propagated effects of small molecules on protein-protein interaction networks. *Front. Bioeng. Biotechnol.* **2015**, *3*, 1–18.

[4] Arkin, M. R., Tang, Y. & Wells, J. A. Small-molecule inhibitors of protein-protein interactions: Progressing toward the reality. *Chem. Biol.* **2014**, *21*, 1102–1114.

[5] Jones, S. & Thornton, J. M. Analysis of protein-protein interaction sites using surface patches. *J. Mol. Biol.* **1997**, *272*, 121–132.

[6] Leutert, M., Entwisle, S. W. & Villén, J. Decoding post-translational modification crosstalk with proteomics. *Mol. Cell. Proteomics.* **2021**, *20*, 0–11.

[7] Wells, J. A. & McClendon, C. L. Reaching for high-hanging fruit in drug discovery at protein-protein interfaces. *Nature,* **2007**, *450*, 1001–1009.

[8] Vassilev, L. T. *et al.* In Vivo Activation of the p53 Pathway by Small-Molecule Antagonists of MDM2. *Science.* **2004**, *303*, 844–848.

[9] Oltersdorf, T. *et al.* An inhibitor of Bcl-2 family proteins induces regression of solid tumours. *Nature.* **2005**, *435*, 677–681.

[10] London, N., Raveh, B. & Schueler-Furman, O. Druggable protein-protein interactions - from hot spots to hot segments. *Curr. Opin. Chem. Biol.* **2013**, *17*, 952–959.

[11] Gorczynski, M. J. *et al.* Allosteric Inhibition of the Protein-Protein Interaction between the Leukemia-Associated Proteins Runx1 and CBFβ. *Chemistry and Biology* vol. 14 1186–1197 at https://doi.org/10.1016/j.chembiol.2007.09.006 (2007).

[12] Roman, D. L., Blazer, L. L., Monroy, C. A. & Neubig, R. R. Allosteric inhibition of the regulator of G protein signaling-Gα protein-protein interaction by CCG-4986. *Mol. Pharmacol.* **2010**, *78*, 360–365.

[13] Giordanetto, F., Schäfer, A. & Ottmann, C. Stabilization of protein-protein interactions by small molecules. *Drug Discov. Today* **2014**, *19*, 1812–1821.

[14] Yoo, Y. J., Kim, H., Park, S. R. & Yoon, Y. J. An overview of rapamycin: from discovery to future perspectives. *J. Ind. Microbiol. Biotechnol.* **2017**, *44*, 537–553.

[15] Guduru, S. K. R. & Arya, P. Synthesis and biological evaluation of rapamycin-derived, next generation small molecules. *Medchemcomm.* **2018**, *9*, 27–43.

[16] Shabek, N. & Zheng, N. Plant ubiquitin ligases as signaling hubs. *Nat. Struct. Mol. Biol.* **2014**, *21*, 293–296.

[17] Chamberlain, P. P. & Cathers, B. E. Cereblon modulators: Low molecular weight inducers of protein degradation. *Drug Discov. Today Technol.* **2019**, *31*, 29–34.

[18] Matyskiela, M. E. *et al.* SALL4 mediates teratogenicity as a thalidomide-dependent cereblon substrate. *Nat. Chem. Biol.* **2018**, *14*, 981–987.

[19] Bussiere, D. E. *et al.* Structural basis of indisulam-mediated RBM39 recruitment to DCAF15 E3 ligase complex. *Nat. Chem. Biol.* **2020**, *16*, 15–23.

[20] Dong, G., Ding, Y., He, S. & Sheng, C. Molecular Glues for Targeted Protein Degradation: From Serendipity to Rational Discovery. *J. Med. Chem.* **2021**, *64*, 10606–10620.

[21] Tanaka, M. *et al.* Design and characterization of bivalent BET inhibitors. *Nat. Chem. Biol.* **12**, 1089–1096 (2016).

[22] Arkin, M. R., Tang, Y. & Wells, J. A. Small-Molecule Inhibitors of Protein-Protein Interactions: Progressing toward the Reality. *Chem. Biol.* **2014**, *21*, 1102–1114.

[23] Pruschy, M. N. *et al.* Mechanistic studies of a signaling pathway activated by the organic dimerizer FK1012. *Chem. Biol.* **1994**, *1*, 163–172.

[24] Nakai, K. Controlling signal transduction with synthetic ligands. *Tanpakushitsu Kakusan Koso.* **2007**, *52*, 1794–1795.

[25] Holsinger, L. J., Spencer, D. M., Austin, D. J., Schreiber, S. L. & Crabtree, G. R. Signal transduction in T lymphocytes using a conditional allele of Sos. *Proc. Natl. Acad. Sci. U. S. A.* **1995**, *92*, 9810–9814.

[26] Graef, I. A., Holsinger, L. J., Diver, S., Schreiber, S. L. & Crabtree, G. R. Proximity and orientation underlie signaling by the non-receptor tyrosine kinase ZAP70. *EMBO Journal.* **1997**, *16*, 5618–5628.

[27] Ho, S. N., Biggar, S. R., Spencer, D. M., Schreiber, S. L. & Crabtree, G. R. Dimeric ligands define a role for transcriptional activation domains in reinitiation. *Nature.* **1996**, *382*, 822–826.

[28] Belshaw, P. J., Ho, S. N., Crabtree, G. R. & Schreiber, S. L. Controlling protein association and subcellular localization with a synthetic ligand that induces heterodimerization of proteins. *Proc. Natl. Acad. Sci. U. S. A.* **1996**, *93*, 4604–4607.

[29] Rivera, V. M. *et al.* Regulation of protein secretion through controlled aggregation in the endoplasmic reticulum. *Science.* **2000**, *287*, 826–830.

[30] Bayle, J. H. *et al.* Rapamycin analogs with differential binding specificity permit orthogonal control of protein activity. *Chem. Biol.* **2006**, *13*, 99–107.

[31] Mootz, H. D., Blum, E. S., Tyszkiewicz, A. B. & Muir, T. W. Conditional protein splicing: A new tool to control protein structure and function in vitro and in vivo. *J. Am. Chem. Soc.* **2003**, *125*, 10561–10569.

[32] Hathaway, N. A. *et al.* Dynamics and memory of heterochromatin in living cells. *Cell.* **2012**, *149*, 1447–1460.

[33] Banaszynski, L. A., Chen, L. chun, Maynard-Smith, L. A., Ooi, A. G. L. & Wandless, T. J. A Rapid, Reversible, and Tunable Method to Regulate Protein Function in Living Cells Using Synthetic Small Molecules. *Cell.* **2006**, *126*, 995–1004.

[34] Nishimura, K., Fukagawa, T., Takisawa, H., Kakimoto, T. & Kanemaki, M. An auxin-based degron system for the rapid depletion of proteins in nonplant cells. *Nat. Methods* **2009**, *6*, 917–922.

[35] Ma, Q. *et al.* Rapid and Orthogonal Logic Gating with a Gibberellin-induced Dimerization System Access. *Nat. Chem. Biol.* **2009**, *27*, 14299–14307.

[36] Gestwicki, J. E., Crabtree, G. R. & Graef, I. A. Harnessing Chaperones to Generate Small-Molecule Inhibitors of Amyloid ß Aggregation. *Science.* **2004**, *306*, 865–869.

[37] Marinec, P. S. *et al.* FK506-binding protein (FKBP) partitions a modified HIV protease inhibitor into blood cells and prolongs its lifetime in vivo. *Proc. Natl. Acad. Sci. U. S. A.* **2009**, *106*, 1336–1341.

[38] Békés, M., Langley, D. R. & Crews, C. M. PROTAC targeted protein degraders: the past is prologue. *Nat. Rev. Drug Discov.* **2022**, *21*, 181–200.

[39] Hu, Y. B., Dammer, E. B., Ren, R. J. & Wang, G. The endosomal-lysosomal system: From acidification and cargo sorting to neurodegeneration. *Transl. Neurodegener.* **2015**, *4*, 1–10.

[40] Kocaturk, N. M. & Gozuacik, D. Crosstalk between mammalian autophagy and the ubiquitin-proteasome system. *Front. Cell Dev. Biol.* **2018**, *6*, 1–27.

[41] Paiva, S. L., Da Silva, S. R., De Araujo, E. D. & Gunning, P. T. Regulating the Master Regulator: Controlling Ubiquitination by Thinking Outside the Active Site. *J. Med. Chem.* **2018**, *61*, 405–421.

[42] Morreale, F. E. & Walden, H. Types of Ubiquitin Ligases. *Cell* **2016**, *165*, 248-248.

[43] Roberts, C. J. Therapeutic protein aggregation: Mechanisms, design, and control. *Trends Biotechnol.* **2014**, *32*, 372–380.

[44] Cheng, B. *et al.* Interaction between amyloidogenic proteins and biomembranes in protein misfolding diseases: Mechanisms, contributors, and therapy. *Biochim. Biophys. Acta - Biomembr.* **2018**, *1860*, 1876–1888.

[45] Karlgren, M., Simoff, I., Keiser, M., Oswald, S. & Artursson, P. CRISPR-Cas9: A new addition to the drug metabolism and disposition tool box. *Drug Metab. Dispos.* **2018**, *46*, 1776–1786.

[46] Lee, K. *et al.* The cutting-edge technologies of siRNA delivery and their application in clinical trials. *Arch. Pharm. Res.* **2018**, *41*, 867–874 (2018).

[47] Neklesa, T. K. & Crews, C. M. Greasy tags for protein removal. *Nature.* **2012**, *487*, 308–309.

[48] Xie, T. *et al.* Pharmacological Targeting of the Pseudokinase Her3. *Nat Chem Biol.* **2014**, *10*, 1006–1012.

[49] Lai, A. C. & Crews, C. M. Induced protein degradation: An emerging drug discovery paradigm. *Nat. Rev. Drug Discov.* **2017**, *16*, 101–114.

[50] Sakamoto, K. M. *et al.* PROTACs: Chimeric molecules that target proteins to the Skp1-Cullin-F box complex for ubiquitination and degradation. *Proc. Natl. Acad. Sci. U. S. A.* **2001**, *98*, 8554–8559.

[51] Sakamoto, K. M. *et al.* Development of PROTACs to target cancer-promoting proteins for ubiquitination and degradation. *Mol. Cell. Proteomics.* **2003**. *2*, 1350–1358.

[52] Min, J. H. *et al.* Structure of an HIF-1α-pVHL complex: Hydroxyproline recognition in signaling. *Science.* **2022**, *296*, 1886–1889.

[53] Schneekloth, J. S. *et al.* Chemical Genetic Control of Protein Levels: Selective in Vivo Targeted Degradation. *Journal of the American Chemical Society* **2004**, *126*, 3748–3754.

[54] Hazen, G. *et al.* Targeting steroid hormone receptors for ubiquitination and degradation in breast and prostate cancer. *Oncogene* **2017**, *27*, 7201–7211.

[55] Henning, R. K. *et al.* Degradation of Akt using protein-catalyzed capture agents. *J. Pept. Sci.* **2016**, *22*, 196–200.

[56] Chu, T. T. *et al.* Specific Knockdown of Endogenous Tau Protein by Peptide-Directed Ubiquitin-Proteasome Degradation. *Cell Chem. Biol.* **2016**, *23*, 453–461.

[57] Schneekloth, A. R., Pucheault, M., Tae, H. S. & Crews, C. M. Targeted intracellular protein degradation induced by a small molecule: En route to chemical proteomics. *Bioorganic Med. Chem. Lett.* **2008**, *18*, 5904–5908.

[58] Sekine, K. *et al.* Small molecules destabilize cIAP1 by activating auto-ubiquitylation. *J. Biol. Chem.* **2008**, *283*, 8961–8968.

[59] Van Molle, I. *et al.* Dissecting fragment-based lead discovery at the von hippel-lindau protein:Hypoxia inducible factor 1α protein-protein interface. *Chem. Biol.* **2012**, *19*, 1300–1312.

[60] Galdeano, C. *et al.* Structure-guided design and optimization of small molecules targeting the protein-protein interaction between the von hippel-lindau (VHL) E3 ubiquitin ligase and the hypoxia inducible factor (HIF) alpha subunit with in vitro nanomolar affinities. *J. Med. Chem.* **2014**, *57*, 8657–8663.

[61] Bondeson, D. P. *et al.* Catalytic in vivo protein knockdown by small-molecule PROTACs. *Nat. Chem. Biol.* **2015**, *11*, 611–617.

[62] Lu, J. *et al.* Hijacking the E3 Ubiquitin Ligase Cereblon to Efficiently Target BRD4. *Chem. Biol.* **2015**, *22*, 755–763.

[63] Winter, G. E. *et al.* Phthalimide conjugation as a strategy for in vivo target protein degradation. *Science (80-.).* **2015**, *348*, 1376–1381.

[64] Raina, K. *et al.* PROTAC-induced BET protein degradation as a therapy for castration-resistant prostate cancer. *Proc. Natl. Acad. Sci. U. S. A.* **2016**, *113*, 7124–7129.

[65] Zengerle, M., Chan, K. H. & Ciulli, A. Selective Small Molecule Induced Degradation of the BET Bromodomain Protein BRD4. *ACS Chem. Biol.* **2015**, *10*, 1770–1777.

[66] Burslem, G. M. *et al.* Targeting BCR-ABL1 in chronic myeloid leukemia by PROTAC-mediated targeted protein degradation. *Cancer Res.* **2019**, *79*, 4744–4753.

[67] Hong, D. *et al.* Recent advances in the development of EGFR degraders: PROTACs and LYTACs. *Eur. J. Med. Chem.* **2022**, *239*, 114533.

[68] Smith, B. E. *et al.* Differential PROTAC substrate specificity dictated by orientation of recruited E3 ligase. *Nat. Commun.* **2019**, *10*, 1–13.

[69] Cromm, P. M., Samarasinghe, K. T. G., Hines, J. & Crews, C. M. Addressing Kinase-Independent Functions of Fak via PROTAC-Mediated Degradation. *J. Am. Chem. Soc.* **2018**, *140*, 17019–17026.

[70] Nunes, J. *et al.* Targeting IRAK4 for Degradation with PROTACs. *ACS Med. Chem. Lett.* **2019**, *10*, 1081–1085.

[71] Farnaby, W. *et al.* BAF complex vulnerabilities in cancer demonstrated via structure-based PROTAC design. *Nat. Chem. Biol.* **2019**, *15*, 672–680.

[72] Bond, M. J., Chu, L., Nalawansha, D. A., Li, K. & Crews, C. M. Targeted Degradation of Oncogenic KRASG12C by VHL-Recruiting PROTACs. *ACS Cent. Sci.* **2020**, *6*, 1367–1375.

[73] Bassi, Z. I. *et al.* Modulating PCAF/GCN5 Immune Cell Function through a PROTAC Approach. *ACS Chem. Biol.* **2018**, *13*, 2862–2867.

[74] Zhao, B. & Burgess, K. PROTACs suppression of CDK4/6, crucial kinases for cell cycle regulation in cancer. *Chem. Commun.* **2019**, *55*, 2704–2707.

[75] Lv, D. *et al.* Development of a BCL-xL and BCL-2 dual degrader with improved anti-leukemic activity,. *Nat. Commun.* **2021**, *12*, 1–14.

[76] Zoppi, V. *et al.* Iterative Design and Optimization of Initially Inactive Proteolysis Targeting Chimeras (PROTACs) Identify VZ185 as a Potent, Fast, and Selective von Hippel-Lindau (VHL) Based Dual Degrader Probe of BRD9 and BRD7. *Journal of Medicinal Chemistry* at https://doi.org/10.1021/acs.jmedchem.8b01413 (2019) vol. 62 699–726.

[77] Silva, M. C. *et al.* Targeted degradation of aberrant tau in frontotemporal dementia patient-derived neuronal cell models. *Elife* **2019**, *8*, 1–31.

[78] Li, Y. *et al.* Discovery of MD-224 as a First-in-Class, Highly Potent, and Efficacious Proteolysis Targeting Chimera Murine Double Minute 2 Degrader Capable of Achieving Complete and Durable Tumor Regression. *J. Med. Chem.* **2019**, *62*, 448–466.

[79]Buhimschi, A. D. *et al.* Targeting the C481S Ibrutinib-Resistance Mutation in Bruton's Tyrosine Kinase Using PROTAC-Mediated Degradation. *Biochemistry* **2018**, *57*, 3564–3575.

[80] Powell, C. E. *et al.* Chemically Induced Degradation of Anaplastic Lymphoma Kinase (ALK). *J. Med. Chem.* **2018**, *61*, 4249–4255.

[81] Ottis, P. *et al.* Assessing Different E3 Ligases for Small Molecule Induced Protein Ubiquitination and Degradation. *ACS Chem. Biol.* **2017**, *12*, 2570–2578.

[82] Coomer, S.; Gilingham, D.G. Exploring DCAF15 for reprogrammable targeted protein degradation. *Bioarxiv* **2019**, 542506.
[83] Zhang, X., Crowley, V. M., Wucherpfennig, T. G., Dix, M. M. & Cravatt, B. F. Electrophilic PROTACs that degrade nuclear proteins by engaging DCAF16. *Nat. Chem. Biol.* **2019**, *15*, 737–746.
[84] Tong, B. *et al.* A Nimbolide-Based Kinase Degrader Preferentially Degrades Oncogenic BCR-ABL. *ACS Chem. Biol.* **2020**, *15*, 1788–1794.
[85] Ward, C. C. *et al.* Covalent Ligand Screening Uncovers a RNF4 E3 Ligase Recruiter for Targeted Protein Degradation Applications. *ACS Chem. Biol.* **2019**, *14*, 2430–2440.
[86] Lipinski, C.A.; Lombardo, F.; Dominy, B.W.; Feeney, P.J. Experimental and Computational Approaches to Estimate Solubility and Permeability in Drug Discovery and Development Settings. *Adv. Drug Deliv. Rev.* **1997**, *23*, 3–25.
[87] Pedrucci, F. *et al.* Proteolysis Targeting Chimeric Molecules: Tuning Molecular Strategies for a Clinically Sound Listening. *Int. J. Mol. Sci.* **2022**, *23*, 6630.
[88] Batta A, Kalra BS, Khirasaria R. Trends in FDA drug approvals over last 2 decades: An observational study. *J Family Med Prim Care.* **2020**, *9*, 105-114.
[89] Fuller, J. C., Burgoyne, N. J. & Jackson, R. M. Predicting druggable binding sites at the protein-protein interface. *Drug Discov. Today* **2009**, *14*, 155–161.
[90] Adjei, A. A. What is the right dose? The elusive optimal biologic dose in phase I clinical trials. *J. Clin. Oncol.* **2006**, *24*, 4054–4055.
[91] Dang, C. V., Reddy, E. P., Shokat, K. M. & Soucek, L. Drugging the 'undruggable' cancer targets. *Nat. Rev. Cancer* **2017**, *17*, 502–508.
[92] Hu, Z. & Crews, C. M. Recent Developments in PROTAC-Mediated Protein Degradation: From Bench to Clinic. *ChemBioChem* **2022**, *23*,.
[93] Hughes, S. J. & Ciulli, A. Molecular recognition of ternary complexes: A new dimension in the structure-guided design of chemical degraders. *Essays Biochem.* **2017**, *61*, 505–516.
[94] Gadd, M. S. *et al.* Structural basis of PROTAC cooperative recognition for selective protein degradation Accession codes Atomic coordinates and structure factors for hsBrd4 BD2-MZ1-hsVHL-hsEloC-hsEloB have been deposited in the Protein Data Bank (PDB) under accession number. *Nat Chem Biol* **2017**, *13*, 514–521.

Chapter 3.

Oestrogen Receptor PROTACs

3. Oestrogen Receptor PROTACs

3.1. ER PROTACs: Introduction and Precedents

3.1.1. Oestrogen Receptor and Breast Cancer

The oestrogen receptor (ER) is a transcription factor implicated in the regulation of various physiological processes such as cell growth, reproduction, development and differentiation. It plays a regulatory role in bone density, brain function, cholesterol mobilization and control of inflammation. In females it is responsible for primary and secondary sexual characteristics and regulation of the menstrual cycle,[1] while in males it is involved in sexual function.[2] Two types of ER exist, ERα and ERβ. ERα was discovered in the 1960s; experimentation using tritium-labelled 17β-estradiol demonstrated the retention of the hormone in oestrogen targeted tissues. This discovery opened the door for subsequent identification and study for the receptor,[3] and 40 years later, ERβ was cloned from a rat prostate cDNA library,[4] demonstrating the existence of a second type of receptor and forcing a re-evaluation of the biology of oestrogen.

Both ERα and ERβ belong to the steroid/thyroid hormone superfamily of nuclear receptors. Both receptors show high homology in their primary sequence and similarities in their structure, however, they differ in tissue expression and in response to synthetic ligands.[5] The binding of a ligand to ER triggers conformational changes, leading to receptor dimerization, receptor-DNA interaction, recruitment of coactivators and other transcription factors or formation of protein complexes.[6]

The natural ligand of ER is 17-β-estradiol (E_2). E_2 can cross the cellular membrane and bind to intracellular ERα and ERβ, initiating signalling events. Ligand binding typically results in dimerization of the receptor, translocation to the nucleus and interaction with chromatin at specific DNA regions, regulating gene expression. Alternatively, E_2 can also affect gene expression through a variety of intracellular signalling events.[7]

a)

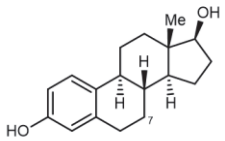

17-β-oestradiol (E2)

b)

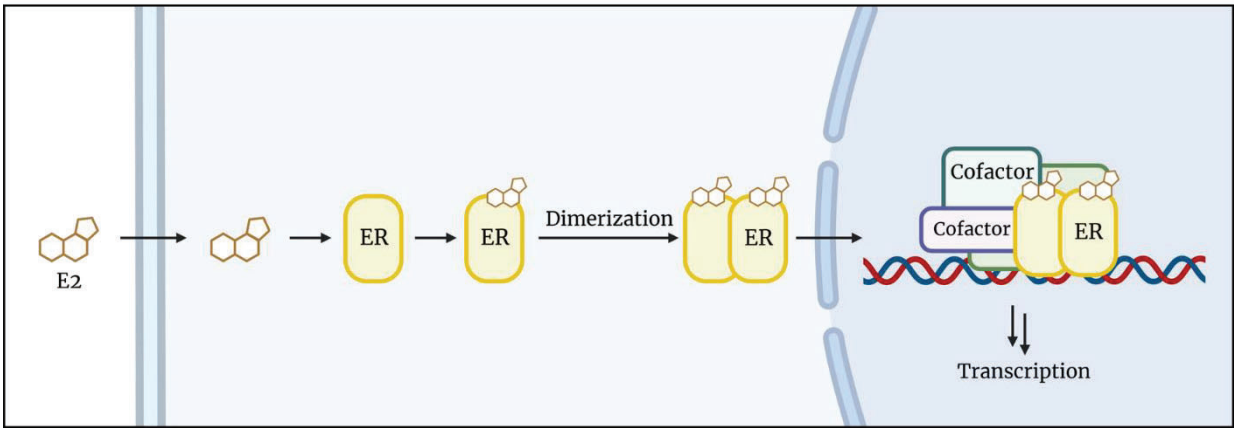

Figure 3.1. **a)** Structure of 17β-oestradiol (E2). **b)** direct activation of ER by E2.

ER signalling also plays a regulatory role in carcinogenesis, as the activated oestrogen-ER complex regulates various genes that are key to cell proliferation and cell cycle progression. It also plays a role in regulating apoptosis and promotes angiogenesis, necessary for tumour progression.[1] The activity of ER has been associated to different types of cancers. The receptor is most notably implicated in breast cancer; however, it is also implicated in ovarian,[8] prostate[9] and colon cancer.[10] ER is the primary target in breast cancer treatment, as 70% of breast cancers are classified as ER-positive (ER+), meaning they respond to hormone therapy,[11] and modulation of this signalling pathway with SERMs (selective oestrogen receptor modulators) and SERDs (selective oestrogen receptor degraders) has been the main strategy in the clinic to treat ER+ breast cancer.

3.1.2 Selective Oestrogen Receptor Modulators

SERMs encompass drugs acting as oestrogen competitors, which bind to the ER and modulate its activity by changing the cofactors with which it associates.[12] The effect of SERMs in modulating the ER and the downstream effect on ER signalling is dependent on the tissue; for example, tamoxifen is known to act as an ER antagonist in breast tissue while having agonistic effect on the uterus, bone and heart.[13] Depending on their chemical structure, SERMs are classified as triphenylethylenes (tamoxifen and derivatives), benzothiophenes (raloxifene), phenylindoles and tetrahydronaphtalenes (**Figure 3.2**).

Tamoxifen is a SERM approved for metastatic breast cancer in the 1970, and is currently the standard treatment against ER+ breast cancer. Tamoxifen's *in vivo* efficacy is attributed to its active metabolites, 4-hydroxytamoxifen (**4OHT**) and endoxifen, which are converted in the liver by P450 enzymes.[14] Tamoxifen binds to the ligand binding domain (LBD) of the ER in a similar way than the natural ligand, however, the dimethylamino side-chain of tamoxifen is exposed outside of the binding pocket and induces conformational changes in the BDL, modifying ER activity.[15] Cellular response to tamoxifen exposure is also dependant on coregulator expression, and depending on the tissue and the cofactors expressed it can act as an antagonist, silencing ER, or as an agonist, promoting activity. Tamoxifen shows agonistic activity in endiometrium tissue and it increases the risk of endometrial cancer over the years.[16] In spite of the side effects, tamoxifen has been the standard of care for breast cancer treatment for several decades, and it has incentivized research on derivatives that might reduce its side effects without compromising efficacy.

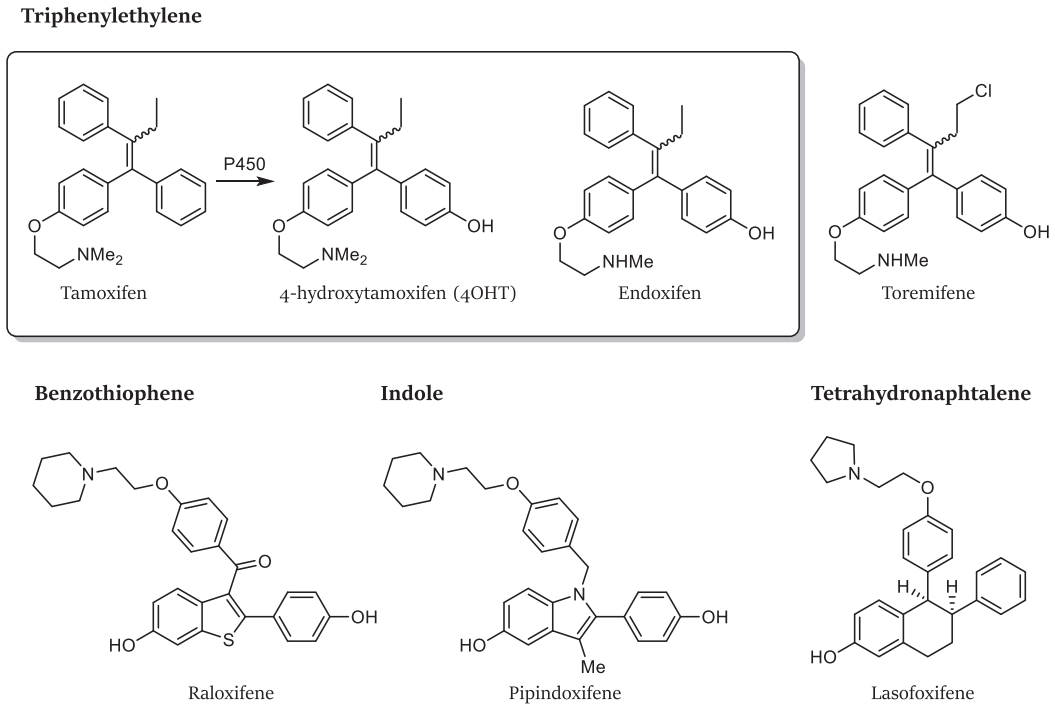

Figure 3.2. Structures of relevant SERMs. Tamoxifen and its active metabolites, **4OHT** and endoxifen. Other SERMS, divided by their chemical scaffold.

Toremifene is a tamoxifen derivative differing in a chloride atom in the ethyl side chain. Toremifene has demonstrated similar efficacy, safety, and side effect profile than tamoxifen, leading to its approval for the treatment of advanced metastatic breast cancer in 1997.[17] Raloxifene belongs to the benzothiophene family of SERMs. It binds to the ER differently than triphenylethylene SERMs, forming a stronger interaction of the side chain's basic nitrogen with an aspartic acid residue conferring it a stronger antistrogenic activity.[18] While raloxifene also inhibits proliferation in breast

cancer cells and does not pose an increased endometrial cancer risk, it displays cross-resistance to breast tumours treated with tamoxifen, and its efficacy in treating advanced breast carcinomas is only moderate.[19] Nevertheless, it received FDA approval in 2007, for reducing the risk of ER+ breast cancer in postmenopausal women at high risk. Other SERMs have been developed and studied in the treatment of ER+ cancer, however, none has surpassed the profile of tamoxifen, resulting in discontinuity at some point during clinical trials.[19]

3.1.3. Selective Oestrogen Receptor Degraders

Despite the cross-resistance observed in ER+ breast cancer towards tamoxifen and other SERMs, the fact that the tumours are still dependant on ER signalling for growth and proliferation suggested that the receptor is still a relevant target for treatment. SERDs (selective oestrogen receptor degraders) are antioestrogens that bind to the ER and destabilize its structure, inhibiting dimerization and inducing degradation of the receptor.[20] SERDs were discovered when the search for endocrine agents to overcome treatment-resistant breast cancers led to compounds with long chain substitutions to the position 7α of estradiol.[21] A long chain (15-19 atoms) prevented the receptor from adopting an agonistic conformation, highlighting a unique mode of action for these compounds. Fulvestrant was derived from these studies, demonstrating efficacy against endometrial cancer and inhibiting the growth of tamoxifen-resistant tumours. Fulvestrant is approved for the treatment of ER+ breast cancer in patients that have progressed on endocrine therapy, as an intramuscular injection. The limitation of bioavailability of fulvestrant and failure to deliver an orally bioavailable formulation have spurred discoveries on orally available SERDs. GW5638 is a prodrug to GW7604 and a tamoxifen analogue. The incorporation of the acrylic acid side-chain induced the destabilization and degradation of ER instead of acting in an agonistic/antagonistic way.[22] Although showing activity towards tamoxifen-resistant MCF7 xenografts, clinical development of the compound was discontinued after phase I clinical trials. GDC0810 and AZD9496 are other SERDs based on triphenylethylene and indole cores respectively, which also incorporate an acrylic acid side-chain; both compounds have been evaluated in clinical studies but have been discontinued.[23,24] Other SERDs currently undergoing clinical evaluation are GDC0927,[25] LSZ102,[26] and elacestrant, the latter having reached phase III trials.[27]

Although fulvestrant remains the only SERD approved for use in the clinic, some of these alternative oral SERDs are currently under clinical development. New SERDs have demonstrated improved bioavailability and pharmacokinetic than fulvestrant in preclinical and early studies, however, the results need to be confirmed in phase III clinical trials before they can reach the clinic.[28]

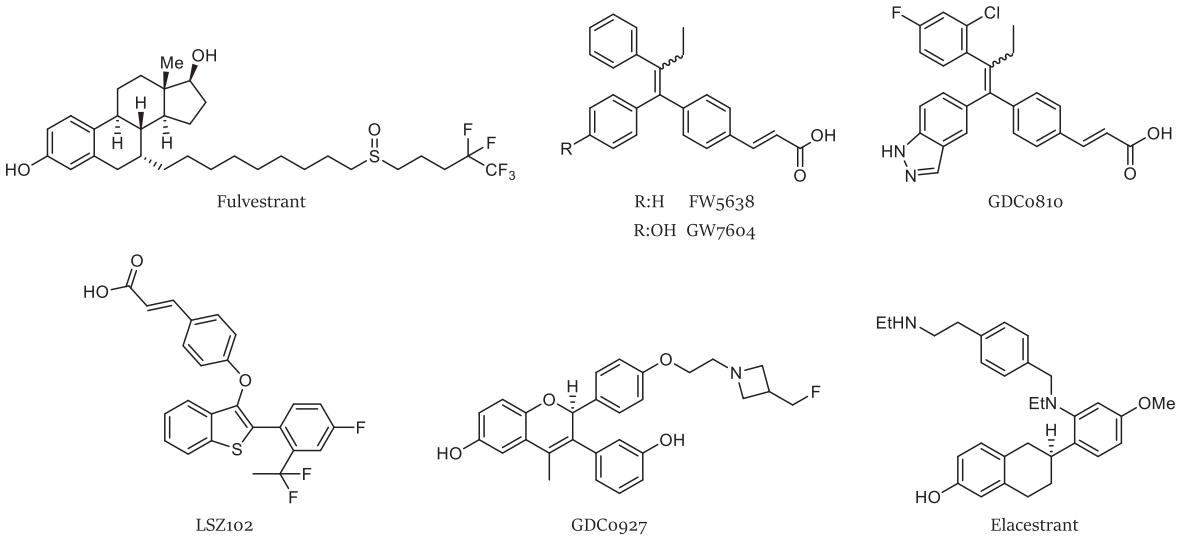

Figure 3.3: Relevant selective oestrogen receptor degraders (SERDS).

Proteolysis targeting chimeras (PROTACs) are heterobifunctional compounds that induce the degradation of a protein by promoting a protein-protein interaction (PPI) between the target and a native E3 ligase, inducing the ubiquitination and subsequent degradation of the protein by the proteasome. Due to its relevance, the ER has remained one of the central targets through the development of PROTAC technology, and ER-targeting PROTACs have been developed and improved over the last 20 years, as this field of research developed.

Early examples of PROTACs employed E_2 to recruit ERα, together with a peptidic sequence with affinity towards an E3 ligase. The first example of a PROTAC achieved degradation of ER at concentrations of 5-10 μM using a phosphopeptide sequence to recruit the E3 ligase $SCF^{\beta TRCP}$.[29] Alternatively, peptidic sequences from hypoxia-inducible factor-1α (HIF-1α) were used to induce ER degradation by recruiting the Von Hippel-Lindau (VHL) E3 ligase.[30] The discovery of small-molecule E3 ligase ligands constituted a breakthrough in the synthesis of new degraders, and more examples of ERα-targeting PROTACs appeared as the field expanded. Several degraders utilizing bestatin derivatives to recruit the cIAP E3 ligase were synthesized using estradiol derivatives[31] and **4OHT**.[32] Other compounds have combined the natural ligand with a small-molecule ligand targeting the VHL E3 ligase.[33] Raloxifene has also been used as ER-targeting warhead, in combination with cIAP and VHL ligands.[34] A raloxifene derivative, which was selected after an extensive structure-activity relationship study considering various warheads and linker structures, provided compounds with DC_{50} values under nanomolar concentrations, surpassing the effect of fulvestrant in MCF-7 cells.[35] Other ER ligands have been used in the design of protein degraders, such as those inspired in existing oral SERDs (AstraZeneca)[36] and compounds based on indole, tetrahydronaphtalene or tetrahydroisoquinoline cores (Arvinas).[37] ARV-471 is an orally bioavailable PROTAC currently being evaluated in phase II clinical trials.[38] There are also more recent examples of peptidic warheads

targeting ER, such as TD-PROTACs[39] or cell-permeable peptide PROTACs,[40] both using a lactam cyclic peptide binding motif targeting ER.

During the past two years and as we conducted our work in the synthesis of ER degraders, new examples of tamoxifen-based PROTACs have also appeared in the literature. Degraders patented by Accutar Biotech combine tamoxifen with the VHL ligand linked by alkyl or polyethylene glycol (PEG) linkers.[41] Genentech has also published the preparation of tamoxifen-based PROTACs using the VHL and a XIAP (X-linked inhibitor of apoptosis protein) ligand.[42] Besides having DC_{50} values on the low nanomolar range, these compounds were combined with antibodies to study their delivery in *in vivo* systems.

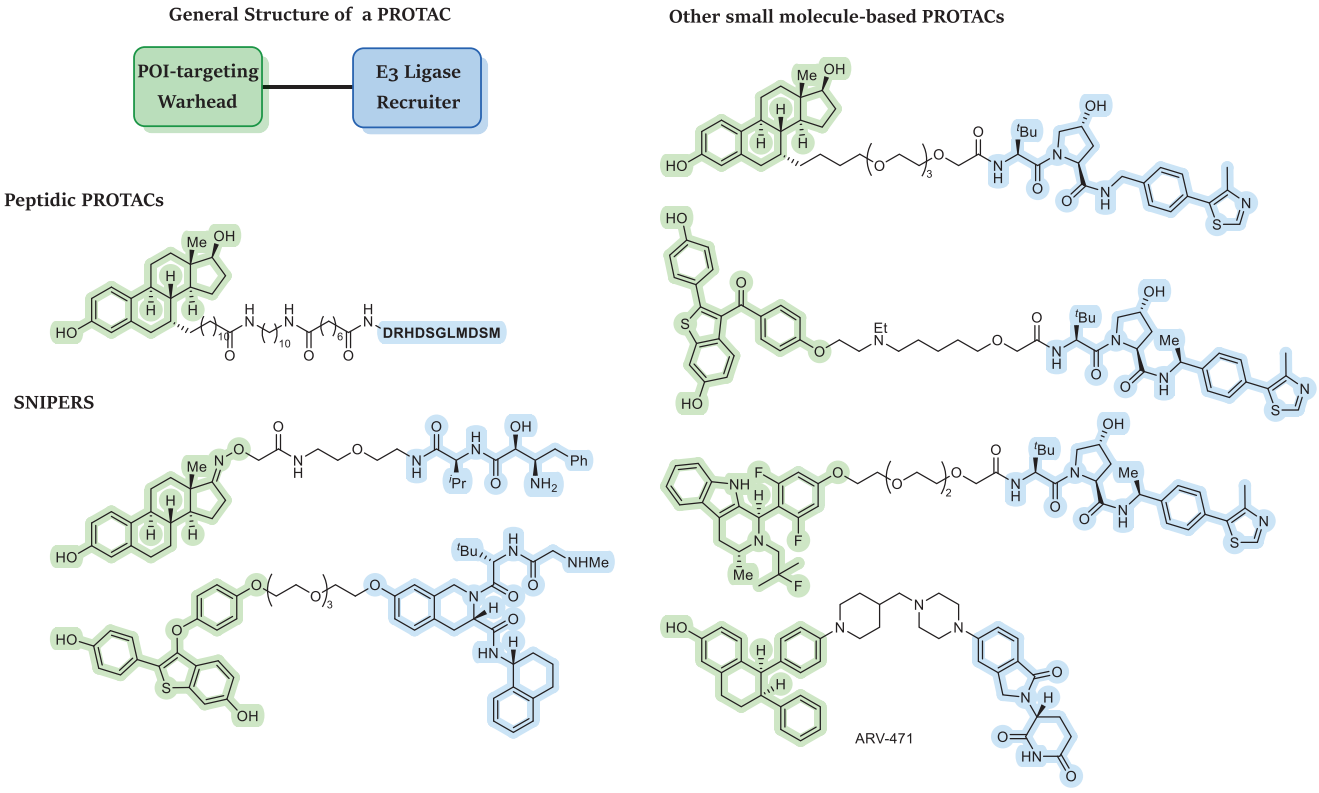

Figure 3.4. Examples of ER-targeting PROTACs.

3.2. ER PROTACs: Objectives

The importance of ER degradation within oncology is indisputable, demonstrated by the ability of some degraders to achieve tumour regression at picomolar concentrations and the presence of an ER PROTAC in clinical trials. Moreover, as a chemical biology tool, PROTACs can be used to help understand the mechanism of action in breast cancer treatment, and study in this direction will be essential for transferring this technology further into the clinical setting.

This project started in 2019 as a collaboration with the Growth Control and Cancer Metastasis research group at the IRB Barcelona, led by Prof. Roger Gomis. The role of ER is central in the study of cell signalling and metastasis in the setting of breast cancer, and a chemical biology tool that allows immediate depletion of ER levels is of great utility in that context. Our aim within that collaboration was **to design and synthesize PROTACs able to target and degrade the oestrogen receptor**.

3.3. Strategy towards the Synthesis of ER PROTACs

In order to facilitate the production of a small library of PROTACs, and inspired by previous work conducted in our laboratory,[43] we decided to employ a "click chemistry" platform based on a Huisgen 1,3-dipolar cycloaddition, also referred to as copper catalysed azide-alkyne cycloaddition (CuAAC).[44] CuAAC is considered a "click reaction", a term coined by Sharpless and co-workers to describe chemical reactions that allow the connection of two molecular blocks in a selective, high yielding manner under mild conditions and with few or no by-products.[45] Originally the synthetic potential of Huisgen 1,3-dipolar cycloadditions between azides and alkynes was limited by requirement for heating and lack of selectivity. However, the introduction of a copper catalyst allowed the cycloaddition to proceed at room temperature and forming exclusively the 1,4-disubstituted triazole.[46]

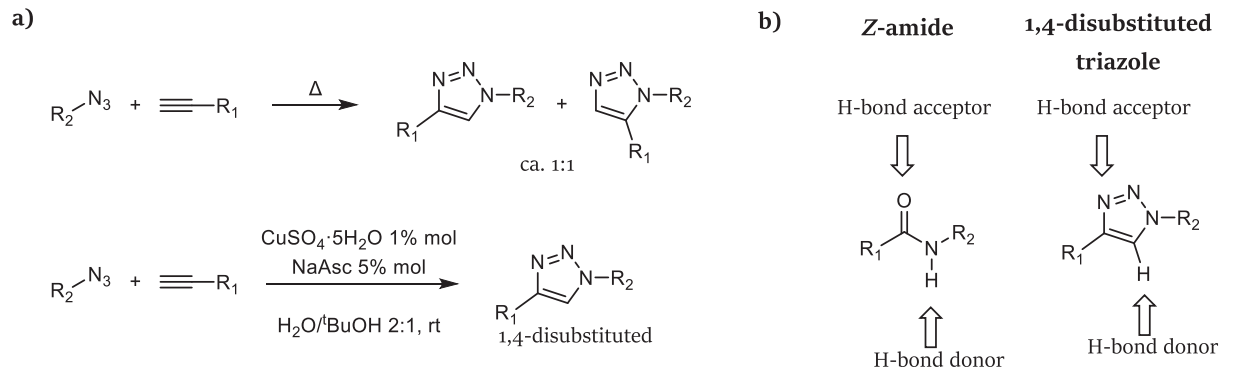

Figure 3.5: a) 1,3-dipolar cycloaddition between an alkyne and an azide (unselective), and catalysed by copper sulphate pentahydrate and sodium ascorbate (regioselective). **b)** hypothesized bioisostericity between *Z*-amides and 1,4-disubstituted triazoles.

This method was first applied to the synthesis of PROTACs by Wurz *et al.*[47] They synthesized CRBN and VHL-based BRD4 PROTACs using a late-stage CuAAC to assemble two advanced intermediates in high yield and under mild conditions. In a similar fashion, we envisaged the linkage of a terminal alkyne to **4OHT** in one end, and the introduction of a terminal azide to thalidomide-based ligands

(**Scheme 3.1**). The linkage of both fragments would yield the final product in a facile way, without cross-reactivity and under mild reaction conditions. The use of CuAAC introduces a triazole into the PROTAC's linker. We considered this would not have a negative impact since triazoles are good amide bioisosteres.[48] Amides are commonly incorporated in linker design, and despite some difference in dipolar moment and substituent distance, both functionalities overlap in terms of hydrogen bond donation/acceptation.

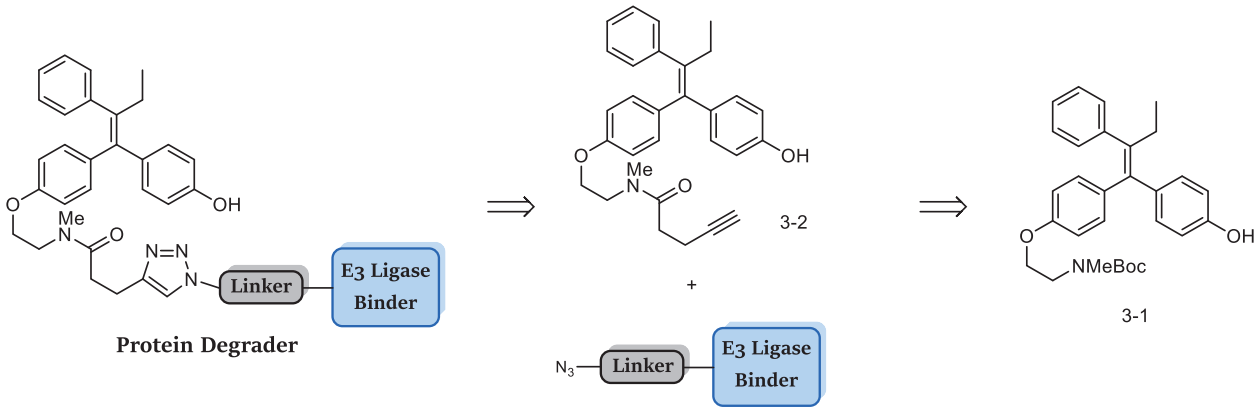

Scheme 3.1. Retrosynthetic analysis of **4OHT**-based PROTACs.

3.4. Synthesis of the Tamoxifen-based Warhead

Based on previous work in our laboratory, we envisaged the preparation of a warhead based on **4OHT**. Based on studies on the binding mode of tamoxifen, we discerned the dimethylamino side-chain as the best attachment point for a potential linker, as it lays outside the LBD of the ER and is less likely to disrupt ligand affinity.[49] Moreover, the amine attachment point was suitable for linkage, either by amide formation or nucleophilic substitution (**Scheme 3.2**). This approach is validated by examples of tamoxifen conjugates and other tamoxifen-based drugs,[50] where the dimethylamino handle has been used to attach antibody conjugates or to synthesize protein degraders.

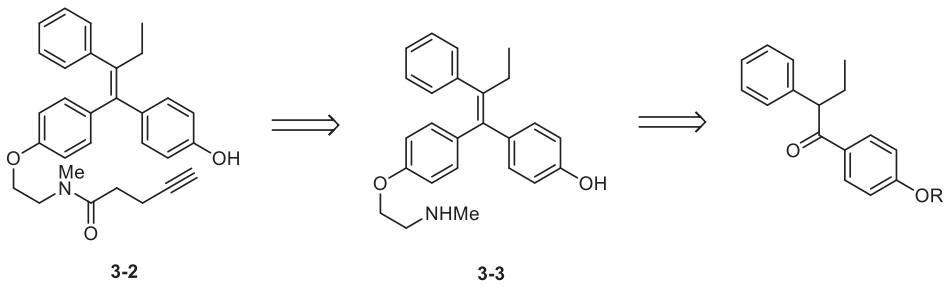

Scheme 3.2. Retrosynthesis of the **4OHT**-based warhead.

We designed a route starting with a Friedel-Crafts acylation between 2-phenylbutanoic acid and allyloxy benzene to afford ketone **3-6** (**Scheme 3.3**). Addition of 4-tetrahydropyranyloxy phenyl lithium to this ketone, followed by deprotection of the THP group gave the mono-protected intermediate **3-7** in good yields. The Williamson ether formation with N-protected N-methyl-2-chloroethanamine allowed direct introduction of the dimethylamino side-chain. After removal of the boc-protecting group, the amide formation with 4-pentynoic acid gave **4OHT** fragment **3-9**. Palladium catalyzed deprotection of the allyl ether in basic conditions afforded the acetylenic **4OHT** fragment **3-2** as a mixture of isomers.

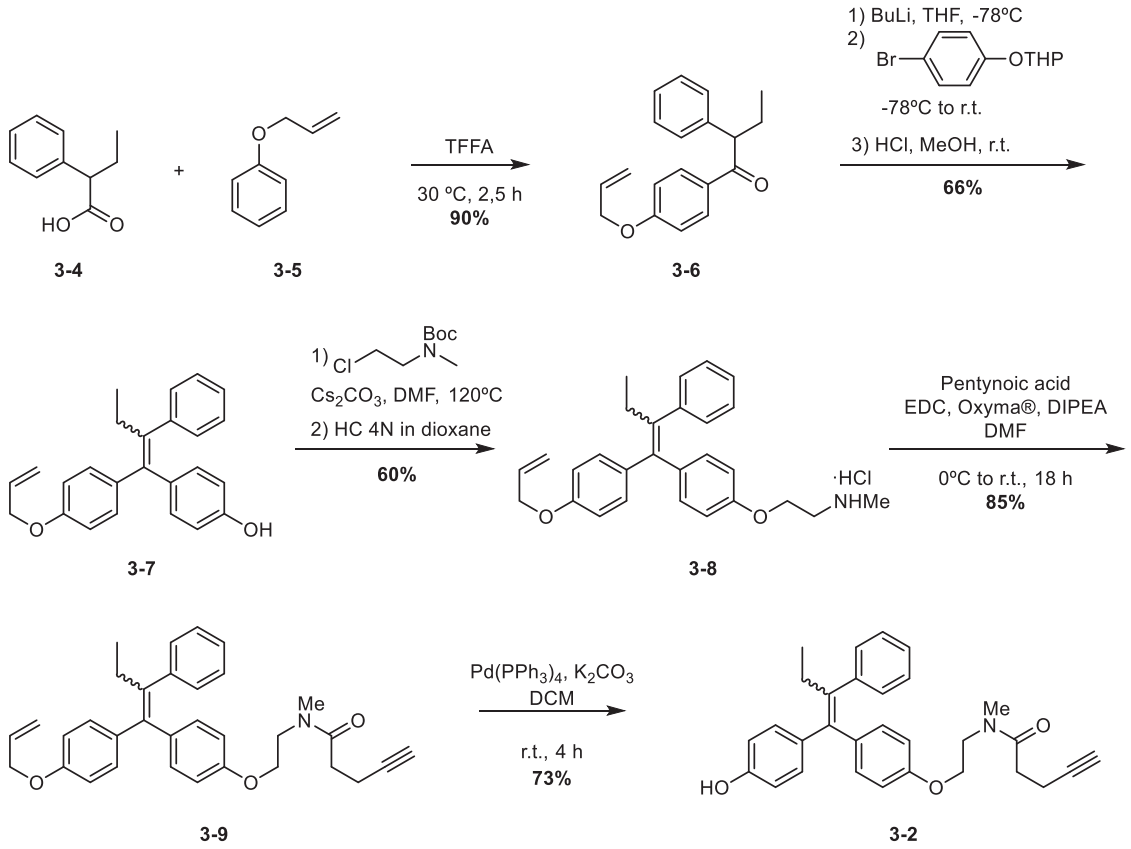

Scheme 3.3: Synthesis of the **4OHT**-based warhead.

3.5. CRBN-based ER PROTACs

3.5.1. Synthesis of CRBN-based ER PROTACs with PEG linkers

Pomalidomide derivatives bearing a terminal azide were synthesized to be coupling partners for the click reaction with the **4OHT**-based warhead. Condensation of 4-fluorophtalic anhydride with 3-aminopiperidine-2,6-dione afforded the fluorothalidomide **3-10** in excellent yield. The SNAr reaction

of **3-10** with four commercially available amino-azides with different lengths of polyethylene glycol (PEG) linkers afforded the azido intermediates **3-11a-d**. Finally, CuAAC of these azides with the acetylenic 4-**OHT** derivative **3-2** afforded the potential PROTACs **TAM-PO-1- 4** in moderate to high yields (**Scheme 3.4**).

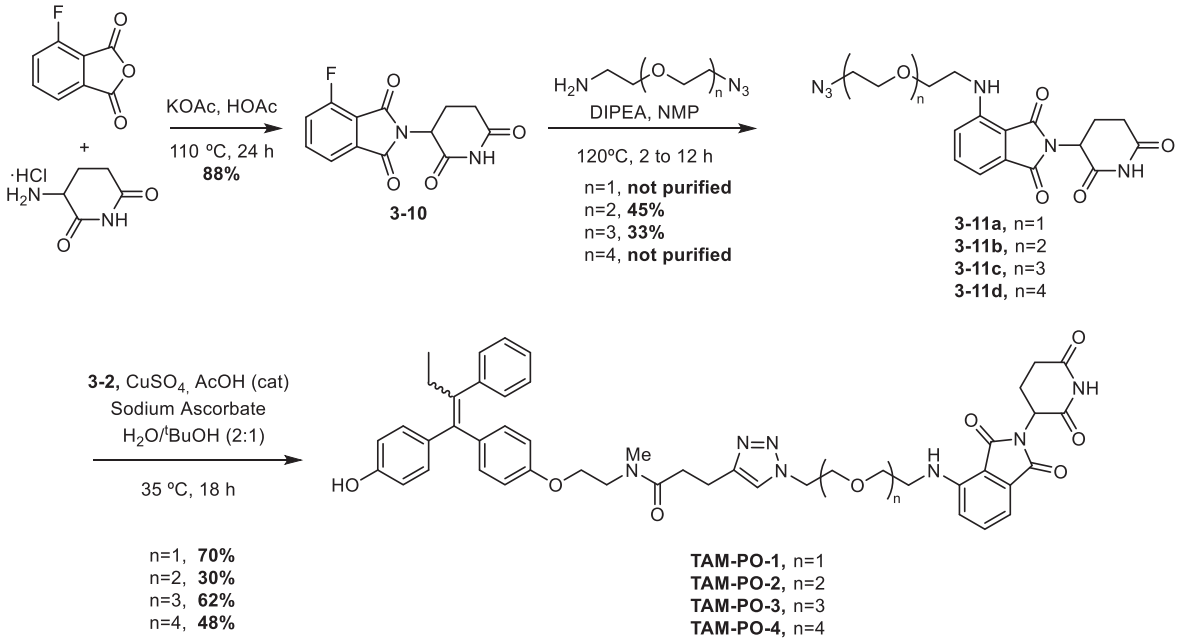

Scheme 3.4. Synthesis of pomalidomide-azide fragments **3-11a-d** and synthesis of PROTACs **TAM-PO-1-4**.

This facile diversification allowed the synthesis of a library of 4 compounds bearing PEG linkers of different lengths. In-vivo evaluation of the four compounds gave us insight into the optimal linker length before attempting further optimization of the degraders.

3.5.2. Synthesis of CRBN-based ER PROTACs with alkyl linkers

Together with pomalidomide, lenalidomide derivatives have been also used in PROTAC design (**Figure 3.6**). We sought to incorporate a lenalidomide derivative into our PROTAC collection to compare its potency with a pomalidomide derivatives of comparable linker length. For some targets it has been reported that the potency of PROTACs with an alkyl or alkynyl group at the 4' of the phthalimide ring is greater than the ones with a 4'-NH group.[51] This influence was also observed with PROTACs targeting p38 MAPK previously developed in our group.[43] We relied on a Sonogashira coupling to introduce a carbon-linked linker to the thalidomide derivative. (**Scheme 3.5**)

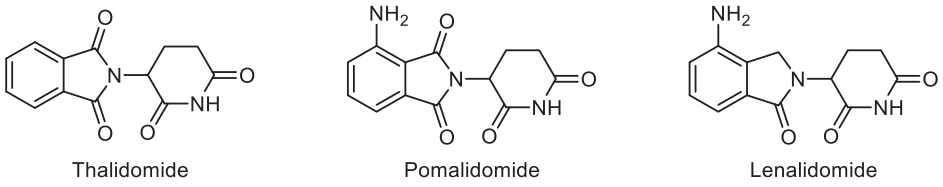

Figure 3.6. Structures of thalidomide, pomalidomide and lenalidomide.

Lenalidomide precursor **3-13** was prepared in two steps from commercially starting materials in excellent yields. **3-13** was then subjected to a Sognogashira cross-coupling reaction to introduce the alkyl chain. The coupling with *N*-Boc-4 pentyn-1-amine afforded the alkylated compound **3-14** in good yield. Deprotection of the carbamate followed by condensation with 6-azidohexanoic acid gave the azido coupling partner **3-18**. At the same time, alkyne **3-14** was hydrogenated and subjected to the same amidation sequence, affording the coupling partner **3-16**.

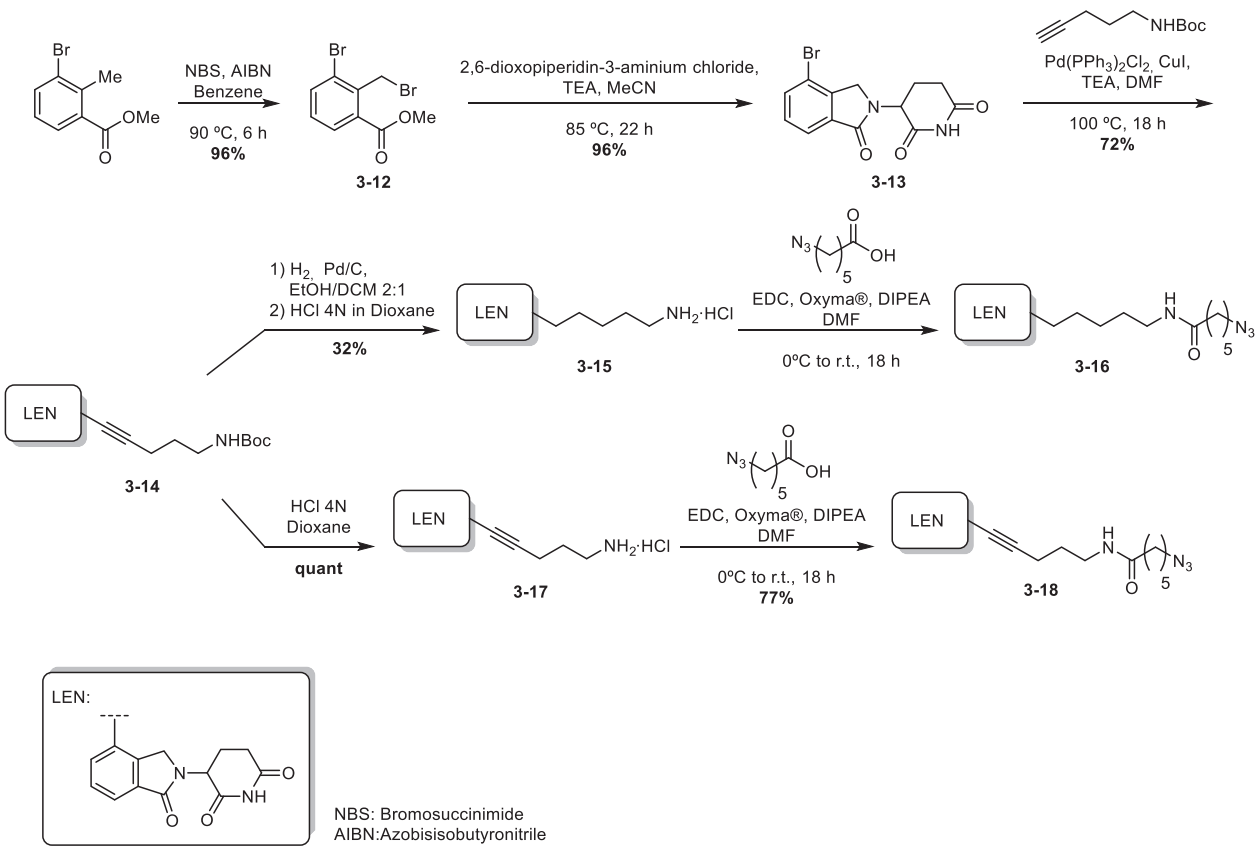

Scheme 3.5. Synthesis of lenalidomide-based azide fragments.

With both fragments in hand, we synthesized the two lenalidomide-based PROTACs under standard CuCCAC conditions with warhead **3-2**, affording compounds **TAM-LEN-1** and **2** in good yields.

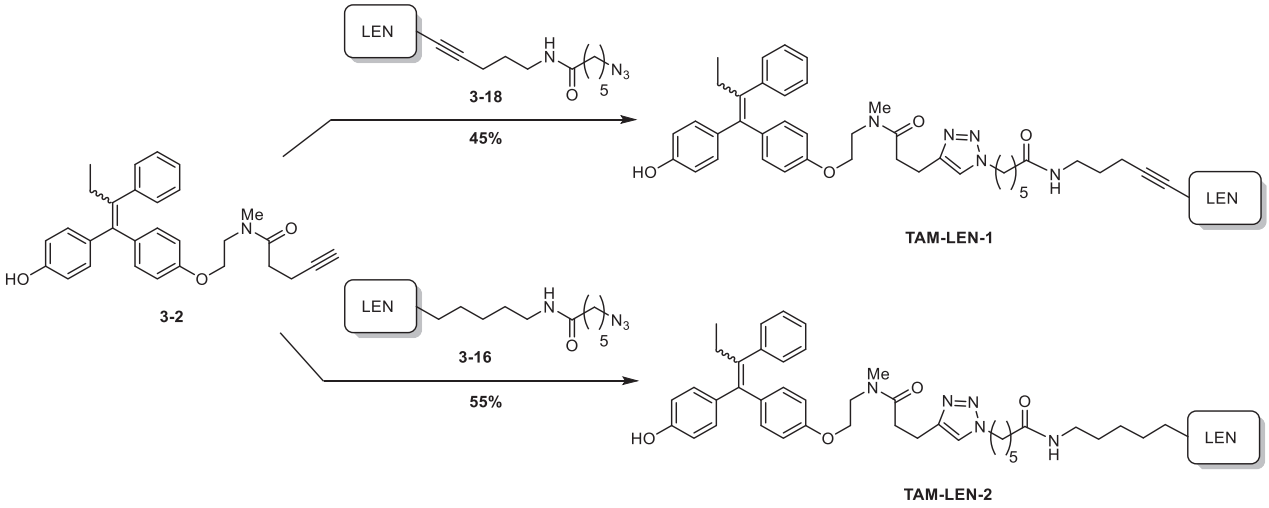

Scheme 3.6. Synthesis of lenalidomide-based ER PROTACs. Reaction conditions: $CuSO_4 \cdot 5\ H_2O$, Sodium ascorbate, *t*-BuOH/H_2O (2:1), 35 °C, 24 hours.

3.5.3. Optimization of the 4OHT Warhead

4OHT exhibits *E*/*Z* isomerism around the double bound. This fact is of biological relevance, as only the *Z* isomer has biological activity, and a 300-fold higher affinity compared to the *E* isomer. Moreover, isomerization between the E and Z isomers of **4OHT** occurs in cell culture media, accounting for the biological activity of *E*-**4OHT** *in vitro*. Interestingly, there is no interconversion observed *in vitro* between the two isomers of tamoxifen.[52]

In order to lock the structure into the active configuration, McCague *et al.*[53] synthesized analogues of **4OHT** with a controlled configuration. The introduction of a methyl group at the 2 position of the phenol ring afforded a compound that did not isomerize under physiological conditions and displayed affinity for ER comparable to that of *Z*-**4OHT**. Attempts to construct a fused ring structure, by linking the ethyl moiety with the phenolic group or fusing the opposed phenolic and phenyl ring afforded compounds with reduced affinity for ER.

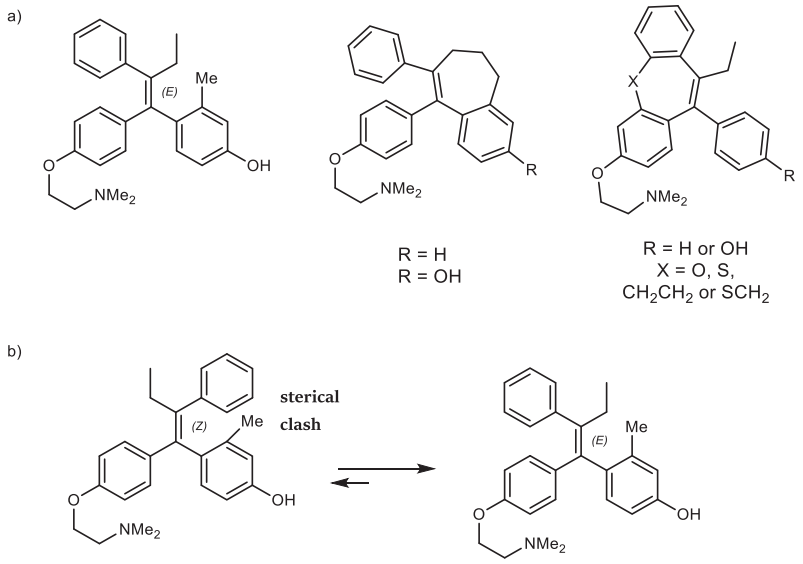

Figure 3.7. a) Non isomerizable analogues of **4OHT**. b) 2-methyl-**4OHT** favours the *E* configuration.[1]

We decided to incorporate this tactic to our ER PROTAC design, hypothesising that the steric hindrance between the ethyl and phenyl groups would afford a mixture enriched in *E* isomer, which would translate into better affinity towards the ER and better PROTAC potency.

The synthesis of the 2-methyl-**4OHT** warhead **3-24** was carried out in a similar way than that of **3-2**. (**Scheme 3.7.**). Ketone **3-6**, readily available from the synthesis of **3-2**, was used as a starting point. Substitution of the allyl protecting group for the more labile THP followed reaction with allyl-protected phenol **3-19**, lithiation and nucleophilic attack to **3-20**. Reaction conditions also sufficed for the deprotection of the THP-protected phenol *trans* to the methyl-bearing aromatic ring. The side chain was introduced *via* substitution to the deprotected phenol *trans* to the 2-methyl aromatic ring, using *N*-protected *N*-methyl-2-chloroethanamine, and followed by amide bond formation with 4-pentynoic acid. Deprotection of the allylic-protected phenol afforded intermediate **3-24**, which was reacted with azido coupling partner **3-11d** to form the PROTAC **TAM(Me)-POM-4**.

[1] Note on the nomenclature: due to a change in priorities following Cahn-Ingold-Prelog rules, when introducing the methyl group at the aromatic ring the active isomer is designated *E*.

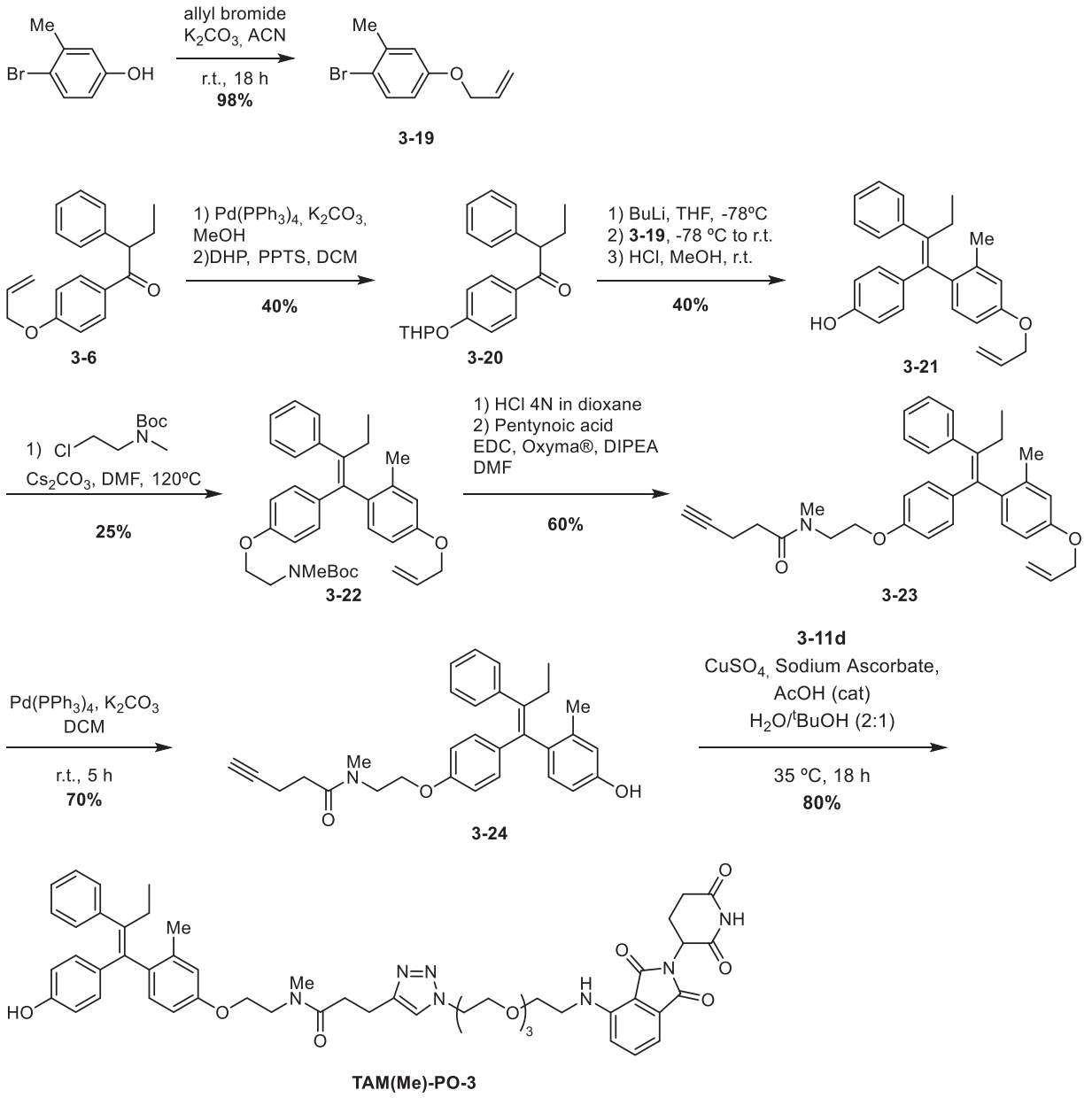

Scheme 3.7. Synthesis of a 2-methyl-**4OHT**-based warhead and PROTAC.

3.5.4. Biological Evaluation of CRBN-based ER PROTACs

The ability of the CRBN-recruiting ER PROTACs to degrade ER was evaluated in MCF-7 and analysed by immunoblotting.[2] **TAM-PO-3** resulted the most active compounds of the TAM-PO series, showing substantial degradation at 5 μM and a consistent concentration/activity relation confirmed by triplicates. Although **TAM-PO-1** showed greater degradation at 1 μM, the results were not consistent and difficult to reproduce. **TAM-PO-3** was selected to study the kinetics of the degradation process,

[2]All the experiments involving the testing of ER degraders were carried out at the Growth Control and Cancer Metastasis Laboratory, at the IRB Barcelona, by Dr. Alicia Llorente and Irene Espuny.

showing no substantial degradation during the first 12 hours (**Figure 3.8b**) and achieving maximum degradation after 24 h of treatment. In order to determine the DC_{50} value of **TAM-PO-3**, MCF-7 cells were treated with **TAM-PO-3** at different concentrations during 24 hours. Quantification of ERα levels normalized to GAPDH levels showed a DC_{50} value of 11.94 nM (**Figure 3.8c**).

Similarly, lenalidomide-based compounds **TAM-LEN-1** and **2** were tested in MCF7 cells and analyzed by Western blotting (**Figure 3.8d**). However, results show activity only at 10 μM, proving less effective in degrading ER than **TAM-PO-3**. Maintaining a similar linker length, the combination of PEG composition and pomalidomide proves to be more effective than the alkyl/amide linker and lenalidomide at inducing degradation of ER.

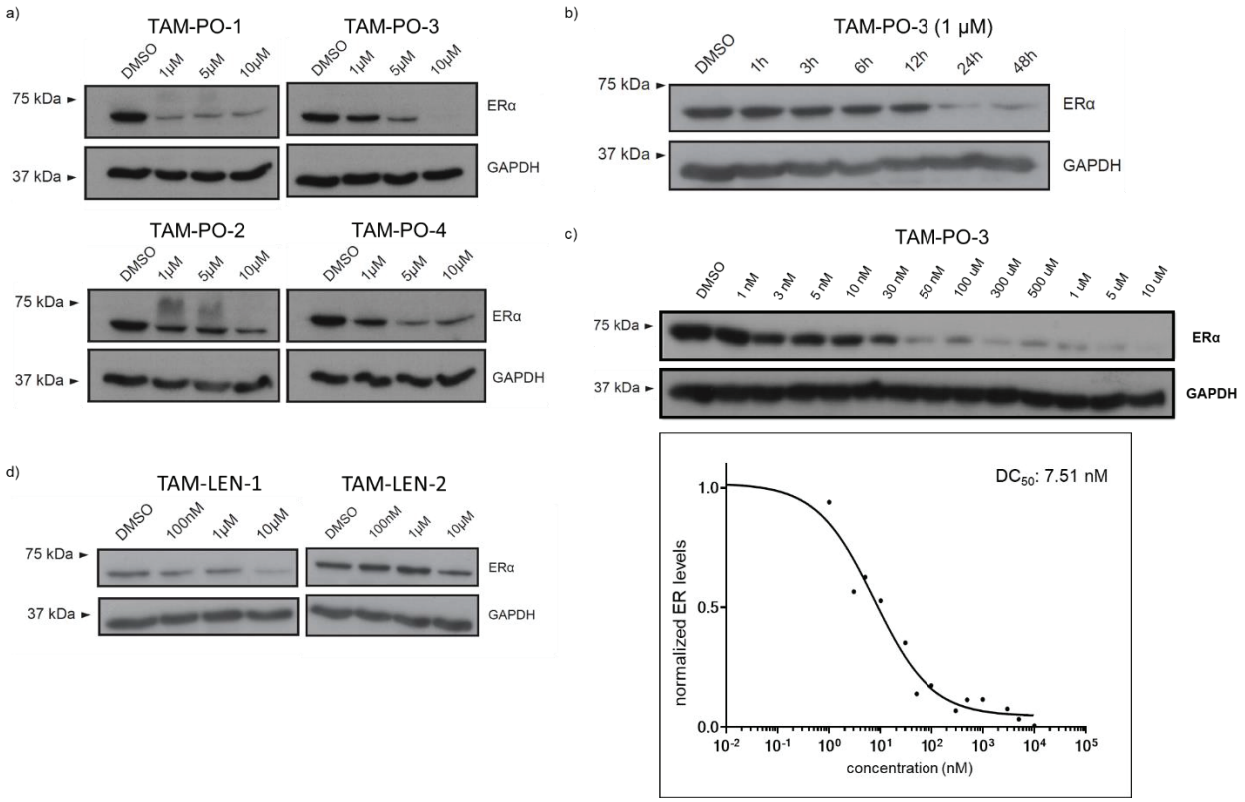

Figure 3.8. Degradation of ERα induced by CRBN-recruiting ER PROTACs. **a)** MCF-7 cells were treated with **TAM-PO-1-4** at different concentrations during 24 hours, and cell lysates were analysed by immunoblotting**. b)** MCF-7 cells were treated with 1 μM **TAM-PO-3** during different time periods (1 to 48 hours). Control cells were treated with DMSO for 48 hours. **c)** MCF-7 cells were treated with **TAM-PO-3** at a wide range of concentrations during 24 hours (representative results from 2 biological replicates). DC_{50} value for **TAM-PO-3** compound, based on quantification of ERα levels normalized to GAPDH levels in MCF-7 cells. d) MCF-7 cells were treated with **TAM-LEN-1** and **2** at different concentrations during 24 hours, and cell lysates were analysed by immunoblotting**.**

Compound **TAM(Me)-PO-3** was also tested, in order to examine if the modification of the warhead does provide more potency towards ER degradation. Western blotting analysis shows that **TAM(Me)-PO-3** provides degradation of the ER at the concentration of 5 nM (**Figure 3.9a**). A dose-response experiment was performed in order to quantify a DC_{50} value of 3.47 nM. This value shows a slight improvement respect **TAM-PO-3**, however, **TAM(Me)-PO-3** only achieves a value of maximum degradation (D_{max}) of about 75% of the original ER loading, in comparison with >80% of **TAM-PO-3**. The introduction of a warhead modification to improve the affinity of the degrader to its target, while improving only slightly the potency, showed limitations in the overall performance in comparison **TAM-PO-3**.

A series of experiments were conducted with **TAM-PO-3** in order to verify that the mechanism of action of the degraders is through the ubiquitin-proteasome system degradation. To demonstrate that the observed degradation effect is CRBN-dependent, a non-effective **TAM-PO-3-Me** compound was synthesized, (see experimental part) possessing a modified version of the pomalidomide fragment methylated at the glutarimide nitrogen, which is known to block the binding activity towards CRBN[54]. **TAM-PO-3-Me** did not degrade ERα at the concentration of 1 μM (**Figure 3.9c**), but some degradation was observed at higher concentrations.

To demonstrate that ERα degradation is through hijacking the ubiquitin-proteasome system, a series of rescue experiments were performed (**Figure 3.9b**) using the proteasome inhibitor Bortezomib (BTZ). Pre-treatment of MCF-7 cells with this proteasome inhibitor for 1 hour, prevented ERα degradation by the **TAM-PO-3**, confirming that the mechanism of action is dependent on the proteasome activity. Pre-treatment with MLN4924, a NEED8-activating enzyme inhibitor (NAEi), also reduced the extent of degradation, indicating that ERα degradation is mostly mediated by E3 ligase activity. However, the persistence of some small degree of degradation suggests that alternative mechanisms other than the ubiquitin-proteasome pathway may also participate. This observation is consistent with the degradation observed using **TAM-PO-3-Me** at higher concentrations.

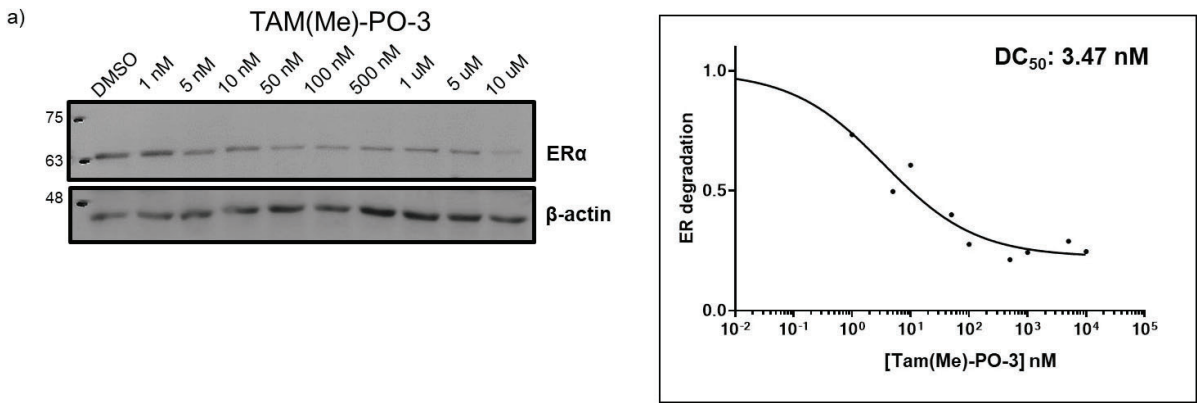

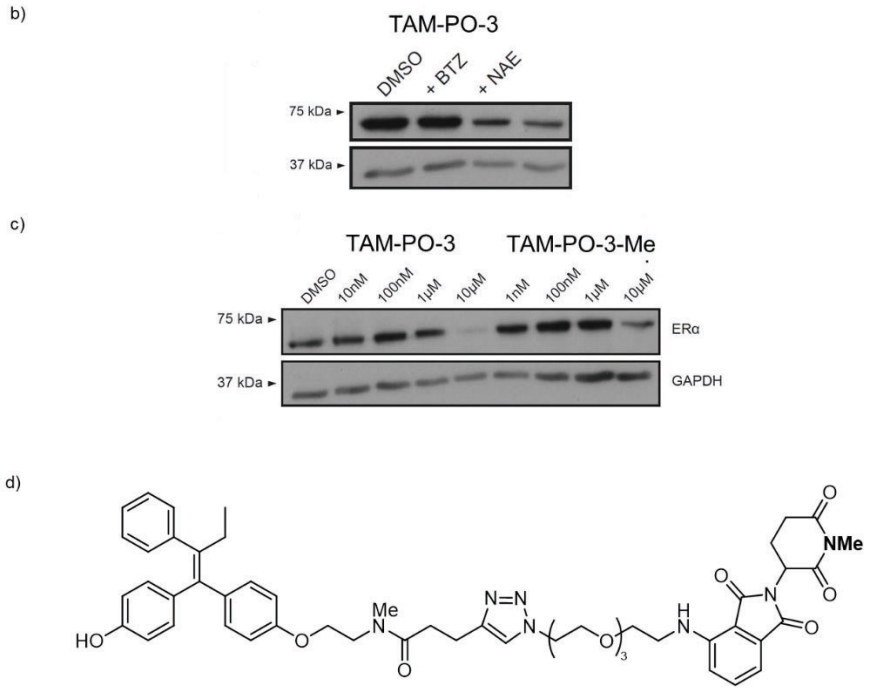

Figure 3.9. a) MCF-7 cells were treated with **TAM(Me)-PO-3** at a wide range of concentrations during 24 hours. DC_{50} value for **TAM(Me)-PO-3** compound, based on quantification of ERα levels normalized to GAPDH levels in MCF-7 cells. **b)** MCF-7 cells were pre-treated for 1 hour with Bortezomib 1 μM or MLN4924 1 μM, and then treated with **TAM-PO-3** at 1 μM during 12 hours. **c)** MCF-7 cells were treated with the inactive compound **TAM-PO-3-Me** at different concentrations for 24 hours. **d)** Chemical structure of the inactive compound **TAM-PO-3-Me**.

From the initial family of PEG-based pomalidomide degraders, only **TAM-PO-3** had a satisfactory degradation profile, although long treatment time was needed to obtain good degradation of ER. None of the efforts aimed at improving the potency of the compound by modifying warhead, linker composition or E3 ligase binder had resulted in a decisive improvement.

3.6. VHL-based ER PROTACs

3.6.1. Synthesis of VHL-based ER PROTACs

The Von Hippel-Lindau (VHL) protein is part of a multiprotein complex possessing E3 ubiquitin ligase activity. VHL is responsible for the recognition of target proteins, including HIF-1α, for proteasomal degradation.[55] The interaction between VHL and HIF-1α is mimicked by a small-molecule ligand, and analogues of this structure have been successfully used in PROTAC design to discover molecules that recruit the VHL E3 ligase to induce degradation of many targets.[56] Given the existence of accessible small-molecule ligands for this E3 ligase, and the modular nature of our ER degraders' synthesis, we decided to incorporate it into our PROTAC design. Thus, we synthesized ER degraders based on **4OHT** and the VHL ligand.

Reaction of 4-methyltiazole with the boc-protected amine **3-25** afforded intermediate **3-26**. Sequential incorporation of hydroxyproline and *tert*-leucine by peptide synthesis afforded fragment **3-28**. Cleavage of the boc-protecting group under acidic conditions yielded the VHL ligand **3-29**.

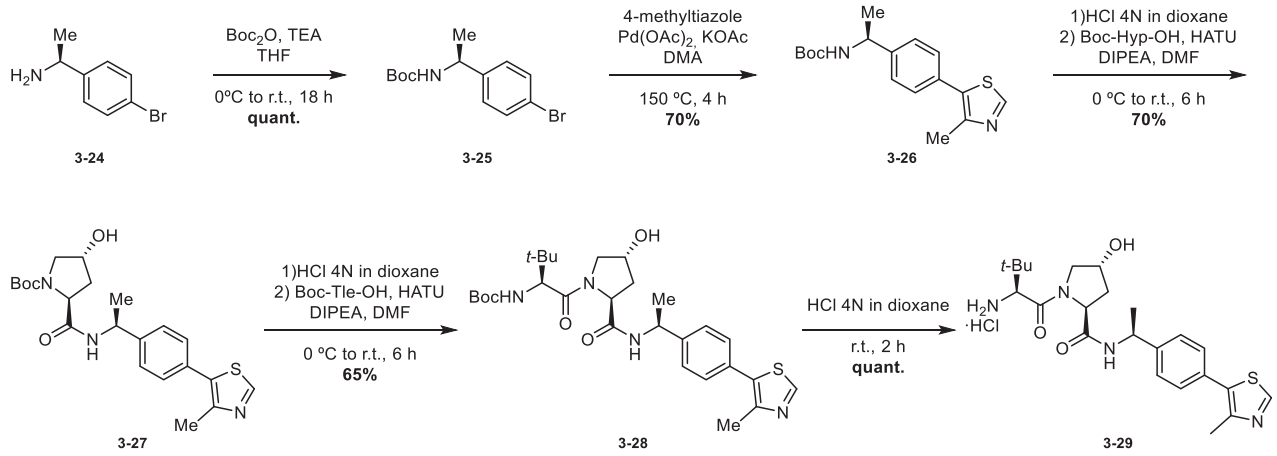

Scheme 3.8. Synthesis of the VHL ligand.

A different set of molecular linkers attached to the VHL ligand were synthesized, bearing all a terminal azide group (**Scheme 3.9**). Fragments **3-30a** and **3-30b** were prepared by direct amidation of the VHL ligand using 4-azidobutanoic acid and 6-azidohexanoic acid. Fragments **3-32a-c** were prepared by first attaching a terminal boc-protected amino acid and performing a second amidation with the corresponding terminal azido acid. Analogous to the thalidomide derivatives, VHL-based degraders were assembled using a CuAAC, yielding compounds **TAM-VHL-1-5** in moderate to good yields.

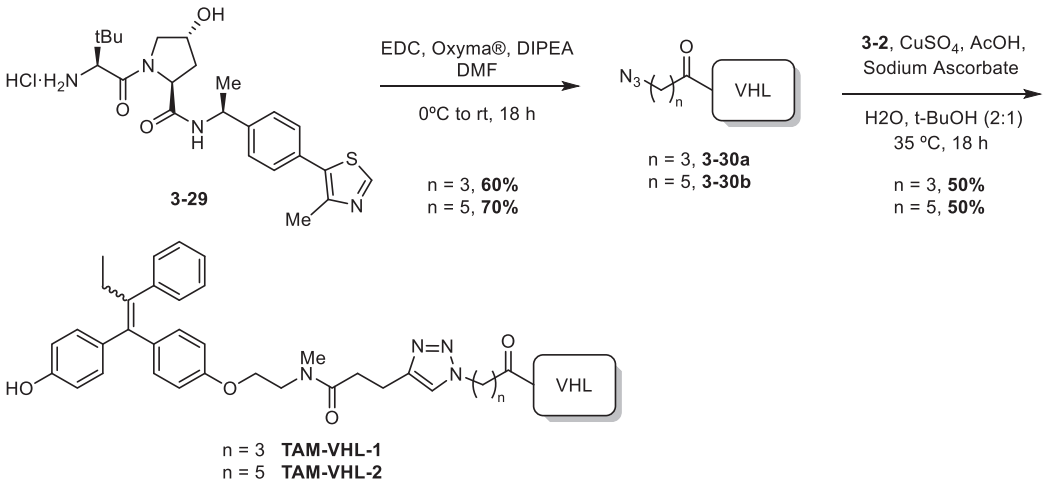

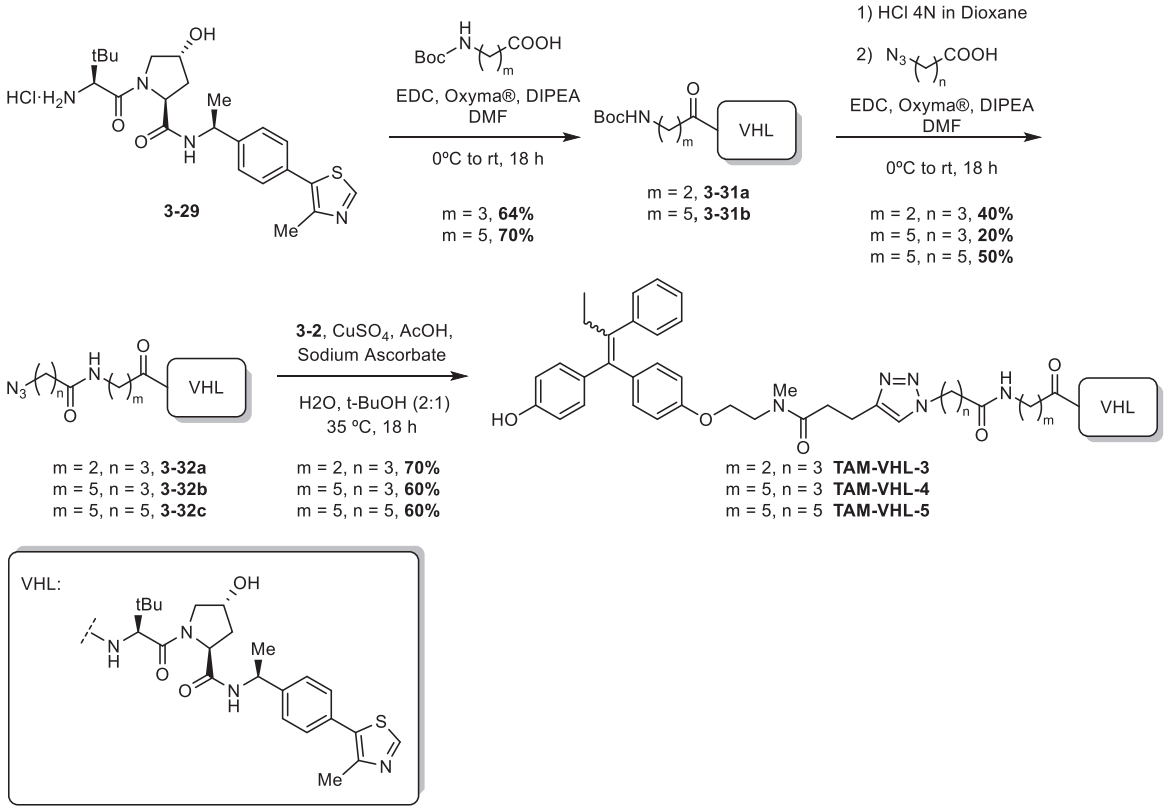

Scheme 3.9. Synthesis of ERα PROTACs **TAM-VHL-1-5**, derived from **4OHT** and VHL-based ligands.

3.6.2. Biological Evaluation of VHL-based ER PROTACs

The efficacy of compounds **TAM-VHL-1-5** degrading ERα was tested by Western blotting (**Figure 3.10a**). Compounds **TAM-VHL-1** and **TAM-VHL-2**, the most potent of the series, showed both substantial degradation of ERα at a concentration of 10 nM.

The DC_{50} values for **TAM-VHL-1** and **TAM-VHL-2** were determined by quantification of Western blotting data. MCF-7 cells were treated with **TAM-VHL-1** and **TAM-VHL-2** at different concentrations during 24 hours, and ERα protein levels normalized to GAPDH protein levels were plotted against PROTAC concentration to obtain DC_{50} values of 4.5 nM and 5.3 nM respectively (**Figure 3.10c**).

A series of rescue experiments were performed (**Figure 3.10d**) to explore the mechanism of action of **TAM-VHL-1** and **2**. Pre-treatment with the proteasome inhibitor Carfilzomib for 30 minutes before PROTAC treatment for 6 hours rescued ERα from being degraded, proving that degradation was proteasome dependent. Moreover, pre-treatment with MLN4924 (NAEi), also prevented degradation of ERα, confirming that binding to the VHL ligand is essential for the mechanism of action.

In parallel, compound **TAM-VHL-1'** (see experimental section) was synthesized using the diastereoisomer of the VHL ligand with the inverted hydroxyl stereocenter, which does not have the ability to bind to VHL.[57] The compound was not able to degrade ERα (**Figure 3.10e**), showing that disruption of the binding with the VHL protein prevents degradation. These experiments show that recruitment of the VHL E3 ligase is essential for **TAM-VHL-1** and **TAM-VHL-2** induced degradation of ERα. These results are consistent with the mechanism of action of bifunctional degraders, proving **TAM-VHL-1** and **TAM-VHL-2** to act as bona fide PROTACs.

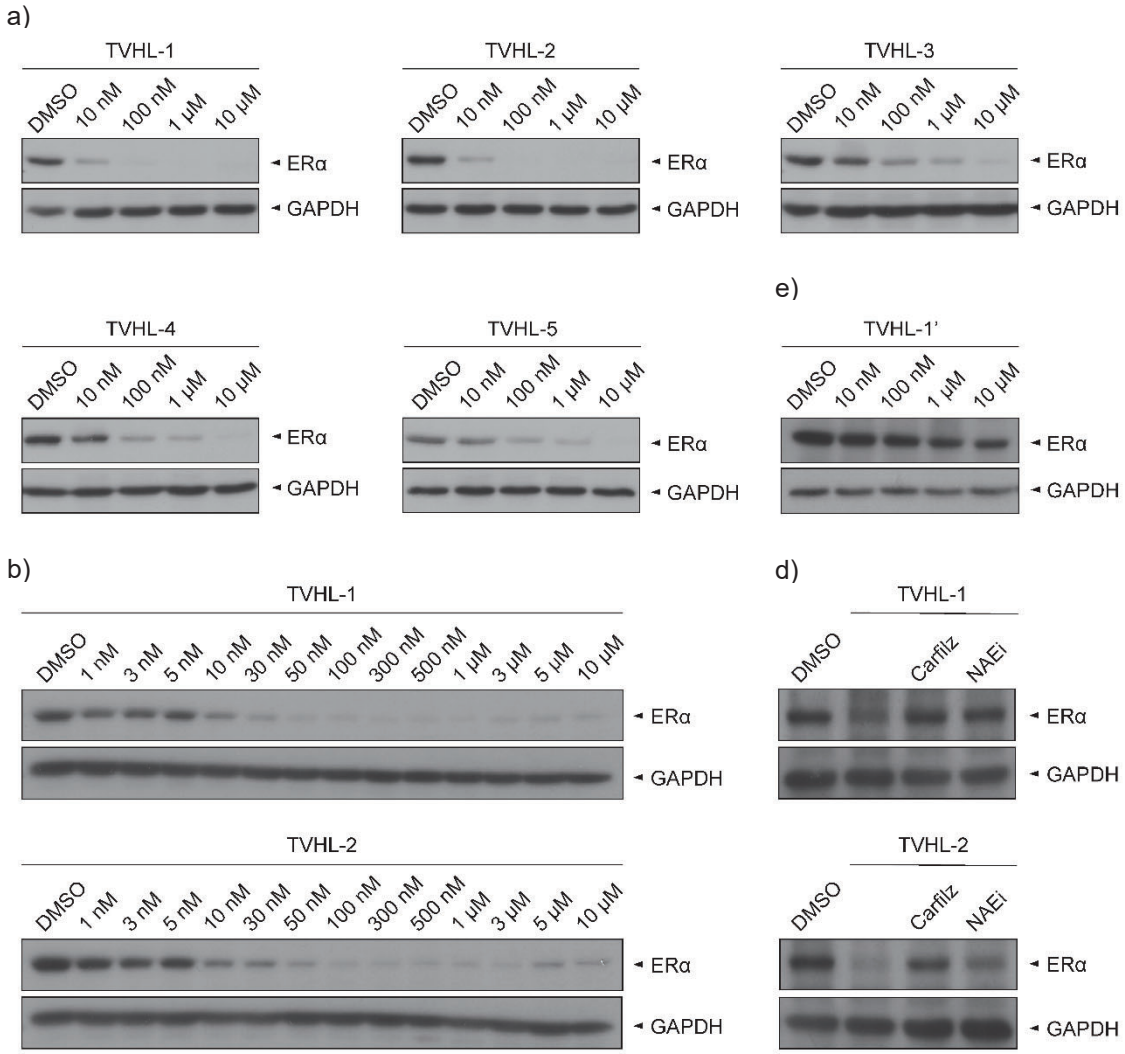

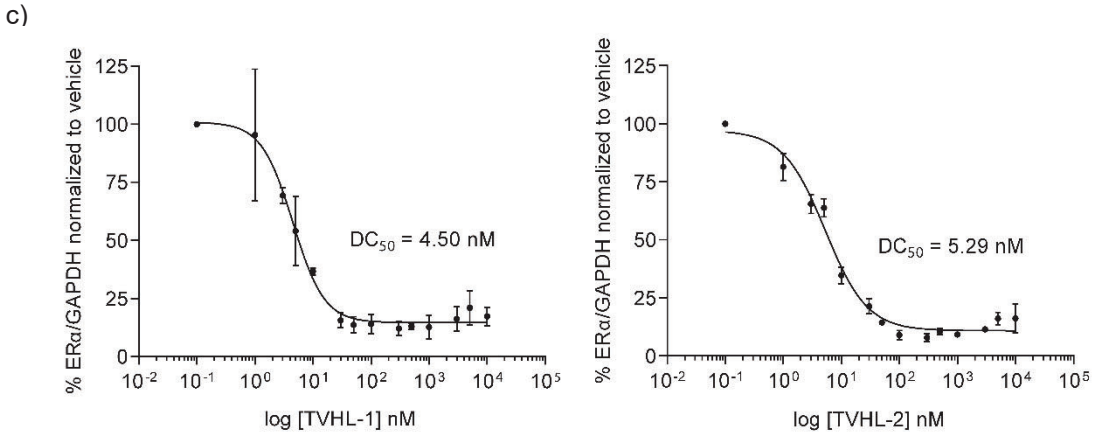

Figure 3.10. **Degradation of ERα induced by TAM-VHL-1-5 compounds. a)** MCF-7 cells were treated with **TAM-VHL-1-5** at different concentrations for 24 hours, and cell lysates were analyzed by immunoblotting. **b)** MCF-7 cells were treated with **TAM-VHL-1** or **TAM-VHL-2** at a wide range of concentrations during 24 hours (representative results from triplicates). **c)** DC_{50} values for **TAM-VHL-1** and **TAM-VHL-2** compounds, based on quantification of ERα levels normalized to GAPDH levels in MCF-7 cells, by triplicates. **d)** MCF-7 cells were pre-treated for 30 minutes with Carfilzomib 1 μM or MLN4924 1 μM, and then treated with **TAM-VHL-1** or **TAM-VHL-2** 500 nM during 6 hours. **e)** MCF-7 cells were treated with the inactive diastereoisomer of **TAM-VHL-1** (**TAM-VHL-1'**) at different concentrations for 24 hours.

3.7. ER PROTACs: Conclusions

In this chapter we describe the synthesis of ER PROTACs based on **4OHT**. A synthesis of **4OHT** previously developed in our laboratory was adapted to incorporate a terminal alkyne, that was used to synthesize various PROTACs bearing CRBN or VHL-recruiting fragments.

The use of pomalidomide derivatives as an E3 recruiting fragment afforded the compounds **TAM-PO-1-4**, of which **TAM-PO-3** shows activity inducing degradation of ER (DC_{50}: 7.51 nM).

We attempted to synthesize analogues of **TAM-PO-3** with improved activity, by using a different CRBN recruiter and by modifying the POI-targeting warhead. **TAM-LEN-1** and **TAM-LEN-2**, bearing lenalidomide instead of pomalidomide, did not show improved degradation of ER. **TAM(Me)-PO-3** was prepared using a modified version of **4OHT** warhead favouring the active isomer, however the degrader had a similar DC_{50} value (3.47 nM) and a lower D_{max} than **TAM-PO-3**. None of these attempts to improve **TAM-PO-3** yielded a better compound.

We synthesized a series of PROTACs recruiting the VHL E3 ligase, using the VHL ligand **3-29**. Compounds **TAM-VHL-1** and **TAM-VHL-2** are potent ER degraders, with DC_{50} values of 4.50 nM and 5.29 nM respectively. These compounds are being used at the Growth Control and Cancer Metastasis Laboratory as chemical biology tools. The synthesis and biological evaluation of VHL-based ER PROTACs has been published in a peer-reviewed journal.[58]

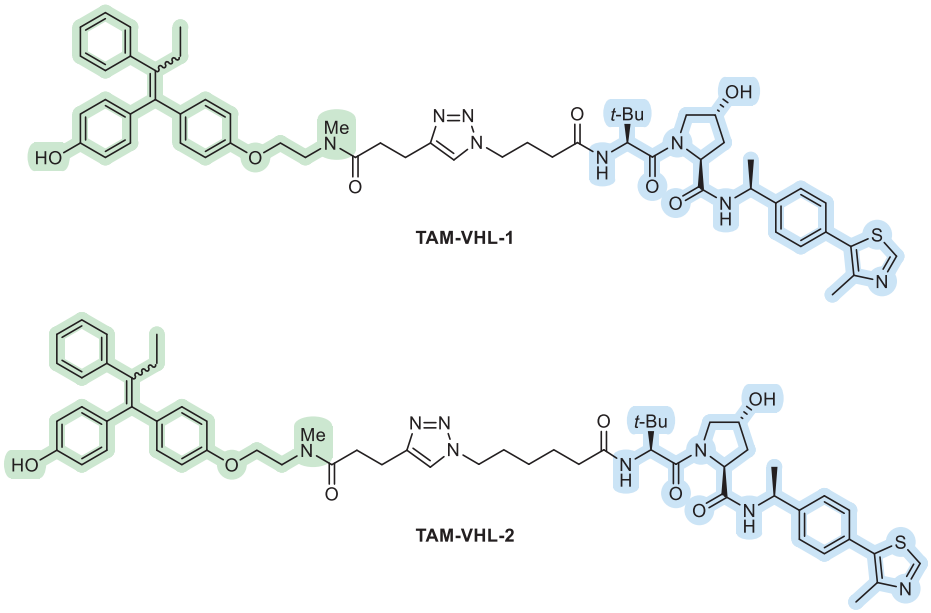

Figure 3.11. Structures of **TAM-VHL-1** and **TAM-VHL-2**.

References

[1] Liang, J. & Shang, Y. Estrogen and cancer. *Annu. Rev. Physiol.* **2013**, *75*, 225–240.

[2]Schulster, M., Bernie, A. M. & Ramasamy, R. The role of estradiol in male reproductive function. *Asian J. Androl.* **2016**, *18*, 435–440.

[3] Nilsson, S. *et al.* Mechanisms of estrogen action. *Physiol. Rev.* **2001**, *81*, 1535–1565.

[4] Kuiper, G. G. J. M., Enmark, E., Pelto-Huikko, M., Nilsson, S. & Gustafsson, J. Å. Cloning of a novel estrogen receptor expressed in rat prostate and ovary. *Proc. Natl. Acad. Sci. U. S. A.* **1996**, *93*, 5925–5930.

[5] Younes, M. & Honma, N. Estrogen Receptor betha. *Arch. Pathol. Lab. Med.* **2011**, *135*, 63–66.

[6] Nilsson, S. *et al.* Mechanisms of estrogen action. *Physiol. Rev.* **2001**, *81*, 1535–1565.

[7] Macgregor, J. I. & Jordan, V. C. Basic guide to the mechanisms of antiestrogen action. *Pharmacol. Rev.* **1998**, *50*, 151–196.

[8] Li, S. *et al.* microRNA-206 overexpression inhibits cellular proliferation and invasion of estrogen receptor α-positive ovarian cancer cells. *Mol. Med. Rep.* **2014**, *9*, 1703–1708.

[9] Price D, Stein B, Sieber P, et al. Toremifene for the prevention of prostate cancer in men with high grade prostatic intraepithelial neoplasia: results of a double-blind, placebo controlled, phase IIB clinical trial. *J Urol* **2006**, *3*, 176.

[10] Edvardsson, K., Ström, A., Jonsson, P., Gustafsson, J.-Åke & Williams, C. Estrogen Receptor β Induces Antiinflammatory and Antitumorigenic Networks in Colon Cancer Cells. *Mol. Endocrinol.* **2011**, *25*, 969–979.

[11] Nagini, S. Breast Cancer: Current Molecular Therapeutic Targets and New Players. *Anticancer. Agents Med. Chem.* **2017**, *17*, 152–163.

[12] Nilsson, S. & Koehler, K. F. Oestrogen receptors and selective oestrogen receptor modulators: Molecular and cellular pharmacology. *Basic Clin. Pharmacol. Toxicol.* **2005**, *96*, 15–25.

[13] Jordan, V. C. Tamoxifen: Catalyst for the change to targeted therapy. *Eur. J. Cancer* **2008**, *44*, 30–38.

[14] Lim, C. K. *et al.* A comparative study of tamoxifen metabolism in female rat, mouse and human liver microsomes. *Carcinogenesis* **1994**, *15*, 589–593.

[15] Shiau, A. K. *et al.* The structural basis of estrogen receptor/coactivator recognition and the antagonism of this interaction by tamoxifen. *Cell* **1998**, *95*, 927–937.

[16] Davies, C. *et al.* Long-term effects of continuing adjuvant tamoxifen to 10 years versus stopping at 5 years after diagnosis of oestrogen receptor-positive breast cancer: ATLAS, a randomised trial. *Lancet* **2013**, *381*, 805–816.

[17] Zhou, W. Bin, Ding, Q., Chen, L., Liu, X. A. & Wang, S. Toremifene is an effective and safe alternative to tamoxifen in adjuvant endocrine therapy for breast cancer: Results of four randomized trials. *Breast Cancer Res. Treat.* **2011**, *128*, 625–631.

[18] Grese, T. A. *et al.* Structure-activity relationships of selective estrogen receptor modulators: Modifications to the 2-arylbenzothiophene core of raloxifene. *J. Med. Chem.* **1997**, *40*, 146–167.

[19] Patel, H. K. & Bihani, T. Selective estrogen receptor modulators (SERMs) and selective estrogen receptor degraders (SERDs) in cancer treatment. *Pharmacol. Ther.* **2018**, *186*, 1–24.

[20] McDonnell, D. P., Wardell, S. E. & Norris, J. D. Oral Selective Estrogen Receptor Downregulators (SERDs), a Breakthrough Endocrine Therapy for Breast Cancer. *J. Med. Chem.* **2015**, *58*, 4883–4887.

[21] Wakeling, A. E. & Bowler, J. Biology and mode of action of pure antioestrogens. *J. Steroid Biochem.* **1988**, *30*, 141–147.

[22] Wu, Y. L. *et al.* Structural basis for an unexpected mode of SERM-Mediated ER antagonism. *Mol. Cell* **2005**, *18*, 413–424.

[23] NCT02338349. (n.d.) A phase I, multicenter, open-label, multi-part, dose-escalation study of RAD1901 in postmenopausal women with advanced estrogen receptor positive and her2-negative breast cancer. ClinicalTrials.gov. https://clinicaltrials.gov/ct2/ show/NCT02338349. Accessed September 20, 2017.

[24] NCT02248090. (n.d.) AZD9496 first time in patients ascending dose study. https:// clinicaltrials.gov/ct2/show/NCT02248090.Accessed September 20, 2017.

[25] NCT02316509. (n.d.) A study of GDC-0927 in postmenopausal women with locally ad- vanced or metastatic estrogen receptor positive breast cancer. https://clinicaltrials. gov/ct2/show/NCT02316509. Accessed September 20, 2017.

[26] Tria, G. S. *et al.* Discovery of LSZ102, a potent, orally bioavailable selective estrogen receptor degrader (SERD) for the treatment of estrogen receptor positive breast cancer. *J. Med. Chem.* **2018**, *61*, 2837–2864.

[27] Bidard, F.-C. *et al.* Elacestrant (oral selective estrogen receptor degrader) Versus Standard Endocrine Therapy for Estrogen Receptor–Positive, Human Epidermal Growth Factor Receptor 2–Negative Advanced Breast Cancer: Results From the Randomized Phase III EMERALD Trial. *J. Clin. Oncol.* **2022**, JCO.22.00338.

[28] Hernando, C. *et al.* Oral selective estrogen receptor degraders (Serds) as a novel breast cancer therapy: Present and future from a clinical perspective. *Int. J. Mol. Sci.* **2021**, *22*,.

[29] Sakamoto, K. M. *et al.* Development of Protacs to target cancer-promoting proteins for ubiquitination and degradation. *Mol. Cell. Proteomics* **2003**, *2*, 1350–1358.

[30] Bargagna-Mohan, P., Baek, S. H., Lee, H., Kim, K. & Mohan, R. Use of PROTACS as molecular probes of angiogenesis. *Bioorganic Med. Chem. Lett.* **2005**, *15*, 2724–2727.

[31] Itoh, Y., Kitaguchi, R., Ishikawa, M., Naito, M. & Hashimoto, Y. Design, synthesis and biological evaluation of nuclear receptor-degradation inducers. *Bioorganic Med. Chem.* **2011**, *19*, 6768–6778.

[32]Ohoka, N. *et al.* Derivatization of inhibitor of apoptosis protein (IAP) ligands yields improved inducers of estrogen receptor degradation. *Journal of Biological Chemistry* at https://doi.org/10.1074/jbc.RA117.001091 (2018) vol. 293 6776–6790.

[33] S.A. Campos, A.H. Harling, John DavidMiah, I.E.D. Smith, Proteolysis Targeting Chimeras (PROTACs) Directed to the Modulation of The Estrogen Receptor, **2014**. WO/2014/108452A1

[34] i) J.D. Harling, I.E.D. Smith, IAP E3 Ligase Directed Proteolysis Targeting Chimeric Molecules, **2016**. WO/2016/169989A1.ii) J.D. Harling, I.E.D. Smith, Novel Compounds, **2019**. US2019/0263798.

[35] Hu, J. *et al.* Discovery of ERD-308 as a Highly Potent Proteolysis Targeting Chimera (PROTAC) Degrader of Estrogen Receptor (ER). *J. Med. Chem.* **2019**, *62*, 1420–1442.

[36] Kargbo, R. B. PROTAC-Mediated Degradation of Estrogen Receptor in the Treatment of Cancer. *ACS Med. Chem. Lett.* **2019**, *10*, 1367–1369.

[37] a) A. P. Crew, C. Crews, H. Dong, E. Ko, J. Wang, Preparation of estrogen-related receptor alpha based PROTAC compounds and associated methods of use. EP2985285, 2016. b) A. P. Crew, Y. Qian, H. Dong, J. Wang, C. M. Crews, Preparation of indole derivatives as estrogen receptor degraders. US20180072711, 2018. c) A. P. Crew, Y. Qian, H. Dong, J. Wang, K. R. Hornberger, C. M. Crews, Tetrahydronaphthalene and tetrahydroisoquinoline derivatives as estrogen receptor degraders and their preparation. WO2018102725, 2018.

[38] https://www.arvinas.com/pipeline-programs/estrogen-receptor

[39] Jiang, Y. *et al.* Development of Stabilized Peptide-Based PROTACs against Estrogen Receptor α. *ACS Chemical Biology* **2018** *13* 628–635.

[40] Dai, Y. *et al.* Development of cell-permeable peptide-based PROTACs targeting estrogen receptor α. *European Journal of Medicinal Chemistry* at https://doi.org/10.1016/j.ejmech.2019.111967 (2020) vol. 187. Reference format

[41] i) J. Fan, K. Liu, Novel Compounds Having Estrogen Receptor Alpha Degradation Activity and Uses Thereof, **2018**. US20180208590. ii) J. Fan, K. Liu, Novel Compounds Having Estrogen Receptor Alpha Degradation Activity and Uses Thereof, **2020**. US20200024269A1

[42] Dragovich, P. S. *et al.* Antibody-mediated delivery of chimeric protein degraders which target estrogen receptor alpha (ERα). *Bioorganic Med. Chem. Lett.* **2020**, *30*, 126907.

[43] Donoghue, C., Cubillos-Rojas, M., Gutierrez-Prat, N., Sanchez-Zarzalejo, C., Verdaguer, X., Riera, A., Nebreda, A.R.. Optimal linker length for small molecule PROTACs that selectively target p38α and p38β for degradation. *Eur. J. Med. Chem.* **2020**, *201*, 112451.

[44] Singh, M. S., Chowdhury, S. & Koley, S. Advances of azide-alkyne cycloaddition-click chemistry over the recent decade. *Tetrahedron* **2016**, *72*, 5257–5283.

[45] Kolb, H. C., Finn, M. G. & Sharpless, K. B. Click Chemistry: Diverse Chemical Function from a Few Good Reactions. *Angew. Chem. Int. Ed.* **2001**, *40*, 2004–2021.

[46] Rostovtsev, V. V., Green, L. G., Fokin, V. V. & Sharpless, K. B. A stepwise huisgen cycloaddition process: Copper(I)-catalyzed regioselective 'ligation' of azides and terminal alkynes. *Angew. Chemie - Int. Ed.* **2002**, *41*, 2596–2599.

[47] Wurz, R. P. *et al.* A 'click Chemistry Platform' for the Rapid Synthesis of Bispecific Molecules for Inducing Protein Degradation. *J. Med. Chem.* **2018**, *61*, 453–461.

[48] Bonandi, E. *et al.* The 1,2,3-triazole ring as a bioisostere in medicinal chemistry. *Drug Discov. Today* **2017**, *22*, 1572–1581.

[49] Chakraborty, S. & Biswas, P. K. Structural insights into selective agonist actions of tamoxifen on human estrogen receptor alpha. *J. Mol. Model.* **2014**, *20*.falta pagina

[50] Burke, P. J., Kalet, B. T. & Koch, T. H. Antiestrogen binding site and estrogen receptor mediate uptake and distribution of 4-hydroxytamoxifen-targeted doxorubicin-formaldehyde conjugate in breast cancer cells. *J. Med. Chem.* **2004**, *47*, 6509–6518.

[51] Zhou, B. *et al.* Discovery of a Small-Molecule Degrader of Bromodomain and Extra-Terminal (BET) Proteins with Picomolar Cellular Potencies and Capable of Achieving Tumor Regression. *J. Med. Chem.* **2018**, *61*, 462–481.

[52] Katzenellenbogen, B. S., Norman, M. J., Eckert, R. L., Peltz, S. W. & Mangel, W. F. Bioactivities, estrogen receptor interactions, and plasminogen activator-inducing activities of tamoxifen and hydroxy-tamoxifen isomers in MCF-7 human breast cancer cells. *Cancer Res.* **1984**, *44*, 112–119.

[53] Foster, A. B. *et al.* Hydroxy derivatives of tamoxifen. *J. Med. Chem.* **1985**, *28*, 1491–1497

[54] Fischer, E. S. *et al.* Structure of the DDB1-CRBN E3 ubiquitin ligase in complex with thalidomide. *Nature* **2014**, *512*, 49–53.

[55] Chitrakar, A., Budda, S. A., Henderson, J. G., Axtell, R. C. & Zenewicz, L. A. E3 Ubiquitin Ligase Von Hippel–Lindau Protein Promotes Th17 Differentiation. *J. Immunol.* **2020**, *205*, 1009–1023.

[56] Galdeano, C. *et al.* Structure-guided design and optimization of small molecules targeting the protein-protein interaction between the von hippel-lindau (VHL) E3 ubiquitin ligase and the hypoxia inducible factor (HIF) alpha subunit with in vitro nanomolar affinities. *Journal of Medicinal Chemistry* at https://doi.org/10.1021/jm5011258 (2014) vol. 57 8657–8663.

[57] P.S. Dragovich, P. Adhikari, R.A. Blake, N. Blaquiere, J. Chen, Y.-X. Cheng, W. den Besten, J. Han, S.J. Hartman, J. He, M. He, E. Rei Ingalla, A. V. Kamath, T. Kleinheinz, T. Lai, D.D. Leipold, C.S. Li, Q. Liu, J. Lu, Y. Lu, F. Meng, L. Meng, C. Ng, K. Peng, G. Lewis Phillips, T.H. Pillow, R.K. Rowntree, J.D. Sadowsky, D. Sampath, L. Staben, S.T. Staben, J. Wai, K. Wan, X. Wang, B. Wei, I.E. Wertz, J. Xin, K. Xu, H. Yao, R. Zang, D. Zhang, H. Zhou, Y. Zhao, Antibody-mediated delivery of chimeric protein degraders which target estrogen receptor alpha (ERα), Bioorg. Med. Chem. Lett. 30 (2020) 126907.

[58] Loren, G., Espuny, I., Llorente, A., Donoghue, C., Verdaguer, X., Gomis, R., Riera, A., Design and optimization of oestrogen receptor PROTACs based on 4-hydroxytamoxifen. *Eur. J. Med. Chem.* **2022**, *243*, 114770.

Chapter 4.

Tousled-like Kinase PROTACs

4 Tousled-like Kinase PROTACs

4.1. TLK PROTACs: Introduction and Objectives

Tousled-like kinases (TLKs) are a group of kinases belonging to a distinct branch of Serine/Threonine kinases expressed across most cell lines and tissues. TLKs and the Tousled Kinase (TSL) are responsible for phosphorylation of ASF1a and ASF1b, two histone chaperones that mediate histone exchange.[1] The activity of these kinases has been linked to regulation of chromatin plasticity, playing a role in many essential cellular processes required for development and aging, such as DNA replication and repair, cell division and transcription.[2] There are two distinct TLK genes in mammals, TLK1 and TLK2, and although being highly similar, they seem to have some specific roles, as well as largely redundant function in genome maintenance.[3]

The TLK2 gene has been reported to be amplified in Oestrogen Receptor (ER)-positive breast cancer.[4] Studies have also suggested its implication in intellectual disability patients.[5] Its implication in cancer have suggested that small-molecule inhibitors of TLK2 could be used as anticancer agents. Work by T. Stracker et al. investigated the activity of small-molecule kinase inhibitors against TLK2, testing other kinase inhibitors and several commercially available compounds.[6] They found that non-specific kinase inhibitors Staurosporine and K-252a abolished TLK2 catalytic activity, while other inhibitors known to target CDK1 (CGP74541A) and GSK3 (Inhibitor XIII) also showed activity against the kinase, as well as the Indirubin derivatives E804 and indirubin-3′-monoxime.[2] More recently, a study developed derivatives based on a bisindole scaffold that inhibit TLK2 with a IC_{50} value of 20 nM showing antiproliferative effects in triple negative breast cancer cells MDA-MB-231.[7]

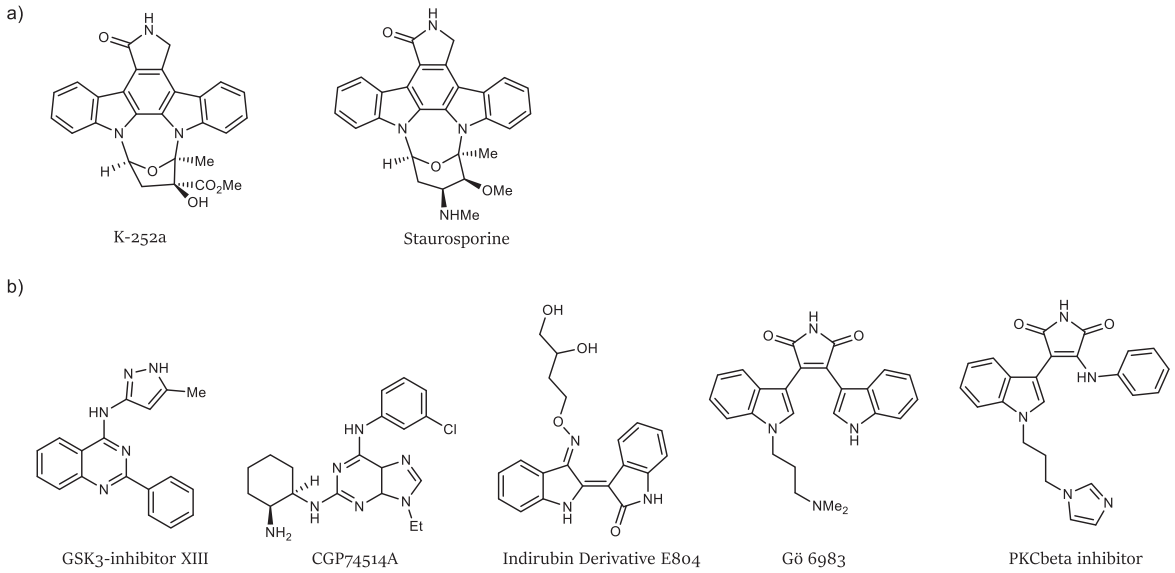

Figure 4.1. a) pan-Kinase inhibitors K-252a and Staurosporine. **b)** compounds targeting TLK2: CDK1 inhibitor CGP74541A, GSK3 inhibitor, bisindolylmaleimide derivatives (targeting PKC), and bisindole derivative Indirubin.

Our search for TLK2 degraders started out as a collaboration with the Stracker Laboratory, at the IRB Barcelona. Based on a recent publication, they had selected a panel of kinase inhibitors showing activity against TLK2. We hypothesized that with the adequate modifications on some of these structures, we could synthesize a TLK-targeting warhead for the synthesis of TLK2 degraders. Following a similar strategy to that described in chapters 3 and 5, we envisaged a modular synthesis based on a copper(I)-catalysed Alkyne-Azide Cycloaddition (CuAAC) to couple a POI-targeting warhead with various E3 ligase recruiting fragments. Our initial objective was to **derivatize TLK2 ligands into warheads functionalized with a terminal linker or alkyne, and then synthesize protein degraders recruiting CRBN or the VHL E3 ubiquitin ligases.**

4.2. Design and Synthesis of TLK PROTACs

Based on structure simplicity and synthetic accessibility, we selected the bisindolylmaleimide scaffold (**Figure 4.1**, gö6983 and PKC beta inhibitor) to design potential TLK degraders. Attachment points for a linker were devised at position 6 of the indole ring and at the indole nitrogen (**Figure 4.2a**). Initially we approached the bisindolylmaleimide core by constructing the tricyclic ring from 6-bromoindole, with the idea to functionalize position 6 at a later stage (**Scheme 4.1**). Following treatment with oxalyl chloride and quenching in methoxide/methanol, intermediate **4-1** was reacted with indole-3-acetamide, affording warhead **4-2** after condensation in acidic media.

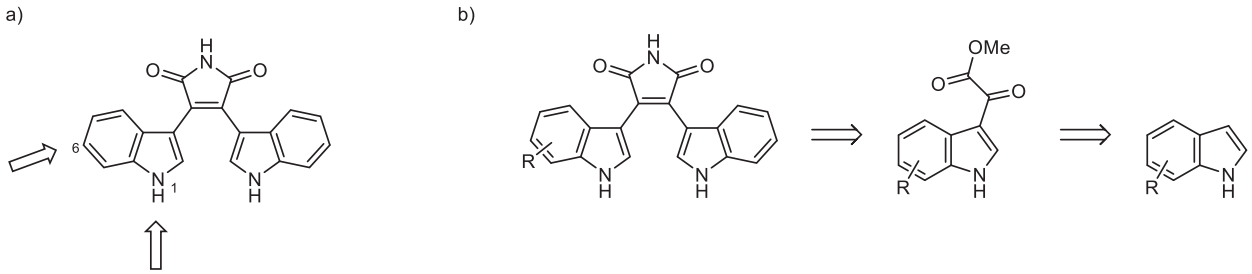

Figure 4.2: a) functionalization points in the bisindolylmaleimide core. **b)** Retrosynthetic analysis of the bisindolylmaleimide scaffold.

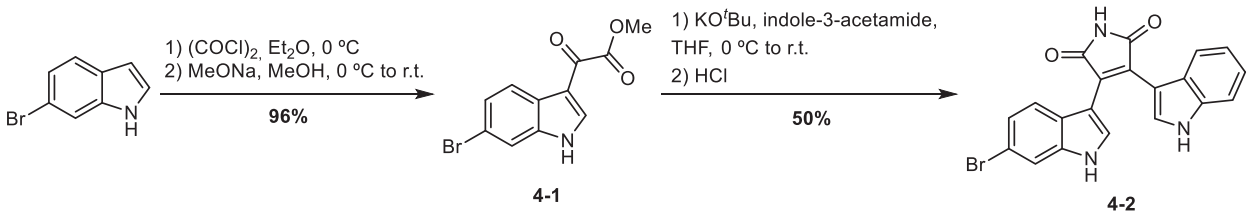

Scheme 4.1: Synthesis of the bromo intermediate **4-2**.

Warhead **4-2** was subjected to Sonogashira and Buchwald-Hartwig conditions using alkyne and amine fragments of diverse complexity. Reaction with boc-protected propargyl amine and pentynoic ester did not show conversion, nor did more complex pomalidomide derivatives bearing a terminal alkyne. Buchwald-Hartwig aminations also proved unsuccessful; not even when attempting to use simpler substrates such as boc-piperazine. At this point, perceiving that an extensive screening of the reaction conditions would be necessary to make this transformation work in acceptable yields, we decided to move to a different synthetic route that was being explored parallel to this one.

As an alternative route to the functionalization of fragment **4-2**, we envisaged an early alkylation of the indole starting material followed by formation of the bisindolylmaleimide structure. Inspired by work by Krumrich *et al.*,[8] who report the synthesis of various bisindolylmaleimide analogues, we decided to introduce the alkyl chain through the indole-3-acetamide fragment. Direct alkylation with trityl-protected bromo propanol afforded intermediate **4-4**, which was converted into the bisindolylmaleimide structure after condensation with fragment **4-5**, derived from indole. The acidic conditions required for the condensation sufficed for the deprotection of the alcohol, which was subsequently converted into the mesylate, followed by substitution with N-methyl-propargylamine.

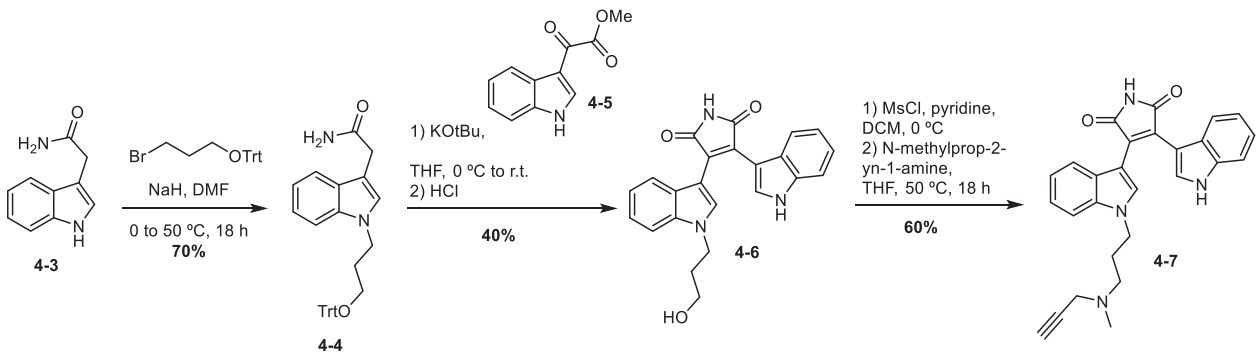

Scheme 4.2: Synthesis of alkylated derivative **4-7**.

Warhead **4-7** was coupled with azide fragments previously described in chapter 3, bearing both CRBN and VHL recruiting warheads. This resulted in the synthesis of two families of potential TLK degraders: **4-8a-d** and **4-9a-f**. The ability of compounds **4-8a-d** and **4-9a-c** compounds to degrade TLK2 was tested in in MCF7 cells, however, degradation of TLK2 was not observed for any of the compounds.

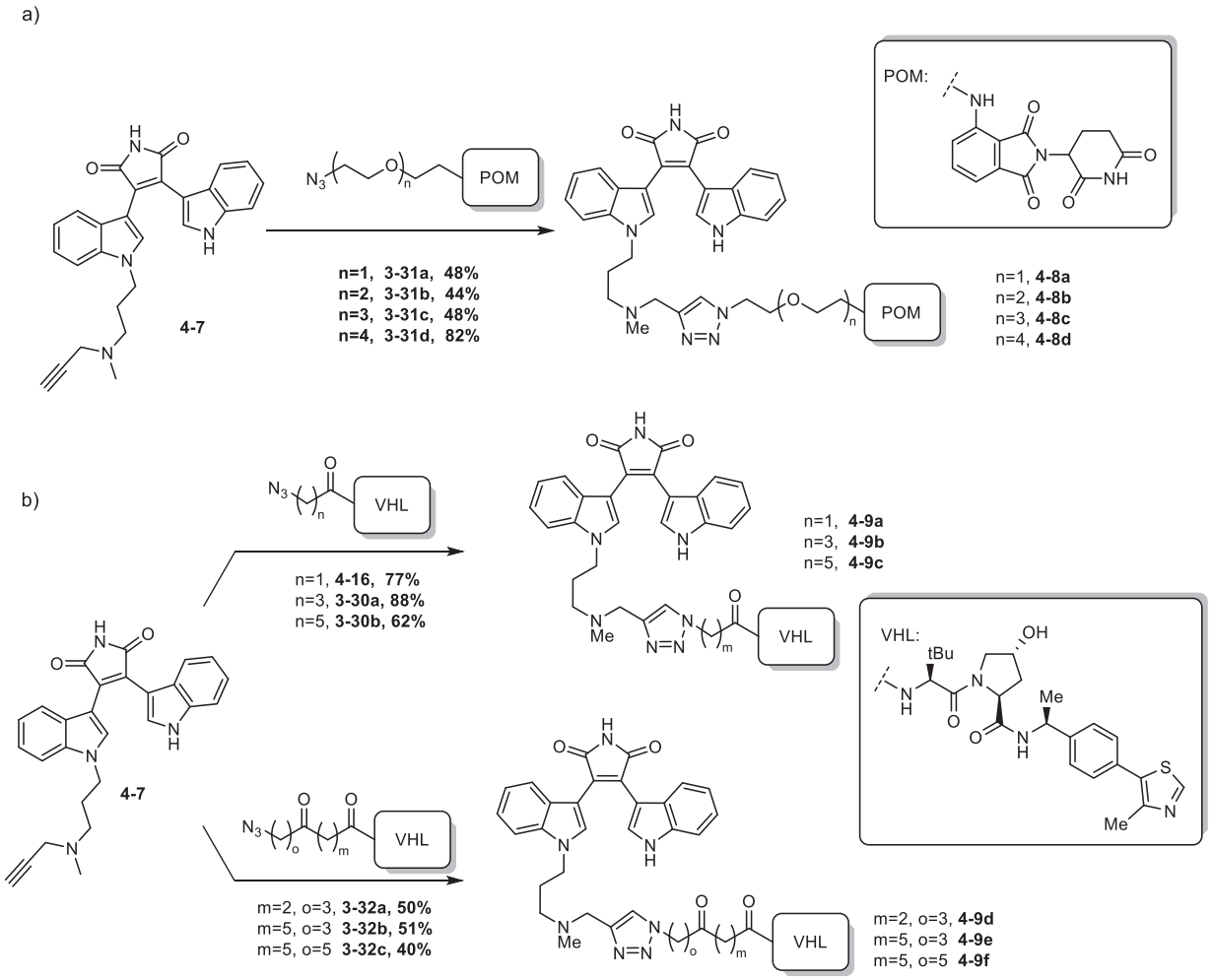

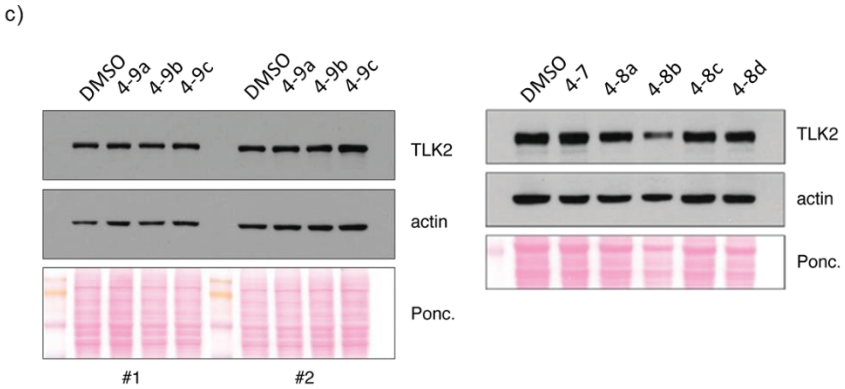

Scheme 4.3: a) Synthesis of potential TLK2 degraders recruiting CRBN. Reaction conditions: $CuSO_4 \cdot 5H_2O$, AcOH (cat), Sodium Ascorbate, H_2O/*t*-BuOH (2:1), 35 °C, 18 h. **b)** Synthesis of potential TLK2 degraders recruiting VHL. Reaction conditions: $CuSO_4 \cdot 5H_2O$, AcOH (cat), Sodium Ascorbate, H_2O/*t*-BuOH (2:1), 35 °C, 18 h. **c)** Biological evaluation of TLK2 degraders. MCF7 cells were treated with 10 μM of the compound for 24 h, cell lysates were analysed by immunoblotting.

We modified the bisindolylmaleimide-based warhead to include more spacing between the ligand and the triazole formed during the CuAAC. Fragment **4-6** was again mesylated and substituted with a piperazine fragment bearing a terminal alkyne, maintaining compatibility with our library of a E3 ligase-azide fragments. Thus, intermediate **4-10** was coupled to pomalidomide- and VHL-based fragments of various linker lengths.

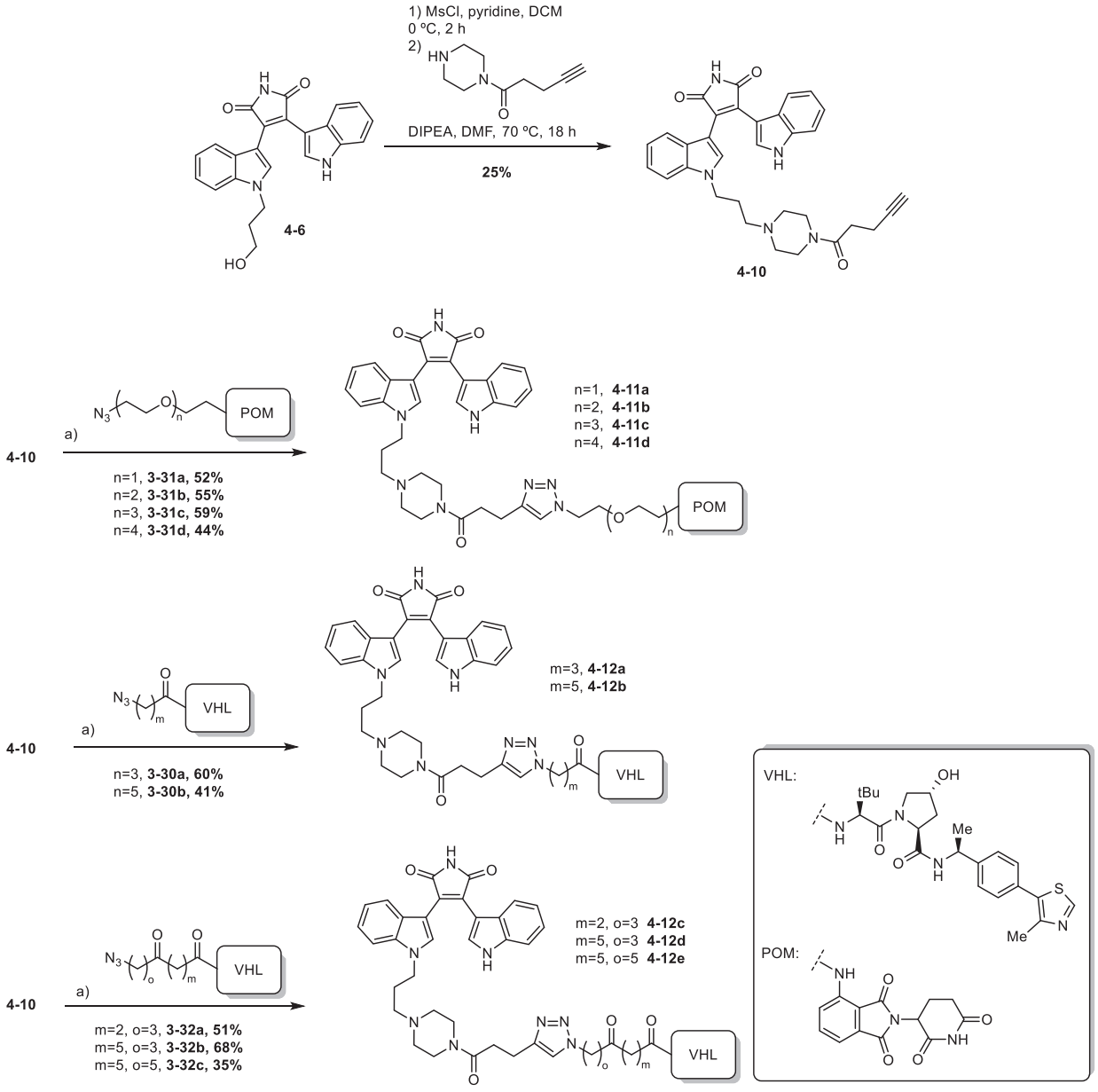

Scheme 4.4: Synthesis of intermediate **4-10** and derivatization into protein degraders. Reaction conditions: a) $CuSO_4 \cdot 5\ H_2O$, AcOH (cat), Sodium Ascorbate, H_2O/*t*-BuOH (2:1), 35 °C, 18 h.

In spite of the failure in the initial cross-coupling approach, we still wanted to explore a different attachment point other than the indole nitrogen. Synthesis of the bisindolylmaleimide core staring from an indole-6-methy ester followed by hydrolisis afforded intermediate **4-15**. Derivatization with propargyl amine, however, did not yield the desired amide **4-16**. Starting from boc-protected 5-aminoindole produced intermediate **4-19**, which was equally reluctant to undergo amidation to afford the alkyne coupling partner **4-20**.

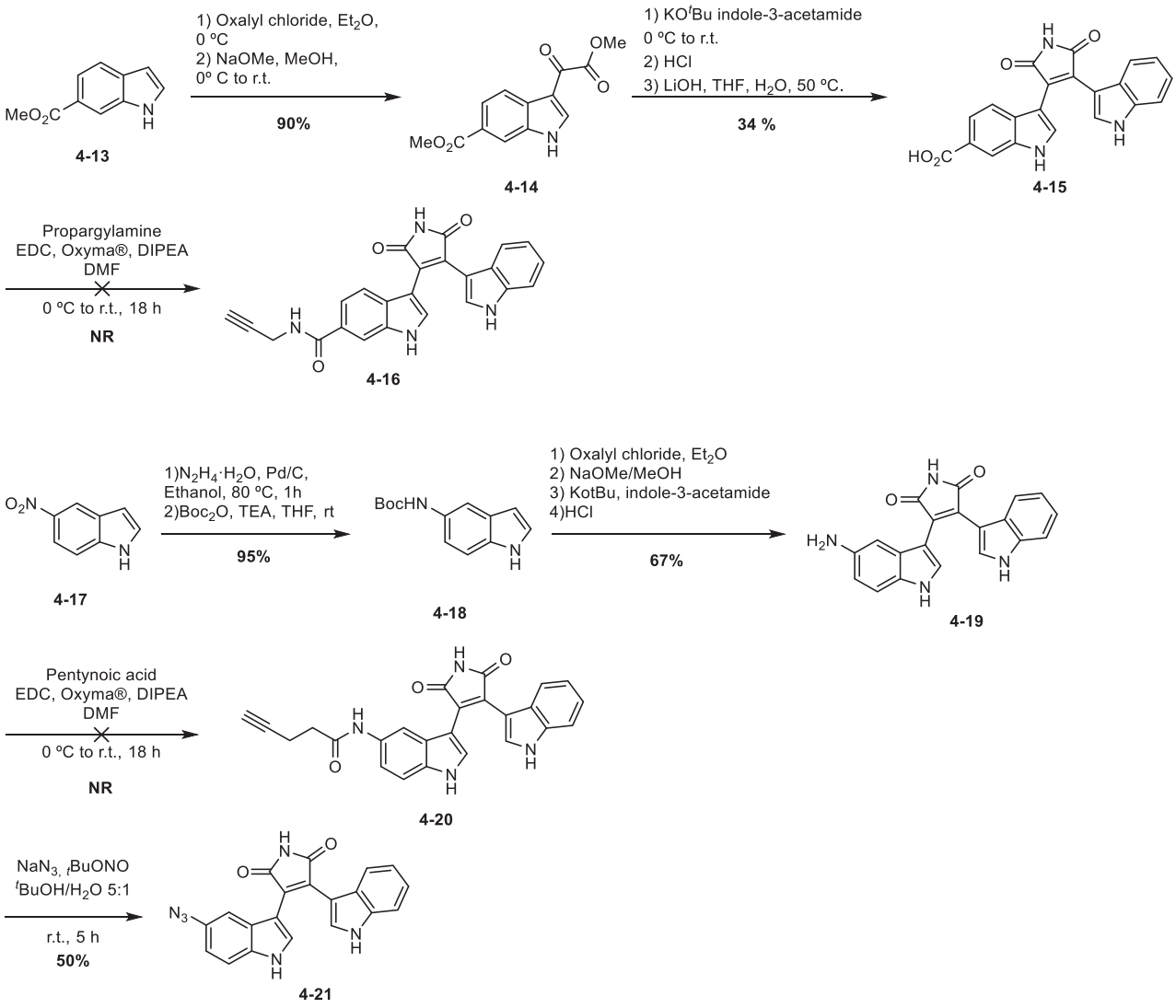

Scheme 4.5: alternative attachment points to the bisindolylmaleimide core a) attempted synthesis of **4-18**. b) attempted synthesis of **4-20**. c) conversion of the amine **4-19** into the azide **4-21**.

Intermediate **4-19** could, however, be converted to the corresponding azide, turning the amine into a diazonium salt in the presence sodium azide. Azide-bearing warhead **4-21** was ready to be coupled to the complementary click partners. However, our initial designs encompassed the inverse reactivity, bearing the terminal azide on the E3 ligase fragments and the terminal alkyne in the POI-

binding warhead. To synthesize degraders derived from **4-21**, we prepared a series of VHL-based fragments bearing a terminal alkyne.

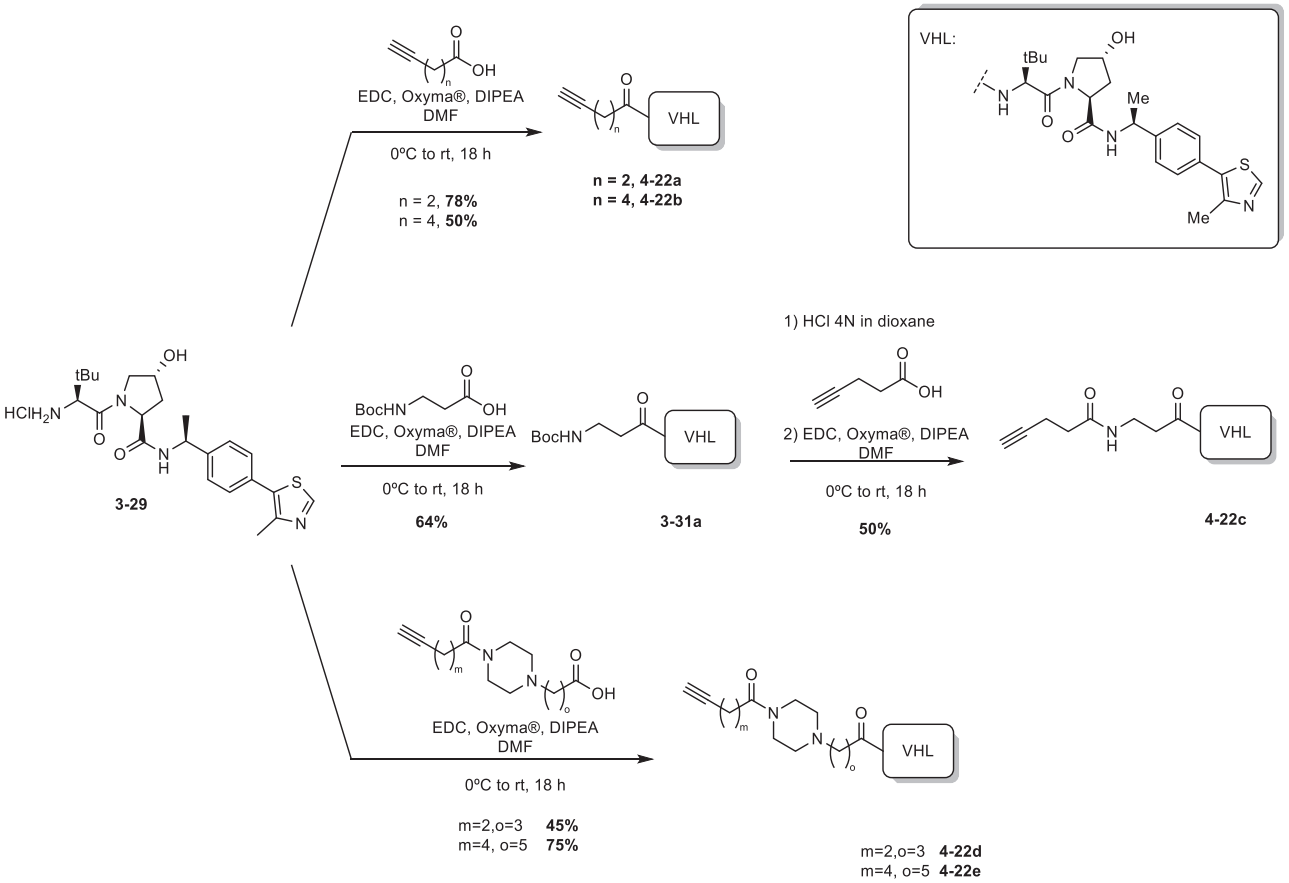

Scheme 4.6: Synthesis of the VHL-alkyne fragments.

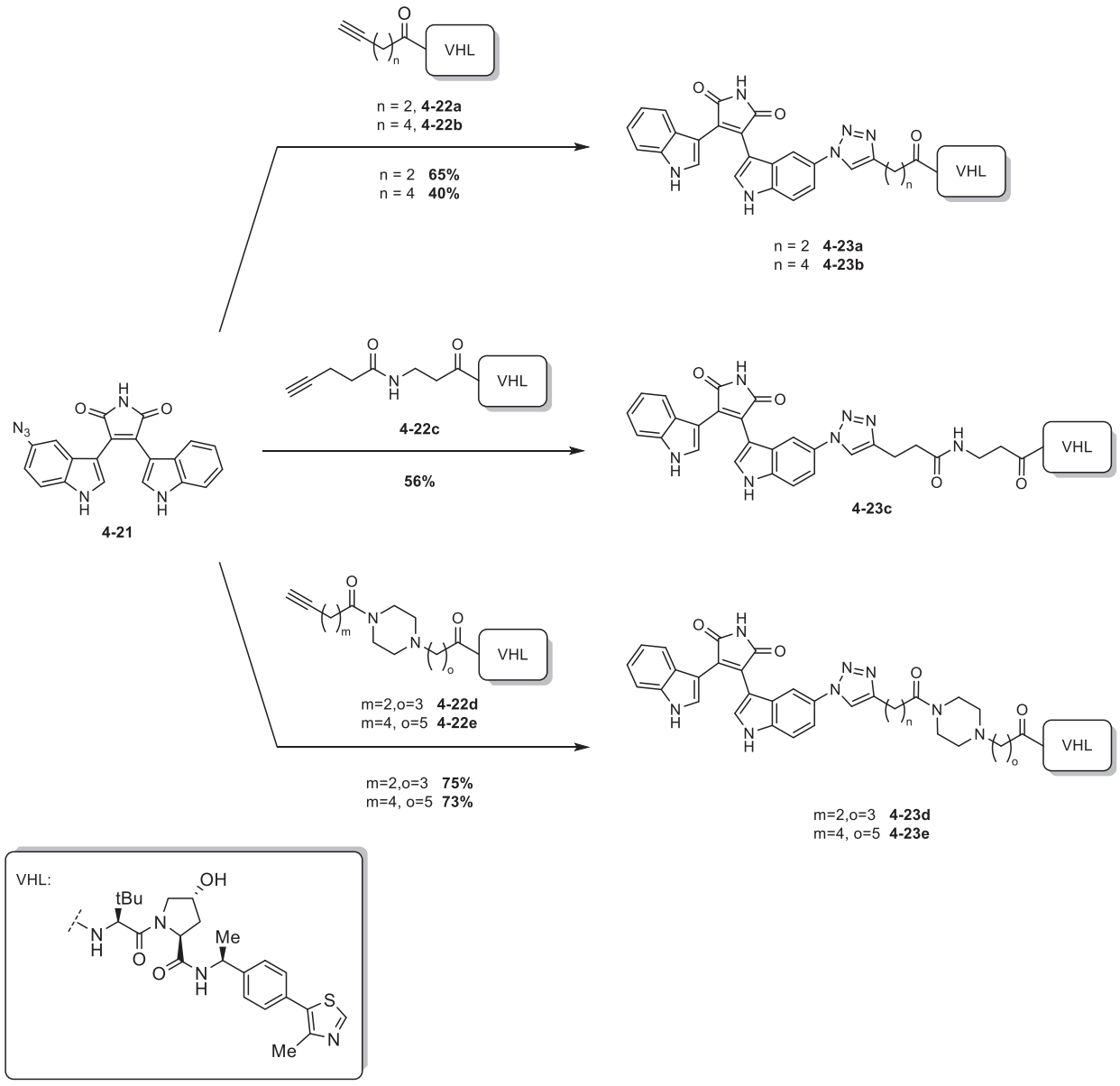

Scheme 4.7: Synthesis of PROTACs derived from warhead **4-21**. Reaction conditions: alkyne fragment, $CuSO_4 \cdot {}_5H_2O$, AcOH (cat), Sodium Ascorbate, H_2O, *t*-BuOH (2:1) 35 °C, 18 h.

With the new families of compounds in hand, based on the N-alkylated-piperazine and the azide warheads, we set out for biological testing of the compounds. The compounds were sent to T. Stracker's laboratory, who in December 2020 had moved to the National Cancer Institute's Centre for Cancer Research. Compounds **4-9d-f**, **4-11a-d**, **4-12a-e** and **4-23a-e** were used to treat Hela-LT cells at a concentration of 10 μM, however, upon treatment, a red precipitate was observed in the plates for most of the compounds. Compounds **49-d**, **4-11a**, **4-11b**, **4-23a** and **4-23b** did not precipitate upon treatment, and their ability to degrade TLK1 was analysed by Western blotting analysis. The results, however, show no degradation of TLK1 for any of the compounds.

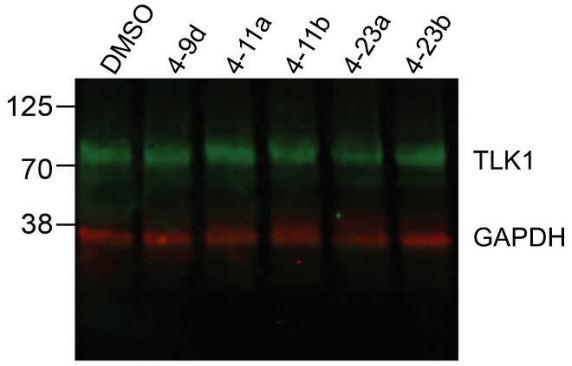

Figure 4.3. a)The tested analogues do not induce degradation of TLK1. Hela-LT cells were treated with the indicated compound at a concentration of 10 μM, cell lysates were analysed by Western blotting.

4.3. TLK PROTACs: Conclusions and Future Work

Based on known inhibitors displaying activity towards TLK2, we have attempted the preparation of TLK degraders by designing a warhead based on the bisindolylmaleimide scaffold. Different synthetic routes towards a bisindolylmaleimide warhead were explored. We synthesized two warheads based on a *N*-alkylation strategy featuring a linker with a terminal alkyne (**4-7** and **4-10**) and one warhead bearing an azide at the 5 position of the indole (**4-21**).

Warheads **4-7** and **4-10**, bearing a terminal alkyne, was paired with VHL and CRBN-recruiting fragments via CuAAC, obtaining the potential degraders **4-8a-d**, **4-9a-f**, **4-11a-d** and **4-12a-e**. Warhead **4-21**, bearing an azide, was coupled with VHL-based fragments with terminal alkynes, obtaining potential degraders **4-23a-e**.

Compounds **4-8a-d** and **4-9a-c** and were tested in MCF7 cells against TLK2 degradation, unfortunately degradation was not observed. Compounds **4-9d-f**, **4-11a-d** and **4-23a-e** have been preliminary tested, however, they do not seem to induce degradation of TLK1 in Hela-LT cells. The effect of the other compounds was not tested by Western blotting because of the precipitation of the compounds upon treatment.

Lacking insight into the issues behind the inactivity of the compounds, we have not pursued synthetic efforts to prepare any other analogues. Our warhead design was based on structural similarities with existing analogues of the inhibitors, however, we did not have a crystal structure of the TLK-inhibitor complex to help our design. We had no certainty that the linker we were constructing would not disrupt important interactions with the protein, and binding assays with the compounds would be needed to asses it. Moreover, TLK has been reported to be mainly a nuclear protein. We have no insight on the permeability of the PROTAC, nor know if the inactivity is due to unproductive engagement with the proteins or because the degrader cannot reach them. Although the project remains open, biological and structural data are needed to determine future directions.

References

[1] Klimovskaia, I. M. *et al.* Tousled-like kinases phosphorylate Asf1 to promote histone supply during DNA replication. *Nat. Commun.* **2014**, *5*, 3394.
[2] Mortuza, G. B. *et al.* Molecular basis of Tousled-Like Kinase 2 activation. *Nat. Commun.* **2018**, *9*,.
[3] Segura-Bayona, S. *et al.* Differential requirements for Tousled-like kinases 1 and 2 in mammalian development. *Cell Death Differ.* **2017**, *24*, 1872–1885.
[4] Kim, J.-A. *et al.* Comprehensive functional analysis of the tousled-like kinase 2 frequently amplified in aggressive luminal breast cancers. *Nat. Commun.* **2016**, *7*, 12991.
[5]Lelieveld, S. H. *et al.* Meta-analysis of 2,104 trios provides support for 10 new genes for intellectual disability. *Nat. Neurosci.* **2016**, *19*, 1194–1196.
[6] Gao, Y. *et al.* A broad activity screen in support of a chemogenomic map for kinase signalling research and drug discovery. *Biochem. J.* **2013**, *451*, 313–328.
[7] Lee, S. B. *et al.* Design, synthesis and biological evaluation of bisindole derivatives as anticancer agents against Tousled-like kinases. *Eur. J. Med. Chem.* **2022**, *227*, 113904.
[8] Faul, M. M., Winneroski, L. L. & Krumrich, C. A. A New, Efficient Method for the Synthesis of Bisindolylmaleimides. *J. Org. Chem.* **1998**, *63*, 6053–6058.

Chapter 5.

p38 PROTACs

Chapter 5. p38 PROTACs

5.1. p38 PROTACs: Introduction

The mitogen-activated protein kinases (MAPKs) are a family of kinases involved in a broad variety of cellular responses, including cell differentiation, gene expression, proliferation, survival and apoptosis.[1] Canonical MAPKs are divided in three families; the extracellular signal-regulated kinases (ERKs), the c-Jun N-terminal kinases (JNKs) and the p38 mitogen-activated protein kinases (p38s). Generally, ERKs are activated by growth factors and mitogens, whereas JNKs and p38 MAPKs respond to cellular stress and inflammatory cytokines.[2]

MAP kinases have almost no catalytic activity in their basal state; they require activation *via* phosphorylation. Thus, their activity is controlled by a phosphorylation cascade that involves other kinases located upstream in the signalling pathway.[3] A three-part signalling module comprises a MAPK kinase kinase (MAP3K), a MAPK kinase (MAP2K) and a MAP kinase (MAPK). Upon stimulation, MAP3Ks are phosphorylated and activated, and trigger sequential phosphorylation and activation of the MAP2Ks and MAPKs downstream. MAPKs are doubly phosphorylated on a conserved motif located within the activation loop of the kinase domain, causing a conformational change that allows the binding of ATP and the substrate.[4]

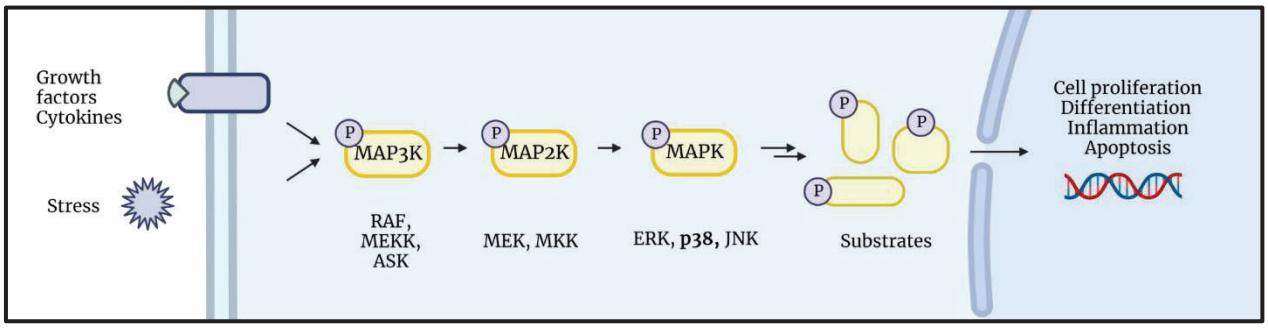

Figure 5.1. Schematic representation of the MAPK pathway.

The p38 MAP kinases are a subfamily of the MAP kinases, and are key regulators of the biosynthesis of pro-inflammatory cytokines. They are activated by cellular stress and play a role in immune response and regulation of cell survival and differentiation.[5] The p38 MAPK kinase family consists in four members (α, β, γ and δ) that display different tissue expression, p38α being the most abundant isoform and ubiquitously expressed in almost all cell types.[6]

MAPKs act on a wide range of cellular functions by phosphorylating downstream targets that include transcription factors, regulatory and structural proteins, protein kinases and phosphatases.[7] The

p38 family members are estimated to phosphorylate over 300 substrates, including MK2/3, MNK1/2 and MSK1/2, which are involved in intracellular stress signal amplification, and regulation of other inflammatory mediators such as TNFα, IL-1β, IL-6 and CXCl2. In particular, p38α contributes to a range of processes that are pivotal for normal tissue functioning, which are frequently deregulated in many pathologies.

Its role in regulating the production of pro-inflammatory cytokines has made p38 an attractive target for a number of stress-related inflammatory diseases, as well as neurodegenerative diseases and cancer.[8] However, in tumor formation, metastasis and dormancy, p38α seems to play a dual role, which is dependent on the tissue and point of progression in the disease.[9] Whereas p38α inhibitors attenuate metastasis of breast cancer,[10] p38 downregulation can facilitate metastatic spread of colon cancer cells from liver to lung.[11] This seemingly contradictory data highlights the complexity of the MAPK signaling pathway and its central position in the regulation of many cellular processes. In spite of this ambiguity, the p38 MAPK pathway have been proposed as a target in the treatment of inflammatory diseases and cancer, and a number of p38 MAPKs inhibitors have been developed and pushed through clinical trials.

Although there have been many attempts to bring a p38 MAPK inhibitor to the market, none have advanced through clinical trials.[12] One reason are the side effects and toxicity observed at higher doses for some of these inhibitors.[13] Because they rely on interactions with the ATP-binding site, which is highly conserved among the kinome, kinase inhibitors typically lack total selectivity. Some inhibitors have exploited particular conformations of the p38 MAPKs in order to gain selectivity, such as the type-I inhibitor PH-797804, that targets the so-called glycine flip at Gly110 of the kinase hinge region,[14] or BIRB-796, which addresses a less-conserved distant site from the ATP-binding domain.[15] Other p38 MAPK inhibitors show kinase selectivity; SB203580 degrades p38α and β over the majority of kinases, although it shows inhibition of other MAPKs. AMG-548 has exquisite potency towards p38α but it also targets JNK2/3. Other inhibitors such as pamapimod or talmapimod also show selectivity against other kinases but fail to distinguish between the α and β isoforms.

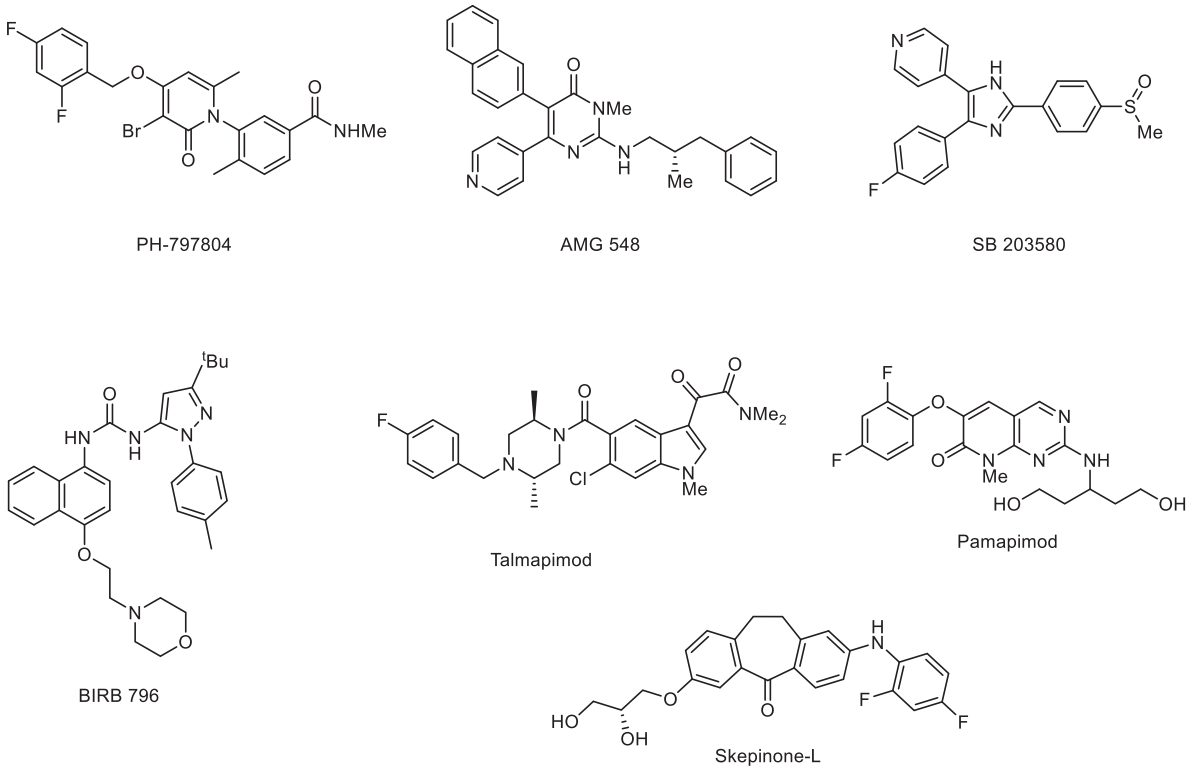

Figure 5.2. Structures of relevant p38 inhibitors.

Due to the difficulty of achieving selectivity across the kinome, targeting kinases selectively with small-molecule traditional inhibitors still remains a challenge. New pharmacological modes of action, such as targeted protein degradation, have gained prominence during the past years and might be able to overcome such issues. In particular, some PROTACs (Proteolysis Targeting Chimaeras) targeting kinase proteins have been able to surpass these limitations, degrading kinase targets selectively.

In 2019, Crews et al. reported isoform-selective p38 degraders based on a kinase inhibitor and recruiting the von Hippel-Lindau (VHL) E3 ligase. A year later, our laboratory reported a series of p38 PROTACs based on the p38 inhibitor **PH-797804** and thalidomide analogues, which recruit the $CRL4^{CRBN}$ E3 ubiquitin ligase. Based on the binding mode of PH, the attachment point to the linker was selected at the methylamide moiety, projecting opposite to the kinase's active site.[16] Ligands based on 5' carboxylic acid thalidomide derivatives, lenalidomide and pomalidomide, were employed as E3 ligase targeting warheads. A series of compounds of varying the linker length featuring alkyl or polyethylene glycol (PEG) linker compositions were prepared, in order to assess the optimal linker length. The most active compound of the series was **NR-7h**, composed of an alkyl linker and a pomalidomide derivative as the E3 ligase binder. The compound achieved DC_{50} values of 24 nM in TD7D cells and 27 nM in MB-MDA 231 cells. It suffered, however, from poor solubility in water, which hindered its study in mouse models, and *in vitro* results did not prove any clear advantage over the inhibitor.

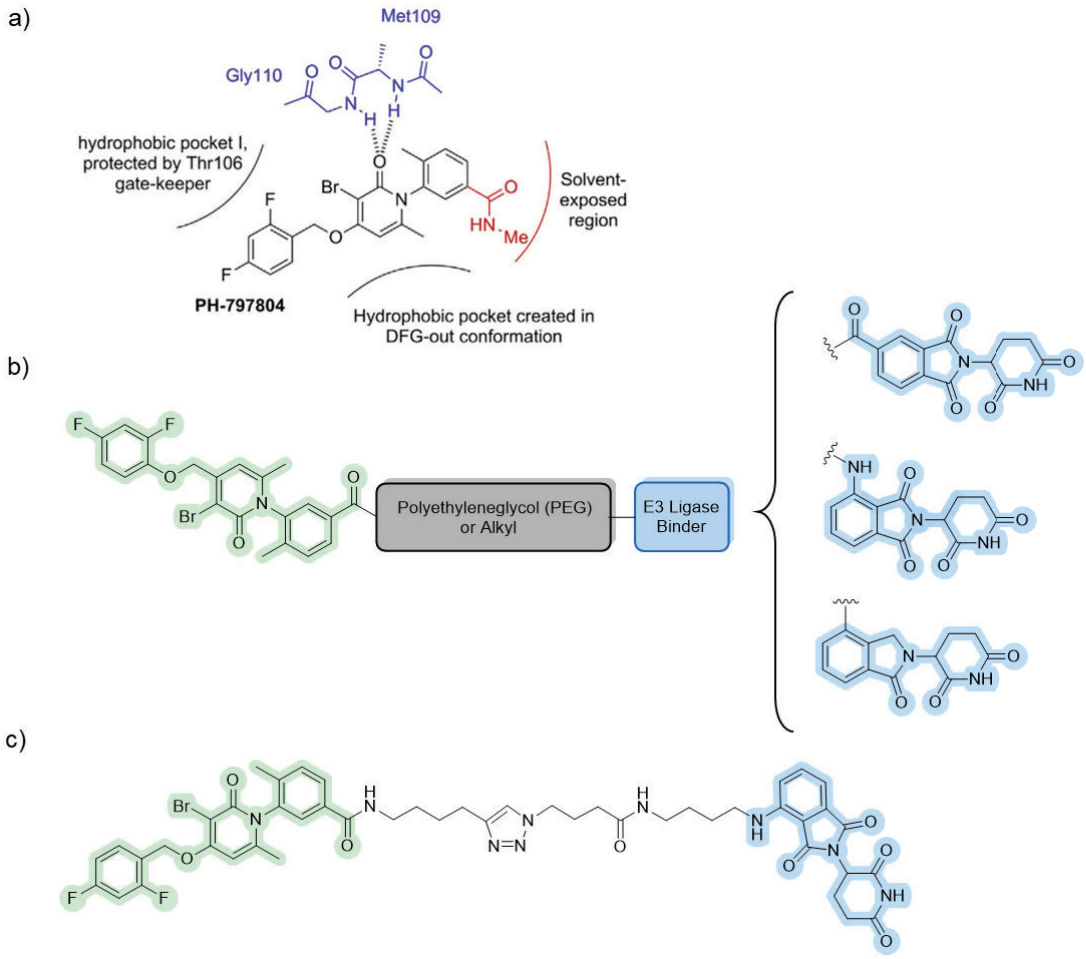

Figure 5.3. a) binding mode of **PH-797804**. **b)** outline of CRBN-targeting p38 PROTACs. **c)** Structure of **NR-7h**.

5.2. p38 PROTACs: Objectives

NR-7h needed optimization to prove that the degradation strategy adds some value over inhibition with the parent inhibitor **PH-797804**. Moreover, we wanted to explore the possible advantages of our PROTACs performing studies *in vivo*. **Our first objective was to synthesize analogues of NR-7h that maintained its potency while improving water solubility.** We tackled the optimization of **NR-7h** through two different strategies: modification of the linker composition to introduce more polar groups, and modification of the E3 ubiquitin ligase recruiter.

After identifying novel p38 degraders, we set of to study how the linker composition affected activity. **The second objective of this chapter was to conduct a structure-activity relationship study on the linker**, in order to find more potent and soluble compounds and to understand the effect of linker composition on PROTAC activity.

5.3. CRBN-based p38 PROTACs

A number of studies have pointed out the importance of the linker in PROTAC activity, highlighting its role in the formation of interactions that promote a cooperative tertiary complex formation.[17,18] The linker is also one of the main domains to carry out a structure-activity relationship (SAR) on a PROTAC, since modifications on the warheads can disturb binding to the target protein or E3 ligase. Linker length is determinant to PROTAC activity, and its composition has a big impact on the compound's properties, such as solubility or cell membrane permeability. Our first strategy to improve the water solubility of **NR-7h** was the modification of the linker composition to introduce more polar groups.

Our initial approach consisted of changing the linker composition of **NR-7h** to polyethylene glycol (PEG) linkers. PEG chains are one of the most common linker motifs in PROTAC design due to their synthetic accessibility, thanks to commercially available bi-functionalized PEG fragments. We hypothesized that their flexibility could be comparable to that of the original alkyl linker of **NR-7h**, while the PEG composition could provide differences in the PROTAC's properties and behavior. PROTACs bearing PEG linkers have been found to possess chameleonic behavior; the flexibility of the PEG chain allows folded conformations that correlates with higher cell permeability and solubility.[19]

Fragment **5-7** was synthesized according to our previous work, following methods described in the literature (**Scheme 5.1**).[20] Condensation of **5-1** and **5-2** under basic conditions afforded intermediate **5-3** in good yields. Bromination of **5-3**, followed by ether formation yielded methyl ester **5-6**. Treatment with NaOH yielded the free acid **5-7**, which was used to prepare functionalized PH-based fragments.

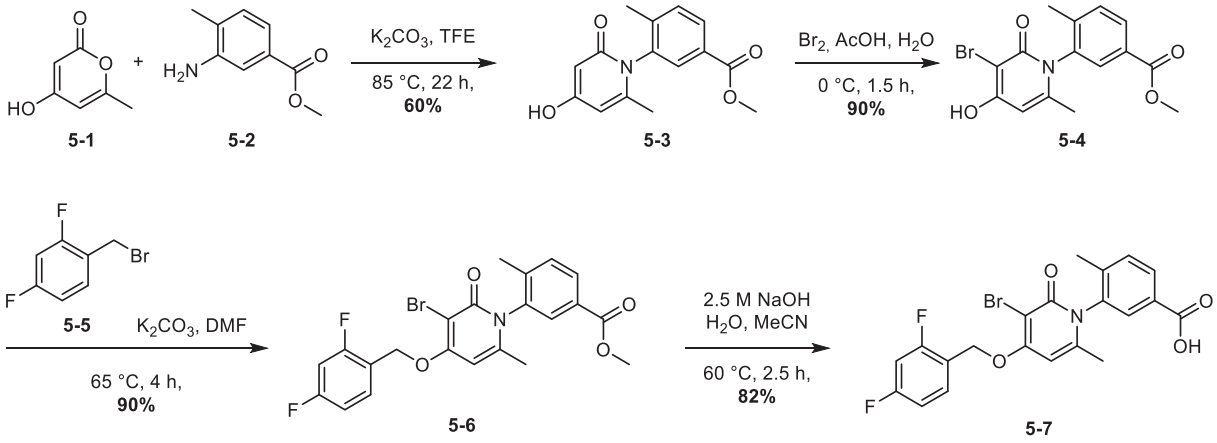

Scheme 5.1: Synthesis of **5-7**.

5-7 was subjected to amide formation conditions with PEG fragments bearing terminal alkynes or azides. As in our previous work, in order to couple two advanced intermediates we relied on a copper-catalyzed alkyne-azide cycloaddition (CuAAC), a type of "click chemistry" described in **chapter 3**. The complementary click fragments were prepared from fluorothalidomide **3-10**. Alkyne-bearing fragments **5-8a** and **5-8b** were synthesized through aromatic nucleophilic substitution, azide-bearing fragments **3-11b** and **3-11c** described in chapter 3 were also used. Compounds **5-10a-d** were prepared under standard CuAAC conditions, yielding four analogs that maintained the linker length of **NR-7h (Scheme 5.2)**.

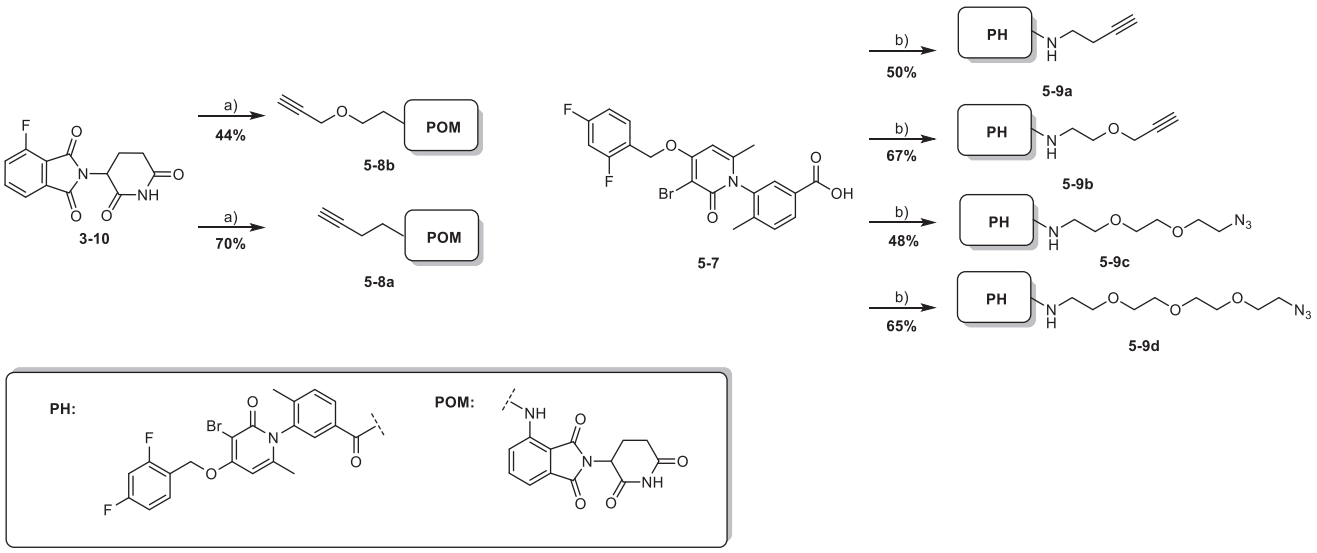

Scheme 5.2: Synthesis of pomalidomide fragments. Reaction conditions: a) corresponding amine, DIPEA, DMA, 120 °C, 2 hours. b) Synthesis of PH fragments. Corresponding amine, EDC·HCl, Oxyma®, DIPEA, DMF, 0 °C to r.t., 18 hours.

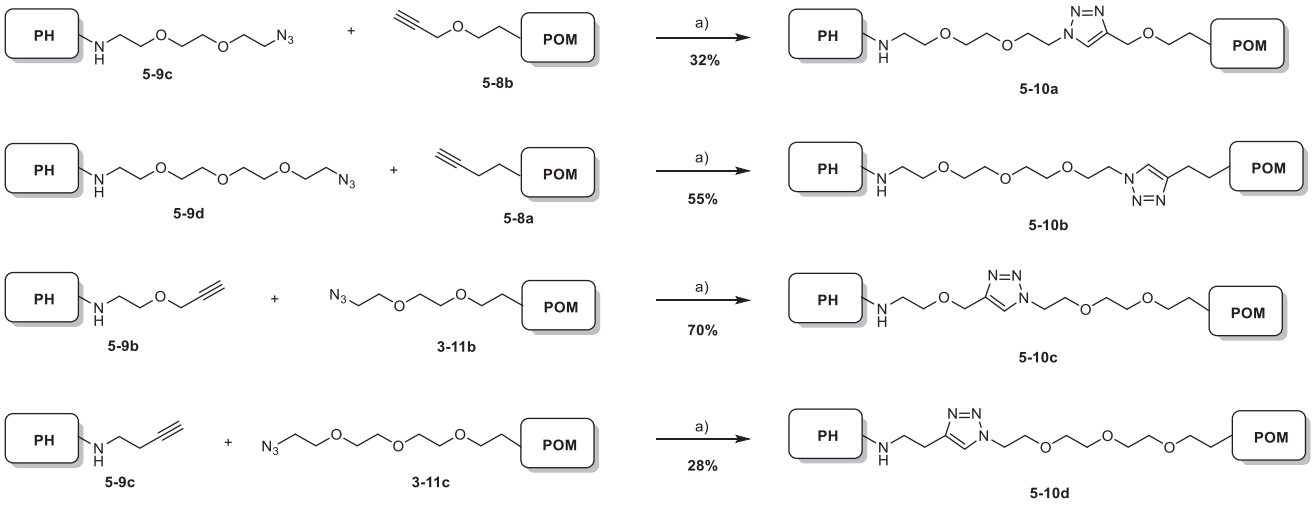

Scheme 5.3: Synthesis of protein degraders **5-10a-d**. Reaction conditions: a) $CuSO_4 \cdot 5H_2O$, Sodium Ascorbate, AcOH, H_2O:*t*-BuOH (2:1), 35 °C, 18 hours.

In addition to the PEG-based linkers, we also devised the introduction of peptidic linkers, hypothesizing they will contribute greatly to the water-solubility of the analogues. Fragment **5-11** was synthesized using solid phase peptide synthesis (SPPS). The amino acid fragment was prepared starting from Fmoc-protected β-alanine, anchored to a 2-chlorotrytyl chloride resin. After addition of two β-alanine units, the free acid fragment **5-7** was coupled to the peptide. After cleavage from the resin, fragment **5-11** was retrieved and subjected to liquid-phase amide formation together with pomalidomide fragment **5-13**. Similarly, **5-16** was prepared by solid phase peptide synthesis starting from Fmoc-protected 2-(2-(2-aminoethoxy)ethoxy)acetic acid. Following addition of a β-alanine unit and SPPS coupling with fragment **5-7**, the compound was cleaved from the resin and coupled with lenalidomide-based fragment **5-15**.

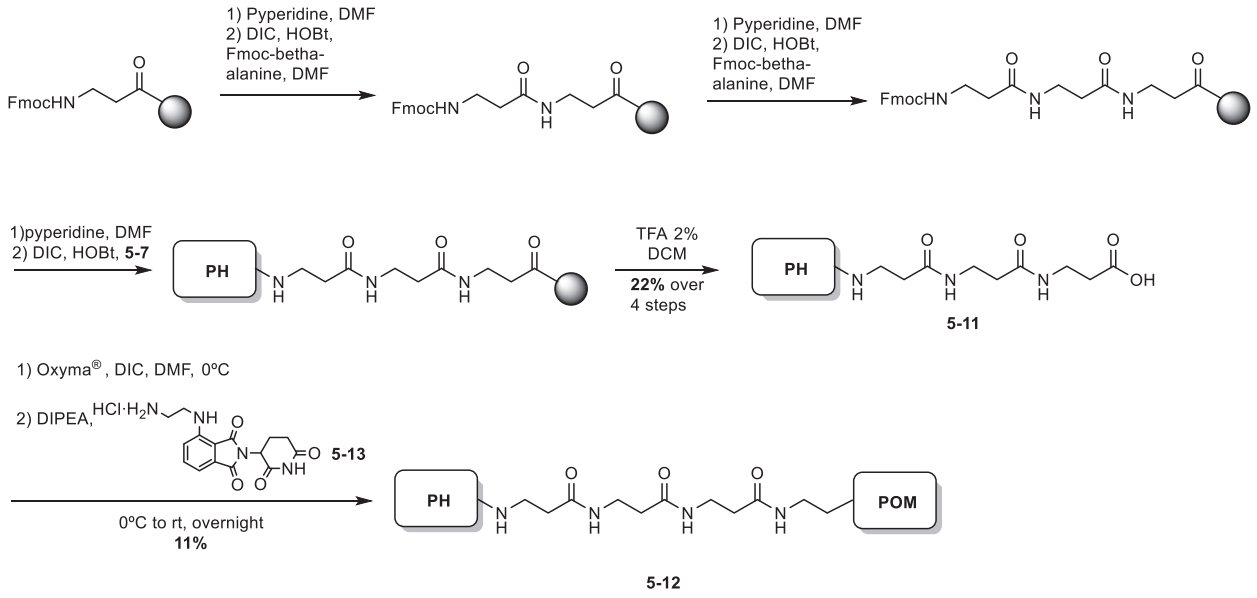

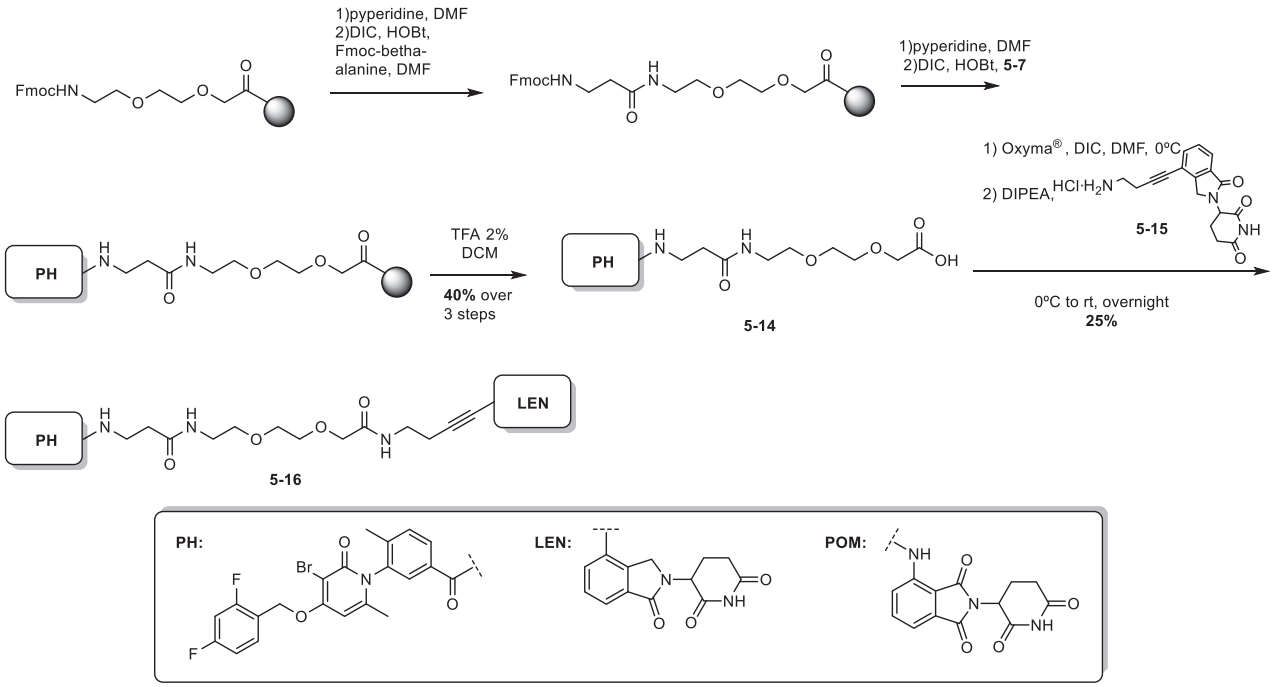

Scheme 5.4. Synthesis of degraders **5-12** and **5-16**.

The ability of PEG-based analogs **5-10a-d** and peptide-based analogs **5-12** and **5-16** to degrade p38 was tested and compared to that of **NR-7h**.[1] Immunoblotting assay showed only modest degradation induced by compounds **5-10a-d**. Compound **5-16** also achieved less degradation than **NR-7h**, while **5-12** displayed no activity. Because **5-16** displays the best potency among the new compounds, its water solubility was tested. The compound was soluble in a 50% weight preparation of cyclodextrin[21] in water, at a concentration of 5 mg/mL. This formulation allowed the administration of the compound *in vivo*. Mice were treated with compound **5-16**, and then p38 levels were analyzed in several tissues by immunoblotting. Unfortunately, degradation was not observed in lung, heart, kidney or liver tissue.

[1] This project is an ongoing collaboration with the Signalling and Cell Cycle laboratory at the IRB Barcelona, led by Prof. A. Nebreda. All the cellular and mice experiments were carried out by Dr. Mónica Cubillos-Rojas.

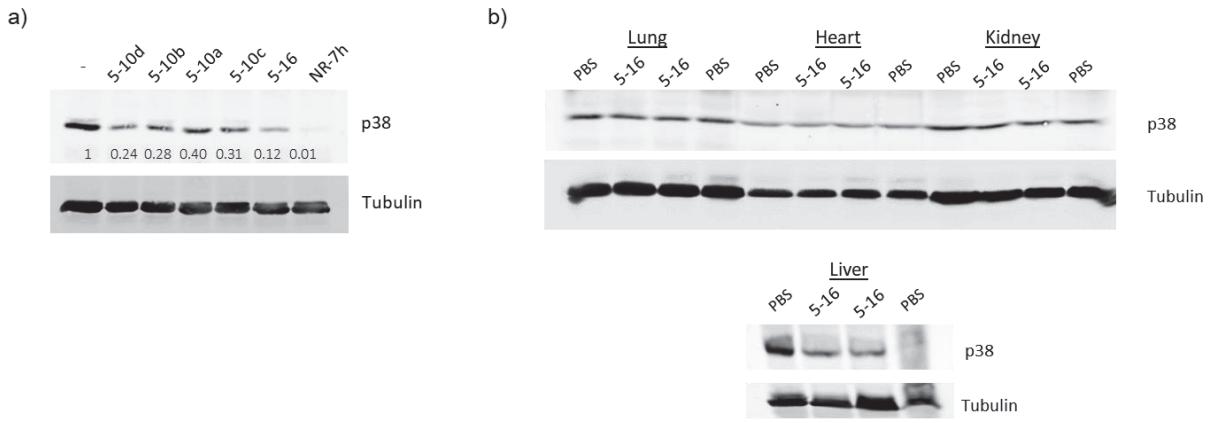

Figure 5.4. **a)** MDA-MB-231 cells were treated with compounds **5-10a-c** and **5-16**, at a concentration of 1 μM for 24 hours, and then cell lysates were analyzed by immunoblotting. **b)** Mice were treated with a single intraperitoneal dose of 15 mg/kg. The tissues were analyzed 18 hours after injection.

5.4. VHL-based p38 PROTACs

All p38 PROTACs developed so far in our laboratory recruited CRBN, the substrate receptor of the $CRL4^{CRBN}$ E3 ubiquitin ligase. Thalidomide derivatives, responsible for the binding to CRBN, exhibit very low water-solubility,[22] probably accounting for the poor solubility of the thalidomide-based PROTACs. The Von Hippel-Lindau E3 ubiquitin ligase is another E3 ligase widely targeted in PROTAC design. VHL is responsible for the recognition of target proteins, including HIF-1α, for proteasomal degradation.[23] The interaction between VHL and HIF-1α is mimicked by a small-molecule ligand, and analogues of this structure have been successfully used in PROTAC design to discover molecules that recruit the VHL E3 ligase to induce degradation of many targets.[24] We hypothesized that PROTACs based on a VHL ligand would exhibit much greater water solubility than those based on thalidomide or derivatives, due to the partial peptidic nature of the ligand's structure. Thus, we designed the synthesis of VHL-based p38 PROTACs.

The VHL ligand was synthesized as described in **chapter 3**. As in our previous work, we decided to prepare VHL fragments based on the terminal amine exit vector, linked a terminal azide. We used VHL-based fragments **3-30b** and **3-32a** and **3-32b**, previously used for the synthesis of ER PROTACs **(chapter 3)**. To be used in a CuAAC, fragment **5-7** was derivatized to the alkyne-bearing warhead **5-17**. The complementary azide and alkyne fragments were subjected to CuAAC conditions, yielding PROTACs **NR-11a-c (Scheme 5.5)**.

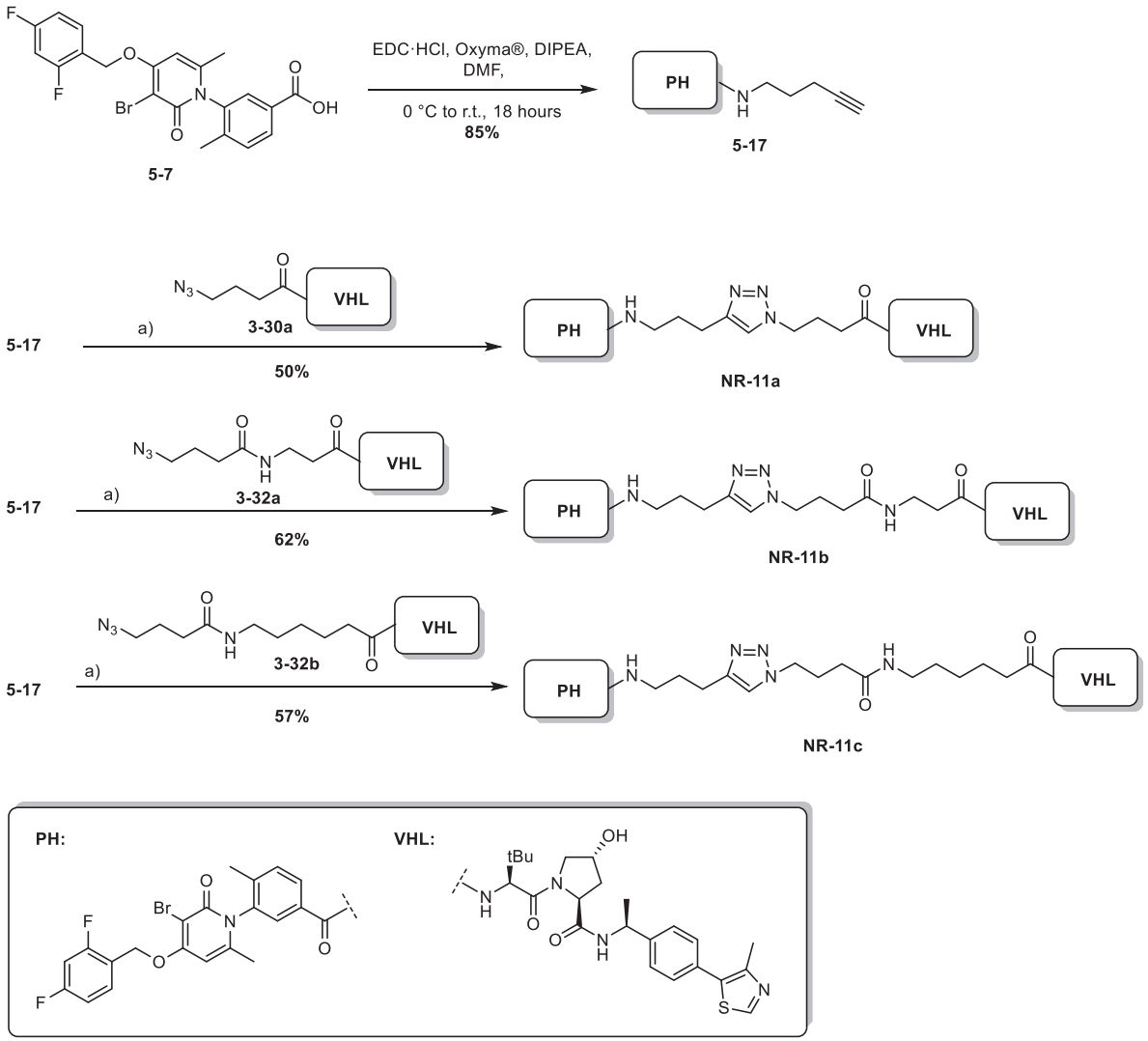

Scheme 5.5. Synthesis of degraders **NR-11a-c**. Reaction conditions: a) $CuSO_4 \cdot 5H_2O$, Sodium Ascorbate, AcOH, H_2O, *t*-BuOH (2:1), 35 °C, 18 hours.

Having degraders **NR-11a-c** in hand, we moved to the evaluation of their biological effect, in collaboration with the Signaling and Cell Cycle laboratory, at the IRB Barcelona. The ability of **NR-11a-c** to degrade p38 was tested a panel of different cell lines (**Figure 5.5a**). Degradation in comparable levels to **NR-7h** was observed in MDA-MB-231 and T47D cells for all three compounds, while in mouse BBL358 cells only **NR-11c** achieved comparable degradation. Based on these results, **NR-11c** was selected for further characterization. Osteosarcoma cell lines U2OS, MG63 and SAOS-2 were selected for further testing. Our previous work showed that **NR-7h** had a poor ability to induce p38α degradation in these cell lines,[16] however, **NR-11c** showed good activity (**Figure 5.5b**).

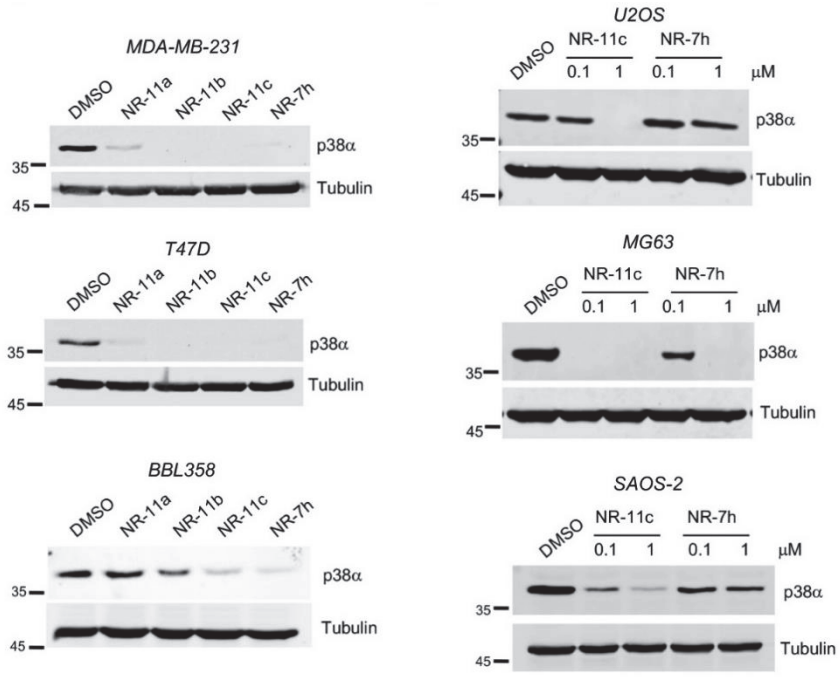

Figure 5.5. **a)** Breast cancer cell lines were incubated with **NR-11a-c** at 1 μM, and 24 h later p38α levels were analyzed in cells lysates by immunoblotting. **b)** Osteosarcoma cell lines were incubated with **NR-11c** and **NR-7h** at 1 or 0.1 μM for 24 h and p38α levels were analyzed in cells lysates by immunoblotting.

The concentration of **NR-11c** required to induce half-maximal degradation (DC_{50}) of p38α in MDA-MB-231 cells was estimated at 11.55 nM (**Figure 5.6a**). Consistent with the "hook effect" reported in bifunctional molecules, we observed a small decreased efficiency of degradation at 10 μM. The treatment time required to induce p38α degradation was analyzed, finding that total degradation was achieved in just 2-4 hours after the addition of **NR-11c** at 1μM (**Figure 5.6b**). The long-term effect of **NR-11c** was also maintained for 72 hours after treatment of the cells with the compound (**Figure 5.6c**). Interestingly, we observed significant degradation of p38α when cells were treated with **NR-11c** for 24 hours and then maintained up to 48 hours after removal of the compound from the media.

To characterize the mechanism of **NR-11c**-induced degradation of p38α, cells were pre-treated with the proteasome inhibitor MG132 or with the NEDD8-Activating Enzyme inhibitor (NAEi), a compound that prevents activation of cullin-RING ubiquitin ligases (**Figure 5.6d**). Degradation of p38α was impaired with both compounds, indicating that **NR-11c** induces p38α degradation by the proteasome pathway in an ubiquitin ligase dependent manner. We also synthesized the inactive isomer **NR-11c***, which is impaired in its ability to engage the E3 ligase. **NR-11c*** did not induce p38α degradation, proving that engagement with the E3 ubiquitin ligase is necessary to induce degradation. (**Figure 5.6d**). The specificity of **NR-11c** was investigated in MDA-MB-231 cells (**Figure 5.6e**), and degradation of the four p38 MAPK family members was analyzed by Western blotting after 24 hours of PROTAC treatment. Interestingly, **NR-11c** specifically degraded p38α, a selectivity not observed for **NR-7h**. Other MAPKs, namely JNK and ERK1/2, were not degraded by **NR-11c**.

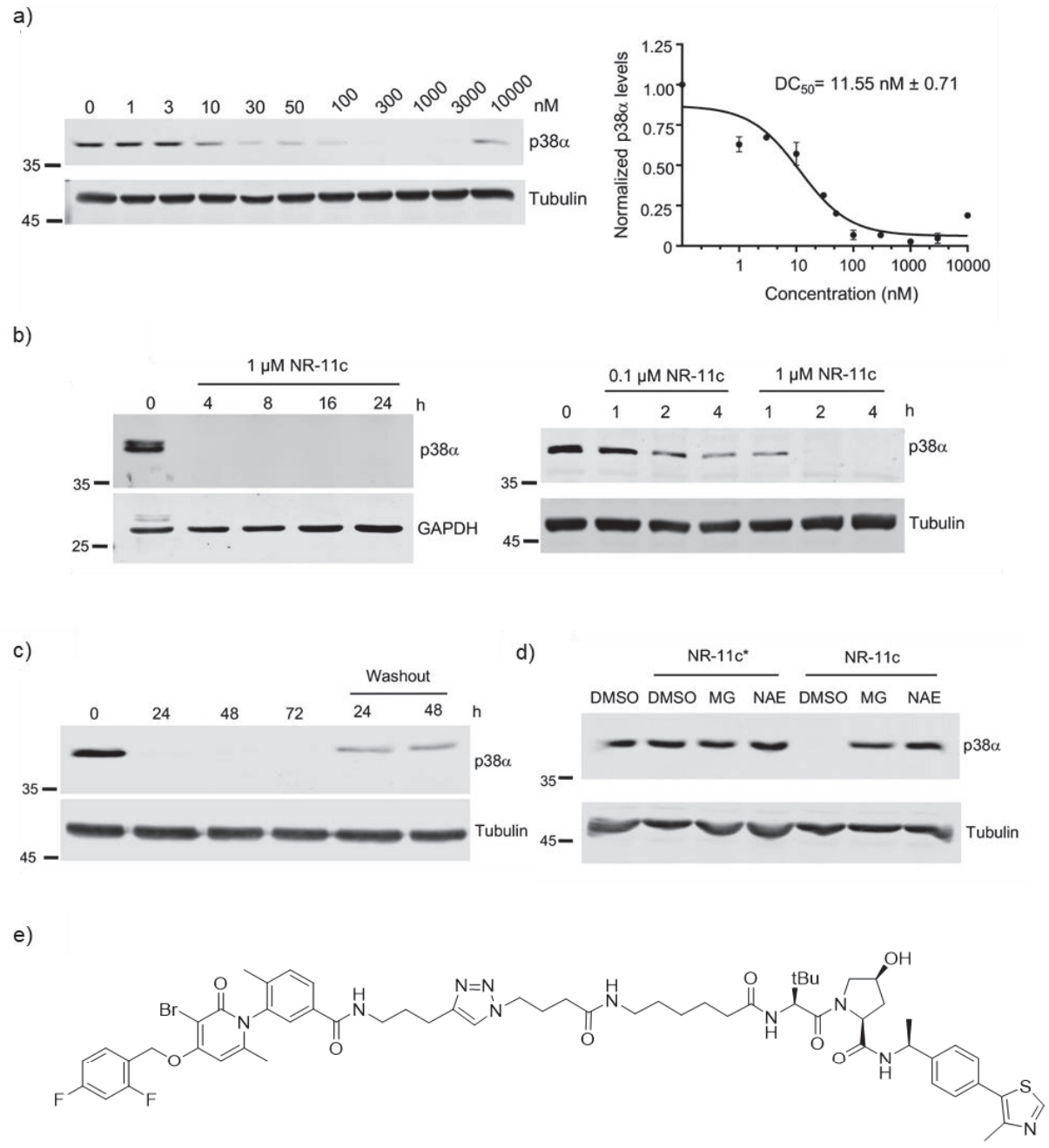
a)
0 1 3 10 30 50 100 300 1000 3000 10000 nM
p38α
Tubulin
35
45
Normalized p38α levels
DC50= 11.55 nM ± 0.71
Concentration (nM)
b)
1 μM NR-11c
0 4 8 16 24 h
p38α
GAPDH
0.1 μM NR-11c
1 μM NR-11c
0 1 2 4 1 2 4 h
Tubulin
c)
Washout
0 24 48 72 24 48 h
d)
NR-11c*
NR-11c
DMSO DMSO MG NAE DMSO MG NAE
e)
Br
F
tBu
OH
S

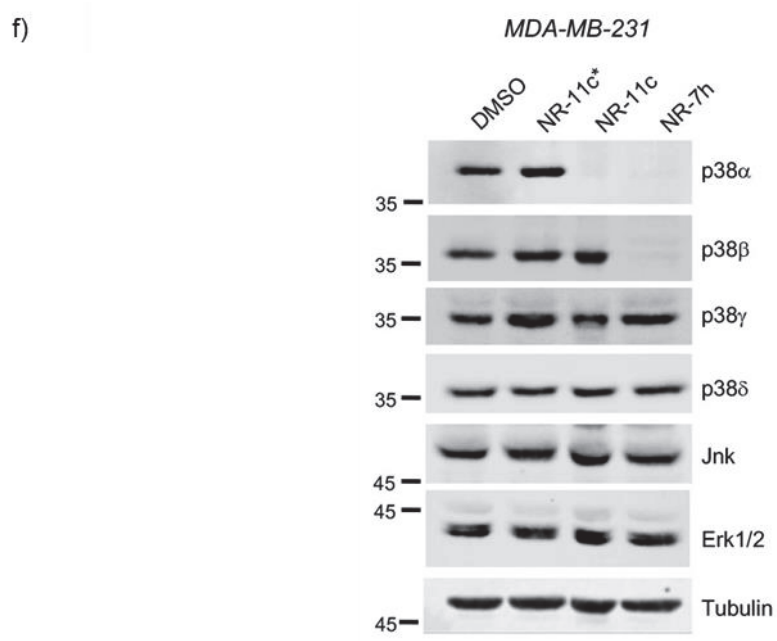

Figure 5.6. a) MDA-MB-231 cells treated with the indicated concentrations of **NR-11c** for 24 h, and then cell lysates were analyzed by immunoblotting. DC_{50} values for p38α degradation were determined based on the quantification of the p38α band. **b)** MDA-MB-231 cells were treated with **NR-11c** at 1 or 0.1 μM for the indicated times and p38α levels were evaluated by immunoblotting. **c)** MDA-MB-231 cells were cultured with **NR-11c** at 1 μM for the indicated times, or after 24 hours the compound was removed and cells were maintained for another 24 or 48 h without compound (washout). Cells lysates were analyzed by immunoblotting. **d) NR-11c** induces degradation of p38α in a proteasome-dependent manner. MDA-MB-231 cells were pre-treated with the proteasome inhibitor MG132 at 20 μM or the NAE inhibitor at 1 μM for 1 h prior to incubation with either NR-11c or the inactive compound NR-11c* at 1 μM for 8 hours. Cells were collected and p38α levels were analyzed by immunoblotting. **e)** Structure of the inactive isomer NR-11c*, displaying inverted stereochemistry at the hydroxyproline alcohol. **f)** NR-11c specifically induces p38α degradation. A. MDA-MB-231 cells were treated with **NR-11c** at 1 μM for 24 hours and cell lysates were then analyzed by immunoblotting using the indicated antibodies.

The solubility of **NR-11c** was tested in a PBS solution containing cyclodextrin, a carbohydrate widely used for enhancing aqueous solubility of drugs.[21] The degrader was soluble, at least, at a concentration of 7 mg/mL, which was enough to conduct in vivo studies. **NR-11** was administered to mice either through tail vein injection or intraperitoneal, and 24 hours later assessed p38α protein levels in different tissues. We found that p38α protein levels were clearly downregulated in the liver from mice treated with **NR-11c** but did not change in lung, kidney or spleen taken from the same mice (**Figure 5.7a**). The effect of **NR-11c** was also evaluated in the context of a tumor (**Figure 5.7b**). Local administration (intratumoral and peritumoral) produced also downregulation of p38α levels in tumors implanted to mice.

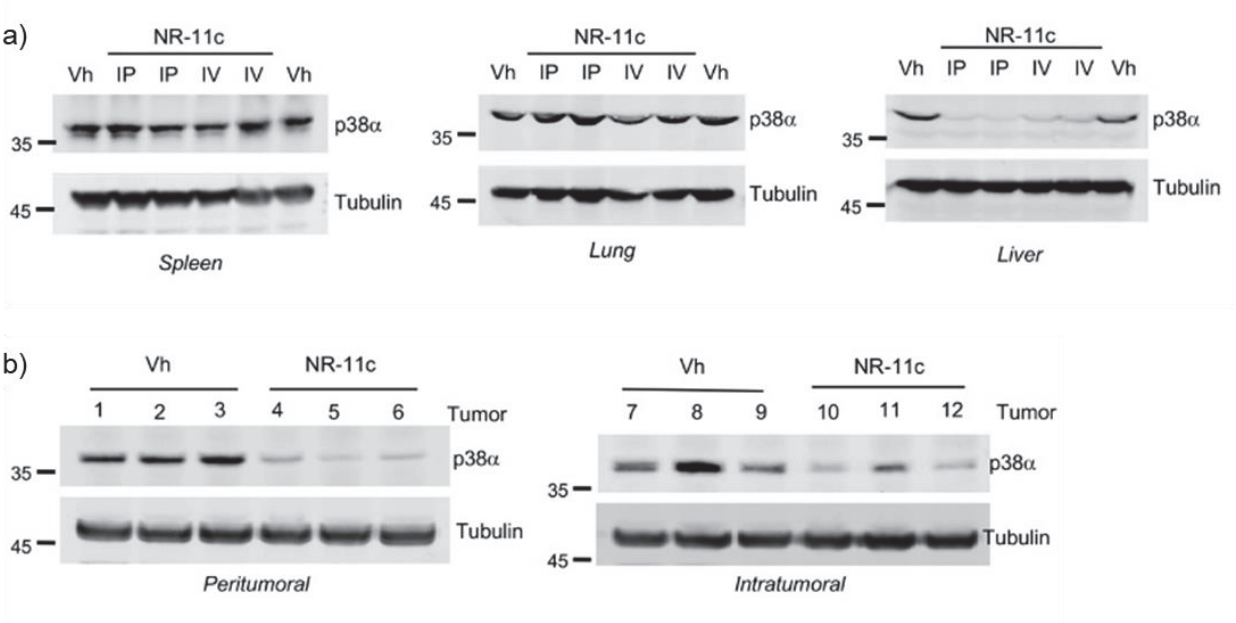

Figure 5.7. Effect of **NR-11c** in mice. **a)** C57BL/6J mice were administered intraperitoneal (IP) or intravenously (IV) with **NR-11c** at 15 mg/kg dissolved in PBS with 50% cyclodextrin or with vehicle (Vh). Mice treated via IP received two doses in 24 hours, while mice treated via IV received only one dose. After 24 hours, the indicated tissues were obtained and p38α protein levels were analyzed by immunoblotting. Tubulin was used as a loading control. **b)** MDA-MB-231 cells implanted in the mammary fat pad of SCID/NOD mice and allowed to grow up to 100-150 mm3 (4-5 weeks). **NR-11c** or Vh were administered via the indicated routes. After 24 hours, mammary tumors were collected and p38α protein levels were analyzed by immunoblotting.

5.5. SAR study on NR-11c analogues

Systemic administration of **NR-11c** to mice resulted in p38α downregulation in the liver, without showing substantial change in lung, kidney or spleen. It has been reported that the linker's chemical composition and length are major determinants of the PROTAC's pharmacokinetic properties and metabolic stability.[25] We hypothesised that it might also be influencing the distribution profile of the degrader, and play a role in the retention of the compound in liver tissue. We conducted a structure-activity relationship (SAR) study on the linker, to determine how linker composition might be affecting the degrader's activity and *in vivo* distribution.

Studies have shown that PROTAC activity can be improved when the linker is rigidified by the addition of groups with restricted rotation such as piperazines, piperidines or alkynes.[26] While designing the SAR study on the linker, we attempted to introduce rigidity at different positions and determine how it affects activity.

5.5.1. Synthesis of analogues with piperidine and piperazaine rings (NR-12a-e and NR14a-f)

We first decided to prepare analogues substituting the amide placed at the linker (between the imidazole and the VHL ligand) for a piperazine. Azide **5-21,** connected to the VHL ligand through a piperazine fragment, was prepared as shown in **scheme 5.6**. Boc-piperazine was alkylated using dibromopropane, followed by substitution using sodium azide to afford fragment **5-19**. The azide intermediate was functionalized using bromo methyl butanoate. After ester hydrolysis and amide formation with the VHL ligand (**3-29**), fragment **5-21** was obtained. This azide was coupled with the previously described alkyne **5-17** to give analogue **NR-12a**.

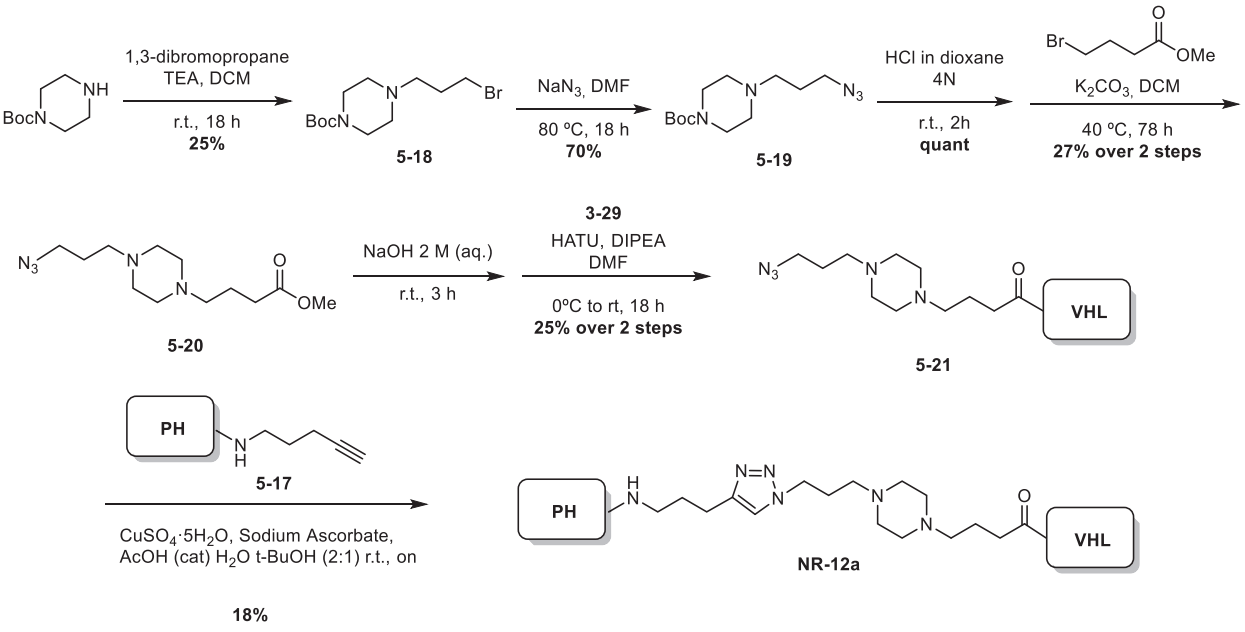

Scheme 5.6. Synthesis of fragments **5-22** and **5-26**.

Then we decided to replace the amide connecting the p38-targeting warhead to the linker for a piperazine ring, via a piperazine amide. We synthesized the key intermediate **5-23** by reaction of fragment **5-7** with boc-piperazine and subsequent boc deprotection, and used the fragment as a platform to design different analogues (**Scheme 5.7**). Our strategy was to test different reactivities at the piperazine nitrogen in order to expand the linker, while also maintaining the linker length close to the one of **NR-11c**.

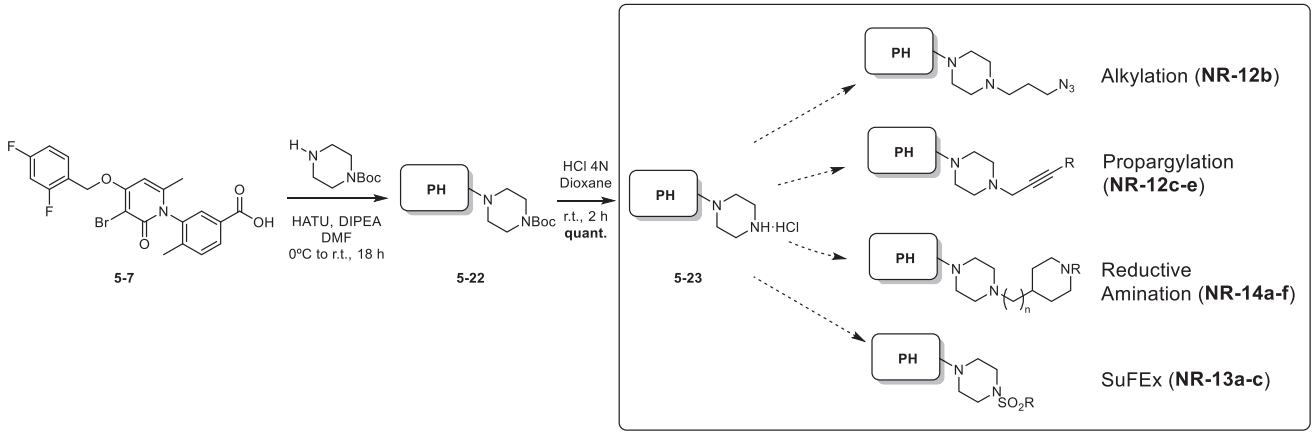

Scheme 5.7. Synthesis of **5-23** and possible derivatization routes.

Direct alkylation of **5-23** was attempted using electrophilic fragments derived from boc-hydroxyaziridine, iodo boc-aziridine and iodo boc-piperidine. Alkylation, however, did not take place or did so in marginal yields. To overcome the problems of the direct alkylation we turned to alkylation of the piperazine fragment before attachment to **5-7**. Previously described piperazine **5-19** was coupled to **5-7** to yield azide **5-25**. A complementary alkyne fragment was prepared by reductive amination, using aldehyde **5-32a**, available in our laboratory, and the VHL ligand (**3-29)**. CuAAC between the two compounds afforded **NR-12b**.

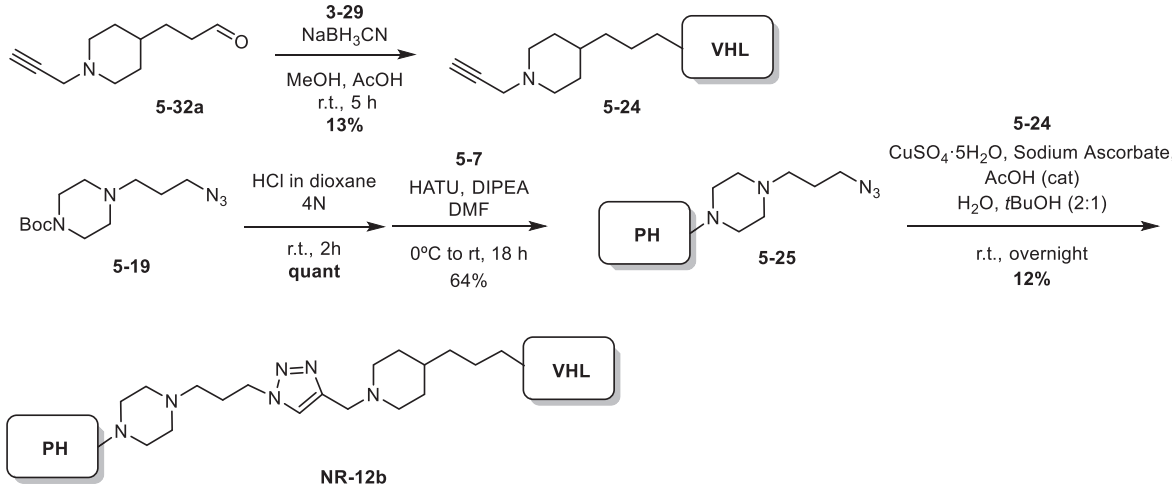

Scheme 5.8. Synthesis of **NR-12b**.

Next, we planned to introduce a terminal alkyne through alkylation of the piperazine fragment, taking advantage of the high electrophilicity of propargyl bromide. Boc-protected piperazine was directly alkylated with propargyl bromide, followed by deprotection and amide formation with **5-7**

(**Scheme 5.7**). This sequence afforded fragment **5-27**, connecting the linker to the PH fragment via a piperazine linkage and bearing a terminal alkyne.

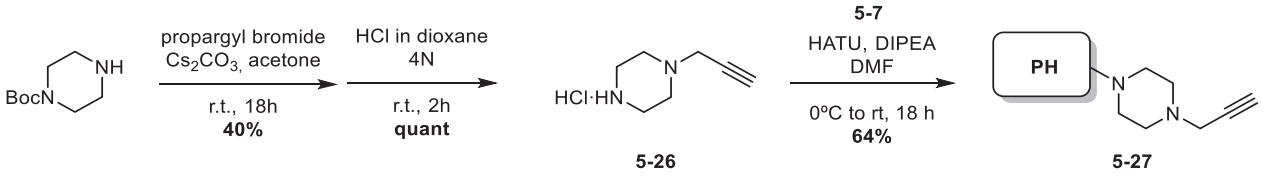

Scheme 5.9. Synthesis of fragments **5-22**.

Taking advantage of this modular approach to the synthesis of PROTACs, we used the previously described VHL-based fragments **3-32b** and **5-26** to couple via CuAAC to fragment **5-27**, yielding **NR-12c** and **NR-12d** (**Scheme 5.10**).

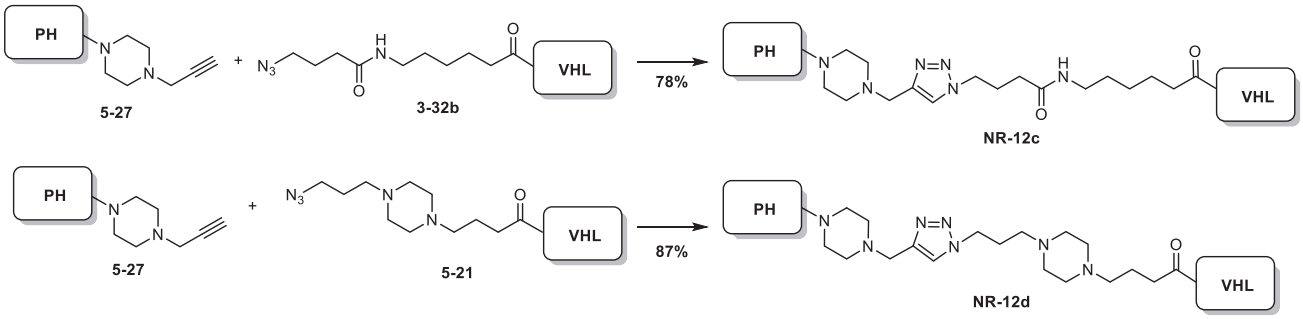

Scheme 5.10. Synthesis of degraders **NR-12a-c**. Reaction conditions: $CuSO_4 \cdot 5H_2O$, Sodium Ascorbate, AcOH (cat) H2O *t*-BuOH (2:1) r.t., overnight.

In order to improve the yields of the piperazine alkylation strategy, we explored their reactivity with butynediol derivatives. But-2-yne-1,4-diol was converted into the mono-tosylate and substituted to fragment **5-23.** The terminal alcohol was again tosylated, followed by substitution with 1-(piperazin-1-yl)pent-4-yn-1-one. Click partner **5-29** was subjected to CuAAC conditions with VHL-ligand derivative **4-16**, affording **NR-12e**.

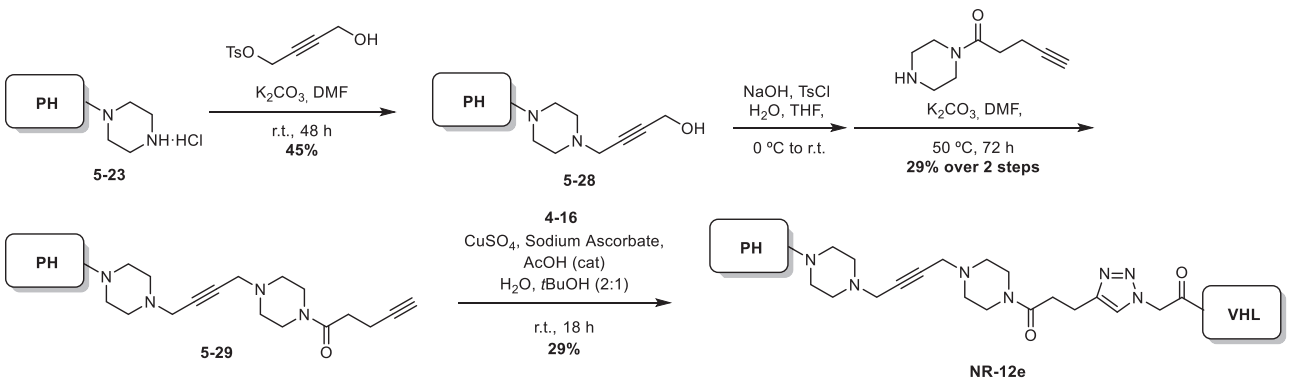

Scheme 5.11. Synthesis of degrader **NR-12e**.

We continued exploring other methods for the alkylation of piperazine fragment **5-23**. We envisaged the preparation of bifunctional piperidine derivatives, bearing a terminal alkyne at one side and an alcohol at the other. Oxidation of the alcohol to aldehyde would allow the alkylation with **5-23** by reductive amination, while the alkyne could be attached to a VHL-ligand fragment bearing a terminal azide.

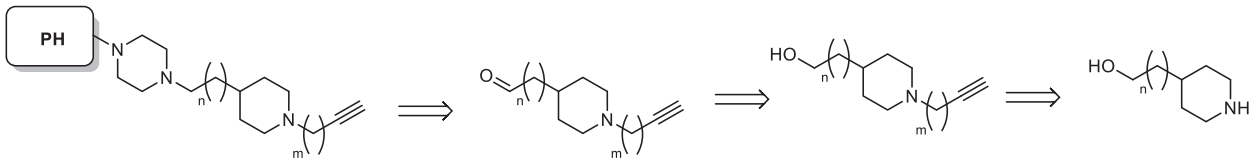

Scheme 5.12: Retrosynthetic analysis of PH-based fragments based on reductive amination linkers.

Three commercially available piperidine-alcohol derivatives were alkylated using propargyl bromide. Alcohols **5-31a-c** were subjected to Swern oxidation conditions, affording the corresponding aldehydes in good yields. Aldehydes **5-32a-c** were then reacted with fragment **5-23** to afford reductive amination adducts **5-33a-c**. The terminal alkynes were then subjected to CuAAC conditions with VHL-ligand azide derivatives of different linker lengths, aiming at a final length similar to that of **NR-11c** but allowing a slight length variation.

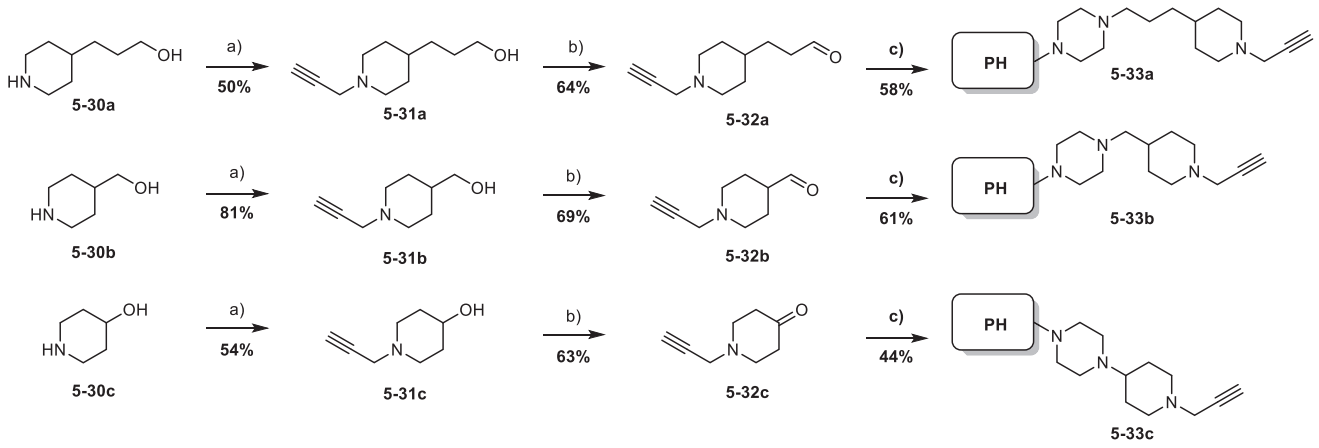

Scheme 5.13. Coupling of the alkyne fragment to PH by reductive amination. Reaction conditions: a) Propargyl bromide, Cs_2CO_3, Acetone, r.t., 18 h; b) Oxalyl chloride, DMSO, DCM, -78 °C then TEA -78 °C to r.t., 18 h; c) **5-23**, $NaBH_3CN$, MeOH, AcOH, 0 °C to r.t., 18 h.

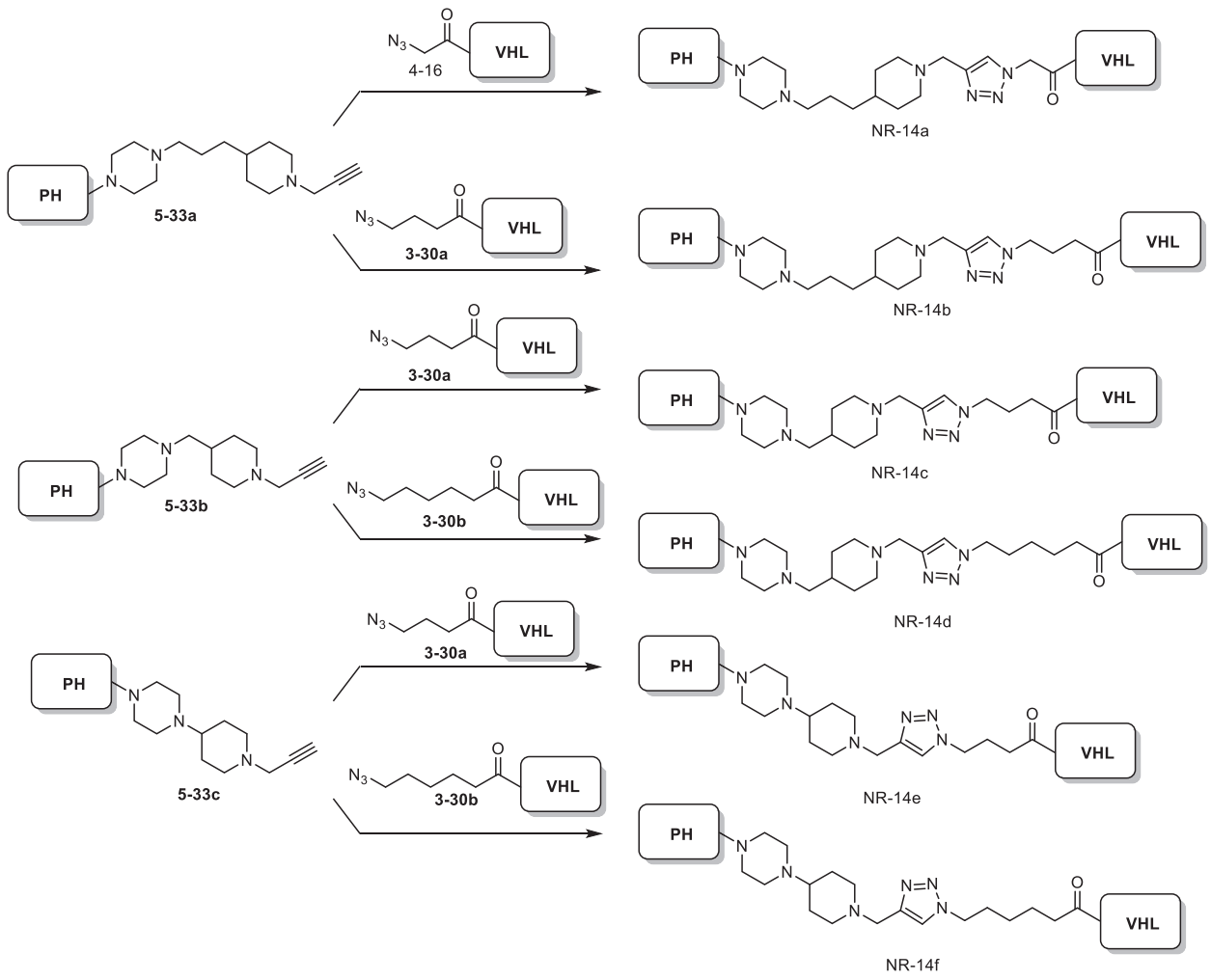

Scheme 5.14. Synthesis of degraders **NR-14a-f**. Reaction conditions: $CuSO_4{\cdot}5H_2O$, Sodium Ascorbate, AcOH (cat) H_2O/*t*-BuOH (2:1) r.t., overnight.

Purification of **NR-14b** was performed in silica flash column chromatography. Attempts to purify **NR-14a**, however, ran into technical complications, due to the need of equilibrating the silica with trimethylamine and the recovery of trimethylamine salts with the product. Together with the very low-scale conditions in which these reactions were run, it posed difficulties in isolating the final products. The rest of the **NR-14** series were simply delivered for cellular testing after reaction work-up, with the idea of doing a preliminary testing of the compounds activity, and potentially resynthesize the active compounds in the future. HPLC-MS analysis was performed on the crudes to assess purity, showing excellent purity (<95%) for **NR-14d** and **NR-14e** and moderate (60-75%) for **NR-14a**, **NR-14e** and **NR-14f**.

5.5.2. Synthesis of analogues with a 1,1'-sulfonyldipiperazine fragment (NR-13a-c and NR-15)

Through this work, most of the syntheses of PROTACs have relied on a late-stage coupling of an azide and an alkyne intermediate via a copper-catalyzed alkyne azide cycloaddition (CuAAC). This strategy has proved useful in delivering final products in good yields that would have been otherwise much harder to prepare. In order to diversify our synthetic tools, we attempted the introduction of another “click” type reaction, to be used in the same fashion as the CuAAC strategy.

The catalytic sulphur(VI) fluoride exchange (SuFEx) is a “click” reaction developed by Sharpless and co-workers in 2014. Classical SuFEx involved substituting a stable S-F bond with aryl silyl ethers to give the corresponding S-O linkage.[27] The scope of the reaction was later expanded with amines,[28][29] organometallic reagents,[30] and other carbon nucleophiles.[31] SuFEx reactions meet the criteria to be considered a “click” reaction, being wide in scope, modular, and able to create function by linking simple building blocks.[32] They also present advantages over the CuAAC; a SuFEx coupling is metal-free, which confers it more significance in the biological application and drug discovery fields. It also allows a greater diversity of connections; the CuAAC requires the express installation of an azide and an alkyne on both building blocks, while SuFEx can link together a variety of functional groups very common to organic chemistry scaffolds.

It is interesting to think of the SuFEx as “molecular plugin”, that allows the connection of two different functionalities. A number of SuFEx connectors have already been developed, including sulfonyl fluoride ($ArSO_2F$), sulfuryl fluoride (SO_2F_2) and surrogates, thionyl tetrafluoride (SOF_4), ethane sulfonyl fluoride (ESF) and 1-Bromoethene-1-sulfonyl fluoride (BESF).[33] Once installed to the coupling partner, all hubs allow the substitution of the stable S-F bond for the preferred nucleophile group under the right activation conditions. The connective hubs differ in the installation method to the “click partner”. While sulfonyl fluorides have to be constructed using traditional synthetic methods, usually by halogen exchange of a sulfonyl chloride, sulfonyl and sulfuryl fluorides allow the substitution on an amine. Ethane sulfonyl fluoride function as a Michael acceptor, while BESF also allow reactivity on the side-chain, orthogonal to the S-F substitution.

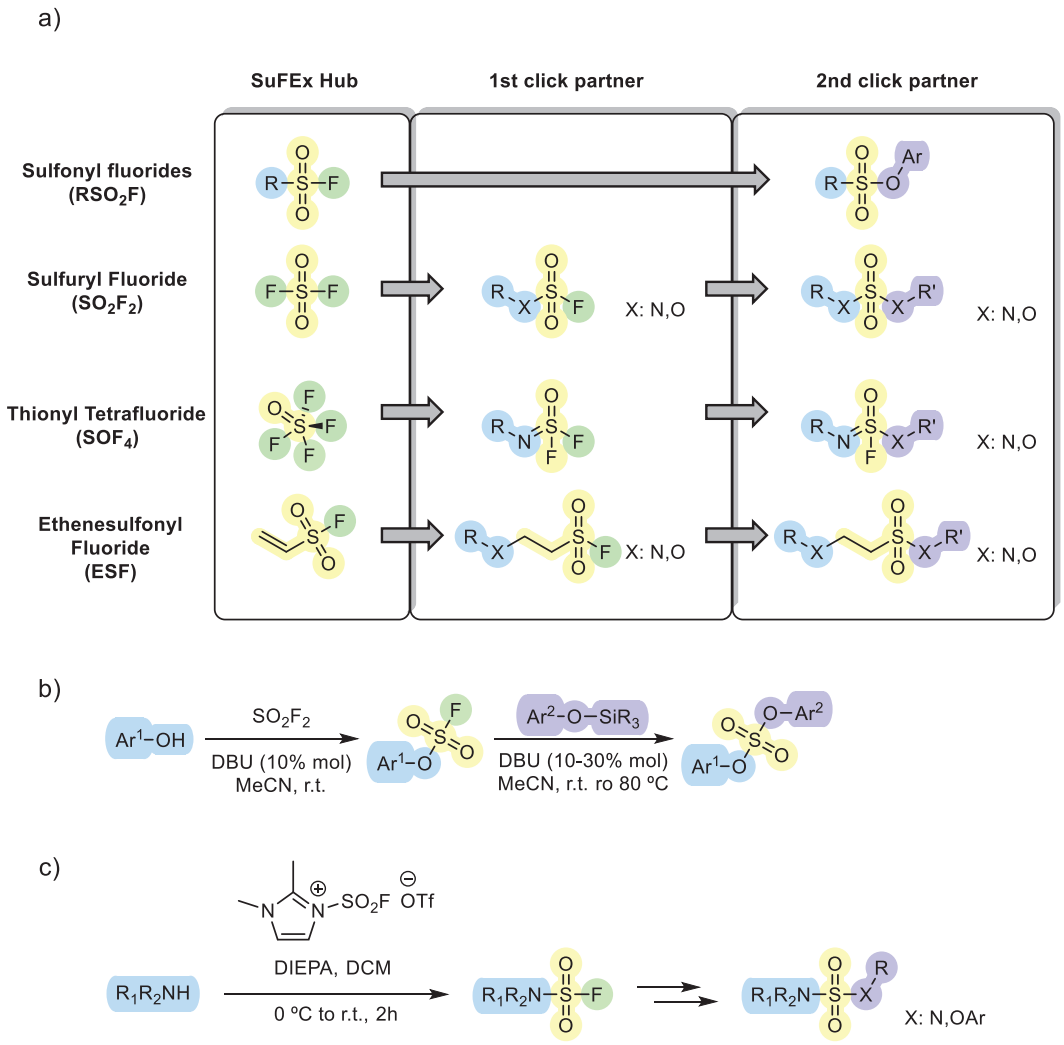

Figure 5.15. SuFEx reactivity. a) Schematic representation of the main sulphur(VI) hubs. **b)** Classical SuFEx chemistry, involving the substitution of a stable S-F bond with aryl silyl ethers. **c)** Reaction of an amine with fluorosulfuryl imidazolium salts, forming a sulfamoyl fluoride.

Sulfuryl fluoride was originally used for the installation of a sulphur(VI) center. Its "plugin" potential was demonstrated by the synthesis of fluorosulfates (RO-SO_2F), which could react efficiently with silyl ethers in the presence of catalytic DBU, forming stable sulphate linked products (**Figure 5.15b**). SO_2F_2 can also be reacted to secondary amines, giving the corresponding sulfamoyl fluorides, that can be further substituted with amines. Recently, fluorosulfuryl imidazolium salts have emerged as a bench stable alternative to sulfuryl fluoride (**Figure 5.15c**). The imidazolium salt displays enhanced reactivity over sulfuryl fluoride; having shorter reaction times for the fluorosulfonylation of phenols and allowing the reaction with primary amines, which were unreactive towards SO_2F_2. Because of the versatility of this sulphur(VI) hub and the commercial availability of fluorosulfuryl imidazolium salts, we decided to employ it in the synthesis of p38 degraders.

The reactivity of fragment **5-23** towards SuFEx was assessed by reaction with the commercial imidazolium salt **5-34** affording sulfamoyl fluoride **5-35**. Reaction with boc-protected piperazine

then did not proceed at room temperature. It has been reported that the synthesis of sulfamides from the corresponding sulfamoyl derivatives requires the addition of a calcium catalyst.[28] We reacted **5-35** and boc-piperazine in the presence of $Ca(NTf_2)_2$ and DABCO, together with gentle heating. After finding the right reaction conditions, we proceeded to derivatize intermediate **5-35** with different piperazine-alkyne fragments, which were later subjected to CuAAC reaction conditions with VHL ligand fragments bearing a terminal azide. Previously synthesized fragments **3-30a, 3-30b** and **4-16** were used, keeping the spacing between the VHL ligand and the terminal azide consistent with the linker length of **NR-11c**.

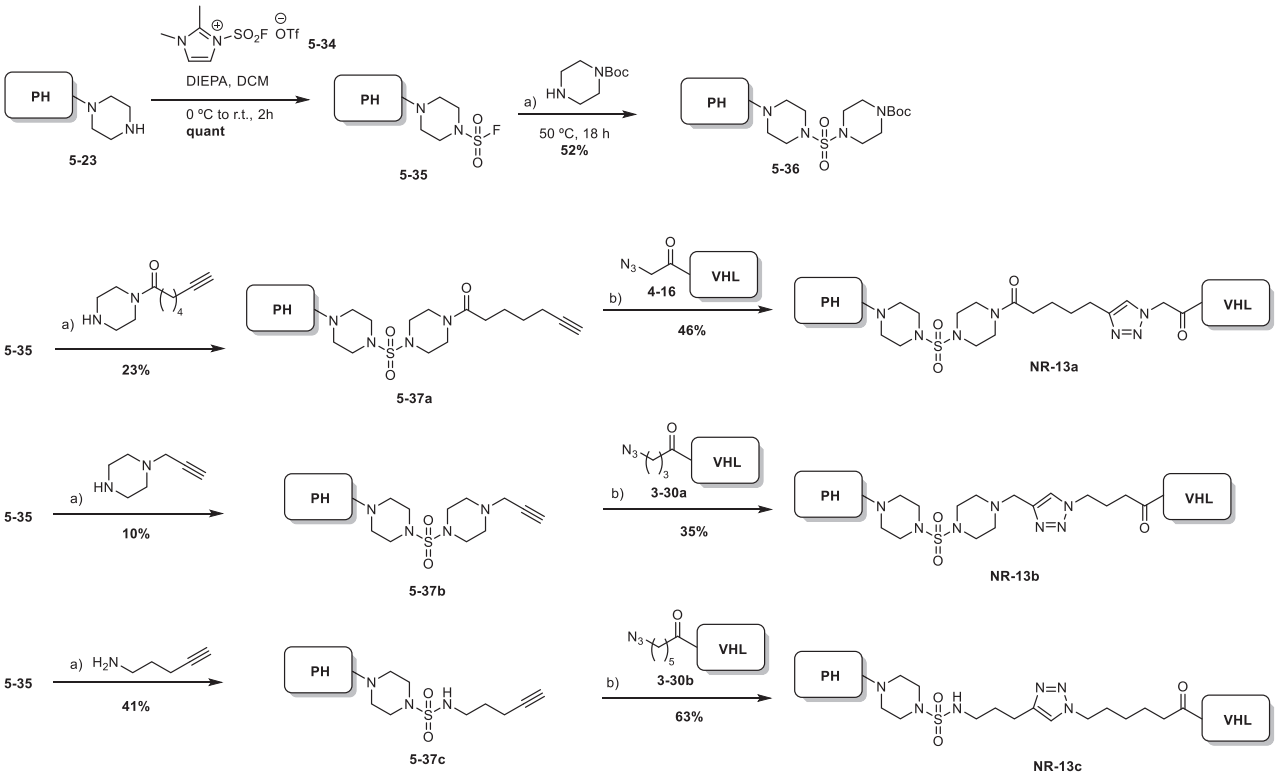

Scheme 5.16. Synthesis of SuFEx adduct **5-35** and synthesis of degraders **NR-13a-c**. Reaction conditions: a) DABCO, $Ca(NTf_2)_2$, THF, 50 °C, 18 h., b) $CuSO_4 \cdot 5H_2O$, Sodium Ascorbate, AcOH (cat.). H_2O *t*-BuOH (2:1) r.t., overnight.

We also sought to interrogate weather the SuFEx coupling could be used as a substitute for the CuAAC. In order to do so, we designed degrader **NR-15** bearing a sulfamide at the middle of the linker. We prepared two fragments to perform the SuFEx, one based on the PH-piperazine warhead and the other on the VHL ligand, both bearing a terminal amine.

The VHL-ligand fragment was prepared from boc-protected piperidine-4-carboxylic acid and **3-29**, followed by conversion into the sulfamoyl fluoride. The click partner **5-41** was prepared by reductive amination with aldehyde **5-40**; which was obtained in two steps from commercial piperidine

derivative **5-30a**. The two piperidine fragments were subjected to SuFEx conditions. After purification of the crude by silica flash column chromatography, the desired product was recovered in a very low yield. Under the described conditions conversion was very low, and most of the starting material was recovered after purification. Although the reaction conditions were not optimized, the amount of **NR-15** obtained was enough to be used in the biological testing of the compound.

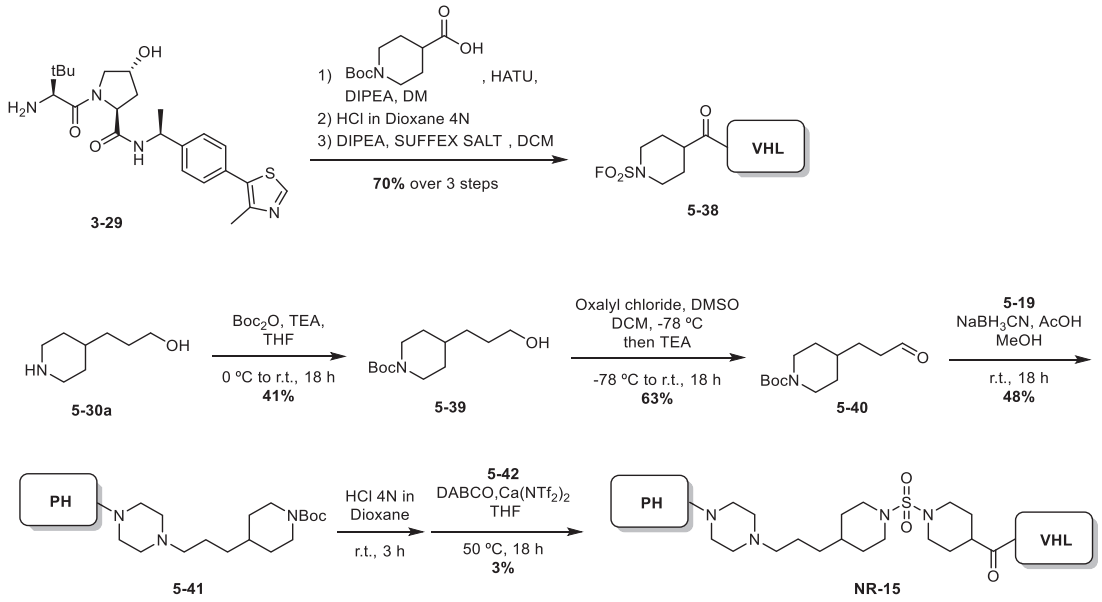

Scheme 5.17. Synthesis of **NR-15**.

5.5.3. Biological Evaluation of the SAR Analogues and Discussion

The ability of the 16 analogues of **NR-11c** to degrade p38α was tested in MB-MDA-231 cancer cells (**Figure 5.9**). **NR-11c** was tested under the same conditions for comparison. Only two analogues, **NR-13c** and **NR-15** achieve comparable degradation levels to **NR-11c**. Compounds **NR-12a,b,d**, **NR-13a,b**, **NR-14b** and **NR-14d** were able to promote substantial degradation of p38α, while the rest of compounds do not show any effect on p38α levels.

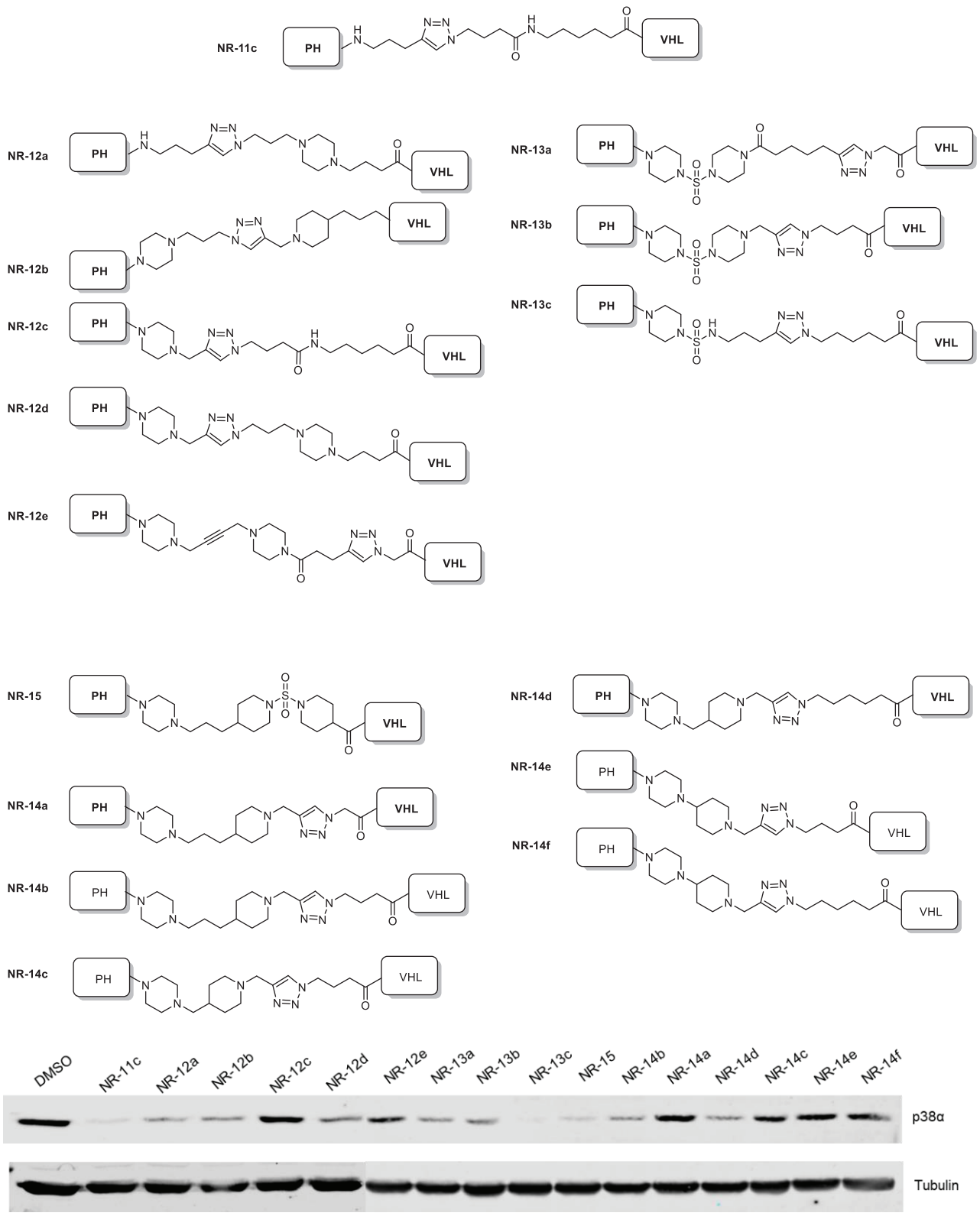

Figure 5.18. Simplified structures of **NR-11c** analogues and induced degradation of p38 by **NR-11c** analogues. MDA-MB-231 cells treated with **NR12-a-d**, **NR-13a-c**, **NR-14a-f** or **NR-15** at a concentration of 1 μM for 24 h, and then cell lysates were analyzed by immunoblotting.

Compounds **NR-12a-d** are structurally similar to **NR-11c**, the linker modifications of these analogues consist of the introduction of piperidine or piperazine moieties at different points of the linker. Substitution of the linker amide for a heterocycle leads to reduced activity in compounds **NR-12a**, **NR-12b**and **NR-12d**. Similarly, the piperazine linkage to the p38-targeting warhead does not seem to provide an increase in activity. The introduction of rigidity through a propargyl di-piperazine system is not well tolerated, resulting in loss of activity in **NR-12e**.

Compounds **NR-13a** and **NR-13b** have a sulfamide linkage of two piperazines close to the PH warhead, and differ slightly in total linker length. While the preparation of these compounds was interesting from the synthetic point of view, as it incorporates the use of SuFEx chemistry, both compounds show reduced activity, similar to that of **NR-12a**. Compound **NR-13c**, however, displays excellent p38 degradation. This analogue features a sulfamide linkage between a primary amine and a piperazine. We hypothesize that by allowing more flexibility than **NR-13a** and **NR-13b**, the linker is able to fold in a more favourable way, improving degradation potency.

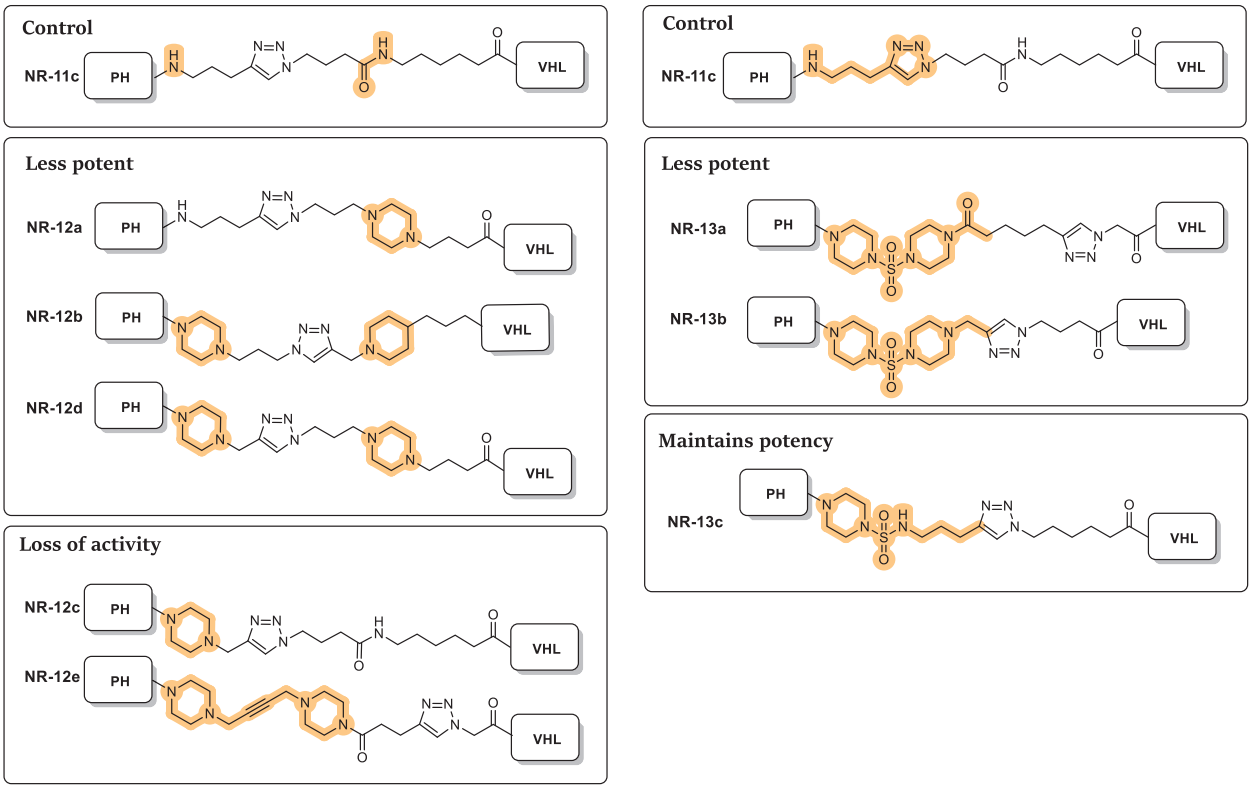

Figure 5.10. Linker SAR, alkylation analogues.

Reductive amination-based linkers proved to be less active than **NR-11c**. **NR-14e** and **NR-14f** show no activity, consistent with the observation that some flexibility is needed at the PH-end of the linker to achieve activity. **NR-14a** and **NR-14c** do not show substantial degradation of p38 either, however

they counterparts **NR-14b** and **NR-14d**, featuring more spacing at the VHL-end of the linker, recover some potency. **NR-15** shows good p38 degradation. This compound shares with **NR-13c** a motif of PH-piperazine attachment followed by a flexible fragment. As this piperazine-propyl-piperidine fragment of **NR-15** is shared by **NR-14b** and **NR-14a**, the improved activity of **NR-15** can be attributed to the rigid sulfamide fragment. **NR-15** shows that introducing rigidity in the linker, spaced by fragments that permit some flexibility and rotation, favours activity. Although we find this trend interesting, structural studies are needed to understand why **NR-15** has better activity than the **NR-14** series, and what are the exact linker conformations and interactions with protein surface that lead to an improved activity.

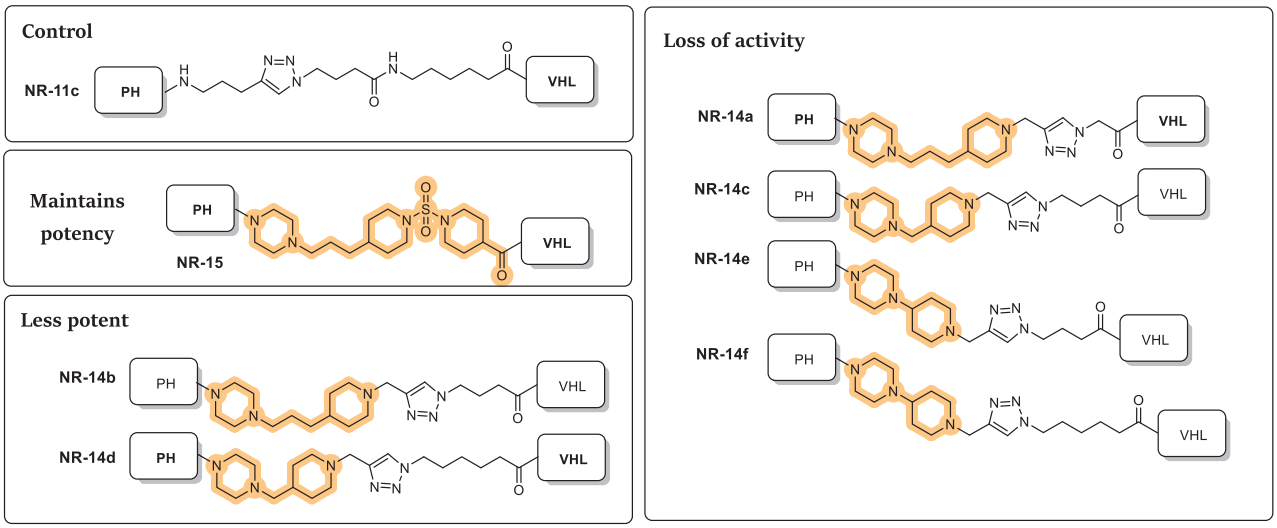

Figure 5.19. Linker SAR, alkylation analogues.

5.6. p38 PROTACs: Conclusions

This chapter shows the synthetic efforts towards the optimization of **NR-7h**, a potent p38 PROTAC with poor water solubility.

Modification of the linker composition of **NR-7h** afforded degraders **5-10a-d**, composed of a PEG-based linker, and **5-12/16** with a peptidic-based linker. The compounds showed a reduced ability to induce degradation of p38 compared to **NR-7h**. Although **5-16** improved in water-solubility respect **NR-7h**, it was not active in vivo.

By exchanging the E3 ligase recruiter of the degrader, we obtained VHL-targeting PROTACs able to induce degradation of p38. The degradation profile of the most potent compound, **NR-11c**, was extensively studied, showing isoform selectivity and activity in a wider range of cell lines than **NR-7h**, which can be attributed to the recruitment of the VHL E3 ubiquitin ligase. The synthesis of the **NR-11** series, its characterization and in vivo study were published.[34]

We performed a SAR study on the linker of **NR-11c**, synthesizing 16 analogues divided in three series based on the linker chemistry; compounds in which amide linkage was substituted by direct alkylation strategies (**NR-12** series), compounds featuring a SuFEx linkage (**NR-13** series) and linkers with a bicyclic piperazine-piperidine system (**NR-14** series and **NR-15**). The most active compounds, with comparable potency to **NR-11c**, are **NR-13c** and **NR-15**, which display excellent p38α degradation. Although all the analogues maintain a linker length similar to that of **NR-11c**, their ability to degrade p38α is variable. This reinforces the notion that linker length is not the only determinant of PROTAC activity, and that the chemical composition plays a crucial role at stablishing interactions with protein surface that lead to a productive ternary complex formation.

Regarding future work in this project, compounds **NR-13c** and **NR-15** have been selected for in vivo study, in order to test their activity in mice. Their distribution profile will be analysed, in order to see if the compounds achieve systemic administration or like **NR-11c**, they degrade p38α exclusively in the liver.

Although the SAR study of the linker provides some data on which scaffolds afford better activity, structural studies are needed to determine the contribution of each modification. In collaboration with the spin-off company Nostrum Biodiscovery, we are planning the computational study of the linker SAR compounds. By computationally docking the compounds with p38α and the VHL E3 ubiquitin ligase, we aim to understand how the linker folds at the protein interface and which interactions favour the formation of the ternary complex, and correlate this data to the ability of each compound to induce degradation of p38α.

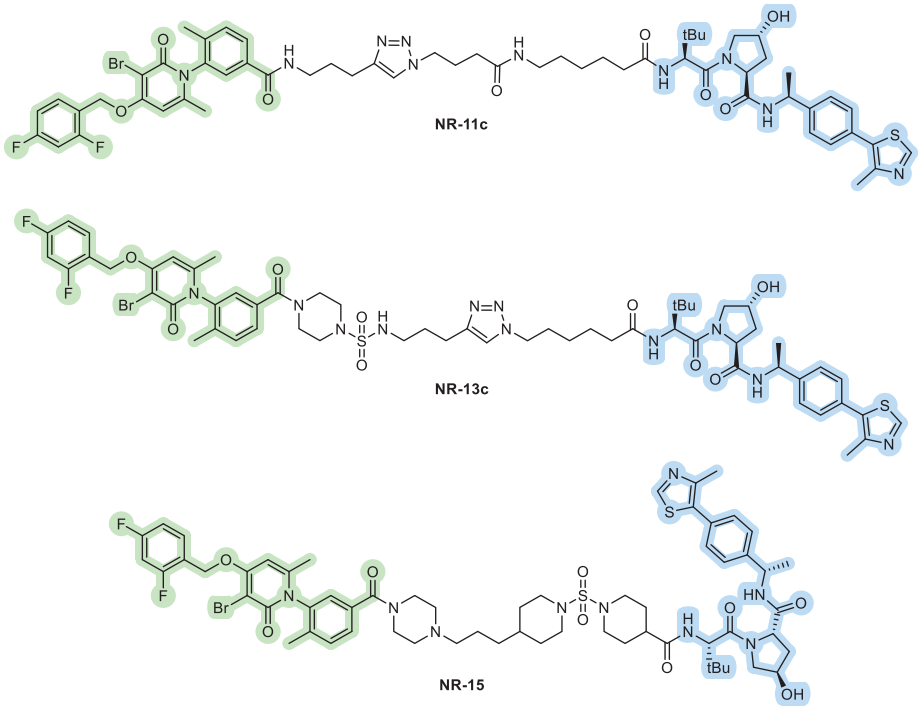

Figure 5.20. Structures of the in vivo active PROTAC **NR-11c**, and the two best candidates from the SAR study, **NR-13c** and **NR-15**.

References

[1] Cuadrado, A. & Nebreda, A. R. Mechanisms and functions of p38 MAPK signalling. *Biochem. J.* **2010**, *429*, 403–417.
[2] Yu, J., Sun, X., Goie, J. Y. G. & Zhang, Y. Regulation of host immune responses against influenza a virus infection by mitogen-activated protein kinases (Mapks). *Microorganisms* **2020**, *8*, 1–17.
[3] Barrantes, I. D. B., Coya, J. M., Maina, F., Arthurd, J. S. C. & Nebreda, A. R. Genetic analysis of specific and redundant roles for p38α and p38β MAPKs during mouse development. *Proceedings of the National Academy of Sciences of the United States of America* at https://doi.org/10.1073/pnas.1015013108 (2011) vol. 108 12764–12769.
[4] Trempolec, N., Dave-Coll, N. & Nebreda, A. R. SnapShot: P38 MAPK substrates. *Cell* **2013**, *152*, 924-924.e1.
[5] Cargnello, M. & Roux, P. P. Activation and function of the MAPKs and their substrates, the MAPK-activated protein kinases. Microbiol Mol. Biol. Rev. 75, 50–83 (2011)
[6] Cuenda, A. & Rousseau, S. p38 MAP-Kinases pathway regulation, function and role in human diseases. *Biochim. Biophys. Acta - Mol. Cell Res.* **2007**, *1773*, 1358–1375.
[7] C. Youssif, M. Cubillos-Rojas, M. Comalada, E. Llonch, C. Perna, N. Djouder, A.R. Nebreda, Myeloid p38alpha signaling promotes intestinal IGF-1 produc- tion and inflammation-associated tumorigenesis, *EMBO Mol. Med*. **2018**, 10, e8403.
[8] Kim, E. K. & Choi, E. Biochimica et Biophysica Acta Pathological roles of MAPK signaling pathways in human diseases. *BBA - Mol. Basis Dis.* **2010**, *1802*, 396–405.
[9] Igea, A. & Nebreda, A. R. The Stress Kinase p38α as a Target for Cancer Therapy. *Cancer Res.* **2015**, *75*, 3997–4002.
[10] Wu, X. *et al.* Ubiquitin-conjugating enzyme Ubc13 controls breast cancer metastasis through a TAK1-p38 MAP kinase cascade. **2014**,.
[11] Urosevic, J. *et al.* Colon cancer cells colonize the lung from established liver metastases through p38 MAPK signalling and PTHLH. **2014**, *16*, 685-694.
[12] Haller, V. *et al.* Expert Opinion on Therapeutic Patents An updated patent review of p38 MAP kinase inhibitors (2014-2019). *Expert Opin. Ther. Pat.* **2020**, *30*, 453–466.
[13] Lee, M. R. & Dominguez, C. MAP Kinase p38 Inhibitors : Clinical Results and an Intimate Look at Their Interactions with p38 Protein. **2005**, *18*, 2979–2994.
[14] Martz KE, Dorn a, Baur B, et al.. Targeting the hinge glycine flip and+the activation loop: novel approach to potent p38α inhibitors.J Med Chem. 2012 Sep 13;55(17):7862–7874
[15] Cirillo, P. F. *et al.* Inhibition of p38 MAP kinase by utilizing a novel allosteric binding site. **2002**, *9*, 268-272.
[16] Donoghue, C., Cubillos-Rojas, M., Gutierrez-Prat, N., Sanchez-Zarzalejo, C., Verdaguer, X., Riera, A., Nebreda, A.R.. Optimal linker length for small molecule PROTACs that selectively target p38α and p38β for degradation. *Eur. J. Med. Chem.* **2020**, *201*, 112451.
[17] Gadd MS, Testa A, Lucas X, Chan KH, Chen W, Lamont DJ, et al. Structural basis of PROTAC cooperative recognition for selective protein degradation. Nat Chem Biol. 2017;13:514-21.
[18] Roy MJ, Winkler S, Hughes SJ, Whitworth C, Galant M, Farnaby W, et al. SPR-measured dissociation kinetics of PROTAC ternary complexes influence target degradation rate. ACS Chem Biol. 2019;14:361-8.
[19] Poongavanam, V. *et al.* Linker-Dependent Folding Rationalizes PROTAC Cell Permeability. *J. Med. Chem.* **2022**, *65*, 13029–13040.
[20] Selness, S. R. *et al.* Discovery of PH-797804, a highly selective and potent inhibitor of p38 MAP kinase. *Bioorganic Med. Chem. Lett.* **2011**, *21*, 4066–4071.
[21] Hydroxypropyl B-cyclodextrin is a carbohydrate widely used for enhancing the aqueous solubility and stability of the drugs. Brewster, M.E.; Loftsson, T. Cyclodextrins as pharmaceutical solubilizers. *Advanced Drug Delivery Reviews* **2007**, *59*, 645-666, doi:10.1016/J.ADDR.2007.05.012.
22 Xing, L. *et al.* Structural bioinformatics-based prediction of exceptional selectivity of p38 MAP kinase inhibitor PH-797804. *Biochemistry* **2009**, *48*, 6402–6411.
[23] Chitrakar, A., Budda, S. A., Henderson, J. G., Axtell, R. C. & Zenewicz, L. A. E3 Ubiquitin Ligase Von Hippel–Lindau Protein Promotes Th17 Differentiation. *J. Immunol.* **2020**, *205*, 1009–1023.
[24] Galdeano, C. *et al.* Structure-guided design and optimization of small molecules targeting the protein-protein interaction between the von hippel-lindau (VHL) E3 ubiquitin ligase and the hypoxia inducible factor (HIF) alpha subunit with in vitro nanomolar affinities. *Journal of Medicinal Chemistry* at https://doi.org/10.1021/jm5011258 (2014) vol. 57 8657–8663.
[25] Goracci, L.; Desantis, J.; Valeri, A.; Castellani, B.; Eleuteri, M.; Cruciani, G. Understanding the Metabolism of Proteolysis Targeting Chimeras (PROTACs): The Next Step toward Pharmaceutical Applications. J. Med. Chem. 2020, 63, 11615–11638.

[26] Han, X. *et al.* Discovery of ARD-69 as a Highly Potent Proteolysis Targeting Chimera (PROTAC) Degrader of Androgen Receptor (AR) for the Treatment of Prostate Cancer. *J. Med. Chem.* **2019**, *62*, 941–964.

[27] Dong, J., Krasnova, L., Finn, M. G. & Barry Sharpless, K. Sulfur(VI) fluoride exchange (SuFEx): Another good reaction for click chemistry. *Angew. Chemie - Int. Ed.* **2014**, *53*, 9430–9448.

[28] Mahapatra, S. *et al.* SuFEx Activation with Ca(NTf2)2: A Unified Strategy to Access Sulfamides, Sulfamates, and Sulfonamides from S(VI) Fluorides. *Org. Lett.* **2020**, *22*, 4389–4394.

[29] Wei, M. *et al.* A Broad-Spectrum Catalytic Amidation of Sulfonyl Fluorides and Fluorosulfates**. *Angew. Chemie* **2021**, *133*, 7473–7480.

[30] Gao, B., Li, S., Wu, P., Moses, J. E. & Sharpless, K. B. SuFEx Chemistry of Thionyl Tetrafluoride (SOF 4) with Organolithium Nucleophiles: Synthesis of Sulfonimidoyl Fluorides, Sulfoximines, Sulfonimidamides, and Sulfonimidates . *Angew. Chemie* **2018**, *130*, 1957–1961.

[31] Smedley, C. J. *et al.* Bifluoride Ion Mediated SuFEx Trifluoromethylation of Sulfonyl Fluorides and Iminosulfur Oxydifluorides. *Angew. Chemie - Int. Ed.* **2019**, *58*, 4552–4556.

[32]Kolb, H. C., Finn, M. G. & Sharpless, K. B. Click Chemistry: Diverse Chemical Function from a Few Good Reactions. *Angew. Chemie - Int. Ed.* **2001**, *40*, 2004–2021.

[33] Barrow, A. S. *et al.* The growing applications of SuFEx click chemistry. *Chem. Soc. Rev.* **2019**, *48*, 4731–4758.

[34] Cubillos-Rojas, M., Loren, G., Hakim, Y. Z., Verdaguer, X., Riera, A., Nebreda, A. R.; Synthesis and Biological Activity of a VHL-Based PROTAC Specific for p38α. *Cancers (Basel).* **2023**, *15*, 611.

Chapter 6

Phosphorylation Inducers

6. Phosphorylation Inducers

6.1. Phosphorylation Inducers: Introduction

In recent years, the field of targeted protein degradation (TPD) has been greatly expanded by the development of PROTACs (proteolysis targeting chimaeras). Following this example, other classes of bifunctional molecules that bind simultaneously to two or more molecules to induce proximity have been developed. PROTACs owe their pharmacological effect to the recruitment of an E3 ligase. Other bifunctional molecules, however, can bind to different biological effectors in order to promote other post-translational modifications (PTM) or effects on the target protein. Examples in the literature range from alternative strategies for degradation to inducing other PTMs such as phosphorylation, acetylation or deubiquitination (**Figure 6.1**).

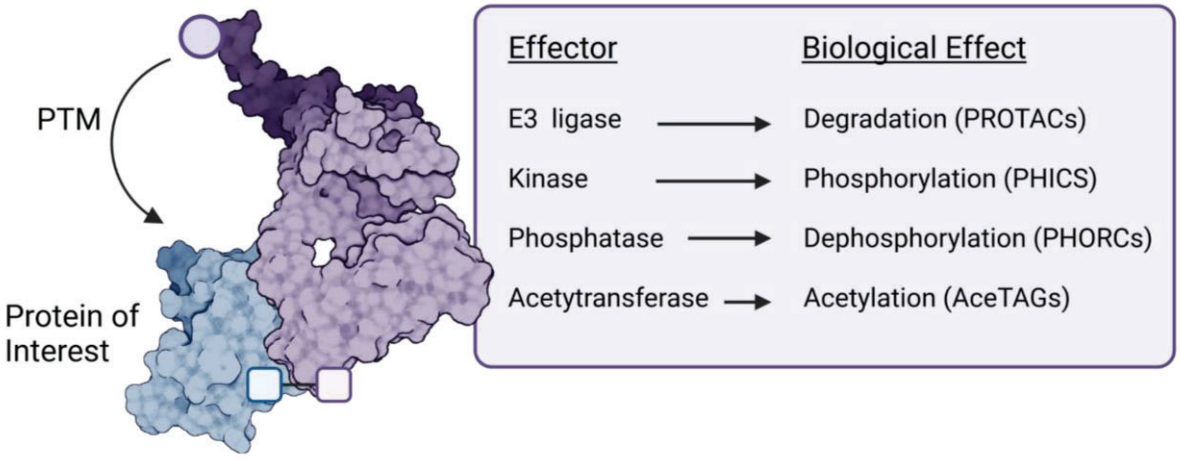

Figure 6.1. General representation of a heterobifunctional molecule triggering a PTM. Possible effectors, their biological effect and the related bifunctional molecule.

Beyond protein degradation, PTMs play important roles in protein biological functions.[1] One of the most important post-translational modifications (PTMs) is phosphorylation, the addition of a phosphoryl (-PO_3^{2-}) group to a protein. Phosphorylation is the most frequent post-translational modification, occurring in more than 13.000 proteins in the human proteome.[2] It regulates enzyme activity, protein structure, stability, cellular localization; its fast kinetics and reversibility confer it the behaviour of a molecular switch that regulates protein function.[3] Because of their broad role in protein regulation and cellular processes, abnormal phosphorylation activity has been linked to several diseases, including cancer[4] and neurodegenerative disorders.[5] The loss of phosphorylation sites due to diseases mutation might disrupt protein function and affect signal transduction, leading to dysregulation and tumour progression. Phosphorylation occurs typically on a serine (Ser),

thereonie (Thr) or tyrosine (Tyr) residue, and it is catalysed by specific protein kinases. The human kinome is comprised by 538 kinases, which catalyse the transfer of γ-phosphate of ATP to Ser, Thr or Tyr residues to the substrate protein. The inverse process of dephosphorylation is catalysed by protein phosphatases, a type of enzyme that hydrolyses the phosphoric acid monoester of a phosphorylated substrate.

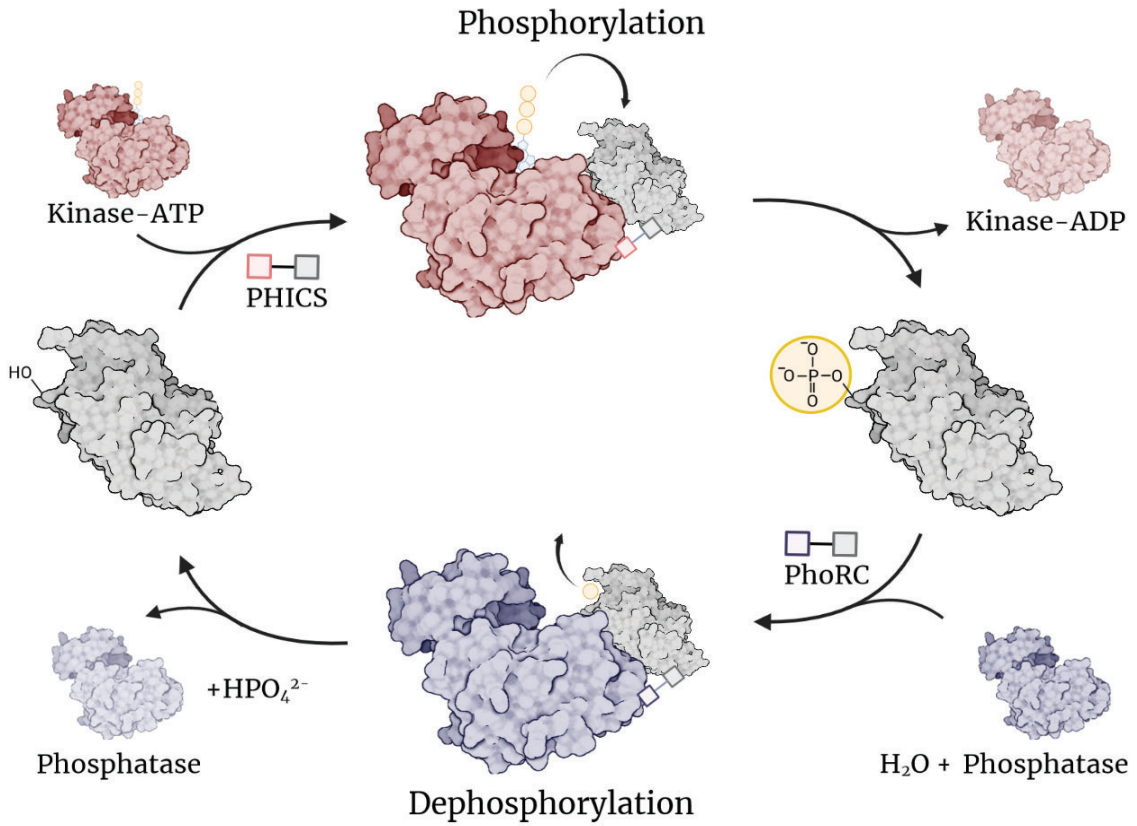

Figure 6.3. Induction of phosphorylation and dephosphorylation by PHICS and PhoRCs.

Due to the relevance of phosphorylation in cellular processes and disease, there is interest in the synthesis of bifunctional molecules that attempt to control phosphorylation levels of a target. PHICS (phosphorylation inducing chimeric small molecules) recruit a protein kinase to induce phosphorylation of a target protein, while PhoRCs (phosphatase recruiting chimeras) do the inverse by engaging a phosphatase. PHICS composed of ligands for bromodomain-containing protein 4 (BRD4) and Bruton's tyrosine kinase (BTK) linked to kinase activators have been successful at inducing phosphorylation of these targets.[6]

PHICs reported in the literature recruit either the AMP-activated protein kinase (AMPK) or protein kinase C (PKC) to induce phosphorylation of the target protein. The need to recruit directly the protein effecting the PTM (the kinase) limits the choice of the ligand, which should not have an

antagonistic effect to the protein that is binding to. This contrasts with PROTAC design; PROTACs recruit a substrate recognition subunit of the E3 ligase complex, while the protein responsible for ubiquitin transfer is the E2 ubiquitin ligase, which remains unaffected by the binding of the ligand. In the case of kinases, the use of an antagonistic ligand would reduce or disable the protein's function.

Similarly, PhoRCs have been designed using a phosphatase activator anchor to recruit a phosphatase. Proof of concept studies have reported PhoRCs to recruit protein phosphatase 1 (PP1) using a tetrapeptide sequence,[7] and protein phosphatase 2A (PP2A) by using a fusion protein.[8] Small-molecule phosphatase recruiters were used to target protein phosphatase 5 (PP5), allowing the synthesis of PP5-recruiting PhoRCs which deactivate the protein ASK1.[9]

6.2. Phosphorylation Inducers: Objectives

Known ligands targeting protein kinases are mostly inhibitors, regardless of whether they bind at the active or allosteric site.[10] Although a growing number of publications demonstrate the potential therapeutic benefits of protein kinase activators,[11] they are largely outnumbered by the amount of inhibitors developed. Although this limits the warhead choice when designing PHICS, it also highlights the need for novel protein kinase activators or ligands without antagonistic effect that can be used in PHICS design.

The starting point of this project was the identification of novel p38α ligands in an *in silico* high-throughput screening campaign. This project, carried out in Dr. Nebreda's group in collaboration with Dr. Orozco (IRB Barcelona) and Dr. Díaz (Nostrum Biodiscovery, NBD),[12] identified potential ligands for p38 from a 2.5 million low-molecular-weight compounds of the ZINC15 database,[13] retrieving 35 compounds showing promising binding profiles. According to their calculations, they identified several of the binders to be allosteric ligands. We hypothesised that these binders, that did not target the ATP binding site, could be used as a kinase-recruiting warheads, and started to explore the synthesis of PHICS using these compounds. Our first objective was **to synthesize p38-recruiting PHICS using a p38 allosteric ligand as warhead.** Based on our experience in building p38 PROTACs, we decided to first **synthesize p38 PROTACs based on the novel ligand** to validate that this scaffold could effectively recruit the kinase, and then move to the **synthesis of PHICS recruiting p38.** This project was carried out as a collaboration with the signalling and cell cycle laboratory at the IRB Barcelona, led by Prof. Nebreda, as a continuation of their discovery of potential p38 allosteric ligands.

Parallel to this, we decided to investigate the synthesis of PHICS targeting an inducible degron TAG system. We set out to **synthesize PKC-targeting PHICS that would engage with the degron tags dTAG and aTAG.** This work was a collaboration with the targeted protein degradation and drug

discovery laboratory at the IRB Barcelona, led by Dr. Mayor-Ruiz., who performed the cellular assays and analysis of the induced phosphorylation.

6.3. Synthesis of Compounds with a p38 Allosteric Ligand

NC-37 is the most potent hit from the *in-silico* screening (**scheme 6.1**). The compound has an inhibitory effect over p38 autophosphorylation and initial calculations pointed out that the compound bound to an allosteric site of p38. In order to prepare bifunctional compounds, however, we selected **6-1**, a less potent compound also found active inhibiting p38 autophosphorylation and featuring a terminal aniline. We envisaged extending the linker from the aniline nitrogen via an amide bond.

Intermediate **6-3** was prepared in two steps from 4-nitrobenzene-1,2-diamine and cyclopentanecarboxylic acid, forming first the corresponding amide followed by condensation in acetic acid. Reduction of the nitro group afforded the amino derivative, which was converted into the sulphonamide by reaction with 2-nitrobenzenesulfonyl, bearing the masked amino handle. Subsequent reduction afforded warhead **6-1** in good yields.

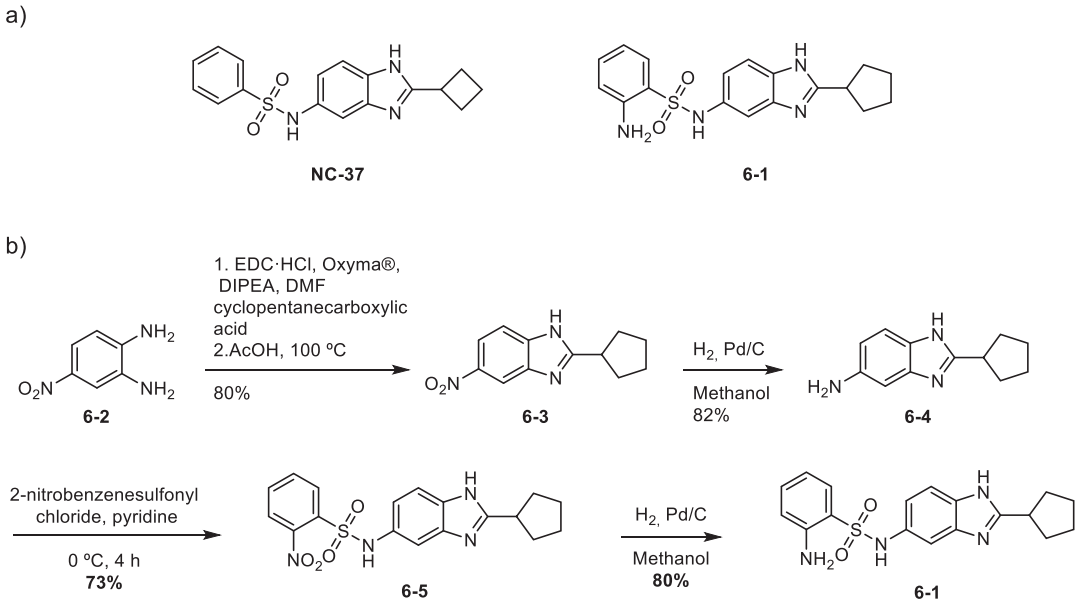

Scheme 6.1. a) Structures of **NC-37** and **6-1**. **b)** Synthesis of **6-1**.

Initially we wanted to assess the potential of **6-1** to engage p38 as part of a bifunctional molecule. To test if the warhead could bind in a productive way to p38, we derivatized **6-1** and synthesized a small family of PROTACs. Reaction of **6-1** with pentynoic acid afforded **6-6**. The terminal alkyne was

the subjected to CuAAC conditions, together with three VHL fragments bearing a terminal azide at different distances.

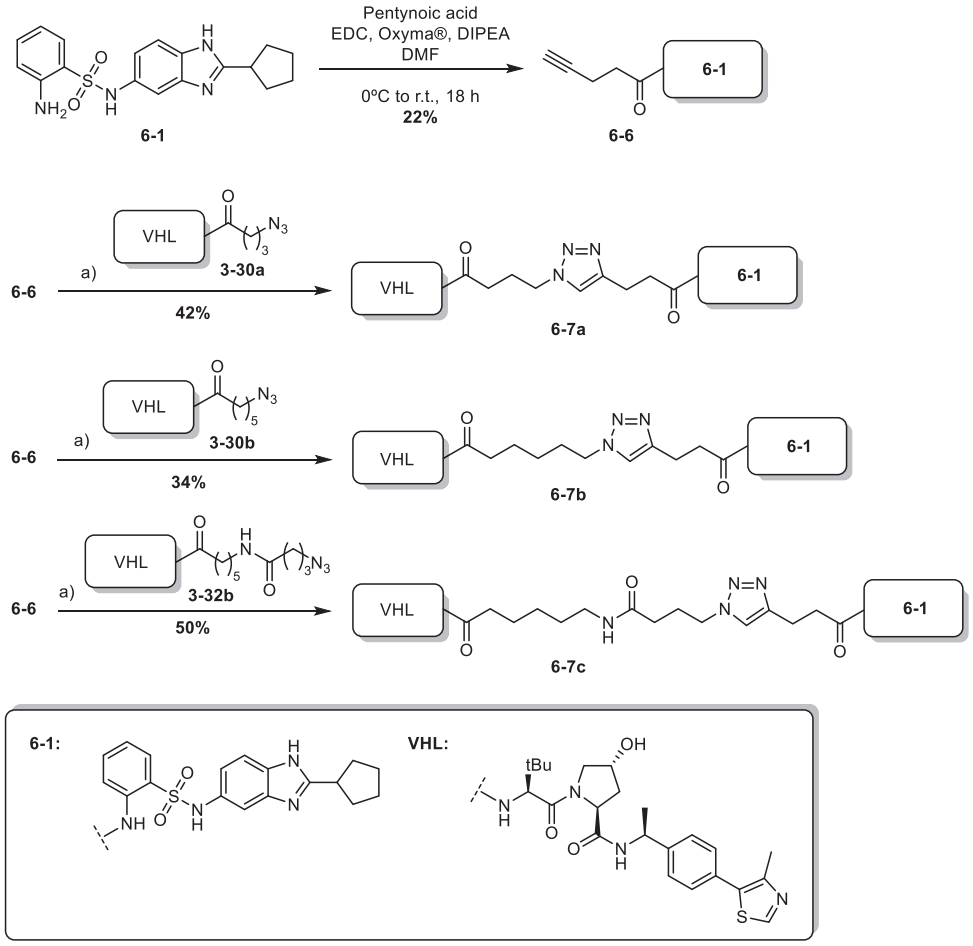

Scheme 6.2. Reaction conditions: a) $CuSO_4 \cdot 5\ H_2O$, Sodium Ascorbate, AcOH (cat) H_2O / *t*-BuOH (2:1) r.t., overnight.

The ability of compounds **6-7a-c** to degrade p38 was tested in cells.[1] Western blotting analysis showed no degradation of p38α. Parallel to the synthesis of **6-7a-c**, structural studies conducted by Dr. Macias, at the IRB Barcelona, solved the binding mode of **NC-37**, revealing the aromatic ring of the sulphonamide substituent was buried in the binding pocket of p38α (PDB: 7z6i).[12] These results explain the inactivity of compounds **6-7a-c**, which most likely do not have the capacity to bind p38. Moreover, the studies show that **NC-37** can bind to several binding sites; it can act as an ATP competitor, although with lower potency than other p38 inhibitors, and also to the hinge pocket and

[1] This project is a collaboration with the Signalling and Cell Cycle laboratory at the IRB Barcelona, led by Prof. A. Nebreda. All the cellular and mice experiments were carried out by Dr. Mónica Cubillos-Rojas.

to an allosteric pocket. These findings partially invalidated our initial hypothesis, since a ligand competing with ATP for binding could inactivate the kinase we want to recruit.

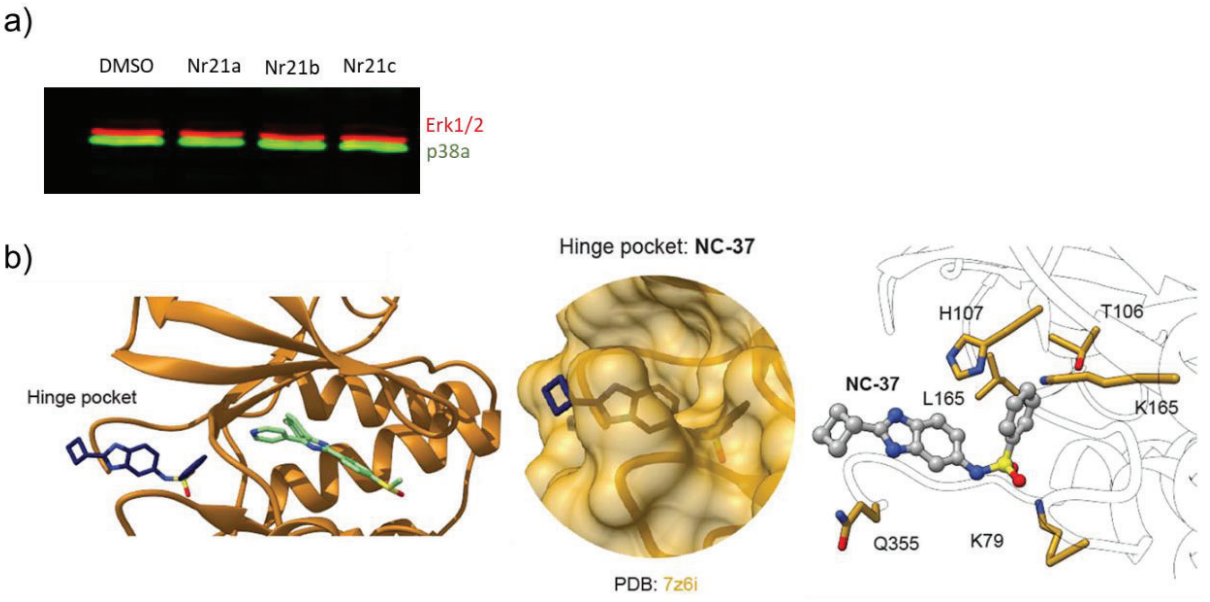

Figure 6.4. a) 6-7a-c do not induce degradation of p38. MDA-MB-231 cells were treated with 1µM of compound for 24hours. Cell lysates were analysed by Western blotting. **b)** binding mode of NC-37. Adapted from González, L. *et* al.

Nonetheless, we hypothesised that the ligand still had potential to recruit the target kinase as an effector, based on its ability to bind to two other regions in the protein and its low potency as a type I inhibitors (with an IC_{50} at the micromolar range). The crystal structure of **NC-37** shows the cyclobutane ring is solvent-exposed, so we hypothesised that substitution for an alkyl chain could still provide binding to the hinge pocket, and that engagement with this site could allow p38 to function as a kinase.

We modified our initial synthesis of **6-1** to introduce an alkyl chain bearing a terminal alkyne at the opposite side of the molecule. Formation of the benzoimidazole core was performed using heptynoic acid instead of cyclopentanecarboxylic acid, under the same conditions. Reduction of the nitro group was performed with iron powder in ammonium chloride to spare the terminal alkyne. Direct sulphonamide formation on **6-8** produced poly-sulfonylatead products; boc-protection of **6-9** was required to obtain **6-11** in acceptable yields. After boc deprotection, warhead **6-11** was subjected to CuAAC conditions with tree different VHL fragments with terminal azides, affording compounds **6-12a-c**. Unfortunately, the potential degraders, showed no activity degrading p38α in cells.[2] The

[2] This project is a collaboration with the Signalling and Cell Cycle laboratory at the IRB Barcelona, led by Prof. A. Nebreda. All the cellular and mice experiments were carried out by Dr. Mónica Cubillos-Rojas.

failure to convert warhead **6-11** into a p38-targeting warhead discouraged us to continue in this direction. More structural studies are needed in order to assess why the compounds are not active, and to see if compounds derived from **6-11** can bind to p38 at the allosteric sites. Moreover, the ability of derivatives of **6-11** to recruit p38 as a kinase effector was still dubious, and we decided to turn to a protein kinase C (PKC) activator for the synthesis of phosphorylation-inducing molecules.

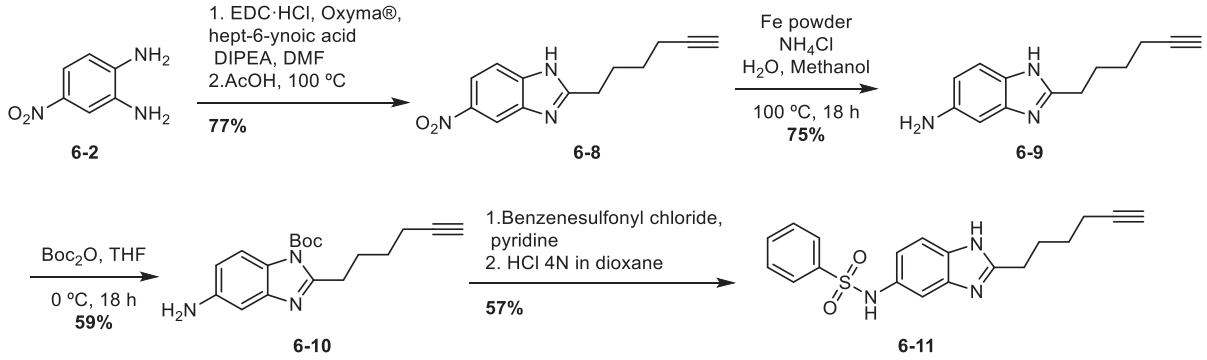

Scheme 6.3. Synthesis of warhead **6-11**.

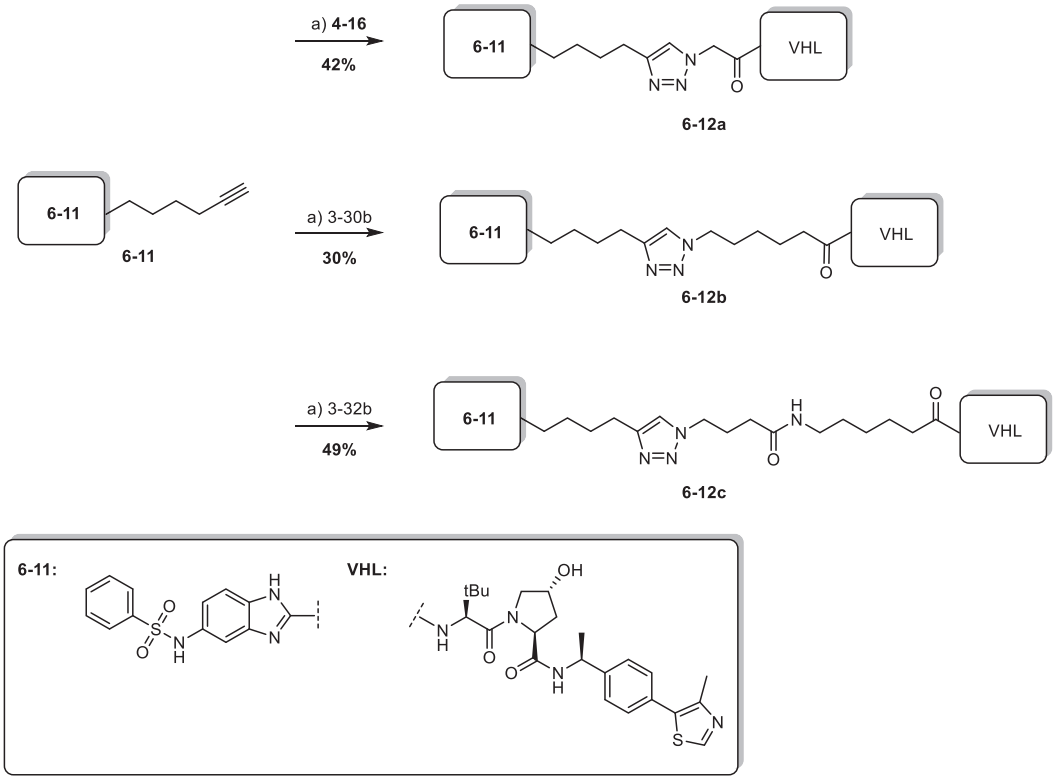

Scheme 6.4. Reaction conditions: a) $CuSO_4 \cdot 5\ H_2O$, Sodium Ascorbate, AcOH (cat), H_2O / *t*-BuOH (2:1), r.t., overnight.

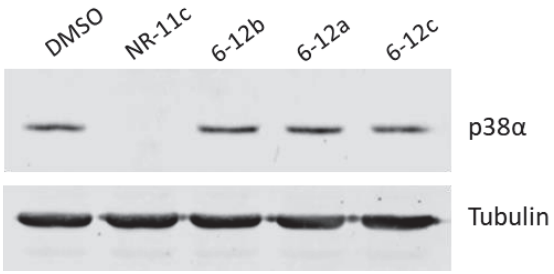

Figure 6.5. 6-12a-c do not induce degradation of p38. MDA-MB-231 cells were treated with 1μM of compound for 24 hours. Cell lysates were analysed by Western blotting. NR-11c, a potent p38 degrader, was used as control.

6.4 Synthesis of Compounds with a PKC Ligand

Currently, there are only a few examples of PHICS reported in the literature. These compounds, recruiting either the AMP-activated protein kinase (AMPK) or the protein kinase C (PKC), are able to induce phosphorylation of a target protein in vitro.[6] We chose to target PKC and synthesize a warhead based on a PKC activator, suitable for the synthesis of PHICS. Initially, and based on our experience in synthesizing p38 PROTACs, we decided to target p38 as the target protein, using a warhead based on the inhibitor PH-797804 (**5-7**).

A PKC-targeting warhead was synthesized similarly to procedures reported in the literature.[6] *L*-tyrosine methyl ester was protected using methyl chloroformate and subjected to nitration conditions to obtain **6-14**. Reduction of the nitro by hydrogenation at 50 bar and acetylation of the aniline and phenol groups afforded **6-15**. The methyl ester was then reduced and subsequently acetylated, and **6-16** was subjected again to nitration conditions. Introduction of this nitro group in the *orto* position was possible thanks to the directing amino group, which is afterwards reduced by conversion to the diazonium salt and subsequent addition of hypophosphorous acid.

Nitro intermediate **6-18** was derivatized using the amino benzylic handle **6-19**, followed by the construction of the lactame ring. Reduction of the amino group using sodium borohydride and copper (II) acetate followed addition of chiral fragment **6-22**. Compound **6-23** was then deprotected simultaneously at the ester and carbamate ends and subjected to cyclization using DPPA. The resulting product was methylated through reductive amination and the amino handle was deprotected under acidic conditions.

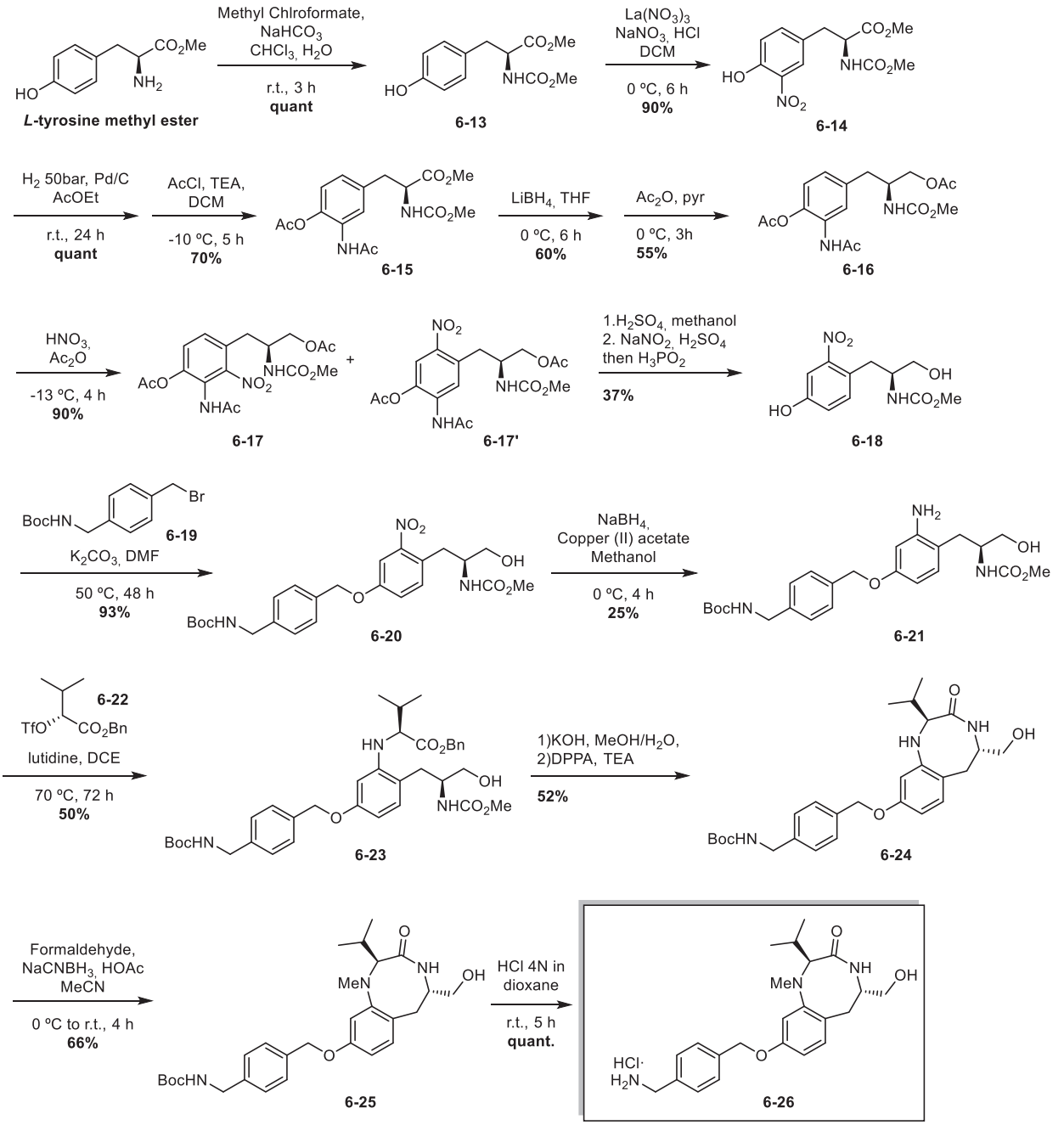

Scheme 6.5. Synthesis of warhead **6-26**, based on a PKC activator.

Warhead **6-26** was derivatized into three different fragments with different linker lengths. Compound **6-27**, bearing a terminal amine, was directly coupled to **5-7** via amide formation. Two terminal azido fragments were also synthesized. **6-28a** was subjected to copper(I)-catalysed alkyne-azide cycloaddition (CuAAC) conditions with PH-based fragment **5-17**, and a longer PH-based fragment was synthesized by addition of a cadaverine and pentynoic acid units, and subjected to CuAAC with **6-28b**.

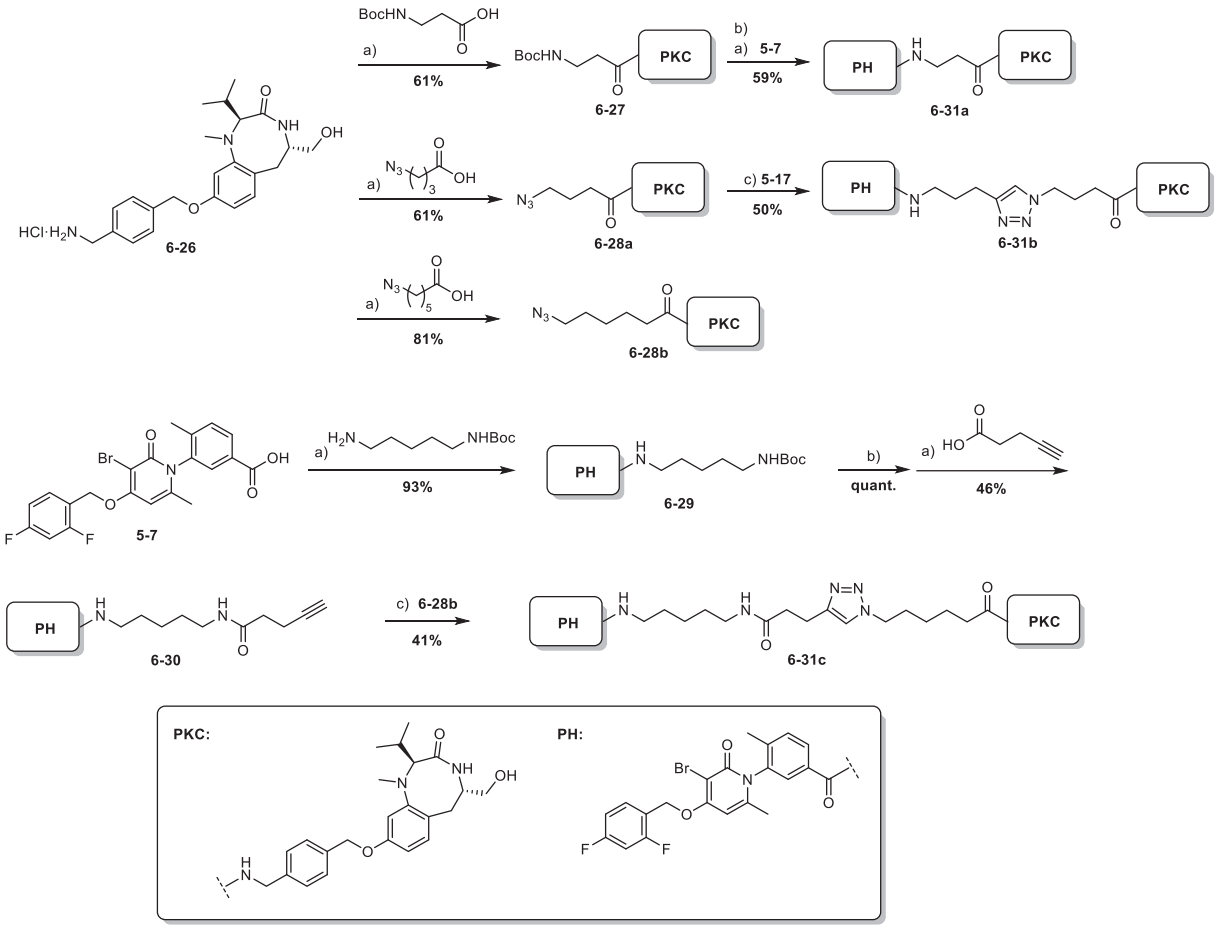

Scheme 6.6. Synthesis of potential p38 PHICS.

The ability of compounds **6-31a-c** to phosphorylate p38 was tested in cells.[3] Unfortunately, phosphorylation of p38 was not observed. We hypothesized that the inactivity of the PHICS was due to the lack of favourable protein-protein interactions (PPI) between PKC and p38. In order to have more chances of finding a protein of interest (POI) that can form favourable interactions with PKC, we decided to incorporate a protein tag into our system, which allows us to test for different POIs using the same compound.

[3] This project is a collaboration with the Targeted protein degradation and drug discovery at the IRB Barcelona, led by Dr. Mayor-Ruiz. All the cellular experiments, including the treatment, Western blot analysis and expression of the mutant proteins, were carried out by Dr. Domostegui.

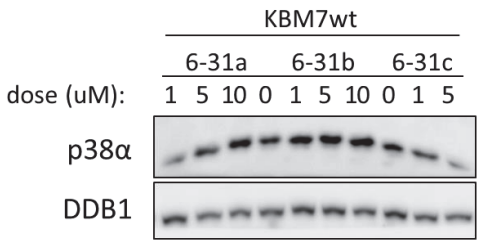

Figure 6.5. potential PHICS 6-31a-c do not induce phosphorylation of p38. KBM7 cells were treated with 1, 5 or 10 μM of compound. Cell lysates were analysed by Western blot using a Phos-tag gel.

6.5 Tag-based PHICS

6.5.1. Protein Degradation and degradation Tags

During the past 20 years, bifunctional protein degraders have consolidated as a technology able to induce degradation of a target protein by hijacking the ubiquitin-proteasome system (UPS). The ability to downregulate protein levels has found application as chemical biology tools.[14] Moreover, this applicability has prompted the development of systems that combine bifunctional molecules with modification of the target protein, allowing better selectivity and control. The combination of bifunctional degraders with chemical genetics has produced tools that allow the study of a protein of interest in a temporal controlled manner and great selectivity. Allele-specific chemical genetics consists in the modification of a protein-ligand pair in a way that the engineered interface is still biochemically competent but orthogonal to the wild-type system.[15] This strategy typically involves the introduction of a hydrophobic “bump” in the ligand, while engineering a corresponding “hole” into the target protein binding pocket. The complementary modifications typically enhance the affinity between the modified ligand-modified protein pair, while drastically reducing the affinity between the modified ligand and the wild-type target protein. This approach, commonly referred to as “bump-and-hole”, has emerged as one of the most powerful chemical genetic tools in recent years, and has been combined with PROTAC technology to deliver very selective degraders that can be integrated in engineered biological systems to target proteins for which there is no known ligand.

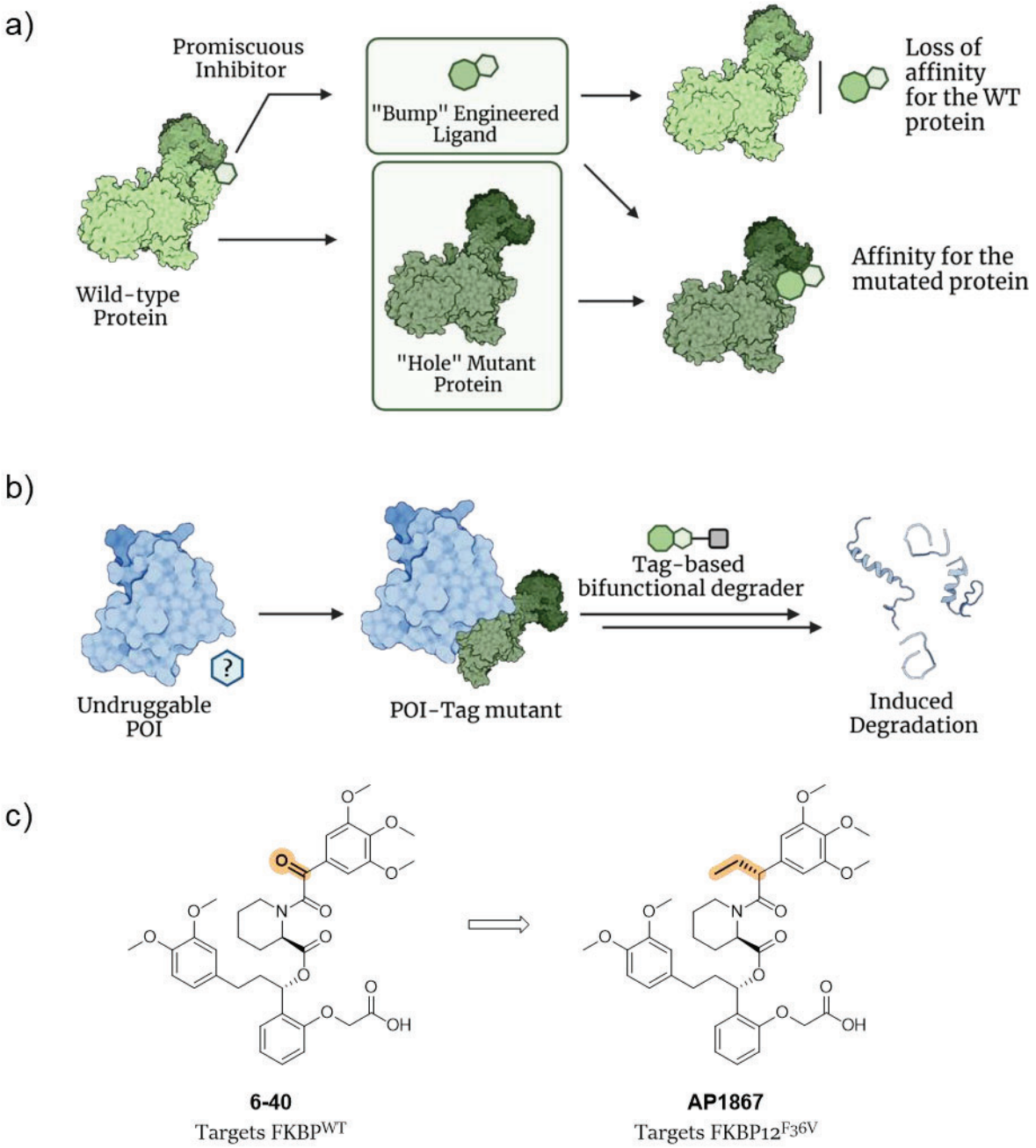

Figure 6.6. a) Schematic representation of the bump and hole strategy. **b)** Schematic representation of a TAG degron system. A POI with unknown ligand is expressed as a mutant with the degron TAG and targeted by a bifunctional degrader, bearing the TAG-specific ligand. c) "Bumped" version of a FKBP12 ligand, AP1867 targets the mutant FKBP12^{F36V} selectively.

One of such systems is the dTAG degrader.[16] The system is based on a PROTAC targeting CRBN and FKBP12. A bump-and-hole pair was engineered for the warhead targeting FKBP12, including a mutated version of the protein with a cavity (FKBP12^{F26V}) and a "bumped" synthetic ligand. The bifunctional degrader constructed with the modified warhead showed affinity for FKBP12^{F26V} but not for the wild type (FKBP12^{wt}). This selectivity permitted degradation of FKBP12^{F26V} chimeras

without affecting the activity of $FKBP12^{WT}$, thus the dTAG degrader could be used to induce degradation of any protein expressed in-frame with the FKBP12 mutant. This same principle has been replicated, producing degradation tags based on proteins others than FKBP12.[17,18]

6.5.2. Synthesis and biological evaluation of TAG-based PHICS

Chemoproteomic tools such as the dTAG degrader system have expanded the scope of bifunctional degraders, allowing degradation of undruggable targets in a selective and controlled way. We wanted to couple the wide scope of a chemoproteomic tool with the application of another post-translational modification, namely phosphorylation.

We devised the synthesis of bifunctional compounds composed of a kinase recruiting warhead and a degradation tag. Targeting a tag instead of a specific target protein would allow us to test for various proteins using the same molecule, and we would have more chances of finding a suitable target.

We chose to use the dTAG and the aTAG systems for the design of the compounds. As described in the introduction, the dTAG consists on expression of an FKBP12 mutant to the protein of interest, which is targeted specifically by a derivative of rapamycin. We also employed the aTAG (Achilles tag) system, a similar technology based on the MTH1 protein, paired with a specific ligand consisting on a 3-amino quinolone core.[19]

The aTAG warhead was synthesized as reported in the literature.[20] Commercial dichloroquinoline **6-32** was substituted selectively at the pyridinic chloride with aniline and then converted into the methyl amide **6-34**. Compound **6-34** was subjected to a Suzuki coupling to introduce the methyl piconilate, which was subsequently hydrolysed to obtain the carboxylic acid warhead **6-37**.

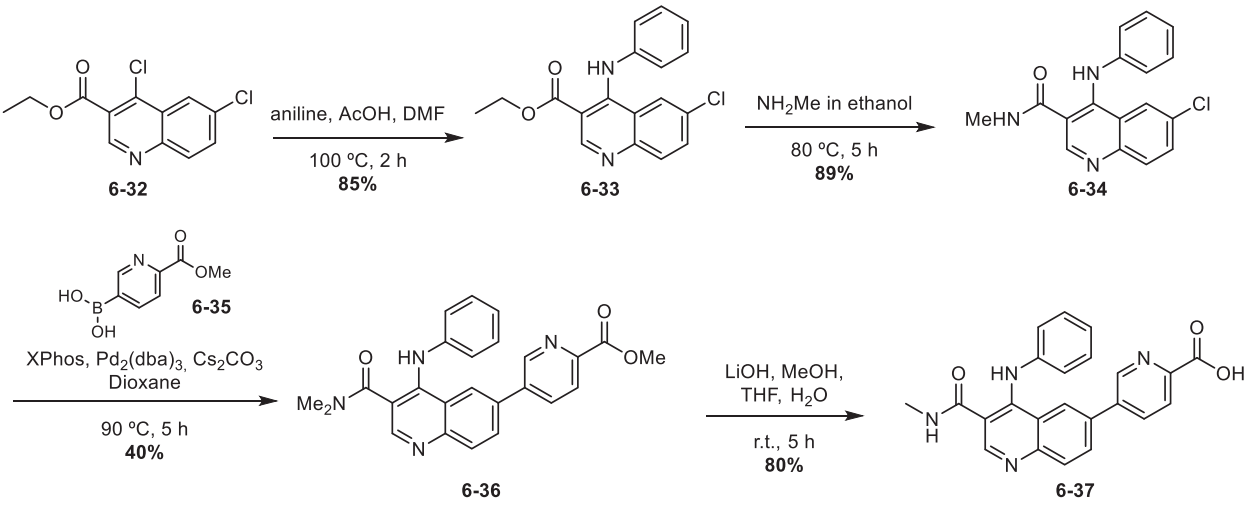

Scheme 6.7. Synthesis of the aTAG warhead **6-37**.

Potential PHICS were synthesized based on the acid warhead **6-37**. Direct amide coupling with the PKC activator **6-26** afforded **6-39a**, with a minimal linker length. Reaction with functionalized PKC derivatives bearing a terminal amide afforded **6-39b-c**; compound **6-39d** bearing a longer linker was synthesized by previous functionalization with butynamine, followed by CuAAC with the PKC warhead-azide **6-28b**.

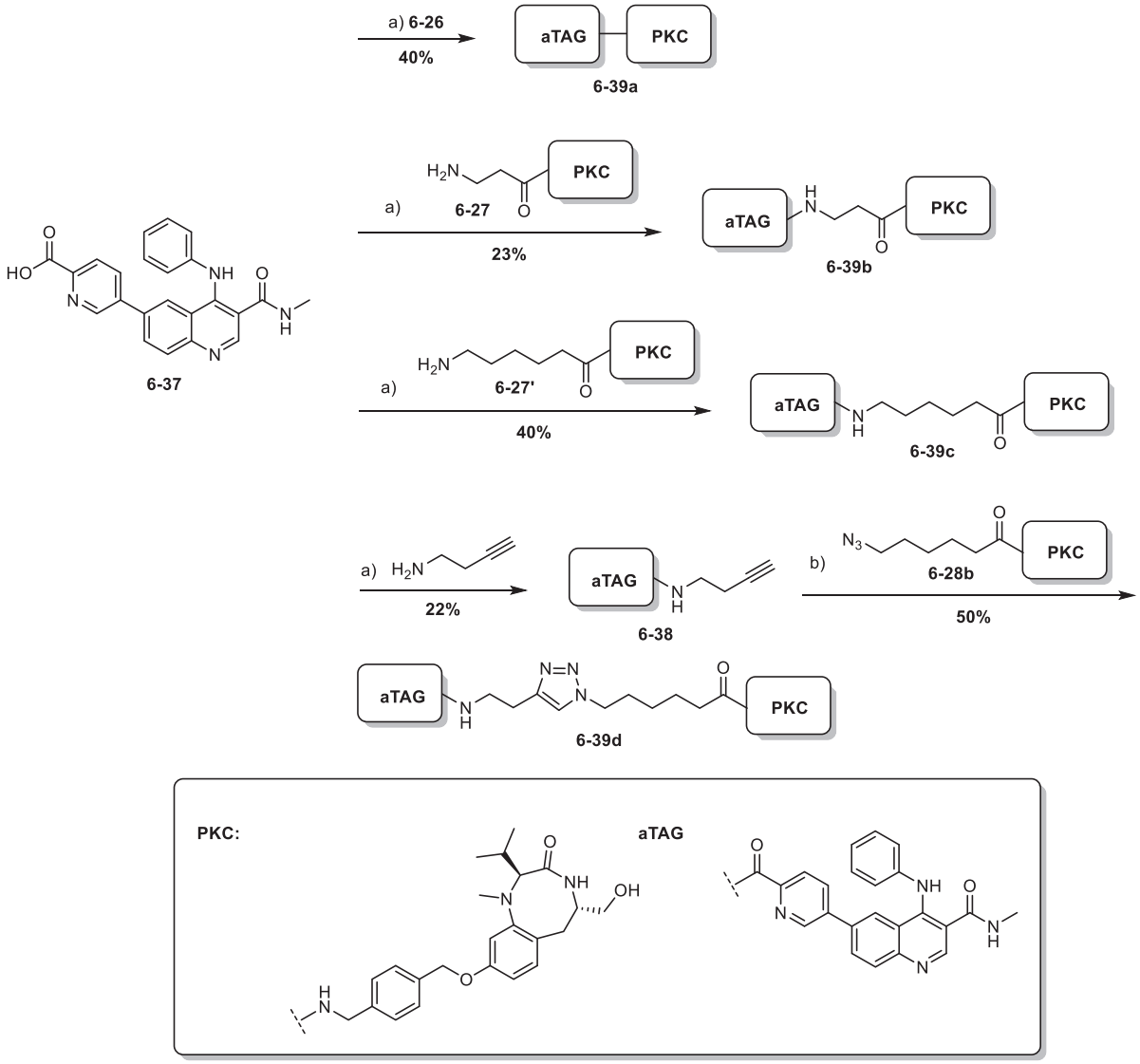

Scheme 6.8. Synthesis of potential PHICS based on the aTAG warhead.

Similarly, dTAG targeting PHICS were synthesized. Warhead **6-40**, available in our laboratory, was coupled to the PKC activator directly or to amino acid derivatives, affording **6-42a** and **b**. Reaction

of **6-40** with butynamine and subsequent CuAAC with PKC warhead-azide fragments afforded compounds **6-42c-d**, with longer linkers.

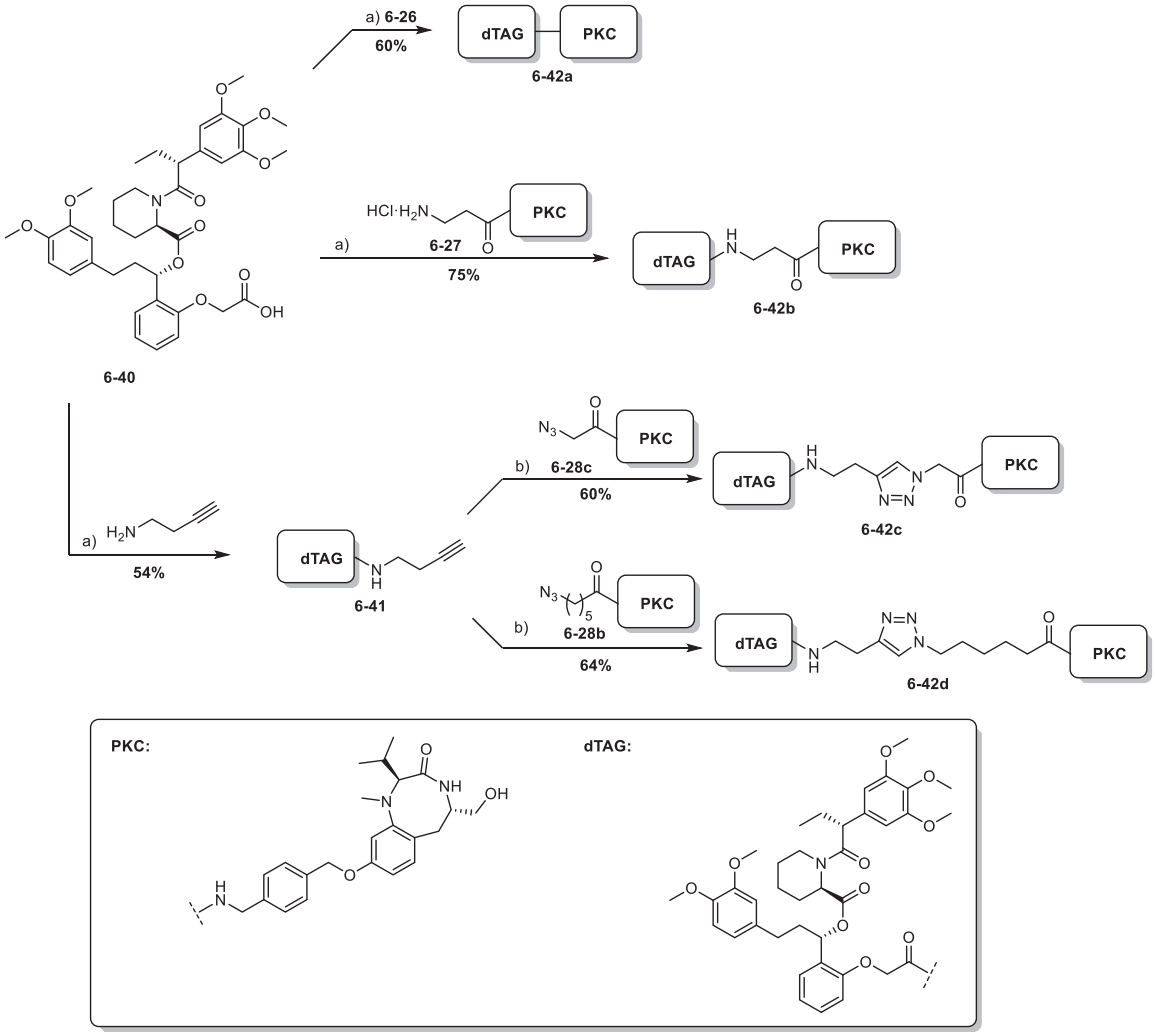

Scheme 6.9. Synthesis of potential PHICS based on the dTAG warhead.

In order to test the ability of compounds **6-39a-d** and **6-42a-d** to induce phosphorylation, we decided to target ERF.[4] ERF is a transcriptional repressor that binds to the DNA and supresses cellular proliferation. Upon mitotic signal and RAS/MAPK pathway activation, ERF is phosphorylated, translocating from the nucleus to the cytoplasm.[21]

The ability of compounds **6-39a-d** or **6-42a-d** to induce ERF phosphorylation was tested in cells overexpressing a dTAG- or aTAG-ERF fusion construct. Treatment with PHICS shows an increase

[4] This project is a collaboration with the Targeted protein degradation and drug discovery laboratory at the IRB Barcelona, led by Dr. Mayor-Ruiz. All the cellular experiments, including the treatment, Western blot analysis and expression of the mutant proteins, were carried out by Dr. Domostegui.

in the intensity of the bands corresponding to the phosphorylated ERF construct, compared with the control (**Figure 6.7a**). Similarly, when the cells are previously treated with a MEK inhibitor, which blocks ERF phosphorylation, treatment with PHICS partially restores phosphorylation. Compounds **6-42a-d** show similar levels of activity at inducing phosphorylation of the ERF-dTAG construct, while in the aTAG series, compounds **6-39a** and **6-39c** seem to exhibit greater potency than the rest.

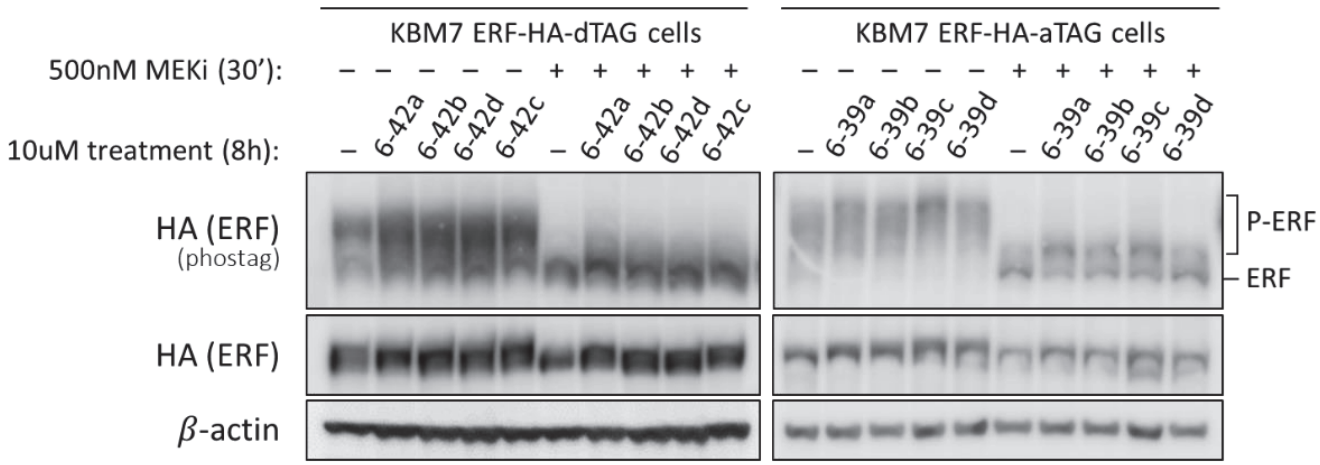

Figure 6.7. PHICS 6-39a-d and 6-42a-d increase phosphorylation levels of ERF constructs. KBM7 cells overexpressing aTAG or dTAG ERF constructs were treated with 1, μM of compound. Cell lysates were analysed by Western blot, using a PhosTag gel.

6.6. Phosphorylation Inducers: Conclusions

In this chapter we describe our attempts to synthesize bifunctional molecules able to induce phosphorylation of a target protein.

Compund **6-1**, initially believed to be an allosteric binder of p38, was derivatized into two warheads amenable for the synthesis of bifunctional compounds. Attachment of an alkyne to the aniline handle afforded warhead **6-6**, bearing a terminal alkyne and thus functionalizable via CuAAC. Introduction of the alkyne at the opposite site of the molecule, substituting the alkane ring, afforded **6-11**. Initially, warheads **6-1** and **6-11** were used to construct PROTACs recruiting the VHL ligand. Potential degraders **6-7a-c** and **6-12a-c**, however, did not induce degradation of p38 in cells. The inability to construct active degraders using **6-1**, discouraged us from synthesizing phosphorylation inducers including this warhead.

Warhead **6-26**, based on a PKC activator, was synthesized. This fragment has been used in the synthesis of PHICS, and its ability to recruit PKC to induce phosphorylation of a target protein *in vitro* has been reported in the literature.[6] Using **6-26** and the p38 inhibitor **PH-797804**, we

constructed potential PHICS inducing phosphorylation of p38 by recruiting PKC. Compounds **6-32a-c** were tested in cells, however, they did not induce phosphorylation of p38.

PHICS targeting a protein tag instead of a defined protein of interest were synthesized. By targeting the dTAG or aTAG tags, any protein of interest expressed in-frame with the tag could be targeted by the potential PHICS, expanding the scope of the compounds and facilitating the identification of a protein of interest favourable to induced phosphorylation. The aTAG ligand was synthesized as described in the literature, while the dTAG ligand was readily available in our laboratory. Both fragments were used to synthesize PKC-based PHICS, bearing different linker lengths.

Compounds **6-39a-d** and **6-42a-d** show potential at inducing phosphorylation of aTAG- or dTAG-ERF constructs. The dTAG-based compounds **6-42a-d** have the ability to similarly increase the levels of phosphorylated ERF-dTAG construct as seen by Western blotting, while the aTAG based compounds **6-39a** and **6-39c** are the most potent compounds of the aTAG series.

Future work requires further validation of compounds **6-39a-d** and **6-42a-d**. *In vitro* testing of their ability to induce phosphorylation of ERF constructs could be easier to quantify than in cells. Moreover, the potential of PHICS **6-39a-d** and **6-42a-d** lies on their ability to induce phosphorylated of any tagged protein. Performing the same experiments in different proteins of interest would test the scope of the compounds and potentially expand it.

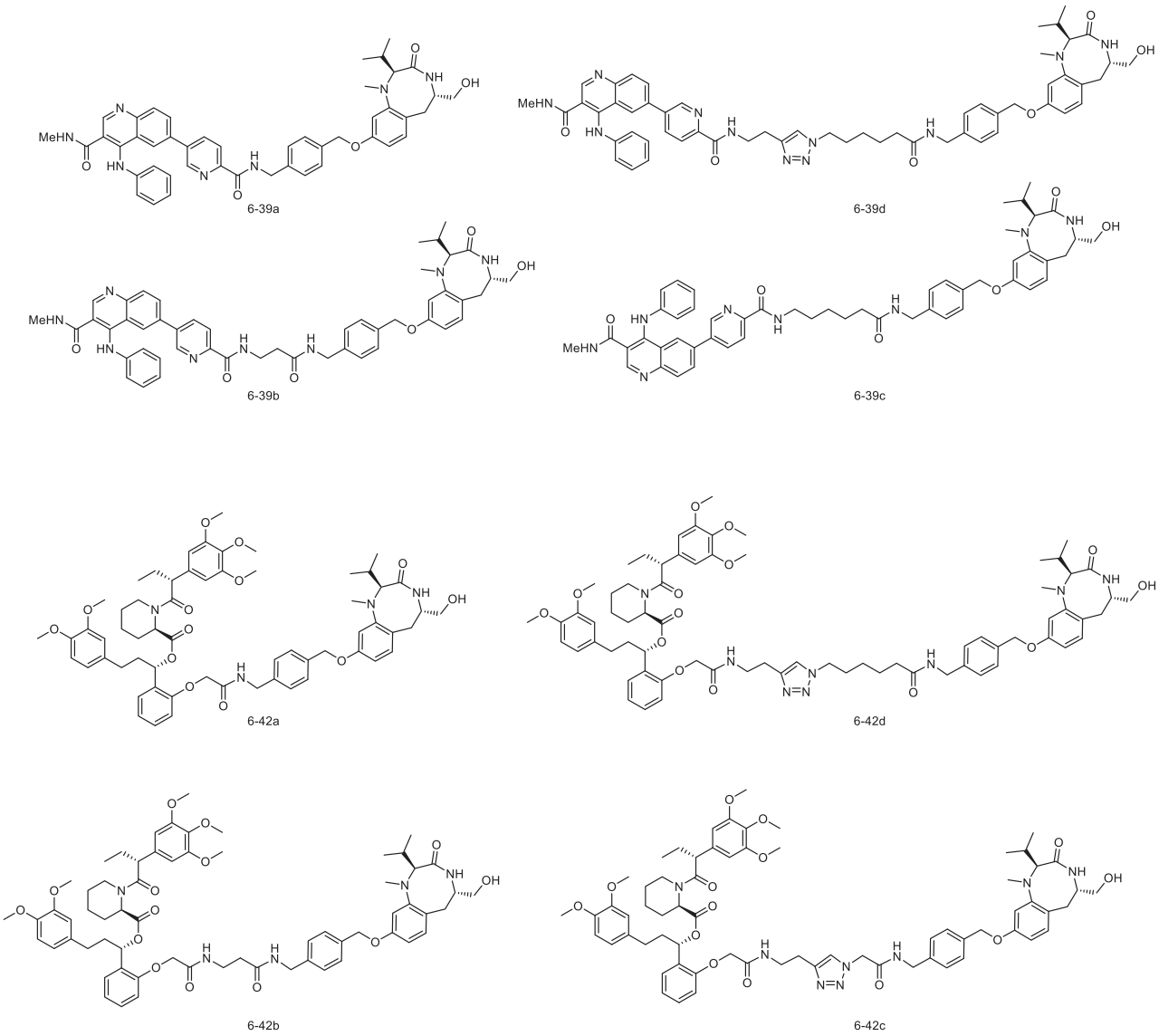

Figure 6.8. Structures of dTAG and aTAG-based PHICS.

References

[1] Hua, L. *et al.* Beyond Proteolysis-Targeting Chimeric Molecules: Designing Heterobifunctional Molecules Based on Functional Effectors. *J. Med. Chem.* **2022**, *65*, 8091–8112.

[2] Vlastaridis, P.; Kyriakidou, P.; Chaliotis, A.; Van de Peer, Y.; Oliver, S. G.; Amoutzias, G. D. Estimating the Total Number of Phosphoproteins and Phosphorylation Sites in Eukaryotic Proteomes. GigaScience 2017, 6, giw015.

[3] Nishi, H., Shaytan, A. & Panchenko, A. R. Physicochemical mechanisms of protein regulation by phosphorylation. *Front. Genet.* **2014**, *5*, 1–10.

[4] Ardito, F., Giuliani, M., Perrone, D., Troiano, G. & Muzio, L. Lo. The crucial role of protein phosphorylation in cell signalingand its use as targeted therapy (Review). *Int. J. Mol. Med.* **2017**, *40*, 271–280.

[5] Morris, M.; Knudsen, G. M.; Maeda, S.; Trinidad, J. C.; Ioanoviciu, A.; Burlingame, A. L.; Mucke, L. Tau Post-Translational Modifications in Wild-Type and Human Amyloid Precursor Protein Transgenic Mice. Nat. Neurosci. 2015, 18, 1183–1189.

[6] Siriwardena, S. U. *et al.* Phosphorylation-Inducing Chimeric Small Molecules. *J. Am. Chem. Soc.* **2020**, *142*, 14052–14057.

[7] Yamazoe, S.; Tom, J.; Fu, Y.; Wu, W.; Zeng, L.; Sun, C.; Liu,
Q.; Lin, J.; Lin, K.; Fairbrother, W. J.; Staben, S. T. Heterobifunctional Molecules Induce Dephosphorylation of Kinases-a Proof of Concept Study. J. Med. Chem. 2020, 63, 2807–2813.

[8] Chen, P. H.; Hu, Z.; An, E.; Okeke, I.; Zheng, S.; Luo, X.; Gong, A.; Jaime-Figueroa, S.; Crews, C. M. Modulation of Phosphoprotein Activity by Phosphorylation Targeting Chimeras (PhosTACs). ACS Chem. Biol. 2021, 16, 2808–2815.
8108

[9] Zhang, Q. *et al.* Protein Phosphatase 5-Recruiting Chimeras for Accelerating Apoptosis-Signal-Regulated Kinase 1 Dephosphorylation with Antiproliferative Activity. *J. Am. Chem. Soc.* **2023**, *145*, 1118–1128.

[10] Ayala-Aguilera, C. C.; Valero, T.; Lorente-Macías, Á .; Baillache, D. J.; Croke, S.; Unciti-Broceta, A. Small molecule kinase inhibitor drugs (1995–2021): medical indication, pharmacology, and synthesis. J. Med. Chem. **2022**, *65* (2), 1047–1131.

[11] Zorn, J. A.; Wells, J. A. Turning enzymes ON with small molecules. Nat. Chem. Biol. **2010**, *6* (3), 179–188.

[12] González, L. *et al.* Characterization of p38α autophosphorylation inhibitors that target the non-canonical activation pathway. *Nat. Commun.* **2023**, *14*, 3318.

[13] Sterling, T. & Irwin, J.J. ZINC 15--Ligand Discovery for Everyone. J Chem Inf Model **2015**, *55*, 2324-37.

[14] Němec, V., Schwalm, M. P., Müller, S. & Knapp, S. PROTAC degraders as chemical probes for studying target biology and target validation. *Chem. Soc. Rev.* **2022**, *51*, 7971–7993.

[15] Slam, K. The Bump-and-Hole Tactic: Expanding the Scope of Chemical Genetics. *Cell Chem. Biol.* **2018**, *25*, 1171–1184.

[16] Nabet, B. *et al.* The dTAG system for immediate and target-specific protein degradation. *Nat. Chem. Biol.* **2018**, *14*, 431–441.

[17] Bond, A. G. *et al.* Development of BromoTag: A "Bump-and-Hole"–PROTAC System to Induce Potent, Rapid, and Selective Degradation of Tagged Target Proteins. *J. Med. Chem.* **2021**, *64*, 15477–15502.

[18] Nishimura, K., Fukagawa, T., Takisawa, H., Kakimoto, T. & Kanemaki, M. An auxin-based degron system for the rapid depletion of proteins in nonplant cells. *Nat. Methods* **2009**, *6*, 917–922.

[19] Veits, G. K. *et al.* Development of an AchillesTAG degradation system and its application to control CAR-T activity. *Curr. Res. Chem. Biol.* **2021**, *1*, 100010.

[20] Compounds for the degradation of BRD9 or MTH1. Current Patent Assignee: C4 THERAPEUTICS INC - US2021/198256, 2021, A1 Patent Family Members: EP3846800 A1; US2021/198256 A1; WO2020/51235 A1; EP3846800 A4

[21] Le Gallic L, Sgouras D, Beal G Jr, Mavrothalassitis G. Transcriptional repressor ERF is a Ras/mitogen-activated protein kinase target that regulates cellular proliferation. Mol Cell Biol. **1999**;*19*(6):4121-33.

Chapter 7.

Conclusions

7. Conclusions

1.- The design and synthesis of several oestrogen receptor (ER) PROTACs based on 4-hydroxytamoxifen (4OHT) is described. A family of compounds based on pomalidomide and polyethylene glycol linkers were synthesized, of which **TAM-PO-1** and **TAM-PO-3** are the most potent. Attempts to synthesize better analogues of **TAM-PO-3** by using modified warheads or alkyl linkers did not yield improved compounds. The synthesis of compounds based on a Von-Hippel Lindau (VHL) ligand and alkyl linkers afforded **TAM-VHL-1** and **TAM-VHL-2**, two potent ER degraders, with DC_{50} values of 4.5 nM and 5.3 nM respectively.

2.- The synthesis of potential PROTACs targeting the tousled-like kinase (TLK) is described. A kinase inhibitor displaying activity towards TLK2 was derivatized into three different warheads, amenable to PROTAC synthesis. The kinase-targeting warheads were combined with different VHL and CRBN-targeting fragments of different linker length and composition. In total, 24 potential TLK degraders were synthesized. Unfortunately, none of the compounds was able to induce TLK degradation in cells.

3.a- Compound **NR-7h**, a p38 PROTAC previously developed in our laboratory, was subjected to a structure-activity relationship study in order to find analogues with improved water solubility. Modification of the linker, by introduction of more polar groups, resulted in PROTACs with reduced potency, lacking *in vivo* activity. Modification of the E3 ligase recruiter, using a VHL-targeting fragment, afforded compounds maintaining the potency of **NR-7h**, and improving its water solubility. **NR-11c** is the most potent of the series, displaying a DC_{50} value of 12 nM. *In vivo* studies in mice of **NR-11c** showed that the compound displays potent degradation of p38α exclusively in the liver, suggesting that the compound is being retained in the organ.

3.b- Analogues of **NR-11c** bearing different linker compositions were synthesized to study the effect of the linker in the compound's activity and distribution. In total, 16 analogues were synthesized. Two compounds, **NR-13c** and **NR-15**, display excellent p38α degradation. This study shows the importance of the linker in determining PROTAC activity; linkers with a similar linker length but different degrees of rigidity and heterocyclic components provided a big variability in PROTAC activity. Future work will consist in testing **NR-13c** and **NR-15** *in vivo* to study their distribution. Moreover, computational studies are currently under way, in order to study the interaction between the structures of **NR-13c** and **NR-15** with p38α and the VHL protein.

4.a- An allosteric ligand of p38 was used as a kinase-recruiting warhead in the synthesis of potential Phosphorylation Inducing Chimaeras (PHICS). The ligand was derivatized at two different points and used to construct PROTACs **6-7a-c** and **6-12a-c**, in order to test its ability to engage p38. However, none of the compounds proved to be active, and the use of this warhead was discontinued.

4.b- A warhead based on a PKC activator was used in the synthesis of compounds **6-31a-c,** potential PHICS targeting the phosphorylation of p38. These compounds, however, did not induce phosphorylation of p38 in cells.

4.c- Potential PHICS based on a PKC activator and aTAG or dTAG ligands were synthesized. The ability of the compounds to induce phosphorylation of a protein of interest was studied in cells overexpressing constructs of ERF with the aTAG or dTAG. Compounds **6-39a-d**, based on the dTAG ligand, increase the phosphorylation levels of the ERF-dTAG constructs with similar activity. Compounds **6-39a-d**, based on the aTAG ligand, induce phosphorylation of ERF-aTAG constructs, being **6-39a** and **6-39c** the most potent PHICS of the series.

Chapter 8.

Experimental Section

8. Experimental Section

8.1. General Methods

Unless otherwise stated, reagents and solvents were purchased from commercial suppliers and used without further purification. Anhydrous THF, Et_2O and DCM were obtained from a solvent purification system (SPS PS-MD-3). Reactions requiring anhydrous conditions were performed in dried glassware under inert nitrogen atmosphere. Thin layer chromatography was carried out using TLC-aluminium sheets with silica gel (Merck 60 F_{254}). Preparative thin layer chromatography was carried out when necessary using TLC-aluminium sheets (Silica Gel 60 F_{254}). Silica gel chromatography was performed using 35-70 mm silica or an automated chromatography system (Interchim PuriFlash 430). Reaction temperature was controlled using baths of ice in water (0 °C), dry ice on acetone (-78 °C), isopropanol bath controlled by a cryocooler (EK 90 Immersion Cooler Thermo Scientific) or heating mantels with silica oil baths.

Instrumentation

NMR spectra were recorded at 23 °C on NMR spectrometers of the *Centres Científics I Tecnològics de la Universtat de Barcelona*. Mercury 400 MHz, Varian VNMRS 400 MHz, Varian VNMRS 500 MHz or Brucker 600 MHz apparatus were employed. ^{1}H and ^{13}C spectra were referenced to internal solvent resonances.

High resolution ESI-MS spectra were recorded in a LTQ-FT Ultra (Thermo Scientific) at the Institute for Research in Biomedecine (IRB Barcelona).

IR spectra were recorded in a Thermo Nicolet 6700 FT-IR spectrometer at the *Departament de Química Orgànica i Inorgànica de la Universitat de Barcelona*, using an ATR system.

HPLC chromatography was performed on a Hewlett-Packard 1050 equipment, with UV detection using a Kinetix EVO C18 50x 4.6 mm, 2.6 μm column (Standard gradient: 10 mM NH_4CO_3 / MeCN (95:5) – (0-100)).

Microwave radiation was applied to reactions where stated using a CEM Discover microwave unit or a Biotage Initiator+ unit.

Melting points were determined using a Büchi M-640 apparatus.

8.2. General Prodecures

General method for amide formation 1 – EDC

A flask charged with the coresponding carboxylic acid (1 eq.), oxyma (1.5 eq.), EDC·HCl (1.5 eq.) and DMF (0.2 M) was purged under nitrogen and stirred at 0 °C and DIPEA (2.5 eq.) was added dropwise. After 15 min the corresponding amine (1.1 eq.) dissolved in a minimum ammount of DMF was added

to the reaction mixture and left stirring overnight. Ethyl acetate and water were added, then the aqueous layer was re-extracted using ethyl acetate, the combined organic layers washed with brine and $CuSO_4$, dried over $MgSO_4$, and then concentrated under reduced pressure.

General method for amide formation 2 – HATU

A flask was charged with the amine or amine hydrochloride (1 eq.), the corresponding carboxylic acid (1 eq.), DMF (0.25 M) and DIPEA (4 eq.). The reaction mixture was stirred at 0 °C and HATU (1.1 eq.) was added. The reaction mixture was let to warm up to room temperature during 2 to 5 h. After reaction completion, water and ethyl acetate were added, the aqueous layer was re-extracted using ethyl acetate, the combined organic layers washed with brine and $CuSO_4$, dried over $MgSO_4$, and then concentrated under reduced pressure.

General method for amide formation 3 – DIC

The carboxylic acid (1 equiv) was dissolved in anhydrous DMF, cooled to 0 °C, then added Oxyma (ethyl cyanohydrox- yiminoacetate) (1.66 equiv) and DIC (N,N0-Diisopropylcarbodii- mide) (1.66 equiv). After 15 min the solution turned yellow, then TEA (1.66 mL) was added, followed by the corresponding amine starting material (1.1 equiv). The reaction was left 18 hours before quenching with water. The mixture was separated between DCM and water, then the aqueous layer re-extracted using DCM. The combined organic layers were washed with brine, dried over magnesium sulphate, and then concentrated under reduced pressure.

General method for CuAAC

A flask was charged with the alkyne (1 eq.), the corresponding azido partner (1 eq.), $CuSO_4$ pentahydrate (0.1 eq.), sodium ascorbate (0.2 eq.), H_2O/*tert*-butanol 2:1 (0.026 M), and acetic acid (2 eq.) and sonicated until a homogeneous suspension was observed and stirred overnight at 35 °C. Brine and dichloromethane were added to the reaction mixture, the aqueous layer was extracted with dichloromethane, dried over $MgSO_4$ and concentrated under reduced pressure.

8.3. Experimental Section – ER PROTACs

2-(2,6-dioxopiperidin-3-yl)-4-fluoroisoindoline-1,3-dione (3-10)

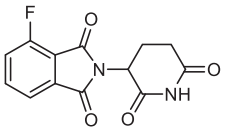

A boiling tube charged with 4-fluoroisobenzofuran-1,3-dione (1.2 g, 7.22 mmol), 2,6-dioxopiperidin-3-aminium chloride (1.33 g, 8.092 mmol), potassium acetate (1.49 g, 15.17 mmol) and acetic acid (16 mL) was sealed and heated to 110 °C for 24h. The reaction mixture was then concentrated and the

dark blue crude solid obtained was purified by flash column chromatography. The product was eluted at 4% MeOH/DCM, affording a white solid (1.75 g, 6.34 mmol, 88%).

^{1}H NMR (400 MHz, $CDCl_3$) δ 8.10 (s, 1H), 7.77 (ddd, *J* = 8, 7, 4 Hz, 1H), 7.71 (dt, *J* = 7, 1 Hz, 1H), 7.43 (td, *J* = 9, 1 Hz, 1H), 5.02 – 4.95 (m, 1H), 2.96 – 2.70 (m, 3H), 2.20 – 2.12 (m, 1H) ppm **^{13}C NMR** (101 MHz, $CDCl_3$) δ 171.08, 168.55, 166.38 (d, *J* = 3.0 Hz), 164.21, 157.91 (d, *J* = 266.7 Hz), 137.20 (d, *J* = 7.6 Hz), 133.99, 122.94 (d, *J* = 19.7 Hz), 120.10 (d, *J* = 3.6 Hz), 117.74 (d, *J* = 12.6 Hz), 50.33, 31.96, 27.40, 21.96.

4-fluoro-2-(1-methyl-2,6-dioxopiperidin-3-yl)isoindoline-1,3-dione (3-10-Me)

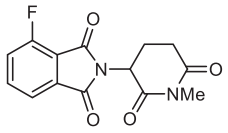

A round flask was charged with 2-(2,6-dioxopiperidin-3-yl)-4-fluoroisoindoline-1,3-dione (400 mg, 1.45 mmol), K_2CO_3 (400 mg, 2.90 mmol), iodomethane (137 µL, 1.59 mmol) and DMF (10 mL) was purged under nitrogen and stirred overnight at room temperature. Ethyl acetate and water were added to the reaction mixture, then the aqueous layer was re-extracted using ethyl acetate (x2), the combined organic layers washed with brine (x3), $CuSO_4$ (x2) and brine (x1), dried over $MgSO_4$, and then concentrated under reduced pressure. The crude was purified by flash column chromatography, the product was eluted at 45% ethyl acetate/hexanes as a yellowish solid (403 mg, 1.39 mmol, 96%).

^{1}H NMR (400 MHz, $CDCl_3$) δ 7.76 (ddd, *J* = 8.3, 7.4, 4.3 Hz, 1H), 7.69 (ddd, *J* = 7.4, 0.9, 0.5 Hz, 1H), 7.46 – 7.37 (m, 1H), 5.02 – 4.93 (m, 1H), 3.20 (s, 3H), 3.05 – 2.95 (m, 1H), 2.86 – 2.72 (m, 2H), 2.16 – 2.08 (m, 1H).

4-((2-(2-azidoethoxy)ethyl)amino)-2-(2,6-dioxopiperidin-3-yl)isoindoline-1,3-dione (3-11a)

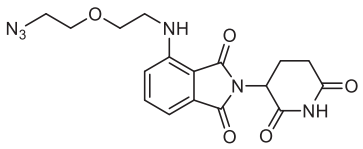

To a solution of **3-10** (4, 96 mg, 0.35 mmol) in NMP (4 mL) in a boiling tube was added 2-(2-azidoethoxy)ethan-1-amine (50 mg, 0.38 mmol) and DIPEA (121 µL, 0.69 mmol), sealed, then heated to 120 °C for 3 h. Ethyl acetate and water were added to the reaction mixture, then the aqueous layer was re-extracted using ethyl acetate (x2), the combined organic layers washed with brine (x3), $CuSO_4$ (x2) and brine (x1), dried over $MgSO_4$, and then concentrated under reduced pressure. The crude was filtered through silica (1% MeOH/DCM) and used without further purification.

4-((2-(2-(2-azidoethoxy)ethoxy)ethyl)amino)-2-(2,6-dioxopiperidin-3-yl)isoindoline-1,3-dione (3-11b)

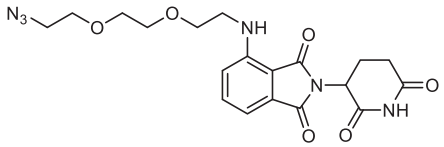

To a solution of **3-10** (300 mg, 1.09 mmol) in NMP (15 mL) in a boiling tube was added 2-(2-(2-azidoethoxy)ethoxy)ethan-1-amine (209 mg, 1.2 mmol) and DIPEA (240 µL, 1.38 mmol), sealed, then heated to 120 °C for 12 h. Ethyl acetate and water were added to the reaction mixture, then the aqueous layer was re-extracted using ethyl acetate (x2), the combined organic layers washed with brine (x3), $CuSO_4$ (x2) and brine (x1), dried over $MgSO_4$, and then concentrated under reduced pressure. . The crude was purified by flash column chromatography, the product was eluted at 2% MeOH/DCM as a yellow solid (210 mg, 0.49 mmol, **45%**).

^{1}H NMR (400 MHz, $CDCl_3$) δ 8.68 (s, 1H), 7.45 (ddd, *J* = 8.6, 7.1, 0.6 Hz, 1H), 7.06 (dd, *J* = 7.1, 0.6 Hz, 1H), 6.89 (d, *J* = 8.5 Hz, 1H), 6.47 (t, *J* = 5.7 Hz, 1H), 4.98 – 4.87 (m, 1H), 3.74 – 3.68 (m, 2H), 3.67 – 3.61 (m, 6H), 3.45 (q, *J* = 5.5 Hz, 2H), 3.35 (dd, *J* = 5.6, 4.5 Hz, 2H), 2.89 – 2.65 (m, 3H), 2.11 – 2.04 (m, 1H). **^{13}C NMR** (101 MHz, $CDCl_3$) δ 171.60, 169.36, 168.72, 167.69, 146.87, 136.06, 132.54, 116.85, 111.65, 110.30, 70.73, 70.72, 70.12, 69.61, 50.72, 48.91, 42.39, 31.44, 22.79. **IR (ATR):** 3092, 2857, 2092, 1692 cm^{-1}. **HRMS (ESI):** calc. $[M+H]^+$: 431.16736; found: 431.16719. **M_p:** 103°C.

4-((2-(2-(2-(2-azidoethoxy)ethoxy)ethoxy)ethyl)amino)-2-(2,6-dioxopiperidin-3-yl)isoindoline-1,3-dione (3-11c)

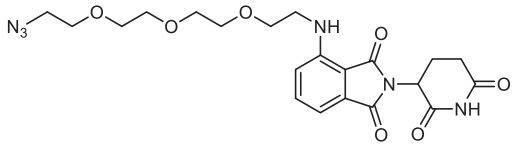

To a solution of **3-10** (75 mg, 0.27 mmol) in NMP (3 mL) in a boiling tube was added 2-(2-(2-(2-azidoethoxy)ethoxy)ethoxy)ethan-1-amine (65 mg, 0.30 mmol) and DIPEA (95 µL, 0.54 mmol), sealed, then heated to 120 °C for 12 h. Ethyl acetate and water were added to the reaction mixture, then the aqueous layer was re-extracted using ethyl acetate (x2), the combined organic layers washed with brine (x3), $CuSO_4$ (x2) and brine (x1), dried over $MgSO_4$, and then concentrated under reduced pressure. . The crude was purified by flash column chromatography, the product was eluted at 1% MeOH/DCM as a yellow solid (43 mg, 0.09 mmol, **33%**).

^{1}H NMR (400 MHz, $CDCl_3$) δ 8.46 (NH, 1H), 7.47 (dd, *J* = 9, 7 Hz, 1H), 7.08 (d, *J* = 7 Hz, 1H), 6.91 (d, *J* = 9 Hz, 1H), 6.47 (NH, t, *J* = 6 Hz, 1H), 4.91 (dd, *J* = 12, 5 Hz, 1H), 3.71 (t, *J* = 5 Hz, 2H), 3.68 – 3.62 (m, 10H), 3.46 (q, *J* = 5 Hz, 2H), 3.36 (t, *J* = 5 Hz, 2H), 2.90 – 2.66 (m, 3H), 2.13 – 2.06 (m, 1H) ppm. **^{13}C NMR** (101 MHz, $CDCl_3$) δ 171.4, 169.4, 168.6, 167.7, 146.9, 136.1, 132.6, 116.9, 111.7, 110.3, 70.8, 70.8, 70.1, 69.6, 50.8, 49.0, 42.5, 31.5,

22.9 ppm. **IR (Film):** 3390, 2107, 1698, 1624, 1324, 1115 cm^{-1}. **HRMS (ESI):** calc. for $[C_{21}H_{27}O_7N_6]^+$: 475.1936; found: 475.1937. **M_p:** 85°C.

4-((14-azido-3,6,9,12-tetraoxatetradecyl)amino)-2-(2,6-dioxopiperidin-3-yl)isoindoline-1,3-dione (3-11d)

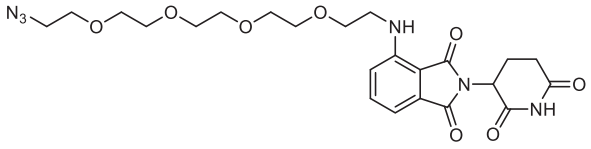

To a solution of **3-10** (100 mg, 0.36 mmol) in NMP (3 mL) in a boiling tube was added 14-azido-3,6,9,12-tetraoxatetradecan-1-amine (106 mg, 0.40 mmol) and DIPEA (125 µL, 0.72 mmol), sealed, then heated to 120 °C for 3 h. Ethyl acetate and water were added to the reaction mixture, then the aqueous layer was extracted using ethyl acetate (x2), the combined organic layers washed with brine (x3), $CuSO_4$ (x2) and brine (x1), dried over $MgSO_4$, and then concentrated under reduced pressure. The crude was filtered through silica (1% MeOH/DCM) and used without further purification.

4-((2-(2-(2-(2-azidoethoxy)ethoxy)ethoxy)ethyl)amino)-2-(1-methyl-2,6-dioxopiperidin-3-yl)isoindoline-1,3-dione (3-11c-Me)

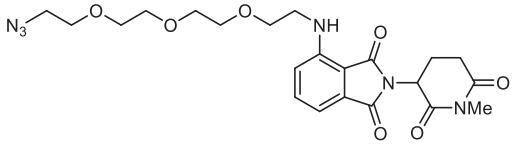

To a solution of **3-10-Me** (100 mg, 0.34 mmol) in NMP (3 mL) in a boiling tube was added 2-(2-(2-(2-azidoethoxy)ethoxy)ethoxy)ethan-1-amine (84 mg, 0.37 mmol) and DIPEA (119 µL, 0.68 mmol), sealed, then heated to 120 °C for 12 h. Ethyl acetate and water were added to the reaction mixture, then the aqueous layer was re-extracted using ethyl acetate (x2), the combined organic layers washed with brine (x3), $CuSO_4$ (x2) and brine (x1), dried over $MgSO_4$, and then concentrated under reduced pressure. The crude was purified by flash column chromatography, the product was eluted at 1% MeOH/DCM as a yellow oil (40 mg, 0.08 mmol, **24%**).

^{1}H NMR (400 MHz, $CDCl_3$) δ 7.47 (ddd, *J* = 8.6, 7.1, 0.6 Hz, 1H), 7.08 (dd, *J* = 7.1, 0.6 Hz, 1H), 6.91 (d, *J* = 8.4 Hz, 1H), 6.46 (t, *J* = 5.9 Hz, 1H), 4.95 – 4.84 (m, 1H), 3.77 – 3.57 (m, 14H), 3.46 (q, *J* = 5.6 Hz, 2H), 3.39 – 3.32 (m, 2H), 3.19 (s, 0H), 2.99 – 2.90 (m, 1H), 2.79 – 2.70 (m, 2H), 2.11 – 2.04 (m, 1H). **^{13}C NMR** (101 MHz, $CDCl_3$) δ 171.4, 169.5, 169.1, 167.9, 146.9, 136.1, 132.6, 116.8, 111.7, 110.5, 70.8, 70.1, 69.6, 50.8, 49.7, 42.5, 32.0, 27.3, 22.2. **IR (ATR):** 2869, 2096, 1701 cm^{-1}. **HRMS (ESI):** calc. $[M+H]^+$: 489.20922; found: 489.20883.

Metyhl 3-bromo-2-(bromomethyl)benzoate (3-12)

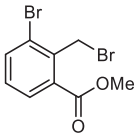

Methyl 3-bromo-2-methylbenzoate (200 mg, 0.87 mmol), NBS (185 mg, 1.04 mmol) and VAZO (1,1'-(diazene-1,2-diyl)bis(cyclohexane-1-carbonitrile), 21 mg, 0.09 mmol) in benzene (2 mL) was heated at 90 °C for 6 h. The solvent was removed under reduced pressure then the crude was purified by column chromatography, affording an off white solid eluted at 10% AcOEt/hexane (256 mg, **96%**).

^{1}H NMR (400 MHz, $CDCl_3$) δ 7.9 (dd, *J* = 7.8, 1.3 Hz, 1H), 7.8 (dd, *J* = 8.0, 1.3 Hz, 1H), 7.2 (t, *J* = 7.9 Hz, 2H), 4.0 (s, 4H), 1.6 (d, *J* = 0.6 Hz, 2H).

3-(4-bromo-1-oxoisoindolin-2-yl)piperidine-2,6-dione (3-13)

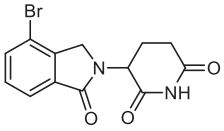

To a solution of Metyhl 3-bromo-2-(bromomethyl)benzoate (288 mg, 0.94 mmol) in MeCN (10 mL) was added triethylamine and 2,6-dioxopiperidin-3-aminium chloride (188 mg, 1.41 mmol) then heated in a pressure tube at 85 °C for 22 h. The solvent was evaporated under reduced pressure and the residue was purified by column chromatography. The product was eluted at 7% MeOH/DCM as a white solid (290 mg, **96%**).

^{1}H NMR (400 MHz, DMSO-d_6) δ 11.0 (s, 1H), 7.9 (dd, *J* = 7.9, 0.9 Hz, 1H), 7.8 (dd, *J* = 7.5, 0.9 Hz, 1H), 7.5 (t, *J* = 7.7 Hz, 1H), 5.1 (dd, *J* = 13.3, 5.1 Hz, 1H), 4.4 (d, *J* = 17.6 Hz, 1H), 4.3 (d, *J* = 17.5 Hz, 1H), 2.9 (ddd, *J* = 17.2, 13.7, 5.4 Hz, 1H), 2.6 – 2.5 (m, 2H), 2.0 (dtd, *J* = 12.8, 5.4, 2.3 Hz, 1H).

***tert*-butyl (5-(2-(2,6-dioxopiperidin-3-yl)-1-oxoisoindolin-4-yl)pent-4-yn-1-yl)carbamate (3-14)**

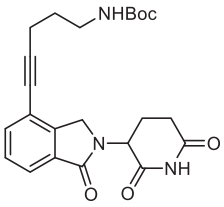

A flask charged with 3-(4-bromo-1-oxoisoindolin-2-yl)piperidine-2,6-dione (**3**, 41 mg, 0.13 mmol), CuI (5 mg, 0.03 mmol), $Pd(PPh_3)_4$ (18 mg, 0.03 mmol) and DMF (4 mL) was degassed with nitrogen, added trimethylamine (1.75 mL) and stirred at 100 °C overnight. The mixture was cooled to room temperature, filtered through celite, washed with AcOEt then concentrated under reduced pressure. Ethyl acetate and water were added, then the aqueous layer was re-extracted using ethyl acetate , the combined organic layers washed with brine and copper sulfate, dried over $MgSO_4$, and then

concentrated under reduced pressure. The crude was purified by flash column chromatography, the product was eluted at 100% AcOEt, affording the product as an incolor oil (48 mg, **72%**).

^{1}H NMR (400 MHz, $CDCl_3$) δ 7.9 – 7.8 (m, 1H), 7.7 – 7.6 (m, 1H), 7.6 – 7.5 (m, 1H), 5.3 – 5.2 (m, 1H), 4.5 – 4.2 (m, 2H), 3.3 – 3.3 (m, 2H), 2.9 – 2.8 (m, 2H), 2.5 (t, *J* = 6.9 Hz, 2H), 2.4 – 2.4 (m, 1H), 2.2 (ddt, *J* = 10.5, 5.2, 2.8 Hz, 1H), 1.8 (p, *J* = 7.0 Hz, 2H), 1.4 (s, 9H).

3-(4-(5-aminopent-1-yn-1-yl)-1-oxoisoindolin-2-yl)piperidine-2,6-dione hydrochloride (3-17)

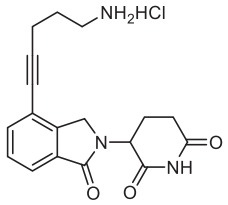

A flask was charged with tert-butyl (5-(2-(2,6-dioxopiperidin-3-yl)-1-oxoisoindolin-4-yl)pent-4-yn-1-yl)carbamate (**8**, 136 mg, 0.31 mmol) and HCl 4N in dioxane (3 mL). After 3h the reaction mixture was concentrated under reduced pressure affording a white solid. The product was used without further purification (90mg, **80%**).

6-azido-N-(5-(2-(2,6-dioxopiperidin-3-yl)-1-oxoisoindolin-4-yl)pent-4-yn-1-yl)hexanamide (3-18)

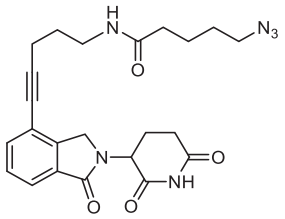

A flask charged with 6-azidohexanoic acid (11 mg, 0.07 mmol), ethyl cyano(hydroxyimino)acetate (17 mg, 0.12 mmol), EDC·HCl (23 mg, 0.12 mmol) and DMF (1 mL) was purged under nitrogen and stirred at 0 °C and DIPEA (31 µL, 0.18 mmol) was added dropwise. After 15 min 3-(4-(5-aminopent-1-yn-1-yl)-1-oxoisoindolin-2-yl)piperidine-2,6-dione hydrochloride (**11**, 30 mg, 0.08 mmol) dissolved in DMF (1 mL) was added to the reaction mixture and stirred overnight. Ethyl acetate and water were added, then the aqueous layer was re-extracted using ethyl acetate, the combined organic layers washed with brine, $CuSO_4$ dried over $MgSO_4$, and then concentrated under reduced pressure. The crude was purified by flash column chromatography, the product was eluted at 3% MeOH/DCM as a colourless oil (26 mg, **77%**).

^{1}H NMR (400 MHz, $CDCl_3$) δ 7.8 (dd, *J* = 7.6, 1.1 Hz, 1H), 7.6 (dd, *J* = 7.6, 1.1 Hz, 1H), 7.4 (t, *J* = 7.6 Hz, 1H), 5.7 (s, 1H), 5.2 (dd, *J* = 13.3, 5.0 Hz, 1H), 4.6 – 4.4 (m, 2H), 3.5 – 3.4 (m, 2H), 3.3 (t, *J* = 6.8 Hz, 2H), 3.0 – 2.8 (m, 3H), 2.5 (t, *J* = 6.9 Hz, 2H), 2.3 – 2.1 (m, 3H), 1.9 – 1.8 (m, 2H), 1.7 – 1.6 (m, 4H), 1.5 – 1.4 (m, 2H). **^{13}C NMR** (101 MHz, CD_3OD) δ 176.3, 175.1, 159.2, 145.5, 135.8, 129.9, 129.6, 123.8, 120.8, 91.0, 77.7, 54.8, 53.7, 52.3, 39.4, 36.9, 32.4, 29.6, 29.3, 27.4, 26.5, 24.0, 17.7.

tert-butyl (5-(2-(2,6-dioxopiperidin-3-yl)-1-oxoisoindolin-4-yl)pentyl)carbamate

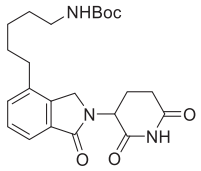

A flask was charged with tert-butyl (5-(2-(2,6-dioxopiperidin-3-yl)-1-oxoisoindolin-4-yl)pent-4-yn-1-yl)carbamate (**8**, 48 mg, 0.11 mmol), Pd/C (24 mg, 0.01 mmol) and ethanol/DCM 1:2 (3.75 mL), degassed with nitrogen and stirred under an hydrogen atmosphere for 24h. The crude was diluted in methanol, filtered through celite and purified by flash column chromatography, the product was eluted at 3% MeOH/DCM as an incolor oil (15 mg, **32%**).

^{1}H NMR (400 MHz, Chloroform-*d*) δ 8.2 (s, 1H), 7.8 – 7.6 (m, 1H), 7.5 – 7.3 (m, 2H), 5.3 (dd, *J* = 13.3, 5.2 Hz, 1H), 4.5 (s, 1H), 4.5 – 4.3 (m, 2H), 3.1 (q, *J* = 6.9 Hz, 2H), 3.0 – 2.8 (m, 2H), 2.7 – 2.6 (m, 2H), 2.4 (qd, *J* = 13.1, 5.2 Hz, 1H), 2.2 (dtd, *J* = 13.0, 5.2, 2.7 Hz, 1H), 1.7 (p, *J* = 7.7 Hz, 2H), 1.6 – 1.5 (m, 2H), 1.5 – 1.3 (m, 11H).

3-(4-(5-aminopentyl)-1-oxoisoindolin-2-yl)piperidine-2,6-dione hydrochloride (3-15)

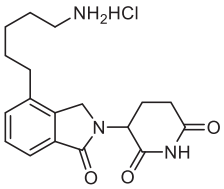

A flask was charged with tert-butyl (5-(2-(2,6-dioxopiperidin-3-yl)-1-oxoisoindolin-4-yl)pentyl)carbamate (15 mg, 0.03 mmol) and HCl 4N in dioxane (1 mL). After 3h the reaction mixture was concentrated under reduced pressure affording an incolor oil, which was used without further purification.

5-azido-N-(5-(2-(2,6-dioxopiperidin-3-yl)-1-oxoisoindolin-4-yl)pentyl)pentanamide (3-16)

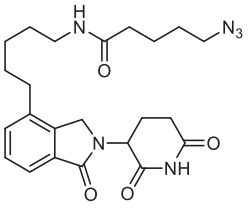

A flask charged with 6-azidohexanoic acid (7 mg, 0.04 mmol), ethyl cyano(hydroxyimino)acetate (7 mg, 0.06 mmol), EDC·HCl (13 mg, 0.06 mmol) and DMF (1 mL) was purged under nitrogen and stirred at 0 °C and DIPEA (29 µL, 0.17 mmol) was added dropwise. After 15 min 3-(4-(5-aminopentyl)-1-oxoisoindolin-2-yl)piperidine-2,6-dione hydrochloride (**9**, 18 mg, 0.05 mmol) dissolved in DMF (1 mL) was added to the reaction mixture and stirred overnight. Ethyl acetate and

water were added, then the aqueous layer was re-extracted using ethyl acetate, the combined organic layers washed with brine, $CuSO_4$, dried over $MgSO_4$, and then concentrated under reduced pressure. The crude was used without further purification.

^{1}H NMR (400 MHz, $CDCl_3$) δ 8.2 (s, 1H), 7.8 – 7.6 (m, 1H), 7.5 – 7.3 (m, 2H), 5.3 (dd, *J* = 13.3, 5.2 Hz, 1H), 4.5 (s, 1H), 4.5 – 4.3 (m, 2H), 3.1 (q, *J* = 6.9 Hz, 2H), 3.0 – 2.8 (m, 2H), 2.7 – 2.6 (m, 2H), 2.4 (qd, *J* = 13.1, 5.2 Hz, 1H), 2.2 (dtd, *J* = 13.0, 5.2, 2.7 Hz, 1H), 1.7 (p, *J* = 7.7 Hz, 2H), 1.6 – 1.5 (m, 2H), 1.5 – 1.3 (m, 11H).

tert-butyl (S)-(1-(4-bromophenyl)ethyl)carbamate (3-25)

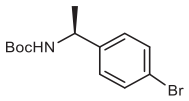

A flame dried flask was charged with **3-24** (1g, 5 mmol), THF (4 ml) and cooled down at 0 °C. Boc anhydride (1.2 g, 5.5 mmol) in THF (3 mL) and trimethylamine (0.76 mL, 5.5 mmol) were added and the reaction mixture was let to warm up at room temperature overnight. Water and ethyl acetate were added to the reaction mixture, the aqueous phase extracted with ethyl acetate, the organic layers combined and washed with brine and dried over $MgSO_4$. The product was dried under reduced pressure to afford **3-25** (1.5 g, **quant.**) as a white solid.

^{1}H NMR (400 MHz, $CDCl_3$) δ 7.45 (d, J = 8.5 Hz, 2H), 7.17 (d, J = 8.2 Hz, 2H), 4.74 (s, 1H), 1.55 (s, 3H), 1.41 (s, 9H).

tert-butyl (S)-(1-(4-(4-methylthiazol-5-yl)phenyl)ethyl)carbamate (3-26)

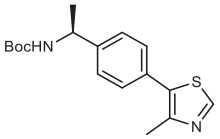

A pressure flask was charged with **3-25** (200 mg, 0.66 mmol), $Pd(OAc)_2$ (1.5 mg, 0.06 mmol) and DMAc (1 mL). KOAc (131 mg, 1.33 mmol) and 4-methyltiazole (0.12 mL, 1.33 mmol) were added and the reaction mixture was stirred at 150 °C for 3 hours. The reaction mixture was filtrated through celite and washed with AcOEt. Water was added and the aqueous phase was washed with AcOEt. The organic layers were combined, washed with brine (x5) and dried over $MgSO_4$. The crude was dried under reduced pressure and purified by flash column chromatography. The product was eluted at 30% AcOEt/Hexane, reported as a yellowish solid (150 mg, **70%**).

^{1}H NMR (400 MHz, $CDCl_3$) δ 8.67 (s, 1H), 7.41 (d, J = 8.1 Hz, 2H), 7.36 (d, J = 8.1 Hz, 2H), 4.82 (s, 1H), 2.53 (s, 3H), 1.46 (d, J = 19.3 Hz, 12H).

(S)-1-(4-(4-methylthiazol-5-yl)phenyl)ethan-1-amine hydrochloride (3-26 HCl)

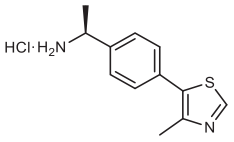

3-26 (690 mg, 2.16 mmol) was stirred in 5 mL HCl/dioxane 4N for 2 h. The solvent was then evaporated affording the hydrochloride salt as a yellowish solid (553 mg, **quant.**).

tert-butyl (4R)-4-hydroxy-2-(((S)-1-(4-(4-methylthiazol-5-yl)phenyl)ethyl)carbamoyl)pyrrolidine-1-carboxylate (3-27)

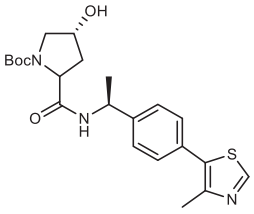

NUM was prepared following general method for amide formation 2, using **3-26 HCl** (553 mg, 2.58 mmol) and Boc-L-hydroxyproline (610 mg, 2.58 mmol). The crude was purified by flash column chromatography, product was eluted at 80% AcOEt/Hexane and reported as a white solid (605 mg, **65%**).

^{1}H NMR (400 MHz, CD_3OD) δ 8.88 (s, 1H), 7.44 (d, J = 3.3 Hz, 4H), 5.13 – 5.02 (m, 2H), 4.44 – 4.29 (m, 2H), 3.60 – 3.42 (m, 2H), 2.48 (s, 3H), 2.20 (s, 1H), 1.93 (ddd, J = 13.1, 8.6, 4.9 Hz, 1H), 1.51 (d, J = 7.1 Hz, 3H), 1.50 – 1.33 (m, 9H).

(4R)-4-hydroxy-N-((S)-1-(4-(4-methylthiazol-5-yl)phenyl)ethyl)pyrrolidine-2-carboxamide (3-27 HCl)

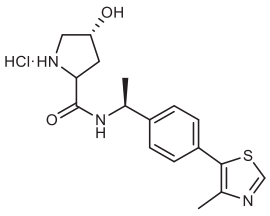

3-26 (646 mg, 1.76 mmol) was stirred in 5 mL of HCl/dioxane 4N for 2 h. The solvent was then evaporated affording the hydrochloride salt as a yellowish solid (650 mg, **quant.**).

tert-butyl ((S)-1-((2R,4R)-4-hydroxy-2-(((S)-1-(4-(4-methylthiazol-5-yl)phenyl)ethyl)carbamoyl)pyrrolidin-1-yl)-3,3-dimethyl-1-oxobutan-2-yl)carbamate (3-28)

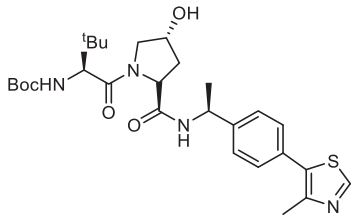

3-28 was prepared following general method for amide formation 2, using **3-27 HCl** (650mg, 1.76 mmol) and Boc-L-*tert*-leucine (407 mg, 1.76 mmol). The crude was purified by flash column chromatography, product was eluted at 75% AcOEt/Hexane and reported as a white solid (721 mg, 75%).

^{1}H NMR (400 MHz, $CDCl_3$) δ 8.67 (s, 1H), 7.58 (d, J = 8.2 Hz, 1H), 7.39 (q, J = 8.2 Hz, 4H), 5.21 (d, J = 8.9 Hz, 1H), 5.13 – 5.02 (m, 1H), 4.80 (t, J = 7.9 Hz, 1H), 4.51 (s, 1H), 4.18 (dd, J = 17.9, 10.2 Hz, 2H), 3.56 (d, J = 12.3 Hz, 1H), 2.76 (s, 1H), 2.62 (s, 1H), 2.14 – 1.97 (m, 1H), 1.51 – 1.38 (m, 12H), 1.05 (s, 9H).

(2R,4R)-1-((S)-2-amino-3,3-dimethylbutanoyl)-4-hydroxy-N-((S)-1-(4-(4-methylthiazol-5-yl)phenyl)ethyl)pyrrolidine-2-carboxamide hydrochloride (3-29)

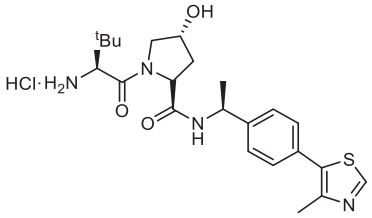

3-28 (700 mg, 1.28 mmol) was stirred in 5 mL of HCl/dioxane 4N for 2 h. The solvent was then evaporated affording the hydrochloride salt as an off-white solid (615 mg, **quant.**).

^{1}H NMR (400 MHz, DMSO-d_6) δ 9.0 (s, 1H), 8.6 (d, *J* = 7.7 Hz, 1H), 8.2 – 8.0 (m, 3H), 7.6 – 7.3 (m, 4H), 4.9 (t, *J* = 7.2 Hz, 1H), 4.5 (t, *J* = 8.4 Hz, 1H), 4.3 (s, 1H), 3.9 (d, *J* = 5.5 Hz, 1H), 3.7 (d, *J* = 11.1 Hz, 1H), 3.5 – 3.5 (m, 1H), 2.5 (s, 3H), 2.1 (dd, *J* = 12.8, 7.6 Hz, 1H), 1.8 (ddd, *J* = 13.1, 9.2, 4.3 Hz, 1H), 1.4 (d, *J* = 7.0 Hz, 3H), 1.0 (s, 9H).

The ^{1}H NMR spectra was consistent with that reported in the literature.[1]

(2R,4S)-1-((S)-2-amino-3,3-dimethylbutanoyl)-4-hydroxy-N-((S)-1-(4-(4-methylthiazol-5-yl)phenyl)ethyl)pyrrolidine-2-carboxamide hydrochloride (3-29*)

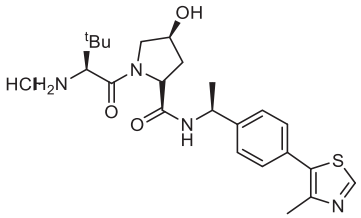

3-29* was prepared as **3-29**, using *cis*-hydroxyproline.

(2S,4R)-1-((S)-2-(4-azidobutanamido)-3,3-dimethylbutanoyl)-4-hydroxy-N-((S)-1-(4-(4-methylthiazol-5-yl)phenyl)ethyl)pyrrolidine-2-carboxamide (3-30a)

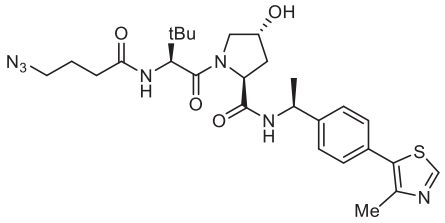

Prepared following general method for amide formation 1, using **3-29** (250 mg, 0.49 mmol) and 4-azidobutanoic acid (63 mg, 0.49 mmol). The crude was purified by flash column chromatography, the product was eluted at 10% methanol/DCM. Obtained as a white solid (50 mg, **60%**).

^{1}H NMR (400 MHz, $CDCl_3$) δ 8.67 (s, 1H), 7.44 – 7.32 (m, 5H), 6.34 (dd, *J* = 9.0, 3.1 Hz, 1H), 5.07 (p, *J* = 7.0 Hz, 1H), 4.69 (t, *J* = 7.8 Hz, 1H), 4.56 (d, *J* = 8.7 Hz, 1H), 4.50 (s, 1H), 4.03 (dt, *J* = 11.5, 1.9 Hz, 1H), 3.61 (dd, *J* = 11.2, 3.9 Hz, 1H), 3.31 (td, *J* = 6.5, 1.9 Hz, 2H), 2.51 (s, 3H), 2.46 (s, 1H), 2.36 – 2.19 (m, 2H), 2.10 – 1.99 (m, 1H), 1.87 (pd, *J* = 6.9, 3.7 Hz, 2H), 1.47 (d, *J* = 7.1 Hz, 3H), 1.03 (s, 9H). **^{13}C NMR** (101 MHz, $CDCl_3$) δ 172.6, 172.0, 169.8, 150.5, 148.6, 143.2, 131.1, 129.7, 126.6, 70.1, 58.7, 57.8, 56.8, 50.8, 49.0, 35.7, 35.3, 33.1, 26.6, 24.8, 22.3, 16.2. **IR (ATR):** 3272, 2971, 2098, 1615, 1066 cm^{-1}. **HRMS (ESI):** calculated for $[C_{25}H_{34}N_7O_4S]^+$: 528.2387, found: 528.2378

(2S,4S)-1-((S)-2-(4-azidobutanamido)-3,3-dimethylbutanoyl)-4-hydroxy-N-((S)-1-(4-(4-methylthiazol-5-yl)phenyl)ethyl)pyrrolidine-2-carboxamide (3-30a*)

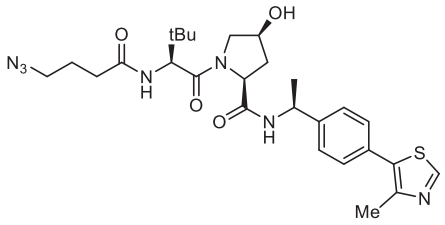

Prepared following general method for amide formation 1, using **3-29*** (20 mg, 0.04 mmol) and 4-azidobutanoic acid (5.3 mg, 0.04 mmol). The crude was purified by flash column chromatography; the product eluted at 10% methanol/DCM yielding **3-30a*** as a white solid (16 mg, 70% yield).

^{1}H NMR (400 MHz, CDCl3) δ 8.68 (d, J = 1.2 Hz, 1H), 7.57 – 7.44 (m, 1H), 7.38 (dd, J = 8.8, 6.1 Hz, 3H), 6.09 (s, 1H), 5.07 (p, J = 7.1 Hz, 1H), 4.58 (d, J = 8.9 Hz, 1H), 4.46 (s, 1H), 3.94 (d, J = 11.2 Hz, 1H), 3.79 (dd, J = 11.2, 4.7 Hz, 1H), 3.24 (td, J = 6.5, 3.1 Hz, 2H), 2.52 (d, J = 11.1 Hz, 4H), 2.46 – 2.11 (m, 4H), 1.99 – 1.72 (m, 2H), 1.50 (d, J = 7.0 Hz, 3H), 1.01 (s, 9H). **HRMS (ESI):** calculated for $[C_{27}H_{38}O_4N_7S]^+$: 556.27005, found: 556.26957.

(2S,4R)-1-((S)-2-(6-azidohexanamido)-3,3-dimethylbutanoyl)-4-hydroxy-N-((S)-1-(4-(4-methylthiazol-5-yl)phenyl)ethyl)pyrrolidine-2-carboxamide (3-30b)

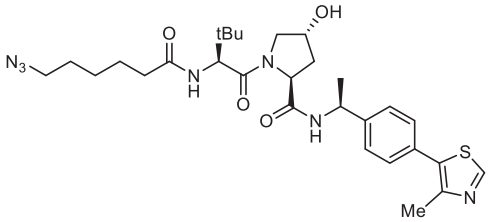

Prepared following general method for amide formation 1, using **3-29** (100 mg, 0.21 mmol) and 6-azidohexanoic acid (27 mg, 0.21 mmol). The crude was purified by flash column chromatography, the product was eluted at 10% methanol/DCM. Obtained as a white solid (85mg, **70%**).

^{1}H NMR (400 MHz, $CDCl_3$) δ 8.66 (s, 1H), 7.43 (d, *J* = 7.9 Hz, 1H), 7.41 – 7.32 (m, 5H), 6.27 (d, *J* = 8.8 Hz, 1H), 5.07 (p, *J* = 7.0 Hz, 1H), 4.57 (d, *J* = 8.9 Hz, 1H), 4.49 (s, 1H), 4.01 (dt, *J* = 11.4, 1.9 Hz, 1H), 3.90 (s, 1H), 3.61 (dd, *J* = 11.2, 3.9 Hz, 1H), 3.23 (t, *J* = 6.8 Hz, 2H), 2.50 (s, 3H), 2.44 (ddd, *J* = 12.7, 7.6, 4.8 Hz, 1H), 2.16 (t, *J* = 7.4 Hz, 2H), 2.02 (ddd, *J* = 12.7, 8.1, 2.4 Hz, 1H), 1.68 – 1.50 (m, 4H), 1.46 (d, *J* = 6.9 Hz, 3H), 1.42 – 1.29 (m, 2H), 1.02 (s, 9H). **^{13}C NMR** (101 MHz, $CDCl_3$) δ 173.3, 172.0, 169.9, 150.5, 148.5, 143.2, 131.0, 129.6, 126.6, 70.0, 58.7, 57.6, 56.8, 51.3, 48.9, 36.2, 35.7, 35.3, 28.6, 26.5, 26.4, 25.1, 22.3, 16.2. **IR (ATR):** 3265, 2971, 2095, 1687, 1614, 1066 cm^{-1}. **HRMS (ESI):** calculated for $[C_{29}H_{42}N_7O_4S]^+$: 584.3014, found: 528.584.3009.

tert-butyl (3-(((S)-1-((2S,4R)-4-hydroxy-2-(((S)-1-(4-(4-methylthiazol-5-yl)phenyl)ethyl)carbamoyl)pyrrolidin-1-yl)-3,3-dimethyl-1-oxobutan-2-yl)amino)-3-oxopropyl)carbamate (3-31a)

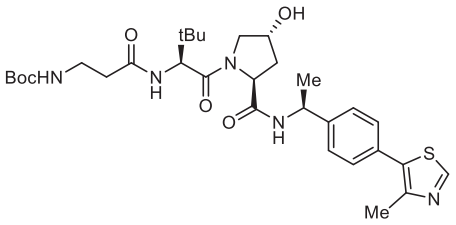

Prepared following general method for amide formation 2, using **3-29** (250 mg, 0.52 mmol) and 3-((tert-butoxycarbonyl)amino)propanoic acid (92 mg, 0.52 mmol). The crude was purified by flash column chromatography, the product was eluted at 5% methanol/DCM. Obtained as a white solid (204 mg, **64%**).

^{1}H NMR (400 MHz, $CDCl_3$) δ 8.67 (s, 1H), 7.49 (d, *J* = 7.8 Hz, 1H), 7.43 – 7.32 (m, 4H), 6.61 (d, *J* = 8.7 Hz, 1H), 5.08 (p, *J* = 7.1 Hz, 1H), 4.75 (t, *J* = 8.0 Hz, 1H), 4.56 (d, *J* = 8.5 Hz, 1H), 4.50 (s, 1H), 4.09 (d, *J* = 11.4 Hz, 1H), 3.60 (dd, *J* = 11.4, 3.6 Hz, 1H), 3.45 – 3.26 (m, 2H), 2.52 (s, 5H), 2.40 – 2.29 (m, 1H), 2.15 – 2.04 (m, 1H), 1.47 (d, *J* = 6.9 Hz, 3H), 1.42 (s, 9H), 1.04 (s, 9H). **^{13}C NMR** (101 MHz, $CDCl_3$) δ 172.2, 169.8, 156.3, 150.5, 148.6, 143.3, 131.7, 131.0, 129.7, 126.6, 79.6, 70.3, 58.6, 57.9, 57.0, 49.0, 37.0, 36.4, 35.7, 35.2, 28.6, 26.6, 22.3, 16.2. **HRMS (ESI):** calculated for $[C_{31}H_{46}N_5O_6S]^+$: 616.31633, found: 616.31548.

tert-butyl (6-(((S)-1-((2S,4R)-4-hydroxy-2-(((S)-1-(4-(4-methylthiazol-5-yl)phenyl)ethyl)carbamoyl)pyrrolidin-1-yl)-3,3-dimethyl-1-oxobutan-2-yl)amino)-6-oxohexyl)carbamate (3-31b)

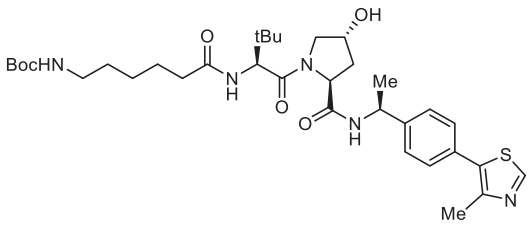

Prepared following general method for amide formation 1, using **3-29** (318 mg, 0.66 mmol) and 6-((tert-butoxycarbonyl)amino)hexanoic acid (153 mg, 0.66 mmol). The crude was purified by flash column chromatography, the product was eluted at 10% methanol/DCM. Obtained as a white solid (300 mg, **70%**).

^{1}H NMR (400 MHz, $CDCl_3$) δ 8.66 (s, 1H), 7.47 (d, *J* = 7.8 Hz, 1H), 7.38 (t, *J* = 6.2 Hz, 4H), 6.26 (d, *J* = 8.7 Hz, 1H), 5.08 (p, *J* = 7.1 Hz, 1H), 4.72 (t, *J* = 7.9 Hz, 1H), 4.56 (d, *J* = 8.7 Hz, 1H), 4.52 – 4.47 (m, 1H), 4.13 – 4.01 (m, 1H), 3.70 – 3.54 (m, 1H), 3.07 (d, *J* = 7.3 Hz, 2H), 2.51 (s, 4H), 2.27 – 2.04 (m, 3H), 1.61 (s, 2H), 1.51 – 1.37 (m, 14H), 1.34 – 1.23 (m, 2H), 1.04 (s, 9H). **^{13}C NMR** (101 MHz, $CDCl_3$) δ 173.8, 172.3, 169.8, 156.2, 150.4, 148.6, 143.3, 131.0, 129.7, 126.6, 79.3, 70.1, 58.6, 57.7, 56.8, 48.9, 40.5, 36.4, 35.6, 35.1, 29.8, 28.6, 26.7, 26.3, 25.3, 22.4, 16.2. **HRMS (ESI):** calculated for $[C_{34}H_{52}N_5O_6S]^+$: 658.36328, found: 658.36249.

(2S,4R)-1-((S)-2-(3-aminopropanamido)-3,3-dimethylbutanoyl)-4-hydroxy-N-((S)-1-(4-(4-methylthiazol-5-yl)phenyl)ethyl)pyrrolidine-2-carboxamide hydrochloride (3-31a HCl)

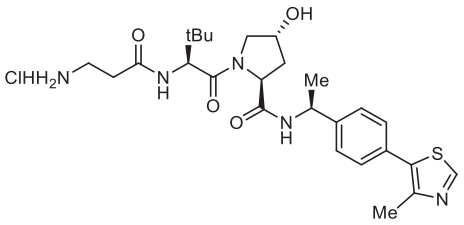

3-31a (268 mg, 0.44 mmol) was dissolved in 4N HCl/dioxane (5 mL) and stirred at room temperature for 3 h. The reaction crude was concentrated under reduced to afford NUM as an off white solid. The product was used without further purification (241 mg, quant.).

(2S,4R)-1-((S)-2-(6-aminohexanamido)-3,3-dimethylbutanoyl)-4-hydroxy-N-((S)-1-(4-(4-methylthiazol-5-yl)phenyl)ethyl)pyrrolidine-2-carboxamide (3-31b HCl)

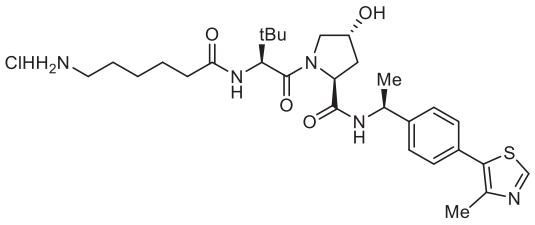

3-31b (79 mg, 0.12 mmol) was dissolved in 4N HCl/dioxane (5 mL) and stirred at rt for 3 h. The reaction crude was concentrated under reduced to afford NUM as an off white solid. The product was used without further purification (71 mg, quant.).

(2S,4R)-1-((S)-2-(3-(4-azidobutanamido)propanamido)-3,3-dimethylbutanoyl)-4-hydroxy-N-((S)-1-(4-(4-methylthiazol-5-yl)phenyl)ethyl)pyrrolidine-2-carboxamide (3-32a)

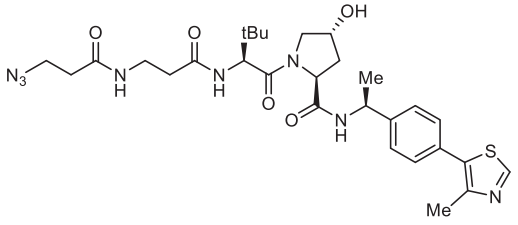

Prepared following general method for amide formation 2, using **3-31a HCl** (55 mg, 0.42 mmol) and 4-azidobutanoic acid (55 mg, 0.42 mmol). The crude was purified by flash column chromatography, the product was eluted at 5% methanol/DCM. Obtained as a white solid (104 mg, **40%**).

^{1}H NMR (500 MHz, $CDCl_3$) δ 8.67 (s, 1H), 7.43 – 7.33 (m, 5H), 6.70 (d, *J* = 8.7 Hz, 1H), 6.46 (t, *J* = 6.1 Hz, 1H), 5.09 (p, *J* = 7.0 Hz, 1H), 4.72 (t, *J* = 8.1 Hz, 1H), 4.56 (d, *J* = 8.7 Hz, 1H), 4.51 (dt, *J* = 4.2, 2.1 Hz, 1H), 4.06 (dt,

J = 11.5, 1.8 Hz, 1H), 3.62 (dd, *J* = 11.4, 3.6 Hz, 1H), 3.59 – 3.36 (m, 2H), 3.32 (td, *J* = 6.6, 1.7 Hz, 2H), 2.55 – 2.41 (m, 5H), 2.35 (ddd, *J* = 15.0, 7.5, 4.9 Hz, 1H), 2.29 – 2.19 (m, 2H), 2.11 (ddt, *J* = 13.6, 8.0, 1.9 Hz, 1H), 1.88 (qd, *J* = 8.0, 7.6, 6.3 Hz, 2H), 1.47 (d, *J* = 6.9 Hz, 3H), 1.04 (s, 9H). **^{13}C NMR** (126 MHz, $CDCl_3$) δ 172.5, 172.4, 172.2, 169.7, 150.5, 148.7, 143.2, 131.7, 131.1, 129.7, 126.6, 70.3, 58.6, 58.2, 57.0, 51.0, 49.0, 36.0, 36.0, 35.9, 35.2, 33.3, 26.7, 24.9, 22.3, 16.2. **HRMS (ESI):** calculated for $[C_{30}H_{43}N_8O_5S]^+$: 627.30716, found: 627.30480.

(2S,4R)-1-((S)-2-(6-(4-azidobutanamido)hexanamido)-3,3-dimethylbutanoyl)-4-hydroxy-N-((S)-1-(4-(4-methylthiazol-5-yl)phenyl)ethyl)pyrrolidine-2-carboxamide (3-32b)

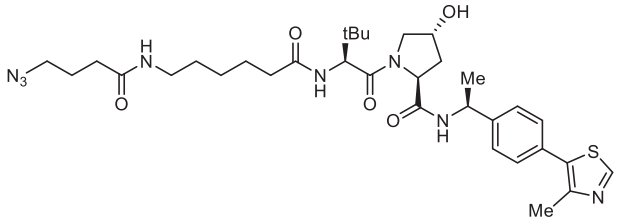

Prepared following general method for amide formation 2, using **3-31b HCl** (150 mg, 0.25 mmol) and 4-azidobutanoic acid (33 mg, 0.25 mmol). The crude was purified by flash column chromatography, the product was eluted at 5% methanol/DCM. Obtained as a white solid (33 mg, **20%**).

^{1}H NMR (400 MHz, $CDCl_3$) δ 8.67 (s, 1H), 7.48 – 7.33 (m, 5H), 6.33 (d, *J* = 8.8 Hz, 1H), 5.95 (t, *J* = 5.8 Hz, 1H), 5.06 (dt, *J* = 13.7, 7.1 Hz, 1H), 4.70 (t, *J* = 8.0 Hz, 1H), 4.57 (d, *J* = 8.7 Hz, 1H), 4.49 (s, 1H), 4.14 – 4.01 (m, 1H), 3.60 (dd, *J* = 11.3, 3.7 Hz, 1H), 3.32 (t, *J* = 6.5 Hz, 2H), 3.20 (q, *J* = 6.9 Hz, 2H), 2.51 (s, 3H), 2.49 – 2.41 (m, 1H), 2.23 (q, *J* = 7.5 Hz, 2H), 2.08 (dtd, *J* = 13.9, 8.1, 7.1, 2.9 Hz, 1H), 1.89 (p, *J* = 6.9 Hz, 2H), 1.59 (dt, *J* = 10.5, 7.5 Hz, 2H), 1.46 (dd, *J* = 6.9, 2.7 Hz, 5H), 1.37 – 1.19 (m, 2H), 1.03 (s, 9H). **^{13}C NMR** (101 MHz, $CDCl_3$) δ 173.7, 172.1, 172.0, 169.9, 150.5, 148.6, 143.3, 131.0, 129.7, 126.6, 70.1, 58.7, 57.7, 56.9, 48.9, 39.4, 36.2, 35.9, 35.3, 33.3, 29.2, 26.6, 26.3, 25.1, 25.0, 22.3, 16.2. **HRMS (ESI):** calculated for $[C_{33}H_{49}N_8O_5S]^+$: 669.35411, found: 669.35288.

(2S,4S)-1-((S)-2-(6-aminohexanamido)-3,3-dimethylbutanoyl)-4-hydroxy-N-((S)-1-(4-(4-methylthiazol-5-yl)phenyl)ethyl)pyrrolidine-2-carboxamide hydrochloride (3-31b* HCl)

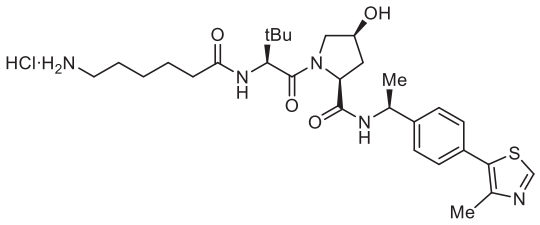

Prepared as **3-31b HCl**, using 3-29* instead of 3-29.

(2S,4S)-1-((S)-2-(6-(4-azidobutanamido)hexanamido)-3,3-dimethylbutanoyl)-4-hydroxy-N-((S)-1-(4-(4-methylthiazol-5-yl)phenyl)ethyl)pyrrolidine-2-carboxamide (3-32b*)

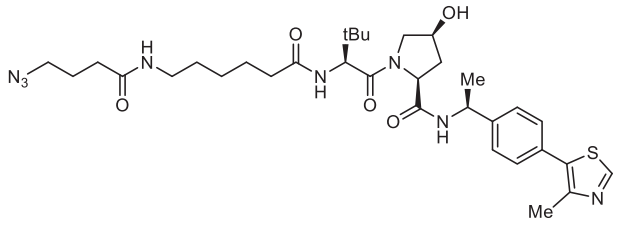

Prepared as **3-32b**, using **3-31b*HCl** instead of **3-31b**. Reported as a white solid (12 mg, 32% yield).

^{1}H NMR (400 MHz, $CDCl_3$) δ 8.69 (d, *J* = 4.0 Hz, 1H), 7.39 (dd, *J* = 8.6, 6.1 Hz, 4H), 6.02 (d, *J* = 5.7 Hz, 1H), 5.90 (d, *J* = 9.0 Hz, 1H), 5.06 (p, *J* = 7.2 Hz, 1H), 4.93 (d, *J* = 9.3 Hz, 1H), 4.63 (dd, *J* = 27.6, 8.9 Hz, 2H), 4.55 – 4.44 (m, 1H), 3.94 (d, *J* = 11.2 Hz, 1H), 3.78 (dd, *J* = 11.2, 4.6 Hz, 1H), 3.35 (t, *J* = 6.6 Hz, 2H), 3.30 – 3.01 (m, 2H), 2.52 (d, *J* = 12.4 Hz, 3H), 2.40 – 2.00 (m, 8H), 1.98 – 1.86 (m, 2H), 1.55 (dd, *J* = 37.0, 7.0 Hz, 5H), 1.35 (q, *J* = 7.1 Hz, 2H), 1.27 – 1.14 (m, 2H), 1.01 (s, 9H). **HRMS (ESI):** calculated for $[C_{33}H_{48}N_8O_5S]^+$: 669.35411, found: 669.35236.

(2S,4R)-1-((S)-2-(6-(6-azidohexanamido)hexanamido)-3,3-dimethylbutanoyl)-4-hydroxy-N-((S)-1-(4-(4-methylthiazol-5-yl)phenyl)ethyl)pyrrolidine-2-carboxamide (3-32c)

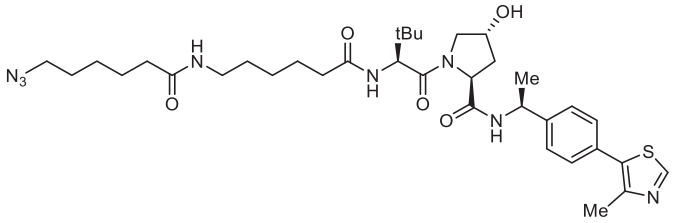

Prepared following general method for amide formation 2, using **3-31b'** (40 mg, 0.25 mmol) and 6-azidohexanoic acid (40 mg, 0.25 mmol). The crude was purified by flash column chromatography, the product was eluted at 5% methanol/DCM. Obtained as a white solid (88 mg, **50%**).

^{1}H NMR (400 MHz, $CDCl_3$) δ 8.65 (d, *J* = 1.3 Hz, 1H), 7.51 (d, *J* = 7.9 Hz, 1H), 7.39 – 7.31 (m, 4H), 6.47 (d, *J* = 8.6 Hz, 1H), 6.04 (t, *J* = 5.8 Hz, 1H), 5.11 – 4.99 (m, 1H), 4.65 (t, *J* = 8.0 Hz, 1H), 4.52 (d, *J* = 8.8 Hz, 1H), 4.48 (d, *J* = 5.8 Hz, 1H), 3.99 (d, *J* = 11.3 Hz, 1H), 3.61 (dd, *J* = 11.2, 3.7 Hz, 1H), 3.29 – 3.19 (m, 2H), 3.15 (q, *J* = 6.7 Hz, 2H), 2.48 (d, *J* = 1.7 Hz, 4H), 2.38 – 2.29 (m, 1H), 2.21 – 2.03 (m, 5H), 1.65 – 1.51 (m, 6H), 1.49 – 1.17 (m, 9H), 1.01 (s, 9H). **^{13}C NMR** (101 MHz, $CDCl_3$) δ 173.8, 173.1, 171.9, 170.1, 150.5, 148.5, 143.4, 131.6, 130.9, 129.6, 126.5, 70.0, 58.9, 57.8, 56.9, 51.3, 48.8, 39.2, 36.4, 36.2, 36.0, 35.2, 29.2, 28.6, 26.6, 26.4, 26.2, 25.3, 25.1, 22.2, 16.1. **HRMS (ESI):** calculated for $[C_{35}H_{53}N_8O_5S]^+$: 697.38541, found: 697.38439.

1-(4-(Allyloxy)phenyl)-2-phenylbutan-1-one (3-6)

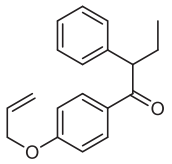

To a flask charged with 2-phenylbutanoic acid (10 g, 60.9 mmol) was added (allyloxy)benzene (8.3 mL, 60.9 mmol) and then TFAA (9.5 mL, 67.0 mmol). The mixture was stirred for 2.5 h at 30 °C, then added dropwise to a saturated solution of $KHCO_3$ and washed with DCM. The combined organic layers were then washed with brine, dried over $MgSO_4$, then concentrated under reduced pressure to afford a colourless oil, which solidified upon standing (16 g, **94%**).

^{1}H NMR (400 MHz, $CDCl_3$) δ: 7.99–7.89 (m, 2H), 7.33–7.26 (m, 4H), 7.23–7.15 (m, 1H), 6.91 – 6.84 (m, 2H), 6.01 (ddt, *J* = 17, 11, 5 Hz, 1H), 5.39 (dq, *J* = 17, 2 Hz, 1H), 5.29 (dq, *J* = 11, 1 Hz, 1H), 4.55 (dt, *J* = 5, 2 Hz, 2H), 4.39 (t, *J* = 7 Hz, 1H), 2.19 (dt, *J* = 14, 7 Hz, 1H), 1.84 (dt, *J* = 14, 7 Hz, 1H), 0.89 (t, *J* = 7 Hz, 3H) ppm. **^{13}C NMR** (101 MHz, $CDCl_3$) δ 198.6, 162.2, 140.0, 132.5, 130.9, 130.1, 128.8, 128.2, 126.8, 118.1, 114.3, 68.8, 55.1, 27.1, 12.3 ppm. **IR (Film):** 3026, 1666, 1597, 1258, 1020, 744 cm^{-1}. **HRMS (ESI):** calc. for $[C_{19}H_{21}O_2]^+$: 281.15361; found: 281.15354. **M_p:** 43°C.

(E/Z)-4-(1-(4-(Allyloxy)phenyl)-2-phenylbut-1-en-1-yl)phenol (3-7)

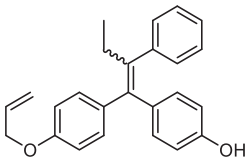

To a flask charged with a solution of 2-(4-bromophenoxy)tetrahydro-2H-pyran (6.9 g, 26.8 mmol) in THF (15 mL) at -78 °C was added dropwise n-BuLi (2.5 M, 10.7 mL, 26.8 mmol). The mixture was maintained between -72 – -68 °C for 45 min. Then, a solution of 1-(4-(allyloxy)phenyl)-2-phenylbutan-1-one (**5**, 5.0 g, 18.0 mmol) in THF (15 mL) was added dropwise. The mixture was allowed to reach rt, stirred overnight and worked up with water and ethyl acetate. The organic layer was washed with brine, dried over $MgSO_4$ and concentrated under reduced pressure to afford 11.7 g of the tertiary alcohol intermediate as a brown oil,. This crude intermediate was dissolved in methanol (40 mL), and conc. HCl (2.0 mL, 26 mmol) was added dropwise at rt. After 1 h, NaOH (1 M, 20 mL) was added until pH 9, diluted with H_2O and extracted with ethyl acetate. The combined organic layers were washed with brine, dried over $MgSO_4$, and concentrated under reduced pressure to afford a brown oil that was purified by flash column chromatography. The desired product **6** eluted at 7% EtOAc/hexanes as an off-white solid, as 1:1 mixture of E/Z stereoisomers (6.12 g, **66%**).

^{1}H NMR (400 MHz, $CDCl_3$) δ 7.12 – 7.00 (m, 7H), 6.84 – 6.80 (m, 2H), 6.67 – 6.63 (m, 2H), 6.42 – 6.37 (m, 2H), 6.01 (ddt, *J* = 17, 11, 5 Hz, 1H), 5.36 (dq, *J* = 17, 2 Hz, 1H), 5.23 (dq, *J* = 11, 1 Hz, 1H), 4.48 (dt, *J* = 5, 2 Hz, 2H), 2.41 (q, *J* = 7 Hz, 2H), 0.85 (t, *J* = 7 Hz, 3H) ppm. **^{13}C NMR** (101 MHz, $CDCl_3$) δ 157.3*, 156.5, 154.2* , 153.3, 142.6* , 142.6, 141.1* , 141.1, 137.7* , 137.7, 136.4* , 136.4, 136.0* , 135.9, 133.4* , 133.3, 132.1* , 131.9, 130.8* , 130.5, 129.7, 127.8, 125.9, 117.7* , 117.5, 114.9* , 114.2, 114.2* , 113.5, 68.8* , 68.6, 29.0* , 29.0, 13.6 ppm. (* denote extra signals belonging to the other isomer). **IR (Film):** 3395, 2964, 1606, 1506, 1231, 844 cm^{-1}. **HRMS (ESI):** calc. for $[C_{25}H_{25}O_2]^+$: 357.18491; found: 357.18526. **M_p:** 120 °C.

2-(4-(1-(4-(allyloxy)phenyl)-2-phenylbut-1-en-1-yl)phenoxy)-N-methylethan-1-amine hydrochloride (3-8)

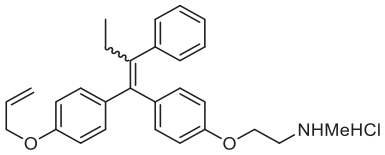

4-(1-(4-(Allyloxy)phenyl)-2-phenylbut-1-en-1-yl)phenol (**6**, 166 mg, 0.47 mmol), Cs_2CO_3 (445 mg, 1.40 mmol) and DMF (1 mL) were stirred for 20 min at 120 °C. *tert*-Butyl (2-chloroethyl)carbamate (108 mg, 0.56 mmol) was added dropwise and the reaction mixture was stirred overnight at 120 °C. Work-up with ethyl acetate and water gave an organic phase that was washed with brine and copper sulfate, dried over $MgSO_4$, and concentrated under reduced pressure. The crude, composed mainly by (E/Z)-2-(4-(1-(4-(allyloxy)phenyl)-2-phenylbut-1-en-1-yl)phenoxy)-*N*-Boc-*N*-methylethan-1-amine (150 mg, 0.29 mmol) was dissolved in 4N HCl/dioxane (2 mL) and stirred at rt for 1 h. The reaction crude was concentrated under reduced pressure and purified by flash column chromatography, the product eluted at 3% MeOH/DCM as a white solid foam (72 mg, 0.17 mmol, **60% over 2 steps**).

N-(2-(4-(1-(4-(Allyloxy)phenyl)-2-phenylbut-1-en-1-yl)phenoxy)ethyl)-N-methylpent-4-ynamide (3-9)

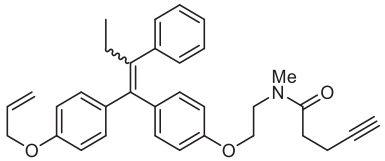

Prepared following general method for amide formation 1, using **3-8** (150 mg, 0.36 mmol) and pent-4-ynoic acid (32 mg, 0.33 mmol). The crude was purified by flash column chromatography, the product was eluted at 25% ethyl acetate in hexanes. Obtained as yellowish thick oil (136 mg, **85%**).

^{1}H NMR (400 MHz, DCCl3) δ 7.20 – 7.07 (m, 7H), 6.96 – 6.83 (m, 2H), 6.80 – 6.72 (m, 2H), 6.59 – 6.49 (m, 2H), 6.03 (dddt, *J* = 40.1, 17.2, 10.6, 5.3 Hz, 1H), 5.49 – 5.17 (m, 2H), 4.59 – 4.33 (m, 2H), 4.19 – 3.94 (m, 2H), 3.71 (ddt, *J* = 41.8, 13.6, 5.3 Hz, 2H), 3.22 – 2.95 (m, 3H), 2.75 – 2.39 (m, 6H), 2.02 – 1.91 (m, 1H), 0.96 – 0.89 (m, 3H). **^{13}C NMR** (101 MHz, cdcl$_3$) δ 171.7, 171.4*, 157.5, 157.4*, 156.6, 156.5*, 156.1*, 142.7, 141.3, 137.8, 136.7, 136.5*, 136.3*, 136.0*, 133.5, 132.2, 132.1*, 132.0, 130.9, 130.8, 130.7, 129.8, 128.0, 126.1, 126.1, 117.8, 117.6, 114.4, 114.1, 113.6, 113.3, 83.8, 83.7*, 83.6*, 83.5*, 69.0, 68.8*, 68.7*, 66.9, 66.6*, 65.3*, 65.0*, 63.2, 60.5, 49.3, 49.2*, 48.3*, 37.6, 37.6*, 34.2*, 34.1*, 32.7, 32.6*, 32.3*, 32.2*, 29.2, 14.5, 13.7. (* denote extra signals belonging to the other isomer) IR: 1649, 1503, 1231 cm^{-1}. **HRMS (ESI):** calc. [M+H]$^+$: 494.26898 ; found: 494.26897.

N-(2-(4-(1-(4-hydroxyphenyl)-2-phenylbut-1-en-1-yl)phenoxy)ethyl)-*N*-methylpent-4-ynamide (3-2)

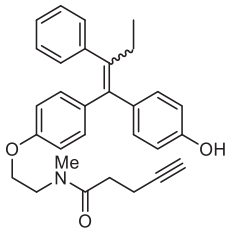

A suspension of *N*-(2-(4-(1-(4-(allyloxy)phenyl)-2-phenylbut-1-en-1-yl)phenoxy)ethyl)-N-methylpent-4-ynamide (**7**, 75 mg, 0.15 mmol), Pd(PPh$_3$)$_4$ (9 mg, 0.01 mmol), K$_2$CO$_3$ (63 mg, 0.46 mmol) and methanol (1 mL) was and stirred under nitrogen at room temperature for 4 h. Ethyl acetate and NH$_4$Cl sat were added, the aqueous layer was re-extracted using ethyl acetate (x2) and the combined organic layers washed with brine, dried over MgSO$_4$ and concentrated under reduced pressure. The crude was purified by flash column chromatography, the product was eluted at 50% ethyl acetate/hexanes as an incolor thick oil (48 mg, 0.11 mmol, **73%**).

^{1}H NMR (400 MHz, DCCl$_3$) δ 7.19 – 7.05 (m, 7H), 6.89 – 6.67 (m, 4H), 6.54 – 6.44 (m, 2H), 4.16 – 3.92 (m, 2H), 3.81 – 3.58 (m, 2H), 3.21 – 2.94 (m, 3H), 2.76 – 2.43 (m, 6H), 1.98 – 1.89 (m, 1H), 0.92 (td, *J* = 7.4, 1.8 Hz, 3H). **^{13}C NMR** (101 MHz, cdcl$_3$) δ 171.8, 171.6*, 157.3, 157.0*, 156.5*, 156.1*, 155.0, 154.0*, 142.8, 142.7*, 141.4, 141.2*, 141.1*, 137.9, 136.8, 136.3*, 136.0, 135.7*, 132.2, 132.1, 130.9, 130.8, 130.8, 129.8, 128.0, 126.1, 126.0, 115.2, 114.5, 114.0, 113.3, 83.7, 83.7*, 83.5*, 83.5*, 68.9, 66.8, 66.5*, 65.3*, 65.0*, 49.3, 49.3*, 48.4*, 37.7, 37.7*, 34.2*, 32.7, 32.6*, 32.3,* 32.2*, 29.2, 14.5, 13.8. (* denote extra signals belonging to the other isomer) **IR (ATR):** 1778, 1603, 1500 cm^{-1}. **HRMS (ESI):** calc. [M+H]$^+$: 454.23767; found: 454.23743.

4-(allyloxy)-1-bromo-2-methylbenzene (3-19)

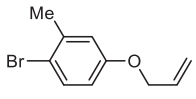

A round flask was loaded with 4-bromo-3-methylphenol (5 g, 26.7 mmol, 1 eq.), allyl bromide (2.54 mL, 29.0 mmol, 1.1 eq.), potassium carbonate (11 g, 80.0 mmol, 3 eq.) and acetonitrile (37 mL, 0.4 M), and stirred overnight at room temperature. The reaction mixture was filtered and extracted with water. The aqueous phase was extracted with ethyl acetate and the organic fractions were

combined, washed with brine, dried over magnesium sulphate and dried under reduced pressure. The reaction crude was used without further purification (colourless oil, 6 g, **98%**).

^{1}H NMR (400 MHz, cdcl$_3$) δ 7.4 (d, *J* = 8.7 Hz, 1H), 6.8 (dt, *J* = 3.1, 0.7 Hz, 1H), 6.6 (ddt, *J* = 8.7, 3.0, 0.6 Hz, 1H), 6.0 (ddtd, *J* = 17.3, 10.5, 5.3, 0.6 Hz, 1H), 5.4 (dqd, *J* = 17.3, 1.6, 0.6 Hz, 1H), 5.3 (dqd, *J* = 10.5, 1.4, 0.5 Hz, 1H), 4.6 – 4.5 (m, 2H), 2.4 (d, *J* = 0.7 Hz, 3H).

1-(4-hydroxyphenyl)-2-phenylbutan-1-one

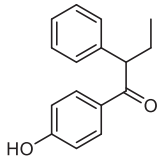

A flask was loaded with **3-6** (3 g, 1.07 mol, 1 eq.), Pd(PPh$_3$)$_4$ (620 mg, 53.6 mmol, 0.05 eq.), K$_2$CO$_3$ (4.4 g, 31.9 mmol, 3 eq.) and methanol (70 mL, 0.15 M), the reaction mixture was stirred under nitrogen at room temperature overnight. The reaction mixture was diluted in ethyl acetate and extracted with NaOH 1M. The aqueous phase was then acidified and extracted with ethyl acetate. The organic phases were combined, washed with brine, dried over magnesium sulphate and dried under reduced pressure. The residue was dissolved again in ethyl acetate and filtered through celite, dried under reduced pressure again to afford a brownish solid. Used without further purification. (1.63 g, **65%**).

1H NMR (400 MHz, CDCl$_3$) δ 8.02 – 7.86 (m, 2H), 7.33 – 7.26 (m, 4H), 7.24 – 7.08 (m, 1H), 6.80 (d, J = 8.7 Hz, 2H), 4.39 (t, J = 7.3 Hz, 1H), 2.28 – 2.11 (m, 1H), 1.84 (dt, J = 13.7, 7.3 Hz, 1H), 0.89 (t, J = 7.4 Hz, 3H).

2-phenyl-1-(4-((tetrahydro-2H-pyran-2-yl)oxy)phenyl)butan-1-one (3-20)

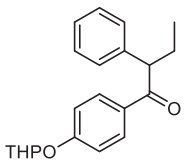

To a flask charged with 1-(4-hydroxyphenyl)-2-phenylbutan-1-one (1.6 g, 7.2 mmol, 1 eq.) dissolved in DCM (14 mL, 0.5M) at 0 °C was added DHP (1.898mL, 21.6 mmol, 3 eq.) then PPTS (0.18 g, 0.07 mmol, 0.1 eq.). The mixture was stirred for 18 h warming to room temperature before separation between DCM and water. The organic layer was then washed with brine, dried over magnesium sulphate, then concentrated under reduced pressure. The product was used without further purification (1.54 g, **65%**).

4-(1-(4-(allyloxy)-2-methylphenyl)-2-phenylbut-1-en-1-yl)phenol (3-21)

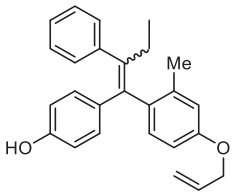

To a flask charged with 4-(allyloxy)-1-bromo-2-methylbenzene (**3-19**, 2.14 g, 9.4 mmol) dissolved in THF (10 mL) at -78 °C was added dropwise 2.5 M n-BuLi (5.1 mL, 9.4 mmol). The mixture was maintained between -72 – -68 °C for 45 min before the dropwise addition of **3-20** (1.54 g, 4.7 mmol) dissolved in THF (15 mL). The mixture was stirred overnight allowing it to reach room temperature, then separated between water and ethyl acetate. The organic layer was washed with brine, dried over magnesium sulphate and concentrated under reduced pressure to afford the tertiary alcohol intermediate as a brown oil. The crude intermediate was dissolved in methanol (10 mL), then concentrated HCl (0.4 mL) was added dropwise to the mixture at rt. After 1 h, 1 M NaOH was added until pH 9, dilution with water and then extracted using ethyl acetate.The combined organic layers were washed with brine, dried over magnesium sulphate, and then concentrated under reduced pressure to afford a brown oil. The residue was purified by flash column chromatography, the product eluted at 7% EtOAc/hexanes as an off-white solid (0.7 g, **40%**).

^{1}H NMR (400 MHz, cdcl$_3$) δ 7.22 – 7.01 (m, 6H), 6.83 – 6.68 (m, 4H), 6.51 – 6.36 (m, 2H), 6.14 – 5.88 (m, 1H), 5.45 – 5.14 (m, 2H), 4.53 (dt, *J* = 5.4, 1.5 Hz, 2H), 4.37* (dt, *J* = 5.4, 1.6 Hz, 2H), 2.36 – 2.21 (m, 2H), 2.10 (s, 3H), 1.98* (s, 3H), 0.99* (t, *J* = 7.4 Hz, 3H), 0.82 (t, *J* = 7.4 Hz, 3H). **^{13}C NMR** (101 MHz, cdcl$_3$) δ 157.5, 153.5, 142.7*, 142.4, 142.3*, 141.5, 137.7, 137.6*, 137.5*, 136.8, 136.0*, 135.7, 135.3*, 134.3, 133.6, 133.5*, 132.5*, 131.7, 130.6, 130.5, 129.8, 129.0, 128.0, 127.6, 126.2, 126.0*, 117.7, 117.6*, 116.6, 116.0*, 114.9, 114.3, 111.6, 111.3*, 68.9, 68.7*, 29.3, 20.7*, 20.2, 14.0*, 13.0. (* denote extra signals belonging to the other isomer) **IR (ATR):** 3402, 2922, 1509, 1170 cm^{-1}. **HRMS (ESI):** calculated for $[C_{26}H_{25}O_2]^-$: 369.186, found: 369.1862. **M_p:** 105°C.

tert-butyl (2-(4-(1-(4-(allyloxy)-2-methylphenyl)-2-phenylbut-1-en-1-yl)phenoxy)ethyl) (methyl)carbamate (3-22)

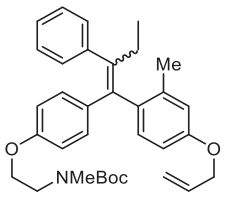

A flask was charged with **3-21** (0.7 g, 1.88 mmol), caesium carbonate (1.8 g, 5.6 mmol) and DMF (4 mL) and stirred for 20 min at 120 °C, then tert-butyl (2-chloroethyl)carbamate (0.44 g, 2.26 mmol) was added. The reaction mixture was stirred overnight at 150 °C. Ethyl acetate and water were added, then the aqueous layer was re-extracted using ethyl acetate, the combined organic layers washed with brine and copper sulfate, dried over MgSO4, and then concentrated under reduced

pressure. The crude was purified by flash column chromatography, product was eluted at 10% ethyl acetate/hexanes. Yellowish oil (400 mg, **40%**).

^{1}H NMR (400 MHz, $CDCl_3$) δ 7.26 – 6.99 (m, 6H), 6.83 – 6.73 (m, 4H), 6.54 – 6.42 (m, 2H), 6.14 – 5.89 (m, 1H), 5.48 – 5.30 (m, 1H), 5.31 – 5.12 (m, 1H), 4.52 (dt, *J* = 5.3, 1.5 Hz, 2H), 4.36* (dt, *J* = 5.3, 1.5 Hz, 2H), 3.92 (s, 2H), 3.52 – 3.41 (m, 2H), 2.97* (s, 3H), 2.89 (s, 3H), 2.39 – 2.20 (m, 2H), 2.11 (s, 3H), 1.99* (s, 3H), 1.46* (s, 9H), 1.42 (s, 9H), 1.00* (t, *J* = 7.3 Hz, 3H), 0.82 (t, *J* = 7.5 Hz, 3H). **^{13}C NMR** (101 MHz, $CDCl_3$) δ 157.6, 157.0, 156.5*, 155.6, 142.6*, 142.4, 142.3*, 141.5, 137.5, 137.5*, 136.8, 135.8*, 135.5, 134.4*, 133.6*, 133.5, 132.4*, 131.5, 130.5*, 130.3, 129.8, 128.9, 128.0, 127.6, 126.1*, 125.9, 117.5, 117.3, 116.5, 115.9, 113.9, 113.2, 111.6, 111.3, 79.6, 68.7, 68.5*, 66.6*, 65.9, 48.4*, 48.3, 36.2*, 35.4, 29.2, 28.5, 20.6, 20.2*, 14.0*, 13.0. **IR (ATR):** 2970, 1691, 1151 cm^{-1}. **HRMS (ESI):** calculated for $[C_{34}H_{41}NNaO_4]^+$:550.2928, found: 550.2913.

2-(4-(1-(4-(allyloxy)-2-methylphenyl)-2-phenylbut-1-en-1-yl)phenoxy)-N-methylethan-1-amine hydrochloride (3-22 HCl)

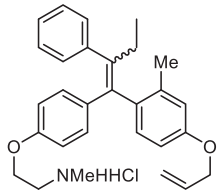

3-22 (400 mg, 0.76 mmol) was dissolved in 4N HCl/dioxane (2 mL) and stirred at room temperature for 2 hours. The reaction crude was concentrated under reduced pressure affording an off white solid. The product was used without further purification (350 mg, **quant.**).

N-(2-(4-(1-(4-(allyloxy)-2-methylphenyl)-2-phenylbut-1-en-1-yl)phenoxy)ethyl)-N-methylpent-4-ynamide (3-23)

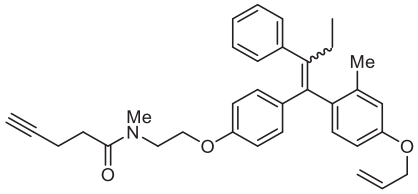

Prepared following general method for amide formation 1, using **3-22 HCl** (360 mg, 0.77 mmol) and pent-4-ynoic acid (76 mg, 0.77 mmol). The crude was purified by flash column chromatography, the product was eluted at 40% ethyl acetate in hexanes. Obtained as an incolor oil (230 mg, **58%**).

^{1}H NMR (400 MHz, cdcl$_3$) δ 7.24 – 7.00 (m, 6H), 6.84 – 6.72 (m, 4H), 6.48 (dd, *J* = 8.9, 2.4 Hz, 2H), 6.15 – 5.90 (m, 1H), 5.47 – 5.17 (m, 2H), 4.54 (dt, *J* = 5.4, 1.5 Hz, 2H), 4.38* (dt, *J* = 5.4, 1.5 Hz, 2H), 4.15 – 3.86 (m, 2H), 3.78 – 3.59 (m, 2H), 3.15* (s, 3H), 3.06 (s, 3H), 3.02* (s, 3H), 2.95* (s, 3H), 2.70 – 2.48 (m, 4H), 2.37 – 2.20 (m, 2H), 2.10 (s, 3H), 1.98* (s, 3H), 1.95 – 1.87 (m, 1H), 0.99* (td, *J* = 7.4, 1.7 Hz, 3H), 0.82 (td, *J* = 7.4, 2.1 Hz, 3H). **^{13}C NMR** (101 MHz, cdcl$_3$) δ 171.0, 157.5, 156.3, 155.9*, 142.3, 141.8*, 141.6, 137.5, 136.7, 135.4, 135.4*, 134.9*, 134.5, 133.5, 132.4*, 131.6*, 131.5, 130.5*, 130.3*, 129.7, 128.9, 127.9, 127.5, 126.1, 125.9, 117.5, 117.3*, 116.5, 115.8, 113.8, 113.1, 111.5, 111.2*, 83.7, 83.5, 68.7*, 68.6, 66.4, 64.9*, 49.0*, 48.0, 37.6, 33.9*, 32.5, 32.1*, 29.2, 27.9*, 20.5*, 20.1, 14.6*, 14.3, 13.9*, 12.9. (* denote extra signals belonging to the other isomer).

IR (ATR): 2969.77, 2357.07, 1646.42, 1239.23 cm^{-1}. **HRMS (ESI):** calculated for $[C_{34}H_{38}NO_3]^+$: 508.2846, found: 508.2831.

N-(2-(4-(1-(4-hydroxy-2-methylphenyl)-2-phenylbut-1-en-1-yl)phenoxy)ethyl)-N-methylpent-4-ynamide (3-24)

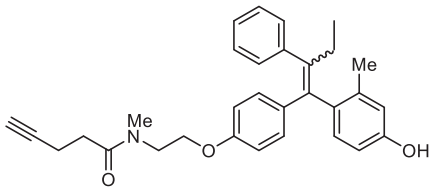

A flask loaded with **3-23** (230 mg, 0.45 mmol), $Pd(PPh_3)_4$ (26 mg, 0.02 mmol), K_2CO_3 (188 mg, 1.35 mmol) and DCM (3 mL) was purged under nitrogen and stirred at room temperature for 5 h. Ethyl acetate and NH_4Cl sat were added, then the aqueous layer was re-extracted using ethyl acetate (x2) and the combined organic layers washed with brine, dried over $MgSO_4$ and concentrated under reduced pressure. The crude was purified by flash column chromatography, the product was eluted at 50% ethyl acetate/hexanes as a white solid foam (145 mg, **70%**).

^{1}H NMR (400 MHz, cdcl$_3$) δ 7.23 – 7.00 (m, 6H), 6.84 – 6.67 (m, 4H), 6.53 – 6.41 (m, 2H), 4.11* (dt, *J* = 16.0, 5.2 Hz, 2H), 3.96 (dt, *J* = 18.1, 5.4 Hz, 2H), 3.80 – 3.71* (m, 2H), 3.70 – 3.60 (m, 2H), 3.10* (dd, *J* = 53.2, 1.6 Hz, 3H), 3.02 (dd, *J* = 44.2, 1.6 Hz, 3H), 2.68 – 2.47 (m, 4H), 2.37 – 2.23 (m, 2H), 2.06 (s, 3H), 1.95* (s, 3H), 1.94 – 1.89 (m, 1H), 0.99* (td, *J* = 7.4, 1.9 Hz, 3H), 0.82 (td, *J* = 7.4, 2.1 Hz, 3H). **^{13}C NMR** (101 MHz, cdcl$_3$) δ 172.0, 171.9, 171.7, 171.7, 157.1, 156.7, 156.3, 155.9, 155.2, 155.2, 154.5, 154.5, 142.7, 142.6, 142.5, 142.4, 142.3, 141.8, 141.6, 137.7, 137.7, 137.6, 137.5, 137.4, 136.9, 136.8, 136.3, 135.9, 135.3, 135.2, 134.8, 134.8, 134.7, 132.6, 131.7, 131.6, 130.7, 130.7, 130.5, 130.4, 129.8, 129.0, 128.1, 128.0, 127.6, 126.2, 126.2, 126.0, 117.2, 116.6, 113.8, 113.2, 112.6, 112.3, 83.6, 83.4, 69.0, 66.8, 66.5, 65.2, 64.9, 49.2, 48.3, 37.7, 34.2, 32.6, 32.5, 32.2, 32.2, 29.3, 28.0, 20.5, 20.0, 14.8, 14.5, 14.0, 13.0. **HRMS (ESI):** calculated for $[C_{31}H_{34}NO_3]^+$: 468.25332, found: 468.25297. **M_p:** 78°C.

3-(1-(2-(2-((2-(2,6-dioxopiperidin-3-yl)-1,3-dioxoisoindolin-4-yl)amino)ethoxy)ethyl)-1H-1,2,3-triazol-4-yl)-N-(2-(4-(1-(4-hydroxyphenyl)-2-phenylbut-1-en-1-yl)phenoxy)ethyl)-N-methylpropanamide (TAM-PO-1)

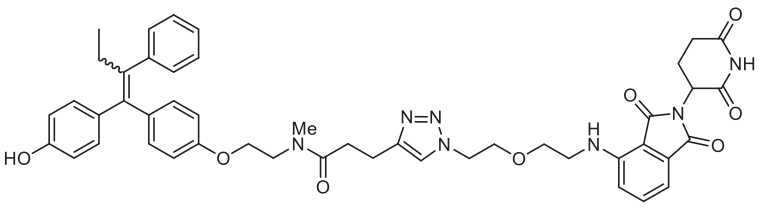

The product was prepared following general method for CuAAC from alkyne **3-2** (32mg, 0.07 mmol) and **3-11a** (50 mg, 0.07 mmol). The crude was purified by flash column chromatography, the product was eluted at 3% MeOH/DCM yielding **TAM-PO-1** as a yellow solid (40 mg, **70%**).

^{1}H NMR (400 MHz, $CDCl_3$) δ 7.73 – 7.62 (m, 1H), 7.50 – 7.37 (m, 1H), 7.17 – 7.00 (m, 7H), 6.87 – 6.64 (m, 5H), 6.51 – 6.39 (m, 3H), 5.04 – 4.92 (m, 1H), 4.53 – 4.41 (m, 2H), 4.11 – 3.90 (m, 2H), 3.85 – 3.74 (m, 2H), 3.69 – 3.56 (m, 4H), 3.44 – 3.35 (m, 2H), 3.12 – 2.90 (m, 5H), 2.85 – 2.68 (m, 6H), 2.50 – 2.40 (m, 2H), 2.14 – 2.06 (m, 1H), 0.90 (t, *J* = 7.4 Hz, 3H) ppm. **^{13}C NMR** (101 MHz, $cdcl_3$) δ 173.0, 172.9*, 172.0, 172.0*, 169.6, 169.1*, 169.1, 167.8, 157.3*, 157.0*, 156.5*, 156.1, 155.4*, 155.3*, 154.4*, 154.4, 147.2, 147.1, 146.7, 142.8*, 142.7, 141.0*, 140.9, 138.0, 136.8*, 136.7*, 136.3, 136.2, 135.8*, 135.6*, 135.4*, 135.2, 132.7, 132.1, 132.1, 130.8, 130.7, 129.8, 127.9, 126.0, 123.2, 116.8, 115.2, 114.5, 114.1, 113.3, 113.3, 112.0, 110.7, 70.6*, 69.9, 69.4, 66.7*, 66.4, 65.7,* 65.4, 50.4, 49.6, 49.1, 48.2*, 48.1, 42.3, 37.6*, 37.4*, 34.6*, 34.5, 32.9*, 32.9*, 32.5*, 32.5, 31.5, 29.1, 23.1, 21.2*, 21.2*, 20.9*, 20.9, 13.7. (* denote extra signals belonging to the other isomer) **IR (ATR):** 1686, 1625, 1496, 723 cm^{-1}. **HRMS (ESI):** calc. $[M+H]^+$: 840.37154; found: 840.36991. **M_p:** 99- 108°C.

3-(1-(2-(2-(2-((2-(2,6-dioxopiperidin-3-yl)-1,3-dioxoisoindolin-4-yl)amino)ethoxy)ethoxy)ethyl)-1H-1,2,3-triazol-4-yl)-N-(2-(4-(1-(4-hydroxyphenyl)-2-phenylbut-1-en-1-yl)phenoxy)ethyl)-N-methylpropanamide (TAM-PO-2)

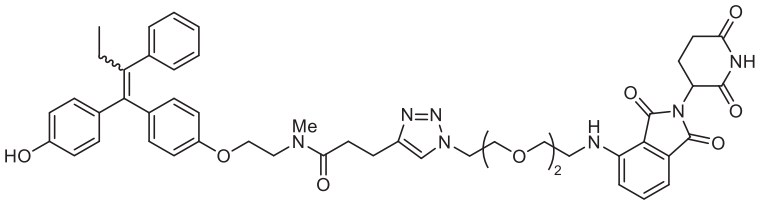

The product was prepared following general method for CuAAC from alkyne **3-2** (32 mg, 0.07 mmol) and **3-11b** (29 mg, 0.07 mmol). The crude was purified by flash column chromatography, the product was eluted at 3% MeOH/DCM yielding **TAM-PO-2** as a yellow solid (18 mg, **30%**).

^{1}H NMR (400 MHz, $CDCl_3$) δ 7.50 – 7.35 (m, 2H), 7.09 – 6.95 (m, 7H), 6.85 – 6.57 (m, 5H), 6.45 – 6.32 (m, 3H), 4.83 (ddt, *J* = 11.4, 3.2, 2.0 Hz, 1H), 4.40 – 4.28 (m, 2H), 4.04 – 3.83 (m, 2H), 3.79 – 3.71 (m, 2H), 3.66 – 3.46 (m, 8H), 3.35 (dq, *J* = 5.3, 3.0 Hz, 2H), 3.04 – 2.83 (m, 5H), 2.79 – 2.59 (m, 5H), 2.47 – 2.32 (m, 2H), 2.03 – 1.98 (m, 1H), 0.86 – 0.80 (m, 3H) ppm. **^{13}C NMR** (101 MHz, $cdcl_3$) δ 172.7*, 172.6*, 172.6*, 172.5, 171.6, 169.5, 168.9, 167.8, 157.3*, 157.0*, 156.5*, 156.1, 155.4*, 155.4*, 154.5*, 154.5, 146.9, 146.7, 142.8*, 142.7, 141.1*, 140.9, 138.0, 136.8*, 136.7*, 136.4, 136.2, 135.7*, 135.6*, 135.3*, 135.2, 132.6, 132.1, 132.1, 130.8, 130.7, 129.8, 127.9, 126.0, 123.1, 116.9, 115.2, 114.5, 114.0, 113.3, 113.3, 111.8, 110.4, 70.7, 70.6, 69.7, 69.4, 66.6*, 66.3*, 65.7*, 65.3, 50.2, 49.3*, 49.2, 49.1*, 48.2*, 48.2, 42.4, 37.6*, 37.5*, 34.5*, 34.4, 32.9*, 32.8*, 32.5*, 32.4, 31.5, 29.1, 22.9, 21.2, 21.2*, 20.9*, 20.9, 13.7. (* denote extra signals belonging to the other isomer). **IR (ATR):** 1698, 1503, 738 cm^{-1}. **HRMS (ESI):** calc. $[M+H]^+$: 884.39775; found: 884.39630. **M_p:** 105- 113°C.

3-(1-(2-(2-(2-(2-((2-(2,6-dioxopiperidin-3-yl)-1,3-dioxoisoindolin-4-yl)amino)ethoxy)ethoxy)ethoxy)ethyl)-1H-1,2,3-triazol-4-yl)-N-(2-(4-(1-(4-hydroxyphenyl)-2-phenylbut-1-en-1-yl)phenoxy)ethyl)-N-methylpropanamide (TAM-PO-3)

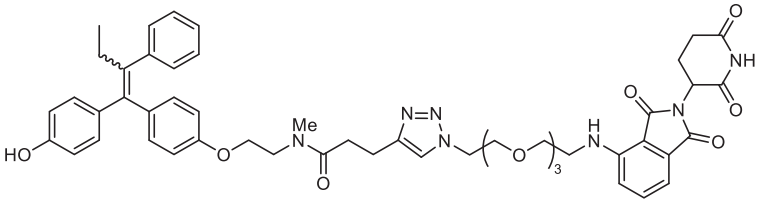

The product was prepared following general method for CuAAC from alkyne **3-2** (23 mg, 0.05 mmol) and **3-11c** (23 mg, 0.05 mmol). The crude was purified by flash column chromatography, the product was eluted at 4% MeOH/DCM yielding **TAM-PO-3** as a yellow solid (23 mg, **62%**).

^{1}H NMR (400 MHz, $CDCl_3$) δ 7.53 – 7.40 (m, 2H), 7.17 – 7.00 (m, 7H), 6.91 – 6.63 (m, 5H), 6.47 (ddd, *J* = 6.7, 5.6, 2.9 Hz, 3H), 4.90 (dd, *J* = 11.8, 5.4 Hz, 1H), 4.40 – 4.24 (m, 2H), 4.10 – 3.81 (m, 2H), 3.81 – 3.50 (m, 14H), 3.43 (q, *J* = 5.4 Hz, 2H), 3.14 – 2.91 (m, 5H), 2.91 – 2.66 (m, 5H), 2.51 – 2.40 (m, 2H), 2.12 – 2.06 (m, 1H), 0.90 (td, *J* = 7.4, 1.7 Hz, 3H) ppm. **^{13}C NMR** (101 MHz, $cdcl_3$) δ 172.5*, 172.5, 171.5, 169.4, 168.7, 167.8, 157.3*, 156.5, 155.3*, 154.4, 146.9, 146.7, 142.7, 141.1, 138.0, 136.2, 132.6, 132.1, 132.1, 130.8, 130.7, 129.8, 127.9, 126.0, 123.1*, 123.0, 117.0, 115.2, 114.5, 114.1, 113.3, 111.8, 110.4, 70.8, 70.7, 70.7, 70.6, 69.6, 66.7*, 66.4, 50.1, 49.2*, 49.0, 48.3*, 48.2, 42.5, 37.6*, 37.5*, 34.5*, 34.4, 32.9*, 32.5, 31.6, 29.1, 22.9, 21.0, 13.8. (* denote extra signals belonging to the other isomer) **IR (ATR):** 1701, 1622, 1114, 729 cm^{-1}. **HRMS (ESI):** calc. $[M+H]^+$: 928.42397; found: 928.42301. **M_p:** 84- 89°C.

3-(1-(14-((2-(2,6-dioxopiperidin-3-yl)-1,3-dioxoisoindolin-4-yl)amino)-3,6,9,12-tetraoxatetradecyl)-1H-1,2,3-triazol-4-yl)-N-(2-(4-(1-(4-hydroxyphenyl)-2-phenylbut-1-en-1-yl)phenoxy)ethyl)-N-methylpropanamide (TAM-PO-4)

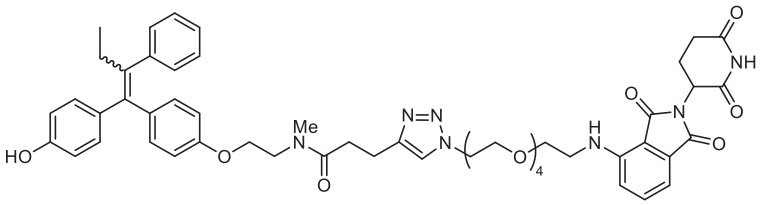

The product was prepared following general method for CuAAC from alkyne **3-2** and **3-11d** (34 mg, 0.07 mmol). The crude was purified by flash column chromatography, the product was eluted at 4% MeOH/DCM as a yellow solid yielding **TAM-PO-4** (31 mg, **48%**).

^{1}H NMR (400 MHz, $CDCl_3$) δ 7.56 – 7.43 (m, 2H), 7.20 – 7.02 (m, 7H), 6.92 – 6.78 (m, 2H), 6.77 – 6.64 (m, 2H), 6.53 – 6.43 (m, 2H), 4.97 – 4.82 (m, 1H), 4.40 – 4.25 (m, 2H), 4.09 – 3.88 (m, 2H), 3.79 – 3.48 (m, 18H), 3.43 (dt, *J* = 5.6, 2.8 Hz, 2H), 3.17 – 2.63 (m, 10H), 2.50 – 2.41 (m, 2H), 2.11 – 2.04 (m, 1H), 0.91 – 0.86 (m, 3H) ppm. **^{13}C NMR** (101 MHz, $cdcl_3$) δ 172.5, 171.5, 169.4, 168.7, 167.8, 157.3*, 157.0*, 156.5*, 156.1, 155.3*, 154.4, 147.0, 146.8, 142.7, 141.1*, 141.0, 138.0, 136.4, 136.2, 135.8*, 135.4, 132.6, 132.1, 132.1, 131.0, 130.7, 129.8, 129.0, 127.9, 126.0, 122.9, 117.0, 115.2, 114.5, 114.1, 113.3, 113.2, 111.8, 110.4, 70.8, 70.7, 70.7, 70.6, 70.5, 69.6, 66.7*, 66.4*, 66.0*, 65.7, 50.1, 49.3*, 49.2*, 49.0, 48.3*, 48.2, 42.5, 37.7*, 37.6*, 34.5*, 34.4, 32.9*, 32.0*, 31.5*, 31.0, 29.5*, 29.1, 22.9*, 22.8, 21.1, 13.7. (* denote extra signals belonging to the other isomer). **IR (ATR):** 1701, 1618.8, 1108, 729 cm^{-1}. **HRMS (ESI):** calc. $[M+H]^+$: 972.45018; found: 972.44833. **M_p:** 112-120°C.

N-(2-(4-(1-(4-hydroxyphenyl)-2-phenylbut-1-en-1-yl)phenoxy)ethyl)-N-methyl-3-(1-(2-(2-(2-((2-(1-methyl-2,6-dioxopiperidin-3-yl)-1,3-dioxoisoindolin-4-yl)amino)ethoxy)ethoxy)ethoxy)ethyl)-1H-1,2,3-triazol-4-yl)propanamide (TAM-PO-3-Me)

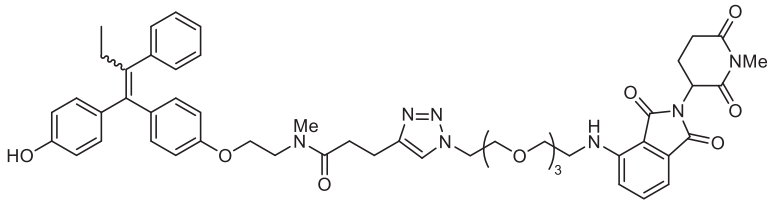

The product was prepared following general method for CuAAC from alkyne **3-2** (18 mg, 0.04 mmol) and **3-11c-Me** (18 mg, 0.04 mmol). The crude was purified by flash column chromatography, the product was eluted at 3% MeOH/DCM yielding **TAM-PO-3-Me** as a yellow solid film (32 mg, **85%**).

^{1}H NMR (400 MHz, $CDCl_3$) δ 7.58 – 7.42 (m, 2H), 7.20 – 7.00 (m, 7H), 6.94 – 6.61 (m, 4H), 6.55 – 6.37 (m, 2H), 4.90 (dd, *J* = 12.1, 5.7 Hz, 1H), 4.41 – 4.29 (m, 2H), 4.12 – 3.88 (m, 1H), 3.81 – 3.51 (m, 14H), 3.43 (q, *J* = 5.5 Hz, 2H), 3.18 (s, 1H), 3.13 – 2.86 (m, 5H), 2.83 – 2.65 (m, 3H), 2.46 (dtd, *J* = 12.6, 7.5, 3.5 Hz, 2H), 2.09 – 2.04 (m, 1H), 0.95 – 0.86 (m, 3H). **^{13}C NMR** (101 MHz, $CDCl_3$) δ 172.4*, 172.4, 171.5, 169.6, 169.2, 167.9, 157.3*, 157.0*, 156.5*, 156.1, 155.3*, 154.4, 146.9, 146.7, 142.8*, 142.7, 141.1*, 141.0, 137.9, 136.8*, 136.7*, 136.4, 136.1, 135.7*, 135.3, 132.6, 132.1, 130.7, 129.8, 127.9, 126.0, 122.9, 116.9, 115.2, 114.5, 114.0, 113.3, 113.2, 111.8, 110.4, 70.8, 70.7, 70.6, 69.7, 69.6, 66.6*, 66.3*, 65.7*, 65.4, 50.2, 49.7, 49.2*, 48.2, 42.5, 37.6*, 37.5*, 34.4*, 34.3, 32.9*, 32.5, 32.0, 29.1, 27.4, 22.2, 21.3*, 21.1, 13.7. (* denote extra signals belonging to the other isomer). **IR (ATR):** 1701, 1683, 1234, 1108 $cm^{-1.}$ **HRMS (ESI):** calc. $[M+H]^+$: 942.43730; found: 942.43962. **M_p:** 72-78°C.

-3-(1-(2-(2-(2-(2-((2-(2,6-dioxopiperidin-3-yl)-1,3-dioxoisoindolin-4-yl)amino)ethoxy)ethoxy)ethoxy)ethyl)-1H-1,2,3-triazol-4-yl)-N-(2-(4-(1-(4-hydroxyphenyl)-2-phenylbut-1-en-1-yl)-3-methylphenoxy)ethyl)-N-methylpropanamide(TAM(Me)-PO-3)

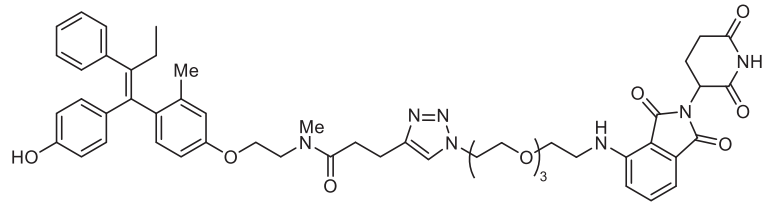

The product was prepared following general method for CuAAC from alkyne **3-24** (20 mg, 0.04 mmol) and **3-11d** (20 mg, 0.04 mmol). The crude was purified by flash column chromatography, the product was eluted at 4% MeOH/DCM yielding **TAM-PO-3-Me** as a yellow solid film (31 mg, **80%**).

^{1}H NMR (400 MHz, $CDCl_3$) δ 8.68 (s, 1H), 7.74 – 7.49 (m, 1H), 7.46 (dd, *J* = 14.4, 6.8 Hz, 1H), 7.20 – 6.96 (m, 7H), 6.89 (d, *J* = 8.5 Hz, 1H), 6.80 – 6.67 (m, 4H), 6.51 – 6.42 (m, 2H), 6.42 – 6.32 (m, 1H), 4.90 (dd, *J* = 11.7, 5.3 Hz, 1H), 4.40 – 4.26 (m, 2H), 4.09 – 3.89 (m, 2H), 3.86 – 3.72 (m, 2H), 3.69 (t, *J* = 5.4 Hz, 2H), 3.65 – 3.51 (m, 10H), 3.44 (q, *J* = 5.5 Hz, 2H), 3.08 – 2.89 (m, 5H), 2.89 – 2.63 (m, 5H), 2.28 (p, *J* = 6.5 Hz, 2H), 2.11 – 2.06 (m, 1H), 2.04 (d, *J* = 5.1 Hz, 3H), 1.93* (d, *J* = 3.3 Hz, 3H), 1.01 – 0.93* (m, 3H), 0.81 – 0.73 (m, 3H). **^{13}C NMR** (101 MHz, $CDCl_3$) δ 172.4, 171.5, 169.4, 168.7, 167.8, 156.4, 156.0, 155.3, 155.2, 146.9, 142.4, 142.4, 141.7, 141.6, 137.7, 137.6, 136.8, 136.8, 136.2, 134.9, 134.9, 134.8, 132.6, 131.6, 131.6, 131.0, 130.7, 130.4, 129.9, 129.0, 128.1, 128.0, 127.6, 126.2, 126.0, 122.9, 117.2, 116.9, 116.7, 113.9, 113.2, 113.2, 112.7, 111.8, 110.4, 70.9, 70.7, 70.7, 70.6, 69.6, 66.4, 65.4, 50.1, 49.2, 49.0, 48.2, 42.5, 37.5, 34.4, 32.9, 31.6, 29.3, 28.0, 22.9, 21.0, 20.5, 20.1, 14.1, 13.0. **IR (ATR):** 2900.73, 1695.60, 1622.60, 1048.51 cm^{-1}. **HRMS (ESI):** calculated for $[C_{52}H_{60}N_7O_{10}]^+$: 942.4396, found: 942.4387. **Mp:** 72 °C.

N-(5-(2-(2,6-dioxopiperidin-3-yl)-1-oxoisoindolin-4-yl)pent-4-yn-1-yl)-6-(4-(3-((2-(4-(1-(4-hydroxyphenyl)-2-phenylbut-1-en-1-yl)phenoxy)ethyl)(methyl)amino)-3-oxopropyl)-1H-1,2,3-triazol-1-yl)hexanamide (TAM-LEN-1)

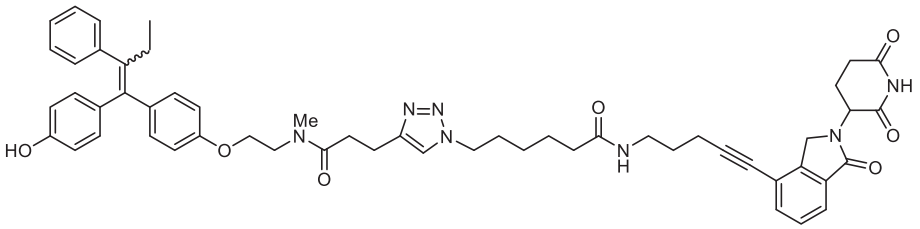

The product was prepared following general method for CuAAC from alkyne **3-2** (13 mg, 0.03 mmol) and **3-18** (11 mg, 0.03 mmol). The crude was purified by flash column chromatography, the product was eluted at 3% MeOH/DCM yielding **TAM-LEN-1** as a yellow solid film (10 mg, **45%**).

^{1}H NMR (400 MHz, $CDCl_3$) δ 8.9 (s, 1H), 7.8 (d, *J* = 7.6 Hz, 1H), 7.5 (d, *J* = 7.5 Hz, 1H), 7.4 (dt, *J* = 37.0, 7.4 Hz, 3H), 7.1 (tq, *J* = 17.8, 7.5 Hz, 6H), 6.9 – 6.6 (m, 4H), 6.5 – 6.3 (m, 2H), 6.0 (s, 1H), 5.2 – 5.2 (m, 1H), 4.5 (qd, *J* = 17.2, 3.4 Hz, 2H), 4.2 – 3.8 (m, 4H), 3.7 – 3.6 (m, 4H), 3.5 – 3.3 (m, 2H), 3.1 – 2.9 (m, 5H), 2.9 – 2.6 (m, 4H), 2.6 – 2.4 (m, 4H), 2.2 – 2.0 (m, 4H), 1.8 – 1.6 (m, 4H), 1.6 – 1.5 (m, 2H), 1.2 (s, 2H), 1.0 – 0.9 (m, 3H). **^{13}C NMR** (101 MHz, $CDCl_3$) δ 171.6, 169.8, 157.2, 154.5, 154.0, 143.9, 134.4, 131.9, 130.6, 129.7, 128.4, 127.8, 125.9, 123.4, 115.2, 114.5, 113.9, 113.1, 58.4, 51.9, 49.7, 48.3, 47.2, 38.6, 37.5, 36.2, 32.7, 31.6, 29.7, 29.0, 25.8, 24.7, 23.2, 18.4, 17.1, 13.6. **HRMS (ESI):** calculated for $[C_{54}H_{60}O_70N_7]^+$: 918.45487; found: 918.45273. **IR (ATR):** 2926.4, 1693.8, 1231.4, 726.7 cm^{-1} **Mp:** 97-107°C.

N-(5-(2-(2,6-dioxopiperidin-3-yl)-1-oxoisoindolin-4-yl)pentyl)-6-(4-(3-((2-(4-(1-(4-hydroxyphenyl)-2-phenylbut-1-en-1-yl)phenoxy)ethyl)(methyl)amino)-3-oxopropyl)-1H-1,2,3-triazol-1-yl)hexanamide (TAM-LEN-2)

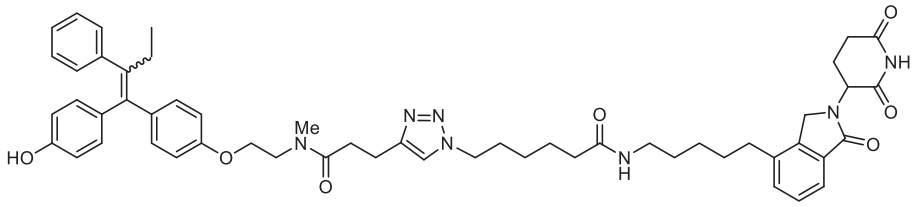

The product was prepared following general method for CuAAC from alkyne **3-2** (27 mg, 0.05 mmol) and **3-16** (22 mg, 0.05 mmol). The crude was purified by flash column chromatography, the product was eluted at 3% MeOH/DCM yielding **TAM-LEN-1** as a yellow solid film (25 mg, **55%**).

^{1}H NMR (400 MHz, $CDCl_3$) δ 7.7 (d, *J* = 7.3 Hz, 1H), 7.4 – 7.3 (m, 2H), 7.2 – 7.0 (m, 8H), 6.8 (dd, *J* = 17.0, 8.6 Hz, 2H), 6.8 – 6.6 (m, 2H), 6.5 – 6.3 (m, 2H), 5.9 (s, 1H), 5.2 (dd, *J* = 13.5, 5.3 Hz, 1H), 4.4 (dd, *J* = 16.2, 3.2 Hz, 1H), 4.3 (dd, *J* = 16.1, 3.9 Hz, 1H), 4.1 – 3.8 (m, 4H), 3.8 – 3.6 (m, 2H), 3.2 – 3.2 (m, 1H), 3.1 – 2.9 (m, 7H), 2.9 – 2.7 (m, 4H), 2.6 – 2.6 (m, 2H), 2.4 (dt, *J* = 14.6, 7.2 Hz, 2H), 2.1 – 2.0 (m, 2H), 1.8 – 1.6 (m, 4H), 1.6 – 1.5 (m, 4H), 1.4 – 1.3 (m, 2H), 1.2 – 1.1 (m, 2H), 0.9 (td, *J* = 7.4, 2.4 Hz, 3H). **^{13}C NMR** (101 MHz, $CDCl_3$) δ 173.3, 171.6, 171.3, 170.1, 170.0, 156.4, 156.0, 154.7, 154.3, 147.0, 142.7, 141.2, 141.0, 140.2, 137.3, 132.1, 132.0, 132.0, 131.4, 131.0, 130.7, 130.6, 129.8, 128.7, 127.9, 126.0, 121.9, 115.3, 114.6, 114.0, 113.3, 84.3, 70.7, 66.7, 60.5, 52.0, 49.8, 48.3, 46.5, 46.1, 39.3, 37.7, 36.3, 32.9*, 31.9*, 31.7, 29.9, 29.5, 29.4, 29.1, 26.5, 26.0, 25.0*,

24.9, 23.5, 13.8. **HRMS (ESI):** calculated for $[C_{54}H_{60}O_70N_7]^+$: 922.48617; found: 922.48424. **IR (ATR):** 2969.8, 1733.8, 1216.9 cm^{-1}. **M_p:**75-82°C.

(2S,4R)-4-hydroxy-1-((S)-2-(4-(4-(3-((2-(4-((E)-1-(4-hydroxyphenyl)-2-phenylbut-1-en-1-yl)phenoxy)ethyl)(methyl)amino)-3-oxopropyl)-1H-1,2,3-triazol-1-yl)butanamido)-3,3-dimethylbutanoyl)-N-((S)-1-(4-(4-methylthiazol-5-yl)phenyl)ethyl)pyrrolidine-2-carboxamide (TAM-VHL-1)

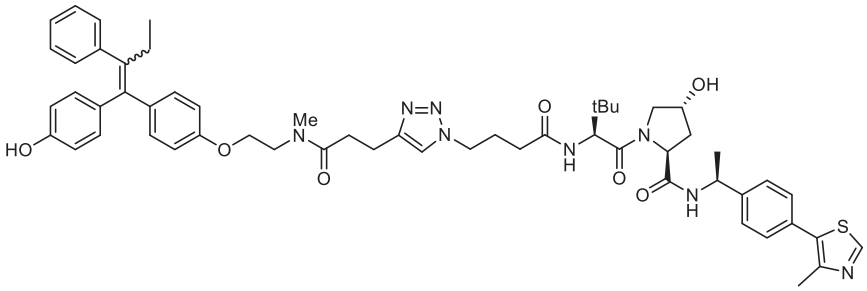

The product was prepared following general method for CuAAC from alkyne **3-2** (18 mg, 0.04 mmol) and **3-30a** (25 mg, 0.04 mmol).The crude was purified by flash column chromatography, the product was eluted at 10% MeOH/DCM yielding **TAM-VHL-1** as a white solid (25 mg, **50 %**).

^{1}H NMR (400 MHz, $CDCl_3$) δ 8.67 (s, 1H), 7.42 – 7.30 (m, 4H), 7.19 – 6.95 (m, 8H), 6.80 (dd, *J* = 8.6, 3.1 Hz, 2H), 6.73 (dd, *J* = 8.2, 5.5 Hz, 1H), 6.66 (dd, *J* = 8.3, 5.7 Hz, 1H), 6.42 (dd, *J* = 38.3, 8.3 Hz, 2H), 5.15 – 5.03 (m, 1H), 4.72 (dq, *J* = 8.6, 4.0 Hz, 1H), 4.49 (t, *J* = 6.2 Hz, 2H), 4.20 – 3.97 (m, 4H), 3.97 – 3.83 (m, 1H), 3.76 – 3.65 (m, 1H), 3.66 – 3.54 (m, 2H), 3.12 – 2.89 (m, 5H), 2.75 (ddt, *J* = 54.6, 23.9, 6.7 Hz, 2H), 2.51 (s, 3H), 2.52 – 2.37 (m, 3H), 2.14 (s, 1H), 2.04 – 1.86 (m, 3H), 1.47 (dd, *J* = 6.9, 4.5 Hz, 3H), 1.05 (d, *J* = 2.8 Hz, 9H), 0.94 – 0.85 (m, 3H) ppm. **^{13}C NMR** (101 MHz, $CDCl_3$) δ 207.0*, 172.4*, 172.4*, 172.3, 172.2, 172.1, 172.0*, 170.0, 169.9, 157.2*, 156.7*, 156.3*, 155.9*, 155.4, 154.5, 150.4, 148.4, 147.2*, 146.9, 143.3, 143.3*, 142.6*, 142.5, 141.1*, 140.9, 137.8*, 137.7*, 137.7*, 137.7, 137.3*, 136.9*, 136.6, 135.5*, 135.5*, 135.1*, 135.0, 132.0, 132.0*, 131.9, 131.7*, 130.8, 130.6, 130.6, 129.7, 129.5, 127.8, 126.5, 125.9, 122.4*, 122.4*, 122.3, 115.2, 114.5, 114.0*, 113.9, 113.2*, 113.1, 70.1, 66.4*, 66.1*, 65.5*, 65.2, 58.6*, 58.5, 58.4*, 58.4*, 58.3, 56.8, 49.2*, 49.1*, 48.9, 48.6, 48.5*, 48.3, 37.7*, 37.7, 36.1*, 36.0*, 35.1, 35.0*, 35.0*, 34.3*, 34.2, 32.7, 32.7*, 32.2, 32.2, 32.0, 32.0*, 31.9, 29.0, 26.6, 25.9, 25.8*, 22.2, 21.1, 16.1, 13.6 ppm. **IR (ATR):** 2955, 1621, 1506, 1235, 727 cm^{-1}. **HRMS (ESI):** calculated for $[C_{57}H_{69}O_7N_8S]^+$: 1009.50044, found: 1009.50085. **M_p:** 96-103 °C.

(2*S*,4R)-4-hydroxy-1-((*S*)-2-(6-(4-(3-((2-(4-((E)-1-(4-hydroxyphenyl)-2-phenylbut-1-en-1-yl)phenoxy)ethyl)(methyl)amino)-3-oxopropyl)-1H-1,2,3-triazol-1-yl)hexanamido)-3,3-dimethylbutanoyl)-*N*-((*S*)-1-(4-(4-methylthiazol-5-yl)phenyl)ethyl)pyrrolidine-2-carboxamide (TAM-VHL-2)

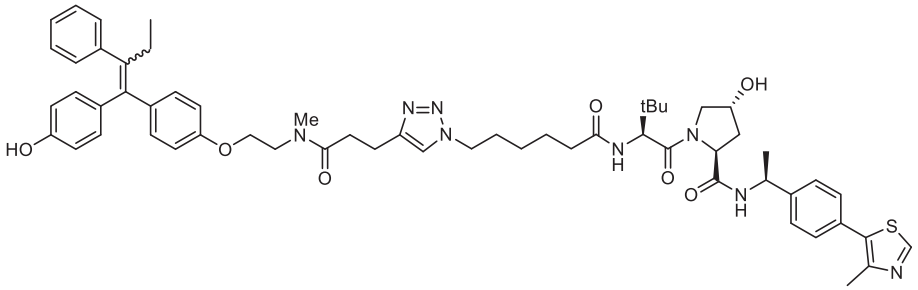

The product was prepared following general method for CuAAC from alkyne **3-2** (18 mg, 0.04 mmol) and **3-30b** (26 mg, 0.04 mmol). The crude was purified by flash column chromatography, the product was eluted at 10% MeOH/DCM yielding **TAM-VHL-2** as a white solid (22 mg, **50 %**).

^{1}H NMR (400 MHz, $CDCl_3$) δ 8.68 (s, 1H), 7.44 – 7.33 (m, 5H), 7.20 – 7.00 (m, 8H), 6.81 (t, *J* = 8.6 Hz, 1H), 6.70 (dt, *J* = 21.9, 8.0 Hz, 2H), 6.48 (dd, *J* = 11.4, 8.4 Hz, 1H), 6.31 (t, *J* = 8.5 Hz, 1H), 5.16 – 5.01 (m, 1H), 4.71 (q, *J* = 9.1, 8.6 Hz, 1H), 4.64 – 4.54 (m, 1H), 4.49 (s, 1H), 4.11 – 3.53 (m, 8H), 3.13 – 2.90 (m, 5H), 2.87 – 2.59 (m, 2H), 2.52 (s, 3H), 2.50 – 2.37 (m, 3H), 2.27 – 2.01 (m, 3H), 1.75 – 1.52 (m, 4H), 1.47 (t, *J* = 6.8 Hz, 3H), 1.18 (dd, *J* = 14.6, 7.5 Hz, 2H), 1.07 – 0.99 (m, 9H), 0.91 (td, *J* = 7.4, 1.8 Hz, 3H) ppm. **^{13}C NMR** (101 MHz, $CDCl_3$) δ 173.5*, 173.4, 172.4*, 172.4*, 172.3, 172.0*, 171.9, 169.9, 157.2*, 156.8*, 156.4*, 155.9, 155.3*, 154.4, 150.4, 148.5, 146.8, 143.2, 142.6, 141.1*, 141.0*, 140.9, 137.8*, 137.8, 136.9*, 136.7*, 136.5, 135.6*, 135.5*, 135.2*, 135.2, 131.9, 131., 130.8, 130.6, 129.7, 129.6, 127.8, 126.5, 125.9, 121.8, 115.2, 114.5, 113.9*, 113.9, 113.2*, 113.1, 70.0, 66.5*, 66.2*, 65.5*, 65.1, 58.7, 57.7, 56.9, 49.7, 49.2*, 49.1*, 48.9, 48.3*, 48.3, 37.7*, 37.6*, 35.8, 35.3, 34.3*, 34.2, 32.8*, 32.7, 32.4*, 32.4, 29.8, 29.0 , 26.5, 25.8* , 25.8 , 24.6 , 22.2 , 21.1, 16.1 , 13.6 ppm. **IR (ATR):** 2958, 1622, 1506, 1237, 727 cm^{-1}. **HRMS (ESI):** calculated for $[C_{59}H_{73}O_7N_8S]^+$: 1037.53174, found: 1037.53229. **M_p:** 82-90 °C.

(2S,4R)-4-hydroxy-1-((S)-2-(3-(4-(4-(3-((2-(4-((E)-1-(4-hydroxyphenyl)-2-phenylbut-1-en-1-yl)phenoxy)ethyl)(methyl)amino)-3-oxopropyl)-1H-1,2,3-triazol-1-yl)butanamido)propanamido)-3,3-dimethylbutanoyl)-N-((S)-1-(4-(4-methylthiazol-5-yl)phenyl)ethyl)pyrrolidine-2-carboxamide (TAM-VHL-3)

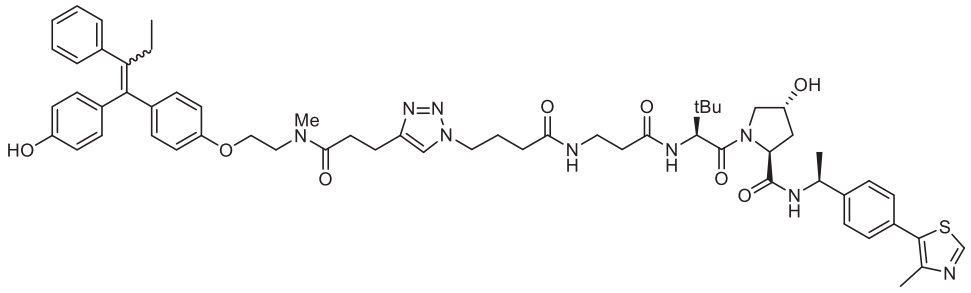

The product was prepared general method for CuAAC from alkyne **3-2** (18 mg, 0.04 mmol) and **3-32a** (25 mg, 0.04 mmol). The crude was purified by flash column chromatography; the product was eluted at 10% MeOH/DCM yielding **TAM-VHL-3** as a white solid (30 mg, **70 %**).

^{1}H NMR (400 MHz, $CDCl_3$) δ 8.70 (s, 1H), 7.66 (s, 1H), 7.38 (s, 5H), 7.19 – 6.99 (m, 8H), 6.89 – 6.62 (m, 4H), 6.49 (d, *J* = 9.0 Hz, 2H), 5.10 (s, 1H), 4.62 (s, 2H), 4.43 (s, 1H), 4.20 – 3.37 (m, 8H), 3.36 – 2.65 (m, 9H), 2.59 – 2.11 (m, 9H), 2.01 (d, *J* = 31.9 Hz, 5H), 1.49 – 1.33 (m, 3H), 1.03 (d, *J* = 3.8 Hz, 9H), 0.91 (td, *J* = 7.6, 2.2 Hz, 3H) ppm. **^{13}C NMR** (101 MHz, $CDCl_3$) δ 172.2, 171.8, 170.3, 156.3, 155.8, 155.4, 154.5, 143.6, 142.5, 141.1, 140.9, 137.7, 137.0, 136.6, 135.6, 135.2, 131.9, 130.6, 129.7, 127.8, 126.6, 125.9, 115.3, 114.6, 114.0, 113.2, 70.2, 67.1, 58.8, 58.0, 57.2, 48.8, 48.4, 46.0, 36.8, 36.2, 36.0, 35.4, 32.7, 29.0, 26.6, 22.4, 13.6 ppm. **IR (ATR):** 2963, 1620, 1506, 1170, 727 cm^{-1}. **HRMS (ESI):** calculated for $[C_{60}H_{74}O_8N_9S]^+$: 1080.53756, found: 1080.53782. **M_p:** 98 °C.

(2S,4R)-4-hydroxy-1-((S)-2-(6-(4-(4-(3-((2-(4-((E)-1-(4-hydroxyphenyl)-2-phenylbut-1-en-1-yl)phenoxy)ethyl)(methyl)amino)-3-oxopropyl)-1H-1,2,3-triazol-1-yl)butanamido)hexanamido)-3,3-dimethylbutanoyl)-N-((S)-1-(4-(4-methylthiazol-5-yl)phenyl)ethyl)pyrrolidine-2-carboxamide (TAM-VHL-4)

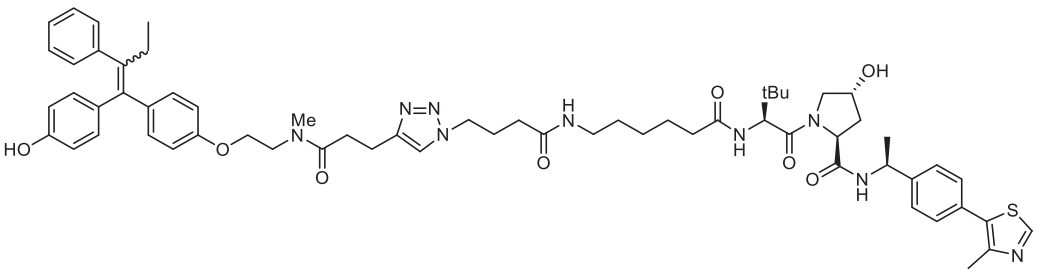

The product was prepared following general method for CuAAC from alkyne **3-2** (18 mg, 0.04 mmol) and **3-32b** (25 mg, 0.04 mmol). The crude was purified by flash column chromatography, the product was eluted at 10% MeOH/DCM yielding **TAM-VHL-4** as a white solid (28 mg, **60 %**).

^{1}H NMR (400 MHz, $CDCl_3$) δ 8.68 (s, 1H), 7.51 – 7.29 (m, 5H), 7.20 – 7.00 (m, 7H), 6.86 – 6.79 (m, 1H), 6.75 – 6.65 (m, 2H), 6.48 (ddd, *J* = 14.9, 8.4, 4.2 Hz, 2H), 6.39 – 6.33 (m, 1H), 5.09 (td, *J* = 7.2, 4.1 Hz, 1H), 4.71 (q, *J* = 8.0 Hz, 1H), 4.62 (dd, *J* = 9.3, 7.5 Hz, 1H), 4.49 (s, 1H), 4.22 – 3.81 (m, 6H), 3.62 (dd, *J* = 9.7, 6.1 Hz, 2H), 3.15 (d, *J* = 6.7 Hz, 2H), 3.12 – 2.90 (m, 5H), 2.90 – 2.59 (m, 2H), 2.52 (s, 3H), 2.50 – 2.39 (m, 3H), 2.17 (tt, *J* = 19.2, 6.6 Hz, 3H), 2.10 – 1.96 (m, 4H), 1.58 (dq, *J* = 20.8, 6.9 Hz, 2H), 1.48 – 1.44 (m, 3H), 1.44 – 1.38 (m, 2H), 1.32 – 1.26 (m, 2H), 1.03 (d, *J* = 5.7 Hz, 9H), 0.91 (td, *J* = 7.4, 1.4 Hz, 3H) ppm. **^{13}C NMR** (101 MHz, $CDCl_3$) δ 173.8, 171.9, 171.7, 169.9, 157.2*, 156.3, 155.3*, 154.4, 150.4, 148.5, 143.3, 142.5, 141.1*, 140.9, 137.8*, 137.7, 136.9*, 136.5, 135.6*, 135.2, 132.0, 131.9, 130.8, 130.6, 129.7, 129.6, 127.8, 126.5, 125.9, 122.3, 115.3, 115.2, 114.5, 113.9, 113.2, 69.9, 66.5*, 66.1*, 65.3*, 65.0, 58.7, 57.5, 57.0, 49.0, 48.9, 48.3, 39.2, 37.6*, 37.5*, 36.0, 35.3, 34.2*, 34.1, 32.7, 32.6, 29.0, 28.8, 26.5, 26.1, 26.0, 24.8, 22.2, 21.0, 16.1, 13.6 ppm. **IR (ATR):** 2925, 1624, 1237, 830 cm^{-1}. **HRMS (ESI):** calculated for $[C_{63}H_{80}O_8N_9S]^+$: 1122.58451, found: 1122.58502. **M_p:** 70-75 °C.

(2S,4R)-4-hydroxy-1-((S)-2-(6-(6-(4-(3-((2-(4-((E)-1-(4-hydroxyphenyl)-2-phenylbut-1-en-1-yl)phenoxy)ethyl)(methyl)amino)-3-oxopropyl)-1H-1,2,3-triazol-1-yl)hexanamido)hexanamido)-3,3-dimethylbutanoyl)-N-((S)-1-(4-(4-methylthiazol-5-yl)phenyl)ethyl)pyrrolidine-2-carboxamide (TAM-VHL-5)

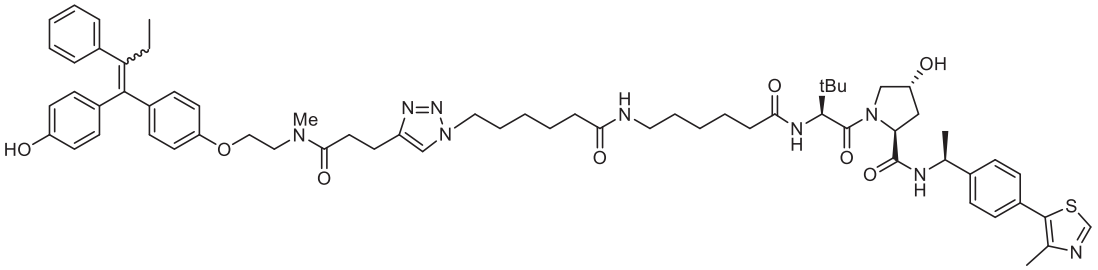

The product was prepared following general method for CuAAC from alkyne **3-2** (18 mg, 0.04 mmol) and **3-32c** (25 mg, 0.04 mmol). The crude was purified by flash column chromatography, the product was eluted at 10% MeOH/DCM yielding **TAM-VHL-5** as white solid (25 mg, **60 %**).

^{1}H NMR (400 MHz, $CDCl_3$) δ 8.68 (s, 1H), 7.46 – 7.29 (m, 6H), 7.19 – 6.99 (m, 7H), 6.87 – 6.77 (m, 1H), 6.76 – 6.60 (m, 2H), 6.54 – 6.38 (m, 2H), 5.99 (dd, *J* = 13.9, 6.4 Hz, 1H), 5.09 (td, *J* = 7.2, 3.7 Hz, 1H), 4.72 (q, *J* = 8.2 Hz, 1H), 4.65 – 4.56 (m, 1H), 4.49 (d, *J* = 10.9 Hz, 1H), 4.12 – 3.57 (m, 8H), 3.17 (p, *J* = 6.9 Hz, 2H), 3.12 – 2.89 (m, 5H), 2.75 (ddt, *J* = 58.3, 26.4, 6.6 Hz, 2H), 2.52 (d, *J* = 2.1 Hz, 3H), 2.50 – 2.40 (m, 3H), 2.28 – 2.03 (m, 5H), 1.73 – 1.52 (m, 6H), 1.50 – 1.36 (m, 5H), 1.32 – 1.11 (m, 4H), 1.07 – 1.00 (m, 9H), 0.91 (td, *J* = 7.4, 1.8 Hz, 3H) ppm.**^{13}C NMR** (101 MHz, $CDCl_3$) δ 173.9, 173.1, 172.2*, 172.0, 169.8, 156.3, 155.4*, 154.5, 150.4, 148.5, 146.9, 143.2, 142.5, 141.2, 137.8, 136.9*, 136.5, 135.4, 131.9, 130.9, 130.6, 129.7, 129.6, 127.8, 126.5, 125.9, 121.8, 115.2, 114.5, 113.9, 113.1, 69.9, 66.5*, 66.2, 58.6, 57.6, 56.9, 49.7, 49.1*, 48.9, 48.3, 39.2, 37.7*, 37.6, 36.2, 36.0, 35.8, 35.2, 32.8, 29.8, 29.0, 28.9, 26.5, 26.0, 25.9, 24.9, 24.8, 22.2, 21.1, 16.1, 13.6 ppm. **IR (ATR):** 2931, 1626, 1051 cm^{-1}. **HRMS (ESI):** calculated for $[C_{65}H_{84}O_8N_9S]^+$: 1150.61581, found: 1150.61685**. M_p:** 80 °C.

(2S,4S)-4-hydroxy-1-((S)-2-(4-(4-(3-((2-(4-((E)-1-(4-hydroxyphenyl)-2-phenylbut-1-en-1-yl)phenoxy)ethyl)(methyl)amino)-3-oxopropyl)-1H-1,2,3-triazol-1-yl)butanamido)-3,3-dimethylbutanoyl)-N-((S)-1-(4-(4-methylthiazol-5-yl)phenyl)ethyl)pyrrolidine-2-carboxamide (TAM-VHL-1*)

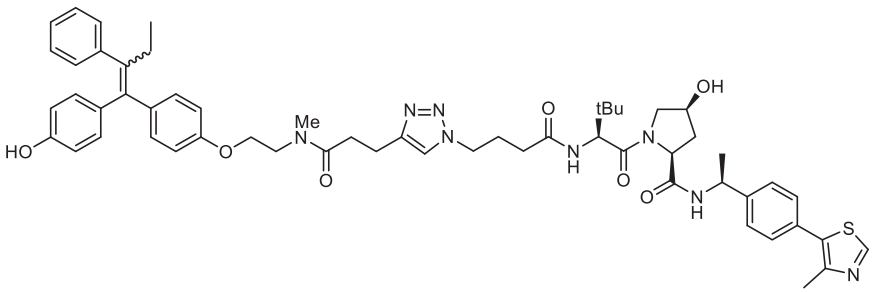

The product was prepared following general method for CuAAC from alkyne **3-2** (7 mg, 0.015 mmol) and **3-30a*** (8.5 mg, 0.015 mmol). The crude was purified by flash column chromatography; the product was eluted at 15% MeOH/DCM yielding **TAM-VHL-1*** as a white wax (9 mg, **60 %**).

^{1}H NMR (400 MHz, $CDCl_3$) δ 8.79 – 8.67 (m, 1H), 7.42 – 7.25 (m, 4H), 7.20 – 7.02 (m, 8H), 6.84 – 6.64 (m, 4H), 6.51 – 6.36 (m, 2H), 5.04 (dt, J = 14.3, 7.2 Hz, 1H), 4.61 (t, J = 8.4 Hz, 1H), 4.50 (dd, J = 11.4, 7.1 Hz, 2H), 4.21 – 3.90 (m, 3H), 3.83 – 3.60 (m, 5H), 3.08 – 2.94 (m, 5H), 2.87 – 2.60 (m, 2H), 2.52 – 2.41 (m, 4H), 2.39 – 1.96 (m, 6H), 1.26 (d, J = 2.6 Hz, 3H), 1.05 – 0.99 (m, 9H), 0.91 (t, J = 7.3 Hz, 3H). **HRMS (ESI):** calculated for $[C_{57}H_{69}O_7N_8S]+$: 1009.50044; found: 1009.49884.

8.4. Experimental Section – TLK PROTACs

methyl 2-(6-bromo-1H-indol-3-yl)-2-oxoacetate (4-1)

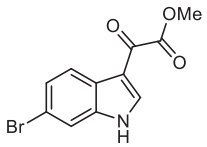

A flame-dried flask was loaded with 6-bromoindole (1.5 g, 7.65 mmol) and Et_2O and cooled down at 0°C, then oxalyl chloride (0.72 mL, 8.4 mmol) was added dropwise. The reaction mixture was allowed to warm up at rt for 1 h, then cooled down at 0°C and a suspension of NaOMe (0.82 g, 15.2 mmol) in MeOH (7.5 mL) was added dropwise. The reaction mixture was allowed to warm up at rt for 1 hour, then water was added. The precipitate was filtered and washed with cold water. The solid was dried and used without further purification. Reported as a yellow solid. (2.1 g, **96%**).

^{1}H NMR (400 MHz, DMSO) δ 12.46 (s, 1H), 8.47 (dd, J = 3.3, 1.1 Hz, 1H), 8.07 (dd, J = 8.5, 0.6 Hz, 1H), 7.40 (dd, J = 8.5, 1.8 Hz, 1H), 3.87 (d, J = 1.1 Hz, 3H).

3-(6-bromo-1H-indol-3-yl)-4-(1H-indol-3-yl)-1H-pyrrole-2,5-dione (4-2)

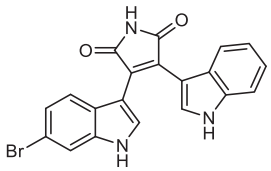

A flame-dried flask was loaded with KO^{t}Bu (0.59 g, 5.3 mmol) and THF (5 mL) and cooled down at at 0°C. A suspension of **4-1** (0.5 g, 1.77 mmol) and indole-3-acetamide (0.34 g, 1.9 mmol) in THF (10 mL) was added slowly. The reaction mixture was kept at 0°C for 30 min and then let warm up at room temperature for 3 hours. The reaction mixture was cooled down at 0°C and HCl conc. (3.6 mL) was added dropwise. The reaction mixture was stirred at room temperature for 1 hour, then water and ethyl acetate were added, the aqueous layer was extracted with ethyl acetate, the organic layers combined, washed with brine, dried over $MgSO_4$ and evaporated under reduced pressure. The

product was purified by silica flash column chromatography, eluted at 35% ethyl acetate/hexanes. Reported as a bright red solid (1.1 g, **50%**).

^{1}H NMR (400 MHz, DMSO-d_6) δ 11.7 (s, 2H), 10.9 (s, 1H), 7.7 (d, J = 17.6 Hz, 2H), 7.5 (dd, J = 1.6, 0.8 Hz, 1H), 7.4 (dt, J = 8.2, 0.9 Hz, 1H), 7.0 (ddd, J = 8.2, 7.0, 1.3 Hz, 1H), 6.7 – 6.7 (m, 3H), 6.6 (ddd, J = 8.0, 6.9, 1.0 Hz, 1H). **HRMS (ESI)**: calculated for $[C_{20}H_{13}N_3O_2Br_1]^+$: 406.01857; found: 406.01871.

2-(1-(3-(trityloxy)propyl)-1H-indol-3-yl)acetamide (4-4)

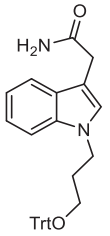

A flame-dried flask was loaded with NaH (60% in oil, 0.56 g, 7 mmol, 1.2 eq.) and DMF (19 mL) and cooled down at 0 °C. Indol-3-acetamide (1 g, 5.7 mmol, 1 eq.) in DMF (5 mL) was added and stirred at 0 °C 30 minutes. Then tityl-protected 3-bromopropan-1-ol was added slowly, reaction mixture was heated up at 50 °C and stirred overnight. Reaciton mixture was quenched by adding ethyl acetate and water. The aqueous phase was extracted with ethyl acetate, the organic layers combined , washed with brine, dried over magnesium sulphate and dried under reduced pressure. The crude was purified by silica flash column chromatography, eluting at 90% ethyl acetate in hexanes. **4-4** was obtained as a red solid (1.9 g, **70%**).

^{1}H NMR (400 MHz, CDCl3) δ 7.53 (dt, J = 7.8, 1.0 Hz, 1H), 7.46 – 7.39 (m, 6H), 7.36 – 7.18 (m, 12H), 7.12 (ddd, J = 7.9, 7.0, 1.0 Hz, 1H), 5.42 (s, 1H), 5.14 (s, 1H), 4.30 (t, J = 6.6 Hz, 2H), 3.61 (d, J = 0.8 Hz, 2H), 3.06 (t, J = 5.7 Hz, 2H), 2.10 (p, J = 6.2 Hz, 2H).

methyl 2-(1H-indol-3-yl)-2-oxoacetate (4-5)

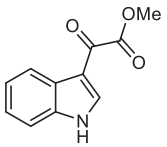

4-5 was prepared following the same procedure as **4-1**, using indole (1 g, 8.5 mmol). Obtained as a yellow solid and used without further purification (1.6 g, **95%**).

^{1}H NMR (400 MHz, DMSO) δ 12.39 (s, 1H), 8.43 (s, 1H), 8.24 – 8.04 (m, 1H), 7.63 – 7.46 (m, 1H), 7.39 – 7.09 (m, 2H), 3.87 (s, 3H). **^{13}C NMR** (101 MHz, DMSO) δ 179.2, 164.4, 138.8, 137.2, 125.9, 124.3, 123.3, 121.6, 113.2, 112.9, 53.0.

3-(1-(3-hydroxypropyl)-1H-indol-3-yl)-4-(1H-indol-3-yl)-1H-pyrrole-2,5-dione (4-6)

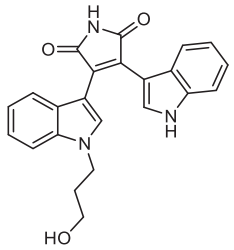

4-6 was prepared following the same procedure as **4-2**, using **4-4** (1.9 g, 4 mmol, 1.1 eq.) and **4-5** (0.74 g, 3.6 mmol, 1 eq.) The product was purified by silica flash column chromatography, eluted at 80% ethyl acetate in hexanes. Obtained as a red solid (0.55 g, **40%**).

^{1}H NMR (400 MHz, $CDCl_3$) δ 8.51 (s, 1H), 7.77 (d, J = 2.8 Hz, 1H), 7.62 (s, 1H), 7.41 – 7.29 (m, 3H), 7.17 – 7.05 (m, 3H), 6.95 (d, J = 8.1 Hz, 1H), 6.88 – 6.79 (m, 1H), 6.76 (ddd, J = 8.1, 7.1, 1.0 Hz, 1H), 4.28 (q, J = 6.7 Hz, 2H), 3.53 (t, J = 5.8 Hz, 2H), 2.07 – 1.99 (m, 2H). **HRMS (ESI):** calculated for $[C_{24}H_{22}N_3O_5S]^+$: 464.12747, found: 464.12739.

3-(3-(4-(1H-indol-3-yl)-2,5-dioxo-2,5-dihydro-1H-pyrrol-3-yl)-1H-indol-1-yl)propyl methanesulfonate (4-6-Ms)

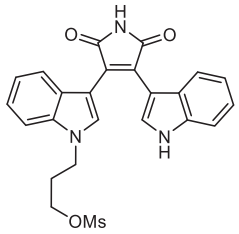

A flask was loaded with **4-6** (577 mg, 1.5 mmol, 1 eq.), dry DCM (15 mL, 0.1 M) and pyridine (4.5 mL, 0.36 mmol, 3 eq.), then MsCl (0.14 mL, 1.8 mmol, 1.2 eq.) was added dropwise and stirred overnight. Water and HCl 1M were added to the reaction mixture, the aqueous phase was extracted with ethyl acetate and dried under reduced pressure. The crude was used without further purification.

3-(1H-indol-3-yl)-4-(1-(3-(methyl(prop-2-yn-1-yl)amino)propyl)-1H-indol-3-yl)-1H-pyrrole-2,5-dione (4-7)

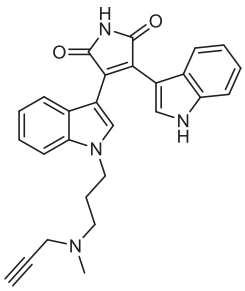

A pressure flask was loaded with 3-(3-(4-(1H-indol-3-yl)-2,5-dioxo-2,5-dihydro-1H-pyrrol-3-yl)-1H-indol-1-yl)propyl methanesulfonate **(4-6-Ms,** 500 mg, 1.1 mmol, 1 eq.), N-methylprop-2-yn-1-amine (196 mg, 2.7 mmol, 2.5 eq.) and THF (7 mL, 0.15M) and stired at 50 °C for 24 hours. Water and ethyl acetate were added, the aqueous layer was extracted with ethyl acetate and the organic layers were combined, washed with brine, dried over magnesium sulphate and dried under reduced pressure. The reaction crude was purified by flash column chromatography; the product was eluted at 50% ethyl acetate in hexanes. Obtained as a red solid, 170 mg, **60%**).

^{1}H NMR (400 MHz, $CDCll_3$) δ 8.58 (s, 1H), 7.74 (d, *J* = 2.8 Hz, 1H), 7.70 (s, 1H), 7.57 (s, 1H), 7.35 – 7.31 (m, 2H), 7.13 – 7.03 (m, 2H), 6.99 – 6.94 (m, 2H), 6.80 – 6.71 (m, 2H), 4.23 (t, *J* = 6.8 Hz, 2H), 3.32 (d, *J* = 2.4 Hz, 2H), 2.37 (t, *J* = 6.6 Hz, 2H), 2.29 (s, 3H), 2.21 (t, *J* = 2.4 Hz, 1H), 1.95 (p, *J* = 6.7 Hz, 2H). **^{13}C NMR** (101 MHz, $CDCl_3$) δ 172.0, 136.2, 135.8, 132.3, 128.8, 128.2, 127.4, 126.2, 125.4, 122.7, 122.2, 122.2, 121.9, 120.3, 120.2, 111.2, 109.7, 107.2, 105.7, 78.3, 73.3, 51.8, 45.6, 44.1, 41.4, 27.5. **IR**: 2971.18, 1691.27, 1066.02 cm^{-1}. **HRMS (ESI)**: calculated for $[C_{27}H_{25}N_4O_2]^+$: 437.1972, found: 437.1966. **M_p**:122°C.

3-(1H-indol-3-yl)-4-(1-(3-(4-(pent-4-ynoyl)piperazin-1-yl)propyl)-1H-indol-3-yl)-1H-pyrrole-2,5-dione (4-10)

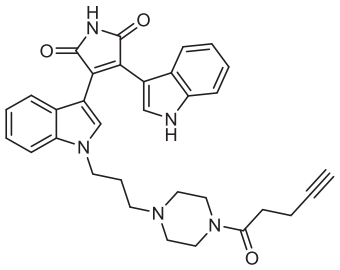

A flame-dried flask was loaded with 1-(piperazin-1-yl)pent-4-yn-1-one hydrochloride (130 mg, 0.65 mmol), DMF (1.5 mL) and DIPEA (0.15 mL, 0.86 mmol) and stired for 10 minutes, then 3-(3-(4-(1H-indol-3-yl)-2,5-dioxo-2,5-dihydro-1H-pyrrol-3-yl)-1H-indol-1-yl)propyl methanesulfonate (NUM, 100 mg, 0.22 mmol) was added and the reaction mixture was stired at 70 °C overnight. Water and ethyl acetate were added to the reaction mixture and the aqueous layer was extracted with ethyl acetate. The organic layers were combined and washed with brine and $CuSO_4$, then dried over $MgSO_4$ and the solvent was evaporated under reduced pressure. The reaction crude was purified by flash column chromatography, the product was eluted at 5% methanol/DCM. Obtained as a red solid (26.5 mg, **23%**).

^{1}H NMR (400 MHz, $CDCl_3$) δ 8.92 (d, *J* = 2.8 Hz, 1H), 8.12 (s, 1H), 7.72 (d, *J* = 2.8 Hz, 1H), 7.66 (s, 1H), 7.34 – 7.27 (m, 2H), 7.12 – 7.00 (m, 3H), 6.92 (d, *J* = 8.0 Hz, 1H), 6.76 (ddd, *J* = 8.1, 7.0, 0.9 Hz, 1H), 6.71 (ddd, *J* = 8.1, 7.0, 1.0 Hz, 1H), 4.23 (t, *J* = 6.5 Hz, 2H), 3.61 (t, *J* = 5.1 Hz, 2H), 3.47 (t, *J* = 5.0 Hz, 2H), 2.56 (d, *J* = 1.8 Hz, 4H), 2.35 (t, *J* = 5.1 Hz, 2H), 2.27 (t, *J* = 5.1 Hz, 2H), 2.22 (t, *J* = 6.6 Hz, 2H), 1.99 – 1.92 (m, 3H). **^{13}C NMR** (101 MHz, $CDCl_3$) δ 172.5, 169.5, 136.3, 136.0, 132.3, 128.7, 128.6, 127.8, 126.4, 125.5, 122.7, 122.4, 122.3, 122.0, 120.4, 120.3, 111.5, 109.7, 107.1, 105.9, 83.7, 69.0, 54.2, 53.3, 52.5, 45.5, 44.0, 41.8, 32.3, 26.7, 14.7. **HRMS (ESI)**: calculated for $[C_{32}H_{32}N_5O_3]^+$: 534.24997, found: 534.24954.

methyl 3-(2-methoxy-2-oxoacetyl)-1H-indole-6-carboxylate (4-14)

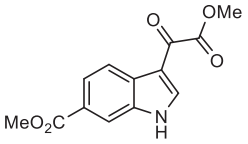

4-14 was prepared following the same procedure as **4-1**, starting from methyl 1H-indole-6-carboxylate (1g). Obtained as a yellow solid and used without further purification (1.27 g, **90%**).

^{1}H NMR (400 MHz, DMSO) δ 12.93 – 12.40 (m, 1H), 8.64 (d, J = 3.4 Hz, 1H), 8.26 – 8.20 (m, 1H), 8.15 (dd, J = 1.6, 0.7 Hz, 1H), 7.86 (dd, J = 8.4, 1.5 Hz, 1H), 3.89 (s, 3H), 3.86 (s, 3H).

3-(5-azido-1H-indol-3-yl)-4-(1H-indol-3-yl)-1H-pyrrole-2,5-dione

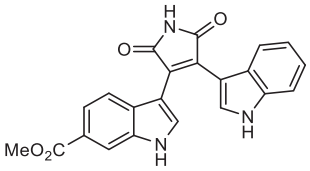

4-19 was prepared following the same procedure as **4-2**, using **4-14** (1.27 g, 4.8 mmol). The product was purified by silica flash column chromatography, eluted at 70% ethyl acetate in hexanes. Obtained as a red solid (0.46 g, **34%**).

^{1}H NMR (400 MHz, DMSO) δ 12.0 (s, 1H), 11.7 (d, J = 2.8 Hz, 1H), 11.0 (s, 1H), 8.0 (d, J = 1.5 Hz, 1H), 7.9 (d, J = 2.8 Hz, 1H), 7.8 (d, J = 2.8 Hz, 1H), 7.4 (d, J = 8.0 Hz, 1H), 7.2 (dd, J = 8.5, 1.6 Hz, 1H), 7.0 (ddd, J = 8.2, 7.0, 1.2 Hz, 1H), 6.9 (d, J = 8.5 Hz, 1H), 6.7 (d, J = 8.0 Hz, 1H), 6.6 (ddd, J = 8.0, 6.9, 1.0 Hz, 1H), 3.8 (s, 3H). **IR:** 3262.1, 1693.8, 1301.0 cm^{-1}. **HRMS (ESI)**: calculated for $[C_{22}H_{16}N_3O_4]^+$: 386.11353, found: 386.11343. **M_p:** 306 °C.

3-(4-(1H-indol-3-yl)-2,5-dioxo-2,5-dihydro-1H-pyrrol-3-yl)-1H-indole-6-carboxylic acid (4-15)

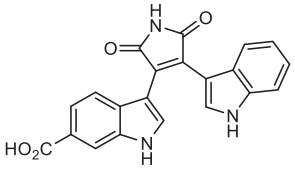

A flask was loaded with 3-(5-azido-1H-indol-3-yl)-4-(1H-indol-3-yl)-1H-pyrrole-2,5-dione (50 mg, 0.13 mmol, 1 eq.), LiOH·H2O (16 mg, 0.39 mmol, 3 eq.) and H2O/THF 1:1 (0.4 mL, 0.35 M). The reaction mixture was stirred overnight at 50 °C and diluted with water, quenched in NH4Cl sat. and extracted with ethyl acetate. The organic phases were combined and dried under reduced pressure. Obtained as a red solid (21 mg, **42% over 2 steps**).

^{1}H NMR (400 MHz, CD3OD) δ 8.1 (dt, J = 1.5, 0.6 Hz, 1H), 8.0 (d, J = 0.4 Hz, 1H), 7.9 (s, 1H), 7.4 (dd, J = 8.2, 1.1 Hz, 1H), 7.3 (ddd, J = 8.5, 1.5, 0.4 Hz, 1H), 7.0 (ddd, J = 8.2, 7.0, 1.2 Hz, 1H), 6.9 (dt, J = 8.5, 0.6 Hz, 1H), 6.8 – 6.7 (m, 1H), 6.7 – 6.6 (m, 1H).

1H-indol-5-amine

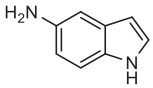

A flame dried flask was loaded with was loaded with 5-nitro-1*H*-indole (1g, 6.12 mmol) and Pd/C (100mg, 0.6 mmol), then ethanol (20 mL) and hydrazine monohydrate (2.3 mL, 30,6 mmol) were added. Reaction mixture was heated up at 80 °C and stired for 1 hour. The reaction mixture was let cool down at room temperature, was filtered over celite, added water and ethyl acetate and the aqueous phase was extracted with ethyl acetate three times. The organic layers were combined, washed with brine and dried over $MgSO_4$, then dried under reduced pressure. The crude product was purified by flash column chromatography, the product was eluted at 55% ethyl acetate/hexanes. Off-white solid (0.72g, **95%**).

^{1}H NMR (400 MHz, CDCl3) δ 7.96 (s, 1H), 7.20 (dt, J = 8.5, 0.8 Hz, 1H), 7.13 (dd, J = 3.1, 2.5 Hz, 1H), 6.95 (dt, J = 2.3, 0.7 Hz, 1H), 6.67 (dd, J = 8.5, 2.2 Hz, 1H), 6.38 (ddd, J = 3.1, 2.0, 1.0 Hz, 1H).

tert-butyl (1H-indol-5-yl)carbamate (4-18)

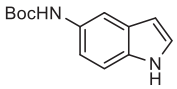

1H-indol-5-amine (0.72 g, 5.45 mmol, 1 eq.) was dissolved in ethyl acetate (88 mL, 0.076 M) and boc-anhydride (3.3 g, 2.5 eq.) was added and stirred at room temperature overnight. The reaction mixture was washed with water and dried under reduced pressure. The crude was purified by silica flash column chromatography, previously equilibrated with TEA 2% in hexane, eluting at 20% ethyl acetate in hexane. Obtained as a yellow oil (1.27 g, **90%**).

^{1}H NMR (400 MHz, CDCl3) δ 8.19 (s, 1H), 7.68 (s, 1H), 7.28 (d, J = 1.3 Hz, 1H), 7.16 (q, J = 2.9, 2.0 Hz, 1H), 7.10 (dd, J = 8.5, 2.1 Hz, 1H), 6.47 (ddd, J = 3.2, 2.0, 1.0 Hz, 2H), 1.53 (s, 7H).

methyl 2-(5-((tert-butoxycarbonyl)amino)-1H-indol-3-yl)-2-oxoacetate

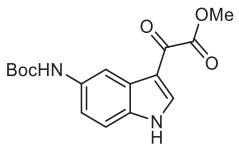

A flame-dried flask was loaded with tert-butyl (1H-indol-5-yl)carbamate (3.3 g, 14.2 mmol) and Et_2O (28 mL) and cooled down at 0°C, then oxalyl chloride (1.34 mL, 15 mmol) was added dropwise. The reaction mixture was allowed to warm up at rt for 3 h and a suspension of NaOMe (1.5 g, 28 mmol) in MeOH (28 mL) was added dropwise. The reaction mixture was allowed to warm up at rt for 4 h, then water was added. The precipitate was filtered and washed with cold water. The product was reported as a dark yellow solid and used without further purification (3.02 g. **65%**).

^{1}H NMR (400 MHz, DMSO) δ 12.28 (s, 1H), 9.30 (s, 1H), 8.35 (dd, J = 8.4, 2.8 Hz, 2H), 7.40 (dd, J = 8.7, 0.7 Hz, 1H), 7.33 (dd, J = 8.7, 2.1 Hz, 1H), 3.88 (s, 3H), 1.49 (s, 9H).

3-(5-amino-1H-indol-3-yl)-4-(1H-indol-3-yl)-1H-pyrrole-2,5-dione (4-19)

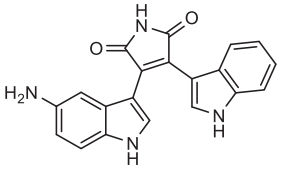

4-19 was prepared following the same procedure as **4-2**, using **4-18** (2 g, 6.3 mmol). The product was purified by silica flash column chromatography, eluted at 80% ethyl acetate in hexanes. Obtained as a red solid (1.4 g, **67%**).

^{1}H NMR (400 MHz, DMSO) δ 11.72 (d, J = 2.7 Hz, 1H), 11.48 (s, 1H), 10.87 (s, 1H), 7.81 (d, J = 2.8 Hz, 1H), 7.47 (d, J = 2.8 Hz, 1H), 7.42 – 7.32 (m, 1H), 7.27 (d, J = 9.2 Hz, 1H), 7.04 – 6.94 (m, 2H), 6.75 – 6.59 (m, 3H). **HRMS (ESI):** calculated for $[C_{20}H_{15}N_4O_2]^+$: 343.11895, found: 343.11888.

3-(5-azido-1H-indol-3-yl)-4-(1H-indol-3-yl)-1H-pyrrole-2,5-dione (4-21)

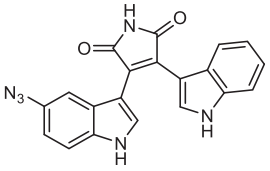

To a round flask containing sodium azide (171 mg, 2.63 mmol) and a mixture of *tert*-butanol/water (5:1, 0.5 mL) was added **4-19** (300 mg, 0.88 mmol) and tert-butyl nitrite (0.6 mL, 5,28 mmol). The reaction mixture was stirred at room temperature during 5 hours, then water and ethyl acetate were

added. The organic layer was extracted with ethyl acetate and the organic layers were combined, washed with brine, dried over $MgSO_4$ and dried under vacuum. The crude was purified by flash column chromatography, the product was eluted with 40% ethyl acetate in hexanes. Obtained as a red solid (160 mg, **50%**).

^{1}H NMR (400 MHz, CD3OD) δ 7.87 (s, 1H), 7.77 (s, 1H), 7.38 – 7.30 (m, 1H), 7.27 (dd, J = 8.6, 0.6 Hz, 1H), 6.96 (ddd, J = 8.2, 7.1, 1.2 Hz, 1H), 6.77 (dt, J = 8.1, 1.0 Hz, 1H), 6.59 – 6.53 (m, 3H), 6.47 (dd, J = 2.2, 0.6 Hz, 1H). **^{13}C NMR** (101 MHz, DMSO) δ 173.4, 173.3, 136.3, 134.1, 131.1, 129.4, 127.9, 127.7, 126.8, 125.9, 122.1, 121.1, 119.7, 114.2, 113.5, 112.2, 110.8, 105.9. **HRMS (ESI):** calculated for $[C_{20}H_{12}N_6O_2]^+$: 368.10163, found: 368.10159.

tert-butyl 4-(pent-4-ynoyl)piperazine-1-carboxylate

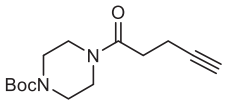

The title compound was prepared following general method for amide formation 2, using 1-boc-piperazine (500 mg, 1 eq.) and 4-pentynoic acid (263 mg, 1 eq.). The product was obtained as a brownish solid and used without further purification.

^{1}H NMR (400 MHz, $CDCl_3$) δ 3.59 (dd, *J* = 6.5, 4.1 Hz, 2H), 3.47 – 3.36 (m, 6H), 2.61 – 2.51 (m, 4H), 2.00 – 1.94 (m, 1H), 1.46 (s, 9H).

tert-butyl 4-(hept-6-ynoyl)piperazine-1-carboxylate

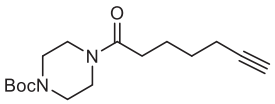

The title compound was prepared following general method for amide formation 2, using 1-boc-piperazine (2 g, 0.01 mol, 1 eq.) and 6-heptynoic acid (1.36 mL, 0.01 mol, 1 eq.). The product was obtained as a beige oil and used without further purification (2.9 g, **85%**).

^{1}H NMR (400 MHz, $CDCl_3$) δ 3.59 (dd, *J* = 7.8, 2.7 Hz, 2H), 3.48 – 3.32 (m, 6H), 2.36 (t, *J* = 7.6 Hz, 2H), 2.23 (td, *J* = 7.0, 2.7 Hz, 2H), 1.95 (t, *J* = 2.7 Hz, 1H), 1.83 – 1.73 (m, 2H), 1.65 – 1.54 (m, 2H), 1.47 (s, 9H). **^{13}C NMR** (101 MHz, $CDCl_3$) δ 171.34, 154.59, 84.06, 80.29, 68.68, 45.41, 43.62, 41.37, 32.76, 28.40, 28.05, 24.26, 18.22. **HRMS (ESI**): calculated for $[C_{16}H_{27}O_3N_2]^+$: 295.20162, found: 295.2150. **IR (ATR):** 3229, 2975, 2930, 2863, 1635, 1422 cm^{-1}.

Methyl 4-(4-(pent-4-ynoyl)piperazin-1-yl)butanoate

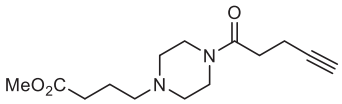

tert-butyl 4-(pent-4-ynoyl)piperazine-1-carboxylate was treated with HCL 4N in dioxane for 2 hours, then dried under reduced pressure.

The reaction crude (480 mg, 2.88 mmol, 1 eq.) was loaded in a pressure flask together with methyl 4-bromobutanoate (0.43 mL, 3.4 mmol, 1.2 eq.), K_2CO_3 (1.2 g, 8.64 mmol, 3 eq.) and DCM (15 mL, 0.2 M) and stirred at 35 °C for 5 days. Water was added to the reaction mixture, extracted with DCM (x3), the organic fractions were combined and washed with brine, dried over $MgSO_4$ and dried under reduced pressure. The crude was purified by flash column chromatography, the product was eluted at 5% methanol/DCM. The product was obtained as a yellowish oil (534 mg, **56%**).

^{1}H NMR (400 MHz, $CDCl_3$) δ 3.67 (s, 3H), 3.61 (t, *J* = 5.2 Hz, 2H), 3.45 (t, *J* = 5.1 Hz, 2H), 2.55 (q, *J* = 3.5 Hz, 4H), 2.46 – 2.32 (m, 8H), 1.97 (dq, *J* = 2.2, 1.3 Hz, 1H), 1.82 (p, *J* = 7.2 Hz, 2H). **^{13}C NMR** (101 MHz, $CDCl_3$) δ 173.9, 169.2, 83.5, 68.7, 57.4, 53.1, 52.7, 51.5, 45.3, 41.7, 32.1, 31.9, 22.0, 14.5. **IR(ATR):** 3269, 2948, 2819, 1731, 1634, 1435 cm^{-1}. **HRMS (ESI):** calculated for $[C_{14}H_{23}O_3N_2]^+$: 267.17032, found: 267.17035.

4-(4-(pent-4-ynoyl)piperazin-1-yl)butanoic acid

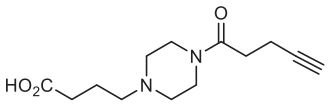

Methyl 4-(4-(pent-4-ynoyl)piperazin-1-yl)butanoate (534 mg, 2 mmol) was dissolved in NaOH 2M (5 mL) and 3 drops of methanol and stirred at room temperature for 4 hours. The pH of the solution was adjusted to 7 using HCl 1M, then evaporated under reduced pressure. The crude was dissolved in methanol, filtered and dried under reduced pressure to afford the product as an off-white solid, which was used without further purification (435 mg, **86%**).

^{1}H NMR (400 MHz, $CDCl_3$) δ 3.67 (s, 3H), 3.61 (t, *J* = 5.2 Hz, 2H), 3.45 (t, *J* = 5.1 Hz, 2H), 2.55 (q, *J* = 3.5 Hz, 4H), 2.46 – 2.32 (m, 8H), 1.97 (dq, *J* = 2.2, 1.3 Hz, 1H), 1.82 (p, *J* = 7.2 Hz, 2H). **^{13}C NMR** (101 MHz, $CDCl_3$) δ 173.9, 169.2, 83.5, 68.7, 57.4, 53.1, 52.7, 51.5, 45.3, 41.7, 32.1, 31.9, 22.0, 14.5.

Methyl 6-(4-(hept-6-ynoyl)piperazin-1-yl)hexanoate

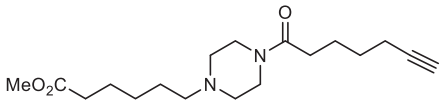

tert-butyl 4-(hept-6-ynoyl)piperazine-1-carboxylate was treated with HCL 4N in dioxane for 2 hours, then dried under reduced pressure.

The reaction crude (600 mg, 2.6 mmol, 1 eq.) was loaded in a pressure flask together with methyl 6-bromohexanoate (0.5 mL, 3.12 mmol, 1.2 eq.), K_2CO_3 (1.1 g, 7.8 mmol, 3 eq.) and DCM (13 mL, 0.2 M) and stirred at 35 °C for 5 days. Water was added to the reaction mixture, extracted with DCM (x3), the organic fractions were combined and washed with brine, dried over $MgSO_4$ and dried under reduced pressure. The crude was purified by flash column chromatography, the product was eluted at 5% methanol/DCM. The product was obtained as a yellowish oil (340 mg, **40%**).

^{1}H NMR (400 MHz, $CDCl_3$) δ 3.67 (s, 3H), 3.62 (t, *J* = 5.1 Hz, 2H), 3.47 (t, *J* = 5.0 Hz, 2H), 2.44 – 2.28 (m, 10H), 2.23 (td, *J* = 7.0, 2.5 Hz, 2H), 1.95 (t, *J* = 2.6 Hz, 1H), 1.76 (p, *J* = 7.5 Hz, 2H), 1.70 – 1.56 (m, 4H), 1.51 (p, *J* = 7.5 Hz, 2H), 1.41 – 1.29 (m, 2H). **^{13}C NMR** (101 MHz, $CDCl_3$) δ 174.1, 171.0, 93.5, 84.1, 68.5, 58.2, 53.4, 52.9, 51.5, 45.5, 41.5, 34.0, 32.6, 28.1, 27.0, 26.4, 24.8, 24.3, 18.2. **HRMS (ESI):** calculated for $[C_{18}H_{31}O_3N_2]^+$: 323.23292, found: 323.23313. **IR (ATR):** 3278, 2935, 2861, 1732, 1635, 1434 cm^{-1}.

6-(4-(hept-6-ynoyl)piperazin-1-yl)hexanoic acid

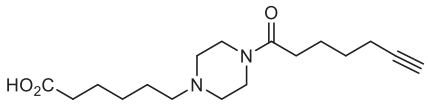

Methyl 6-(4-(hept-6-ynoyl)piperazin-1-yl)hexanoate (NUM, 300 mg, 0.93 mmol) was dissolved in NaOH 2M (3 mL) and 3 drops of methanol and stirred at room temperature for 4 hours. The pH of the solution was adjusted to 7 using HCl 1M, then evaporated under reduced pressure. The crude was dissolved in methanol, filtered and dried under reduced pressure to afford the product as an off-white solid, which was used without further purification (250 mg, **87%**).

(2S,4R)-1-((S)-2-(2-azidoacetamido)-3,3-dimethylbutanoyl)-4-hydroxy-N-((S)-1-(4-(4-methylthiazol-5-yl)phenyl)ethyl)pyrrolidine-2-carboxamide (4-16)

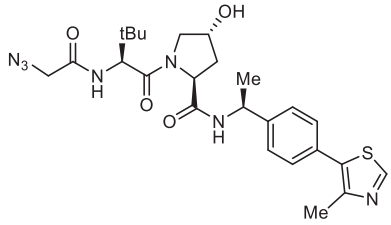

Prepared following general method for amide formation 2, using **3-29**, 200 mg, 0.42 mmol) and azidoacetic acid (42 mg, 0.42 mmol). The crude was purified by flash column chromatography, the product was eluted at 5% methanol/DCM and reported as an off-white solid (200 mg, **90%**).

^{1}H NMR (400 MHz, $CDCl_3$) δ 8.68 (s, 1H), 7.46 – 7.33 (m, 5H), 7.03 (d, *J* = 8.8 Hz, 1H), 5.08 (p, *J* = 7.0 Hz, 1H), 4.70 (t, *J* = 7.8 Hz, 1H), 4.57 (d, *J* = 8.9 Hz, 1H), 4.52 (s, 1H), 4.07 – 3.94 (m, 3H), 3.65 (dd, *J* = 11.2, 3.9 Hz, 1H), 2.51 (s, 3H), 2.45 (ddd, *J* = 12.7, 7.5, 4.7 Hz, 1H), 2.11 – 2.01 (m, 1H), 1.49 (d, *J* = 6.9 Hz, 3H), 1.05 (s, 9H). **^{13}C NMR** (101 MHz, $CDCl_3$) δ 171.2 (C), 169.8 (C), 167.2 (C), 150.5 (C), 148.6 (C), 143.2 (C), 131.0 (C), 129.7 (CH), 126.5 (CH), 70.2 (CH), 58.8 (CH), 57.6 (CH), 56.9 (CH_2), 52.5 (CH_2), 49.0 (CH), 36.0 (C), 35.7(CH_2), 26.6 (CH_3), 22.3 (CH_3), 16.2 (CH_3). **IR (ATR):** 3296.45, 2959.11, 2103.19, 1621.26 cm^{-1}. **HRMS (ESI):** calculated for $[C_{25}H_{34}N_7O_4S]^+$: 528.2387, found: 528.2378.

(2S,4R)-1-((S)-3,3-dimethyl-2-(pent-4-ynamido)butanoyl)-4-hydroxy-N-((S)-1-(4-(4-methylthiazol-5-yl)phenyl)ethyl)pyrrolidine-2-carboxamide (4-22a)

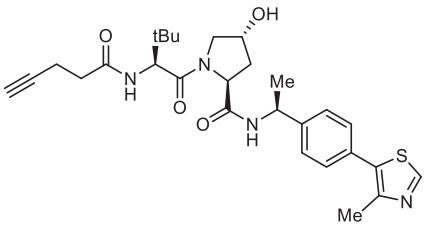

Prepared following general method for amide formation 2, using **3-29** (50 mg, 0.10 mmol) and pent-4-ynoic acid (11 mg, 0.10 mmol). The crude was purified by flash column chromatography, the product was eluted at 5% methanol/DCM and reported as an off-white solid (42 mg, **78%**).

^{1}H NMR (400 MHz, Chloroform-*d*) δ 7.4 (d, *J* = 7.9 Hz, 1H), 7.4 – 7.3 (m, 4H), 6.5 (d, *J* = 8.6 Hz, 1H), 5.1 (p, *J* = 7.0 Hz, 1H), 4.7 (t, *J* = 7.8 Hz, 1H), 4.6 (d, *J* = 8.6 Hz, 1H), 4.0 (d, *J* = 11.2 Hz, 1H), 3.6 (dd, *J* = 11.2, 3.8 Hz, 1H), 2.6 – 2.3 (m, 8H), 2.1 – 2.0 (m, 2H), 1.5 (d, *J* = 6.9 Hz, 3H), 1.0 (s, 9H). **^{13}C NMR** (101 MHz, Chloroform-*d*) δ 171.9, 171.7, 169.9, 143.3, 131.1, 129.7, 128.9, 126.6, 82.9, 70.1, 69.9, 58.7, 57.8, 56.8, 48.9, 35.8, 35.4, 35.3, 26.6, 22.3, 16.2, 15.0. **HRMS (ESI):** calculated for $[C_{28}H_{37}N_4O_4S]^+$: 525.25300, found: 525.25264. **IR (ATR):** 3290.2, 2361.3, 1622.9, 1540.7 cm^{-1}. **M_p:** 130–132°C.

(2R,4R)-1-((S)-2-(hept-6-ynamido)-3,3-dimethylbutanoyl)-4-hydroxy-N-((S)-1-(4-(4-methylthiazol-5-yl)phenyl)ethyl)pyrrolidine-2-carboxamide (4-22b)

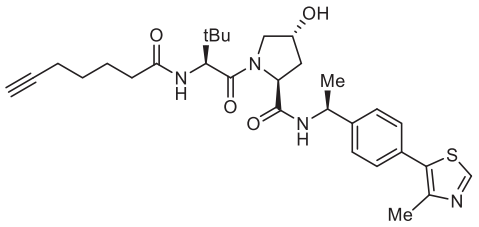

Prepared following general method for amide formation 2, using **3-29** (50 mg, 0.10 mmol) and hept-6-ynoic acid (15 mg, 0.10 mmol). The crude was purified by flash column chromatography, the product was eluted at 5% methanol/DCM and reported as an off-white solid (30 mg, **50%**).

^{1}H NMR (400 MHz, Chloroform-*d*) δ 8.6 (s, 1H), 7.7 – 7.4 (m, 1H), 7.4 – 7.3 (m, 4H), 6.2 (d, *J* = 8.7 Hz, 1H), 5.0 (p, *J* = 7.0 Hz, 1H), 4.6 (t, *J* = 7.9 Hz, 1H), 4.5 (d, *J* = 8.7 Hz, 1H), 4.4 (dd, *J* = 4.4, 2.4 Hz, 1H), 4.0 (d, *J* = 11.2 Hz, 1H), 3.6 (dd, *J* = 11.3, 3.8 Hz, 1H), 2.5 – 2.4 (m, 4H), 2.2 – 2.1 (m, 4H), 2.0 – 1.9 (m, 1H), 1.9 (t, *J* = 2.6 Hz, 1H), 1.7 – 1.6 (m, 2H), 1.5 – 1.4 (m, 2H), 1.4 (d, *J* = 6.9 Hz, 3H), 1.0 (s, 9H). **^{13}C NMR** (101 MHz, Chloroform-*d*) δ 173.4, 172.2, 169.8, 143.3, 131.0, 129.7, 128.9, 126.6, 84.0, 70.1, 68.9, 58.7, 57.7, 56.8, 49.0, 35.9, 35.7, 35.2, 27.9, 26.6, 24.7, 22.3, 18.3, 16.2. **HRMS (ESI):** calculated for $[C_{30}H_{41}N_4O_4S]^+$: 553.28430, found: 553.28396. **M_p:** 198–200°C.

(2R,4R)-1-((S)-2-(hept-6-ynamido)-3,3-dimethylbutanoyl)-4-hydroxy-N-((S)-1-(4-(4-methylthiazol-5-yl)phenyl)ethyl)pyrrolidine-2-carboxamide (4-22c)

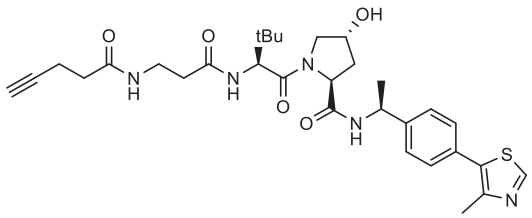

Prepared following general method for amide formation 2, using 3-31a (50 mg, 0.10 mmol) and hept-6-ynoic acid (15 mg, 0.10 mmol). The crude was purified by flash column chromatography, the product was eluted at 5% methanol/DCM and reported as an off-white solid (30 mg, **50%**).

^{1}H NMR (400 MHz, Chloroform-*d*) δ 8.6 (s, 1H), 7.7 – 7.4 (m, 1H), 7.4 – 7.3 (m, 4H), 6.2 (d, *J* = 8.7 Hz, 1H), 5.0 (p, *J* = 7.0 Hz, 1H), 4.6 (t, *J* = 7.9 Hz, 1H), 4.5 (d, *J* = 8.7 Hz, 1H), 4.4 (dd, *J* = 4.4, 2.4 Hz, 1H), 4.0 (d, *J* = 11.2 Hz, 1H), 3.6 (dd, *J* = 11.3, 3.8 Hz, 1H), 2.5 – 2.4 (m, 4H), 2.2 – 2.1 (m, 4H), 2.0 – 1.9 (m, 1H), 1.9 (t, *J* = 2.6 Hz, 1H), 1.7 – 1.6 (m, 2H), 1.5 – 1.4 (m, 2H), 1.4 (d, *J* = 6.9 Hz, 3H), 1.0 (s, 9H). **^{13}C NMR** (101 MHz, Chloroform-*d*) δ 173.4, 172.2, 169.8, 143.3, 131.0, 129.7, 128.9, 126.6, 84.0, 70.1, 68.9, 58.7, 57.7, 56.8, 49.0, 35.9, 35.7, 35.2, 27.9, 26.6, 24.7, 22.3, 18.3, 16.2. **HRMS (ESI):** calculated for $[C_{30}H_{41}N_4O_4S]^+$: 553.28430, found: 553.28396. **M_p:** 198–200°C.

(2S,4R)-1-((S)-3,3-dimethyl-2-(4-(4-(pent-4-ynoyl)piperazin-1-yl)butanamido)butanoyl)-4-hydroxy-N-((S)-1-(4-(4-methylthiazol-5-yl)phenyl)ethyl)pyrrolidine-2-carboxamide (4-22d)

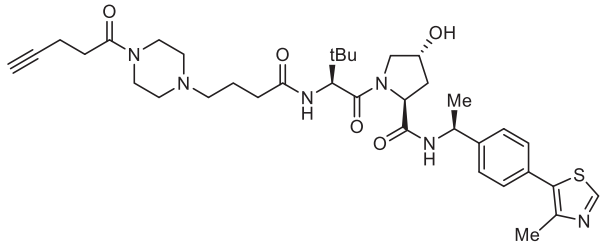

Prepared following general method for amide formation 2, using **3-29** (50 mg, 0.10 mmol) and 4-(4-(pent-4-ynoyl)piperazin-1-yl)butanoic acid (25 mg, 0.10 mmol). The crude was purified by flash column chromatography, the product was eluted at 10% methanol/DCM and reported as a white solid (31 mg, **45%**).

^{1}H NMR (400 MHz, $CDCl_3$) δ 8.71 – 8.64 (m, 1H), 7.38 (q, *J* = 7.0, 5.1 Hz, 4H), 5.07 (q, *J* = 7.0 Hz, 1H), 4.75 – 4.61 (m, 1H), 4.59 – 4.51 (m, 1H), 4.48 (s, 1H), 4.11 – 3.96 (m, 1H), 3.63 – 3.53 (m, 3H), 3.45 (t, *J* = 4.9 Hz, 2H), 2.54 – 2.48 (m, 3H), 2.44 – 2.27 (m, 9H), 2.20 (ddt, *J* = 10.0, 7.2, 3.2 Hz, 4H), 2.06 (dd, *J* = 13.6, 8.3 Hz, 1H), 1.94 (q, *J* = 2.3 Hz, 1H), 1.73 (q, *J* = 7.2 Hz, 2H), 1.59 (dq, *J* = 14.5, 6.3 Hz, 4H), 1.51 – 1.41 (m, 5H), 1.30 (t, *J* = 7.8 Hz, 2H), 1.10 – 0.97 (m, 9H). **^{13}C NMR** (101 MHz, CD3OD) δ 174.1, 171.8 , 170.8, 170.6, 151.5, 147.7, 144.2, 131.9, 130.1, 129.1, 126.2, 82.5, 69.6, 68.8, 59.2, 57.9, 57.0, 56.6, 52.5, 52.2, 48.7, 44.5, 40.7, 37.5, 35.0, 32.8, 31.5, 29.3, 25.7, 21.6, 21.0, 14.4. **HRMS (ESI):** calculated for $[C_{36}H_{51}O_5\ N_6S]^+$: 679.36362, found: 679.36212. **IR(ATR):** 3292, 2956, 1621, 838 cm^{-1}. **M_p:** 100 °C.

(2S,4R)-1-((S)-2-(6-(4-(hept-6-ynoyl)piperazin-1-yl)hexanamido)-3,3-dimethylbutanoyl)-4-hydroxy-N-((S)-1-(4-(4-methylthiazol-5-yl)phenyl)ethyl)pyrrolidine-2-carboxamide (4-22e)

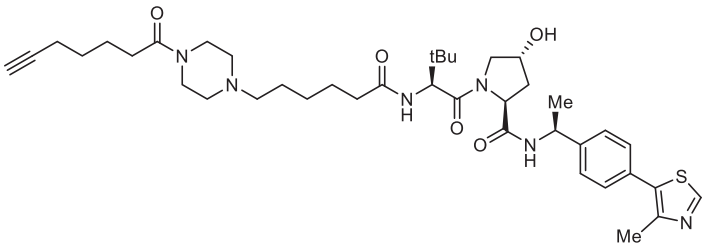

Prepared following general method for amide formation 2, using **3-29** (100 mg, 0.20 mmol) and 6-(4-(hept-6-ynoyl)piperazin-1-yl)hexanoic acid (64 mg, 0.20 mmol). The crude was purified by flash column chromatography, the product was eluted at 9% methanol/DCM and reported as a white solid (110 mg, **75%**).

^{1}H NMR (400 MHz, $CDCl_3$) δ 8.71 – 8.64 (m, 1H), 7.38 (q, *J* = 7.0, 5.1 Hz, 4H), 5.07 (q, *J* = 7.0 Hz, 1H), 4.75 – 4.61 (m, 1H), 4.59 – 4.51 (m, 1H), 4.48 (s, 1H), 4.11 – 3.96 (m, 1H), 3.63 – 3.53 (m, 3H), 3.45 (t, *J* = 4.9 Hz, 2H), 2.54 – 2.48 (m, 3H), 2.44 – 2.27 (m, 9H), 2.20 (ddt, *J* = 10.0, 7.2, 3.2 Hz, 4H), 2.06 (dd, *J* = 13.6, 8.3 Hz, 1H), 1.94 (q, *J* = 2.3 Hz, 1H), 1.73 (q, *J* = 7.2 Hz, 2H), 1.59 (dq, *J* = 14.5, 6.3 Hz, 4H), 1.51 – 1.41 (m, 5H), 1.30 (t, *J* = 7.8 Hz, 2H), 1.10 – 0.97 (m, 9H). **^{13}C NMR** (101 MHz, $CDCl_3$) δ 173.9, 171.7, 171.4, 170.0, 150.4 , 148.4, 143.2, 131.6, 130.8, 129.5, 126.4, 84.1, 69.7, 68.6, 58.7, 57.4, 57.3, 56.9, 53.4, 52.7, 48.8, 48.7, 45.4, 41.4, 36.2, 35.7, 35.3, 32.6, 28.0, 26.9, 26.4, 26.2, 25.2, 24.3, 22.1, 16.0. **HRMS (ESI):** calculated for $[C_{40}H_{59}O_5N_6S]^+$: 735.42622, found: 735.42691. **IR (ATR):** 3290, 2932, 2359, 1619, 840 cm^{-1}. **M_p:** 71 °C.

4-((2-(2-(4-(((3-(3-(4-(1H-indol-3-yl)-2,5-dioxo-2,5-dihydro-1H-pyrrol-3-yl)-1H-indol-1-yl)propyl)(methyl)amino)methyl)-1H-1,2,3-triazol-1-yl)ethoxy)ethyl)amino)-2-(2,6-dioxopiperidin-3-yl)isoindoline-1,3-dione (4-8a)

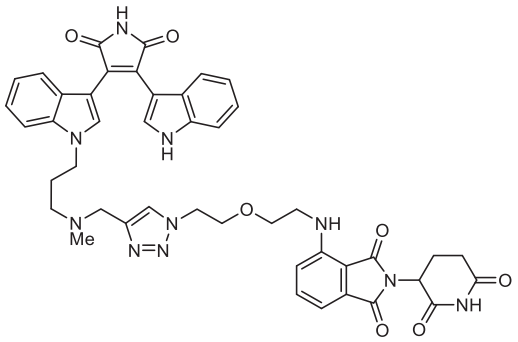

The product was prepared following the general method for CuAAC using **4-7** (16 mg, 0.03 mmol) and **3-31a** (11.5 mg, 0.03 mmol). The crude was purified by flash column chromatography, the product was eluted at 4% MeOH/DCM and reported as a red solid (12 mg, **48%**).

^{1}H NMR (500 MHz, $CDCl_3$) δ 8.74 (s, 1H), 7.73 – 7.60 (m, 3H), 7.47 (dd, *J* = 8.4, 7.2 Hz, 1H), 7.34 – 7.28 (m, 2H), 7.13 – 7.03 (m, 4H), 6.93 (dt, *J* = 8.1, 0.9 Hz, 1H), 6.84 (d, *J* = 8.5 Hz, 1H), 6.75 (dddd, *J* = 13.8, 8.0, 7.0, 1.0 Hz, 2H), 6.57 (t, *J* = 5.6 Hz, 1H), 4.89 (dd, *J* = 12.2, 5.5 Hz, 1H), 4.58 – 4.48 (m, 2H), 4.19 (t, *J* = 6.6 Hz, 2H), 3.91 – 3.83 (m, 2H), 3.75 – 3.56 (m, 4H), 3.39 (td, *J* = 5.3, 2.3 Hz, 2H), 2.82 – 2.61 (m, 3H), 2.41 – 2.34 (m, 2H), 2.21 (s, 3H), 2.12 – 2.07 (m, 1H), 2.03 (d, *J* = 9.7 Hz, 2H). **^{13}C NMR** (126 MHz, $CDCl_3$) δ 172.3, 172.2, 171.6, 170.0, 169.2, 167.7 (d, *J* = 2.2 Hz), 147.0, 144.3, 136.4, 136.3, 136.0, 132.6, 132.6, 129.0, 128.5, 127.7, 126.3, 125.7, 124.5, 122.8, 122.4, 122.3, 122.1, 120.5, 120.3, 117.1, 112.3, 111.4, 110.8, 109.8, 107.3, 105.6, 69.8, 69.6, 53.4, 52.1, 50.5, 49.1, 44.5, 42.3, 41.4, 31.4, 27.0, 23.1. **HRMS (ESI):** calculated for $[C_{46}H_{47}N_{10}O_8]^+$: 867.3573, found: 867.3566.

4-((2-(2-(2-(4-(((3-(3-(4-(1H-indol-3-yl)-2,5-dioxo-2,5-dihydro-1H-pyrrol-3-yl)-1H-indol-1-yl)propyl)(methyl)amino)methyl)-1H-1,2,3-triazol-1-yl)ethoxy)ethoxy)ethyl)amino)-2-(2,6-dioxopiperidin-3-yl)isoindoline-1,3-dione (4-8b)

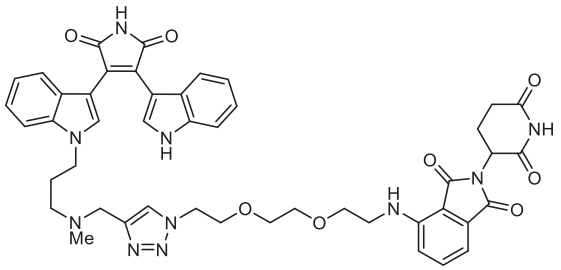

The product was prepared following the general method for CuAAC using **4-7** (24 mg, 0.06 mmol) and **3-31b** (23 mg, 0.06 mmol). The crude was purified by flash column chromatography, the product was eluted at 4% MeOH/DCM and reported as a red solid (21 mg, **44%**).

^{1}H NMR (500 MHz, $CDCl_3$) δ 8.79 (s, 1H), 8.08 (d, *J* = 1.9 Hz, 1H), 7.66 (d, *J* = 2.7 Hz, 1H), 7.64 (s, 1H), 7.60 (s, 1H), 7.54 – 7.43 (m, 1H), 7.30 (ddt, *J* = 8.3, 3.6, 0.9 Hz, 2H), 7.13 – 6.99 (m, 5H), 6.85 (d, *J* = 8.5 Hz, 1H), 6.78 (ddt, *J* = 8.2, 7.0, 1.2 Hz, 2H), 6.52 (t, *J* = 5.4 Hz, 1H), 4.88 (dd, *J* = 12.5, 5.4 Hz, 1H), 4.52 (td, *J* = 5.4, 1.6 Hz, 2H), 4.17 (t, *J* = 6.7 Hz, 2H), 3.90 (t, *J* = 5.5 Hz, 2H), 3.72 – 3.49 (m, 10H), 3.47 – 3.37 (m, 2H), 2.82 – 2.62 (m, 3H), 2.39 (q, *J* = 6.6 Hz, 2H), 2.22 (s, 3H), 2.09 – 2.05 (m, 1H), 2.03 – 1.97 (m, 2H). **^{13}C NMR** (126 MHz, $CDCl_3$) δ 172.2, 172.1, 171.7, 169.7, 169.3, 167.8, 146.8, 144.4 (d, *J* = 21.0 Hz), 136.3, 136.3, 136.0, 132.7, 132.5, 129.9, 129.0, 128.5, 126.3, 125.5, 124.3, 122.8, 122.5, 122.4, 122.2, 120.5, 120.4, 116.9, 112.0, 111.4, 110.5, 109.8, 107.2, 105.7, 70.7, 70.6, 69.8, 69.3, 53.6, 52.4, 50.3, 49.1, 44.5, 42.4, 41.4, 31.6, 27.0, 23.1. **HRMS (ESI):** calculated for $[C_{44}H_{43}N_{10}O_7]^+$: 823.3311, found: 823.3298. **IR (ATR):** 2987.9, 1602.7, 1505.1 cm^{-1}.

4-((2-(2-(2-(2-(4-(((3-(3-(4-(1H-indol-3-yl)-2,5-dioxo-2,5-dihydro-1H-pyrrol-3-yl)-1H-indol-1-yl)propyl)(methyl)amino)methyl)-1H-1,2,3-triazol-1-yl)ethoxy)ethoxy)ethoxy)ethyl)amino)-2-(2,6-dioxopiperidin-3-yl)isoindoline-1,3-dione (4-8c)

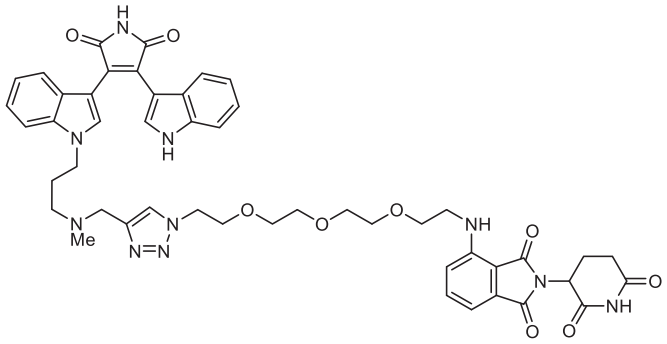

The product was prepared following the general method for CuAAC using **4-7** (20 mg, 0.05 mmol) and **3-31c** (22 mg, 0.05 mmol). The crude was purified by flash column chromatography, the product was eluted at 4% MeOH/DCM and reported as a red solid (20 mg, **48%**).

^{1}H NMR (500 MHz, $CDCl_3$) δ 9.02 (s, 1H), 8.87 (s, 1H), 7.97 (s, 1H), 7.69 (d, *J* = 2.7 Hz, 1H), 7.60 (s, 1H), 7.46 – 7.41 (m, 2H), 7.32 – 7.28 (m, 2H), 7.13 – 7.03 (m, 4H), 6.97 (d, *J* = 8.1 Hz, 1H), 6.85 (d, *J* = 8.5 Hz, 1H), 6.80 (ddd, *J* = 8.1, 7.0, 1.0 Hz, 1H), 6.75 (ddd, *J* = 8.1, 7.0, 1.0 Hz, 1H), 6.47 (t, *J* = 5.6 Hz, 1H), 4.89 (dd, *J* = 12.2, 5.4 Hz, 1H), 4.44 (t, 2H), 4.18 (t, *J* = 6.5 Hz, 2H), 3.85 (t, *J* = 5.2 Hz, 2H), 3.67 – 3.58 (m, 10H), 3.51 (s, 2H), 3.40 (q, *J* = 5.5 Hz, 2H), 2.84 – 2.64 (m, 2H), 2.30 (t, *J* = 6.7 Hz, 2H), 2.19 (s, 3H), 2.11 – 2.02 (m, 1H), 1.97 (p, *J* = 6.6 Hz, 2H). **^{13}C NMR** (126 MHz, $CDCl_3$) δ 172.4, 171.5, 169.5, 168.9, 167.8, 146.9, 144.5, 136.3, 136.2, 136.1, 132.6, 132.6, 128.8, 128.7, 127.9, 126.4, 125.4, 124.0, 122.7, 122.5, 122.3, 122.1, 120.5, 120.4, 116.9, 111.8, 111.5, 110.4, 109.8, 107.0, 105.7, 70.8, 70.7, 70.6, 69.6, 69.5, 53.4, 52.4, 50.2, 49.0, 44.2, 42.4, 41.5, 31.6, 27.1, 22.9. **HRMS (ESI):** calculated for $[C_{48}H_{51}N_{10}O_9]^+$: 911.3835, found: 911.382.

4-((14-(4-(((3-(3-(4-(1H-indol-3-yl)-2,5-dioxo-2,5-dihydro-1H-pyrrol-3-yl)-1H-indol-1-yl)propyl)(methyl)amino)methyl)-1H-1,2,3-triazol-1-yl)-3,6,9,12-tetraoxatetradecyl)amino)-2-(2,6-dioxopiperidin-3-yl)isoindoline-1,3-dione (4-8d)

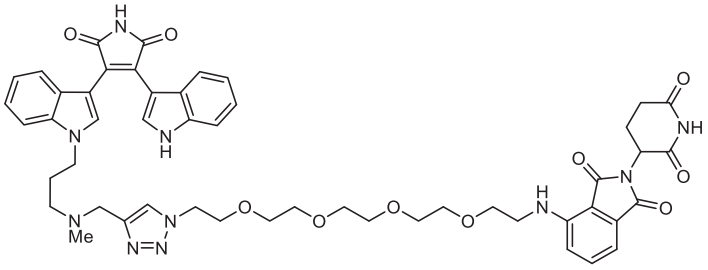

The product was prepared following the general method for CuAAC using **4-7** (20 mg, 0.05 mmol) and **3-31d** (24 mg, 0.05 mmol). The crude was purified by flash column chromatography, the product was eluted at 5% MeOH/DCM and reported as a red solid (36 mg, **82%**).

^{1}H NMR (500 MHz, $CDCl_3$) δ 9.12 (d, *J* = 2.8 Hz, 1H), 8.00 (s, 1H), 7.70 (d, *J* = 2.8 Hz, 1H), 7.59 (s, 1H), 7.47 – 7.40 (m, 2H), 7.31 (dd, *J* = 8.1, 7.0 Hz, 2H), 7.13 – 7.02 (m, 4H), 7.00 – 6.95 (m, 1H), 6.85 (d, *J* = 8.5 Hz, 1H), 6.80 (ddd, *J* = 8.1, 7.0, 0.9 Hz, 1H), 6.75 (ddd, *J* = 8.1, 7.1, 1.0 Hz, 1H), 6.47 (t, *J* = 5.6 Hz, 1H), 4.92 – 4.85 (m, 1H), 4.43 (dd, *J* = 5.8, 4.6 Hz, 2H), 4.18 (t, *J* = 6.5 Hz, 2H), 3.82 (t, *J* = 5.2 Hz, 2H), 3.67 – 3.56 (m, 14H), 3.52 (s, 2H), 3.40 (q, *J* = 5.5 Hz, 2H), 2.87 – 2.62 (m, 3H), 2.30 (t, *J* = 6.7 Hz, 2H), 2.19 (s, 3H), 2.12 – 2.03 (m, 1H), 1.97 (p, *J* = 6.7 Hz, 2H). **^{13}C NMR** (126 MHz, $CDCl_3$) δ 172.4, 171.5, 169.4, 168.9, 167.8, 146.9, 144.4, 136.4, 136.2, 132.6, 132.5, 128.8, 128.0, 126.4, 125.4, 124.0, 122.7, 122.4, 122.3, 122.1, 120.4, 120.3, 116.9, 111.8, 111.6, 110.4, 109.8, 107.0, 105.7, 70.8, 70.7, 70.6, 70.5, 69.6, 69.5, 53.3, 52.4, 50.2, 49.0, 44.2, 42.5, 41.5, 31.5, 27.2, 22.9. **HRMS (ESI):** calculated for $[C_{50}H_{55}N_{10}O_{10}]^+$: 955.4097, found: 955.4088.

(2S,4R)-1-((S)-2-(2-(4-(((3-(3-(4-(1H-indol-3-yl)-2,5-dioxo-2,5-dihydro-1H-pyrrol-3-yl)-1H-indol-1-yl)propyl)(methyl)amino)methyl)-1H-1,2,3-triazol-1-yl)acetamido)-3,3-dimethylbutanoyl)-4-hydroxy-N-((S)-1-(4-(4-methylthiazol-5-yl)phenyl)ethyl)pyrrolidine-2-carboxamide (4-9a)

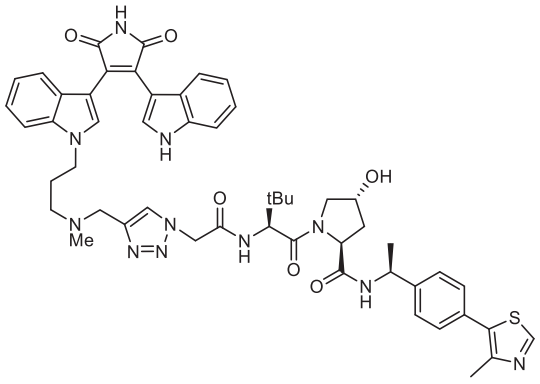

The product was prepared following the general method for CuAAC using **4-7** (20 mg, 0.05 mmol) and **4-16** (24 mg, 0.05 mmol) .The crude was purified by flash column chromatography, the product was eluted at 8% MeOH/DCM and reported as a red **solid** (34 mg, **77%**).

^{1}H NMR (400 MHz, CD_3OD) δ 8.85 (s, 1H), 7.78 – 7.72 (m, 2H), 7.61 (d, *J* = 11.0 Hz, 1H), 7.43 – 7.37 (m, 4H), 7.34 – 7.26 (m, 2H), 7.07 – 6.92 (m, 3H), 6.77 – 6.65 (m, 2H), 6.54 (ddd, *J* = 8.1, 7.0, 1.0 Hz, 1H), 5.23 – 5.09 (m, 2H), 4.99 (q, *J* = 7.0 Hz, 1H), 4.63 – 4.56 (m, 2H), 4.42 – 4.37 (m, 1H), 4.29 – 4.20 (m, 3H), 3.84 (d, *J* = 11.1 Hz, 1H), 3.71 (dd, *J* = 11.0, 3.9 Hz, 1H), 3.65 – 3.52 (m, 2H), 2.46 (s, 3H), 2.35 – 2.26 (m, 2H), 2.19 (s, 4H), 2.04 – 1.88 (m, 3H), 1.48 (d, *J* = 7.0 Hz, 3H), 1.06 (s, 9H). **^{13}C NMR** (101 MHz, CD_3OD) δ 175.1 (d, *J* = 4.5 Hz), 173.2, 171.8, 167.8, 152.8, 149.1, 145.6, 137.8, 137.5, 133.1, 132.4, 131.5, 130.5, 130.4, 130.2, 129.8, 128.9, 128.0,

127.6, 127.4, 127.0, 126.8, 123.1, 123.0, 122.9, 122.5, 120.9, 120.6, 112.6, 110.8, 107.4, 107.0, 71.0, 60.7, 59.6, 58.0, 54.3, 52.8, 52.5, 50.2, 45.0, 42.0, 38.8, 36.6, 28.3, 27.0, 22.4, 15.8. **HRMS (ESI):** calculated for $[C_{52}H_{58}O_6N_{11}S]^+$: 964.42868, found: 964.42879.

(2S,4R)-1-((S)-2-(4-(4-(((3-(3-(4-(1H-indol-3-yl)-2,5-dioxo-2,5-dihydro-1H-pyrrol-3-yl)-1H-indol-1-yl)propyl)(methyl)amino)methyl)-1H-1,2,3-triazol-1-yl)butanamido)-3,3-dimethylbutanoyl)-4-hydroxy-N-((S)-1-(4-(4-methylthiazol-5-yl)phenyl)ethyl)pyrrolidine-2-carboxamide (4-9b)

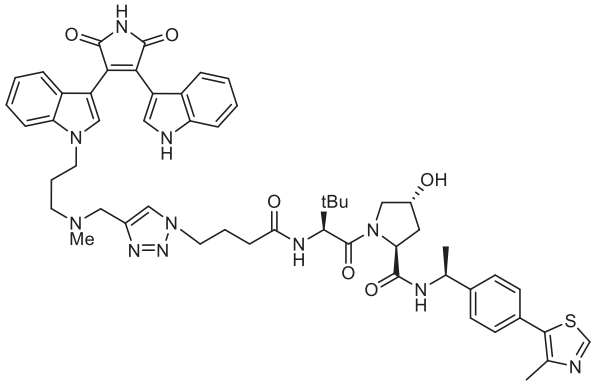

The product was prepared following the general method for CuAAC using **4-7** (20 mg, 0.05 mmol) and **3-30a** (25 mg, 0.05 mmol) .The crude was purified by flash column chromatography, the product was eluted at 8% MeOH/DCM and reported as a red solid (40 mg, **88%**).

^{1}H NMR (400 MHz, CD_3OD) δ 8.86 (s, 1H), 7.81 – 7.69 (m, 2H), 7.65 (s, 1H), 7.44 – 7.37 (m, 4H), 7.35 – 7.29 (m, 2H), 7.04 (ddd, *J* = 8.2, 7.0, 1.2 Hz, 1H), 6.98 – 6.92 (m, 2H), 6.75 – 6.67 (m, 2H), 6.54 (ddd, *J* = 8.1, 7.0, 1.0 Hz, 1H), 4.98 (q, *J* = 6.7 Hz, 1H), 4.62 – 4.54 (m, 2H), 4.43 (d, *J* = 4.8 Hz, 1H), 4.29 (dt, *J* = 18.3, 6.7 Hz, 4H), 3.89 (d, *J* = 11.0 Hz, 1H), 3.74 (dd, *J* = 11.0, 4.0 Hz, 1H), 3.62 (s, 2H), 2.46 (s, 3H), 2.36 – 2.24 (m, 4H), 2.23 – 2.09 (m, 6H), 2.00 – 1.91 (m, 3H), 1.48 (d, *J* = 7.0 Hz, 3H), 1.04 (s, 9H). **^{13}C NMR** (101 MHz, CD_3OD) δ 175.0, 174.3, 173.2, 172.3, 152.8, 149.1, 145.6, 144.7, 137.8, 137.5, 133.3, 133.1, 131.5, 130.5, 130.2, 129.8, 128.9, 128.0, 127.6, 127.4, 126.9, 125.3, 123.1, 123.0, 123.0, 122.5, 120.6, 110.9, 107.5, 107.0, 71.0, 60.6, 59.3, 58.0, 54.4, 52.6, 50.5, 50.1, 45.0, 42.0, 38.8, 36.4, 33.0, 28.3, 27.3, 27.1, 22.4, 15.8. **HRMS (ESI):** calculated for $[C_{54}H_{62}O_6N_{11}S]^+$: 992.45998, found: 992.46017.

(2S,4R)-1-((S)-2-(6-(4-(((3-(3-(4-(1H-indol-3-yl)-2,5-dioxo-2,5-dihydro-1H-pyrrol-3-yl)-1H-indol-1-yl)propyl)(methyl)amino)methyl)-1H-1,2,3-triazol-1-yl)hexanamido)-3,3-dimethylbutanoyl)-4-hydroxy-N-((S)-1-(4-(4-methylthiazol-5-yl)phenyl)ethyl)pyrrolidine-2-carboxamide (4-9c)

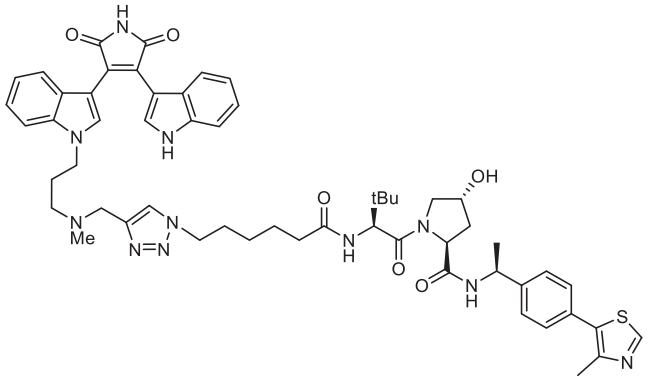

The product **was** prepared following the general method for CuAAC using **4-7** (20 mg, 0.05 mmol) and **3-30b** (27 mg, 0.05 mmol) .The crude was purified by flash column chromatography, the product was eluted at 8% MeOH/DCM and reported as a red solid (29 mg, **62%**).

^{1}H NMR (400 MHz, CD_3OD) δ 8.8 (d, *J* = 1.1 Hz, 1H), 7.8 (d, *J* = 1.1 Hz, 1H), 7.7 – 7.6 (m, 2H), 7.5 – 7.3 (m, 6H), 7.1 – 7.0 (m, 1H), 6.9 (t, *J* = 7.7 Hz, 2H), 6.7 – 6.6 (m, 2H), 6.6 – 6.5 (m, 1H), 5.0 (q, *J* = 7.0 Hz, 1H), 4.7 – 4.5 (m, 2H), 4.4 (s, 1H), 4.2 (dt, *J* = 13.7, 6.7 Hz, 4H), 3.9 (d, *J* = 11.0 Hz, 1H), 3.7 (d, *J* = 11.3 Hz, 3H), 2.5 (d, *J* = 1.2 Hz, 3H), 2.4 – 2.3 (m, 2H), 2.3 – 2.1 (m, 6H), 2.1 – 1.9 (m, 3H), 1.8 (p, *J* = 7.3 Hz, 2H), 1.6 (dt, *J* = 14.7, 7.2 Hz, 2H), 1.5 (dd, *J* = 7.0, 1.2 Hz, 3H), 1.4 – 1.2 (m, 2H), 1.1 – 1.0 (m, 9H). **^{13}C NMR** (101 MHz, CD_3OD) δ 174.2, 173.6, 173.6, 171.8, 170.9, 151.4, 147.6, 144.2, 142.1, 136.4, 136.1, 131.9, 131.6, 131.0, 130.1, 129.1, 128.8, 128.4, 127.4, 126.6, 126.2, 126.0, 125.5, 124.1, 121.7, 121.6, 121.5, 121.1, 119.5, 119.2, 111.1, 109.4, 106.0, 105.7, 69.6, 59.2, 57.6, 56.6, 52.7, 50.8, 49.8, 48.7, 43.5, 40.5, 37.4, 36.2, 35.0, 34.8, 29.4, 26.5, 25.7, 24.8, 21.0, 14.4. **HRMS (ESI):** calculated for $[C_{56}H_{66}O_6N_{11}S]^+$: 1020.49128, found: 102.49135.

(2S,4R)-1-((S)-2-(3-(4-(4-(((3-(3-(4-(1H-indol-3-yl)-2,5-dioxo-2,5-dihydro-1H-pyrrol-3-yl)-1H-indol-1-yl)propyl)(methyl)amino)methyl)-1H-1,2,3-triazol-1-yl)butanamido)propanamido)-3,3-dimethylbutanoyl)-4-hydroxy-N-((S)-1-(4-(4-methylthiazol-5-yl)phenyl)ethyl)pyrrolidine-2-carboxamide (4-9d)

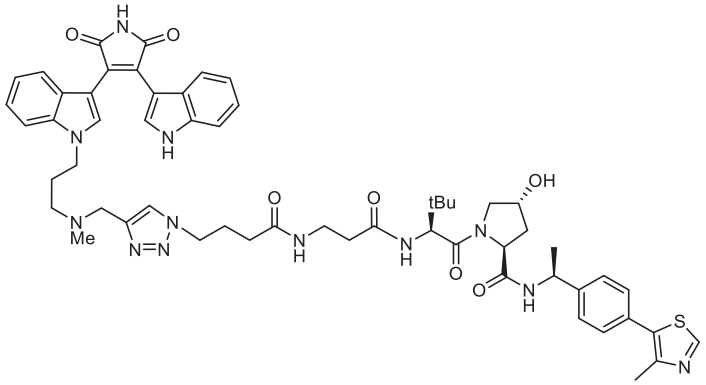

The product was prepared following the general method for CuAAC using **4-7** (7 mg, 0.016 mmol) and **3-32a** (10 mg, 0.016 mmol) .The crude was purified by flash column chromatography, the product was eluted at 7% MeOH/DCM and reported as a red solid (8 mg, **50%**).

^{1}H NMR (400 MHz, CD_3OD) δ 8.75 (s, 1H), 7.67 (d, *J* = 2.5 Hz, 1H), 7.64 (s, 1H), 7.58 – 7.49 (m, 1H), 7.30 (s, 5H), 7.25 – 7.18 (m, 1H), 6.94 (ddd, *J* = 8.2, 7.0, 1.2 Hz, 1H), 6.88 – 6.81 (m, 2H), 6.65 – 6.53 (m, 2H), 6.43

(ddd, *J* = 8.1, 7.0, 1.0 Hz, 1H), 4.89 (q, *J* = 7.0 Hz, 1H), 4.52 – 4.43 (m, 2H), 4.32 (dt, *J* = 4.6, 2.6 Hz, 1H), 4.20 (dt, *J* = 18.0, 6.6 Hz, 4H), 3.80 (dt, *J* = 11.3, 1.7 Hz, 1H), 3.69 – 3.57 (m, 3H), 3.40 – 3.27 (m, 2H), 2.40 – 2.21 (m, 7H), 2.21 – 1.80 (m, 11H), 1.38 (d, *J* = 7.0 Hz, 3H), 0.92 (d, *J* = 9.1 Hz, 9H). **^{13}C NMR** (101 MHz, CD_3OD) δ 173.6, 173.1, 172.3, 171.9, 170.9, 151.4, 147.7, 144.2, 136.4, 136.1, 131.6, 130.1, 129.1, 128.8, 128.4, 127.4, 126.6, 126.2, 125.9, 125.5, 121.7, 121.6, 121.6, 121.1, 119.5, 119.2, 111.1, 109.4, 106.1, 105.7, 69.7, 59.2, 57.9, 56.5, 52.9, 51.0, 49.3, 48.8, 43.5, 40.5, 37.5, 35.7, 34.9, 34.9, 32.2, 26.6, 25.9, 25.6, 21.0, 14.4. **HRMS (ESI):** calculated for $[C_{57}H_{67}O_7N_{12}S]^+$: 1063.49709, found: 1063.49773.

(2S,4R)-1-((S)-2-(6-(4-(4-(((3-(3-(4-(1H-indol-3-yl)-2,5-dioxo-2,5-dihydro-1H-pyrrol-3-yl)-1H-indol-1-yl)propyl)(methyl)amino)methyl)-1H-1,2,3-triazol-1-yl)butanamido)hexanamido)-3,3-dimethylbutanoyl)-4-hydroxy-N-((S)-1-(4-(4-methylthiazol-5-yl)phenyl)ethyl)pyrrolidine-2-carboxamide (4-9e)

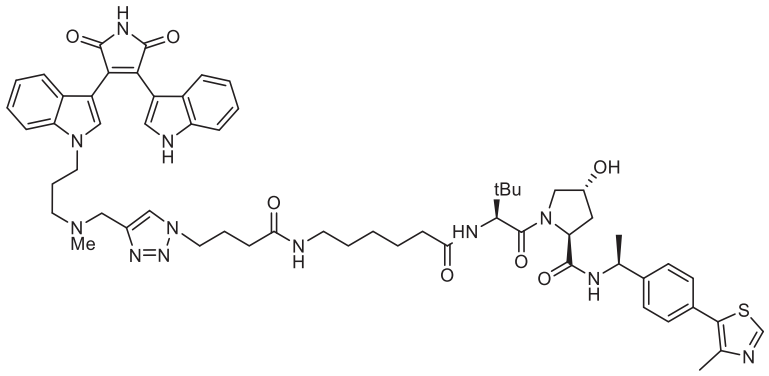

The product was prepared following the general method for CuAAC using **4-7** (17 mg, 0.039 mmol) and **3-32b** (27 mg, 0.039 mmol) .The crude was purified by flash column chromatography, the product was eluted at 7% MeOH/DCM and reported as a red solid (22 mg, **51%**).

^{1}H NMR (400 MHz, CD_3OD) δ 8.84 (s, 1H), 7.83 – 7.68 (m, 2H), 7.63 (d, *J* = 1.7 Hz, 1H), 7.44 – 7.28 (m, 6H), 7.03 (tdd, *J* = 8.3, 3.5, 1.1 Hz, 1H), 6.94 (dtd, *J* = 7.0, 3.6, 1.2 Hz, 2H), 6.74 – 6.63 (m, 2H), 6.52 (ddd, *J* = 8.1, 7.0, 1.0 Hz, 1H), 4.98 (q, *J* = 6.9 Hz, 1H), 4.64 – 4.49 (m, 2H), 4.41 (s, 1H), 4.28 (dt, *J* = 21.0, 6.6 Hz, 4H), 3.87 (d, *J* = 11.0 Hz, 1H), 3.73 (dd, *J* = 11.0, 3.9 Hz, 1H), 3.70 – 3.54 (m, 2H), 3.12 (t, *J* = 7.0 Hz, 2H), 2.44 (d, *J* = 9.1 Hz, 3H), 2.40 – 1.92 (m, 15H), 1.64 – 1.53 (m, 2H), 1.48 (d, *J* = 7.0 Hz, 5H), 1.35 – 1.27 (m, 2H), 1.02 (s, 9H). **^{13}C NMR** (101 MHz, CD_3OD) δ 174.5, 173.6, 172.8, 171.8, 170.9, 151.4, 149.3, 147.6, 144.2, 136.4, 136.1, 131.6, 130.1, 129.1, 129.0, 128.8, 128.4, 127.4, 126.6, 126.2, 126.2, 125.9, 125.5, 121.7, 121.6, 121.5, 121.1, 119.5, 119.2, 111.1, 109.4, 106.0, 105.6, 69.5, 59.2, 57.6, 56.6, 55.2, 49.3, 48.7, 43.6, 39.8, 38.9, 37.8, 37.4, 35.1, 35.0, 32.1, 28.6, 26.8, 26.1, 25.9, 25.6, 25.2, 21.0, 14.4. **HRMS (ESI):** calculated for $[C_{60}H_{73}O_7N_{12}S]^+$: 1005.54404, found: 1105.54485.

(2S,4R)-1-((S)-2-(6-(6-(4-(((3-(3-(4-(1H-indol-3-yl)-2,5-dioxo-2,5-dihydro-1H-pyrrol-3-yl)-1H-indol-1-yl)propyl)(methyl)amino)methyl)-1H-1,2,3-triazol-1-yl)hexanamido)hexanamido)-3,3-dimethylbutanoyl)-4-hydroxy-N-((S)-1-(4-(4-methylthiazol-5-yl)phenyl)ethyl)pyrrolidine-2-carboxamide (4-9f)

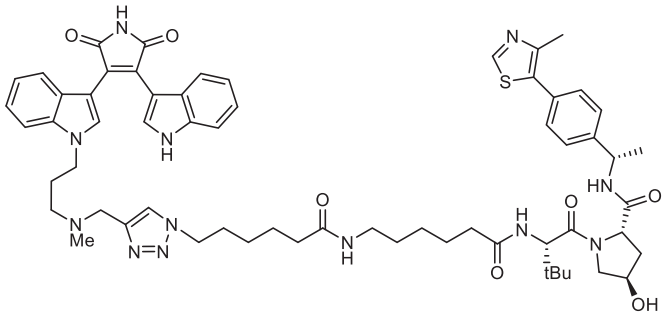

The product was prepared following the general method for CuAAC using **4-7** (20 mg, 0.046 mmol) and **3-32c** (32 mg, 0.046 mmol) .The crude was purified by flash column chromatography, the product was eluted at 8% MeOH/DCM and reported as a red solid (21 mg, **40%**).

^{1}H NMR (400 MHz, CD3OD) δ 8.84 (s, 1H), 7.76 (d, *J* = 1.5 Hz, 1H), 7.64 (d, *J* = 5.8 Hz, 2H), 7.43 – 7.35 (m, 5H), 7.35 – 7.28 (m, 1H), 7.02 (ddd, *J* = 8.3, 7.0, 1.1 Hz, 1H), 6.97 – 6.91 (m, 2H), 6.74 – 6.61 (m, 2H), 6.54 – 6.46 (m, 1H), 4.98 (q, *J* = 7.0 Hz, 1H), 4.67 – 4.50 (m, 2H), 4.45 – 4.39 (m, 1H), 4.25 (d, *J* = 7.0 Hz, 4H), 3.87 (d, *J* = 10.7 Hz, 1H), 3.73 (dd, *J* = 11.0, 4.0 Hz, 1H), 3.68 – 3.56 (m, 2H), 3.12 (t, *J* = 7.0 Hz, 2H), 2.45 (d, *J* = 3.8 Hz, 3H), 2.39 – 2.09 (m, 9H), 2.06 – 1.90 (m, 4H), 1.80 (t, *J* = 7.6 Hz, 2H), 1.58 (ddd, *J* = 15.2, 8.2, 6.1 Hz, 4H), 1.47 (dd, *J* = 7.1, 2.2 Hz, 5H), 1.37 – 1.23 (m, 4H), 1.03 (s, 9H). **^{13}C NMR** (101 MHz, CD3OD) δ 174.5, 174.3, 173.6, 173.6, 171.8, 170.9, 151.4, 147.6, 144.2, 136.4, 136.1, 131.7, 130.1, 129.1, 128.8, 128.3, 127.4, 126.6, 126.2, 125.9, 125.5, 121.7, 121.6, 121.5, 121.1, 119.5, 119.2, 111.1, 109.4, 106.1, 105.6, 69.5, 59.2, 57.6, 56.6, 54.9, 49.8, 48.7, 43.6, 40.6, 38.8, 37.4, 35.3, 35.1, 35.0, 29.5, 28.7, 26.2, 25.7, 25.2, 24.9, 21.0, 14.4. **HRMS (ESI):** calculated for $[C_{62}H_{77}O_7N_{12}S]^+$: 1133.5754, found: 1133.57554.

4-((2-(2-(4-(3-(4-(3-(3-(4-(1H-indol-3-yl)-2,5-dioxo-2,5-dihydro-1H-pyrrol-3-yl)-1H-indol-1-yl)propyl)piperazin-1-yl)-3-oxopropyl)-1H-1,2,3-triazol-1-yl)ethoxy)ethyl)amino)-2-(2,6-dioxopiperidin-3-yl)isoindoline-1,3-dione (4-11a)

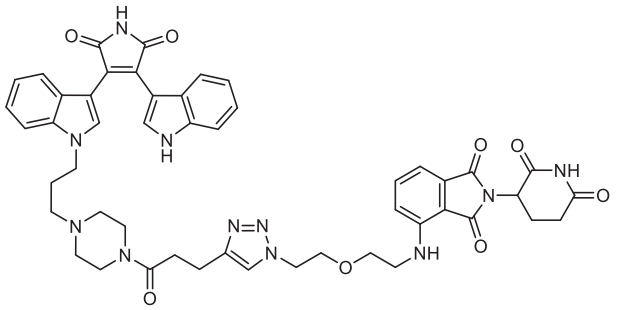

The product was prepared following the general method for CuAAC using **4-10** (11 mg, 0.021 mmol) and **3-31a** (8 mg, 0.021 mmol) .The crude was purified by flash column chromatography, the product was eluted at 4% MeOH/DCM and reported as a red solid (10 mg, **52%**).

^{1}H NMR (400 MHz, $CDCl_3$) δ 9.59 (d, *J* = 2.8 Hz, 1H), 7.87 (s, 1H), 7.80 – 7.74 (m, 2H), 7.57 – 7.46 (m, 2H), 7.36 – 7.26 (m, 2H), 7.18 – 7.09 (m, 2H), 7.03 (ddd, *J* = 8.2, 7.0, 1.2 Hz, 1H), 6.93 – 6.83 (m, 3H), 6.72 (ddd, *J* = 8.1, 7.0, 1.0 Hz, 1H), 6.52 (t, *J* = 5.4 Hz, 1H), 5.05 (dd, *J* = 12.2, 5.6 Hz, 1H), 4.65 – 4.43 (m, 2H), 4.16 (t, *J* = 6.3 Hz, 2H), 3.91 – 3.80 (m, 2H), 3.73 – 3.66 (m, 2H), 3.54 – 3.39 (m, 4H), 3.32 (t, *J* = 5.1 Hz, 2H), 3.06 (ddq, *J* = 22.7, 15.1, 7.5 Hz, 2H), 2.89 – 2.71 (m, 5H), 2.20 – 1.99 (m, 7H), 1.86 (p, *J* = 6.4 Hz, 2H). **^{13}C NMR** (101 MHz, $CDCl_3$) δ 172.2, 170.9, 169.6, 169.2, 167.6, 147.0, 146.5, 136.3, 136.2, 136.1, 132.6, 132.3, 128.8, 128.6, 128.1, 126.3, 124.9, 123.0, 122.5, 122.4, 122.2, 121.9, 120.3, 120.2, 116.6, 111.9, 111.5, 110.7, 109.6, 106.6, 105.7, 69.8, 69.3, 53.7, 52.6, 52.3, 50.4, 48.9, 45.4, 43.6, 42.1, 41.6, 32.7, 31.4, 26.1, 23.0, 21.1.

4-((2-(2-(2-(4-(3-(4-(3-(3-(4-(1H-indol-3-yl)-2,5-dioxo-2,5-dihydro-1H-pyrrol-3-yl)-1H-indol-1-yl)propyl)piperazin-1-yl)-3-oxopropyl)-1H-1,2,3-triazol-1-yl)ethoxy)ethoxy)ethyl)amino)-2-(2,6-dioxopiperidin-3-yl)isoindoline-1,3-dione (4-11b)

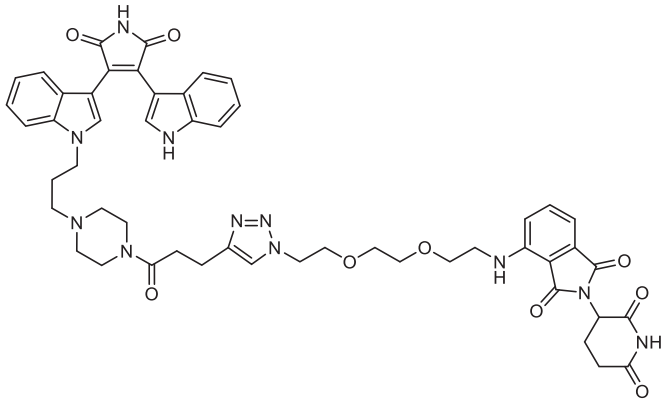

The product was prepared following the general method for CuAAC **4-10** (10 mg, 0.019 mmol) and **3-31b** (8 mg, 0.019 mmol) .The crude was purified by flash column chromatography, the product was eluted at 6% MeOH/DCM and reported as a red solid (10 mg, **55%**).

^{1}H NMR (400 MHz, $CDCl_3$) δ 9.6 – 9.5 (m, 1H), 8.1 (s, 1H), 7.8 (d, *J* = 2.9 Hz, 1H), 7.6 – 7.5 (m, 2H), 7.5 (q, *J* = 7.6 Hz, 1H), 7.3 (d, *J* = 8.2 Hz, 2H), 7.2 – 7.0 (m, 3H), 7.0 – 6.8 (m, 3H), 6.7 (t, *J* = 7.6 Hz, 1H), 6.5 (dt, *J* = 11.3, 5.5 Hz, 1H), 4.9 (dt, *J* = 11.2, 4.8 Hz, 1H), 4.5 (dt, *J* = 13.8, 5.2 Hz, 2H), 4.2 (d, *J* = 6.8 Hz, 2H), 3.9 – 3.8 (m, 2H), 3.7 – 3.3 (m, 14H), 3.1 – 2.9 (m, 2H), 2.8 (qt, *J* = 14.5, 8.9 Hz, 5H), 2.3 – 2.0 (m, 7H), 1.9 (s, 3H). **^{13}C NMR** (101 MHz, $CDCl_3$) δ 172.4, 172.3, 171.6, 170.5, 169.4, 168.8, 167.7, 146.7, 146.6, 136.2, 136.1, 136.0, 132.5, 132.2, 128.8, 128.7, 126.3, 125.1, 122.8, 122.5, 122.3, 122.2, 121.9, 120.3, 120.2, 116.8, 111.6, 111.5, 109.6, 106.7, 105.7, 70.7, 70.6, 70.5, 70.5, 70.4, 69.6, 69.4, 69.3, 53.8, 52.8, 52.2, 50.0, 48.9, 45.3, 43.7, 42.3, 41.5, 32.5, 31.4, 26.2, 22.7, 21.1. **HRMS (ESI):** calculated for $[C_{51}H_{54}O_9N_{11}]^+$: 964.41005, found: 964.40922.

4-((2-(2-(2-(2-(4-(3-(4-(3-(3-(4-(1H-indol-3-yl)-2,5-dioxo-2,5-dihydro-1H-pyrrol-3-yl)-1H-indol-1-yl)propyl)piperazin-1-yl)-3-oxopropyl)-1H-1,2,3-triazol-1-yl)ethoxy)ethoxy)ethoxy)ethyl)amino)-2-(2,6-dioxopiperidin-3-yl)isoindoline-1,3-dione (4-11c)

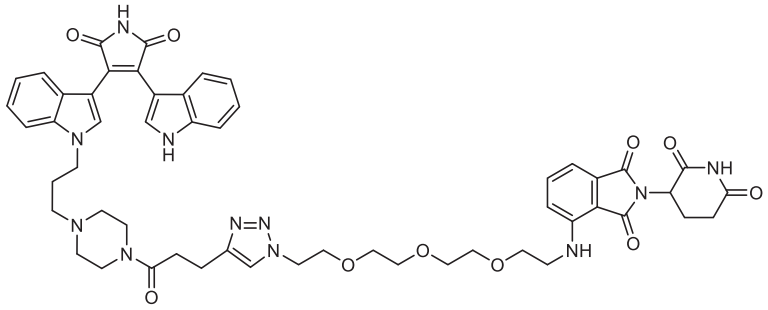

The product was prepared following the general method for CuAAC using **4-10** (25 mg, 0.047 mmol) and **3-31c** (23 mg, 0.047 mmol) .The crude was purified by flash column chromatography, the product was eluted at 6% MeOH/DCM and reported as a red solid (28 mg, **59%**).

^{1}H NMR (400 MHz, $CDCl_3$) δ 9.74 (d, *J* = 2.9 Hz, 1H), 8.57 (s, 1H), 7.74 (d, *J* = 2.8 Hz, 1H), 7.54 (d, *J* = 12.4 Hz, 2H), 7.42 (dd, *J* = 8.5, 7.1 Hz, 1H), 7.31 – 7.22 (m, 2H), 7.17 (d, *J* = 8.1 Hz, 1H), 7.12 – 7.02 (m, 2H), 6.99 (ddd, *J* = 8.2, 6.9, 1.2 Hz, 1H), 6.90 – 6.75 (m, 3H), 6.67 (ddd, *J* = 8.1, 7.0, 1.0 Hz, 1H), 6.47 (t, *J* = 5.6 Hz, 1H), 4.98 – 4.86 (m, 1H), 4.47 – 4.40 (m, 2H), 4.14 (t, *J* = 6.5 Hz, 2H), 3.81 (t, *J* = 5.2 Hz, 2H), 3.68 (t, *J* = 5.3 Hz, 2H), 3.65 – 3.47 (m, 10H), 3.42 (q, *J* = 5.4 Hz, 2H), 3.33 (d, *J* = 6.2 Hz, 2H), 3.03 (t, *J* = 7.3 Hz, 2H), 2.87 – 2.64 (m, 5H), 2.12 (tdd, *J* = 19.5, 7.1, 4.5 Hz, 7H), 1.93 – 1.83 (m, 2H). **^{13}C NMR** (101 MHz, $CDCl_3$) δ 172.6, 172.6, 171.8, 170.5, 169.3, 168.9, 167.7, 146.8, 146.6, 136.2, 136.2, 136.0, 132.5, 132.2, 128.9, 128.3, 128.0, 126.4, 125.1, 122.9, 122.4, 122.3, 122.1, 121.9, 120.2, 120.1, 116.8, 111.6, 111.5, 110.2, 109.6, 106.6, 105.8, 70.7, 70.5, 70.5, 70.5, 69.4, 69.4, 53.9, 52.8, 52.3, 50.0, 48.9, 45.3, 43.7, 42.3, 41.5, 32.6, 31.4, 26.3, 22.7, 21.2. **HRMS (ESI):** calculated for $[C_{53}H_{58}O_{10}N_{11}]^+$: 1008.43626, found: 1008.43602.

4-((14-(4-(3-(4-(3-(3-(4-(1H-indol-3-yl)-2,5-dioxo-2,5-dihydro-1H-pyrrol-3-yl)-1H-indol-1-yl)propyl)piperazin-1-yl)-3-oxopropyl)-1H-1,2,3-triazol-1-yl)-3,6,9,12-tetraoxatetradecyl)amino)-2-(2,6-dioxopiperidin-3-yl)isoindoline-1,3-dione (4-11d)

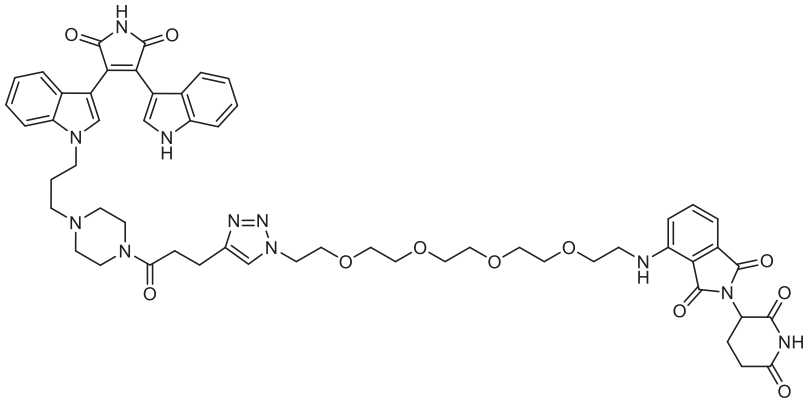

The product was prepared following the general method for CuAAC using **4-10** (15 mg, 0.028 mmol) and **3-31d** (15 mg, 0.028 mmol) .The crude was purified by flash column chromatography, the product was eluted at 8% MeOH/DCM and reported as a red solid (13 mg, **44%**).

^{1}H NMR (400 MHz, $CDCl_3$) δ 9.6 (d, *J* = 2.8 Hz, 1H), 9.0 (s, 1H), 8.2 (s, 1H), 7.8 (d, *J* = 2.8 Hz, 1H), 7.5 (d, *J* = 9.9 Hz, 2H), 7.4 (dd, *J* = 8.5, 7.1 Hz, 1H), 7.3 (dd, *J* = 8.2, 0.9 Hz, 2H), 7.2 (dt, *J* = 8.1, 1.0 Hz, 1H), 7.1 – 7.0 (m, 2H), 7.0 (ddd, *J* = 8.2, 7.1, 1.2 Hz, 1H), 6.9 – 6.8 (m, 3H), 6.7 (ddd, *J* = 8.1, 7.0, 1.0 Hz, 1H), 6.5 (t, *J* = 5.6 Hz,

1H), 4.9 (dd, *J* = 12.1, 5.4 Hz, 1H), 4.5 (t, *J* = 5.1 Hz, 2H), 4.2 (t, *J* = 6.4 Hz, 2H), 3.8 (t, *J* = 5.1 Hz, 2H), 3.7 – 3.5 (m, 16H), 3.4 (q, *J* = 5.4 Hz, 2H), 3.3 (t, *J* = 5.0 Hz, 2H), 3.0 (t, *J* = 7.3 Hz, 2H), 2.9 – 2.6 (m, 5H), 2.2 – 2.0 (m, 7H), 1.9 (dd, *J* = 12.6, 6.3 Hz, 2H). **^{13}C NMR** (101 MHz, $CDCl_3$) δ 172.4, 172.3, 171.5, 170.4, 169.3, 168.7, 167.7, 146.8, 146.6, 136.2, 136.1, 136.0, 132.5, 132.2, 128.8, 128.4, 128.0, 126.4, 125.1, 122.8, 122.4, 122.3, 122.2, 121.9, 120.2, 120.1, 116.8, 111.6, 111.5, 110.2, 109.6, 106.6, 105.8, 70.7, 70.6, 70.6, 70.5, 70.4, 69.5, 69.4, 53.9, 52.8, 52.3, 50.1, 48.9, 45.3, 43.7, 42.3, 41.6, 32.6, 31.4, 26.3, 22.8, 21.2. **HRMS (ESI):** calculated for $[C_{55}H_{62}O_{11}N_{11}]^+$: 1052.46248, found: 1052.46266.

(2S,4R)-1-((S)-2-(4-(4-(3-(4-(3-(3-(4-(1H-indol-3-yl)-2,5-dioxo-2,5-dihydro-1H-pyrrol-3-yl)-1H-indol-1-yl)propyl)piperazin-1-yl)-3-oxopropyl)-1H-1,2,3-triazol-1-yl)butanamido)-3,3-dimethylbutanoyl)-4-hydroxy-N-((S)-1-(4-(4-methylthiazol-5-yl)phenyl)ethyl)pyrrolidine-2-carboxamide (4-12a)

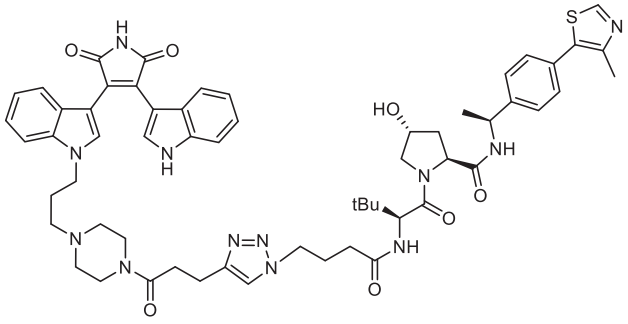

The product was prepared following the general method for CuAAC using **4-10** (15 mg, 0.026 mmol) and **3-30a** (14 mg, 0.026 mmol). The crude was purified by flash column chromatography, the product was eluted at 5% MeOH/DCM and reported as a red solid (17 mg, **60%**).

^{1}H NMR (400 MHz, CD3OD) δ 8.84 (s, 1H), 7.76 (d, *J* = 3.1 Hz, 1H), 7.72 (s, 1H), 7.61 (d, *J* = 6.8 Hz, 1H), 7.44 – 7.35 (m, 5H), 7.32 (dd, *J* = 8.1, 0.8 Hz, 1H), 7.07 – 6.91 (m, 3H), 6.73 (dt, *J* = 8.0, 1.0 Hz, 1H), 6.67 (ddd, *J* = 8.1, 7.1, 0.9 Hz, 1H), 6.55 (ddd, *J* = 8.1, 7.0, 1.0 Hz, 1H), 4.98 (q, *J* = 7.0 Hz, 1H), 4.59 (s, 1H), 4.59 – 4.53 (m, 1H), 4.46 – 4.41 (m, 1H), 4.35 (t, *J* = 6.8 Hz, 2H), 4.25 (t, *J* = 6.4 Hz, 2H), 3.89 (d, *J* = 11.0 Hz, 1H), 3.73 (dd, *J* = 11.0, 3.9 Hz, 1H), 3.57 – 3.43 (m, 4H), 2.96 (q, *J* = 11.8, 9.5 Hz, 2H), 2.75 (t, *J* = 7.3 Hz, 2H), 2.45 (s, 3H), 2.35 – 2.08 (m, 11H), 2.03 – 1.88 (m, 3H), 1.47 (d, *J* = 7.0 Hz, 3H), 1.02 (d, *J* = 10.3 Hz, 9H). **^{13}C NMR** (101 MHz, CD3OD) δ 173.6, 172.9, 171.8, 170.9, 151.4, 144.2, 136.4, 136.2, 131.7, 130.1, 129.1, 128.7, 128.3, 127.6, 126.6, 126.2, 126.0, 125.4, 122.6, 121.6, 121.5, 121.1, 119.5, 119.2, 111.1, 109.4, 106.0, 105.6, 89.6, 69.6, 59.2, 57.8, 56.6, 54.0, 52.7, 52.2, 49.0, 48.7, 45.2, 43.4, 41.4, 37.4, 34.9, 31.8, 31.4, 26.2, 25.9, 25.6, 25.6, 21.0, 20.8, 14.4. **HRMS (ESI):** calculated for $[C_{59}H_{69}O_7N_{12}S]^+$: 1089.51274, found: 1089.51251.

(2S,4R)-1-((S)-2-(6-(4-(3-(4-(3-(3-(4-(1H-indol-3-yl)-2,5-dioxo-2,5-dihydro-1H-pyrrol-3-yl)-1H-indol-1-yl)propyl)piperazin-1-yl)-3-oxopropyl)-1H-1,2,3-triazol-1-yl)hexanamido)-3,3-dimethylbutanoyl)-4-hydroxy-N-((S)-1-(4-(4-methylthiazol-5-yl)phenyl)ethyl)pyrrolidine-2-carboxamide (4-12b)

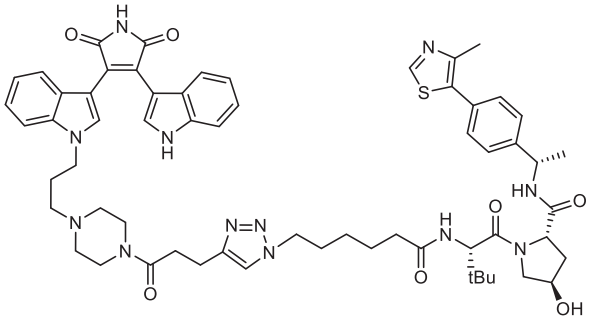

The product was prepared following the general method for CuAAC using **4-10** (12 mg, 0.022 mmol) and 3-30b (14 mg, 0.022 mmol). The crude was purified by flash column chromatography, the product was eluted at 6% MeOH/DCM and reported as a red solid (10 mg, **41%**).

^{1}H NMR (500 MHz, CD_3OD) δ 8.84 (s, 1H), 7.76 (d, *J* = 2.5 Hz, 1H), 7.70 (s, 1H), 7.62 (s, 1H), 7.44 – 7.35 (m, 5H), 7.32 (dt, *J* = 8.2, 0.9 Hz, 1H), 7.03 (ddd, *J* = 8.3, 7.0, 1.2 Hz, 1H), 7.00 – 6.90 (m, 2H), 6.73 (dt, *J* = 8.0, 1.0 Hz, 1H), 6.67 (ddd, *J* = 8.1, 7.0, 0.9 Hz, 1H), 6.55 (ddd, *J* = 8.1, 7.0, 1.0 Hz, 1H), 4.98 (q, *J* = 6.9 Hz, 1H), 4.60 (s, 1H), 4.58 – 4.53 (m, 1H), 4.41 (d, *J* = 4.2 Hz, 1H), 4.31 (t, *J* = 7.0 Hz, 2H), 4.26 (t, *J* = 6.5 Hz, 2H), 3.89 – 3.83 (m, 1H), 3.72 (dd, *J* = 11.0, 3.9 Hz, 1H), 3.52 (s, 2H), 3.46 (t, *J* = 5.1 Hz, 2H), 2.97 (t, *J* = 7.3 Hz, 2H), 2.74 (t, *J* = 7.3 Hz, 2H), 2.45 (s, 3H), 2.24 (pd, *J* = 7.2, 4.7 Hz, 6H), 2.21 – 2.14 (m, 3H), 1.98 – 1.88 (m, 3H), 1.88 – 1.80 (m, 2H), 1.62 (p, *J* = 7.4 Hz, 2H), 1.48 (d, *J* = 7.0 Hz, 3H), 1.34 – 1.25 (m, 3H), 1.02 (s, 9H). **^{13}C NMR** (126 MHz, CD_3OD) δ 175.7, 175.0, 175.0, 173.2, 172.4, 172.3, 152.8, 149.1, 145.6, 137.8, 137.6, 133.1, 131.5, 130.5, 130.1, 129.8, 129.0, 128.0, 127.6, 127.4, 126.8, 123.7, 123.0, 122.9, 122.5, 120.9, 120.6, 112.5, 110.8, 107.4, 107.1, 71.0, 60.6, 59.0, 58.0, 55.4, 54.1, 53.6, 51.1, 50.1, 46.6, 44.8, 42.8, 38.8, 36.4, 36.2, 33.2, 30.9, 27.6, 27.1, 27.0, 26.2, 22.4, 22.2, 15.8. **HRMS (ESI):** calculated for $[C_{61}H_{73}O_7N_{12}S]^+$: 1117.54404, found: 1117.54473.

4-(4-(3-(4-(3-(3-(4-(1H-indol-3-yl)-2,5-dioxo-2,5-dihydro-1H-pyrrol-3-yl)-1H-indol-1-yl)propyl)piperazin-1-yl)-3-oxopropyl)-1H-1,2,3-triazol-1-yl)-N-(3-(((S)-1-((2S,4R)-4-hydroxy-2-(1-(((S)-1-(4-(4-methylthiazol-5-yl)phenyl)ethyl)amino)vinyl)pyrrolidin-1-yl)-3,3-dimethyl-1-oxobutan-2-yl)amino)-3-oxopropyl)butanamide (4-12c)

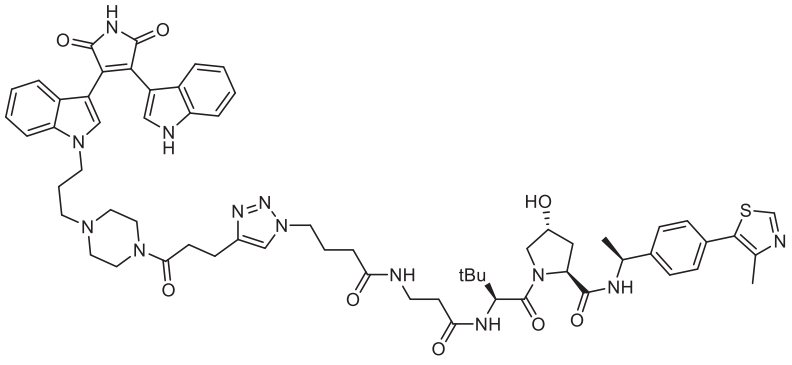

The product was prepared following the general method for CuAAC using **4-10** (9 mg, 0.017 mmol) and **3-32a** (11 mg, 0.017 mmol). The crude was purified by flash column chromatography, the product was eluted at 4% MeOH/DCM and reported as a red solid (10 mg, **51%**).

^{1}H NMR (500 MHz, CD_3OD) δ 8.83 (d, *J* = 8.3 Hz, 1H), 7.76 (d, *J* = 0.8 Hz, 1H), 7.74 (s, 1H), 7.66 – 7.62 (m, 1H), 7.45 – 7.35 (m, 5H), 7.34 – 7.29 (m, 1H), 7.03 (ddd, *J* = 8.3, 7.1, 1.1 Hz, 1H), 7.00 – 6.90 (m, 2H), 6.67 (ddd, *J* = 8.0, 7.0, 0.9 Hz, 1H), 6.55 (ddd, *J* = 8.1, 7.0, 1.0 Hz, 1H), 5.02 – 4.95 (m, 1H), 4.62 – 4.52 (m, 2H), 4.43 – 4.38 (m, 1H), 4.39 – 4.33 (m, 2H), 4.30 – 4.23 (m, 2H), 3.94 – 3.82 (m, 1H), 3.71 (dd, *J* = 11.0, 3.9 Hz, 1H), 3.53 (d, *J* = 5.2 Hz, 2H), 3.47 (t, *J* = 5.2 Hz, 2H), 3.45 – 3.32 (m, 2H), 3.01 – 2.94 (m, 2H), 2.75 (t, *J* = 7.4 Hz, 2H), 2.49 – 2.42 (m, 5H), 2.26 (s, 4H), 2.21 – 2.09 (m, 7H), 1.98 – 1.87 (m, 3H), 1.48 (d, *J* = 7.1 Hz, 3H), 1.01 (d, *J* = 14.3 Hz, 9H). **^{13}C NMR** (126 MHz, CD_3OD) δ 175.0, 175.0, 174.5, 173.6, 173.3, 172.4, 172.3, 152.8, 149.1, 147.7, 145.6, 137.8, 137.6, 133.1, 131.5, 130.5, 130.1, 129.8, 129.0, 128.0, 127.6, 127.3, 126.8, 123.8, 123.0, 122.9, 122.5, 120.9, 120.6, 112.5, 110.8, 107.5, 107.1, 71.0, 60.5, 59.2, 57.9, 55.4, 54.1, 53.6, 50.6, 50.2, 46.6, 44.8, 42.8, 38.9, 37.1, 36.3, 36.3, 33.5, 33.3, 27.6, 27.4, 27.1, 22.4, 22.2, 15.8. **HRMS (ESI)**: calculated for $[C_{62}H_{74}O_8N_{13}S]^+$: 1160.54985, found: 1160.55030.

(2S,4R)-1-((S)-2-(6-(4-(4-(3-(4-(3-(3-(4-(1H-indol-3-yl)-2,5-dioxo-2,5-dihydro-1H-pyrrol-3-yl)-1H-indol-1-yl)propyl)piperazin-1-yl)-3-oxopropyl)-1H-1,2,3-triazol-1-yl)butanamido)hexanamido)-3,3-dimethylbutanoyl)-4-hydroxy-N-((S)-1-(4-(4-methylthiazol-5-yl)phenyl)ethyl)pyrrolidine-2-carboxamide (4-12d)

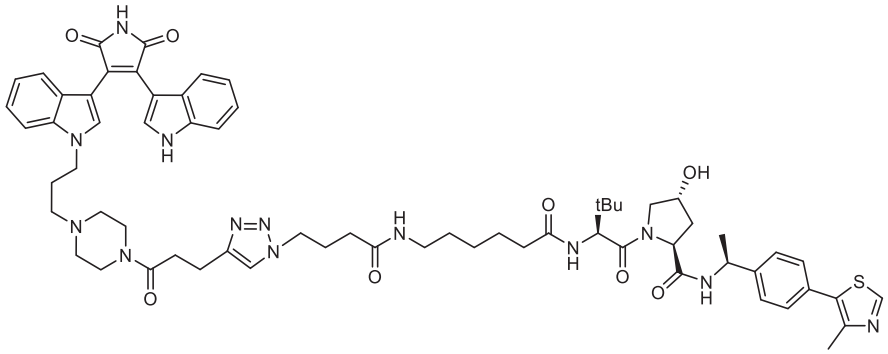

The product was prepared following the general method for CuAAC using **4-10** (12 mg, 0.02 mmol) and **3-32b** (15 mg, 0.022 mmol). The crude was purified by flash column chromatography, the product was eluted at 7% MeOH/DCM and reported as a red solid (18 mg, **68%**).

^{1}H NMR (500 MHz, CD_3OD) δ 8.85 (s, 1H), 7.76 (d, *J* = 1.5 Hz, 1H), 7.73 (s, 1H), 7.62 (d, *J* = 2.6 Hz, 1H), 7.43 – 7.36 (m, 5H), 7.32 (dt, *J* = 8.1, 0.9 Hz, 1H), 7.03 (ddd, *J* = 8.3, 7.0, 1.2 Hz, 1H), 7.01 – 6.92 (m, 2H), 6.73 (dt, *J* = 8.1, 1.0 Hz, 1H), 6.68 (ddd, *J* = 8.0, 7.0, 0.9 Hz, 1H), 6.55 (ddd, *J* = 8.1, 7.0, 1.0 Hz, 1H), 4.98 (q, *J* = 6.9 Hz, 1H), 4.61 (s, 1H), 4.58 – 4.53 (m, 1H), 4.44 – 4.40 (m, 1H), 4.38 – 4.34 (m, 2H), 4.26 (t, *J* = 6.4 Hz, 2H), 3.86 (d, *J* = 10.9 Hz, 1H), 3.72 (dd, *J* = 11.0, 4.0 Hz, 1H), 3.52 (s, 2H), 3.46 (d, *J* = 5.2 Hz, 2H), 3.13 (t, *J* = 7.0 Hz, 2H), 2.97 (t, *J* = 7.4 Hz, 2H), 2.74 (t, *J* = 7.3 Hz, 2H), 2.45 (s, 3H), 2.32 – 2.21 (m, 6H), 2.21 – 2.09 (m, 7H), 1.99 – 1.88 (m, 3H), 1.64 – 1.56 (m, 2H), 1.47 (t, *J* = 7.0 Hz, 5H), 1.38 – 1.29 (m, 2H), 1.01 (s, 9H). **^{13}C NMR** (126 MHz, CD_3OD) δ 174.5, 173.6, 173.6, 172.9, 171.8, 170.9, 151.4, 147.7, 146.6, 144.2, 136.4, 136.2, 131.6, 130.1, 129.1, 128.7, 128.3, 127.6, 126.6, 126.2, 125.9, 125.4, 122.3, 121.6, 121.5, 121.1, 119.5, 119.2, 111.1, 109.4, 106.0, 105.6, 69.5, 59.1, 57.6, 56.6, 54.0, 52.7, 52.2, 49.2, 48.7, 45.2, 43.4, 41.3, 38.9, 37.4, 35.0, 32.1, 31.8, 28.6, 26.2, 26.1, 26.0, 25.6, 25.2, 21.0, 20.7, 14.4. **HRMS (ESI):** calculated for $[C_{65}H_{80}O_8N_{13}S]^+$: 1202.59680, found: 1202.59699.

(2S,4R)-1-((S)-2-(6-(6-(4-(3-(4-(3-(3-(4-(1H-indol-3-yl)-2,5-dioxo-2,5-dihydro-1H-pyrrol-3-yl)-1H-indol-1-yl)propyl)piperazin-1-yl)-3-oxopropyl)-1H-1,2,3-triazol-1-

yl)hexanamido)hexanamido)-3,3-dimethylbutanoyl)-4-hydroxy-N-((S)-1-(4-(4-methylthiazol-5-yl)phenyl)ethyl)pyrrolidine-2-carboxamide (4-12e)

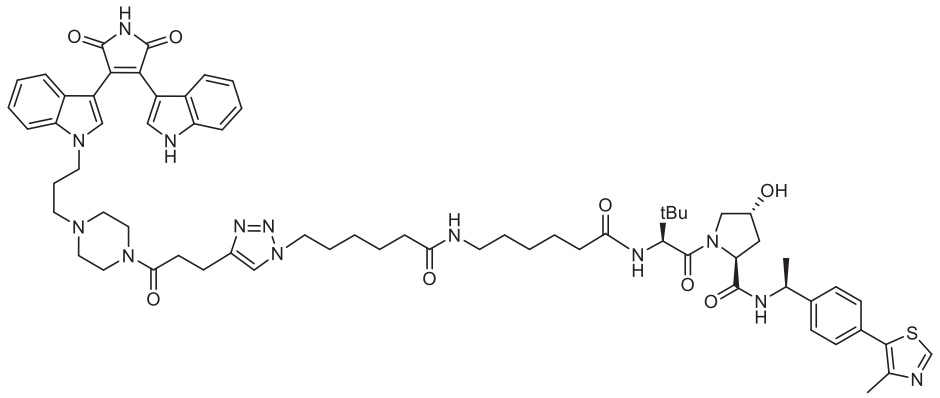

The product was prepared following the general method for CuAAC using **4-10** (11 mg, 0.021 mmol) and **3-32c** (14 mg, 0.021 mmol). The crude was purified by flash column chromatography, the product was eluted at 10% MeOH/DCM and reported as a red solid (9 mg, **35%**).

^{1}H NMR (400 MHz, CD_3OD) δ 8.85 (s, 1H), 7.77 (d, *J* = 1.3 Hz, 1H), 7.71 (s, 1H), 7.63 (s, 1H), 7.45 – 7.35 (m, 5H), 7.32 (dt, *J* = 8.2, 0.9 Hz, 1H), 7.08 – 6.91 (m, 3H), 6.73 (dt, *J* = 8.1, 1.0 Hz, 1H), 6.68 (ddd, *J* = 8.0, 7.0, 0.9 Hz, 1H), 6.55 (ddd, *J* = 8.2, 7.1, 1.0 Hz, 1H), 4.99 (q, *J* = 6.9 Hz, 1H), 4.65 – 4.60 (m, 1H), 4.60 – 4.54 (m, 1H), 4.42 (s, 1H), 4.32 (t, *J* = 7.0 Hz, 2H), 4.26 (t, *J* = 6.5 Hz, 2H), 3.87 (d, *J* = 10.8 Hz, 1H), 3.73 (dd, *J* = 11.0, 3.9 Hz, 1H), 3.53 (s, 2H), 3.47 (d, *J* = 5.3 Hz, 2H), 3.12 (t, *J* = 7.0 Hz, 2H), 2.97 (t, *J* = 7.3 Hz, 2H), 2.74 (t, *J* = 7.3 Hz, 2H), 2.46 (s, 3H), 2.30 – 2.22 (m, 6H), 2.16 (dt, *J* = 19.4, 7.2 Hz, 5H), 2.02 – 1.76 (m, 5H), 1.67 – 1.52 (m, 4H), 1.47 (dd, *J* = 9.4, 7.0 Hz, 5H), 1.32 (s, 4H), 1.03 (s, 9H). **^{13}C NMR** (101 MHz, CD_3OD) δ 174.5, 173.6, 173.6, 171.8, 170.9, 149.6, 147.7, 146.6, 144.2, 136.4, 136.2, 131.7, 130.1, 129.1, 128.7, 128.3, 127.6, 126.6, 126.2, 125.9, 125.4, 123.3, 121.6, 121.5, 121.1, 119.5, 119.2, 111.1, 109.4, 106.0, 105.7, 69.5, 59.1, 57.6, 56.6, 54.0, 52.7, 52.2, 49.6, 48.7, 45.2, 43.4, 41.4, 38.8, 37.4, 35.4, 35.1, 35.0, 31.8, 29.5, 28.7, 26.2, 25.6, 25.6, 25.2, 24.9, 21.0, 20.8, 20.4, 14.3. **HRMS (ESI):** calculated for $[C_{67}H_{84}O_8N_{13}S]^+$: 1230.62810, found: 1230.62783.

(2S,4R)-1-((S)-2-(3-(1-(3-(4-(1H-indol-3-yl)-2,5-dioxo-2,5-dihydro-1H-pyrrol-3-yl)-1H-indol-5-yl)-1H-1,2,3-triazol-4-yl)propanamido)-3,3-dimethylbutanoyl)-4-hydroxy-N-((S)-1-(4-(4-methylthiazol-5-yl)phenyl)ethyl)pyrrolidine-2-carboxamide (4-23a)

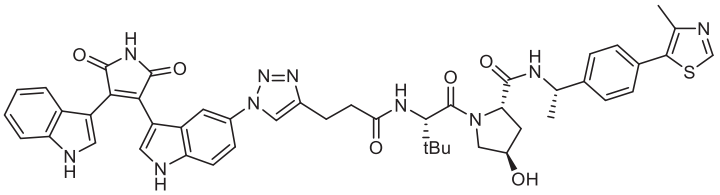

The product was prepared following the general method for CuAAC using **4-21** (14 mg, 0.038 mmol) and **4-22a** (20 mg, 0.038 mmol). The crude was purified by flash column chromatography, the product was eluted at 4% MeOH/DCM and reported as a red solid (22 mg, **65%**).

^{1}H NMR (400 MHz, CD_3OD) δ 8.86 (s, 2H), 7.95 (d, *J* = 11.8 Hz, 1H), 7.74 (s, 1H), 7.51 – 7.26 (m, 8H), 7.01 (t, *J* = 7.5 Hz, 1H), 6.92 – 6.78 (m, 2H), 6.64 (dt, *J* = 10.2, 6.7 Hz, 1H), 5.00 – 4.94 (m, 1H), 4.64 – 4.52 (m, 2H), 4.44 (s, 1H), 3.91 (t, *J* = 11.9 Hz, 1H), 3.76 (dd, *J* = 11.2, 4.0 Hz, 1H), 2.97 (t, *J* = 8.1 Hz, 2H), 2.66 (ddd, *J* =

30.9, 14.3, 7.2 Hz, 2H), 2.44 (d, *J* = 12.1 Hz, 3H), 2.16 (q, *J* = 13.0, 11.7 Hz, 1H), 2.02 – 1.86 (m, 1H), 1.47 (d, *J* = 7.0 Hz, 3H), 0.96 (d, *J* = 12.0 Hz, 9H). **^{13}C NMR** (101 MHz, CD_3OD) δ 173.4, 173.3, 171.8, 170.8, 150.7, 148.3, 147.6, 144.2, 136.2, 136.0, 130.8, 130.1, 129.8, 129.1, 128.6, 128.1, 127.8, 126.2, 126.0, 125.7, 122.0, 120.8, 120.0, 119.5, 115.2, 113.6, 112.1, 111.2, 106.9, 106.3, 69.6, 59.2, 57.8, 56.6, 48.7, 37.3, 35.0, 34.6, 25.6, 21.0, 21.0, 14.4. **HRMS (ESI):** calculated for $[C_{48}H_{49}O_6N_{10}S]^+$: 893.35518, found: 893.35578.

(2S,4R)-1-((S)-2-(5-(1-(3-(4-(1H-indol-3-yl)-2,5-dioxo-2,5-dihydro-1H-pyrrol-3-yl)-1H-indol-5-yl)-1H-1,2,3-triazol-4-yl)pentanamido)-3,3-dimethylbutanoyl)-4-hydroxy-N-((S)-1-(4-(4-methylthiazol-5-yl)phenyl)ethyl)pyrrolidine-2-carboxamide (4-23b)

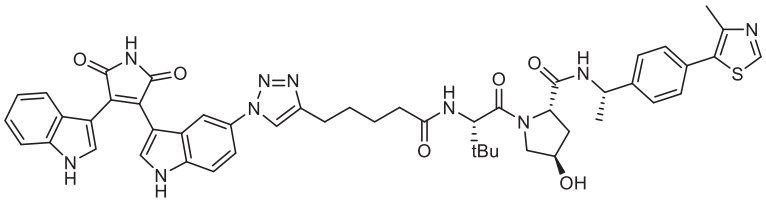

The product was prepared following the general method for CuAAC using **4-21** (25 mg, 0.068mmol) and **4-22b** (37 mg, 0.068 mmol). The crude was purified by flash column chromatography, the product was eluted at 4% MeOH/DCM and reported as a red solid (25 mg, **40%**).

^{1}H NMR (400 MHz, CD3OD) δ 8.78 (s, 1H), 7.98 – 7.91 (m, 1H), 7.87 – 7.80 (m, 1H), 7.71 – 7.64 (m, 1H), 7.43 – 7.23 (m, 9H), 7.11 (t, *J* = 6.2 Hz, 1H), 6.93 (q, *J* = 7.7 Hz, 1H), 6.82 (d, *J* = 8.0 Hz, 1H), 6.69 (d, *J* = 1.9 Hz, 1H), 6.65 – 6.57 (m, 2H), 4.97 – 4.86 (m, 1H), 4.63 – 4.53 (m, 2H), 4.37 (s, 1H), 3.85 (d, *J* = 10.8 Hz, 1H), 3.70 (dd, *J* = 11.0, 4.2 Hz, 1H), 2.61 (s, 3H), 2.35 (d, *J* = 22.5 Hz, 7H), 2.11 (dd, *J* = 13.1, 7.8 Hz, 1H), 1.89 (ddt, *J* = 13.2, 8.8, 3.8 Hz, 1H), 1.70 – 1.57 (m, 6H), 1.39 (dd, *J* = 8.2, 3.7 Hz, 4H), 1.00 (q, *J* = 8.2, 5.9 Hz, 12H). **^{13}C NMR** (101 MHz, CD3OD) δ 174.5, 173.4, 173.2, 171.8, 171.0, 151.4, 147.7, 144.2, 136.1, 135.9, 130.8, 130.0, 129.7, 129.0, 128.8, 128.6, 127.9, 127.8, 126.2, 125.8, 125.6, 121.9, 120.9, 119.9, 119.5, 115.1, 113.6, 112.0, 111.2, 106.8, 106.2, 69.5, 59.2, 57.9, 56.6, 48.7, 37.3, 35.0, 34.9, 28.5, 25.7, 24.9, 24.5, 20.9, 14.4. **HRMS (ESI):** calculated for $[C_{50}H_{53}O_6N_{10}S]^+$: 921.38648, found: 921.38685.

(2S,4R)-1-((S)-2-(3-(3-(1-(3-(4-(1H-indol-3-yl)-2,5-dioxo-2,5-dihydro-1H-pyrrol-3-yl)-1H-indol-5-yl)-1H-1,2,3-triazol-4-yl)propanamido)propanamido)-3,3-dimethylbutanoyl)-4-hydroxy-N-((S)-1-(4-(4-methylthiazol-5-yl)phenyl)ethyl)pyrrolidine-2-carboxamide (4-23c)

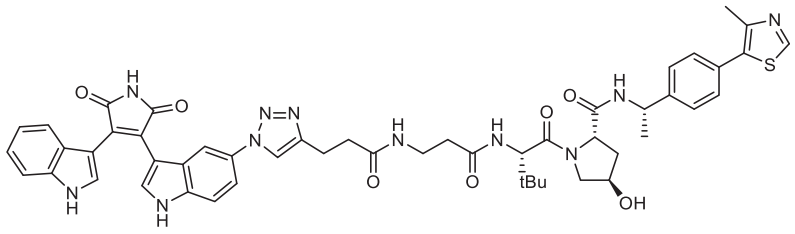

The product was prepared following the general method for CuAAC using **4-21** (9 mg, 0.024 mmol) and **4-22c** (15 mg, 0.024 mmol). The crude was purified by flash column chromatography, the product was eluted at 6% MeOH/DCM and reported as a red solid (13 mg, **56%**).

^{1}H NMR (500 MHz, CD_3OD) δ 8.84 (s, 1H), 7.98 (d, *J* = 2.8 Hz, 1H), 7.75 (s, 1H), 7.46 (dd, *J* = 8.7, 0.6 Hz, 1H), 7.43 – 7.35 (m, 6H), 7.29 – 7.24 (m, 1H), 7.01 (ddd, *J* = 8.2, 7.0, 1.1 Hz, 1H), 6.89 – 6.84 (m, 2H), 6.65 (ddd, *J* = 8.1, 7.0, 1.0 Hz, 1H), 4.96 (q, *J* = 7.0 Hz, 1H), 4.63 – 4.53 (m, 2H), 4.41 (dq, *J* = 4.1, 2.5, 1.9 Hz, 1H), 3.89 (dt, *J* = 11.3, 1.7 Hz, 1H), 3.75 – 3.67 (m, 1H), 3.54 – 3.39 (m, 2H), 3.00 – 2.88 (m, 2H), 2.58 – 2.40 (m, 7H), 2.17 (ddt, *J* = 13.1, 7.7, 2.0 Hz, 1H), 1.94 (ddd, *J* = 13.4, 9.2, 4.5 Hz, 1H), 1.43 (d, *J* = 7.0 Hz, 3H), 1.02 (d, *J* = 6.0 Hz, 9H). **^{13}C NMR** (126 MHz, CD_3OD) δ 174.8, 174.7, 174.6, 173.7, 173.3, 172.4, 152.8, 148.0, 145.6, 137.6, 137.4, 132.2, 131.5, 131.2, 130.4, 130.4, 130.0, 129.4, 129.4, 127.6, 127.5, 127.2, 127.1, 123.4, 122.3, 121.5, 121.0, 116.6, 115.0, 113.5, 112.7, 108.3, 107.7, 71.1, 60.6, 59.3, 57.9, 50.2, 38.8, 37.2, 36.5, 36.3, 36.3, 27.0, 22.4, 22.3, 15.8. **HRMS (ESI):** calculated for $[C_{51}H_{54}O_7N_{11}S]^+$: 964.39229, found: 964.39288.

(2S,4R)-1-((S)-2-(4-(4-(3-(1-(3-(4-(1H-indol-3-yl)-2,5-dioxo-2,5-dihydro-1H-pyrrol-3-yl)-1H-indol-5-yl)-1H-1,2,3-triazol-4-yl)propanoyl)piperazin-1-yl)butanamido)-3,3-dimethylbutanoyl)-4-hydroxy-N-((S)-1-(4-(4-methylthiazol-5-yl)phenyl)ethyl)pyrrolidine-2-carboxamide(4-23d)

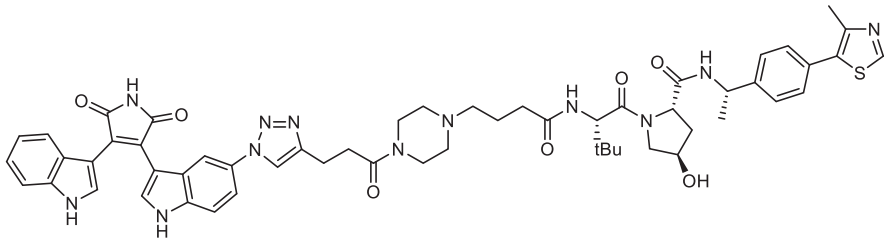

The product was prepared following the general method for CuAAC using **4-21** (14 mg, 0.038 mmol) and **4-22d** (25 mg, 0.038 mmol). The crude was purified by flash column chromatography, the product was eluted at 8% MeOH/DCM and reported as a red solid (30 mg, **75%**).

^{1}H NMR (400 MHz, CD_3OD) δ 8.87 (s, 1H), 8.01 (s, 1H), 7.75 (s, 1H), 7.48 (d, *J* = 0.6 Hz, 1H), 7.45 – 7.34 (m, 6H), 7.03 (ddd, *J* = 8.2, 7.1, 1.1 Hz, 1H), 6.94 – 6.87 (m, 2H), 6.87 – 6.82 (m, 1H), 6.68 (ddd, *J* = 8.1, 7.0, 1.0 Hz, 1H), 5.01 (q, *J* = 7.0 Hz, 1H), 4.68 – 4.53 (m, 2H), 4.45 (dt, *J* = 4.4, 2.2 Hz, 1H), 3.90 (dt, *J* = 11.4, 1.5 Hz, 1H), 3.76 (dd, *J* = 11.0, 3.9 Hz, 1H), 3.71 – 3.62 (m, 2H), 3.54 (q, *J* = 5.1, 4.6 Hz, 2H), 3.00 (t, *J* = 7.2 Hz, 2H), 2.82 – 2.71 (m, 2H), 2.51 – 2.28 (m, 11H), 2.25 – 2.15 (m, 1H), 1.96 (ddd, *J* = 13.4, 9.1, 4.5 Hz, 1H), 1.86 – 1.75 (m, 2H), 1.51 (d, *J* = 7.0 Hz, 3H), 1.06 (s, 9H). **^{13}C NMR** (101 MHz, CD_3OD) δ 174.09, 173.38, 173.28, 171.84, 171.11, 170.85, 151.44, 147.65, 146.51, 144.21, 136.21, 136.01, 131.94, 130.83, 130.09, 129.70, 129.07, 128.54, 128.07, 128.02, 126.21, 126.05, 125.66, 122.00, 120.86, 120.33, 119.57, 115.14, 113.54, 112.15, 111.27, 106.87, 106.33, 69.56, 59.21, 57.68, 56.95, 56.64, 52.69, 52.42, 48.73, 45.06, 41.19, 37.44, 35.09, 32.88, 31.84, 25.64, 22.05, 20.97, 20.77, 14.39.

(2S,4R)-1-((S)-2-(6-(4-(5-(1-(3-(4-(1H-indol-3-yl)-2,5-dioxo-2,5-dihydro-1H-pyrrol-3-yl)-1H-indol-5-yl)-1H-1,2,3-triazol-4-yl)pentanoyl)piperazin-1-yl)hexanamido)-3,3-dimethylbutanoyl)-4-hydroxy-N-((S)-1-(4-(4-methylthiazol-5-yl)phenyl)ethyl)pyrrolidine-2-carboxamide (4-23e)

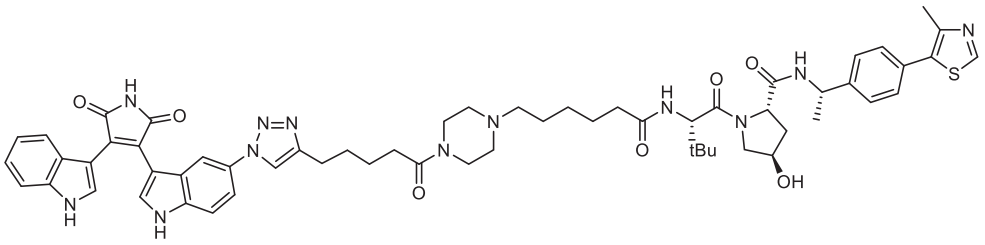

The product was prepared following the general method for CuAAC using **4-21** (13 mg, 0.035 mmol) and **4-22e** (25 mg, 0.035 mmol). The crude was purified by flash column chromatography, the product was eluted at 8% MeOH/DCM and reported as a red solid (28 mg, **73%**).

^{1}H NMR (400 MHz, CD_3OD) δ 8.76 (s, 1H), 7.95 (d, *J* = 6.0 Hz, 1H), 7.63 (d, *J* = 1.8 Hz, 1H), 7.38 (d, *J* = 8.7 Hz, 1H), 7.34 – 7.25 (m, 6H), 6.92 (ddd, *J* = 8.1, 7.0, 1.1 Hz, 1H), 6.83 (dt, *J* = 8.1, 1.0 Hz, 1H), 6.68 (d, *J* = 2.1 Hz, 1H), 6.63 – 6.52 (m, 2H), 4.90 (q, *J* = 7.0 Hz, 1H), 4.53 (s, 1H), 4.50 – 4.46 (m, 1H), 4.33 (dt, *J* = 4.4, 2.2 Hz, 1H), 3.79 (dt, *J* = 11.3, 1.8 Hz, 1H), 3.69 – 3.60 (m, 1H), 3.57 – 3.43 (m, 2H), 3.40 (t, *J* = 5.1 Hz, 2H), 2.60 (t, *J* = 7.0 Hz, 2H), 2.40 – 2.30 (m, 7H), 2.27 (t, *J* = 5.0 Hz, 1H), 2.14 (dddd, *J* = 27.9, 13.1, 9.4, 6.7 Hz, 5H), 1.86 (ddt, *J* = 13.3, 9.1, 4.6 Hz, 1H), 1.62 (dq, *J* = 11.3, 6.9, 5.9 Hz, 2H), 1.56 – 1.44 (m, 4H), 1.39 (d, *J* = 7.0 Hz, 3H), 1.37 – 1.30 (m, 2H), 1.22 – 1.13 (m, 2H), 0.94 (s, 9H). **^{13}C NMR** (101 MHz, CD_3OD) δ 174.5, 173.4, 173.3, 172.5, 171.8, 170.9, 151.5, 147.7, 144.2, 136.2, 136.0, 131.0, 130.1, 129.7, 129.1, 128.6, 128.0, 127.8, 126.2, 126.0, 125.6, 122.0, 121.0, 120.0, 119.6, 115.2, 113.6, 112.2, 111.2, 106.9, 106.4, 69.6, 59.2, 57.8, 57.6, 56.6, 52.9, 52.5, 48.7, 45.0, 41.0, 37.4, 35.1, 35.0, 32.4, 28.4, 26.6, 25.7, 25.3, 24.4, 21.0, 14.4.

8.5. Experimental Section - p38 PROTACs

Methyl 3-(4-hydroxy-6-methyl-2-oxopyridin-1(2*H*)-yl)-4-methylbenzoate (5-3)

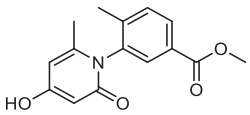

Methyl 3-amino-4-methylbenzoate (40.0 g, 242 mmol) 4-hydroxy-6-methyl-2H-pyran-2-one (45.8 g, 363 mmol) and catalytic potassium carbonate (4.0 g, 29 mmol) were mixed in trifluoroethanol (80 mL) and heated to 85 °C for 22 h. The mixture was removed from the oil bath and allowed to cool before addition of ethyl acetate. The precipitation of the product was observed and collected by filtration, washed with further ethyl acetate to afford **5-3** as a pale yellow/white solid (39.3 g, 144 mmol, **60%**). The NMR spectra were consistent with that reported in the literature.[2]

^{1}H NMR (400 MHz, DMSO-d_6) δ 10.71 (bs, 1H), 7.92 (dd, *J* = 8, 2 Hz, 1H), 7.63 (d, *J* = 2 Hz, 1H), 7.54 (dt, *J* = 8, 1 Hz, 1H), 5.94 (dd, *J* = 3, 1 Hz, 1H), 5.58 (dd, *J* = 3, 1 Hz, 1H), 3.85 (s, 3H), 2.03 (s, 3H), 1.77 (t, *J* = 2 Hz, 3H) ppm.

Methyl 3-(5-bromo-4-hydroxy-6-methyl-2-oxopyridin-1(2*H*)-yl)-4-methylbenzoate (5-4)

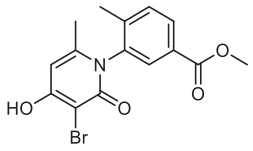

To a suspension of **5-3** (39.3 g, 144 mmol) in AcOH (160 mL) H_2O (41 mL) at 0 °C, in minimal exposure to light, was added a solution of Br_2 (7.7 mL, 150 mmol) in AcOH (40 mL) dropwise over 45 min then left another 10 minutes until no more starting material could be observed by TLC. The mixture was then diluted with water (400 mL), precipitation was observed. The product was obtained by filtration, washed with water (100 mL) and then cold acetonitrile (75 mL), and then dried in the desiccator over 48 h to afford **2** as a faint beige solid (45.7 g, 130 mmol, **90%**). The NMR spectra were consistent with that reported in the literature.[2]

^{1}H NMR (400 MHz, DMSO-d_6) δ 11.54 (s, 1H), 7.93 (dd, J = 8, 2 Hz, 1H), 7.69 (d, J = 2 Hz, 1H), 7.54 (d, J = 8 Hz, 1H), 6.11 (d, J = 1 Hz, 1H), 3.82 (s, 3H), 2.01 (s, 3H), 1.76 (d, J = 1 Hz, 3H) ppm.

Methyl 3-(5-bromo-4-((2,4-difluorobenzyl)oxy)-6-methyl-2-oxopyridin-1(2*H*)-yl)-4-methylbenzoate (5-6)

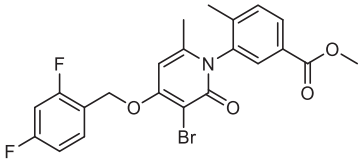

5-4 (45.7 g, 130 mmol) and K_2CO_3 (26.9 g, 195 mmol) were dissolved in DMF (116 mL) and heated to 65 °C. 2,4-Diflouorobenzyl chloride (**5-5,** 17.6 mL, 143 mmol) was then added dropwise and heating was maintained for 3.5 h. The reaction mixture was then removed from the oil bath and allowed to cool for 30 min before decanting it into stirring water (300 mL) at 0 °C causing precipitation. The precipitate was collected by filtration and washed with more water (300 mL) to afford a light orange solid. The crude solid was then triturated using methanol to afford **3** as a white solid (56.1 g, 117 mmol, **90%**). The NMR spectra were consistent with that reported in the literature.[2]

^{1}H NMR (400 MHz, $CDCl_3$) δ 8.03 (dd, J = 8, 2 Hz, 1H), 7.76 (d, J = 2 Hz, 1H), 7.62 (td, J = 8, 6 Hz, 1H), 7.44 (dt, J = 8, 1 Hz, 1H), 7.02 – 6.95 (m, 1H), 6.89 (ddd, J = 10, 9, 3 Hz, 1H), 6.13 (d, J = 1 Hz, 1H), 5.27 (q, J = 1 Hz, 2H), 3.89 (s, 3H), 2.14 (s, 3H), 1.93 (d, J = 1 Hz, 3H) ppm.

3-(5-Bromo-4-((2,4-difluorobenzyl)oxy)-6-methyl-2-oxopyridin-1(2*H*)-yl)-4-methylbenzoic acid (5-7)

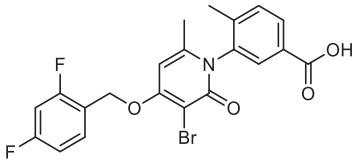

To a flask charged with **5-6** (20.0 g, 42 mmol), suspended in MeCN (70 mL) and water (50 mL), was added 2.5 M NaOH (18.4 mL, 46 mmol) and the reaction mixture was heated to 65 °C for 1 h, at which point the mixture became homogenous. After a second hour at this temperature the reaction mixture was removed from the oil bath and allowed to cool, then acidified to pH 5 using concentrated HCl under a stream of N_2 and stirred for a further hour. The yellow precipitate was then collected by filtration and washed with H_2O (100 mL) then cold MeCN (100 mL) to afford **4** as a white solid (15.9 g, 34 mmol, **82%**). The NMR spectra were consistent with that reported in the literature.[2]

^{1}H NMR (400 MHz, DMSO-d_6) δ 13.08 (s, 1H), 7.93 (dd, *J* = 8, 2 Hz, 1H), 7.73 – 7.65 (m, 2H), 7.54 (d, *J* = 8 Hz, 1H), 7.34 (ddd, *J* = 10, 9, 3 Hz, 1H), 7.18 (td, *J* = 9, 3 Hz, 1H), 6.71 (s, 1H), 5.33 (s, 2H), 2.01 (s, 3H), 1.89 (s, 3H) ppm.

3-(3-bromo-4-((2,4-difluorobenzyl)oxy)-6-methyl-2-oxopyridin-1(2H)-yl)-4-methyl-N-(pent-4-yn-1-yl)benzamide (5-17)

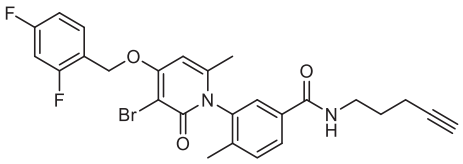

Prepared following general method for amide formation 3, using **5-7** and pent-4-yn-1-aminium chloride. The crude was purified by flash column chromatography, the product was eluted at 70% ethyl acetate in hexanes, yielding **5-17** as a white solid (**73%**).

The NMR spectra were consistent with that reported in the literature.[3]

^{1}H NMR (400 MHz, $CDCl_3$) δ 7.82 (dd, *J* = 8, 2 Hz, 1H), 7.61 (td, *J* = 9, 6 Hz, 1H), 7.54 (d, *J* = 2 Hz, 1H), 7.37 (dd, *J* = 8, 1 Hz, 1H), 7.00 – 6.93 (m, 1H), 6.91 (NH, t, *J* = 6 Hz, 1H), 6.83 (ddd, *J* = 10, 9, 3 Hz, 1H), 6.14 (d, *J* = 1 Hz, 1H), 5.20 (s, 2H), 3.45 – 3.25 (m, 2H), 2.22 (td, *J* = 7, 3 Hz, 2H), 2.08 (s, 3H), 1.96 (t, *J* = 3 Hz, 1H), 1.92 (d, *J* = 1 Hz, 3H), 1.71 (p, *J* = 7 Hz, 2H) ppm.

3-(3-bromo-4-((2,4-difluorobenzyl)oxy)-6-methyl-2-oxopyridin-1(2H)-yl)-N-(but-3-yn-1-yl)-4-methylbenzamide (5-9a)

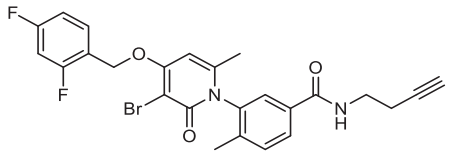

Prepared following general method for amide formation 3, using **5-7** and but-3-yn-1-aminium chloride. The product was purified by silica flash column chromatography, eluting at 70% ethyl acetate/hexanes, as a white solid (**50 %**).

H1 NMR was consistent with that reported in the literature.[3]

^{1}H NMR (400 MHz, $CDCl_3$) δ 7.73 (dd, *J* = 8, 2 Hz, 1H), 7.54 (td, *J* = 8, 6 Hz, 1H), 7.45 (d, *J* = 2 Hz, 1H), 7.31 (dd, *J* = 8, 1 Hz, 1H), 6.90 (tdd, *J* = 9, 3, 1 Hz, 1H), 6.85 (NH, t, *J* = 6 Hz, 1H), 6.78 (ddd, *J* = 10, 9, 3 Hz, 1H), 6.08 (d, *J* = 1 Hz, 1H), 5.16 (s, 2H), 3.38 (dtd, *J* = 43, 13, 7 Hz, 2H), 2.34 (td, *J* = 7, 3 Hz, 2H), 2.03 (s, 3H), 1.92 (t, *J* = 3 Hz, 1H), 1.85 (s, 3H) ppm.

3-(3-bromo-4-((2,4-difluorobenzyl)oxy)-6-methyl-2-oxopyridin-1(2H)-yl)-4-methyl-N-(2-(prop-2-yn-1-yloxy)ethyl)benzamide (5-9b)

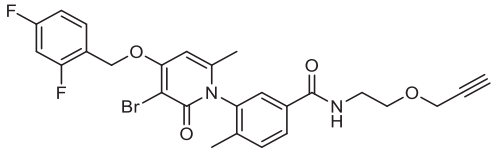

The product was prepared following general method for amide formation 1, using **5-7** (50 mg, 0.11 mmol) and 2-(prop-2-yn-1-yloxy)ethan-1-amine (12 mg, 0.12 mmol).The product was purified by silica flash column cromatography, eluted at 75% AcOEt/hexanes. Reported as an incolor oil (40 mg, **67**%).

^{1}H NMR (400 MHz, $CDCl_3$) δ 7.8 (dd, *J* = 7.9, 1.9 Hz, 1H), 7.6 (td, *J* = 8.5, 6.3 Hz, 1H), 7.5 (d, *J* = 1.9 Hz, 1H), 7.3 (d, *J* = 8.0 Hz, 1H), 7.0 – 6.8 (m, 3H), 6.1 (d, *J* = 0.9 Hz, 1H), 5.2 (s, 2H), 4.1 (d, *J* = 2.4 Hz, 2H), 3.7 – 3.4 (m, 2H), 2.4 (t, *J* = 2.4 Hz, 1H), 2.1 (s, 3H), 1.9 (d, *J* = 0.8 Hz, 3H). **^{13}C NMR** (101 MHz, $CDCl_3$) δ 166.2, 163.3, 163.1 (dd, *J* = 250.1, 11.9 Hz), 160.6, 160.1 (dd, *J* = 249.6, 12.0 Hz), 146.4, 138.8, 137.6, 134.2, 131.5, 130.3 (dd, *J* = 9.9, 5.2 Hz), 128.4, 126.8, 118.7 (dd, *J* = 14.1, 3.7 Hz), 112.0 (dd, *J* = 21.4, 3.6 Hz), 104.0 (t, *J* = 25.2 Hz), 96.9, 96.4, 79.7, 74.9, 68.6, 64.5 (d, *J* = 4.1 Hz), 58.4, 39.8, 21.7, 17.4.

N-(2-(2-(2-azidoethoxy)ethoxy)ethyl)-3-(3-bromo-4-((2,4-difluorobenzyl)oxy)-6-methyl-2-oxopyridin-1(2H)-yl)-4-methylbenzamide (5-9c)

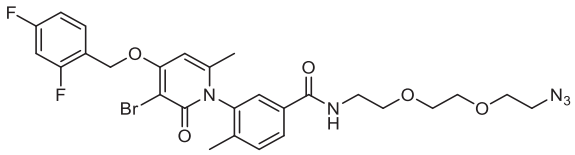

The product was prepared following general method for amide formation 1, using **5-7** (50 mg, 0.11 mmol) and 2-(2-(2-azidoethoxy)ethoxy)ethan-1-amine (19 mg, 0.12 mmol). The product was purified by silica flash column cromatography, eluted at 5% MeOH/DCM. Reported as an incolor oil (33 mg, **48%**).

^{1}H NMR (400 MHz, $CDCl_3$) δ 7.8 (dd, *J* = 8.1, 1.9 Hz, 1H), 7.6 (td, *J* = 8.7, 6.7 Hz, 1H), 7.5 (d, *J* = 1.8 Hz, 1H), 7.4 (d, *J* = 8.1 Hz, 1H), 7.0 – 6.8 (m, 3H), 6.1 (d, *J* = 1.0 Hz, 1H), 5.2 (s, 2H), 3.7 – 3.5 (m, 10H), 3.4 – 3.3 (m, 2H), 2.1 (s, 3H), 1.9 (d, *J* = 0.8 Hz, 3H). **^{13}C NMR** (101 MHz, $CDCl_3$) δ 166.4, 163.3, 163.1 (dd, *J* = 250.2, 12.0 Hz), 160.5, 161.6 – 158.3 (m), 146.3, 139.0, 137.7, 134.4, 131.6, 130.5 (dd, *J* = 9.9, 5.1 Hz), 128.3, 126.8, 118.8 (d, *J* = 14.1 Hz), 112.1 (dd, *J* = 21.3, 3.6 Hz), 104.1 (t, *J* = 25.3 Hz), 97.0, 96.2, 70.6, 70.3, 70.2, 69.8, 64.5 (d, *J* = 4.1 Hz), 50.7, 39.9, 21.6, 17.5.

N-(2-(2-(2-(2-azidoethoxy)ethoxy)ethoxy)ethyl)-3-(3-bromo-4-((2,4-difluorobenzyl)oxy)-6-methyl-2-oxopyridin-1(2H)-yl)-4-methylbenzamide(5-9d)

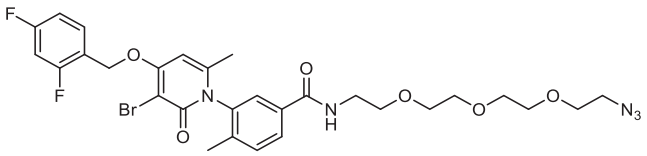

The product was prepared following method for amide formation 1, using **5-7** (50 mg, 0.11 mmol) and 2-(2-(2-(2-azidoethoxy)ethoxy)ethoxy)ethan-1-amine (26 mg, 0.12 mmol). The product was purified by silica flash column cromatography, eluted at 8% MeOH/DCM. Reported as an incolor oil (47 mg, **65%**).

^{1}H NMR (400 MHz, $CDCl_3$) δ 7.8 (dd, *J* = 7.9, 1.9 Hz, 1H), 7.6 (td, *J* = 8.5, 6.3 Hz, 1H), 7.5 (d, *J* = 1.9 Hz, 1H), 7.4 (dd, *J* = 7.9, 0.8 Hz, 1H), 7.2 – 7.1 (m, 1H), 7.0 – 6.9 (m, 1H), 6.8 (ddd, *J* = 10.2, 8.7, 2.5 Hz, 1H), 6.1 (d, *J* = 0.9 Hz, 1H), 5.2 (s, 3H), 3.7 – 3.5 (m, 14H), 3.3 (dd, *J* = 5.6, 4.5 Hz, 2H), 2.1 (s, 3H), 1.9 (d, *J* = 0.8 Hz, 3H). **^{13}C NMR** (101 MHz, $CDCl_3$) δ 166.4, 164.8 – 161.7 (m), 163.2, 160.5, 160.2 (dd, *J* = 249.7, 12.2 Hz), 146.4, 138.8, 137.6, 134.4, 131.5, 130.4 (dd, *J* = 9.9, 5.3 Hz), 128.3, 126.8, 121.1 – 117.2 (m), 112.0 (dd, *J* = 21.4, 3.7 Hz), 104.0 (t, *J* = 25.3 Hz), 96.9, 96.2, 70.7, 70.6, 70.3, 70.1, 69.7, 64.5 (d, *J* = 4.2 Hz), 50.7, 39.9, 21.6, 17.4.

1-(3-(3-bromo-4-((2,4-difluorobenzyl)oxy)-6-methyl-2-oxopyridin-1(2H)-yl)-4-methylphenyl)-1,5-dioxo-9,12-dioxa-2,6-diazatetradecan-14-oic acid (5-14)

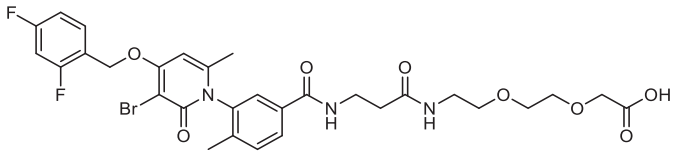

2-chlorotrytil resin (200 mg, 1.5 mmol/g) was suspended in 2 mL of dry DCM during 30 minutes. 1-(9H-fluoren-9-yl)-3-oxo-2,7,10-trioxa-4-azadodecan-12-oic acid (116 mg, 0.3 mmol, 1 eq.) and DIPEA (0.5 mL, 10 eq.) were dissolved in 1 mL of DCM and the minimum amount of DMF to solubilize the mixture, then added to th eresine and shaked for 1 hour. The resin was filtered and washed with DMF (x3) and DCM (x3). The Fmoc group was deprotected upon treatment with 40% piperidine in DCM/DMF 1:1 (10 min) and 20% piperidine in DMF (15 min), DMF washes were performed after Fmoc deprotection (x5).

HOBt (55 mg, 1.5 eq.) and Fmoc-β-Ala (140 mg, 1.5 eq.) were dissolved in a minimum amount of DMF and DIC (69 μL, 1.5 eq.) was added. The pre-activated aminoacid was added in the reaction vessel with the resin and stirred at room temperature during 1.5 hours. The ninhydrin test was performed to monitor the amino acid coupling. After a negative ninhidrin test, DMF washes (3x1 min) were performed. The Fmoc group was deprotected upon treatment with 40% piperidine in DCM/DMF 1:1 (10 min) and 20% piperidine in DMF (15 min), DMF washes were performed after Fmoc deprotection (x5).

5-7 (209 mg, 1.5 eq.) and HOBt (55 mg, 1.5 eq.) were dissolved in a minimum amount of DMF and DIC (69 μL, 1.5 eq.) was added. The pre-activated aminoacid was added in the reaction vessel with the resin and stirred at room temperature during 1.5 hours. The ninhydrin test was performed to monitor the amino acid coupling. After a negative ninhidrin test, DMF washes (3x1 min) were performed. The Fmoc group was deprotected upon treatment with 40% piperidine in DCM/DMF 1:1 (10 min) and 20% piperidine in DMF (15 min), DMF washes were performed after Fmoc deprotection (x5).

Hydrolisis from the resin was performed by treating the resin with 2% TFA in DCM and stirring for 40 minutes. After 2 hours the filtrate was recovered in a round flask, the resin was washed with DCM (x3) and the combined filtrates were dried under reduced pressure (yellow oil, 229 mg). The product was dissolved in a minimum amount of DCM and precipitated in diethyl ether. The solid was recovered by filtration (45 mg, **22%**).

^{1}H NMR (400 MHz, $CDCl_3$) δ 7.8 (dd, *J* = 7.9, 1.8 Hz, 1H), 7.7 (t, *J* = 5.6 Hz, 1H), 7.7 – 7.5 (m, 2H), 7.4 (d, *J* = 8.1 Hz, 1H), 7.3 (s, 1H), 7.0 – 6.9 (m, 1H), 6.9 (ddd, *J* = 10.2, 8.7, 2.5 Hz, 1H), 6.2 (s, 1H), 5.3 (s, 2H), 4.1 (s, 2H), 3.7 – 3.3 (m, 10H), 2.5 (t, *J* = 7.0 Hz, 2H), 2.1 (s, 3H), 1.9 (s, 3H). **^{13}C NMR** (101 MHz, $CDCl_3$) δ 172.5, 171.9, 166.4, 163.6, 163.3 (d, *J* = 320.3 Hz), 160.8, 160.2 (d, *J* = 227.1 Hz), 146.6, 138.8, 137.4, 133.7, 131.5, 130.3, 128.6, 126.9, 118.4, 111.9 (d, *J* = 24.6 Hz), 104.0 (t, *J* = 25.3 Hz), 96.8, 96.6, 71.1, 69.9, 69.6, 68.4, 64.5,

39.2, 37.0, 35.8, 21.5, 17.3. **IR (ATR):** 3015.09, 1697.4, 745.1 cm^{-1}. **HRMS (ESI):** calculated for $[C_{30}H_{33}N_3O_8BrF_2]^+$: 680.14136, found: 680.14106. **M_p:** 112°C.

3-(3-(3-(3-(3-bromo-4-((2,4-difluorobenzyl)oxy)-6-methyl-2-oxopyridin-1(2H)-yl)-4-methylbenzamido)propanamido)propanamido)propanoic acid (5-14)

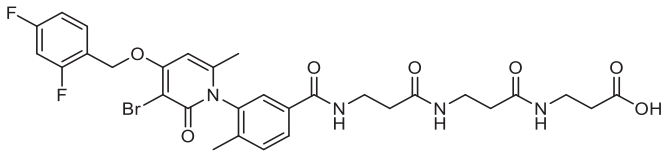

The product was prepared as **5-14**, using 2-chlorotrytil resin to obtain peptides with carboxylic acid as its C-terminal. After inmobilization of the first Fmoc-β-Ala and Fmoc deprotection, 2 more units of Fmoc-β-Ala were coupled following the procedure described **for 5-14**. After Fmoc deprotection **5-7** was incorporated and the peptide was cleaved from the resin and obtained as an incolor film. The product was used without further purification (80 mg, **40%**).

tert-butyl 4-(3-(3-bromo-4-((2,4-difluorobenzyl)oxy)-6-methyl-2-oxopyridin-1(2H)-yl)-4-methylbenzoyl)piperazine-1-carboxylate (5-18)

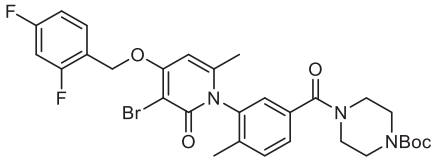

The product was prepared following general method for amide formation 2, using **5-7** (1 g, 2 mmol) 1 Boc-piperazine (0.4 g, 2 mmol). The product was purified by silica flash column chromatography, eluted at 75% AcOEt in hexanes. Reported as an off-white solid (1.2 g, **90%**).

^{1}H NMR (400 MHz, $CDCl_3$) δ 7.54 (td, *J* = 8.5, 6.3 Hz, 1H), 7.40 – 7.31 (m, 2H), 7.06 (d, *J* = 1.4 Hz, 1H), 6.95 – 6.86 (m, 1H), 6.81 (ddd, *J* = 10.2, 8.7, 2.5 Hz, 1H), 6.08 (s, 1H), 5.19 (s, 2H), 3.92 – 3.07 (m, 8H), 2.02 (s, 3H), 1.86 (s, 3H), 1.39 (s, 9H). **^{13}C NMR** (101 MHz, $CDCl_3$) δ 169.2, 164.2 (d, *J* = 324.4 Hz), 163.1, 163.1 (dd, *J* = 250.0, 12.0 Hz), 160.4, 160.2 (dd, *J* = 249.6, 12.0 Hz), 154.5, 146.0, 137.7 (d, *J* = 8.0 Hz), 134.7, 131.8, 130.6 (dd, *J* = 9.8, 5.1 Hz), 128.2, 126.9, 118.7 (dd, *J* = 14.2, 3.7 Hz), 112.0 (dd, *J* = 21.3, 3.7 Hz), 104.0 (t, *J* = 25.3 Hz), 96.9, 96.1, 80.4, 64.4 (d, *J* = 4.0 Hz), 47.7, 44.9 – 41.9 (m), 28.4, 21.6, 17.4.

3-bromo-4-((2,4-difluorobenzyl)oxy)-6-methyl-1-(2-methyl-5-(piperazine-1-carbonyl)phenyl)pyridin-2(1H)-one (5-19)

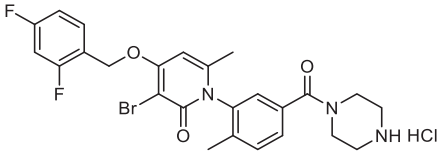

5-18 (1 g, 1.58 mmol) was stirred in 10 mL HCl/dioxane 4N for 2 h. The solvent was then evaporated affording the hydrochloride salt as a white solid (885 mg, **quant.**). The product was used without further purification.

4-hydroxybut-2-yn-1-yl 4-methylbenzenesulfonate

A round flask was charged with but-2-yne-1,4-diol (1 g, 14.7 mmol, 1 eq.), , pyridine (1.86 mL, 23.1 mmol, 1.5 eq.) and DCM (10 mL, 1.5 M), cooled down at 0 °C and tosyl chloride (2.86 g, 14.7, 1eq.) was added portionwise. The reaction mixture was let warming up to room temperature overnight. Water and ethyl acetate were added and the aqueous layer was extracted with ethyl acetate (x3). The organic fractions were combined, washed with brine, dried over $MgSO_4$ and dried under reduced pressure. The crude was purified by silica flash column chromatography, eluting at 30% ethyl acetate in hexanes. Reported as a colourless oil (706 mg, **20%**).

^{1}H NMR (400 MHz, cdcl$_3$) δ 7.8 (d, *J* = 8.3 Hz, 2H), 7.4 – 7.3 (m, 2H), 4.7 (t, *J* = 1.8 Hz, 2H), 4.2 (t, *J* = 1.8 Hz, 2H), 2.5 (s, 3H).

4-(benzyloxy)-3-bromo-1-(5-(4-(4-hydroxybut-2-yn-1-yl)piperazine-1-carbonyl)-2-methylphenyl)-6-methylpyridin-2(1H)-one (5-27)

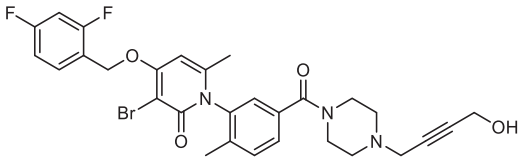

A flask was loaded with **5-19** (500 mg, 0.88 mmol, 1 eq.), 4-hydroxybut-2-yn-1-yl 4-methylbenzenesulfonate (211 mg, 0.88 mmol, 1 eq.), potassium carbonate (297 mg, 2.2 mmol, 2.5 eq.) and DMF (1.35 mL, 0.65 M) and stirred at room temperature over two days. Water and ethyl acetate were added, the aqueous phase was extracted with ethyl acetate, the organic phases combined, washed with brine (x4), dried over magnesium sulphate and dried under reduced pressure. The crude was purified by silica flash column chromatography, eluting at 8% methanol in DCM. Reported as a white solid (241mg, **45%**).

^{1}H NMR (400 MHz, $CDCl_3$) δ 7.6 (td, *J* = 8.5, 6.3 Hz, 1H), 7.5 – 7.4 (m, 2H), 7.1 (d, *J* = 1.6 Hz, 1H), 7.0 – 6.9 (m, 1H), 6.9 (ddd, *J* = 10.2, 8.7, 2.5 Hz, 1H), 6.1 (s, 0H), 5.3 (s, 1H), 4.3 (t, *J* = 1.9 Hz, 2H), 4.0 – 3.4 (m, 4H), 3.3 (t, *J* = 2.0 Hz, 2H), 2.5 (d, *J* = 37.2 Hz, 4H), 2.1 (s, 3H), 1.9 (s, 2H). **^{13}C NMR** (101 MHz, $CDCl_3$) δ 169.1, 163.2, 163.2 (dd, *J* = 250.2, 12.0 Hz), 160.6, 160.3 (dd, *J* = 249.6, 12.0 Hz), 146.2, 137.7, 137.5, 135.0, 131.7, 130.6 (dd, *J* = 9.9, 5.2 Hz), 128.4, 127.0, 118.7 (dd, *J* = 14.1, 3.9 Hz), 112.1 (dd, *J* = 21.4, 3.7 Hz), 104.1 (t, *J* = 25.3 Hz), 97.1, 96.2, 84.3, 80.0, 64.5 (d, *J* = 4.2 Hz), 52.3, 51.8, 51.1, 47.8, 47.2, 42.2, 21.7, 17.4. **HRMS (ESI):** calc. for $[C_{29}H_{29}O_4N_3BrF_2]^+$: 600.13040, found 600.13050. **IR (ATR):** 3323, 1654, 1505, 1342, 450 cm^{-1}.

4-(4-(3-(4-(benzyloxy)-3-bromo-6-methyl-2-oxopyridin-1(2H)-yl)-4-methylbenzoyl)piperazin-1-yl)but-2-yn-1-yl 4-methylbenzenesulfonate (5-27 Ts)

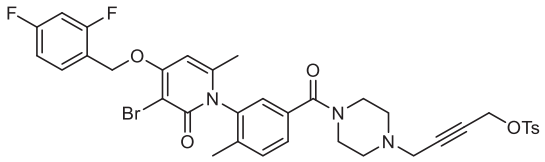

A round flask was charged with **5-27** (150 mg, 0.25 mmol, 1 eq.), , sodium hydroxide (15 mg, 0.38 mmol, 1.5 eq.) in water (0.45 mL) and THF (0.45 mL), cooled down at 0 °C and tosyl chloride (52 mg, 0.28 mmol, 1.1 eq.) in THF (0.45 mL) was added. The reaction mixture was let warming up to room temperature overnight. Water and ethyl acetate were added and the aqueous layer was extracted with ethyl acetate (x3). The organic fractions were combined, washed with brine, dried over $MgSO_4$ and dried under reduced pressure. The crude was filtered through a silica pad, rinsed with 5% methanol and used without further purification (yellowish wax, 38 mg).

4-(benzyloxy)-3-bromo-6-methyl-1-(2-methyl-5-(4-(4-(4-(pent-4-ynoyl)piperazin-1-yl)but-2-yn-1-yl)piperazine-1-carbonyl)phenyl)pyridin-2(1H)-one (5-28)

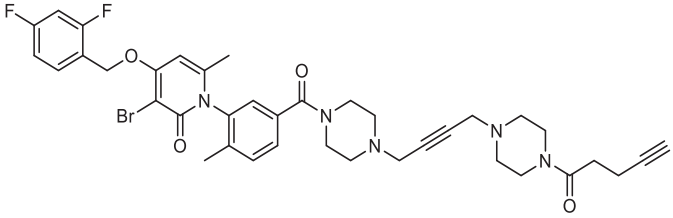

A flask was loaded with **5-27 Ts** (38 mg, 0.053 mmol, 1 eq.), 1-(piperazin-1-yl)pent-4-yn-1-one (num, 834 mg, 0.053 mmol, 1 eq.), potassium carbonate (17 mg, 0.13 mmol, 2.5 eq.) and DMF (0.1 mL, 0.5M) and stirred at 50 °C for 72 h. Water and ethyl acetate were added and the aqueous layer was extracted with ethyl acetate (x3). The organic fractions were combined, washed with brine, dried over $MgSO_4$ and dried under reduced pressure. The crude was purified by silica flash column chromatography, eluting at 8% methanol in DCM. Reported as an off-white oil (11 mg, **29%**).

^{1}H NMR (400 MHz, $CDCl_3$) δ 7.54 (q, *J* = 7.9 Hz, 1H), 7.46 – 7.28 (m, 2H), 7.07 (s, 1H), 6.91 (t, *J* = 8.1 Hz, 1H), 6.81 (t, *J* = 9.6 Hz, 1H), 6.06 (s, 1H), 5.20 (s, 2H), 3.88 – 3.11 (m, 10H), 2.46 (d, *J* = 16.0 Hz, 10H), 2.02 (d, *J* = 2.1 Hz, 3H), 1.90 (dt, *J* = 2.6, 1.4 Hz, 1H), 1.86 (d, *J* = 2.5 Hz, 3H), 1.76 – 1.40 (m, 4H). **IR(ATR)**: 2918, 1651, 1433, 1342, 997 cm^{-1}.

tert-butyl 4-(prop-2-yn-1-yl)piperazine-1-carboxylate

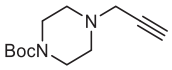

A flask was loaded with 1-boc-piperazine (500 mg, 2.68 mmol, 1eq.), propargyl bromide (290 μL of a solution 80% in toluene, 2.68 mmol, 1 eq.), Cs_2CO_3 (2.6 g, 8 mmol, 3 eq.) and acetone (10.7 mL, 0.25 M). The reaction mixture was stirred overnight at room temperature, then water and ethyl acetate were added. The aqueous phase was extracted with ethyl acetate (x3), organic fractions were combined, washed with brine, dried over $MgSO_4$ and dried under reduced pressure. The crude was purified by silica flash column chromatography, eluting at 75% AcOEt in hexanes. The product was then stirred with HCl in dioxane 4N for 3 h at room temperature and dried under reduced pressure. The reaction crude was dissolved in water and ethyl acetate, the aqueous phase was basified to pH 9 and extracted with ethyl acetate (x3). The organic phases were combined, washed with brine, dried over $MgSO_4$ and dried under reduced pressure. The product was obtained as a brown oil and used without further purification (600 mg; **40%**).

^{1}H NMR (400 MHz, $CDCl_3$) δ 3.27 (d, *J* = 2.4 Hz, 2H), 2.92 (t, *J* = 4.9 Hz, 4H), 2.53 (s, 4H), 2.24 (t, *J* = 2.4 Hz, 1H).

1-(prop-2-yn-1-yl)piperazine hydrochloride (5-21)

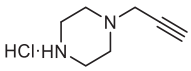

***tert*-butyl 4-(prop-2-yn-1-yl)piperazine-1-carboxylate** (600 g, 2.7 mmol) was stirred in 10 mL HCl/dioxane 4N for 2 h. The solvent was then evaporated affording the hydrochloride salt as an off-white solid (433 mg, **quant.**). The product was used without further purification.

tert-butyl 4-(3-bromopropyl)piperazine-1-carboxylate (5-23)

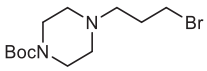

A pressure flask was loaded with 1-boc-piperazine (1 g, 5 mmol, 1 eq.), 1,3-dibromopropane (0.6 mL, 5 mmol, 1 eq.), trimthylamine (0.8 mL, 5.5 mmol, 1.1 eq.) and DCM (15 mL, 0.35 M) was stirred at room temperature for overnight. Water was added to the reaction mixture, and the aqueous phase was extracted with DCM (x3). The organic layers were combined, washed with brine, dried over dried over $MgSO_4$ and dried under reduced pressure. The crude was purified by silica flash column chromatography (equilibrated with 2% $E_{t3}N$ in hexane), eluting at 40% AcOEt/hexanes. Reported as a yellow wax (383 mg, **25%**).

^{1}H NMR (400 MHz, $CDCl_3$) δ 3.46 (t, *J* = 6.6 Hz, 2H), 3.41 (t, *J* = 5.1 Hz, 4H), 2.47 (t, *J* = 7.0 Hz, 2H), 2.37 (t, *J* = 5.1 Hz, 4H), 2.07 – 1.97 (m, 2H), 1.45 (s, 9H).

tert-butyl 4-(3-azidopropyl)piperazine-1-carboxylate (5-24)

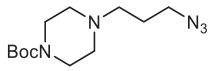

A flask loaded with **5-23** (380 mg, 1.24 mmol, 1 eq.), sodium azide (161 mg, 2.48 mmol, 2 eq.) and DMF (4.4 mL, 0.28 M) was stirred at 80 °C overnight. The mixture was diluted in ethyl acetate and water, the aqueous layer was extracted with ethyl acetate (x2), the organic phases were combined, washed with brine (x5), dried over dried over $MgSO_4$ and dried under reduced pressure. The product was obtained as a colorless oil and used without further purification (327 mg, **70%**).

^{1}H NMR (400 MHz, $CDCl_3$) δ 3.42 (t, *J* = 5.1 Hz, 4H), 3.35 (t, *J* = 6.7 Hz, 2H), 2.42 (t, *J* = 7.0 Hz, 2H), 2.37 (t, *J* = 5.1 Hz, 4H), 1.76 (p, *J* = 6.9 Hz, 2H), 1.46 (s, 9H). **^{13}C NMR** (101 MHz, $CDCl_3$) δ 154.6, 79.5, 55.1, 52.9, 49.4, 43.3, 28.3, 26.1.

1-(3-azidopropyl)piperazine hydrochloride (5-24 HCl)

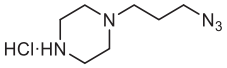

5-24 (320 mg, 1.18 mmol) was stirred in 5 mL HCl/dioxane 4N for 2 h. The solvent was then evaporated affording the hydrochloride salt as an off-white solid (242 mg, **quant.**). The product was used without further purification.

3-bromo-4-((2,4-difluorobenzyl)oxy)-6-methyl-1-(2-methyl-5-(4-(prop-2-yn-1-yl)piperazine-1-carbonyl)phenyl)pyridin-2(1H)-one (5-22)

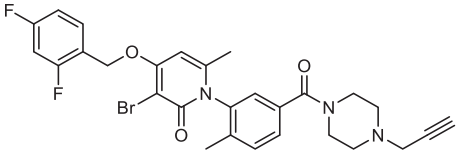

The product was prepared following general method for amide formation 2, using **5-7** (1.3 g, 2.8 mmol) and 1-(prop-2-yn-1-yl)piperazine hydrochloride (450 mg, 2.8 mmol). The crude was purified by silica flash column chromatography, eluting at 4% methanol in DCM. Reported as an off-white oil (1.6 g, **64%**).

^{1}H NMR (400 MHz, $CDCl_3$) δ 7.59 (td, *J* = 8.5, 6.3 Hz, 1H), 7.46 – 7.36 (m, 2H), 7.12 (d, *J* = 1.6 Hz, 1H), 6.96 (dddd, *J* = 8.5, 8.0, 2.5, 1.1 Hz, 1H), 6.87 (ddd, *J* = 10.2, 8.7, 2.5 Hz, 1H), 6.12 (d, *J* = 0.9 Hz, 1H), 5.25 (d, *J* = 1.2 Hz, 2H), 3.93 – 3.38 (m, 3H), 3.32 (d, *J* = 2.4 Hz, 2H), 2.73 – 2.42 (m, 0H), 2.26 (t, *J* = 2.4 Hz, 1H), 2.08

(s, 3H), 1.92 (d, *J* = 0.8 Hz, 3H). **^{13}C NMR** (101 MHz, $CDCl_3$) δ 169.0, 163.2, 163.2 (dd, *J* = 250.3, 12.0 Hz), 160.5, 160.3 (dd, *J* = 249.6, 12.0 Hz), 146.1, 137.7, 137.5, 135.1, 131.7, 130.7 – 130.6 (m), 128.3, 126.9, 118.7 (dd, *J* = 14.2, 3.9 Hz), 112.1 (dd, *J* = 21.4, 3.6 Hz), 104.1 (t, *J* = 25.3 Hz), 97.0, 96.1, 78.2, 73.9, 64.4 (d, *J* = 4.2 Hz), 52.1, 51.6, 47.8, 46.9, 42.2, 21.7, 17.4. **HRMS (ESI):** calc. for $[C_{28}H_{27}O_2N_3BrF_2]^+$: 270.11984, found 570.12190. **IR (ATR):** 2920, 2851, 1619, 1342 cm^{-1} **M_p:** 88 °C.

1-(5-(4-(3-azidopropyl)piperazine-1-carbonyl)-2-methylphenyl)-3-bromo-4-((2,4-difluorobenzyl)oxy)-6-methylpyridin-2(1H)-one (5-34)

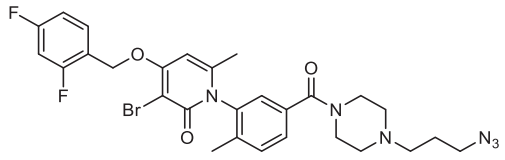

The product was prepared following general method for amide formation 1, using **7-5** (230 mg, 0.50 mmol) and 1-(3-azidopropyl)piperazine hydrochloride (100 mg, 0.5 mmol). The crude was purified by silica flash column chromatography, eluting at 5% methanol in DCM. The product was obtained as an off-white solid (194 mg, **64%**).

^{1}H NMR (400 MHz, $CDCl_3$) δ 7.53 (q, *J* = 8.1 Hz, 1H), 7.34 (t, *J* = 6.3 Hz, 2H), 7.07 (s, 1H), 6.89 (td, *J* = 8.4, 2.4 Hz, 1H), 6.86 – 6.73 (m, 1H), 6.12 (s, 1H), 5.19 (s, 2H), 3.86 – 3.33 (m, 4H), 3.28 (t, *J* = 6.6 Hz, 2H), 2.57 – 2.22 (m, 6H), 2.01 (s, 3H), 1.86 (s, 3H), 1.70 (h, *J* = 7.2 Hz, 2H). **^{13}C NMR** (101 MHz, $CDCl_3$) δ 168.7, 163.0, 162.9 (dd, *J* = 250.2, 11.9 Hz), 160.2, 160.1 (dd, *J* = 249.8, 12.0 Hz), 146.0, 137.5, 137.2, 134.8, 131.5, 130.5 (dd, *J* = 9.9, 5.2 Hz), 128.1, 126.7, 118.6 (dd, *J* = 14.4, 3.8 Hz), 111.8 (dd, *J* = 21.3, 3.7 Hz), 103.8 (t, *J* = 25.3 Hz), 96.7, 96.0, 64.3 (d, *J* = 4.1 Hz), 54.8, 53.0, 52.6, 49.2, 47.6, 42.0, 25.8, 21.4, 17.2. **HRMS (ESI):** calc. for $[C_{28}H_{30}O_3N_6BrF_2]^+$: 615.15253, found 615.15276 **IR(ATR):** 2920, 2093, 1506, 1341 cm^{-1}. **M_p:** 65 °C.

piperidin-4-ylmethanol hydrochloride

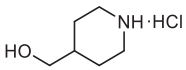

***tert*-butyl 4-(hydroxymethyl)piperidine-1-carboxylate** (1.12 g, 5.23 mmol) was stirred in 15 mL HCl/dioxane 4N for 4 h. The solvent was then evaporated affording the hydrochloride salt as an off-white solid (790 mg, **quant.**). The product was used without further purification.

^{1}H NMR (400 MHz, DMSO-*d6*) δ 9.08 (s, 1H), 8.74 (s, 1H), 3.23 (dd, *J* = 13.4, 9.1 Hz, 4H), 2.95 – 2.63 (m, 2H), 1.88 – 1.68 (m, 2H), 1.61 (ddd, *J* = 8.2, 5.8, 3.0 Hz, 1H), 1.40 – 1.27 (m, 2H).

3-(1-(prop-2-yn-1-yl)piperidin-4-yl)propan-1-ol (5-30a)

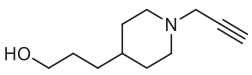

A round flask was loaded with 3-(piperidin-4-yl)propan-1-ol (1.0 g, 7.1 mmol, 1 eq.), caesium carbonate (6.9 g, 21.3 mmol, 3 eq.), acetone (31 mL, 0.23 M) and purged under nitrogen atmosphere.

Propargyl bromide was added (80% in toluene, 0.75 mL, 6.8 mmol, 0.95 eq.) and the reaction mixture was stirred at room temperature overnight. The reaction mixture was filtrated, evaporated under reduced pressure, dissolved in ethyl acetate and washed with water and brine. The organic layer was dried over magnesium sulphate and dried under reduced pressure. The crude was purified by silica flash column chromatography, eluting at 5% methanol/ethyl acetate. Reported as an ochre oil (646 mg, 3.56 mmol, **50%**).

^{1}H NMR (400 MHz, $CDCl_3$) δ 3.63 (t, *J* = 6.6 Hz, 2H), 3.28 (d, *J* = 2.4 Hz, 2H), 2.87 (ddd, *J* = 12.2, 3.6, 1.6 Hz, 2H), 2.25 – 2.11 (m, 3H), 1.75 – 1.65 (m, 2H), 1.64 – 1.51 (m, 2H), 1.38 – 1.18 (m, 5H). **^{13}C NMR** (101 MHz, $CDCl_3$) δ 79.1 (d, *J* = 5.9 Hz), 73.1 (d, *J* = 26.9 Hz), 63.8 – 61.8 (m), 52.6, 47.8 – 46.9 (m), 35.1, 32.6, 32.3, 30.1. **HRMS (ESI):** calc. for $[C_{11}H_{20}ON]^+$: 182.15394, found 182.15414.

3-(1-(prop-2-yn-1-yl)piperidin-4-yl)propanal (5-31a)

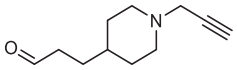

A flame-dried flask was loaded with oxalyl chloride (364 µL, 4.24 mmol, 1.2 eq.), DCM (8.8 mL) and cooled down to -78 °C. DMSO (550 µL, 7.77 mmol, 2.2 eq.) in DCM (1.7 mL) was added dropwise and the reaction mixture was stirred for 5 minutes. **5-30a (**640 mg, 3.53 mmol, 1 eq.) was added in DCM (1.7 mL) dropwise, and the reaction mixture was stirred at -78 °C for 15 minutes. Triethylamine (2.5 mL, 35 mmol, 10 eq.) was added dropwise, and the reaction mixture was let to warm up to room temperature overnight. The reaction mixture was diluted in DCM and washed with HCl 1M. The aqueous phase was basified (pH10-12), extracted with DCM (x5), washed with brine, dried over magnesium sulphate and dried under reduced pressure. The reaction crude was purified by silica flash column chromatography, eluting at 1% methanol/ethyl acetate. Reported as a yellowish oil (408 mg, 2.26 mmol, **64%**).

^{1}H NMR (400 MHz, $CDCl_3$) δ 9.76 (t, *J* = 1.8 Hz, 1H), 3.27 (d, *J* = 2.4 Hz, 2H), 2.93 – 2.79 (m, 2H), 2.44 (td, *J* = 7.6, 1.8 Hz, 2H), 2.22 (t, *J* = 2.4 Hz, 1H), 2.20 – 2.09 (m, 2H), 1.76 – 1.65 (m, 2H), 1.58 (td, *J* = 7.7, 5.9 Hz, 2H), 1.35 – 1.19 (m, 3H). **^{13}C NMR** (101 MHz, $CDCl_3$) δ 201.9, 78.7, 72.8, 52.1, 52.0, 51.9, 46.8, 40.9, 34.4, 31.6, 28.1. **HRMS (ESI):** calc. for $[C_{11}H_{18}ON]^+$: 180.13829, found 180.13829.

(1-(prop-2-yn-1-yl)piperidin-4-yl)methanol (5-30b)

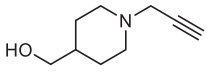

A round flask was loaded with piperidin-4-ylmethanol hydrochloride (790 mg, 5.2 mmol, 1 eq.), caesium carbonate (5 g, 15.6 mmol, 3 eq.), acetone (22 mL, 0.23 M) and purged under nitrogen atmosphere. Propargyl bromide was added (80% in toluene, 0.55 mL, 5.0 mmol, 0.95 eq.) and the reaction mixture was stirred at room temperature overnight. The reaction mixture was filtrated, evaporated under reduced pressure, dissolved in ethyl acetate and washed with water and brine. The organic layer was dried over magnesium sulphate and dried under reduced pressure. The crude

was purified by silica flash column chromatography, eluting at 5% methanol/ethyl acetate. Reported as an ochre oil (642 mg, **81%**).

^{1}H NMR (400 MHz, $CDCl_3$) δ 3.50 (d, *J* = 6.4 Hz, 2H), 3.35 – 3.27 (m, 2H), 2.91 (dt, *J* = 11.0, 3.1 Hz, 2H), 2.26 – 2.14 (m, 3H), 1.82 – 1.73 (m, 2H), 1.58 – 1.45 (m, 1H), 1.39 – 1.28 (m, 2H). **^{13}C NMR** (101 MHz, $CDCl_3$) δ 79.0 (d, *J* = 6.8 Hz), 73.2 (d, *J* = 29.8 Hz), 67.9 – 67.2 (m), 52.2 (t, *J* = 14.3 Hz), 48.0 – 46.8 (m), 38.1, 28.7. **HRMS (ESI):** calc. for $[C_9H_{16}ON]^+$: 154.12264, found 154.12315.

1-(prop-2-yn-1-yl)piperidine-4-carbaldehyde (5-31b)

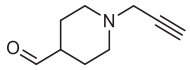

A flame-dried flask was loaded with oxalyl chloride (345 µL, 3.96 mmol, 1.2 eq.), DCM (8.2 mL) and cooled down to -78 °C. DMSO (515 µL, 7.26 mmol, 2.2 eq.) in DCM (1.6 mL) was added dropwise and the reaction mixture was stirred for 5 minutes. **5-30b** (505 mg, 3.3 mmol, 1 eq.) was added in DCM (1.6 mL) dropwise, and the reaction mixture was stirred at -78 °C for 15 minutes. Triethylamine (2.3 mL, 33 mmol, 10 eq.) was added dropwise, and the reaction mixture was let to warm up to room temperature overnight. The reaction mixture was diluted in DCM and washed with HCl 1M. The aqueous phase was basified (pH10-12), extracted with DCM (x5), washed with brine, dried over magnesium sulphate and dried under reduced pressure. The reaction The reaction ncrude was purified by silica flash column chromatography, eluting at 1% methanol/ethyl acetate. Reported as a yellowish oil (343 mg, 2.27 mmol, **69%**).

^{1}H NMR (400 MHz, $CDCl_3$) δ 9.41 (s, 1H), 3.07 (tt, *J* = 6.7, 2.7 Hz, 2H), 2.59 (qd, *J* = 7.2, 3.5 Hz, 2H), 2.18 – 1.95 (m, 4H), 1.78 – 1.60 (m, 2H), 1.59 – 1.38 (m, 2H). **^{13}C NMR** (101 MHz, $CDCl_3$) δ 203.3 (d, *J* = 14.3 Hz), 78.6 (d, *J* = 5.9 Hz), 73.2 (d, *J* = 26.2 Hz), 51.0 (dd, *J* = 19.8, 13.7 Hz), 47.1, 46.9, 25.2. **HRMS (ESI):** calc. for $[C_9H_{14}ON]^+$: 152.10699, found 152.10712.

1-(prop-2-yn-1-yl)piperidin-4-ol (5-30c)

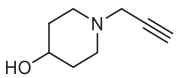

A round flask was loaded with piperidin-4-ol (1 g, 9.9 mmol, 1 eq.), caesium carbonate (9.7 g, 29.7 mmol, 3 eq.), acetone (43 mL, 0.23 M) and purged under nitrogen atmosphere. Propargyl bromide was added (80% in toluene, 1.04 mL, 9.4 mmol, 0.95 eq.) and the reaction mixture was stirred at room temperature overnight. The reaction mixture was filtrated, evaporated under reduced pressure, dissolved in ethyl acetate and washed with water and brine. The organic layer was dried over magnesium sulphate and dried under reduced pressure. The crude was purified by silica flash column chromatography, eluting at 4% methanol/ethyl acetate. Reported as a yellow oil (750 mg, **54%**).

^{1}H NMR (400 MHz, $CDCl_3$) δ 3.61 (tt, *J* = 8.6, 4.1 Hz, 1H), 3.23 (dd, *J* = 2.5, 0.5 Hz, 2H), 2.85 (s, 1H), 2.29 (ddd, *J* = 12.3, 10.1, 3.0 Hz, 2H), 2.22 – 2.18 (m, 1H), 1.91 – 1.79 (m, 2H), 1.55 (dtd, *J* = 13.1, 9.4, 3.8 Hz, 2H). **^{13}C NMR** (101 MHz, $cdcl_3$) δ 78.9 (d, *J* = 5.9 Hz), 73.3 (d, *J* = 26.3 Hz), 67.1 (d, *J* = 20.8 Hz), 49.9, 46.9 (d, *J* = 5.9 Hz), 34.3. **HRMS (ESI):** calc. for $[C_8H_{14}ON]^+$: 140.10699, found 104.10721.

1-(prop-2-yn-1-yl)piperidin-4-one (5-31c)

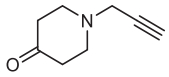

A flame-dried flask was loaded with oxalyl chloride (555 µL, 6.4 mmol, 1.2 eq.), DCM (13.5mL) and cooled down to -78 °C. DMSO (840 µL, 11.9 mmol, 2.2 eq.) in DCM (2.7 mL) was added dropwise and the reaction mixture was stirred for 5 minutes. **5-30c (**750 mg, 5.39 mmol, 1 eq.) was added in DCM (2.7 mL) dropwise, and the reaction mixture was stirred at -78 °C for 15 minutes. Triethylamine (3.85 mL, 53.9 mmol, 10 eq.) was added dropwise, and the reaction mixture was let to warm up to room temperature overnight. The reaction mixture was diluted in DCM and washed with HCl 1M. The aqueous phase was basified (pH10-12), extracted with DCM (x5), washed with brine, dried over magnesium sulphate and dried under reduced pressure. The reaction The reaction ncrude was purified by silica flash column chromatography, eluting at 1% methanol/ethyl acetate. Reported as a yellowish oil (468 mg, 23.41 mmol, **63%**).

^{1}H NMR (400 MHz, $CDCl_3$) δ 3.23 (ddt, *J* = 11.8, 5.8, 2.7 Hz, 2H), 2.64 (dt, *J* = 9.5, 5.6 Hz, 4H), 2.26 (dq, *J* = 10.0, 5.4 Hz, 4H), 2.20 – 2.13 (m, 1H). **^{13}C NMR** (101 MHz, $CDCl_3$) δ 207.7, 78.2 (d, *J* = 6.6 Hz), 73.6 (d, *J* = 29.0 Hz), 51.6, 46.2 (d, *J* = 4.6 Hz), 40.9. **HRMS (ESI):** calc. for $[C_8H_{12}ON]^+$: 138.09134, found 138.09149.

3-bromo-4-((2,4-difluorobenzyl)oxy)-6-methyl-1-(2-methyl-5-(4-((1-(prop-2-yn-1-yl)piperidin-4-yl)methyl)piperazine-1-carbonyl)phenyl)pyridin-2(1H)-one (5-32b)

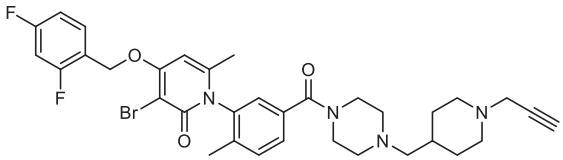

5-7 (300 mg, 0.56 mmol, 1 eq.), **5-31b** (85 mg, 0.56 mmol, 1 eq.), acetic acid (28 µL, catalytic) and methanol (5.6 mL, 0.1 M) were loaded in a round flash and stirred under nitrogen for 1 hour. Then sodium cyanoborohydride (53 mg, 0.56 mmol, 1.5 eq.) was added and the reaction mixture was stirred overnight at room temperature. Water was added to the reaction mixture and extracte with ethyl acetate. The organic layers were combined, washed with brine, dried over magnesium sulphate and dried under reduced pressure. The crued was purified by silica gel flash column chromatography, eluting at 6% methanol/DCM. Reported as a colorless oil (354 mg, **61%**).

^{1}H NMR (400 MHz, $CDCl_3$) δ 7.52 (td, *J* = 8.5, 6.3 Hz, 1H), 7.37 – 7.28 (m, 2H), 7.05 (d, *J* = 1.5 Hz, 1H), 6.94 – 6.85 (m, 1H), 6.80 (ddd, *J* = 10.2, 8.7, 2.5 Hz, 1H), 6.09 (s, 1H), 5.18 (s, 2H), 3.82 – 3.32 (m, 4H), 3.23 (d, *J* = 2.5 Hz, 2H), 2.82 (dt, *J* = 11.8, 3.3 Hz, 2H), 2.47 – 2.04 (m, 9H), 2.00 (s, 3H), 1.85 (s, 3H), 1.69 (dd, *J* = 13.4,

3.6 Hz, 2H), 1.40 (ddt, *J* = 11.3, 7.6, 3.7 Hz, 1H), 1.29 – 1.09 (m, 2H). **^{13}C NMR** (101 MHz, $CDCl_3$) δ 168.7, 163.0, 162.9 (dd, *J* = 250.2, 12.1 Hz), 160.3, 160.1 (dd, *J* = 249.8, 12.1 Hz), 146.0, 137.3 (d, *J* = 36.4 Hz), 135.0, 131.5, 130.5 (dd, *J* = 9.8, 5.2 Hz), 128.1, 126.8, 118.6 (dd, *J* = 14.2, 3.8 Hz), 111.8 (dd, *J* = 21.4, 3.7 Hz), 103.9 (t, *J* = 25.3 Hz), 96.7, 96.0, 78.8, 73.2, 64.3, 64.3, 64.2, 53.7, 53.3, 52.2, 47.9, 47.1, 42.2, 32.5, 30.5, 21.4, 17.2. **HRMS (ESI):** calc. for $[C_{34}H_{38}O_3N_4BrF_2]^+$: 667.20899, found 667.21155.

3-bromo-4-((2,4-difluorobenzyl)oxy)-6-methyl-1-(2-methyl-5-(4-(3-(1-(prop-2-yn-1-yl)piperidin-4-yl)propyl)piperazine-1-carbonyl)phenyl)pyridin-2(1H)-one (5-32a)

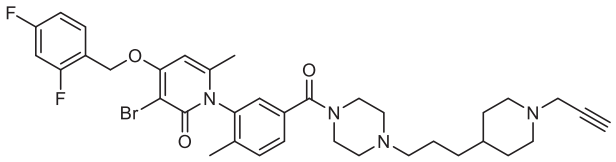

5-7 (450 mg, 0.84 mmol, 1 eq.), **5-31a** (152 mg, 0.84 mmol, 1 eq.), acetic acid (39 µL, catalytic) and methanol (8.4 mL, 0.1 M) were loaded in a round flash and stirred under nitrogen for 1 hour. Then sodium cyanoborohydride (80 mg, 1.26 mmol, 1.5 eq.) was added and the reaction mixture was stirred overnight at room temperature. Water was added to the reaction mixture and extracte with ethyl acetate. The organic layers were combined, washed with brine, dried over magnesium sulphate and dried under reduced pressure. The crued was purified by silica gel flash column chromatography, eluting at 6% methanol/DCM. Reported as a colorless oil (338 mg, **58%**).

^{1}H NMR (400 MHz, $CDCl_3$) δ 7.54 (td, *J* = 8.4, 4.8 Hz, 1H), 7.42 – 7.31 (m, 2H), 7.07 (d, *J* = 1.5 Hz, 1H), 6.97 – 6.85 (m, 1H), 6.81 (ddt, *J* = 11.1, 8.8, 2.5 Hz, 1H), 3.88 – 3.34 (m, 6H), 3.23 (d, *J* = 2.5 Hz, 2H), 2.82 (d, *J* = 11.0 Hz, 2H), 2.54 – 2.21 (m, 6H), 2.21 – 2.08 (m, 3H), 2.01 (s, 3H), 1.87 (s, 3H), 1.64 (d, *J* = 10.5 Hz, 2H), 1.41 (d, *J* = 8.3 Hz, 1H), 1.26 – 1.12 (m, 4H). **^{13}C NMR** (101 MHz $CDCl_3$) δ 163.1, 163.1 (d, *J* = 238.4 Hz), 160.4, 160.2 (d, *J* = 234.9 Hz), 146.1, 137.6, 137.2, 135.1, 131.6 (d, *J* = 26.4 Hz), 130.4, 128.2 (d, *J* = 26.8 Hz), 126.9, 126.7, 118.7 (d, *J* = 16.2 Hz), 112.0 (d, *J* = 22.1 Hz), 104.0 (t, *J* = 26.5 Hz), 96.9, 96.1, 95.9, 79.2, 72.8, 64.3, 58.7, 53.5, 52.6, 47.9, 47.2, 42.3, 35.2, 34.2, 32.3, 24.0, 21.6, 21.5, 17.4, 17.3. **HRMS (ESI):** calc. for $[C_{36}H_{42}O_3N_4BrF_2]^+$: 695.24029, found 695.24225.

3-bromo-4-((2,4-difluorobenzyl)oxy)-6-methyl-1-(2-methyl-5-(4-(1-(prop-2-yn-1-yl)piperidin-4-yl)piperazine-1-carbonyl)phenyl)pyridin-2(1H)-one (5-32c)

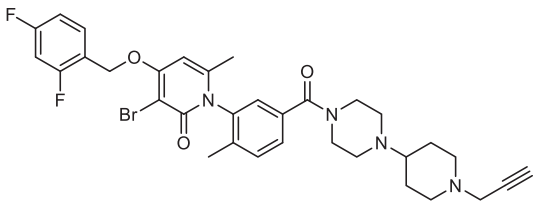

5-7 (400 mg, 0.75 mmol, 1 eq.), **5-31c** (85 mg, 0.75 mmol, 1 eq.), acetic acid (28 µL, catalytic) and methanol (5.6 mL, 0.1 M) were loaded in a round flash and stirred under nitrogen for 1 hour. Then sodium cyanoborohydride (53 mg, 0.85 mmol, 1.5 eq.) was added and the reaction mixture was stirred overnight at room temperature. Water was added to the reaction mixture and extracte with

ethyl acetate. The organic layers were combined, washed with brine, dried over magnesium sulphate and dried under reduced pressure. The crued was purified by silica gel flash column chromatography, eluting at 7% methanol/DCM. Reported as a colorless oil (216 mg, **44%**).

^{1}H NMR (400 MHz, $CDCl_3$) δ 7.63 – 7.47 (m, 1H), 7.48 – 7.29 (m, 2H), 7.12 (s, 1H), 6.94 – 6.85 (m, 1H), 6.80 (ddt, *J* = 10.1, 5.7, 2.5 Hz, 1H), 6.14 (s, 1H), 5.19 (s, 2H), 3.95 – 3.21 (m, 6H), 3.00 – 2.77 (m, 2H), 2.71 – 2.10 (m, 7H), 2.00 (s, 3H), 1.89 (s, 3H), 1.84 – 1.71 (m, 2H), 1.65 – 1.42 (m, 2H), 1.30 (t, *J* = 7.2 Hz, 1H). **HRMS (ESI):** calc. for $[C_{33}H_{36}O_3N_4BrF_2]^+$: 653.19334, found 653.19604.

4-(3-(3-bromo-4-((2,4-difluorobenzyl)oxy)-6-methyl-2-oxopyridin-1(2H)-yl)-4-methylbenzoyl)piperazine-1-sulfonyl fluoride (5-36)

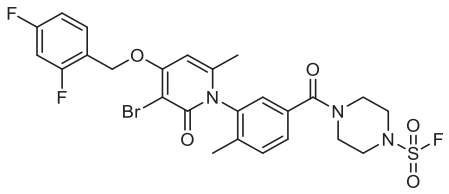

A flask was loaded with **5-7** (100 mg, 0.15 mmol, 1 eq.), DCM (0.8 mL, 0.2 M), DIPEA (30 µL, 0.17 mmol, 1.1 eq.) and cooled down at 0 °C. 1-(Fluorosulfonyl)-2,3-dimethyl-1H-imidazol-3-ium trifluoromethanesulfonate (51 mg, 0.15 mmol, 1 eq.) was added and the reaction mixture was let to warm up to room temperature. After 2 hours, water and ethyl acetate were added, the aqueous layer was extracted with ethyl acetate, the organic layers were combined, washed with brine, dried over magnesium sulphate and dried under reduced pressure. The crude was purified by silica flash column chromatography, eluted at 60% ethyl acetate in hexanes. The product was obtained as a white solid (92 mg, **quantitative**).

^{1}H NMR (400 MHz, $CDCl_3$) δ 7.53 (td, *J* = 8.5, 6.3 Hz, 1H), 7.36 (s, 1H), 7.09 (s, 0H), 6.95 – 6.85 (m, 1H), 6.85 – 6.75 (m, 1H), 6.09 (s, 1H), 5.18 (s, 2H), 3.51 (d, *J* = 112.5 Hz, 9H), 2.02 (s, 2H), 1.86 (s, 2H). **^{13}C NMR** (101 MHz, $CDCl_3$) δ 169.3, 163.1, 163.1 (dd, *J* = 250.3, 12.0 Hz), 160.4, 160.2 (dd, *J* = 249.5, 12.0 Hz), 145.8, 138.3, 137.9, 133.7, 131.9, 130.5 (dd, *J* = 9.8, 5.1 Hz), 128.2, 127.1, 118.6 (dd, *J* = 14.2, 3.9 Hz), 112.0 (dd, *J* = 21.4, 3.7 Hz), 104.0 (t, *J* = 25.3 Hz), 97.0, 96.1, 64.4 (d, *J* = 4.3 Hz), 47.0, 21.5, 17.4. **IR (ATR)**: 1645, 1415, 1202, 751 cm $^{-1}$ **HRMS (ESI):** calculated for $[C_{25}H_{24}O_5N_3BrF_3S]^+$: 614.05667, found: 614.05661.

tert-butyl 4-((4-(3-(3-bromo-4-((2,4-difluorobenzyl)oxy)-6-methyl-2-oxopyridin-1(2H)-yl)-4-methylbenzoyl)piperazin-1-yl)sulfonyl)piperazine-1-carboxylate (5-37)

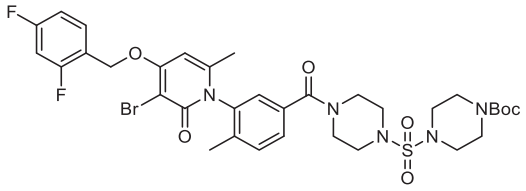

A flask loaded with **5-36** (32 mg, 0.05 mmol, 1 eq.), 1-Bocpiperazine (10 mg, 0.05 mmol, 1 eq.), DABCO (17 mg, 0.15 mmol, 3 eq.), calcium(II) bis(trifluoromethanesulfonimide) (34 mg, 0.06 mmol,

1.1 eq.) and THF (0.1 mL, 0.5 M) was sealed, heated up at 50 °C and stirred overnight. Water and ethyl acetate were added to the reaction mixture, the aqueous phase was extracted with ethyl acetate, the organic layers combined, washed with brine, dried over magnesium sulphate and dried under reduced pressure. The crude was purified by silica flash column chromatography, eluted at 75% ethyl acetate in hexanes. The product was obtained as a white wax (21 mg, **52%**).

^{1}H NMR (400 MHz, $CDCl_3$) δ 7.54 (td, *J* = 8.5, 6.3 Hz, 1H), 7.37 (d, *J* = 1.1 Hz, 2H), 7.06 (t, *J* = 1.1 Hz, 1H), 7.04 – 6.86 (m, 1H), 6.82 (ddd, *J* = 10.2, 8.7, 2.5 Hz, 1H), 6.07 (s, 1H), 5.20 (s, 2H), 3.88 – 3.04 (m, 16H), 2.03 (s, 3H), 1.87 (s, 3H), 1.40 (s, 9H). **^{13}C NMR** (101 MHz, $CDCl_3$) δ 169.2, 163.1, 163.1 (dd, *J* = 250.4, 12.0 Hz), 160.4, 160.2 (dd, *J* = 249.6, 12.1 Hz), 154.4, 145.9, 137.9, 137.7, 134.2, 131.9, 130.5 (dd, *J* = 9.8, 5.2 Hz), 128.2, 127.0, 118.6 (dd, *J* = 14.2, 3.9 Hz), 112.0 (dd, *J* = 21.3, 3.7 Hz), 104.0 (t, *J* = 25.2 Hz), 97.0, 96.1, 80.5, 64.4 (d, *J* = 4.2 Hz), 46.3, 28.4, 21.5, 17.4. **IR (ATR):** 2923, 1643, 1421, 1155, 734 cm^{-1}. **HRMS (ESI):** calculated for $[C_{34}H_{41}O_7N_5BrF_2S]^+$: 780.18726, found: 780.18842.

3-bromo-4-((2,4-difluorobenzyl)oxy)-1-(5-(4-((4-(hept-6-ynoyl)piperazin-1-yl)sulfonyl)piperazine-1-carbonyl)-2-methylphenyl)-6-methylpyridin-2(1H)-one (5-38a)

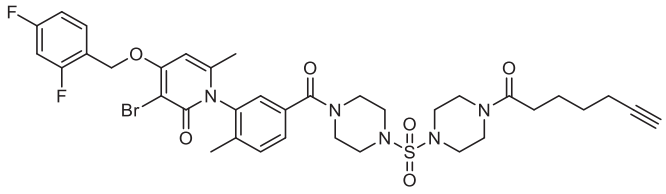

A flask loaded with 4-(3-(3-bromo-4-((2,4-difluorobenzyl)oxy)-6-methyl-2-oxopyridin-1(2H)-yl)-4-methylbenzoyl)piperazine-1-sulfonyl fluoride (num, 50 mg, 0.08 mmol, 1 eq.), 1-(piperazin-1-yl)hept-6-yn-1-one hydrochloride (19 mg, 0.08 mmol, 1 eq.), DABCO (28 mg, 0.16 mmol, 3 eq.), calcium(II) bis(trifluoromethanesulfonimide) (54 mg, 0.0.09 mmol, 1.1 eq.) and THF (0.16 mL, 0.5 M) was sealed, heated up at 50 °C and stirred overnight. Water and ethyl acetate were added to the reaction mixture, the aqueous phase was extracted with ethyl acetate, the organic layers combined, washed with brine, dried over magnesium sulphate and dried under reduced pressure. The crude was purified by silica flash column chromatography, eluted at 3% methanol in DCM. The product was obtained as a white solid (15 mg, **23%**, 50% conversion).

^{1}H NMR (400 MHz, $CDCl_3$) δ 7.61 (td, *J* = 8.5, 6.2 Hz, 1H), 7.44 (dd, *J* = 3.5, 1.1 Hz, 2H), 7.17 – 7.10 (m, 1H), 7.03 – 6.93 (m, 1H), 6.88 (ddd, *J* = 10.2, 8.7, 2.5 Hz, 1H), 6.14 (s, 1H), 5.26 (s, 2H), 3.90 – 3.13 (m, 16H), 2.35 (t, *J* = 7.5 Hz, 2H), 2.23 (td, *J* = 7.0, 2.7 Hz, 2H), 2.14 – 2.03 (m, 3H), 1.98 – 1.90 (m, 4H), 1.81 – 1.69 (m, 2H), 1.59 (q, *J* = 7.2 Hz, 2H). **^{13}C NMR** (101 MHz, $CDCl_3$) δ 171.4, 169.3, 163.3, 163.2 (dd, *J* = 250.3, 11.9 Hz), 160.3 (dd, *J* = 249.5, 12.0 Hz), 146.0, 138.1, 137.8, 134.3, 132.0, 130.6 (dd, *J* = 9.9, 5.2 Hz), 128.4, 127.1, 118.7 (dd, *J* = 14.1, 3.7 Hz), 112.1 (dd, *J* = 21.4, 3.7 Hz), 104.1 (t, *J* = 25.3 Hz), 97.1, 96.2, 84.1, 68.8, 64.5 (d, *J* = 4.1 Hz), 47.2 – 46.1 (m), 45.3, 41.2, 32.8, 28.1, 24.3, 21.6, 18.3, 17.5. **IR (ATR):** 2921, 1636, 1342, 1156, 736 cm^{-1}. **HRMS (ESI):** calculated for $[C_{36}H_{41}O_6N_5BrF_2S]^+$: 788.19235, found: 788.20227.

4-(3-(3-bromo-4-((2,4-difluorobenzyl)oxy)-6-methyl-2-oxopyridin-1(2H)-yl)-4-methylbenzoyl)-N-(pent-4-yn-1-yl)piperazine-1-sulfonamide (5-38c)

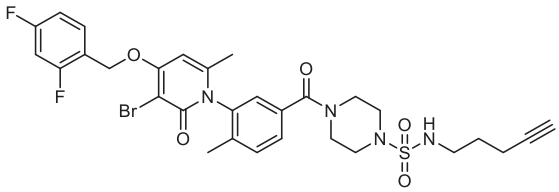

A flask loaded with 4-(3-(3-bromo-4-((2,4-difluorobenzyl)oxy)-6-methyl-2-oxopyridin-1(2H)-yl)-4-methylbenzoyl)piperazine-1-sulfonyl fluoride (num, 58 mg, 0.094 mmol, 1 eq.), pent-4-yn-1-amine hydrochloride (11.4 mg, 0.094 mmol, 1 eq.), DABCO (32 mg, 0.28 mmol, 3 eq.), calcium(II) bis(trifluoromethanesulfonimide) (63 mg, 0.10 mmol, 1.1 eq.) and THF (0.19 mL, 0.5 M) was sealed, heated up at 50 °C and stirred overnight. Water and ethyl acetate were added to the reaction mixture, the aqueous phase was extracted with ethyl acetate, the organic layers combined, washed with brine, dried over magnesium sulphate and dried under reduced pressure. The crude was purified by silica flash column chromatography, the product eluted at 80% ethyl acetate in hexanes. The product was obtained as a yellowish wax (26 mg, **41%**).

^{1}H NMR (400 MHz, $CDCl_3$) δ 7.60 (td, *J* = 8.5, 6.3 Hz, 1H), 7.43 (d, *J* = 1.1 Hz, 2H), 7.17 – 7.12 (m, 1H), 7.02 – 6.93 (m, 1H), 6.88 (ddd, *J* = 10.2, 8.7, 2.5 Hz, 1H), 6.15 (d, *J* = 0.9 Hz, 1H), 5.26 (d, *J* = 1.4 Hz, 2H), 4.68 (t, *J* = 6.2 Hz, 1H), 3.94 – 3.40 (m, 4H), 3.35 – 3.05 (m, 6H), 2.27 (td, *J* = 6.8, 2.7 Hz, 2H), 2.09 (s, 3H), 2.00 (t, *J* = 2.7 Hz, 1H), 1.94 (s, 3H), 1.79 – 1.71 (m, 2H). **^{13}C NMR** (101 MHz, $CDCl_3$) δ 169.3, 163.4, 163.2 (dd, *J* = 250.2, 12.1 Hz), 160.6, 160.3 (dd, *J* = 249.6, 12.0 Hz), 146.1, 137.9, 137.8, 134.4, 131.9, 130.7 (dd, *J* = 9.7, 5.1 Hz), 128.3, 127.1, 118.7 (dd, *J* = 14.2, 3.8 Hz), 112.1 (dd, *J* = 21.3, 3.7 Hz), 104.1 (t, *J* = 25.3 Hz), 96.3, 83.0, 69.9, 64.5 (d, *J* = 4.1 Hz), 46.3, 42.8, 28.3, 21.7, 17.5, 15.9. **IR (ATR):** 2920, 1643, 1343, 1139, 723 cm^{-1}. **HRMS (ESI):** calculated for $[C_{30}H_{32}O_5N_4BrF_2S]^+$: 677.12394, found: 677.12351.

3-bromo-4-((2,4-difluorobenzyl)oxy)-6-methyl-1-(2-methyl-5-(4-((4-(prop-2-yn-1-yl)piperazin-1-yl)sulfonyl)piperazine-1-carbonyl)phenyl)pyridin-2(1H)-one (5-38b)

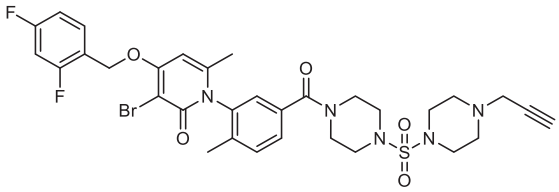

A flask loaded with 4-(3-(3-bromo-4-((2,4-difluorobenzyl)oxy)-6-methyl-2-oxopyridin-1(2H)-yl)-4-methylbenzoyl)piperazine-1-sulfonyl fluoride (num, 58 mg, 0.094 mmol, 1 eq.), 1-(prop-2-yn-1-yl)piperazine (13 mg, 0.094 mmol, 1 eq.), DABCO (16 mg, 0.14 mmol, 1.5 eq.), calcium(II) bis(trifluoromethanesulfonimide) (63 mg, 0.10 mmol, 1.1 eq.) and THF (0.19 mL, 0.5 M) was sealed, heated up at 50 °C and stirred overnight. Water and ethyl acetate were added to the reaction mixture, the aqueous phase was extracted with ethyl acetate, the organic layers combined, washed with brine, dried over magnesium sulphate and dried under reduced pressure. The crude was

purified by silica flash column chromatography, eluted at 80% ethyl acetate in hexanes. The product was obtained as a yellowish wax (7 mg, **10%**).

^{1}H NMR (400 MHz, $CDCl_3$) δ 7.54 (td, *J* = 8.5, 6.3 Hz, 1H), 7.37 (d, *J* = 1.1 Hz, 2H), 7.06 (d, *J* = 1.1 Hz, 1H), 6.93 – 6.91 (m, 1H), 6.82 (ddd, *J* = 10.2, 8.7, 2.5 Hz, 1H), 6.07 (s, 1H), 5.20 (s, 2H), 3.85 – 3.01 (m, 16H), 2.54 (t, *J* = 5.0 Hz, 2H), 2.23 (t, *J* = 2.4 Hz, 1H), 2.03 (s, 3H), 1.87 (s, 3H). **^{13}C NMR** (101 MHz, $CDCl_3$) δ 169.3, 163.2, 164.6 – 161.8 (m), 161.7 – 157.8 (m), 146.0, 138.0, 137.9, 134.4, 132.0, 130.6 (dd, *J* = 9.8, 5.2 Hz), 128.4, 127.1, 118.7 (dd, *J* = 14.0, 3.9 Hz), 112.1 (dd, *J* = 21.2, 3.8 Hz), 104.2 (t, *J* = 25.3 Hz), 97.1, 96.2, 78.1, 74.0, 64.5 (d, *J* = 4.2 Hz), 51.3, 47.3 – 45.7 (m), 21.7, 17.5. **IR(ATR):** 2921, 1644, 1343, 932, 727 cm^{-1}. **HRMS (ESI):** calculated for $[C_{32}H_{35}O_5N_5BrF_2S]^+$: 718.15049, found: 718.15045.

tert-butyl 4-(3-hydroxypropyl)piperidine-1-carboxylate (5-39)

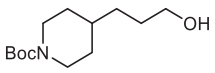

A flask loaded with 3-(piperidin-4-yl)propan-1-ol (500 mg, 3.5 mmol, 1 eq.), TEA (0.35 mL, 1.1 eq.) and THF (2.8 mL, 1.25 M) was stirred at 0°C and boc anhydride (884 mg, 3.87 mmol, 1.1 eq.) was added. The reaction mixture was stirred overnight. Water and ethyl acetate were added to the reaction mixture, the aqueous phase was extracted with ethyl acetate, the organic layers combined, washed with brine, dried over magnesium sulphate and dried under reduced pressure. The crude was purified by silica flash column chromatography, the product eluted at 80% ethyl acetate in hexanes. The product was obtained as a colorless oil (217 mg, **41%**).

^{1}H NMR (400 MHz, $CDCl_3$) δ 4.07 (s, 2H), 3.64 (t, J = 6.8 Hz, 2H), 2.67 (t, J = 12.9 Hz, 2H), 1.74 – 1.53 (m, 5H), 1.45 (s, 11H), 1.08 (qd, J = 12.4, 4.4 Hz, 2H).

tert-butyl 4-(3-oxopropyl)piperidine-1-carboxylate (5-40)

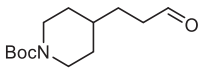

A flask was loaded with **5-39** (217 mg, 0.89 mmol, 1 eq.), dry DCM (2.2 mL, 0.4 M) and stirred at 0 °C. Dess-Martin periodinane (416 mg, 0.98 mmol, 1.1 eq.) was added and stirred for 3.5 hours, allowing it to reach room temperature. The reaction mixture was diluted in DCM and a saturated solution of Na_2S_2O3 was added. The aqueous fraction was extracted with DCM, the organic phases were combined, washed with $NaHCO_3$, brine, dried over magnesium sulphate and dried under reduced pressure. The crude was purified by silica flash column chromatography, the product eluted at 4% methanol in DCM. The product was obtained as a colorless oil (140 mg, **65%**).

^{1}H NMR (400 MHz, $CDCl_3$) δ 9.71 (t, J = 1.7 Hz, 1H), 4.02 (d, J = 13.1 Hz, 2H), 2.59 (t, J = 12.5 Hz, 2H), 2.40 (td, J = 7.5, 1.7 Hz, 2H), 1.67 – 1.46 (m, 4H), 1.38 (s, 10H), 1.03 (qd, J = 12.3, 4.4 Hz, 2H).

***tert*-butyl 4-(3-(4-(3-(3-bromo-4-((2,4-difluorobenzyl)oxy)-6-methyl-2-oxopyridin-1(2H)-yl)-4-methylbenzoyl)piperazin-1-yl)propyl)piperidine-1-carboxylate (5-41)**

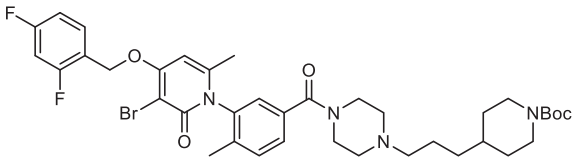

5-19 (38mg, 0.07 mmol, 1 eq.), **5-40** (16 mg, 0.07 mmol), acetic acid (3 µL, catalytic) and methanol (0.66 mL) were loaded in a round flash and stirred under nitrogen for 1 hour. Then sodium cyanoborohydride (6 mg, 0.01 mmol, 1.5 eq.) was added and the reaction mixture was stirred overnight at room temperature. Water was added to the reaction mixture and extracte with ethyl acetate. The organic layers were combined, washed with brine, dried over magnesium sulphate and dried under reduced pressure. The crued was purified by silica gel flash column chromatography, eluting at 8% methanol/DCM. Reported as a white sticky film (24 mg, **48%**)

^{1}H NMR (400 MHz, $CDCl_3$) δ 7.54 (td, *J* = 8.5, 6.2 Hz, 1H), 7.43 – 7.29 (m, 2H), 7.07 (d, *J* = 1.5 Hz, 1H), 6.98 – 6.86 (m, 1H), 6.82 (ddd, *J* = 10.2, 8.7, 2.5 Hz, 1H), 6.27 – 5.95 (m, 1H), 5.20 (d, *J* = 1.4 Hz, 2H), 4.15 – 3.43 (m, 8H), 2.67 – 2.21 (m, 6H), 2.02 (s, 3H), 1.87 (s, 3H), 1.62 – 1.43 (m, 4H), 1.38 (s, 9H), 1.35 – 0.90 (m, 5H). **^{13}C NMR** (101 MHz, $CDCl_3$) δ 163.1, 163.1 (dd, *J* = 250.2, 12.1 Hz), 160.4, 160.2 (dd, *J* = 249.5, 12.1 Hz), 154.9 (d, *J* = 2.9 Hz), 146.0, 137.6 (d, *J* = 12.8 Hz), 134.7, 131.6, 130.5 (dd, *J* = 9.8, 5.1 Hz), 128.2, 126.9, 118.6 (dd, *J* = 14.1, 3.8 Hz), 112.0 (dd, *J* = 21.3, 3.7 Hz), 104.0 (t, *J* = 25.3 Hz), 96.9, 96.1, 79.3, 64.4, 64.3, 58.4, 52.9, 47.3, 44.0, 41.7, 35.8, 35.5, 34.1, 32.1, 31.8, 31.4, 29.7, 28.5, 23.2, 21.5, 17.3.

3-bromo-4-((2,4-difluorobenzyl)oxy)-6-methyl-1-(2-methyl-5-(4-(3-(piperidin-4-yl)propyl)piperazine-1-carbonyl)phenyl)pyridin-2(1H)-one hydrochloride (5-41 HCl)

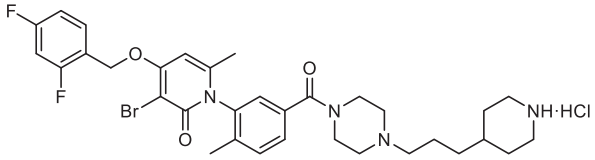

5-41 (24 mg, 0.032 mmol) was stirred in 2 mL HCl/dioxane 4N for 1 h. The solvent was then evaporated affording the hydrochloride salt as a white film (23 mg, **quant.**). The product was used without further purification.

4-(but-3-yn-1-ylamino)-2-(2,6-dioxopiperidin-3-yl)isoindoline-1,3-dione (5-8a)

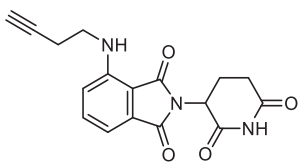

To a solution of **3-10** (38 mg, 0.14 mmol, 1eq.)) in NMP (1.5 mL, 0.09 M) in a pressure tube was added 1-amine-3-butyne (11 mg, 0.15 mmol, 1,1 eq.) and DIPEA (50 µL, 0.28 mmol, 2 eq.), sealed, then heated to 150 °C overnight Ethyl acetate and water were added to the reaction mixture, then the aqueous layer was re-extracted using ethyl acetate (x2), the combined organic layers washed with brine (x3), $CuSO_4$ (x2) and brine (x1), dried over $MgSO_4$, and then concentrated under reduced pressure. . The crude was filtered through a silica plug (ethyl acetate/hexanes 1:1) and used without further purification (20 mg, **44%**).

^{1}H NMR (400 MHz, CDCl3) δ 8.18 (s, 1H), 7.51 (ddd, J = 8.5, 7.1, 0.6 Hz, 1H), 7.12 (dd, J = 7.1, 0.6 Hz, 1H), 6.92 (d, J = 8.5 Hz, 1H), 6.48 (t, J = 6.1 Hz, 1H), 4.92 (dd, J = 12.2, 5.3 Hz, 1H), 3.48 (q, J = 6.7 Hz, 2H), 2.93 – 2.68 (m, 4H), 2.54 (td, J = 6.9, 2.7 Hz, 2H), 2.07 (t, J = 2.6 Hz, 1H). **^{13}C NMR** (126 MHz, $CDCl_3$) 8 170.8, 169.3, 168.2, 167.5, 146.4, 136.2, 132.6, 116.5, 112.0, 110.6, 80.6, 70.8, 48.9, 41.3, 31.4, 22.8, 19.4.

2-(2,6-dioxopiperidin-3-yl)-4-((2-(prop-2-yn-1-yloxy)ethyl)amino)isoindoline-1,3-dione (5-8b)

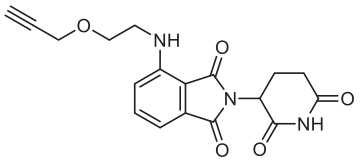

To a solution of **3-10** (50 mg, 0.18 mmol) in NMP (1.5 mL, 0.21 M) in a boiling tube was added 2-(prop-2-yn-1-yloxy)ethan-1-amine (20 mg, 0.20 mmol, 1.1 eq.) and DIPEA (63 µL, 0.36 mmol, 2 eq.), sealed, then heated to 120 °C for 1.5 h. Ethyl acetate and water were added to the reaction mixture, then the aqueous layer was re-extracted using ethyl acetate (x2), the combined organic layers washed with brine (x3), $CuSO_4$ (x2) and brine (x1), dried over $MgSO_4$, and then concentrated under reduced pressure. . The crude was filtered through a silica plug (methanol 2% in DCM) and used without further purification (45 mg, **70%**).

^{1}H NMR (400 MHz, $CDCl_3$) δ 8.4 (s, 1H), 7.5 – 7.4 (m, 1H), 7.1 (d, *J* = 7.1 Hz, 1H), 6.9 (d, *J* = 8.6 Hz, 1H), 6.5 (t, *J* = 5.8 Hz, 1H), 4.9 (dd, *J* = 11.8, 5.3 Hz, 1H), 4.2 (d, *J* = 2.2 Hz, 2H), 3.8 (t, *J* = 5.3 Hz, 2H), 3.5 (q, *J* = 5.4 Hz, 2H), 3.0 – 2.6 (m, 3H), 2.5 (t, *J* = 2.4 Hz, 1H), 2.1 – 2.0 (m, 1H).

tert-butyl (4-(2-(2,6-dioxopiperidin-3-yl)-1-oxoisoindolin-4-yl)but-3-yn-1-yl)carbamate

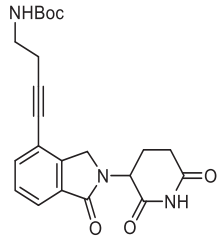

A flask charged with **3-13** (200 mg, 0.62 mmol, 1eq.), CuI (24 mg, 0.12 mmol, 0.2 eq.), $Pd(PPh_3)_4$ (87 mg, 0.12 mmol, 0.2 eq.) and DMF (15 mL, 0.04 M) was degassed with nitrogen, added trimethylamine (7 mL, 92 mmol, 150 eq.) and stirred at 100 °C for 2 days. The mixture was cooled to room temperature, filtered through celite, washed with ethyl acetate then concentrated under reduced pressure. Ethyl acetate and water were added, then the aqueous layer was re-extracted using ethyl acetate , the combined organic layers washed with brine and copper sulfate, dried over $MgSO_4$, and then concentrated under reduced pressure. The crude was purified by flash column chromatography, the product was eluted at 100% ethyl acetate, affording the product as a yellowish oil (212 mg, **83%**).

^{1}H NMR (400 MHz, DMSO-*d*) δ 11.0 (s, 1H), 7.7 (dd, *J* = 7.6, 1.1 Hz, 1H), 7.6 (dd, *J* = 7.6, 1.1 Hz, 1H), 7.5 (t, *J* = 7.6 Hz, 1H), 7.0 (d, *J* = 7.2 Hz, 1H), 5.1 (dd, *J* = 13.3, 5.1 Hz, 1H), 4.5 (d, *J* = 17.9 Hz, 1H), 4.3 (d, *J* = 17.9 Hz, 1H), 3.2 (q, *J* = 6.6 Hz, 2H), 3.0 – 2.8 (m, 1H), 2.6 – 2.5 (m, 4H), 2.1 – 1.9 (m, 1H), 1.4 (s, 9H).

tert-butyl (2-((2-(2,6-dioxopiperidin-3-yl)-1,3-dioxoisoindolin-4-yl)amino)ethyl)carbamate

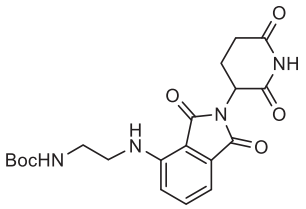

To a solution of **3-10** (200 mg, 0.72 mmol, 1eq.) in NMP (5 mL, 0.15 M) in a pressure tube was added tert-butyl (2-aminoethyl)carbamate (176 mg, 0.79 mmol, 1,1 eq.) and DIPEA (251 µL, 1.44 mmol, 2 eq.), sealed, then heated to 80 °C overnight Ethyl acetate and water were added to the reaction mixture, then the aqueous layer was re-extracted using ethyl acetate (x2), the combined organic layers washed with brine (x3), $CuSO_4$ (x2) and brine (x1), dried over $MgSO_4$, and then concentrated under reduced pressure. . The crude was purified by flash column chromatography, the product was eluted at 50% ethyl acetate in hexanes, affording the product as a yellow oil (55 mg, **18%**).

^{1}H NMR (400 MHz, $CDCl_3$) δ 8.0 (s, 1H), 7.5 (t, *J* = 8.0 Hz, 1H), 7.1 (d, *J* = 7.4 Hz, 1H), 7.0 (d, *J* = 8.5 Hz, 1H), 6.4 (s, 1H), 5.0 – 4.9 (m, 1H), 3.4 (t, *J* = 6.1 Hz, 2H), 3.4 (t, *J* = 6.0 Hz, 2H), 3.0 – 2.7 (m, 3H), 2.2 – 2.1 (m, 1H), 2.0 (d, *J* = 1.2 Hz, 2H), 1.5 – 1.4 (m, 9H).

methyl 4-(4-(3-azidopropyl)piperazin-1-yl)butanoate (5-25)

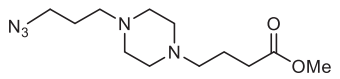

A pressure flask was loaded with **5-24 HCl** (365 mg, 1.77 mmol, 1 eq.), methyl 4-bromobutanoate (267 µL, 2.12 mmol, 1.2 eq.), potassium carbonate (734 mg, 3.5 mmol, 3 eq.) and DCM (10 mL, 0.13 M) was stirred at 40 °C during 5 days. Water was added to the reaction mixture, the aqueous layer was extracted with DCM (x3), the organic fractions were combined, washed with brine, dried over magnesium sulphate and dried under reduced pressure. The crude was purified by silica flash column chromatography, eluting at 4% methanol/DCM. Reported as an incolor oil (250 mg, **38%**).

^{1}H NMR (400 MHz, $CDCl_3$) δ 3.67 (s, 3H), 3.33 (t, *J* = 6.8 Hz, 2H), 2.42 (dd, *J* = 16.6, 9.5 Hz, 10H), 2.35 (td, *J* = 7.3, 3.9 Hz, 4H), 1.87 – 1.71 (m, 4H). **^{13}C NMR** (101 MHz, $CDCl_3$) δ 174.0, 57.6, 55.3, 53.2, 53.1, 51.5, 49.6, 32.0, 26.3, 22.2. **IR (ATR):** 2945, 2809, 2091, 1734, 1155 cm^{-1}. **HRMS (ESI):** calculated for $[C_{12}H_{24}O_2N_5]^+$: 270.19245, found: 270.19249.

4-(4-(3-azidopropyl)piperazin-1-yl)butanoic acid (5-25 acid)

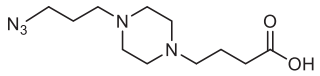

5-25 was stirred in NaOH 2M (5 mL) for 6 hours. The reaction mixture was acidified to pH 3, then evaporated under reduced pressure. The residue was dissolved in DCM and filtered. Product was obtained as a white solid and used without further purification (122 mg, **71**%).

(2S,4R)-1-((S)-2-(4-(4-(3-azidopropyl)piperazin-1-yl)butanamido)-3,3-dimethylbutanoyl)-4-hydroxy-N-((S)-1-(4-(4-methylthiazol-5-yl)phenyl)ethyl)pyrrolidine-2-carboxamide

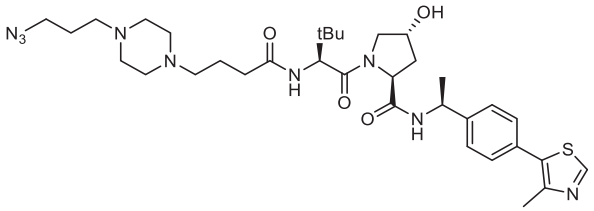

The product was prepared following general method for amide formation 2, using **3-29** (72 mg, 0.15 mmol) and **5-25 acid** (38 mg, 0.15 mmol). The crude was purified by silica flash column chromatography, eluting at 5% methanol in DCM. The product was obtained as a yellowish wax (26 mg, **25%**).

^{1}H NMR (400 MHz, CD_3OD) δ 8.85 (s, 1H), 8.42 (d, *J* = 7.5 Hz, 1H), 7.50 – 7.35 (m, 4H), 4.99 (dd, *J* = 9.5, 4.8 Hz, 1H), 4.82 (s, 4H), 4.64 – 4.46 (m, 2H), 4.46 – 4.36 (m, 1H), 3.89 (d, *J* = 11.0 Hz, 1H), 3.73 (dd, *J* = 11.0, 4.0 Hz, 1H), 3.39 (t, *J* = 6.5 Hz, 2H), 3.34 – 2.59 (m, 10H), 2.51 – 2.38 (m, 4H), 2.26 – 2.17 (m, 1H), 1.95 – 1.87 (m, 2H), 1.87 – 1.69 (m, 2H), 1.49 (d, *J* = 7.0 Hz, 3H), 1.04 (s, 9H). **^{13}C NMR** (101 MHz, CD_3OD) δ 173.8, 171.8,

170.9, 151.5, 147.7, 144.2, 132.0, 130.1, 129.1, 126.3, 69.6, 59.3, 58.2, 56.6, 56.4, 53.9, 51.3, 50.4, 48.8, 37.6, 34.9, 32.3, 29.3, 25.7, 25.6, 25.0, 21.0, 20.2, 14.5. **HRMS (ESI):** calculated for $[C_{34}H_{52}O_4N_9S]^+$: 682.38446, found: 682.38575. **IR(ATR):** 3418, 2091, 1621, 832 cm^{-1}. **M_p:** 115 °C.

(2R,4R)-1-((S)-3,3-dimethyl-2-((3-(1-(prop-2-yn-1-yl)piperidin-4-yl)propyl)amino)butanoyl)-4-hydroxy-N-((S)-1-(4-(4-methylthiazol-5-yl)phenyl)ethyl)pyrrolidine-2-carboxamide (5-33)

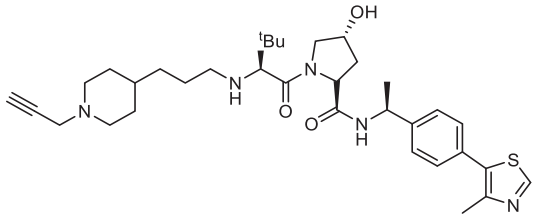

3-29 (92 mg, 0.2 mmol, 1 eq.), **5-31a** (32 mg, 0.18 mmol, 1 eq.), acetic acid (20 µL, catalytic) and methanol (1.8mL, 0.1 M) were loaded in a round flash and stirred under nitrogen for 1 hour. Then sodium cyanoborohydride (17 mg, 0.27 mmol, 1.5 eq.) was added and the reaction mixture was stirred overnight at room temperature. Water was added to the reaction mixture and extracte with ethyl acetate. The organic layers were combined, washed with brine, dried over magnesium sulphate and dried under reduced pressure. The crued was purified by silica gel flash column chromatography, eluting at 8% methanol/DCM. **5-33** was obtained as a colorless film (14 mg, **13%**).

^{1}H NMR (500 MHz, $CDCl_3$) δ 8.67 (s, 1H), 7.83 (d, J = 7.8 Hz, 1H), 7.46 – 7.34 (m, 5H), 5.04 (p, J = 7.1 Hz, 1H), 4.86 (dd, J = 8.4, 5.4 Hz, 1H), 4.62 (p, J = 4.5 Hz, 1H), 3.62 (d, J = 4.3 Hz, 2H), 3.28 (d, J = 2.5 Hz, 2H), 3.10 (s, 1H), 2.93 – 2.83 (m, 2H), 2.72 (dt, J = 13.3, 5.4 Hz, 1H), 2.52 (s, 4H), 2.34 (ddd, J = 11.1, 8.4, 5.9 Hz, 4H), 2.23 (t, J = 2.4 Hz, 1H), 2.18 (t, J = 11.0 Hz, 2H), 1.92 (ddd, J = 13.1, 8.4, 4.5 Hz, 1H), 1.73 – 1.64 (m, 2H), 1.52 – 1.36 (m, 5H), 1.00 (s, 12H).**^{13}C NMR** (126 MHz, CDCl3) δ 176.4, 169.7, 150.4, 148.6, 143.4, 131.8, 131.0, 129.7, 126.6, 79.0, 73.3, 70.2, 67.5, 60.5, 58.2, 55.8, 52.7, 49.3, 49.1, 47.3, 35.4, 35.2, 34.0, 32.2, 29.8, 27.6, 26.9, 22.5, 16.2. **HRMS (ESI):** calc. for $[C_{34}H_{50}O_3N_5S]^+$: 608.36289, found 608.36316. **M_p:** 71 °C.

3-(3-bromo-4-((2,4-difluorobenzyl)oxy)-6-methyl-2-oxopyridin-1(2H)-yl)-N-(2-(2-(2-(2-(4-(2-((2-(2,6-dioxopiperidin-3-yl)-1,3-dioxoisoindolin-4-yl)amino)ethyl)-1H-1,2,3-triazol-1-yl)ethoxy)ethoxy)ethoxy)ethyl)-4-methylbenzamide (5-10b)

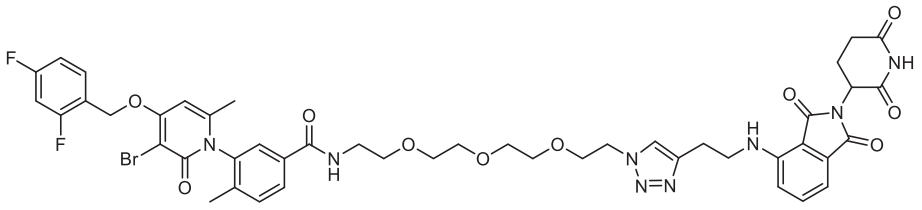

The product was prepared following general method for CuAAC, using **5-9** (32 mg, 0.05 mmol) and **5-8a** (15 mg, 0.05 mmol). The product was purified by silica flash column chromatography, eluted at 5% MeOH/DCM. Reported as a yellow solid film (27 mg, **55%**).

^{1}H NMR (400 MHz, $CDCl_3$) δ 8.9 (s, 2H), 7.8 (dt, *J* = 8.0, 1.2 Hz, 2H), 7.6 – 7.5 (m, 2H), 7.5 (dd, *J* = 5.2, 1.8 Hz, 1H), 7.5 (dd, *J* = 8.5, 7.1 Hz, 1H), 7.4 (dd, *J* = 8.0, 2.1 Hz, 2H), 7.1 – 7.0 (m, 1H), 7.0 – 6.8 (m, 3H), 6.4 (t, *J* = 5.9 Hz, 1H), 6.1 (dd, *J* = 2.1, 0.9 Hz, 1H), 5.2 (s, 2H), 4.9 – 4.8 (m, 1H), 4.4 (t, *J* = 5.2 Hz, 2H), 3.8 (td, *J* = 5.3, 1.4 Hz, 2H), 3.7 – 3.5 (m, 14H), 3.0 (t, *J* = 6.6 Hz, 2H), 2.9 – 2.6 (m, 3H), 2.1 (s, 4H), 1.9 (d, *J* = 2.1 Hz, 4H). **^{13}C NMR** (101 MHz, $CDCl_3$) δ 171.6, 169.5, 168.8, 167.7, 166.8, 163.3, 164.8 – 161.7 (m), 161.7 – 158.6 (m), 160.6, 146.7, 146.4, 138.8, 137.6, 136.2, 134.6, 132.6, 131.5, 130.6 (dd, *J* = 9.6, 5.0 Hz), 128.5, 126.9, 123.1, 118.7 (d, *J* = 14.4 Hz), 116.9, 112.3 – 111.8 (m), 111.8, 110.4, 104.1 (t, *J* = 25.2 Hz), 96.9, 96.2, 70.4, 70.2, 69.8, 69.5, 64.5 (d, *J* = 4.0 Hz), 50.2, 49.0, 42.2, 39.9, 31.5, 25.8, 22.9, 21.6, 17.4. **HRMS (ESI):** calculated for $[C_{46}H_{48}N_8O_{10}BrF_2]^+$: 989.26394, found: 989.26355. **IR (ATR):** 1737, 1641, 1352 cm^{-1}. **M_p:** 106-111°C.

3-(3-bromo-4-((2,4-difluorobenzyl)oxy)-6-methyl-2-oxopyridin-1(2H)-yl)-N-(2-(1-(2-(2-(2-((2-(2,6-dioxopiperidin-3-yl)-1,3-dioxoisoindolin-4-yl)amino)ethoxy)ethoxy)ethoxy)ethyl)-1H-1,2,3-triazol-4-yl)ethyl)-4-methylbenzamide (5-10d)

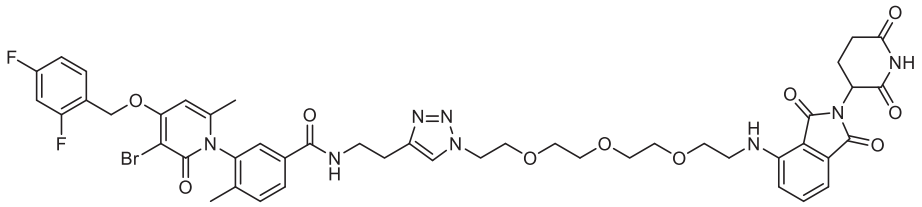

The product was prepared following general method for CuAAC, using **5-9c** (30 mg, 0.08 mmol) and **3-11c** (33 mg, 0.08 mmol). The product was purified by silica flash column chromatography, eluted at 5% MeOH/DCM. Reported as a yellow solid film (23 mg, **28%**).

^{1}H NMR (400 MHz, $CDCl_3$) δ 8.8 (s, 1H), 7.8 (dd, *J* = 8.0, 1.8 Hz, 1H), 7.6 – 7.6 (m, 2H), 7.5 (dd, *J* = 4.6, 1.8 Hz, 1H), 7.5 (dd, *J* = 8.5, 7.1 Hz, 1H), 7.4 (dd, *J* = 8.4, 2.3 Hz, 2H), 7.1 (dd, *J* = 7.1, 0.6 Hz, 1H), 7.0 – 6.9 (m, 1H), 6.9 – 6.8 (m, 2H), 6.5 (t, *J* = 5.6 Hz, 1H), 6.1 (d, *J* = 0.9 Hz, 1H), 5.2 (s, 2H), 4.9 (dt, *J* = 11.5, 5.4 Hz, 1H), 4.5 (t, *J* = 5.1 Hz, 2H), 3.9 – 3.8 (m, 2H), 3.7 – 3.6 (m, 12H), 3.4 (q, *J* = 5.4 Hz, 2H), 2.9 (d, *J* = 6.8 Hz, 2H), 2.9 – 2.7 (m, 3H), 2.1 (d, *J* = 3.2 Hz, 0H), 2.1 (s, 3H), 1.9 (d, *J* = 0.8 Hz, 3H). **^{13}C NMR** (101 MHz, $CDCl_3$) δ 171.5, 169.3, 168.7, 167.6, 166.2, 163.2, 164.6 – 161.4 (m), 160.4, 160.0 (d, *J* = 237.5 Hz), 146.8, 146.3, 138.8, 137.5, 136.0, 134.2, 132.5, 131.4, 130.3, 128.2, 126.7, 122.8, 118.7 (d, *J* = 14.3 Hz), 116.8, 111.9 (d, *J* = 17.7 Hz), 111.6, 110.3, 103.9 (t, *J* = 25.2 Hz), 96.8, 96.2, 70.7, 70.6, 70.5, 69.4, 64.3, 50.1, 48.9, 42.4, 39.3, 31.4, 25.4, 22.8, 21.5, 17.3. **IR (ATR):** 2921, 1694, 1643, 1349 cm^{-1}. **HRMS (ESI):** calculated for $[C_{46}H_{48}N_8O_{10}BrF_2]^+$: 989.26394, found: 989.26333. **M_p:** 109-114°C.

3-(3-bromo-4-((2,4-difluorobenzyl)oxy)-6-methyl-2-oxopyridin-1(2H)-yl)-N-(2-((1-(2-(2-(2-((2-(2,6-dioxopiperidin-3-yl)-1,3-dioxoisoindolin-4-yl)amino)ethoxy)ethoxy)ethyl)-1H-1,2,3-triazol-4-yl)methoxy)ethyl)-4-methylbenzamide (5-10c)

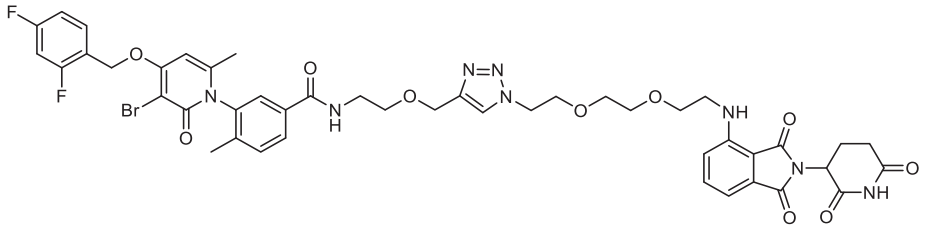

The product was prepared following general method for CuAAC, using **5-9b** (25 mg, 0.05 mmol) and **3-11b** (20 mg, 0.05 mmol). The product was purified by silica flash column chromatography, eluted at 5% MeOH/DCM. Reported as a yellow solid film (32mg, **70%**).

^{1}H NMR (400 MHz, $CDCl_3$) δ 9.0 (d, *J* = 77.7 Hz, 1H), 7.8 – 7.8 (m, 1H), 7.8 – 7.7 (m, 2H), 7.6 – 7.5 (m, 2H), 7.5 – 7.4 (m, 2H), 7.3 (t, *J* = 7.2 Hz, 1H), 7.3 (d, *J* = 0.5 Hz, 1H), 7.1 – 7.0 (m, 1H), 7.0 – 6.9 (m, 1H), 6.9 (td, *J* = 9.0, 2.7 Hz, 2H), 6.5 (q, *J* = 5.4 Hz, 1H), 6.1 (d, *J* = 2.2 Hz, 1H), 5.2 (s, 2H), 4.9 (ddd, *J* = 17.7, 12.1, 5.7 Hz, 1H), 4.6 – 4.4 (m, 4H), 4.3 (dd, *J* = 11.6, 4.8 Hz, 2H), 3.9 – 3.8 (m, 2H), 3.7 – 3.5 (m, 8H), 3.4 (t, *J* = 5.0 Hz, 2H), 2.8 – 2.6 (m, 3H), 2.1 (d, *J* = 3.3 Hz, 4H), 1.9 (s, 3H). **^{13}C NMR** (101 MHz, $CDCl_3$) δ 171.7, 169.5, 169.0 (d, *J* = 8.2 Hz), 167.6 (d, *J* = 3.8 Hz), 166.6 (d, *J* = 5.8 Hz), 163.3 (d, *J* = 4.7 Hz), 163.1 (dd, *J* = 249.4, 12.8 Hz), 160.5, 160.2 (dd, *J* = 249.2, 12.0 Hz), 146.8 (d, *J* = 4.3 Hz), 146.5 (d, *J* = 9.9 Hz), 138.9, 137.6 (d, *J* = 8.2 Hz), 136.2, 134.3 (d, *J* = 5.9 Hz), 132.7 (d, *J* = 2.7 Hz), 131.5, 131.0, 130.5 (d, *J* = 5.8 Hz), 128.9, 128.6, 126.9, 124.2, 118.7 (d, *J* = 14.0 Hz), 116.8 (d, *J* = 4.6 Hz), 112.0 (d, *J* = 21.5 Hz), 111.7, 110.4, 104.1 (t, *J* = 25.0 Hz), 96.8, 96.2, 70.5, 70.5, 69.6, 69.3, 69.2, 69.1, 66.1 (d, *J* = 30.5 Hz), 64.5, 64.2, 50.4, 49.0, 42.4, 40.0, 31.5, 22.9, 21.6, 17.4. **IR (ATR):** 2957, 1724, 1262 cm^{-1}. **HRMS (ESI):** calculated for $[C_{45}H_{46}N_8O_{10}BrF_2]^+$: 975.24828, found: 975.24788. **M_p:** 87-128°C.

3-(3-bromo-4-((2,4-difluorobenzyl)oxy)-6-methyl-2-oxopyridin-1(2H)-yl)-N-(2-(2-(2-(4-((2-((2-(2,6-dioxopiperidin-3-yl)-1,3-dioxoisoindolin-4-yl)amino)ethoxy)methyl)-1H-1,2,3-triazol-1-yl)ethoxy)ethoxy)ethyl)-4-methylbenzamide (5-10a)

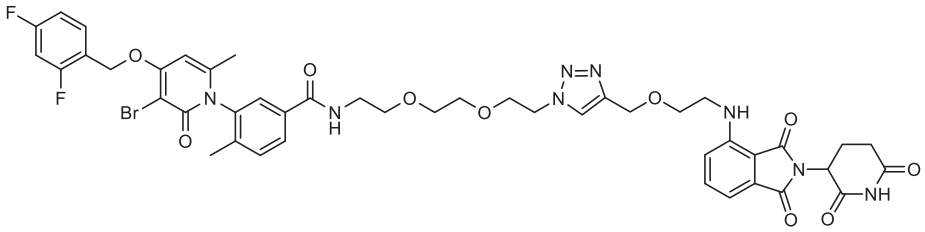

The product was prepared following general method for CuAAC, using **5-9c** (32 mg, 0.05 mmol) and **5-8b** (15 mg, 0.05 mmol). The product was purified by silica flash column chromatography, eluted at 5% MeOH/DCM. Reported as a yellow solid film (16, **32%**).

^{1}H NMR (400 MHz, $CDCl_3$) δ 9.2 (d, *J* = 19.3 Hz, 1H), 7.9 (s, 1H), 7.8 (ddd, *J* = 8.3, 6.7, 1.8 Hz, 1H), 7.7 (d, *J* = 4.5 Hz, 1H), 7.6 (tdd, *J* = 8.6, 6.3, 2.4 Hz, 1H), 7.5 – 7.5 (m, 2H), 7.5 – 7.4 (m, 1H), 7.4 (dd, *J* = 8.0, 4.7 Hz, 1H), 7.3 – 7.2 (m, 1H), 7.1 (dt, *J* = 7.2, 0.7 Hz, 1H), 7.0 – 6.9 (m, 1H), 6.9 – 6.8 (m, 2H), 6.4 (s, 1H), 6.1 (d, *J* = 5.1 Hz, 1H), 5.2 (d, *J* = 6.1 Hz, 2H), 4.9 (td, *J* = 11.9, 6.9 Hz, 1H), 4.7 (s, 2H), 4.4 (d, *J* = 19.4 Hz, 2H), 4.3 – 4.2 (m,

2H), 3.8 (t, *J* = 5.4 Hz, 2H), 3.8 – 3.7 (m, 2H), 3.6 (d, *J* = 3.0 Hz, 6H), 3.4 (d, *J* = 5.1 Hz, 2H), 2.8 – 2.6 (m, 3H), 2.1 – 2.1 (m, 1H), 2.1 (d, *J* = 5.5 Hz, 3H), 1.9 (dd, *J* = 2.2, 0.7 Hz, 3H). **^{13}C NMR** (101 MHz, $CDCl_3$) δ 172.1 (d, *J* = 2.3 Hz), 169.6, 169.1 (d, *J* = 4.6 Hz), 167.8, 167.6, 166.7, 163.3, 163.1 (dd, *J* = 250.3, 12.1 Hz), 161.6 – 158.9 (m), 160.5, 146.9 (d, *J* = 3.0 Hz), 146.4, 139.0 (d, *J* = 4.1 Hz), 137.7, 136.2, 134.4, 132.6, 131.6 (d, *J* = 5.0 Hz), 131.0, 130.9 – 130.2 (m), 128.9, 128.5 (d, *J* = 5.5 Hz), 126.9, 124.4, 118.7 (d, *J* = 14.6 Hz), 117.0, 112.0 (dd, *J* = 21.4, 3.7 Hz), 111.8, 110.4 (d, *J* = 1.8 Hz), 104.1 (t, *J* = 25.3 Hz), 96.9, 96.2, 70.3 (d, *J* = 5.1 Hz), 69.8 (dd, *J* = 40.1, 11.5 Hz), 69.4, 68.1, 66.3, 64.8, 64.5 (d, *J* = 4.3 Hz), 50.1, 49.0, 42.3, 39.9, 39.8, 31.4, 23.1, 21.6, 17.4. **IR (ATR):** 2969, 1737, 1365, 1217 cm^{-1}. **HRMS (ESI):** calculated for $[C_{45}H_{46}N_8O_{10}BrF_2]^+$: 975.24828, found: 975.24811. **M_p:** 95-111°C.

3-(3-bromo-4-((2,4-difluorobenzyl)oxy)-6-methyl-2-oxopyridin-1(2H)-yl)-N-(17-(2-(2,6-dioxopiperidin-3-yl)-1-oxoisoindolin-4-yl)-3,12-dioxo-7,10-dioxa-4,13-diazaheptadec-16-yn-1-yl)-4-methylbenzamide (5-16)

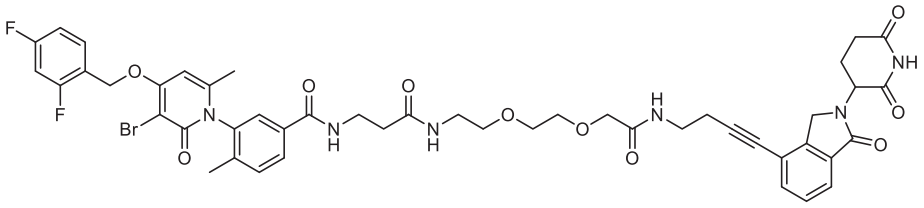

The product was prepared following general method for amide formation 1, using **5-11** (29 mg, 0.04 mmol) and **5-13** (14 mg, 0.04 mmol). The product was purified by silica flash column cromatography, eluted at 7% MeOH/DCM. Reported as a white dense oil (10 mg, **25%**).

^{1}H NMR (400 MHz, $CDCl_3$) δ 7.9 – 7.8 (m, 1H), 7.7 – 7.5 (m, 4H), 7.4 (td, J = 7.6, 1.8 Hz, 1H), 7.4 – 7.3 (m, 2H), 7.1 – 6.9 (m, 1H), 6.9 – 6.8 (m, 1H), 6.8 (s, 1H), 6.2 (d, J = 5.0 Hz, 1H), 5.3 – 5.1 (m, 3H), 4.5 – 4.2 (m, 10H), 3.9 (t, J = 3.5 Hz, 2H), 3.6 – 3.2 (m, 5H), 2.9 – 2.8 (m, 2H), 2.7 (d, J = 9.6 Hz, 2H), 2.6 – 2.3 (m, 3H), 2.1 (s, 3H), 1.9 (d, J = 2.7 Hz, 3H), 1.8 – 1.7 (m, 2H).* **HPLC-MS:** retention time 4.36 min; $[M]^{2+}$ calculated: 486.92, found: 487.0; purity: 76.46%.
*Assignation of the ^{1}H NMR spectra is tentative due to the complexity of the sample.

3-(3-bromo-4-((2,4-difluorobenzyl)oxy)-6-methyl-2-oxopyridin-1(2H)-yl)-N-(3-((3-((3-((2-((2-(2,6-dioxopiperidin-3-yl)-1,3-dioxoisoindolin-4-yl)amino)ethyl)amino)-3-oxopropyl)amino)-3-oxopropyl)amino)-3-oxopropyl)-4-methylbenzamide (5-12)

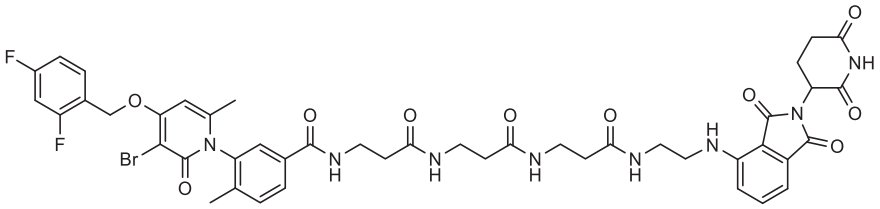

The product was prepared following general method for amide formation 1, using **5-14** (80 mg, 0.12 mmol) and **5-15** (46 mg, 0.13 mmol). The product was purified by silica flash column chromatography, eluted at 8% MeOH/DCM. Reported as a white solid (13 mg, **11%**).

HRMS (ESI): calculated for $[C_{45}H_{46}N_8O_{10}BrF_2]^+$: 9785.24828, found: 975.24756. **IR (ATR):** 1737.8, 1365.4, 1216.8 cm^{-1}. **M_p:** 154-475°C

(2S,4R)-1-((S)-2-(4-(4-(2-(3-(3-bromo-4-((2,4-difluorobenzyl)oxy)-6-methyl-2-oxopyridin-1(2H)-yl)-4-methylbenzamido)ethyl)-1H-1,2,3-triazol-1-yl)butanamido)-3,3-dimethylbutanoyl)-4-hydroxy-N-((S)-1-(4-(4-methylthiazol-5-yl)phenyl)ethyl)pyrrolidine-2-carboxamide (NR-11a)

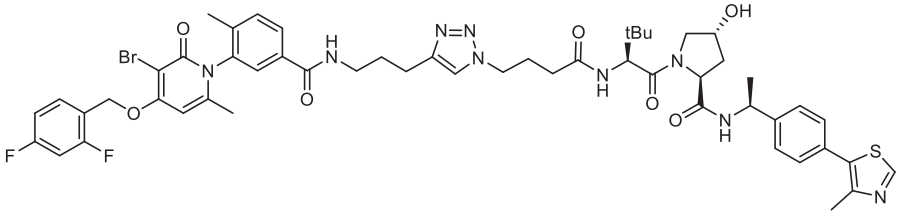

Compound **NR-11a** was prepared following general method for amide formation 1, starting from **5-17** (40 mg, 0.08 mmol) and **3-30a** (43 mg, 0.08 mmol). The crude was purified by flash column chromatography, eluting with 7% MeOH/DCM. **NR-11a** was obtained as a white solid (45 mg, **50%**).

^{1}H NMR (400 MHz, CD_3OD) δ 8.86 (s, 1H), 8.60 – 8.47 (m, 1H), 7.88 (dd, *J* = 12.0, 8.4 Hz, 2H), 7.77 (s, 1H), 7.69 – 7.57 (m, 2H), 7.53 – 7.43 (m, 1H), 7.40 (d, *J* = 1.3 Hz, 4H), 7.10 – 6.98 (m, 2H), 6.65 (s, 1H), 5.34 (s, 2H), 4.98 (dddq, *J* = 9.5, 7.1, 4.8, 2.4, 2.0 Hz, 1H), 4.58 (td, *J* = 8.4, 4.7 Hz, 2H), 4.41 (dt, *J* = 4.2, 2.1 Hz, 1H), 4.37 (t, *J* = 6.8 Hz, 2H), 3.89 (d, *J* = 11.0 Hz, 1H), 3.73 (dd, *J* = 11.0, 3.9 Hz, 1H), 3.39 (d, *J* = 6.9 Hz, 2H), 2.75 (q, *J* = 12.6, 10.0 Hz, 2H), 2.46 (s, 3H), 2.38 – 2.08 (m, 5H), 2.07 (d, *J* = 3.4 Hz, 3H), 2.01 – 1.84 (m, 6H), 1.48 (dd, *J* = 7.0, 2.4 Hz, 3H), 1.10 – 0.95 (m, 9H). **^{13}C NMR** (101 MHz, CD_3OD) δ 172.9, 171.8, 170.9, 167.1, 164.5, 163.4 (d, *J* = 242.2 Hz), 161.0, 160.8 (ddd, *J* = 243.2, 121.2, 12.3 Hz), 151.5, 147.2, 144.2, 139.2, 137.7, 133.8, 131.3, 131.2, 130.1, 129.1, 128.0, 126.6, 126.2, 126.0, 122.4, 119.0 (d, *J* = 14.6 Hz), 111.3 (dd, *J* = 21.7, 3.8 Hz), 103.5 (t, *J* = 25.7 Hz), 97.2, 95.4, 69.6, 64.8 (d, *J* = 3.8 Hz), 59.1, 57.8, 56.6, 49.1, 48.7, 39.0, 37.4, 34.9, 31.5, 28.7, 25.9, 25.7, 22.4, 21.0, 20.0, 15.9, 14.5. **HRMS (ESI):** calculated for $[C_{53}H_{61}O_7N_9BrF_2S]^+$: 1084.35606, found 1084.34834.

(2S,4R)-1-((S)-2-(3-(4-(4-(2-(3-(3-bromo-4-((2,4-difluorobenzyl)oxy)-6-methyl-2-oxopyridin-1(2H)-yl)-4-methylbenzamido)ethyl)-1H-1,2,3-triazol-1-yl)butanamido)propanamido**)-3,3-dimethylbutanoyl)-4-hydroxy-N-((S)-1-(4-(4-methylthiazol-5-yl)phenyl)ethyl)pyrrolidine-2-carboxamide (NR-11b)**

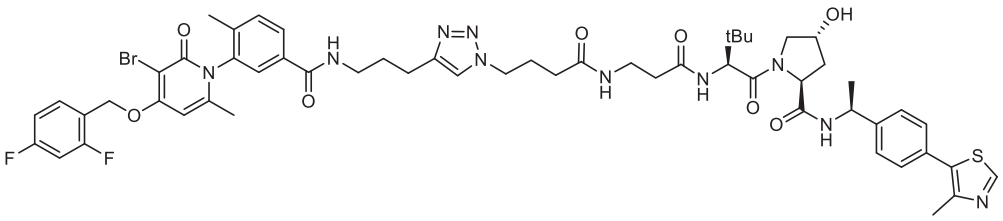

Compound **NR-11b** was prepared following general method for CuAAC, starting **5-17** (40 mg, 0.08 mmol) and **3-32a** (48 mg, 0.08 mmol). The crude was purified by flash column chromatography, eluting with 7% MeOH/DCM. **NR-11b** was obtained as a white solid (57 mg, **62%**).

^{1}H NMR (400 MHz, CD_3OD) δ 8.87 (s, 1H), 7.86 (dt, *J* = 8.0, 1.9 Hz, 1H), 7.79 (s, 1H), 7.70 – 7.59 (m, 2H), 7.50 (d, *J* = 8.0 Hz, 1H), 7.47 – 7.31 (m, 5H), 7.08 – 6.99 (m, 2H), 6.65 (d, *J* = 1.1 Hz, 1H), 5.35 (s, 2H), 4.99 (qd, *J* = 7.0, 2.2 Hz, 1H), 4.63 – 4.52 (m, 2H), 4.39 (q, *J* = 7.1, 6.4 Hz, 3H), 3.93 – 3.84 (m, 1H), 3.76 – 3.66 (m, 1H), 3.49 – 3.32 (m, 4H), 2.76 (t, *J* = 7.4 Hz, 2H), 2.45 (dt, *J* = 6.7, 3.0 Hz, 5H), 2.22 – 1.88 (m, 12H), 1.48 (dd, *J* = 7.0, 2.4 Hz, 3H), 1.02 (s, 9H). **^{13}C NMR** (101 MHz, CD_3OD) δ 173.1, 172.2, 171.8, 170.8, 167.1, 164.5, 163.4 (d, *J* = 241.8 Hz), 161.0, 160.9 (dd, *J* = 243.2, 12.4 Hz), 151.5, 147.2, 144.3, 139.2, 137.7, 133.8, 131.3, 131.3, 131.2, 131.2, 130.1, 129.1, 129.1, 128.0, 126.6, 126.2, 125.9, 122.3, 119.0 (d, *J* = 14.7 Hz), 111.3 (dd, *J* = 21.6, 3.8 Hz), 103.5 (t, *J* = 25.7 Hz), 97.2, 95.4, 69.6, 64.8 (d, *J* = 3.8 Hz), 59.1, 57.8, 56.5, 49.3, 48.7, 39.0, 37.5, 35.7, 34.9, 34.9, 32.1, 28.7, 25.9, 25.7, 22.4, 21.0, 20.0, 15.9, 14.5. **HRMS (ESI):** calculated for $[C_{56}H_{66}O_8N_{10}BrF_2S]^+$: 1155.39318, found 1155.38474.

(2S,4R)-1-((S)-2-(6-(4-(4-(2-(3-(3-bromo-4-((2,4-difluorobenzyl)oxy)-6-methyl-2-oxopyridin-1(2H)-yl)-4-methylbenzamido)ethyl)-1H-1,2,3-triazol-1-yl)butanamido)hexanamido)-3,3-dimethylbutanoyl)-4-hydroxy-N-((S)-1-(4-(4-methylthiazol-5-yl)phenyl)ethyl)pyrrolidine-2-carboxamide (NR-11c)

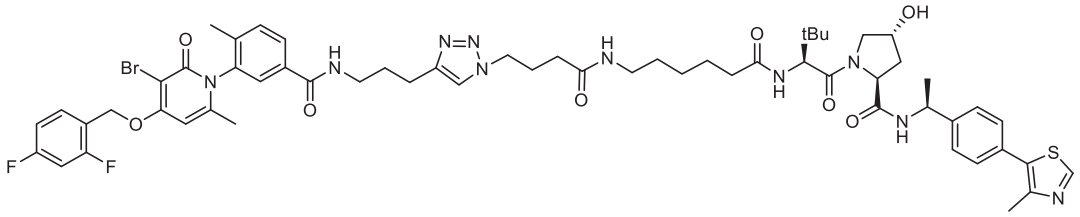

Compound **NR-11c** was prepared following general method for CuAAC, starting **5-17** (35 mg, 0.07 mmol) and **3-32b** (45 mg, 0.07 mmol). The crude was purified by flash column chromatography, eluting with 12% MeOH/DCM. **NR-11c** was obtained as a white solid (48 mg, **57%**).

^{1}H NMR (400 MHz, CD_3OD) δ 8.86 (s, 1H), 7.86 (dt, *J* = 8.0, 1.6 Hz, 1H), 7.77 (s, 1H), 7.71 – 7.58 (m, 2H), 7.51 (d, *J* = 8.1 Hz, 1H), 7.48 – 7.34 (m, 4H), 7.04 (t, *J* = 8.6 Hz, 2H), 6.66 (d, *J* = 1.0 Hz, 1H), 5.35 (s, 2H), 4.99 (q, *J* = 7.0 Hz, 1H), 4.65 – 4.54 (m, 2H), 4.41 (dq, *J* = 4.0, 2.0 Hz, 1H), 4.37 (td, *J* = 5.6, 4.8, 1.8 Hz, 2H), 3.89 – 3.83 (m, 1H), 3.73 (dd, *J* = 11.0, 4.0 Hz, 1H), 3.40 (td, *J* = 6.9, 2.5 Hz, 2H), 3.13 (t, *J* = 7.0 Hz, 2H), 2.76 (t, *J* = 7.5 Hz, 2H), 2.46 (d, *J* = 6.6 Hz, 3H), 2.26 (p, *J* = 7.2 Hz, 3H), 2.16 (dt, *J* = 5.9, 2.8 Hz, 4H), 2.08 (s, 3H), 2.02 – 1.90 (m, 6H), 1.60 (dt, *J* = 15.3, 7.6 Hz, 2H), 1.53 – 1.43 (m, 5H), 1.42 – 1.25 (m, 2H), 1.01 (d, *J* = 9.7 Hz, 9H). **^{13}C NMR** (101 MHz, CD_3OD) δ 174.4, 172.9, 171.8, 170.9, 167.1, 164.5, 163.5 (d, *J* = 241.6 Hz), 161.0, 160.9 (dd, *J* = 243.5, 12.9 Hz), 151.4, 147.2, 147.0, 144.3, 139.2, 137.7, 133.8, 131.4, 131.3, 131.2, 130.1, 129.1, 128.0, 126.6, 126.2, 122.1, 119.0 (d, *J* = 14.6 Hz), 112.0 – 109.9, 103.5 (t, *J* = 25.7 Hz), 97.2, 95.4, 69.5, 64.8 (d, *J* = 3.8 Hz), 59.1, 57.6, 56.6, 49.2, 48.7, 38.9, 38.9, 37.4, 35.1, 35.0, 32.1, 28.7, 28.6, 26.2, 26.0, 25.7, 25.2, 22.4, 21.0, 20.0, 15.9, 14.4. **HRMS (ESI):** calculated for $[C_{59}H_{72}O_8N_{10}BrF_2S]+$: 1197.44013, found 1197.43677.

(2S,4S)-1-((S)-2-(6-(4-(4-(3-(3-(3-bromo-4-((2,4-difluorobenzyl)oxy)-6-methyl-2-oxopyridin-1(2H)-yl)-4-methylbenzamido)propyl)-1H-1,2,3-triazol-1-yl)butanamido)hexanamido)-3,3-dimethylbutanoyl)-4-hydroxy-N-((S)-1-(4-(4-methylthiazol-5-yl)phenyl)ethyl)pyrrolidine-2-carboxamide (NR-11c*)

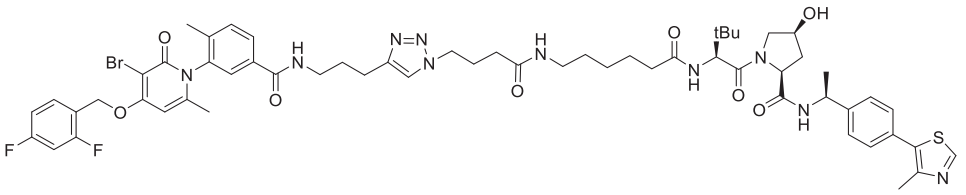

NR-11c* was prepared following general method for CuAAC, starting from **5-17** (10 mg, 0.019 mmol) and **3-32b*** (12 mg, 0.019 mmol). The crude was purified by flash column chromatography, eluting with 11% MeOH/DCM. **NR-11c*** was obtained as a white solid (12.5 mg, **55%**).

HRMS (ESI): calculated for $[C_{59}H_{72}O_8N_{10}BrF_2S]^+$: 1197.44013, found 1197.43914.

(2S,4R)-1-((S)-2-(4-(4-(3-(4-(3-(3-(3-bromo-4-((2,4-difluorobenzyl)oxy)-6-methyl-2-oxopyridin-1(2H)-yl)-4-methylbenzamido)propyl)-1H-1,2,3-triazol-1-yl)propyl)piperazin-1-yl)butanamido)-3,3-dimethylbutanoyl)-4-hydroxy-N-((S)-1-(4-(4-methylthiazol-5-yl)phenyl)ethyl**)pyrrolidine-2-carboxamide (12a)**

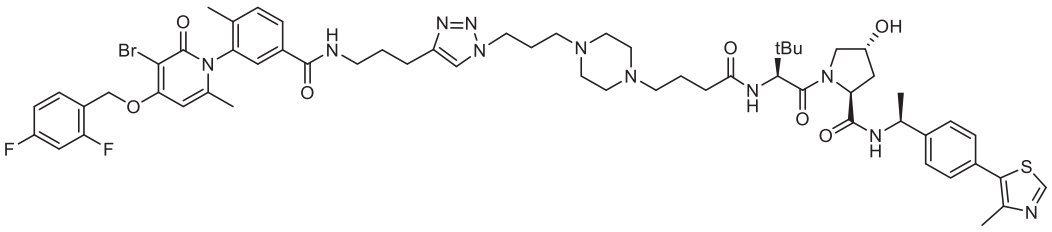

12a was prepared following general method for CuAAC, starting from **5-17** (39 mg, 0.07 mmol) and **5-26** (50 mg, 0.07 mmol). The crude was purified by flash column chromatography, eluting with 13% MeOH/DCM. The product was reported as a white solid (15 mg, **18%**).

^{1}H NMR (400 MHz, CD_3OD) δ 8.87 (s, 1H), 7.71 – 7.61 (m, 1H), 7.57 – 7.47 (m, 2H), 7.46 – 7.38 (m, 4H), 7.26 (d, *J* = 1.7 Hz, 1H), 7.10 – 7.01 (m, 2H), 6.66 (s, 1H), 5.36 (s, 2H), 5.00 (q, *J* = 7.0 Hz, 1H), 4.58 (t, *J* = 8.3 Hz, 1H), 4.44 (s, 1H), 4.33 (s, 1H), 4.11 (t, *J* = 6.3 Hz, 2H), 3.86 (d, *J* = 11.0 Hz, 1H), 3.74 (dd, *J* = 10.9, 4.1 Hz, 1H), 3.66 – 3.50 (m, 4H), 2.67 – 2.28 (m, 15H), 2.25 – 2.14 (m, 1H), 2.08 (s, 3H), 2.01 (s, 4H), 1.86 (q, *J* = 7.4, 6.9 Hz, 2H), 1.69 – 1.54 (m, 4H), 1.50 (d, *J* = 7.0 Hz, 3H), 1.38 (p, *J* = 7.8 Hz, 2H), 1.03 (s, 9H). **HPLC-MS:** retention time 4.797 min; $[M+2]^{2+}$ calculated: 606.64, found: 605.6; purity: 95.94%. **HRMS (ESI):** calculated for $[C_{60}H_{76}O_7N_{11}BrF_2S]^{2+}$: 605.73952, found 605.74069.

(2S,4R)-1-((S)-2-((3-(4-((1-(3-(4-(3-(3-bromo-4-((2,4-difluorobenzyl)oxy)-6-methyl-2-oxopyridin-1(2H)-yl)-4-methylbenzoyl)piperazin-1-yl)propyl)-1H-1,2,3-triazol-4-yl)methyl)piperazin-1-yl)propyl)amino)-3,3-dimethylbutanoyl)-4-hydroxy-N-((S)-1-(4-(4-methylthiazol-5-yl)phenyl)ethyl)pyrrolidine-2-carboxamide (12b)

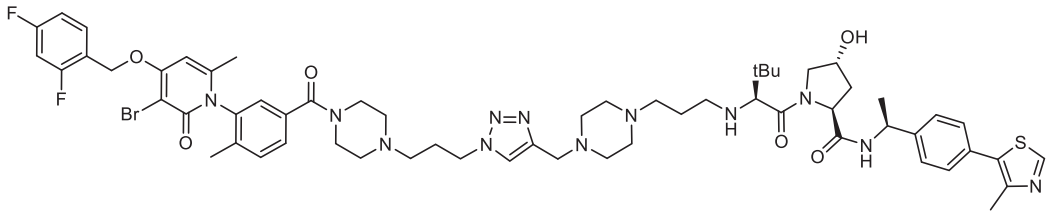

12a was prepared following general method for CuAAC, starting from **5-33** (12 mg, 0.02 mmol) and **5-34** (12 mg, 0.02 mmol). The crude was purified by flash column chromatography, eluting with 20% MeOH/DCM. The product was reported as a white solid film (3 mg, **12%**).

^{1}H NMR (400 MHz, $CDCl_3$) δ 7.6 (q, J = 7.7 Hz, 1H), 7.5 – 7.5 (m, 2H), 7.5 – 7.3 (m, 6H), 7.2 – 7.1 (m, 1H), 7.0 (t, J = 8.5 Hz, 1H), 6.9 – 6.9 (m, 1H), 6.4 (t, J = 9.4 Hz, 2H), 6.1 (s, 1H), 5.3 (s, 2H), 5.1 (p, J = 7.1 Hz, 1H), 4.7 – 4.6 (m, 1H), 4.6 (d, J = 8.8 Hz, 1H), 4.5 (s, 1H), 4.4 (t, J = 6.3 Hz, 2H), 4.0 (d, J = 11.3 Hz, 1H), 3.8 – 3.5 (m, 3H), 3.2 (q, J = 6.4 Hz, 2H), 2.5 (s, 6H), 2.3 – 2.0 (m, 11H), 1.9 (s, 3H), 1.7 – 1.5 (m, 2H), 1.5 – 1.4 (m, 5H), 1.4 – 1.1 (m, 8H), 1.1 – 0.9 (m, 9H).*

*Assignation of the ^{1}H NMR spectra is tentative due to the complexity of the sample.

(2S,4R)-1-((S)-2-(6-(4-(4-((4-(3-(3-bromo-4-((2,4-difluorobenzyl)oxy)-6-methyl-2-oxopyridin-1(2H)-yl)-4-methylbenzoyl)piperazin-1-yl)methyl)-1H-1,2,3-triazol-1-yl)butanamido)hexanamido)-3,3-dimethylbutanoyl)-4-hydroxy-N-((S)-1-(4-(4-methylthiazol-5-yl)phenyl)ethyl)pyrrolidine-2-carboxamide (12c)

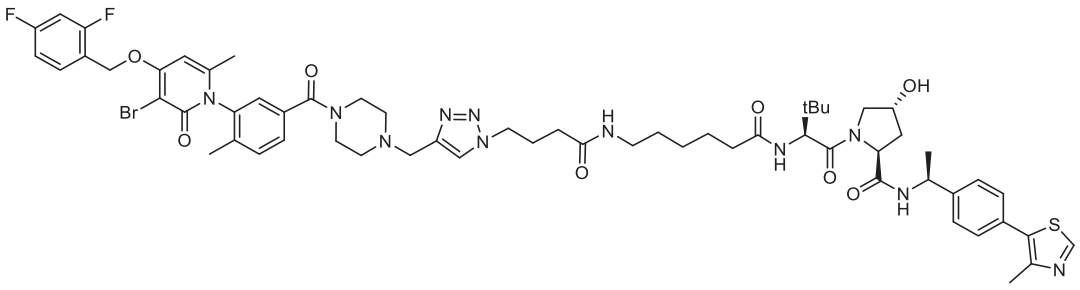

12c was prepared following general method for CuAAC, starting from **5-22** (18 mg, 0.03 mmol) and **3-32b** (18 mg, 0.03 mmol). The crude was purified by flash column chromatography, eluting with 12% MeOH/DCM. The product was reported as a white solid (27 mg, **78%**).

^{1}H NMR (500 MHz, $CDCl_3$) δ 8.66 (s, 1H), 7.63 – 7.49 (m, 3H), 7.38 (dd, *J* = 11.9, 2.9 Hz, 6H), 7.11 (d, *J* = 7.4 Hz, 1H), 7.00 – 6.93 (m, 1H), 6.87 (ddd, *J* = 10.9, 8.8, 2.5 Hz, 1H), 6.54 (d, *J* = 8.1 Hz, 1H), 6.46 (t, *J* = 10.0 Hz, 1H), 6.14 (s, 1H), 5.25 (s, 2H), 5.08 (p, *J* = 7.0 Hz, 1H), 4.66 (td, *J* = 8.1, 4.0 Hz, 1H), 4.58 (d, *J* = 8.9 Hz, 1H), 4.47 (s, 1H), 4.40 (s, 2H), 4.03 (d, *J* = 11.3 Hz, 1H), 3.92 – 3.39 (m, 5H), 3.15 (q, *J* = 6.5 Hz, 2H), 2.62 – 2.03 (m, 20H), 1.92 (s, 3H), 1.71 – 1.52 (m, 2H), 1.51 – 1.37 (m, 5H), 1.24 (s, 2H), 1.01 (s, 9H).

(2S,4R)-1-((S)-2-(4-(4-(3-(4-((4-(3-(3-bromo-4-((2,4-difluorobenzyl)oxy)-6-methyl-2-oxopyridin-1(2H)-yl)-4-methylbenzoyl)piperazin-1-yl)methyl)-1H-1,2,3-triazol-1-yl)propyl)piperazin-1-yl)butanamido)-3,3-dimethylbutanoyl)-4-hydroxy-N-((S)-1-(4-(4-methylthiazol-5-yl)phenyl)ethyl)pyrrolidine-2-carboxamide (12d)

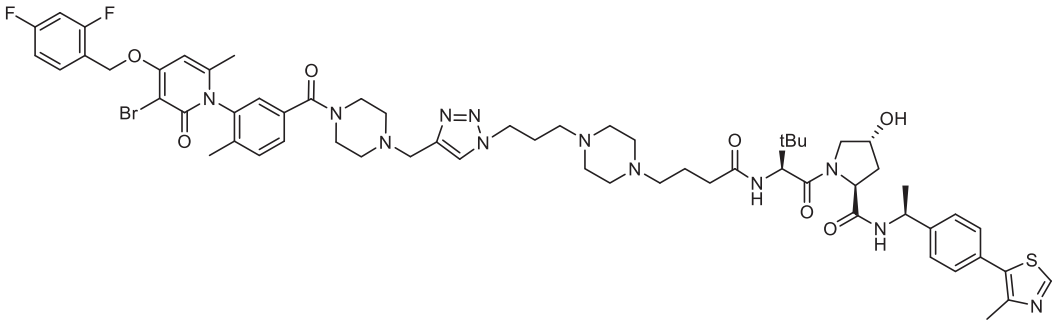

12d was prepared following general method for CuAAC, starting from **5-22** (10 mg, 0.015 mmol) and **5-26** (8.3 mg, 0.015 mmol). The crude was purified by flash column chromatography, eluting with 14% MeOH/DCM. The product was reported as a white solid (16 mg, **87%**).

^{1}H NMR (400 MHz, $CDCl_3$) δ 8.6 (s, 1H), 7.8 (s, 1H), 7.6 – 7.5 (m, 1H), 7.5 – 7.3 (m, 6H), 7.1 (s, 1H), 7.1 – 7.0 (m, 1H), 6.9 (ddd, J = 10.2, 8.7, 2.5 Hz, 1H), 6.2 (d, J = 0.8 Hz, 1H), 5.5 (s, 2H), 5.3 (s, 2H), 5.1 (q, J = 6.7 Hz, 1H), 4.8 (t, J = 8.5 Hz, 1H), 4.6 (s, 1H), 4.4 (d, J = 6.1 Hz, 3H), 4.0 (d, J = 11.3 Hz, 1H), 3.8 (s, 2H), 3.6 – 3.5 (m, 4H), 2.9 (s, 6H), 2.5 (s, 7H), 2.4 – 2.1 (m, 8H), 2.1 – 2.0 (m, 5H), 1.9 (s, 3H), 1.2 (s, 8H), 1.1 (s, 9H).* **HPLC-MS:** retention time 4.73 min; $[M]^{2+}$ calculated: 626.17, found: 626.1; purity: 95.16%. **HRMS (ESI):** calculated for $[C_{62}H_{78}O_7N_{12}BrF_2S]^+$: 1251.49831, found: 1251.49725.
*Assignation of the ^{1}H NMR spectra is tentative due to the complexity of the sample.

(2S,4R)-1-((S)-2-(2-(4-(3-(4-(4-(4-(3-(3-bromo-4-((2,4-difluorobenzyl)oxy)-6-methyl-2-oxopyridin-1(2H)-yl)-4-methylbenzoyl)piperazin-1-yl)but-2-yn-1-yl)piperazin-1-yl)-3-oxopropyl)-1H-1,2,3-triazol-1-yl)acetamido)-3,3-dimethylbutanoyl)-4-hydroxy-N-((S)-1-(4-(4-methylthiazol-5-yl)phenyl)ethyl)pyrrolidine-2-carboxamide (12e)

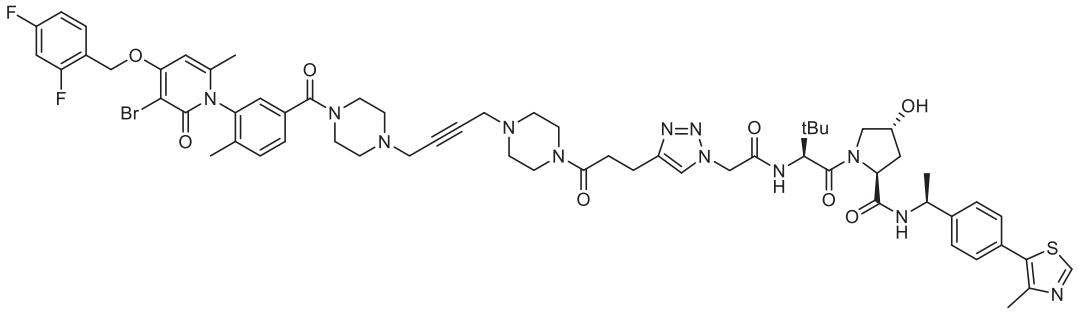

12e was prepared following general method for CuAAC, starting from **5-28** (10 mg, 0.014 mmol) and **4-16** (7.4 mg, 0.014 mmol). The crude was purified by flash column chromatography, eluting with 15% MeOH/DCM. The product was reported as a white solid (5 mg, **29%**).

HRMS (ESI): calc. for $[C_{63}H_{74}O_8N_{12}BrF_2S]^+$: 1277.46192, found 1277.4623. **HPLC-MS:** retention time 4.64 min; $[M]^{2+}$ calculated: 638.15, found: 638.2; purity: 78.5%.

(2S,4R)-1-((S)-2-(2-(4-(5-(4-((4-(3-(3-bromo-4-((2,4-difluorobenzyl)oxy)-6-methyl-2-oxopyridin-1(2H)-yl)-4-methylbenzoyl)piperazin-1-yl)sulfonyl)piperazin-1-yl)-5-oxopentyl)-1H-1,2,3-triazol-1-yl)acetamido)-3,3-dimethylbutanoyl)-4-hydroxy-N-((S)-1-(4-(4-methylthiazol-5-yl)phenyl)ethyl)pyrrolidine-2-carboxamide (13a)

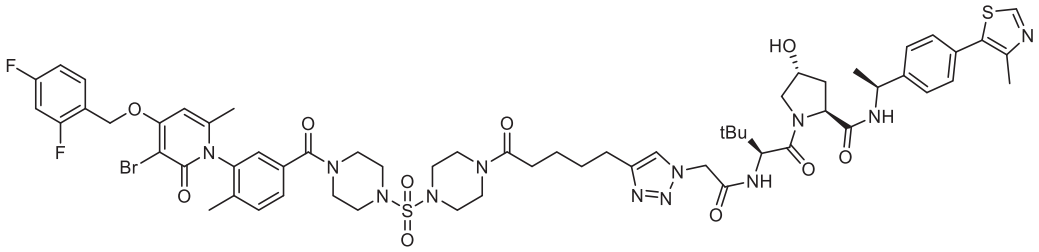

13a was prepared following general method for CuAAC, starting from **5-38a** (12 mg, 0.015 mmol) and **4-16** (8 mg, 0.015 mmol). The crude was purified by flash column chromatography, eluting at 14% MeOH/DCM. The product was reported as a white solid (9 mg, **46%**).

^{1}H NMR (400 MHz, CD_3OD) δ 8.87 (s, 1H), 7.76 (d, *J* = 1.6 Hz, 1H), 7.65 (dt, *J* = 8.9, 7.3 Hz, 1H), 7.57 – 7.47 (m, 2H), 7.45 – 7.37 (m, 4H), 7.31 (dd, *J* = 5.5, 1.6 Hz, 1H), 7.11 – 7.00 (m, 2H), 6.66 (s, 1H), 5.36 (s, 2H), 5.27 – 5.13 (m, 2H), 5.00 (q, *J* = 7.0 Hz, 1H), 4.58 – 4.50 (m, 1H), 4.41 (s, 1H), 3.88 – 3.43 (m, 10H), 3.36 – 3.09 (m, 8H), 2.74 (t, *J* = 7.2 Hz, 2H), 2.48 (s, 3H), 2.42 (q, *J* = 7.8 Hz, 2H), 2.16 (s, 1H), 2.08 (s, 3H), 2.01 (s, 3H), 1.97 – 1.86 (m, 1H), 1.73 (q, *J* = 7.4 Hz, 2H), 1.63 (p, *J* = 7.3 Hz, 2H), 1.50 (d, *J* = 7.0 Hz, 3H), 1.06 (s, 9H). **HRMS (ESI):** calc. for $[C_{61}H_{74}O_{10}N_{12}BrF_2S_2]^+$: 1315.42759, found 1315.42382. **HPLC-MS:** retention time 4.96 min; $[M]^{2+}$ calculated: 658.18, found: 658.1; purity: 99.14%.

(2S,4R)-1-((S)-2-(4-(4-((4-((4-(3-(3-bromo-4-((2,4-difluorobenzyl)oxy)-6-methyl-2-oxopyridin-1(2H)-yl)-4-methylbenzoyl)piperazin-1-yl)sulfonyl)piperazin-1-yl)methyl)-1H-1,2,3-triazol-1-yl)butanamido)-3,3-dimethylbutanoyl)-4-hydroxy-N-((S)-1-(4-(4-methylthiazol-5-yl)phenyl)ethyl)pyrrolidine-2-carboxamide (13b)

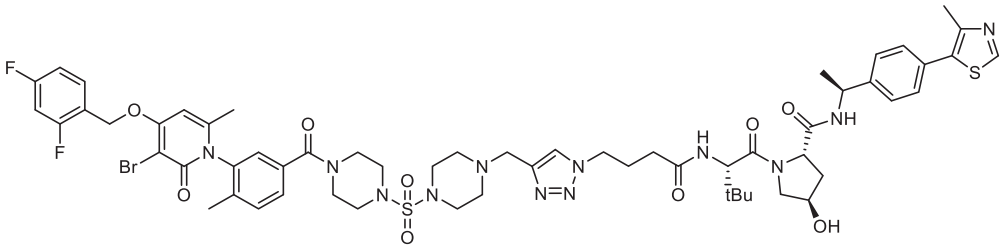

13b was prepared following general method for CuAAC, starting from **5-38b** (15 mg, 0.02 mmol) and **3-30a** (1mg, 0.02 mmol). The crude was purified by flash column chromatography, eluting at 14% MeOH/DCM. The product was reported as a white solid (9 mg, **35%**).

HRMS (ESI): calc. for $[C_{59}H_{72}O_9N_{12}BrF_2S_2]^+$: 1273.41382, found 1273.41326.

(2S,4S)-1-((S)-2-(6-(4-(3-((4-(3-(3-bromo-4-((2,4-difluorobenzyl)oxy)-6-methyl-2-oxopyridin-1(2H)-yl)-4-methylbenzoyl)piperazine)-1-sulfonamido)propyl)-1H-1,2,3-triazol-1-yl)hexanamido)-3,3-dimethylbutanoyl)-4-hydroxy-N-((S)-1-(4-(4-methylthiazol-5-yl)phenyl)ethyl)pyrrolidine-2-carboxamide (13c)

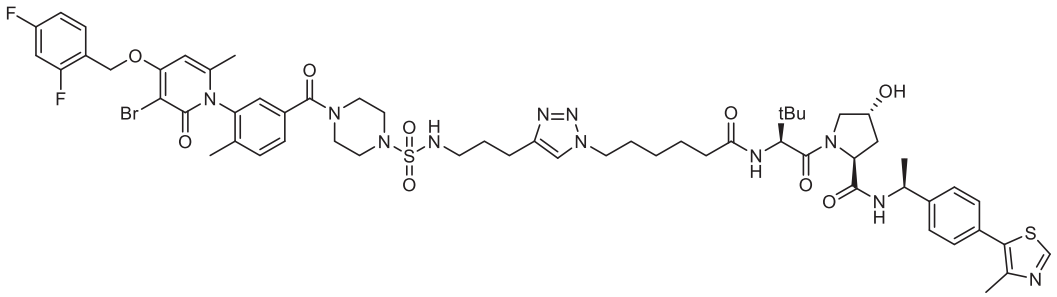

13c was prepared following general method for CuAAC, starting from **5-38c** (26 mg, 0.038 mmol) and **3-30b** (23 mg, 0.038 mmol). The crude was purified by flash column chromatography, eluting at 8% MeOH/DCM. The product was reported as a white solid (30mg, **63%**).

^{1}H NMR (400 MHz, $CDCl_3$) δ 8.66 (s, 1H), 7.64 – 7.37 (m, 2H), 7.49 – 7.33 (m, 6H), 6.97 (t, *J* = 8.3 Hz, 1H), 6.92 – 6.83 (m, 1H), 6.70 (t, *J* = 8.9 Hz, 1H), 6.35 – 6.17 (m, 1H), 6.15 (s, 1H), 5.25 (s, 2H), 5.09 (p, *J* = 7.1 Hz, 1H), 4.64 (q, *J* = 8.2 Hz, 1H), 4.55 – 4.45 (m, 2H), 4.28 (t, *J* = 6.7 Hz, 2H), 4.11 (dd, *J* = 7.1, 1.2 Hz, 1H), 3.97 (d, *J* = 11.2 Hz, 1H), 3.60 (d, *J* = 11.2 Hz, 4H), 3.09 (dq, *J* = 24.5, 6.5 Hz, 6H), 2.78 (tt, *J* = 15.2, 7.8 Hz, 2H), 2.51 (d, *J* = 1.1 Hz, 3H), 2.29 (td, *J* = 8.6, 4.2 Hz, 1H), 2.23 – 2.01 (m, 6H), 2.01 – 1.75 (m, 9H), 1.60 – 1.42 (m, 5H), 0.99 (s, 9H). **HRMS (ESI):** calc. for $[C_{59}H_{73}O_9N_{11}BrF_2S_2]^+$: 1260.42, found 1260.41801. **HPLC-MS:** retention time 4.98 min; $[M]^{2+}$ calculated: 630.6, found: 630.6; purity: 98.2%.

(2S,4R)-1-((S)-2-(2-(4-((4-(3-(4-(3-(3-bromo-4-((2,4-difluorobenzyl)oxy)-6-methyl-2-oxopyridin-1(2H)-yl)-4-methylbenzoyl)piperazin-1-yl)propyl)piperidin-1-yl)methyl)-1H-1,2,3-triazol-1-yl)acetamido)-3,3-dimethylbutanoyl)-4-hydroxy-N-((S)-1-(4-(4-methylthiazol-5-yl)phenyl)ethyl)pyrrolidine-2-carboxamide (NR-14a)

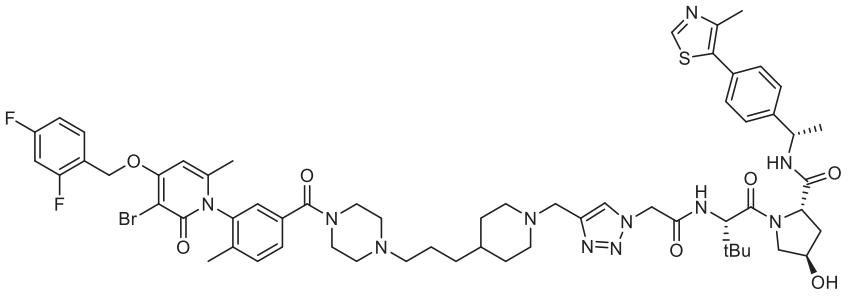

14a was prepared following general method for CuAAC, starting from **5-32a** (30 mg, 0.044 mmol) and **4-16** (23 mg, 0.044 mmol). After work-up, the reaction crude was used in cellular assays without further purification.

^{1}H NMR (400 MHz, $CDCl_3$) δ 8.6 (s, 1H), 7.6 (ddd, J = 12.4, 9.3, 5.2 Hz, 2H), 7.4 – 7.3 (m, 6H), 7.2 – 7.1 (m, 3H), 7.0 – 6.9 (m, 2H), 6.9 – 6.8 (m, 1H), 6.2 (s, 1H), 5.3 (s, 2H), 5.1 (s, 2H), 4.5 (d, J = 61.1 Hz, 3H), 4.2 – 3.2 (m, 8H), 2.9 (d, J = 11.2 Hz, 2H), 2.8 – 2.3 (m, 9H), 2.3 – 1.9 (m, 11H), 1.7 (d, J = 10.6 Hz, 2H), 1.6 – 1.3 (m,

9H), 1.1 – 0.9 (m, 9H).* **HPLC-MS:** retention time 4.95 min; $[M]^{2+}$ calculated: 611.65, found: 611.5; purity: 62.19%.
*Assignation of the ^{1}H NMR spectra is tentative due to the complexity of the spectra.

(2S,4R)-1-((S)-2-(4-(4-((4-(3-(4-(3-(3-bromo-4-((2,4-difluorobenzyl)oxy)-6-methyl-2-oxopyridin-1(2H)-yl)-4-methylbenzoyl)piperazin-1-yl)propyl)piperidin-1-yl)methyl)-1H-1,2,3-triazol-1-yl)butanamido)-3,3-dimethylbutanoyl)-4-hydroxy-N-((S)-1-(4-(4-methylthiazol-5-yl)phenyl)ethyl)pyrrolidine-2-carboxamide (NR-14b)

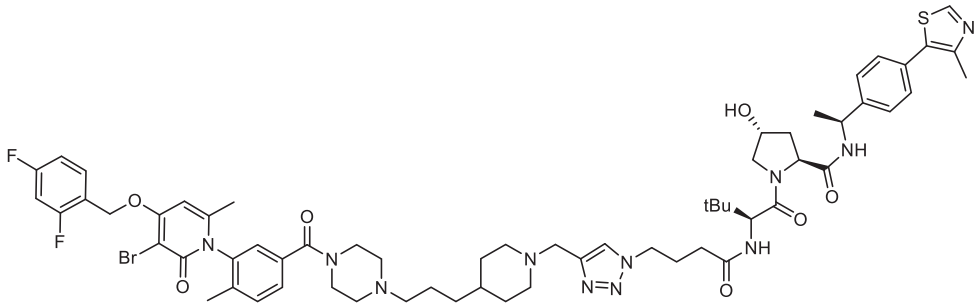

14b was prepared following general method for CuAAC, starting from **5-32a** (42 mg, 0.062 mmol) and **3-30a** (34 mg, 0.062 mmol). The crude was purified by flash column chromatography, eluting at 12% MeOH/DCM. The product was reported as a white solid (29 mg, **38%**).

HRMS (ESI): calc. for $[C_{63}H_{79}O_7N_{11}BrF_2S]^+$: 1250.50562, found 1250.50306. **HPLC-MS:** retention time 4.96 min; $[M]^{2+}$ calculated: 625.68, found: 625.6; purity: 90.04%.

(2S,4R)-1-((S)-2-(4-(4-((4-((4-(3-(3-bromo-4-((2,4-difluorobenzyl)oxy)-6-methyl-2-oxopyridin-1(2H)-yl)-4-methylbenzoyl)piperazin-1-yl)methyl)piperidin-1-yl)methyl)-1H-1,2,3-triazol-1-yl)butanamido)-3,3-dimethylbutanoyl)-4-hydroxy-N-((S)-1-(4-(4-methylthiazol-5-yl)phenyl)ethyl)pyrrolidine-2-carboxamide (NR-14c)

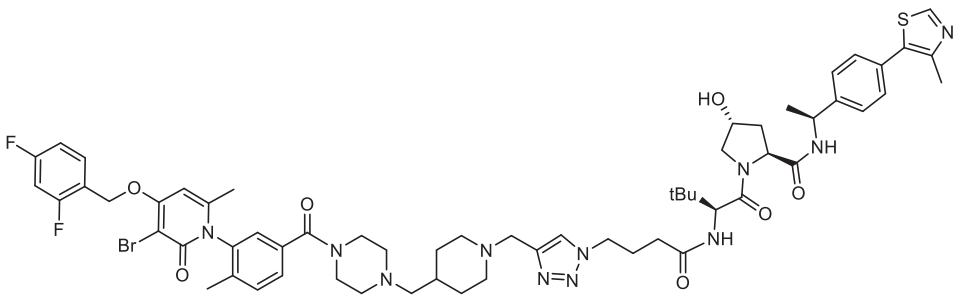

14c was prepared following general method for CuAAC, starting from **5-32b** (35 mg, 0.052 mmol) and **3-30a** (29 mg, 0.052 mmol). After work-up, the reaction crude was used in cellular assays without further purification. Posar el pes? donar alguna explicació més?

^{1}H NMR (400 MHz, $CDCl_3$) δ 8.7 (s, 1H), 7.6 (td, J = 8.5, 6.3 Hz, 1H), 7.5 – 7.3 (m, 6H), 7.1 – 7.1 (m, 1H), 7.0 – 6.9 (m, 1H), 6.9 (ddd, J = 10.1, 8.7, 2.5 Hz, 1H), 6.8 – 6.7 (m, 1H), 6.1 (d, J = 2.2 Hz, 1H), 5.3 (s, 2H), 5.1 (p, J = 7.0 Hz, 1H), 4.8 (t, J = 8.1 Hz, 1H), 4.5 (d, J = 7.7 Hz, 2H), 4.4 – 4.3 (m, 2H), 4.1 (d, J = 11.3 Hz, 1H), 3.9 – 3.3 (m, 7H), 3.1 (d, J = 13.4 Hz, 2H), 2.6 – 2.0 (m, 14H), 1.9 (s, 3H), 1.8 (d, J = 12.7 Hz, 2H), 1.5 (d, J = 6.9 Hz, 5H), 1.3 (s, 8H), 1.0 (s, 9H).* **HPLC-MS:** retention time 4.85 min; $[M]^{2+}$ calculated: 611.65, found: 611.6; purity: 94.65%.
*Assignation of the ^{1}H NMR spectra is tentative due to the complexity of the spectra.

(2S,4R)-1-((S)-2-(6-(4-((4-((4-(3-(3-bromo-4-((2,4-difluorobenzyl)oxy)-6-methyl-2-oxopyridin-1(2H)-yl)-4-methylbenzoyl)piperazin-1-yl)methyl)piperidin-1-yl)methyl)-1H-1,2,3-triazol-1-yl)hexanamido)-3,3-dimethylbutanoyl)-4-hydroxy-N-((S)-1-(4-(4-methylthiazol-5-yl)phenyl)ethyl)pyrrolidine-2-carboxamide (NR-14d)

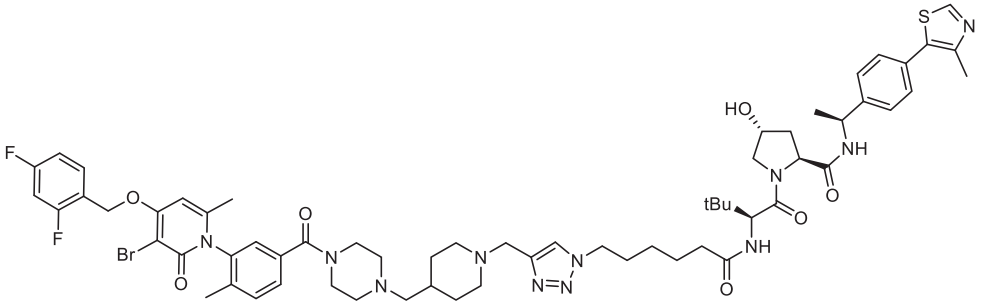

14d was prepared following general method for CuAAC, starting from **5-32b** (23 mg, 0.034 mmol) and **3-30b** (20 mg, 0.034 mmol). After work-up, the reaction crude was used in cellular assays without further purification.

^{1}H NMR (400 MHz, $CDCl_3$) δ 8.7 (s, 1H), 7.7 – 7.5 (m, 2H), 7.5 – 7.3 (m, 6H), 7.1 – 7.1 (m, 1H), 7.0 (dddd, J = 9.1, 8.1, 2.4, 1.1 Hz, 1H), 6.9 (ddd, J = 10.2, 8.7, 2.5 Hz, 1H), 6.1 (d, J = 0.9 Hz, 1H), 5.3 (s, 2H), 5.1 (p, J = 7.0 Hz, 1H), 4.7 (t, J = 7.9 Hz, 1H), 4.6 (d, J = 8.9 Hz, 1H), 4.5 (s, 1H), 4.3 (hept, J = 6.9 Hz, 2H), 4.0 (d, J = 11.2 Hz, 1H), 3.8 – 3.3 (m, 8H), 3.0 (d, J = 11.2 Hz, 2H), 2.5 – 2.0 (m, 21H), 1.9 (d, J = 0.8 Hz, 3H), 1.9 – 1.7 (m, 2H), 1.6 (ddp, J = 21.9, 14.6, 7.2 Hz, 1H), 1.5 – 1.4 (m, 3H), 1.3 – 1.3 (m, 2H), 1.0 (s, 9H).* **HPLC-MS:** retention time 4.92 min; $[M]^{2+}$ calculated: 625.68, found: 625.6; purity: 93.50%.
*Assignation of the ^{1}H NMR spectra is tentative due to the complexity of the spectra.

(2S,4R)-1-((S)-2-(4-(4-((4-(4-(3-(3-bromo-4-((2,4-difluorobenzyl)oxy)-6-methyl-2-oxopyridin-1(2H)-yl)-4-methylbenzoyl)piperazin-1-yl)piperidin-1-yl)methyl)-1H-1,2,3-triazol-1-yl)butanamido)-3,3-dimethylbutanoyl)-4-hydroxy-N-((S)-1-(4-(4-methylthiazol-5-yl)phenyl)ethyl)pyrrolidine-2-carboxamide (NR-14e)

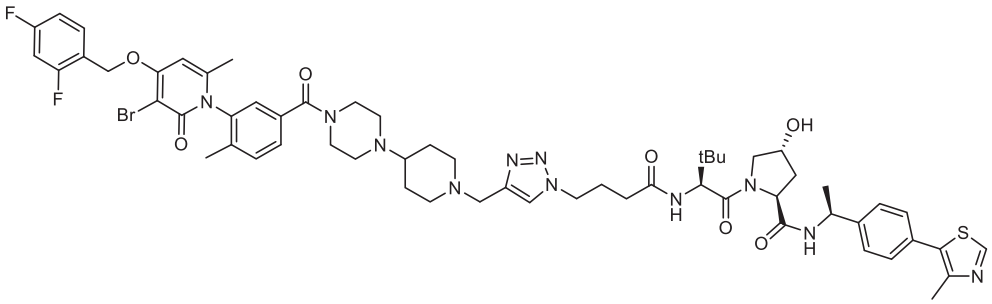

14e was prepared following general method for CuAAC, starting from **5-32c** (23 mg, 0.034 mmol) and **3-30a** (19 mg, 0.034 mmol). After work-up, the reaction crude was used in cellular assays without further purification.

^{1}H NMR (400 MHz, $CDCl_3$) δ 8.7 (d, J = 1.2 Hz, 1H), 7.7 – 7.5 (m, 2H), 7.5 – 7.3 (m, 6H), 7.1 (dt, J = 3.9, 1.7 Hz, 1H), 7.0 – 6.9 (m, 1H), 6.9 (ddd, J = 10.0, 8.8, 2.5 Hz, 1H), 6.7 (d, J = 8.4 Hz, 1H), 6.2 – 6.1 (m, 1H), 5.2 (s, 2H), 5.1 – 5.0 (m, 1H), 4.7 (q, J = 7.6 Hz, 1H), 4.5 – 4.5 (m, 2H), 4.4 (tq, J = 14.1, 7.3 Hz, 1H), 4.1 (dd, J = 17.8, 11.2 Hz, 1H), 3.9 – 3.3 (m, 7H), 3.0 (d, J = 10.7 Hz, 2H), 2.6 – 2.4 (m, 7H), 2.4 – 2.0 (m, 13H), 2.0 – 1.8 (m, 4H), 1.8 (d, J = 12.2 Hz, 2H), 1.6 (q, J = 13.3 Hz, 2H), 1.5 (d, J = 6.9 Hz, 3H), 1.0 (s, 9H).* **HPLC-MS:** retention time 4.71 min; $[M]^{2+}$ calculated: 604.64, found: 604.6; purity: 64.47%.
*Assignation of the ^{1}H NMR spectra is tentative due to the complexity of the spectra.

(2S,4R)-1-((S)-2-(6-(4-((4-(4-(3-(3-bromo-4-((2,4-difluorobenzyl)oxy)-6-methyl-2-oxopyridin-1(2H)-yl)-4-methylbenzoyl)piperazin-1-yl)piperidin-1-yl)methyl)-1H-1,2,3-triazol-1-yl)hexanamido)-3,3-dimethylbutanoyl)-4-hydroxy-N-((S)-1-(4-(4-methylthiazol-5-yl)phenyl)ethyl)pyrrolidine-2-carboxamide (NR-14f)

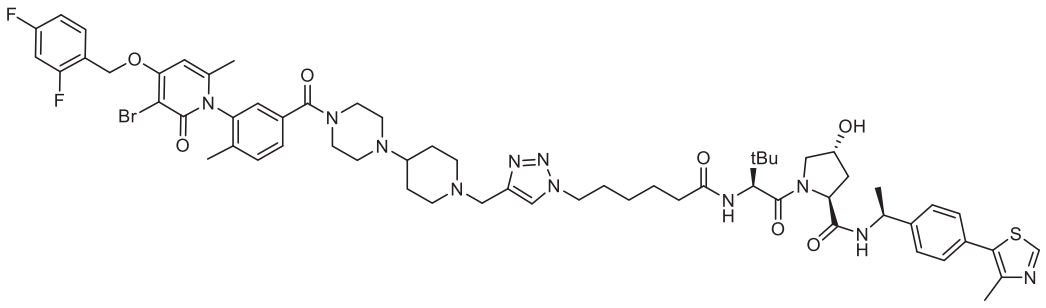

14f was prepared following general method for CuAAC, starting from **5-32c** (23 mg, 0.034 mmol) and **3-30b** (20 mg, 0.034 mmol). After work-up, the reaction crude was used in cellular assays without further purification.

1H NMR (400 MHz, $CDCl_3$) δ 8.6 (d, J = 1.1 Hz, 1H), 7.6 – 7.5 (m, 2H), 7.4 – 7.3 (m, 6H), 7.1 – 7.0 (m, 1H), 7.0 – 6.9 (m, 1H), 6.9 (ddd, J = 10.1, 8.7, 2.5 Hz, 1H), 6.3 – 6.1 (m, 1H), 5.2 (s, 2H), 5.0 (q, J = 6.6 Hz, 1H), 4.7 –

4.5 (m, 2H), 4.4 (s, 1H), 4.3 (t, J = 6.9 Hz, 1H), 4.0 (dd, J = 11.5, 6.8 Hz, 1H), 3.8 – 3.3 (m, 6H), 3.0 (d, J = 11.3 Hz, 1H), 2.7 – 2.1 (m, 21H), 2.1 – 2.0 (m, 5H), 1.9 – 1.8 (m, 5H), 1.8 (d, J = 11.5 Hz, 1H), 1.6 (ddd, J = 23.8, 17.0, 10.0 Hz, 4H), 1.5 (d, J = 6.9 Hz, 3H), 1.0 (d, J = 4.3 Hz, 8H).* **HPLC-MS:** retention time 4.78 min; $[M]^{2+}$ calculated: 618.66, found: 618.6; purity: 70.44%.
*Assignation of the ^{1}H NMR spectra is tentative due to the complexity of the spectra.

1-((4-(3-(4-(3-(3-bromo-4-((2,4-difluorobenzyl)oxy)-6-methyl-2-oxopyridin-1(2H)-yl)-4-methylbenzoyl**)piperazin-1-yl)propyl)piperidin-1-yl)sulfonyl)-N-((S)-1-((2S,4R)-4-hydroxy-2-(((S)-1-(4-(4-methylthiazol-5-yl)phenyl)ethyl)carbamoyl)pyrrolidin-1-yl)-3,3-dimethyl-1-oxobutan-2-yl)piperidine-4-carboxamide (NR-15)**

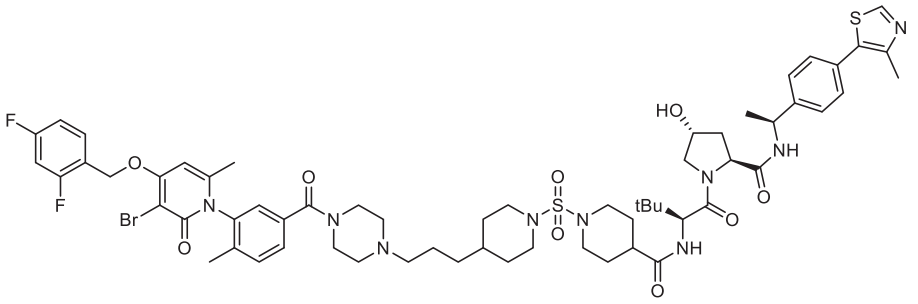

A flask loaded with **5-42** (30 mg, 0.05 mmol, 1 eq.), **5-41 HCl** (23 mg, 0.05 mmol, 1 eq.), DABCO (6 mg, 0.07 mmol, 1.5 eq.), calcium(II) bis(trifluoromethanesulfonimide) (24 mg, 0.05 mmol, 1.1 eq.) and THF (0.1 mL, 0.5 M) was stirred at 50 °C overnight. Water and ethyl acetate were added to the reaction mixture, the aqueous phase was extracted with ethyl acetate, the organic layers combined, washed with brine, dried over magnesium sulphate and dried under reduced pressure. The crude was purified by silica flash column chromatography, eluted at 10% methanol/DCM. Reported as a colorless film (2 mg, **3%**). *Note: most of the starting material was recovered after crude purification, assuming a low conversion.*

^{1}H NMR (400 MHz, CD_3OD) δ 8.8 (s, 1H), 8.4 (d, J = 7.5 Hz, 1H), 7.7 (d, J = 8.9 Hz, 1H), 7.6 (d, J = 3.0 Hz, 1H), 7.6 – 7.5 (m, 1H), 7.5 – 7.4 (m, 2H), 7.4 – 7.3 (m, 4H), 7.2 (s, 1H), 7.0 (t, J = 9.0 Hz, 2H), 6.6 (s, 1H), 5.3 (s, 2H), 4.9 (t, J = 7.1 Hz, 1H), 4.6 – 4.4 (m, 3H), 4.3 (s, 1H), 4.3 – 4.1 (m, 2H), 3.8 – 3.6 (m, 2H), 3.6 (q, J = 6.4 Hz, 6H), 2.9 – 2.8 (m, 4H), 2.7 (q, J = 11.8 Hz, 4H), 2.4 (s, 3H), 2.0 (s, 3H), 1.9 (s, 3H), 1.9 – 1.4 (m, 16H), 1.4 (d, J = 7.0 Hz, 3H), 0.9 (s, 9H).* **HRMS (ESI):** calc. for $[C_{62}H_{79}O_9N_9BrF_2S_2]^+$: 1274.46057, found 1274.45881. **HPLC-MS:** retention time 5.33 min; $[M]^{2+}$ calculated: 637.69, found: 637.6; purity: 71.85%.
*Assignation of the ^{1}H NMR spectra is tentative due to the complexity of the spectra.

8.6. Experimental Section – Phosphorylation Inducers

N-(2-amino-5-nitrophenyl)cyclopentanecarboxamide

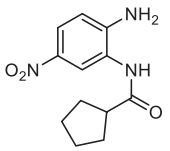

The compound was prepared following general method for amide formation 1, using 4-nitrobenzene-1,2-diamine (200 mg, 1.3 mmol, 1 eq.) and cyclopentanecarboxylic acid (140 mg, 1.1 mmol. 1.2 eq.). After work-up the crude was used without further purification.

^{1}H NMR (400 MHz, DMSO-*d6*) δ 9.1 (s, 1H), 8.3 (d, J = 2.7 Hz, 1H), 8.0 (s, 1H), 7.8 (dd, J = 9.0, 2.7 Hz, 1H), 6.8 (d, J = 9.0 Hz, 1H), 6.4 (s, 1H), 2.9 – 2.8 (m, 1H), 2.0 – 1.8 (m, 2H), 1.8 – 1.6 (m, 4H), 1.6 – 1.4 (m, 2H).

2-cyclopentyl-5-nitro-1H-benzo[d]imidazole (6-3)

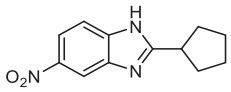

N-(2-amino-5-nitrophenyl)cyclopentanecarboxamide (200 mg, 0.80 mmol) was suspended in acetic acid (5.3 mL, 0.15 M) and stirred at 100 °C overnight. The reaction mixture was then evaporated under reduce pressure and the crude was purified by silica flash column chromatography, eluting at 50% acetate in hexanes. The product was obtained as a brownish solid, 148 mg, **80% over 2 steps**.

^{1}H NMR (400 MHz, $CDCl_3$) δ 9.6 (s, 1H), 8.6 (s, 1H), 8.2 (dd, J = 8.9, 2.2 Hz, 1H), 7.5 (s, 1H), 3.4 (p, J = 8.3 Hz, 1H), 2.3 – 2.2 (m, 2H), 2.1 – 1.7 (m, 6H).

2-cyclopentyl-1H-benzo[d]imidazol-5-amine (6-4)

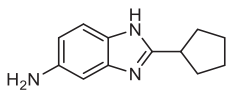

6-3 (148 mg, 0.64 mmol, 1 eq.) was disolved in metanol (20 mL, 0.03 M) and stirred under hydrogen atmosphere (1 bar, balloon) for 18 hours. The reaction mixture was filtered over celite, rinsed with methanol and dried under reduced pressure. The product was obtained as an off-white solid (105 mg, **82%**).

The NMR spectra is consistent with that reported in the literature.[4]

^{1}H NMR (400 MHz, $cdcl_3$) δ 7.33 (s, 1H), 6.76 (s, 1H), 6.60 (ddd, *J* = 8.4, 2.2, 0.9 Hz, 1H), 3.24 (p, *J* = 8.3 Hz, 1H), 2.21 – 2.07 (m, 2H), 1.99 – 1.85 (m, 2H), 1.85 – 1.73 (m, 2H), 1.73 – 1.58 (m, 2H).

N-(2-cyclopentyl-1H-benzo[d]imidazol-5-yl)-2-nitrobenzenesulfonamide (6-5)

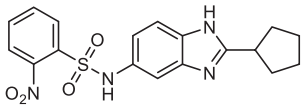

A round flask was loaded with **6-4** (100 mg, 0.49 mmol, 1 eq.) and pyridine (7.14 mL, 0.68 M), cooled down at 0 °C and 2-nitrobenzenesulfonyl chloride (80 µL, 110 mmol, 1.1 eq.) was added dropwise. The reaction mixture was stirred at 0 °C for 4 hours, then water was added. The reaction mixture was extracted with DCM (x3), the organic layers were combined, washed with brine (x2), saturated copper sulphate (x3), dried over magnesium sulphate and dried under reduced pressure. The crude was purified by silica flash column chromatography, eluting at 80% ethyl acetate in hexanes. The product was reported as a yellowish oil (138 mg, **73%**).

^{1}H NMR (500 MHz, DMSO-*d6*) δ 12.12 (s, 1H), 10.44 (s, 1H), 7.98 – 7.85 (m, 2H), 7.85 – 7.70 (m, 2H), 7.40 – 7.27 (m, 1H), 7.21 (s, 1H), 6.91 (d, *J* = 8.5 Hz, 1H), 3.21 (p, *J* = 8.2 Hz, 1H), 2.06 – 1.98 (m, 2H), 1.87 – 1.78 (m, 2H), 1.77 – 1.68 (m, 2H), 1.68 – 1.57 (m, 2H). **^{13}C NMR** (126 MHz, DMSO-*d6*) δ 170.8, 160.0, 150.1, 148.5, 134.8, 132.8, 131.9, 130.4, 124.9, 124.4, 118.9, 117.4, 105.1, 39.4, 32.2, 25.6. **IR (ATR):** 3334, 2944, 1537, 1360, 1152 cm^{-1}. **HRMS(ESI):** calculated for $[C_{18}H_{19}O_4N_4S]^+$: 387.11215, found: 387.11199.

2-amino-N-(2-cyclopentyl-1H-benzo[d]imidazol-5-yl)benzenesulfonamide (6-1)

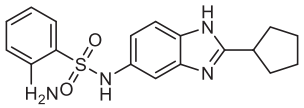

A round flask was loaded with **6-5** (138 mg, 0.36 mmol, 1 eq.), Pd/C 10% (14 mg, 10% weight) and methanol (11.5 mL, 0.03 M), purged under nitrogen and put under hydrogen atmosphere (1 atm). The reaction was stirred at room temperature overnight. The reaction mixture was filtrated through a celite pad, rinsed with methanol and dried under reduced pressure. The product was obtained as an off-white wax and was used without further purification (112 mg).

^{1}H NMR (500 MHz, DMSO-*d6*) δ 7.41 (dd, *J* = 8.0, 1.6 Hz, 1H), 7.24 (d, *J* = 8.4 Hz, 1H), 7.14 (ddd, *J* = 8.5, 7.1, 1.7 Hz, 2H), 6.81 (d, *J* = 8.6 Hz, 1H), 6.71 (dd, *J* = 8.3, 1.1 Hz, 1H), 6.47 (ddd, *J* = 8.1, 7.0, 1.1 Hz, 1H), 3.23 – 3.13 (m, 1H), 2.05 – 1.94 (m, 2H), 1.86 – 1.78 (m, 2H), 1.78 – 1.69 (m, 2H), 1.69 – 1.59 (m, 2H). **IR (ATR):** 3749, 2963, 1541, 4470 cm^{-1}. **HRMS(ESI):** calculated for $[C_{18}H_{21}O_2N_4S]^+$: 357.13797, found: 357.13745.

N-(2-(N-(2-cyclopentyl-1H-benzo[d]imidazol-5-yl)sulfamoyl)phenyl)pent-4-ynamide (6-6)

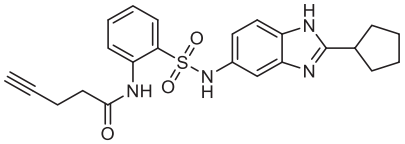

The product was prepared following general method for amide formation 1, **6-1** (300 mg, 0.84 mmol) and 4-pentynoic acid (75 mg, 0.76 mmol). The crude was purified by silica flash column

chromatography, eluting at 80% ethyl acetate in hexanes. The product was reported as a brown oil (67 mg, **22%**).

^{1}H NMR (500 MHz, CD_3OD) δ 7.54 (dd, *J* = 8.2, 1.5 Hz, 1H), 7.49 – 7.44 (m, 2H), 7.16 (ddd, *J* = 8.5, 7.0, 1.6 Hz, 1H), 7.10 (dd, *J* = 8.5, 2.0 Hz, 1H), 6.69 (dd, *J* = 8.3, 1.1 Hz, 1H), 6.52 (ddd, *J* = 8.2, 7.0, 1.1 Hz, 1H), 2.15 (q, *J* = 2.6 Hz, 4H), 2.10 – 2.00 (m, 2H), 1.99 – 1.97 (m, 1H), 1.86 – 1.67 (m, 4H), 1.67 – 1.53 (m, 2H). **^{13}C NMR** (126 MHz, CD_3OD) δ 172.2, 161.7, 148.2, 138.8, 134.9, 131.2, 129.8, 124.3, 118.6, 117.3, 117.0, 115.5, 114.3, 81.8, 68.8, 39.4, 35.5, 31.9, 25.2, 13.1. **IR (ATR):** 2365, 1689, 1621, 148, 1454, 1141, 836 cm^{-1}. **HRMS(ESI):** calculated for $[C_{23}H_{25}O_3N_4S]^+$: 437.16419, found: 437.16358

N-(2-amino-5-nitrophenyl)hept-6-ynamide

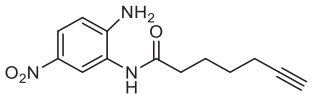

The product was prepared following general method for amide formation 2, using 4-nitrobenzene-1,2-diamine (500 mg, 3.27 mmol, 1 eq.) and 6-heptynoic acid (411 µL, 3.27 mmol, 1 eq.) and stirred overnight at room temperature. The crude was purified by silica flash column chromatography, eluting at 70% ethyl acetate in hexanes. Reported as a yellow solid (660 mg, **77%**).

^{1}H NMR (400 MHz, DMSO-*d6*) δ 9.15 (s, 0H), 8.25 (d, *J* = 2.7 Hz, 0H), 7.83 (dd, *J* = 9.0, 2.7 Hz, 0H), 6.75 (d, *J* = 9.0 Hz, 0H), 6.46 (s, 1H), 2.77 (t, *J* = 2.7 Hz, 0H), 2.38 (t, *J* = 7.4 Hz, 1H), 2.20 (td, *J* = 7.0, 2.7 Hz, 1H), 1.69 (ddd, *J* = 12.5, 8.8, 6.2 Hz, 1H), 1.57 – 1.44 (m, 1H). **^{13}C NMR** (101 MHz, DMSO-*d6*) δ 177.9, 155.1, 141.7, 128.9, 127.9, 127.5, 119.9, 90.6, 77.6, 41.5, 33.9, 30.4, 23.8. **IR(ATR):** 3333, 1629, 1478, 1331 cm^{-1}. **HRMS (ESI):** calculated for $[C_{13}H_{16}O_3N_3]^+$: 262.11862, found: 262.11874.

2-(hex-5-yn-1-yl)-5-nitro-1H-benzo[d]imidazole (6-8)

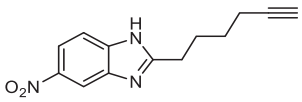

N-(2-amino-5-nitrophenyl)hept-6-ynamide (num, 660 mg, 2.71 mmol) was suspended in acetic acid (5.3 mL, 0.51 M) and stirred at 100 °C overnight. Water and ethyl acetate were added to the reaction mixture, the aqueous phase was extracted with ethyl acetate. The organic layers were combined, washed with saturated potassium bicarbonate (x5), washed with brine, dried over magnesium sulphate and dried under reduced pressure. The product was reported as a light brown solid and used without further purification (521 mg, **85%**).

^{1}H NMR (400 MHz, DMSO-*d6*) δ 8.38 (s, 0H), 7.65 (d, *J* = 8.9 Hz, 0H), 2.90 (t, *J* = 7.5 Hz, 1H), 2.77 (t, *J* = 2.6 Hz, 0H), 2.22 (td, *J* = 7.1, 2.7 Hz, 1H), 1.88 (p, *J* = 7.7 Hz, 1H), 1.61 – 1.47 (m, 1H). **^{13}C NMR** (101 MHz, DMSO-*d6*) δ 142.2, 117.2, 84.2, 71.4, 28.0, 27.5, 26.3, 17.4. I**R (ATR):** 3281, 1938, 1513, 1462, 1333 cm^{-1}. **HRMS (ESI):** calculated for $[C_{13}H_{14}O_2N_3]^+$: 244.10805, found: 244.10803

2-(hex-5-yn-1-yl)-1H-benzo[d]imidazol-5-amine (6-9)

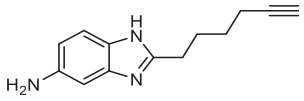

A round flask was loaded with **6-8** (1.5 g, 6.2 mmol, 1 eq.), ammonium chloride (0.33 g, 6.2 mmol, 1 eq.) and iron powder (1.7 g, 31 mmol, 5 eq.) and a 1:1 mixture of water and methanol (258 mL, 0.024 M). The reaction mixture was stirred at 100 °C overnight. The reaction mixture was filtered through a celite pad, rinsed with ethyl acetate, evaporated until the aqueous phase was left, extracted with ethyl acetate and dried under reduced pressure. The crude was purified by silica flash column chromatography, eluting at 100% ethyl acetate. The product was obtained as an ochre oil (970 mg, **75%**).

^{1}H NMR (400 MHz, $CDCl_3$) δ 7.34 (d, *J* = 8.4 Hz, 1H), 6.78 (d, *J* = 2.1 Hz, 1H), 6.66 – 6.58 (m, 1H), 2.86 (t, *J* = 7.7 Hz, 2H), 2.20 (td, *J* = 7.0, 2.7 Hz, 2H), 2.00 – 1.86 (m, 3H), 1.61 (tt, *J* = 9.6, 6.2 Hz, 2H). **IR (ATR):** 3383, 2927, 1633, 1422 cm^{-1}. **HRMS (ESI):** calculated for $[C_{13}H_{16}N_3]^+$: 214.13387, found: 214.13392.

tert-butyl 5-amino-2-(hex-5-yn-1-yl)-1H-benzo[d]imidazole-1-carboxylate (6-10)

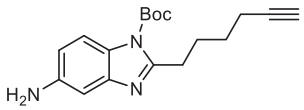

The product was prepared using general method for boc protection, using **6-9** (91 mg, 0.43 mmol). The crude was purified by silica flash column chromatography, eluting at 50% ethyl acetate in hexanes. The product was obtained as an ochre oil (80 mg, **59%**).

^{1}H NMR (400 MHz, CD_3OD) δ 7.60 (s, 1H), 7.26 (dd, *J* = 8.6, 0.7 Hz, 1H), 6.99 (dd, *J* = 8.6, 2.0 Hz, 1H), 4.84 (s, 2H), 2.75 (t, *J* = 7.6 Hz, 2H), 2.17 – 1.98 (m, 3H), 1.87 – 1.75 (m, 2H), 1.41 (s, 11H). **^{13}C NMR** (101 MHz, CD_3OD) δ 156.6, 155.7, 138.9, 136.4, 135.5, 116.1, 115.7, 105.4, 84.5, 80.6, 69.8, 29.2, 29.1, 28.8, 28.3, 18.7. **IR (ATR):** 3343, 1690, 1529, 1150, 620 cm^{-1}. **HRMS (ESI):** calculated for $[C_{18}H_{24}O_2N_3]^+$: 314.18630, found: 314.18567.

tert-butyl 2-(hex-5-yn-1-yl)-5-(phenylsulfonamido)-1H-benzo[d]imidazole-1-carboxylate (6-11')

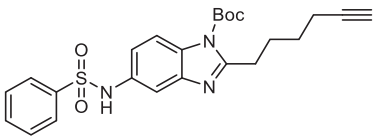

6-10 (78 mg, 0.25 mmol, 1 eq.) was dissolved in pyridine (1.25 mL, 0.2 M) and cooled down at 0 °C. Benzenesulfonyl chloride (31 µL, 0.25 mmol, 1 eq.). The reaction was stirred fo r3 hours, letting warm up to room temperature. Water and ethyl acetate were added to the reaction mixture, the aqueous phase was extracted with ethyl acetate. The organic layers were combined, washed a copper

sulphate solution, brine, dried over magnesium sulphate and dried under reduced pressure. The crude was purified by silica flash column chromatography, eluting at 20% ethyl acetate in hexanes. The product was obtained a yellowish oil (69 mg, **60%**).

^{1}H NMR (400 MHz, $CDCl_3$) δ 8.18 – 8.13 (m, 1H), 7.98 – 7.80 (m, 3H), 7.63 – 7.38 (m, 4H), 6.87 (s, 1H), 6.74 (s, 1H), 3.17 – 3.05 (m, 2H), 2.22 (tdd, *J* = 7.1, 2.7, 1.1 Hz, 2H), 2.01 – 1.95 (m, 2H), 1.94 (t, *J* = 2.6 Hz, 1H), 1.72 – 1.59 (m, 2H), 1.51 (d, *J* = 12.2 Hz, 9H). **^{13}C NMR** (101 MHz, $CDCl_3$) δ 171.3, 153.1, 152.9, 142.6, 138.5 (d, *J* = 3.1 Hz), 137.8, 136.0, 135.8, 134.7, 129.7, 126.8, 126.6, 119.9, 117.0, 116.6, 113.8, 110.0, 104.2, 84.2, 68.7, 29.4, 28.4, 28.4, 28.2, 28.1, 26.8, 26.7, 18.3. **IR (ATR):** 2972, 1719, 1367, 1154,586 cm^{-1}

N-(2-(hex-5-yn-1-yl)-1H-benzo[d]imidazol-5-yl)benzenesulfonamide hydrochloride (6-11)

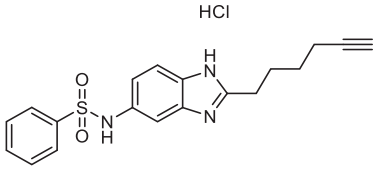

6-11' (60 mg, 0.13 mmol) was stirred in 2 mL of HCl/dioxane 4N for 2 h. The solvent was then evaporated affording the hydrochloride salt as a white solid (50 mg, **quant.**).

(2S,4R)-1-((S)-2-(4-(4-(3-((2-(N-(2-cyclopentyl-1H-benzo[d]imidazol-5-yl)sulfamoyl)phenyl)amino)-3-oxopropyl)-1H-1,2,3-triazol-1-yl)butanamido)-3,3-dimethylbutanoyl)-4-hydroxy-N-((S)-1-(4-(4-methylthiazol-5-yl)phenyl)ethyl)pyrrolidine-2-carboxamide (6-7a)

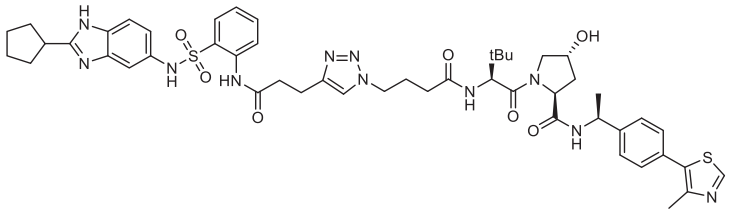

The product was prepared following general method for CuAAC, using **6-6** (22 mg, 0.05 mmol) and **3-30a** (28 mg, 0.05 mmol). The product was purified by silica flash column chromatography, eluted at 7% MeOH/DCM. Reported as a white solid (21 mg, **42%**).

^{1}H NMR (400 MHz, CD_3OD) δ 8.86 (s, 1H), 7.67 (dd, *J* = 8.2, 1.6 Hz, 1H), 7.57 – 7.43 (m, 2H), 7.43 – 7.37 (m, 4H), 7.37 – 7.23 (m, 1H), 7.20 – 7.10 (m, 1H), 6.83 (dd, *J* = 8.4, 1.1 Hz, 1H), 6.67 (ddd, *J* = 8.2, 7.0, 1.1 Hz, 1H), 4.99 (qd, *J* = 7.0, 3.5 Hz, 1H), 4.63 – 4.54 (m, 2H), 4.50 – 4.37 (m, 1H), 4.38 – 4.26 (m, 2H), 3.91 – 3.86 (m, 1H), 3.74 (dd, *J* = 11.0, 3.9 Hz, 1H), 3.41 – 3.33 (m, 1H), 2.83 (t, *J* = 7.1 Hz, 2H), 2.50 – 2.40 (m, 5H), 2.32 – 2.03 (m, 7H), 2.02 – 1.83 (m, 5H), 1.83 – 1.70 (m, 2H), 1.48 (d, *J* = 7.0 Hz, 3H), 1.03 (s, 9H). **^{13}C NMR** (101 MHz, CD_3OD) δ 174.3, 174.3, 173.2, 172.3, 163.1, 152.9, 149.6, 149.1, 147.2, 145.6, 136.3, 133.3, 132.7, 131.5, 131.2, 130.5, 127.6, 125.7, 123.7, 120.0, 118.7, 116.8, 71.0, 59.3, 58.0, 50.4, 50.2, 40.8, 38.8, 37.2, 36.3, 33.3, 32.9, 27.3, 27.1, 26.5, 22.4, 21.3, 15.8. **IR (ATR):** 2923, 2355, 1633, 1142 cm^{-1}. **HRMS (ESI):** calculated for $[C_{50}H_{62}O_7N_{11}S_2]^+$: 992.42696, found: 992.42627.

(2S,4R)-1-((S)-2-(6-(4-(3-((2-(N-(2-cyclopentyl-1H-benzo[d]imidazol-5-yl)sulfamoyl)phenyl)amino)-3-oxopropyl)-1H-1,2,3-triazol-1-yl)hexanamido)-3,3-dimethylbutanoyl)-4-hydroxy-N-((S)-1-(4-(4-methylthiazol-5-yl)phenyl)ethyl)pyrrolidine-2-carboxamide (6-7b)

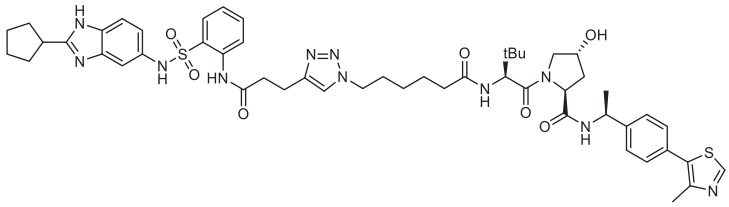

The product was prepared following general method for CuAAC, using **6-6** (14 mg, 0.03 mmol) and **3-30b** (19 mg, 0.03 mmol). The product was purified by silica flash column chromatography, eluted at 8% MeOH/DCM. Reported as a white solid (11 mg, **34%**).

^{1}H NMR (500 MHz, MeOD) δ 8.88 (s, 1H), 7.67 (dd, *J* = 8.2, 1.6 Hz, 1H), 7.49 (s, 2H), 7.46 – 7.36 (m, 4H), 7.33 (ddd, *J* = 8.5, 7.0, 1.7 Hz, 1H), 7.19 – 7.09 (m, 1H), 6.86 – 6.81 (m, 1H), 6.67 (ddd, *J* = 8.2, 7.0, 1.1 Hz, 1H), 4.99 (d, *J* = 7.0 Hz, 1H), 4.64 – 4.49 (m, 2H), 4.43 (dp, *J* = 4.2, 1.9 Hz, 1H), 4.27 (t, *J* = 7.0 Hz, 2H), 3.91 – 3.84 (m, 1H), 3.74 (dd, *J* = 11.0, 4.0 Hz, 1H), 3.36 (d, *J* = 7.9 Hz, 1H), 2.83 (t, *J* = 7.2 Hz, 2H), 2.55 – 2.35 (m, 5H), 2.33 – 2.12 (m, 5H), 2.00 – 1.71 (m, 7H), 1.69 – 1.56 (m, 2H), 1.49 (d, *J* = 7.1 Hz, 2H), 1.28 (q, *J* = 7.8, 7.0 Hz, 3H), 1.02 (s, 9H). **^{13}C NMR** (126 MHz, MeOD) δ 175.7, 174.2, 173.2, 172.3, 152.9, 149.7, 145.7, 136.3, 132.7, 131.5, 130.5, 127.6, 125.7, 120.0, 118.7, 116.8, 71.0, 60.6, 59.1, 58.0, 51.1, 50.1, 40.9, 38.8, 37.3, 36.4, 36.2, 33.3, 30.9, 27.1, 27.0, 26.6, 26.2, 22.4, 21.4, 15.8. **IR (ATR):** 2919, 1560, 1417, 1142 cm^{-1}. **HRMS (ESI):** calculated for $[C_{52}H_{66}O_7N_{11}S_2]^+$: 1020.45826, found: 1020.45740.

(2S,4R)-1-((S)-2-(6-(4-(4-(3-((2-(N-(2-cyclopentyl-1H-benzo[d]imidazol-5-yl)sulfamoyl)phenyl)amino)-3-oxopropyl)-1H-1,2,3-triazol-1-yl)butanamido)hexanamido)-3,3-dimethylbutanoyl)-4-hydroxy-N-((S)-1-(4-(4-methylthiazol-5-yl)phenyl)ethyl)pyrrolidine-2-carboxamide (6-7c)

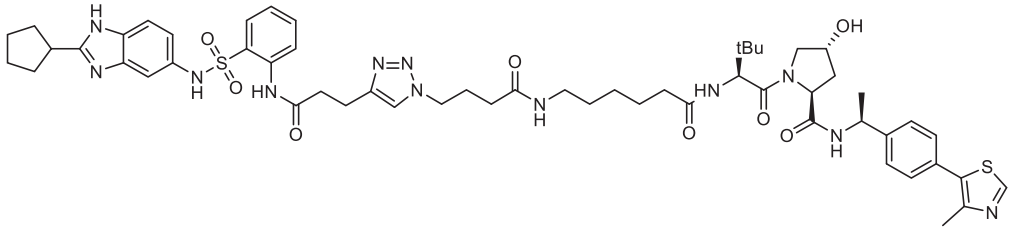

The product was prepared following general method for CuAAC, using **6-6**, (20 mg, 0.05 mmol) and **3-32b** (30 mg, 0.05 mmol). The product was purified by silica flash column chromatography, eluted at 8% MeOH/DCM. Reported as a white solid (25 mg, **50%**).

^{1}H NMR (500 MHz, CD_3OD) δ 8.86 (s, 1H), 7.84 – 7.75 (m, 1H), 7.66 (dd, *J* = 8.2, 1.6 Hz, 1H), 7.49 (d, *J* = 4.3 Hz, 2H), 7.46 – 7.38 (m, 4H), 7.38 – 7.29 (m, 1H), 7.15 (dt, *J* = 8.4, 1.7 Hz, 1H), 6.83 (dd, *J* = 8.4, 1.1 Hz, 1H), 6.67 (ddd, *J* = 8.2, 7.0, 1.1 Hz, 1H), 5.00 (qd, *J* = 7.1, 5.3 Hz, 1H), 4.69 – 4.52 (m, 2H), 4.46 – 4.35 (m, 1H), 4.31 (t, *J* = 6.6 Hz, 2H), 3.90 – 3.81 (m, 1H), 3.74 (dd, *J* = 11.0, 4.0 Hz, 1H), 3.43 – 3.34 (m, 1H), 3.13 (td, *J* = 7.0, 2.3 Hz, 2H), 2.82 (q, *J* = 6.4, 5.7 Hz, 2H), 2.45 (d, *J* = 13.9 Hz, 5H), 2.34 – 2.07 (m, 9H), 2.01 – 1.80 (m, 5H),

1.82 – 1.70 (m, 2H), 1.59 (ddd, *J* = 16.2, 8.1, 2.7 Hz, 2H), 1.55 – 1.39 (m, 5H), 1.38 – 1.29 (m, 2H), 1.02 (s, 9H). **^{13}C NMR** (126 MHz, CD_3OD) δ 175.9, 174.3, 174.2, 173.3, 172.3, 152.9, 149.7, 149.1, 147.2, 145.7, 137.3, 136.3, 134.8, 133.4, 132.7, 131.5, 131.3, 130.5, 127.6, 127.3, 125.7, 123.7, 120.0, 118.7, 116.8, 71.0, 60.6, 59.0, 58.0, 50.6, 50.1, 40.9, 40.3, 38.8, 37.2, 36.5, 36.4, 33.5, 33.3, 30.0, 27.5, 27.3, 27.1, 26.6, 26.5, 26.5, 22.4, 21.4, 15.8. **IR(ATR):** 2918, 1633, 1146, 1143 cm^{-1}. **HRMS (ESI):** calculated for $[C_{56}H_{73}O_8N_{12}S_2]^+$: 1105.51102, found: 1105.51154.

(2S,4R)-1-((S)-3,3-dimethyl-2-(2-(4-(4-(5-(phenylsulfonamido)-1H-benzo[d]imidazol-2-yl)butyl)-1H-1,2,3-triazol-1-yl)acetamido)butanoyl)-4-hydroxy-N-((S)-1-(4-(4-methylthiazol-5-yl)phenyl)ethyl)pyrrolidine-2-carboxamide (6-12a)

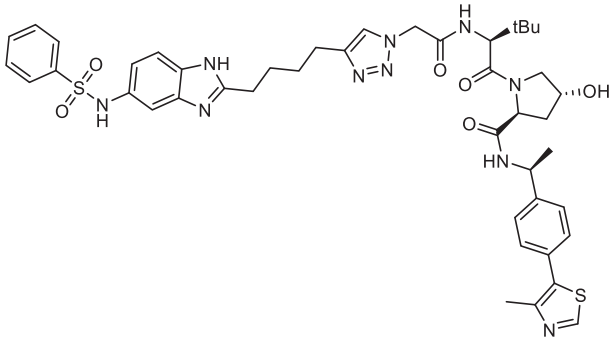

The product was prepared following general method for CuAAC, using **6-11** (9 mg, 0.024 mmol) and **4-16** (13.5 mg, 0.024 mmol). The product was purified by silica flash column chromatography, eluted at 15% MeOH/DCM. Reported as a white solid (9 mg, **42%**).

^{1}H NMR (400 MHz, CD_3OD) δ 8.85 (d, *J* = 14.5 Hz, 1H), 7.74 (s, 1H), 7.65 (d, *J* = 7.4 Hz, 2H), 7.57 – 7.25 (m, 9H), 6.88 (d, *J* = 7.8 Hz, 1H), 5.20 (q, *J* = 16.4 Hz, 2H), 4.97 (q, *J* = 7.0 Hz, 1H), 4.67 – 4.51 (m, 2H), 4.41 (dt, *J* = 4.3, 2.1 Hz, 1H), 3.83 (dt, *J* = 11.3, 1.7 Hz, 1H), 3.72 (dd, *J* = 11.0, 3.9 Hz, 1H), 2.88 (s, 2H), 2.71 (t, *J* = 7.2 Hz, 2H), 2.47 (s, 3H), 2.27 – 2.10 (m, 1H), 1.94 (ddd, *J* = 13.3, 9.1, 4.5 Hz, 1H), 1.84 (s, 2H), 1.69 (s, 3H), 1.47 (d, *J* = 7.0 Hz, 3H), 1.05 (s, 9H). **HRMS (ESI):** calculated for $[C_{44}H_{53}O_6N_{10}S_2]^+$: 881.35855, found: 881.36294.

(2S,4R)-1-((S)-3,3-dimethyl-2-(6-(4-(4-(5-(phenylsulfonamido)-1H-benzo[d]imidazol-2-yl)butyl)-1H-1,2,3-triazol-1-yl)hexanamido)butanoyl)-4-hydroxy-N-((S)-1-(4-(4-methylthiazol-5-yl)phenyl)ethyl)pyrrolidine-2-carboxamide (6-12b)

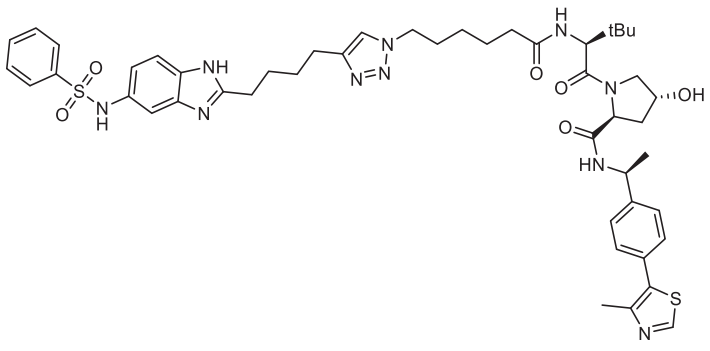

The product was prepared following general method for CuAAC, using **6-11** (14 mg, 0.039 mmol) and **3-30b** (8.5 mg, 0.024 mmol). The product was purified by silica flash column chromatography, eluted at 15% MeOH/DCM. Reported as an off-white solid (11 mg, **30%**).

^{1}H NMR (400 MHz, CD_3OD) δ 8.84 (s, 1H), 8.00 – 7.83 (m, 1H), 7.69 (dd, *J* = 8.5, 1.3 Hz, 2H), 7.62 (s, 1H), 7.57 – 7.48 (m, 2H), 7.46 – 7.36 (m, 4H), 7.30 (d, *J* = 8.6 Hz, 1H), 7.24 (s, 1H), 6.93 – 6.84 (m, 1H), 5.00 (q, *J* = 7.0 Hz, 1H), 4.53 (dd, *J* = 9.6, 2.1 Hz, 1H), 4.45 – 4.37 (m, 2H), 4.23 (td, *J* = 7.1, 1.4 Hz, 2H), 3.97 (d, *J* = 11.0 Hz, 1H), 3.88 (dd, *J* = 11.0, 4.6 Hz, 1H), 2.86 (t, *J* = 7.4 Hz, 2H), 2.71 (q, *J* = 7.4 Hz, 2H), 2.45 (s, 3H), 2.41 – 2.04 (m, 6H), 1.91 – 1.50 (m, 8H), 1.42 (d, *J* = 7.0 Hz, 3H), 1.04 (s, 9H). **HRMS (ESI):** calculated for $[C_{48}H_{61}O_6N_{10}S_2]^+$: 937.42115, found: 937.42767.

(2S,4R)-1-((S)-3,3-dimethyl-2-(6-(4-(4-(4-(5-(phenylsulfonamido)-1H-benzo[d]imidazol-2-yl)butyl)-1H-1,2,3-triazol-1-yl)butanamido)hexanamido)butanoyl)-4-hydroxy-N-((S)-1-(4-(4-methylthiazol-5-yl)phenyl)ethyl)pyrrolidine-2-carboxamide (6-12c)

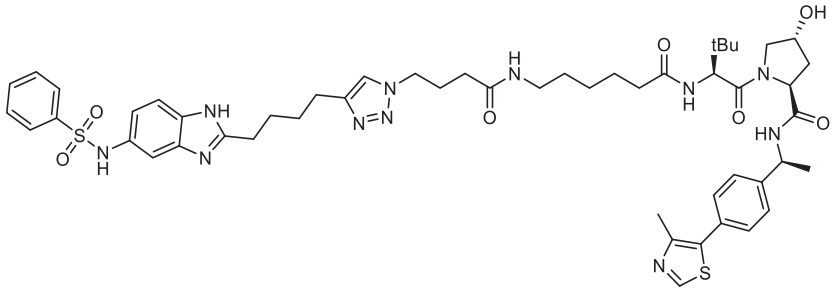

The product was prepared following general method for CuAAC, using **6-11** (6.5 mg, 0.018 mmol) and **3-32b** (12.3 mg, 0.018 mmol). The product was purified by silica flash column chromatography, eluted at 15% MeOH/DCM. Reported as an off-white solid (9 mg, **49%**).

^{1}H NMR (400 MHz, CD_3OD) δ 8.87 (s, 1H), 7.77 – 7.63 (m, 3H), 7.53 – 7.47 (m, 1H), 7.47 – 7.24 (m, 8H), 6.88 (d, *J* = 8.2 Hz, 1H), 4.99 (q, *J* = 7.1 Hz, 1H), 4.70 – 4.52 (m, 2H), 4.43 (dp, *J* = 4.4, 2.0 Hz, 1H), 4.40 – 4.34 (m, 2H), 3.88 (dt, *J* = 11.2, 1.8 Hz, 1H), 3.76 (s, 1H), 3.13 (t, *J* = 7.0 Hz, 2H), 2.88 (s, 2H), 2.72 (t, *J* = 7.4 Hz, 2H), 2.47 (s, 3H), 2.37 – 2.07 (m, 7H), 1.95 (ddd, *J* = 13.3, 9.0, 4.5 Hz, 1H), 1.90 – 1.80 (m, 2H), 1.71 (t, *J* = 7.6 Hz, 2H), 1.60 (tt, *J* = 14.3, 6.9 Hz, 2H), 1.48 (t, *J* = 7.1 Hz, 5H), 1.41 – 1.30 (m, 2H), 1.03 (s, 9H). **HRMS (ESI):** calculated for $[C_{52}H_{68}O_7N_{11}S_2]^+$: 1022.47391, found: 1022.48162.

methyl (methoxycarbonyl)-L-tyrosinate (6-13)

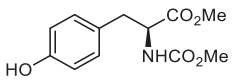

A round flask was filled with methyl L-tyrosinate (1g, 5 mmol), NaHCO3 (0.63 mg, 7.5 mmol) and water (6.6 mL). The reaction mixture was cooled down at 0 °C and a solution of methyl chloroformate (0.48 mL, 6 mmol) in chloroform (3.3 mL) was added dropwise. The reaction mixture was let to warm up during 3 h and water was added. The mixture was exctracted with DCM (x3), the organic layers washed with $NaHCO_3$, combined, dried over $MgSO_4$ and dried under reduced pressure. The product was obtained as a white solid (1.3 g, **quant.**).

^{1}H NMR (400 MHz, $CDCl_3$) δ 7.0 (d, J = 8.1 Hz, 2H), 6.7 (d, J = 8.0 Hz, 2H), 5.2 (s, 1H), 5.1 (d, J = 8.3 Hz, 1H), 4.6 (d, J = 7.4 Hz, 1H), 3.7 (s, 3H), 3.7 (s, 3H), 3.0 (q, J = 9.8 Hz, 2H).

methyl (S)-3-(4-hydroxy-3-nitrophenyl)-2-((methoxycarbonyl)amino)propanoate (6-14)

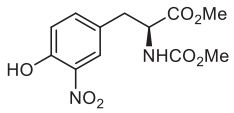

A flask was loaded with $NaNO_3$ (15.3 g, 0.18 mol), $La(NO_3)_3{\cdot}6H_2O$ (0.8 g, 1.8 mmol) and HCl 6N (285 mL) and cooled down at 0 °C. A solution of **6-13** (45 g, 0.18 mol) in DCM (550 mL) was added dropwise over 2 h, then the ice bath was removed and stired for 4 h. Water and DCM were added to the reaction mixture, the aqueous phase was extracted with DCM, the organic phases were combined and washed with water, brine, dried over $MgSO_4$. The crude was dried under reduced pressure and purified by flash column chromatography. The product was eluted at ??? % AcOEt/Hexane, reported as a yellow oil (48 g, **90%**).

^{1}H NMR (400 MHz, $CDCl_3$) δ 7.9 (d, J = 2.2 Hz, 1H), 7.4 (ddd, J = 8.6, 2.3, 0.5 Hz, 1H), 7.1 (d, J = 8.6 Hz, 1H), 5.2 (s, 1H), 4.6 (d, J = 7.2 Hz, 1H), 3.8 (s, 3H), 3.7 (s, 3H), 3.2 (dd, J = 14.1, 5.5 Hz, 1H), 3.0 (dd, J = 14.1, 6.0 Hz, 1H).

methyl (S)-3-(3-amino-4-hydroxyphenyl)-2-((methoxycarbonyl)amino)propanoate

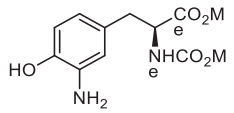

6-14 (48g, 0.16 mol) was dissolved in AcOEt (450 mL) and transferred to a high pressure reactor. Pd/C was added (2.9 g, 1.6 mmol), the reactor was purged with N_2, H_2 (10 bar) and loaded with H_2 (30 bar). The reactor was filled with H_2 as the pressure went down, once stable it was left stirring overnight. The reactor was emptied, reaction mixture was filtered and the filtrate was evaporated under reduced pressure. Product was obtained as a white solid (43.5 g, 0.16 mol, **quant**.).

^{1}H NMR (400 MHz, $CDCl_3$) δ 6.6 (d, J = 8.0 Hz, 1H), 6.5 (s, 1H), 6.4 (d, J = 7.6 Hz, 1H), 5.1 (d, J = 8.3 Hz, 1H), 4.6 – 4.5 (m, 1H), 3.7 (s, 3H), 3.7 (s, 3H), 2.9 (d, J = 4.9 Hz, 2H).

(S)-2-acetamido-4-(3-acetoxy-2-((methoxycarbonyl)amino)propyl)phenyl acetate (6-15)

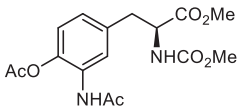

A round flask was charged with **methyl (S)-3-(3-amino-4-hydroxyphenyl)-2-((methoxycarbonyl)amino)propanoate** (43.5 g, 0.16 mol), triethylamine (79 mL, 0.57 mol) and DCM (500 mL) and cooled down at -10 °C. Acetyl chloride (23 mL, 0.32 mol) was added dropwise and the reaction mixture was stirred at -10 °C for 5 h. Water and DCM were added to the reaction mixture, the aqueous phase was extracted with DCM, the organic phases were combined and washed with water, brine, dried over $MgSO_4$. The crude was dried under reduced pressure and purified by flash column chromatography. Product was eluted at 100% AcOEt, reported as a white solid foam (39.5 g, **70%**)

^{1}H NMR (400 MHz, $CDCl_3$) δ 8.0 (s, 1H), 7.2 (s, 1H), 7.1 (d, J = 8.2 Hz, 1H), 7.0 – 6.8 (m, 1H), 5.2 (d, J = 8.4 Hz, 1H), 4.6 (d, J = 7.5 Hz, 1H), 3.8 (s, 3H), 3.7 (s, 3H), 3.1 (d, J = 5.7 Hz, 2H), 2.4 (s, 3H), 2.2 (s, 3H).

(S)-2-acetamido-4-(3-hydroxy-2-((methoxycarbonyl)amino)propyl)phenyl acetate

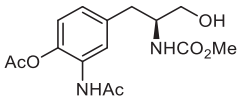

A flame-dried round flask was charged with **(S)-2-acetamido-4-(3-acetoxy-2-((methoxycarbonyl)amino)propyl)phenyl acetate (17 g, 48.3 mmol**) and THF (400 mL). Reaction mixture was cooled down at 0 °C and $LiBH_4$ (3.3 g, 145 mmol) was added slowly. Reaction mixture was monitored until no more starting material was observed by TLC (aprox. 6 h). Reaction mixture was cooled down at 0 °C and water was added slowly. AcOEt was added, the aqueous layer was separated and extracted with AcOEt, the organic layers were combined and washed with brine, dried over $MgSO_4$ and dried under reduced pressure. The product was used without further purification.

(S)-2-acetamido-4-(3-acetoxy-2-((methoxycarbonyl)amino)propyl)phenyl acetate (6-16)

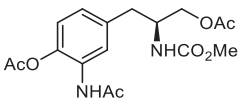

A flask was loaded with **(S)-2-acetamido-4-(3-hydroxy-2-((methoxycarbonyl)amino)propyl)phenyl acetate** (48.3 mmol) and pyridine (240 mL), cooled down at 0 °C and Ac_2O (17 mL, 180 mmol) was added slowly. After 3 hours, reaction mixture was dried under reduced pressure. The residue was dissolved in AcOEt, washed with $CuSO_4$, $NaHCO_3$

and dried under reduced pressure. The product was obtained as a white solid and used without further purification (14.7 g).

^{1}H NMR (400 MHz, $CDCl_3$) δ 8.0 (s, 1H), 7.2 (d, J = 13.2 Hz, 1H), 7.1 (d, J = 8.2 Hz, 1H), 7.0 (s, 1H), 4.9 (s, 1H), 4.2 – 4.0 (m, 3H), 3.6 (s, 3H), 2.8 (t, J = 6.7 Hz, 2H), 2.4 (s, 3H), 2.2 (s, 3H), 2.1 (s, 3H).

(S)-2-acetamido-4-(3-acetoxy-2-((methoxycarbonyl)amino)propyl)-5-nitrophenyl acetate (6-17+6-17')

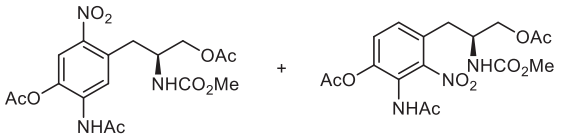

6-16 (2 g, 5.4 mmol) and Ac_2O (21 mL) were cooled down at -13 °C and NHO_3 (1 mL, 16.2 mmol) was added dropwise. Reaction mixture was kept at -13 °C for 4 h, then AcOEt and H2O were added. The aqueous phase was extracted with AcOEt, the organic phases were combined and washed with brine, dried over $MgSO_4$ and dried under vacuum. The crude purified by flash column chromatography, eluted at 60% ethyl acetate in hexanes. **6-17** and **6-17'** were obtained as a mixture of isomers (1.93 g, 4.7 mmol, **86%**).

methyl (S)-(1-hydroxy-3-(4-hydroxy-2-nitrophenyl)propan-2-yl)carbamate (6-18)

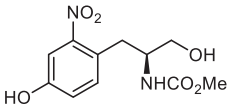

A mixture of 6-17 and 6-17' (4.3 g, 10.4 mmol) was dissolved in methanol (87 mL) and H_2SO_4 1N (87 mL) and stirred at 60 °C overnight. The reaction mixture was dried in the rotatory evaporator to get rid of the methanol, then cooled down at 0°C. $NaNO_2$ (0.72 g, 11.4 mmol) were added and reaction mixture was stirred at 0°C for 1 hour. H_3PO_2 (1.4 mL, 15.6 mmol) was added to the reaction mixture, and after a few minutes it was warmed up at 70 °C. After 5 hours the reaction was stopped, water and ethyl acetate were added to the mixture, the phases were separated and the aqueous phase was extracted with ethyl acetate. The organic layers were combined, dried over magnesium sulphate and dried under reduced pressure. The reaction crude was purified by silica flash column chromatography, the product was eluted at 4 % methanol in DCM. **6-18** was obtained as a red solid (1 g, **37%**).

^{1}H NMR (400 MHz, CD_3OD) δ 7.3 (d, J = 2.6 Hz, 1H), 7.2 (d, J = 8.5 Hz, 1H), 7.0 (dd, J = 8.4, 2.6 Hz, 1H), 6.7 (d, J = 8.4 Hz, 1H), 4.0 – 3.9 (m, 2H), 3.7 – 3.5 (m, 4H), 3.2 (dd, J = 13.8, 4.5 Hz, 1H), 2.7 (dd, J = 13.8, 9.7 Hz, 1H).

methyl (S)-(1-(4-((4-(((tert-butoxycarbonyl)amino)methyl)benzyl)oxy)-2-nitrophenyl)-3-hydroxypropan-2-yl)carbamate (6-20)

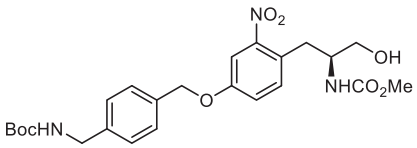

A flask was loaded with **6-18** (330 mg, 1.22 mmol), potassium carbonate (337 mg, 2.44 mmol), DMF (9.4 mL), purged under nitrogen and then tert-butyl (4-(hydroxymethyl)benzyl)carbamate(385 mg, 1.25 mmol) was added dissolved in DMF (2 mL). The reaction mixture was heated at 50 °C and stirred over 48 hours. Water and ethyl acetate were added to the mixture, the phases were separated and the aqueous phase was extracted with ethyl acetate. The organic layers were combined, dried over magnesium sulphate and dried under reduced pressure. The reaction crude was purified by silica flash column chromatography, the product was eluted at 60% ethyl acetate in hexanes. Obtained as an off-white solid foam (412 mg, **93%**).

^{1}H NMR (400 MHz, CDCl3) δ 7.5 (s, 1H), 7.4 – 7.4 (m, 2H), 7.4 – 7.3 (m, 3H), 7.2 (dd, J = 8.5, 2.7 Hz, 1H), 5.2 (s, 1H), 5.1 (s, 2H), 4.9 (s, 1H), 4.3 (d, J = 5.9 Hz, 2H), 4.0 (ddq, J = 8.4, 6.2, 4.1 Hz, 1H), 3.8 – 3.5 (m, 5H), 3.1 (dd, J = 14.2, 6.2 Hz, 1H), 3.0 (d, J = 10.0 Hz, 1H), 1.5 (d, J = 1.3 Hz, 9H).

methyl (S)-(1-(2-amino-4-((4-(((tert-butoxycarbonyl)amino)methyl)benzyl)oxy)phenyl)-3-hydroxypropan-2-yl)carbamate (6-21)

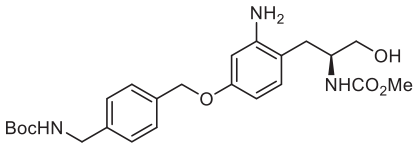

6-20 (920 mg, 1.88 mmol) was dissolved in methanol (31 mL) and a saturated solution of copper (II) acetate in methanol (12 mL) was added. The solution was cooled down at 0 °C and $NaBH_4$ (1 g, 28.2 mmol) was added slowly. The reaction was let to warm up to room temperature and stirred until starting material consumption. The reaction mixture was filtered through celite, rinsed with DCM and evaporated under reduced pressure. The crude was dissolved in ethyl acetate, washed with water, brine, dried over magnesium sulphate and dried under reduced pressure. The crude was used without further purification (827 mg).

^{1}H NMR (400 MHz, CDCl3) δ 7.4 (d, J = 7.8 Hz, 2H), 7.3 – 7.2 (m, 2H), 6.9 (d, J = 8.2 Hz, 1H), 6.4 – 6.2 (m, 2H), 5.4 (s, 1H), 5.0 (s, 2H), 4.9 (s, 1H), 4.5 – 4.3 (m, 3H), 3.9 – 3.4 (m, 6H), 2.8 (d, J = 14.7 Hz, 1H), 2.7 – 2.6 (m, 1H), 1.5 (s, 9H).

benzyl (S)-3-methyl-2-(((trifluoromethyl)sulfonyl)oxy)butanoate (6-22)

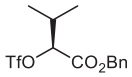

A flame-dried flask was loaded with benzyl (S)-2-hydroxy-3-methylbutanoate (520 mg, 2.5 mmol) dissolved in DCM (3.3 mL) and 2,6-lutidine (378 µL, 3.2 mmol), cooled down at -78 °C and Tf_2O (504 µL, 3.1 mmol) was added dropwise. After 2 hours, the reaction mixture was diluted in DCM and quenched by the addition of water. The layers were separated, the aqueous layer was extracted with DCM, the organic fractions were combined, washed with brine, dried over magnesium sulphate and dried under reduced pressure. The crude was used without further purification (reddish oil, 705 mg).

^{1}H NMR (400 MHz, CDCl3) δ 7.4 (d, J = 2.1 Hz, 5H), 5.3 – 5.2 (m, 2H), 5.0 (d, J = 4.0 Hz, 1H), 2.4 (pd, J = 6.9, 4.0 Hz, 1H), 1.1 (d, J = 6.9 Hz, 3H), 1.0 (d, J = 6.9 Hz, 3H).

benzyl (5-((4-(((tert-butoxycarbonyl)amino)methyl)benzyl)oxy)-2-((S)-3-hydroxy-2-((methoxycarbonyl)amino)propyl)phenyl)-L-valinate (6-23)

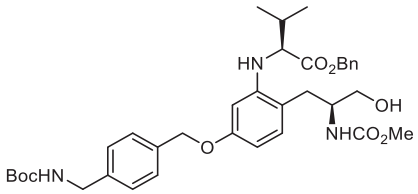

A flame-dried flask was loaded with **6-21** (827 mg, 1.8 mmol theoretical), **6-22** (612 mg, 0.58 mmol theoretical), 2,6-lutidine (0.3 mL, 2.7 mmol) and DCE (20 mL). The reaction mixture was stirred at 70 °C during 72 hours. The reaction mixture was dried under reduced pressure, the crude was redissolved in DCM, dried into a silica dry load and purified by silica flash column chromatography. The product was eluted at 50% ethyl acetate in hexanes. Reported as an incolor film (492 mg, **42%** over 2 steps). Starting material was also recovered (320 mg, calculated conversion: 61%).

^{1}H NMR (400 MHz, CDCl3) δ 7.3 (d, J = 8.1 Hz, 2H), 7.3 (d, J = 1.8 Hz, 2H), 7.0 (d, J = 8.2 Hz, 1H), 6.3 (dd, J = 8.2, 2.4 Hz, 1H), 6.2 (d, J = 2.4 Hz, 1H), 5.5 (s, 1H), 5.1 (d, J = 2.2 Hz, 2H), 4.9 – 4.8 (m, 2H), 4.3 (d, J = 6.0 Hz, 2H), 3.9 (d, J = 6.6 Hz, 1H), 3.7 (s, 1H), 3.7 (s, 3H), 3.6 – 3.4 (m, 2H), 2.9 – 2.7 (m, 2H), 2.2 – 2.1 (m, 1H), 1.5 (s, 9H), 1.1 – 1.0 (m, 3H), 1.0 (d, J = 6.7 Hz, 3H).

tert-butyl (4-((((2S,5S)-5-(hydroxymethyl)-2-isopropyl-3-oxo-1,2,3,4,5,6-hexahydrobenzo[e][1,4]diazocin-9-yl)oxy)methyl)benzyl)carbamate(6-24)

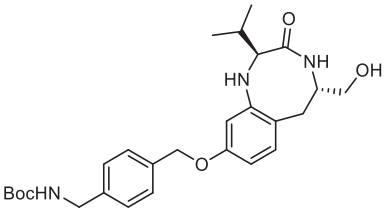

6-23 (706 mg, 1.08 mmol) was dissolved in methanol (18.4 mL), then KOH 2N (9.2mL) was added and the reaction mixture was stirred at 70 °C overnight. The reaction mixture was neutralized to pH 7 and dried thoroughly under reduced pressure.

The reaction crude was dissolved in DMF (90 mL), then TEA (305 µL 2 mmol) and DPPA (350 µL 1.5 mmol) were added. The reaction mixture was stirred 3 hours at room temperature. Water and ethyl acetate were added to the mixture, the phases were separated and the aqueous phase was extracted with ethyl acetate. The organic layers were combined, dried over magnesium sulphate and dried under reduced pressure. The reaction crude was purified by silica flash column chromatography, the product was eluted at 50% ethyl acetate in hexanes. Obtained as an off-white solid foam (284 mg, **54%**).

tert-butyl (4-((((2S,5S)-5-(hydroxymethyl)-2-isopropyl-1-methyl-3-oxo-1,2,3,4,5,6-hexahydrobenzo[e][1,4]diazocin-9-yl)oxy)methyl)benzyl)carbamate (6-25)

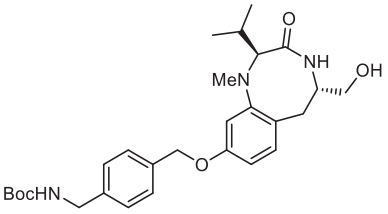

6-24 (284mg, 0.58 mmol) was dissolved in MeCN (12 mL) and cooled down at 0 °C. Formaldehyde (0.47 mL, 37% in water) was added, followed by $NaBH_3CN$ (111 mg, 2.9 mmol) and HOAc (59 µL). The reaction mixture was stirred 5 hours, and then water and ethyl acetate were added. The phases were separated and the aqueous phase was extracted with ethyl acetate. The organic layers were combined, dried over magnesium sulphate and dried under reduced pressure. The reaction crude was purified by silica flash column chromatography, the product was eluted at 40% ethyl acetate in hexanes. Obtained as a white solid (192 mg, **66%**).

The NMR is consistent with that reported in the literature.[5]

^{1}H NMR (400 MHz, $CDCl_3$) δ 7.4 (d, J = 7.8 Hz, 2H), 7.3 – 7.2 (m, 2H), 6.9 (d, J = 8.3 Hz, 1H), 6.7 (s, 1H), 6.6 (d, J = 2.5 Hz, 1H), 6.5 (dd, J = 8.3, 2.5 Hz, 1H), 5.0 (s, 2H), 4.9 (s, 1H), 4.3 (d, J = 6.0 Hz, 2H), 3.9 (s, 1H), 3.7 (d, J = 11.0 Hz, 1H), 3.5 (dd, J = 17.9, 9.1 Hz, 2H), 3.0 (dd, J = 16.8, 7.9 Hz, 1H), 2.7 (s, 3H), 2.5 – 2.3 (m, 1H), 1.5 (s, 9H), 1.0 (d, J = 6.4 Hz, 3H), 0.8 (d, J = 6.7 Hz, 3H).

(2S,5S)-9-((4-(aminomethyl)benzyl)oxy)-5-(hydroxymethyl)-2-isopropyl-1-methyl-1,4,5,6-tetrahydrobenzo[e][1,4]diazocin-3(2H)-one hydrochloride (6-26)

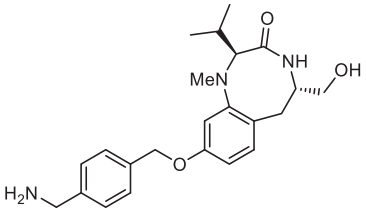

6-25 (190 mg, 0.38 mmol) was stirred in 5 mL of HCl/dioxane 4N for 2 h. The solvent was then evaporated affording the hydrochloride salt as a white solid (165 mg, **quant.**).

tert-butyl (3-((4-((((2S,5S)-5-(hydroxymethyl)-2-isopropyl-1-methyl-3-oxo-1,2,3,4,5,6-hexahydrobenzo[e][1,4]diazocin-9-yl)oxy)methyl)benzyl)amino)-3-oxopropyl)carbamate (6-27)

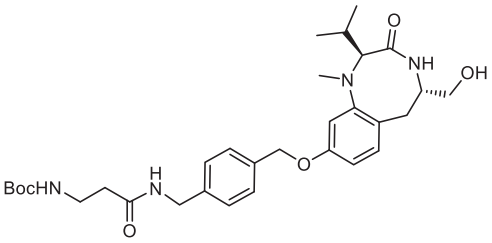

NUM was prepared following general method for amide formation 2, using **6-26** (15 mg, 0.03 mmol) and 3-((tert-butoxycarbonyl)amino)propanoic acid (6.5 mg, 0.053 mmol). The crude was purified by flash column chromatography, product was eluted at 4% methanol/DCM and reported as an off white solid (12 mg, 0.02 mmol, **61%**).

^{1}H NMR (500 MHz, $CDCl_3$) δ 7.37 (d, *J* = 7.8 Hz, 2H), 7.32 – 7.24 (m, 2H), 6.92 (d, *J* = 8.4 Hz, 1H), 6.56 (d, *J* = 2.5 Hz, 1H), 6.48 (d, *J* = 8.6 Hz, 2H), 6.25 (s, 1H), 5.21 (s, 1H), 5.01 (s, 2H), 4.48 – 4.36 (m, 2H), 3.95 (s, 1H), 3.72 – 3.65 (m, 1H), 3.50 (dd, *J* = 10.7, 8.6 Hz, 1H), 3.41 (q, *J* = 6.2 Hz, 3H), 3.01 (dd, *J* = 16.7, 7.9 Hz, 1H), 2.73 (d, *J* = 6.4 Hz, 4H), 2.47 – 2.34 (m, 3H), 1.42 (s, 9H), 1.04 (d, *J* = 6.5 Hz, 3H), 0.85 (d, *J* = 6.7 Hz, 3H). **HRMS (ESI):** calculated for $[C_{31}H_{45}O_6N_4]^+$: 569.33336, found: 569.33228.

3-amino-N-(4-((((2S,5S)-5-(hydroxymethyl)-2-isopropyl-1-methyl-3-oxo-1,2,3,4,5,6-hexahydrobenzo[e][1,4]diazocin-9-yl)oxy)methyl)benzyl)propanamide hydrochloride (6-27-HCl)

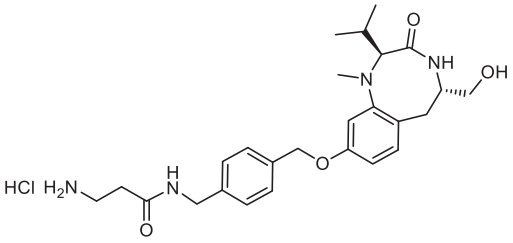

6-27 (10 mg, 0.021 mmol) was dissolved in 4N HCl/dioxane (3 mL) and stirred at rt for 3 h. The reaction crude was concentrated under reduced to afford the corresponding hydrochloride and used without further purification (10 mg, **quant**.).

tert-butyl (6-((4-((((2S,5S)-5-(hydroxymethyl)-2-isopropyl-1-methyl-3-oxo-1,2,3,4,5,6-hexahydrobenzo[e][1,4]diazocin-9-yl)oxy)methyl)benzyl)amino)-6-oxohexyl)carbamate (6-27')

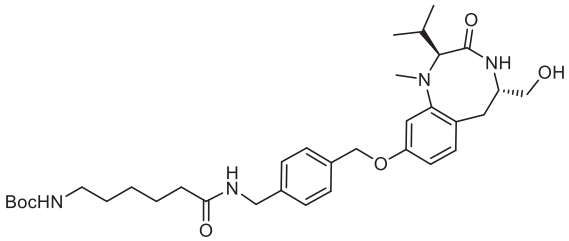

NUM was prepared following general method for amide formation 2, using **6-26** (30 mg, 0.06 mmol) and 6-((tert-butoxycarbonyl)amino)hexanoic acid (27 mg, 0.066 mmol). The crude was purified by flash column chromatography, product was eluted at 4% methanol/DCM and reported as an off white solid (35 mg, 0.057 mmol, **85%**).

^{1}H NMR (400 MHz, $CDCl_3$) δ 7.37 (d, *J* = 7.9 Hz, 2H), 7.31 – 7.24 (m, 2H), 6.92 (d, *J* = 8.3 Hz, 1H), 6.57 (d, *J* = 2.5 Hz, 2H), 6.47 (dd, *J* = 8.3, 2.5 Hz, 1H), 6.05 (d, *J* = 6.0 Hz, 1H), 5.01 (s, 2H), 4.61 (t, *J* = 6.3 Hz, 1H), 4.42 (dd, *J* = 5.8, 2.2 Hz, 2H), 3.94 (s, 1H), 3.68 (dd, *J* = 10.8, 3.9 Hz, 1H), 3.50 (dd, *J* = 10.8, 8.6 Hz, 1H), 3.43 (d, *J* = 8.8 Hz, 1H), 3.05 (dq, *J* = 30.8, 8.0, 7.5 Hz, 3H), 2.78 – 2.63 (m, 4H), 2.50 – 2.34 (m, 1H), 2.26 – 2.15 (m, 2H), 1.72 – 1.62 (m, 2H), 1.55 – 1.39 (m, 11H), 1.35 (q, *J* = 8.2 Hz, 2H), 1.04 (d, *J* = 6.5 Hz, 3H), 0.85 (d, *J* = 6.7 Hz, 3H). **HRMS (ESI):** calculated for $[C_{34}H_{51}O_6N_4]^+$: 611.38031, found: 611.38061.

6-amino-N-(4-((((2S,5S)-5-(hydroxymethyl)-2-isopropyl-1-methyl-3-oxo-1,2,3,4,5,6-hexahydrobenzo[e][1,4]diazocin-9-yl)oxy)methyl)benzyl)hexanamide hydrochloride (6-27'-HCl)

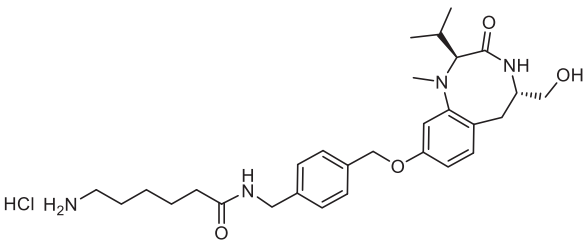

6-27' (35 mg, 0.057 mmol) was dissolved in 4N HCl/dioxane (3 mL) and stirred at rt for 3 h. The reaction crude was concentrated under reduced to afford the corresponding hydrochloride as an off white solid. The product was used without further purification (31 mg, **quant.**).

4-azido-N-(4-((((2S,5S)-5-(hydroxymethyl)-2-isopropyl-1-methyl-3-oxo-1,2,3,4,5,6-hexahydrobenzo[e][1,4]diazocin-9-yl)oxy)methyl)benzyl)butanamide (6-28a)

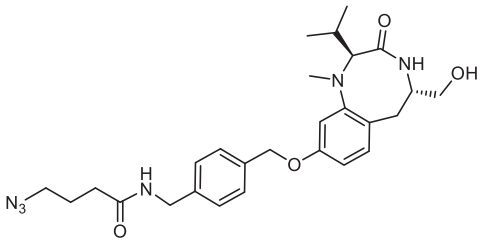

NUM was prepared following general method for amide formation 2, using **6-26** (30 mg, 0.058 mmol) and 4-azidobutanoic acid (7.5 mg, 0.058 mmol). The crude was purified by flash column chromatography, product was eluted at 5% methanol/DCM and reported as an off white solid (18 mg, 0.035 mmol, **61%**).

^{1}H NMR (400 MHz, CD_3OD) δ 8.05 – 7.90 (m, 2H), 7.90 – 7.75 (m, 2H), 7.53 (d, *J* = 8.4 Hz, 1H), 7.30 (d, *J* = 2.6 Hz, 1H), 7.14 (dd, *J* = 8.4, 2.5 Hz, 1H), 5.60 (s, 2H), 4.94 (s, 2H), 4.83 (s, 1H), 4.17 (dd, *J* = 11.0, 4.8 Hz, 1H), 4.10 – 4.01 (m, 2H), 3.95 – 3.89 (m, 2H), 3.55 – 3.37 (m, 2H), 3.31 (s, 3H), 3.02 – 2.96 (m, 1H), 2.91 (t, *J* = 7.4 Hz, 2H), 2.52 – 2.41 (m, 2H), 1.66 (d, *J* = 6.6 Hz, 3H), 1.49 (d, *J* = 6.8 Hz, 3H). **^{13}C NMR** (101 MHz, CD_3OD) δ 174.3, 173.5, 158.4, 152.8, 138.3, 136.5, 132.0, 127.4, 127.3, 124.7, 108.9, 107.5, 72.8, 64.4, 54.0, 50.5, 42.5, 36.3, 35.3, 32.5, 28.2, 24.8, 19.3, 18.6. **HRMS (ESI):** calculated for $[C_{27}H_{37}O_4N_6]^+$: 509.28708, found: 509.28707.

6-azido-N-(4-((((2S,5S)-5-(hydroxymethyl)-2-isopropyl-1-methyl-3-oxo-1,2,3,4,5,6-hexahydrobenzo[e][1,4]diazocin-9-yl)oxy)methyl)benzyl)hexanamide (6-28b)

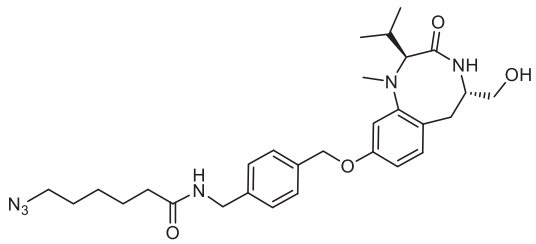

NUM was prepared following general method for amide formation 2, using **6-26** (16 mg, 0.034 mmol) and 6-azidohexanoic acid (27 mg, 0.034 mmol). The crude was purified by flash column chromatography, product was eluted at 4% methanol/DCM and reported as an off white solid (15 mg, 0.028 mmol, **81%**).

^{1}H NMR (500 MHz, $CDCl_3$) δ 7.38 (d, *J* = 8.2 Hz, 2H), 7.30 – 7.27 (m, 2H), 6.92 (d, *J* = 8.3 Hz, 1H), 6.57 (d, *J* = 2.5 Hz, 1H), 6.53 (d, *J* = 3.0 Hz, 1H), 6.47 (dd, *J* = 8.3, 2.6 Hz, 1H), 5.84 (d, *J* = 6.1 Hz, 1H), 5.00 (s, 2H), 4.43 (d, *J* = 5.6 Hz, 2H), 3.93 (s, 1H), 3.69 (dd, *J* = 10.7, 4.0 Hz, 1H), 3.51 (dd, *J* = 10.7, 8.8 Hz, 1H), 3.45 (d, *J* = 8.8 Hz, 1H), 3.27 (t, *J* = 6.8 Hz, 2H), 3.03 (dd, *J* = 16.8, 7.9 Hz, 1H), 2.75 (s, 3H), 2.72 (d, *J* = 2.2 Hz, 1H), 2.41 (dp, *J* = 8.9, 6.6 Hz, 1H), 2.22 (t, *J* = 7.5 Hz, 2H), 1.73 – 1.58 (m, 4H), 1.45 – 1.38 (m, 2H), 1.04 (d, *J* = 6.4 Hz, 3H), 0.85 (d, *J* = 6.7 Hz, 3H). **^{13}C NMR** (126 MHz, $CDCl_3$) δ 173.7, 172.7, 158.5, 152.8, 138.2, 136.5, 132.5, 128.3, 128.2, 107.3, 107.0, 70.3, 69.9, 66.1, 54.5, 51.4, 43.5, 36.8, 36.6, 35.3, 28.7, 28.4, 26.5, 25.3, 20.5, 20.0. **HRMS (ESI):** calculated for $[C_{29}H_{41}O_4N_6]^+$: 537.32, found: 537.32.

2-azido-N-(4-((((2S,5S)-5-(hydroxymethyl)-2-isopropyl-1-methyl-3-oxo-1,2,3,4,5,6-hexahydrobenzo[e][1,4]diazocin-9-yl)oxy)methyl)benzyl)acetamide (6-28c)

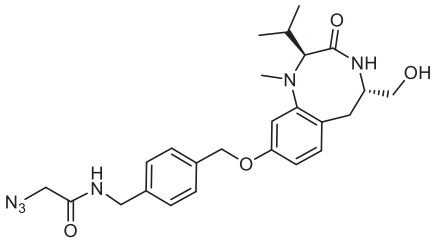

6-28c was prepared following general method for amide formation 2, using **6-26** (13 mg, 0.03 mmol) and 2-azidoacetic acid (3 mg, 0.03 mmol). The crude was purified by flash column chromatography, product was eluted at 5% methanol/DCM and reported as an off white solid (7 mg, 0.015 mmol, **50%**).

^{1}H NMR (400 MHz, $CDCl_3$) δ 7.41 (d, *J* = 7.9 Hz, 2H), 7.30 (d, *J* = 7.9 Hz, 2H), 6.94 (d, *J* = 8.4 Hz, 1H), 6.88 – 6.80 (m, 1H), 6.65 (s, 1H), 6.60 (d, *J* = 2.5 Hz, 1H), 6.49 (dd, *J* = 8.3, 2.5 Hz, 1H), 5.01 (s, 2H), 4.48 (d, *J* = 5.8 Hz, 2H), 4.05 (s, 2H), 3.98 (d, *J* = 10.9 Hz, 1H), 3.71 (dd, *J* = 10.8, 4.0 Hz, 1H), 3.52 (s, 1H), 3.47 (d, *J* = 8.8 Hz, 1H), 3.03 (dd, *J* = 16.9, 7.9 Hz, 1H), 2.79 (d, *J* = 2.3 Hz, 1H), 2.76 (s, 3H), 2.48 – 2.35 (m, 1H), 1.05 (d, *J* = 6.4 Hz, 3H), 0.86 (d, *J* = 6.7 Hz, 3H). **IR (ATR):** 3288, 2920, 2106, 1629, 1501, 1323 cm^{-1}. **HRMS (ESI):** calculated for $[C_{25}H_{33}O_4N_6]^+$: 481.25578, found: 481.25595.

tert-butyl (5-(3-(3-bromo-4-((2,4-difluorobenzyl)oxy)-6-methyl-2-oxopyridin-1(2H)-yl)-4-methylbenzamido)pentyl)carbamate (6-29)

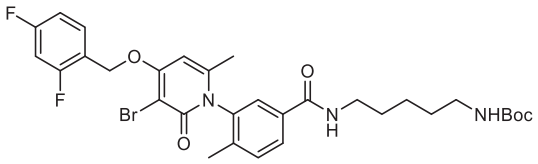

6-29 was prepared following general method for amide formation 2, using **5-7** (100 mg, 0.22 mmol) and boc-cadaverine (45 mg, 0.22 mmol). The crude was purified by flash column chromatography, product was eluted at 5% methanol/DCM and reported as an off white solid (129 mg, **93%**).

^{1}H NMR (500 MHz, $CDCl_3$) δ 7.8 (dd, J = 8.0, 1.8 Hz, 1H), 7.6 (dd, J = 8.5, 6.3 Hz, 1H), 7.4 – 7.3 (m, 1H), 7.2 (t, J = 5.7 Hz, 1H), 7.0 – 6.9 (m, 1H), 6.8 (ddd, J = 10.3, 8.7, 2.5 Hz, 1H), 6.2 (d, J = 0.8 Hz, 1H), 5.2 (s, 2H), 4.9 (t, J = 5.9 Hz, 1H), 3.4 – 3.0 (m, 4H), 2.1 (s, 3H), 1.9 (s, 3H), 1.6 – 1.4 (m, 13H), 1.3 (ddd, J = 9.0, 6.8, 3.2 Hz, 2H). **IR (ATR):** 2936, 1642, 1505, 1167, 841 cm^{-1}. **P_f:** 68 °C. **HRMS (ESI):** calculated for $[C_{31}H_{37}O_5N_3BrF_2]^+$: 648.18792, found: 648.18612.

3-(3-bromo-4-((2,4-difluorobenzyl)oxy)-6-methyl-2-oxopyridin-1(2H)-yl)-4-methyl-N-(5-(pent-4-ynamido)pentyl)benzamide (6-30)

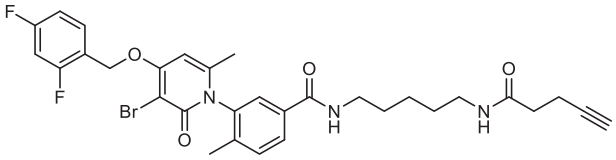

6-29 (129 mg, 0.2 mmol) was dissolved in 4N HCl/dioxane (3 mL) and stirred at room temperature for 3 h. The reaction crude was concentrated under reduced to afford the corresponding hydrochloride as an off white solid. The crude was used in the preparation of **6-30**.

6-30 was prepared following general method for amide formation 2, using **6-29 HCl** (58 mg, 0.10 mmol) and pentynoic acid (10 mg, 0.10 mmol). The crude was purified by flash column chromatography, product was eluted at 4% methanol/DCM and reported as an off white solid (30 mg, **46%**).

^{1}H NMR (400 MHz, CDCl3) δ 7.8 (dt, J = 8.0, 1.6 Hz, 1H), 7.6 – 7.5 (m, 2H), 7.3 (d, J = 8.0 Hz, 1H), 7.2 (t, J = 5.8 Hz, 1H), 7.0 – 6.9 (m, 1H), 6.8 (dddd, J = 10.1, 8.7, 2.6, 1.3 Hz, 1H), 6.4 (t, J = 5.7 Hz, 1H), 6.2 (s, 1H), 3.2 (dq, J = 37.6, 6.1 Hz, 4H), 2.5 – 2.4 (m, 2H), 2.4 – 2.2 (m, 2H), 2.1 (s, 3H), 2.0 (td, J = 2.6, 1.2 Hz, 1H), 1.9 (s, 3H), 1.5 (t, J = 7.8 Hz, 4H), 1.4 – 1.2 (m, 2H).

3-(3-bromo-4-((2,4-difluorobenzyl)oxy)-6-methyl-2-oxopyridin-1(2H)-yl)-N-(3-((4-((((2S,5S)-5-(hydroxymethyl)-2-isopropyl-1-methyl-3-oxo-1,2,3,4,5,6-hexahydrobenzo[e][1,4]diazocin-9-yl)oxy)methyl)benzyl)amino)-3-oxopropyl)-4-methylbenzamide (6-31a)

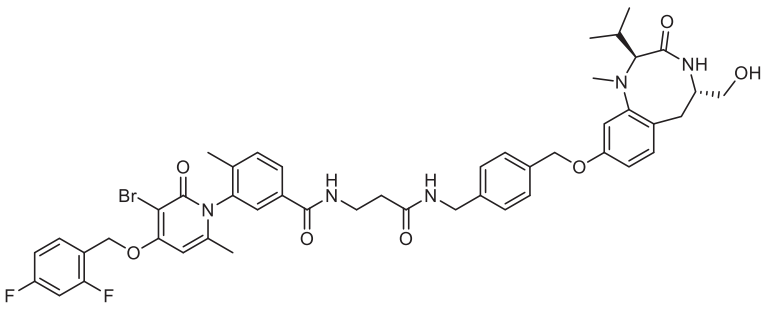

6-31a was prepared following general method for amide formation 2, using **6-27-HCl**, (13 mg, 0.026 mmol) and **5-7** (16 mg, 0.026 mmol). The crude was purified by flash column chromatography, the product was eluted at 7% methanol/DCM and reported as an off white solid (14 mg, 0.015 mmol, **59%**).

^{1}H NMR (400 MHz, $CDCl_3$) δ 7.7 (dd, J = 27.4, 7.9 Hz, 1H), 7.6 – 7.6 (m, 1H), 7.5 (s, 1H), 7.4 – 7.1 (m, 6H), 6.9 (t, J = 8.9 Hz, 1H), 6.9 – 6.7 (m, 2H), 6.6 – 6.4 (m, 1H), 6.4 – 6.3 (m, 1H), 6.3 (s, 1H), 6.2 (s, 1H), 5.2 – 5.1 (m, 2H), 4.9 (s, 1H), 4.5 – 4.2 (m, 2H), 4.0 (d, J = 45.7 Hz, 1H), 3.7 – 3.5 (m, 2H), 3.5 – 3.2 (m, 4H), 3.1 – 2.8 (m, 1H), 2.7 (d, J = 9.6 Hz, 4H), 2.5 – 2.3 (m, 4H), 2.1 – 2.0 (m, 3H), 1.9 – 1.8 (m, 3H), 1.0 (dd, J = 6.5, 2.3 Hz, 3H), 0.8 (d, J = 7.2 Hz, 3H). **HRMS (ESI):** calculated for $[C_{47}H_{51}O_7N_5BrF_2]^+$: 914.29344, found: 914.29390.

3-(3-bromo-4-((2,4-difluorobenzyl)oxy)-6-methyl-2-oxopyridin-1(2H)-yl)-N-(3-(1-(4-((4-((((2S,5S)-5-(hydroxymethyl)-2-isopropyl-1-methyl-3-oxo-1,2,3,4,5,6-hexahydrobenzo[e][1,4]diazocin-9-yl)oxy)methyl)benzyl)amino)-4-oxobutyl)-1H-1,2,3-triazol-4-yl)propyl)-4-methylbenzamide (6-31b)

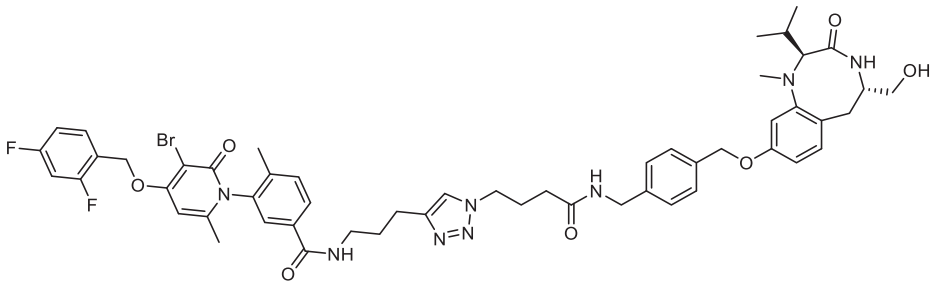

6-31b was prepared following **General method for CuAAC**, using **6-28a** (9 mg, 0.018 mmol) and **5-17** (9.5 mg, 0.018 mmol). The crude was purified by flash column chromatography, the product was eluted at 10% methanol/DCM and reported as an off white solid (9 mg, **50%**).

^{1}H NMR (400 MHz, CDCl3) δ 7.5 (dd, J = 15.2, 7.0 Hz, 2H), 7.5 (d, J = 15.4 Hz, 1H), 7.3 – 7.2 (m, 4H), 7.2 (d, J = 7.8 Hz, 2H), 7.0 (s, 1H), 6.9 – 6.9 (m, 2H), 6.9 – 6.8 (m, 1H), 6.5 (d, J = 2.6 Hz, 1H), 6.1 (d, J = 0.9 Hz, 1H), 5.2 (s, 2H), 4.9 (d, J = 2.5 Hz, 2H), 4.5 (d, J = 10.8 Hz, 1H), 4.3 – 4.2 (m, 4H), 3.9 (dd, J = 8.6, 4.2 Hz, 1H), 3.8 – 3.6 (m, 1H), 3.5 – 3.3 (m, 2H), 3.0 (d, J = 1.2 Hz, 3H), 2.9 (d, J = 12.6 Hz, 1H), 2.7 (s, 2H), 2.6 (dd, J = 14.3, 2.1 Hz, 1H), 2.1 – 1.8 (m, 14H), 0.8 (d, J = 6.5 Hz, 3H), 0.7 (d, J = 6.7 Hz, 3H). **HRMS (ESI):** calculated for $[C_{53}H_{58}O_7N_8BrF_2]^+$: 1035.35744, found: 1035.36229. $[M_{-2H}+H]^+$

3-(3-bromo-4-((2,4-difluorobenzyl)oxy)-6-methyl-2-oxopyridin-1(2H)-yl)-N-(5-(3-(1-(6-((4-((((2S,5S)-5-(hydroxymethyl)-2-isopropyl-1-methyl-3-oxo-1,2,3,4,5,6-hexahydrobenzo[e][1,4]diazocin-9-yl)oxy)methyl)benzyl)amino)-6-oxohexyl)-1H-1,2,3-triazol-4-yl)propanamido)pentyl)-4-methylbenzamide (6-31c)

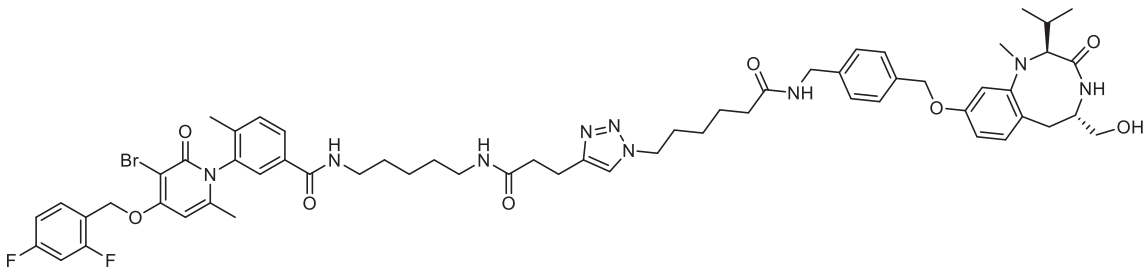

6-31c was prepared following **General method for CuAAC**, using **6-28b** (13 mg, 0.025 mmol) and **6-30** (16 mg, 0.025 mmol). The crude was purified by flash column chromatography; the product was eluted at 10% methanol/DCM and reported as an off white solid (12 mg, **41%**).

Ethyl 6-chloro-4-(phenylamino)quinoline-3-carboxylate (6-33)

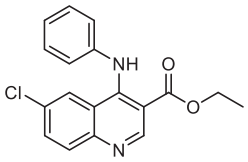

Ethyl 4,6-dichloroquinoline-3-carboxylate (1 g, 3.7 mmol, 1 eq.), aniline (0.4 mL, 4.4 mmol, 1.2 eq.), acetic acid (0.2 mL, 0.22 mmol, 1 eq.) and DNF (14.8 mL, 0.25 M) were loaded in a sealed tube and stirred at 100 °C during 1.5 hours. The reaction mixture was mixed with a saturated solution of potassium carbonate and extracted with ethyl acetate. The organic layers were combined, dried over magnesium sulphate and dried under reduced pressure. The crude was purified by silica gel column chromatography, eluting at 65% ethyl acetate in hexanes. The product was obtained as a yellow solid (1 g, **85%**).

The ^{1}H NMR spectra is consistent with that reported in the literature.[6]

^{1}H NMR (400 MHz, DMSO-*d6*) δ 9.7 (s, 1H), 8.9 (s, 1H), 8.2 (d, J = 2.3 Hz, 1H), 8.0 (d, J = 8.9 Hz, 1H), 7.8 (dd, J = 9.0, 2.3 Hz, 1H), 7.3 (dd, J = 8.8, 7.0 Hz, 2H), 7.1 – 7.0 (m, 4H), 3.9 (q, J = 7.1 Hz, 2H), 1.1 (t, J = 7.1 Hz, 3H).

6-chloro-N-methyl-4-(phenylamino)quinoline-3-carboxamide (6-34)

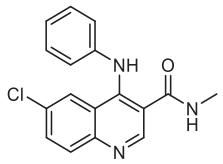

A flask was loaded with num (1.1 g, 3.36 mmol, 1 eq.) and methylamine (33% w I nethanol, 39 mL, 95 eq.) was stirred at 80 °C in a sealed flask during 5 hours. The reaction mixture was transferred to a round flask and dried under reduced pressure. The crude product was used without further purification (yellow solid, 1.03 g, **89%**).

The ^{1}H NMR spectra is consistent with that reported in the literature.[6]

^{1}H NMR (400 MHz, DMSO-*d6*) δ 9.81 (s, 1H), 8.78 (s, 1H), 8.47 (d, *J* = 4.8 Hz, 1H), 8.07 (d, *J* = 2.4 Hz, 1H), 7.95 (d, *J* = 9.0 Hz, 1H), 7.74 (dd, *J* = 8.9, 2.3 Hz, 1H), 7.30 – 7.20 (m, 2H), 7.03 (t, *J* = 7.3 Hz, 1H), 6.98 (d, *J* = 7.8 Hz, 2H), 2.52 (d, *J* = 4.6 Hz, 3H).

methyl 5-(3-(methylcarbamoyl)-4-(phenylamino)quinolin-6-yl)picolinate (6-36)

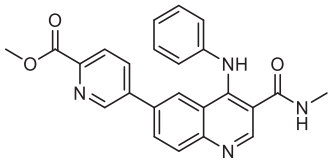

An oven-dried pressure tube was charged with a solution of **6-36** (456.08 mg, 1 .46 mmol) in dioxane (10 mL) and cesium carbonate (1.19 g, 3.66 mmol) and (6-methoxycarbonyl-3-pyridyl)boronic acid (317.66 mg, 1.76 mmol) were added. The reaction mixture was purged with nitrogen for 5 minutes and XPhos (224.95 mg, 292.58 mhio) and $Pd_2(dba)_3$ (133.96 mg, 146.29 mhio) were added. The reaction mixture was heated to 100°C for 4 hours and cooled to room temperature. The reaction mixture was diluted with water and the product was extracted with ethyl acetate. The combined organic layers were dried over anhydrous sodium sulfate, filtered and concentrated under reduced pressure. The crude mixture was purified by column chromatography on silica (4% methanol inDCM) to yield **6-36 (** 510 mg, 1.20 mmol, **81.76%** yield)

5-(3-(methylcarbamoyl)-4-(phenylamino)quinolin-6-yl)picolinic acid (6-37)

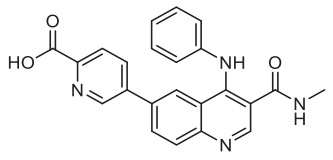

6-36 (94 mg 0.23 mmol 1 eq.) was dissolved in THF (0.5 mL, 0.48 M), MeOH (0.25 mL, 0.24 M) and H_2O (0.5 mL, 0.48 M),and LiOH (18 mg, 0.45 mmol, 2 eq.) was added. The reaction mixture was stirred at room temperature 5 hours. Reaction mixture was extracted with ethyl acetate, the aqueous phase was acidified to pH 4 and evaporated under reduced pressure. The residue was dissolved in acetonitrile, filtered and evaporated again. **6-37** obtained as a yellow solid and used without further purification (70 mg, 80%).

6-(6-(but-3-yn-1-ylcarbamoyl)pyridin-3-yl)-N-methyl-4-(phenylamino)quinoline-3-carboxamide (6-38)

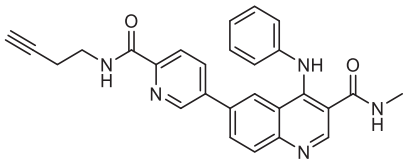

6-38 was prepared following general method for amide formation 2, using **6-37** (82 mg, 0.20 mmol) and but-3-yn-1-amine hydrochloride (22 mg, 0.20 mmol). The crude was purified by flash column chromatography, product was eluted at 2% methanol/DCM and reported as a yellow solid (20 mg, 0.044 mmol, **22%**).

^{1}H NMR (400 MHz, $CDCl_3$) δ 10.76 (s, 1H), 8.88 (s, 1H), 8.41 (dd, *J* = 2.3, 0.8 Hz, 1H), 8.27 (t, *J* = 6.1 Hz, 1H), 8.13 (dd, *J* = 8.1, 0.8 Hz, 1H), 8.07 (d, *J* = 8.7 Hz, 1H), 7.91 (d, *J* = 2.0 Hz, 1H), 7.86 (dd, *J* = 8.7, 2.1 Hz, 1H), 7.59 (dd, *J* = 8.1, 2.3 Hz, 1H), 7.41 – 7.31 (m, 2H), 7.24 – 7.19 (m, 1H), 7.14 – 7.07 (m, 2H), 6.53 (s, 1H), 3.65 (q, *J* = 6.6 Hz, 2H), 3.08 (d, *J* = 4.8 Hz, 3H), 2.54 (td, *J* = 6.7, 2.7 Hz, 2H), 2.06 (t, *J* = 2.6 Hz, 1H). **HRMS (ESI):** calculated for $[C_{27}H_{24}O_2N_5]^+$: 450.19245, found: 450.19187.

6-(6-((4-((((2S,5S)-5-(hydroxymethyl)-2-isopropyl-1-methyl-3-oxo-1,2,3,4,5,6-hexahydrobenzo[e][1,4]diazocin-9-yl)oxy)methyl)benzyl)carbamoyl)pyridin-3-yl)-N-methyl-4-(phenylamino)quinoline-3-carboxamide(6-39a)

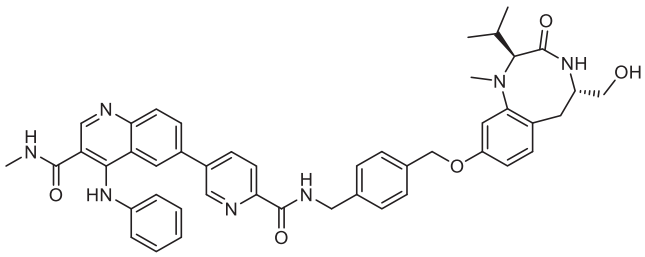

6-39a was prepared following general method for amide formation 2, using **6-37** (9.2 mg, 0.023 mmol) and **6-26** (10 mg, 0.023 mmol). The crude was purified by flash column chromatography, product was eluted at 6% methanol/DCM and reported as a yellow solid (7 mg, 0.089 mmol, **40%**).

HRMS (ESI): calculated for $[C_{46}H_{48}O_5N_7]^+$: 778.37114, found: 778.37158.

6-(6-((3-((4-((((2S,5S)-5-(hydroxymethyl)-2-isopropyl-1-methyl-3-oxo-1,2,3,4,5,6-hexahydrobenzo[e][1,4]diazocin-9-yl)oxy)methyl)benzyl)amino)-3-oxopropyl)carbamoyl)pyridin-3-yl)-N-methyl-4-(phenylamino)quinoline-3-carboxamide (6-39b)

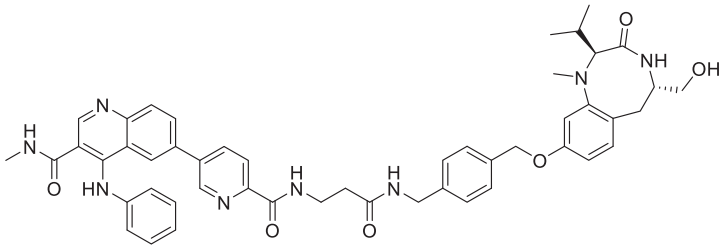

6-39b was prepared following general method for amide formation 2, using **6-37** (10 mg, 0.025 mmol) and **6-27-HCl** (13 mg, 0.025 mmol). The crude was purified by flash column chromatography, product was eluted at 5% methanol/DCM and reported as a yellow solid (5 mg, 0.058 mmol, **23%**).

^{1}H NMR (400 MHz, CD_3OD) δ 8.68 (s, 1H), 8.50 (d, *J* = 2.1 Hz, 1H), 8.15 (d, *J* = 1.9 Hz, 1H), 7.96 (dd, *J* = 9.4, 7.5 Hz, 2H), 7.92 – 7.83 (m, 2H), 7.25 (t, *J* = 7.8 Hz, 2H), 7.13 – 7.01 (m, 6H), 6.67 (d, *J* = 8.4 Hz, 1H), 6.48 (d, *J* = 2.5 Hz, 1H), 6.21 (dd, *J* = 8.4, 2.5 Hz, 1H), 4.73 (s, 0H), 4.27 (d, *J* = 4.6 Hz, 2H), 4.10 (s, 1H), 3.63 (t, *J* = 6.4 Hz, 2H), 3.54 – 3.44 (m, 1H), 3.37 (dd, *J* = 11.0, 7.7 Hz, 1H), 3.32 (d, *J* = 7.8 Hz, 1H), 2.74 (t, *J* = 5.5 Hz, 1H), 2.64 (s, 4H), 2.52 (d, *J* = 11.4 Hz, 5H), 2.22 (dt, *J* = 13.7, 6.8 Hz, 1H), 0.94 (d, *J* = 6.6 Hz, 3H), 0.74 (d, *J* = 6.7 Hz, 3H). **HRMS (ESI):** calculated for $[C_{49}H_{53}O_6N_8]^+$: 849.40826, found: 849.40844.

6-(6-((6-((4-((((2S,5S)-5-(hydroxymethyl)-2-isopropyl-1-methyl-3-oxo-1,2,3,4,5,6-hexahydrobenzo[e][1,4]diazocin-9-yl)oxy)methyl)benzyl)amino)-6-oxohexyl)carbamoyl)pyridin-3-yl)-N-methyl-4-(phenylamino)quinoline-3-carboxamide (6-39c)

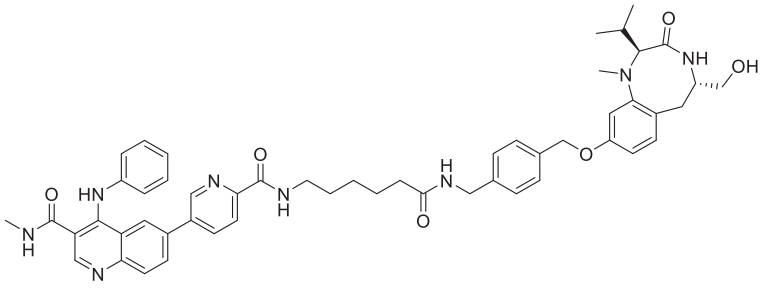

6-39c was prepared following general method for amide formation 2, **6-37** (10 mg, 0.025 mmol) and **6-27'-HCl** (16 mg, 0.025 mmol). The crude was purified by flash column chromatography, product was eluted at 6% methanol/DCM and reported as a yellow solid (9 mg, 0.010 mmol, **40%**).

^{1}H NMR (400 MHz, CD_3OD) δ 8.71 (d, *J* = 44.3 Hz, 2H), 8.42 – 8.23 (m, 1H), 8.16 – 7.97 (m, 4H), 7.46 – 7.13 (m, 10H), 6.88 (d, *J* = 8.4 Hz, 1H), 6.66 (d, *J* = 2.5 Hz, 1H), 6.47 (dd, *J* = 8.4, 2.5 Hz, 1H), 4.93 (s, 2H), 4.34 (d, *J* = 4.6 Hz, 2H), 4.22 (s, 1H), 3.65 – 3.51 (m, 1H), 3.51 – 3.35 (m, 4H), 2.86 (t, *J* = 5.4 Hz, 1H), 2.71 (s, 4H), 2.68 (s, 3H), 2.40 – 2.30 (m, 1H), 2.26 (t, *J* = 7.3 Hz, 2H), 1.67 (dp, *J* = 22.1, 7.2 Hz, 4H), 1.42 (d, *J* = 7.1 Hz,

2H), 1.05 (d, *J* = 6.6 Hz, 3H), 0.87 (d, *J* = 6.7 Hz, 3H). **HRMS (ESI):** calculated for $[C_{52}H_{59}O_6N_8]^+$: 891.45521, found: 891.45502.

6-(6-((2-(1-(6-((4-((((2S,5S)-5-(hydroxymethyl)-2-isopropyl-1-methyl-3-oxo-1,2,3,4,5,6-hexahydrobenzo[e][1,4]diazocin-9-yl)oxy)methyl)benzyl)amino)-6-oxohexyl)-1H-1,2,3-triazol-4-yl)ethyl)carbamoyl)pyridin-3-yl)-N-methyl-4-(phenylamino)quinoline-3-carboxamide (6-39d)

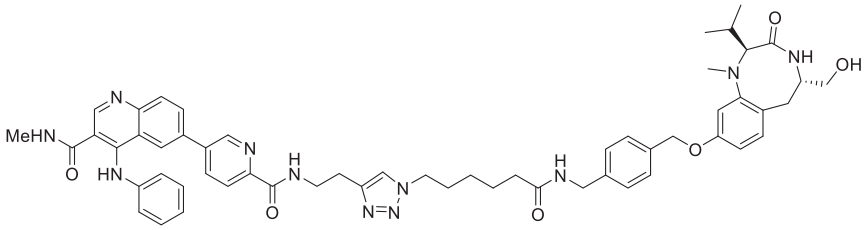

6-39d was prepared following general method for CuAAC, using using **6-38** (7 mg, 0.016 mmol) and **6-28b** (8.3 mg, 0.016 mmol). The crude was purified by flash column chromatography, eluted at 7% MeOH/DCM. Reported as a yellow solid, 8 mg, 0.008 mmol, **50%**).

HRMS (ESI): calculated for $[C_{56}H_{64}O_6N_{11}]^+$: 986.50356, found: 986.50270.

S)-1-(2-(2-(but-3-yn-1-ylamino)-2-oxoethoxy)phenyl)-3-(3,4-dimethoxyphenyl)propyl (R)-1-((R)-2-(3,4,5-trimethoxyphenyl)butanoyl)piperidine-2-carboxylate (6-31)

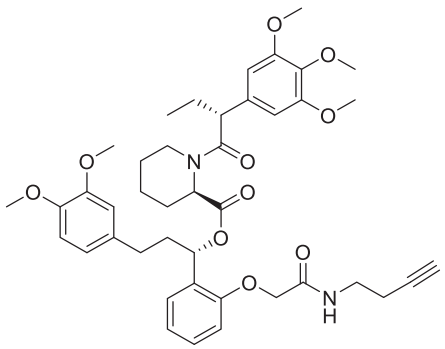

6-31 was prepared following general method for amide formation 2, **using 6-30** (35 mg, 0.05 mmol) and but-3-yn-1-amine hydrochloride (5 mg, 0.05 mmol). The crude was purified by flash column chromatography, product was eluted at 4% methanol/DCM and reported as an off white solid (20 mg, 0.27 mmol, **54%**).

^{1}H NMR (400 MHz, $CDCl_3$) δ 7.41 – 7.28 (m, 1H), 7.23 – 7.04 (m, 1H), 6.88 (td, *J* = 7.5, 1.0 Hz, 1H), 6.83 – 6.73 (m, 2H), 6.66 (td, *J* = 4.9, 2.8 Hz, 2H), 6.50 – 6.35 (m, 2H), 6.15 (dd, *J* = 7.9, 6.1 Hz, 1H), 5.49 (d, *J* = 5.3 Hz, 1H), 4.69 – 4.42 (m, 2H), 3.91 – 3.80 (m, 9H), 3.79 (s, 3H), 3.70 (s, 3H), 3.57 (t, *J* = 7.2 Hz, 1H), 3.49 – 3.21 (m, 2H), 2.70 – 2.49 (m, 2H), 2.49 – 2.36 (m, 2H), 2.33 (td, *J* = 6.9, 2.7 Hz, 2H), 2.26 (d, *J* = 14.0 Hz, 1H), 2.14 – 2.00 (m, 2H), 1.94 (ddd, *J* = 13.8, 9.6, 6.5 Hz, 1H), 1.87 (t, *J* = 2.6 Hz, 1H), 1.81 – 1.50 (m, 4H), 1.42 (dt,

J = 12.9, 3.8 Hz, 1H), 1.30 – 1.15 (m, 2H), 0.92 – 0.74 (m, 3H). **HRMS (ESI):** calculated for $[C_{42}H_{53}O_{10}N_2]^+$: 745.36947, found: 745.37024.

(S)-3-(3,4-dimethoxyphenyl)-1-(2-(2-((4-((((2S,5S)-5-(hydroxymethyl)-2-isopropyl-1-methyl-3-oxo-1,2,3,4,5,6-hexahydrobenzo[e][1,4]diazocin-9-yl)oxy)methyl)benzyl)amino)-2-oxoethoxy)phenyl)propyl (R)-1-((R)-2-(3,4,5-trimethoxyphenyl)butanoyl)piperidine-2-carboxylate (6-32a)

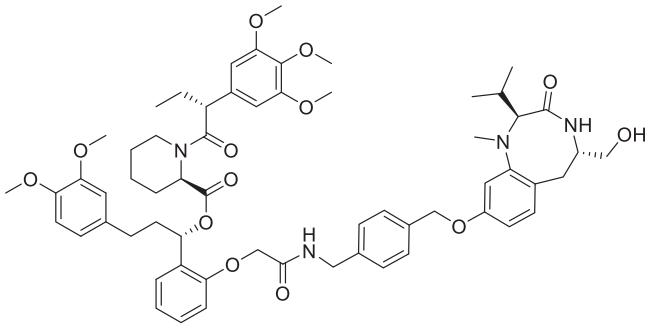

6-32a was prepared following general method for amide formation 2, using **6-26** (10 mg, 0.023 mmol) and **6-30** (16 mg, 0.023 mmol). The crude was purified by flash column chromatography, product was eluted at 3% methanol/DCM and reported as an off white solid (15 mg, 0.014 mmol, **60%**).

^{1}H NMR (400 MHz, $CDCl_3$) δ 7.72 (dt, *J* = 63.4, 6.2 Hz, 1H), 7.40 – 7.23 (m, 2H), 7.23 – 7.11 (m, 3H), 6.94 – 6.82 (m, 2H), 6.82 – 6.71 (m, 2H), 6.71 – 6.58 (m, 2H), 6.55 (d, *J* = 2.5 Hz, 1H), 6.51 – 6.40 (m, 3H), 6.10 (dd, *J* = 8.0, 6.2 Hz, 1H), 5.49 – 5.38 (m, 1H), 4.95 (d, *J* = 2.2 Hz, 2H), 4.76 – 4.31 (m, 4H), 3.92 – 3.74 (m, 11H), 3.67 (s, 7H), 3.51 (dd, *J* = 12.1, 8.2 Hz, 3H), 3.05 (dd, *J* = 16.9, 7.7 Hz, 1H), 2.85 – 2.65 (m, 4H), 2.65 – 2.31 (m, 4H), 2.12 – 1.57 (m, 8H), 1.57 – 1.30 (m, 3H), 1.05 (d, *J* = 6.4 Hz, 3H), 0.91 – 0.82 (m, 6H). **HRMS (ESI):** calculated for $[C_{61}H_{77}O_{13}N_4]^+$: 1073.54816, found: 1073.54759.

(S)-3-(3,4-dimethoxyphenyl)-1-(2-(2-((3-((4-((((2S,5S)-5-(hydroxymethyl)-2-isopropyl-1-methyl-3-oxo-1,2,3,4,5,6-hexahydrobenzo[e][1,4]diazocin-9-yl)oxy)methyl)benzyl)amino)-3-oxopropyl)amino)-2-oxoethoxy)phenyl)propyl (R)-1-((R)-2-(3,4,5-trimethoxyphenyl)butanoyl)piperidine-2-carboxylate (6-32b)

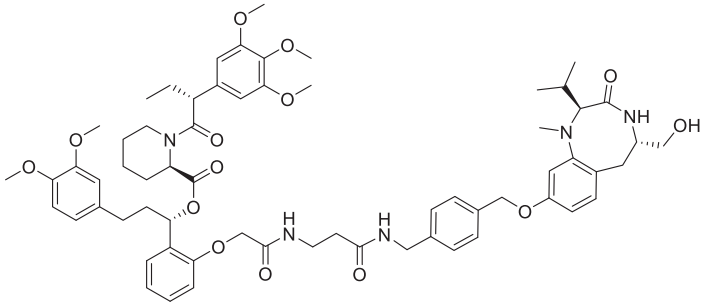

6-32b was prepared following general method for amide formation 2, using **6-27-HCl** (10 mg, 0.021 mmol) and **6-30** (15 mg, 0.021 mmol). The crude was purified by flash column chromatography, product was eluted at 3% methanol/DCM and reported as an off white solid (18 mg, 0.016 mmol, **75%**).

^{1}H NMR (400 MHz, $CDCl_3$) δ 7.43 – 7.13 (m, 6H), 6.96 – 6.80 (m, 2H), 6.81 – 6.63 (m, 6H), 6.50 – 6.34 (m, 4H), 6.12 (dd, *J* = 8.3, 5.8 Hz, 1H), 5.44 (d, *J* = 5.4 Hz, 1H), 4.98 (s, 2H), 4.65 – 4.24 (m, 4H), 4.02 – 3.61 (m, 18H), 3.61 – 3.35 (m, 4H), 3.13 – 2.93 (m, 1H), 2.73 (d, *J* = 3.6 Hz, 4H), 2.67 – 1.17 (m, 17H), 1.04 (d, *J* = 6.4 Hz, 3H), 0.95 – 0.78 (m, 6H). **HRMS (ESI):** calculated for $[C_{64}H_{82}O_{14}N_5]^+$: 1144.58528, found: 1144.58506.

(S)-3-(3,4-dimethoxyphenyl)-1-(2-(2-((2-(1-(2-((4-((((2S,5S)-5-(hydroxymethyl)-2-isopropyl-1-methyl-3-oxo-1,2,3,4,5,6-hexahydrobenzo[e][1,4]diazocin-9-yl)oxy)methyl)benzyl)amino)-2-oxoethyl)-1H-1,2,3-triazol-4-yl)ethyl)amino)-2-oxoethoxy)phenyl)propyl (R)-1-((R)-2-(3,4,5-trimethoxyphenyl)butanoyl)piperidine-2-carboxylate (6-32c)

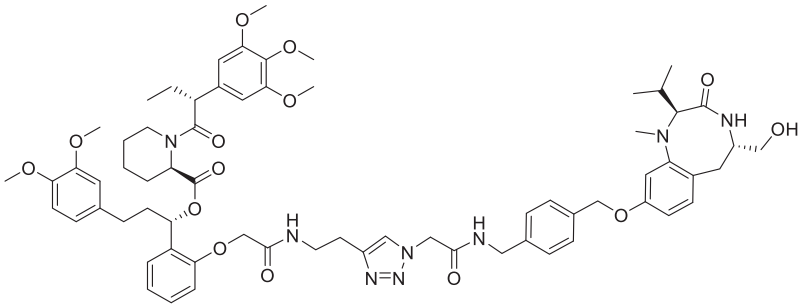

6-32c was prepared following general method for CuAAC, using **6-28c** (8.7 mg, 0.018 mmol) and **6-31** (13.4 mg, 0.018 mmol). The crude was purified by flash column chromatography, product was eluted at 7% methanol/DCM and reported as an off white solid (15 mg, 0.011 mmol, **60%**).

^{1}H NMR (400 MHz, $CDCl_3$) δ 7.44 – 7.13 (m, 6H), 7.04 (p, *J* = 7.1, 6.6 Hz, 1H), 6.93 – 6.59 (m, 5H), 6.55 – 6.37 (m, 4H), 6.13 (dd, *J* = 7.9, 6.0 Hz, 1H), 5.48 – 5.42 (m, 1H), 5.06 – 4.85 (m, 4H), 4.51 – 4.22 (m, 4H), 4.01 – 3.62 (m, 18H), 3.61 – 3.35 (m, 4H), 3.05 – 2.76 (m, 5H), 2.71 (d, *J* = 4.4 Hz, 4H), 2.68 – 2.19 (m, 5H), 2.14 – 1.86 (m, 4H), 1.70 (d, *J* = 34.4 Hz, 5H), 1.04 (d, *J* = 6.4 Hz, 3H), 0.92 – 0.83 (m, 6H). **HRMS (ESI):** calculated for $[C_{67}H_{85}O_{14}N_8]^+$: 1225.61798, found: 1225.61806.

(S)-3-(3,4-dimethoxyphenyl)-1-(2-(2-((2-(1-(6-((4-((((2S,5S)-5-(hydroxymethyl)-2-isopropyl-1-methyl-3-oxo-1,2,3,4,5,6-hexahydrobenzo[e][1,4]diazocin-9-yl)oxy)methyl)benzyl)amino)-6-oxohexyl)-1H-1,2,3-triazol-4-yl)ethyl)amino)-2-oxoethoxy)phenyl)propyl (R)-1-((R)-2-(3,4,5-trimethoxyphenyl)butanoyl)piperidine-2-carboxylate (6-32d)

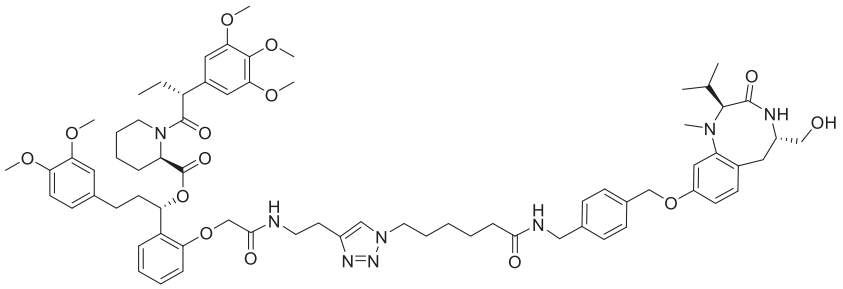

6-32d was prepared following general method for CuAAC, using **6-28b**, 3.6 mg, 0.007 mmol) and **6-31** (5 mg, 0.007 mmol). The crude was purified by flash column chromatography, product was eluted at 7% methanol/DCM and reported as an off white solid (6 mg, 0.0045 mmol, **64%**).

^{1}H NMR (400 MHz, $CDCl_3$) δ 7.55 – 7.18 (m, 9H), 6.93 – 6.62 (m, 6H), 6.53 – 6.23 (m, 3H), 6.14 (t, *J* = 7.0 Hz, 1H), 5.44 (s, 1H), 5.03 (d, *J* = 4.5 Hz, 2H), 4.68 – 4.35 (m, 4H), 4.22 (t, *J* = 7.2 Hz, 2H), 4.01 (s, 1H), 3.89 – 3.62 (m, 16H), 3.59 – 3.42 (m, 4H), 3.36 (d, *J* = 8.6 Hz, 1H), 3.08 – 2.78 (m, 4H), 2.72 (s, 4H), 2.67 – 2.21 (m, 6H), 2.12 – 1.77 (m, 5H), 1.77 – 1.58 (m, 8H), 1.04 (d, *J* = 6.4 Hz, 3H), 0.86 (dd, *J* = 10.8, 7.0 Hz, 6H). **HRMS (ESI):** calculated for $[C_{71}H_{93}O_{14}N_8]^+$: 1281.68058, found: 1281.68069.

References

[1] Crew, A.; Berlin, M.; Dong. H.; Ishchenko, A.; Cacace, P.; Chandler.; Tau Protein Targeting Compounds and Associated Methods of Use, WO2021/11913, 2021, A1.

[2] Selness, S. R.; Devraj, R. V.; Devadas, B.; Walker, J. K.; Boehm, T. L.; Durley, R. C.; Shieh, H.; Xing, L.; Rucker, P. V.; Jerome, K. D.; et al. Discovery of PH-797804, a Highly Selective and Potent Inhibitor of P38 MAP Kinase. *Bioorganic Med. Chem. Lett.* **2011**, *21* (13), 4066–4071. https://doi.org/10.1016/j.bmcl.2011.04.121.

[3] Donoghue, C., Cubillos-Rojas, M., Gutierrez-Prat, N., Sanchez-Zarzalejo, C., Verdaguer, X., Riera, A., Nebreda, A.R.. Optimal linker length for small molecule PROTACs that selectively target p38α and p38β for degradation. *Eur. J. Med. Chem.* **2020**, *201*, 112451.

[4] NOSTRUM BIODISCOVERY S L; BARCELONA SUPERCOMPUTING CENTER CENTRO NAC DE SUPERCOMPUTACION BSC CNS; UNIVERSITAT DE BARCELONA; GOVERNMENT OF SPAIN - WO2020/120576, 2020, A1 Patent Family Members: WO2020/120576 A1

[5] Siriwardena, S. U. *et al.* Phosphorylation-Inducing Chimeric Small Molecules. *J. Am. Chem. Soc.* **2020**, *142*, 14052–14057.

[6] Nasveschuk C. G.; Yin N.; Jackson K. L.; Veits G. K.; Moustakim M.; Yap J. L.; Zeid R. Compound for the Degradation of BRD9 or MTH1. US2021/198256, 2021, A1.

Appendix 1: List of Final Compounds

Oestrogen Receptor PROTACs

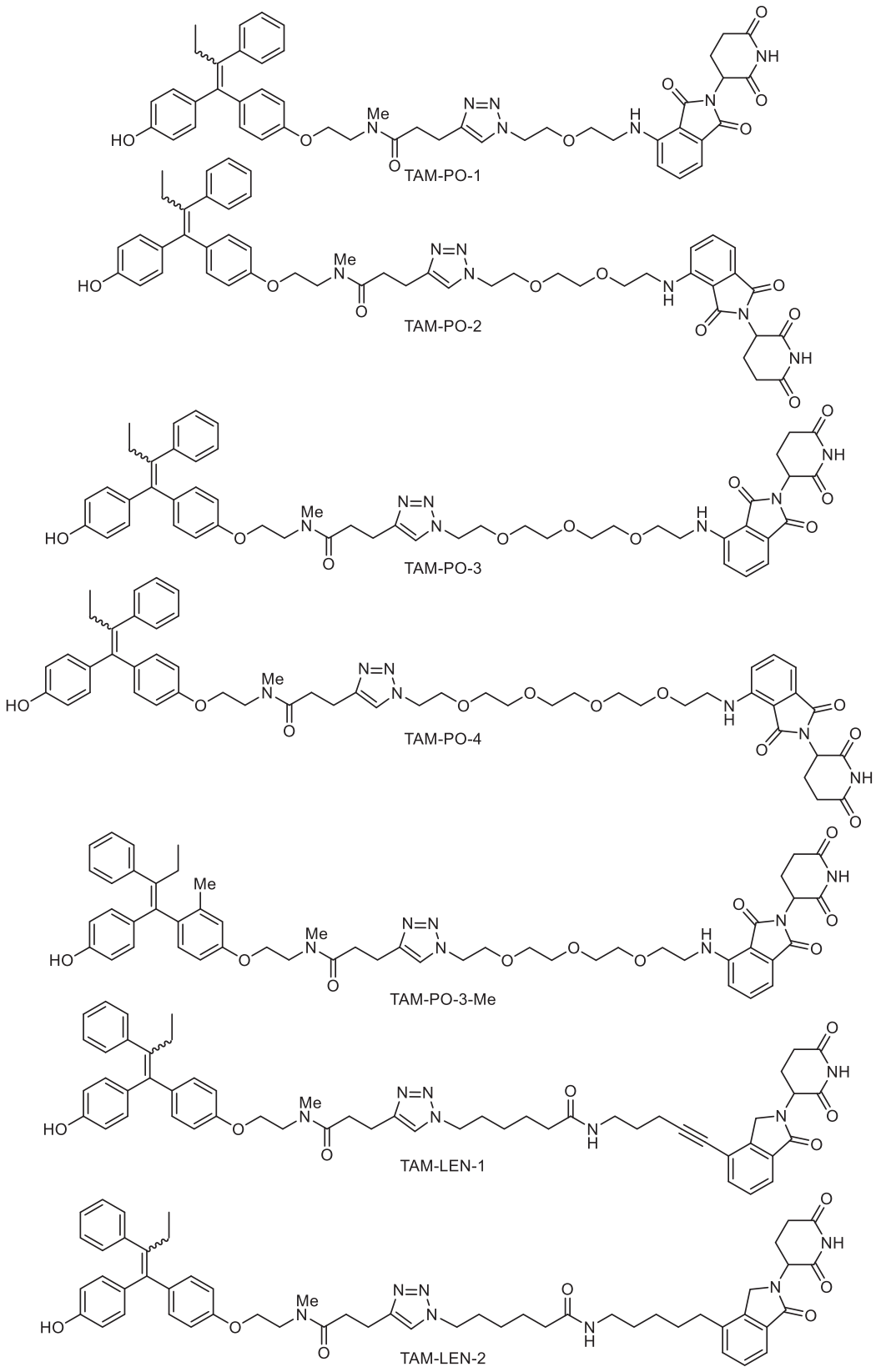

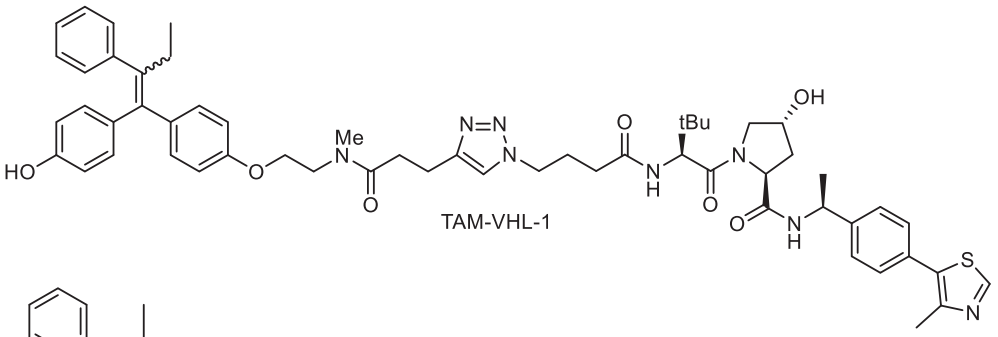

TAM-VHL-1

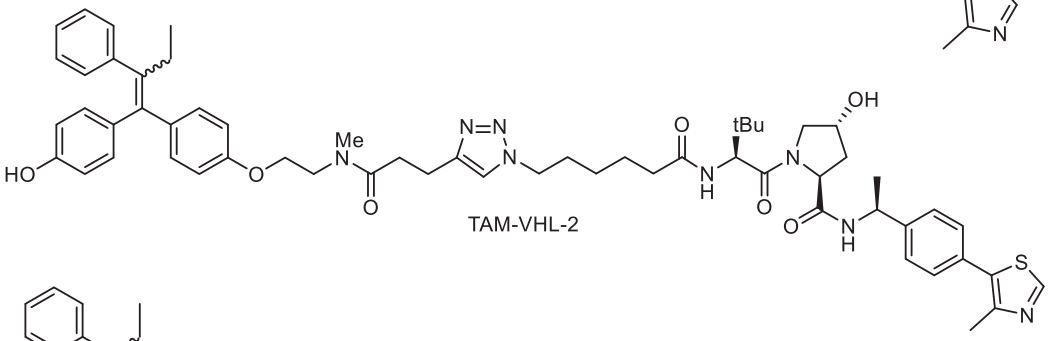

TAM-VHL-2

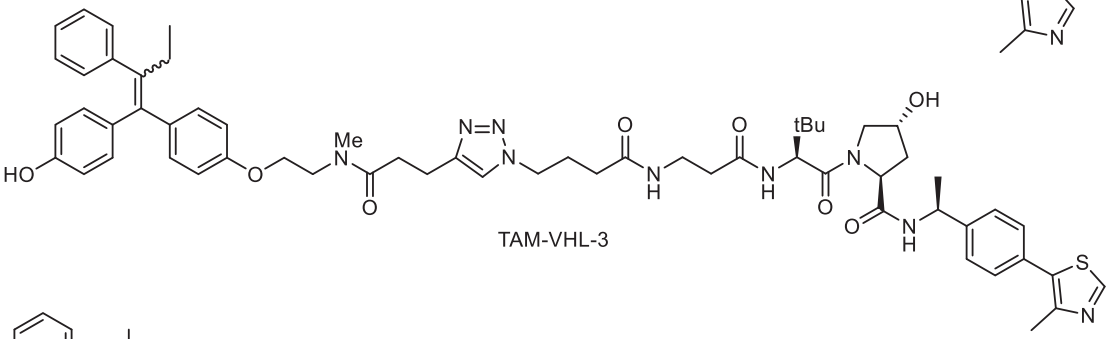

TAM-VHL-3

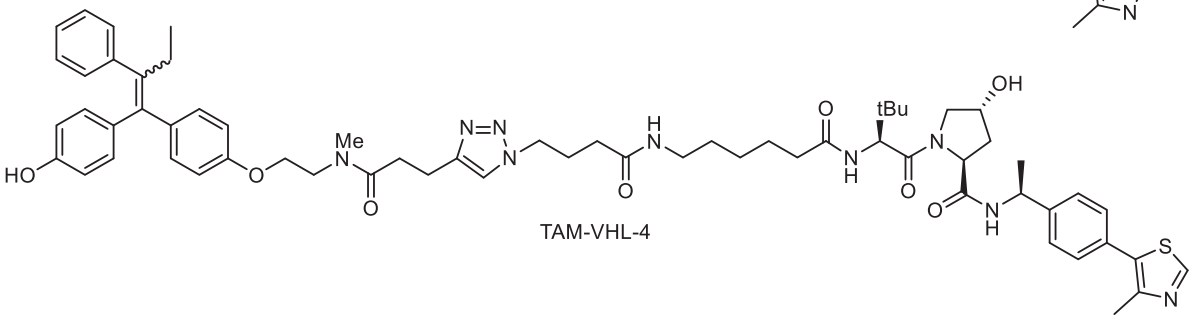

TAM-VHL-4

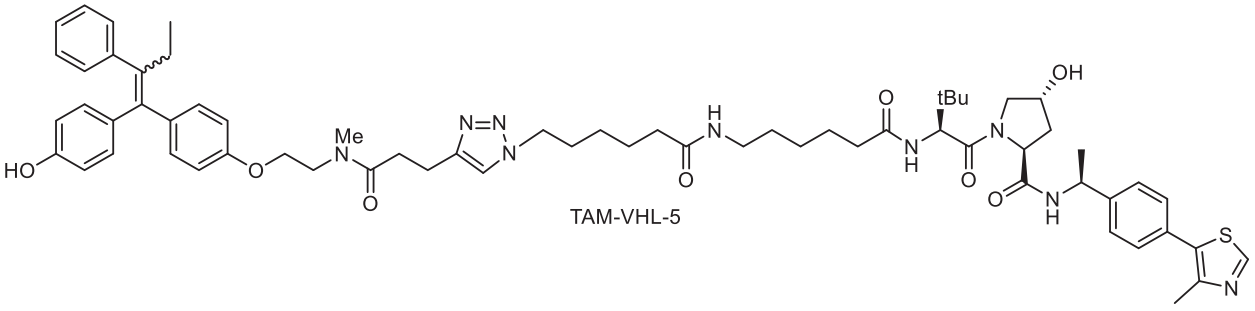

TAM-VHL-5

TLK PROTACs

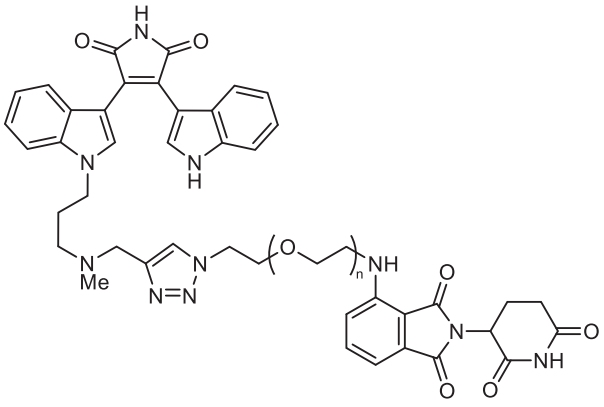

n=1, **4-8a**
n=2, **4-8b**
n=3, **4-8c**
n=4, **4-8d**

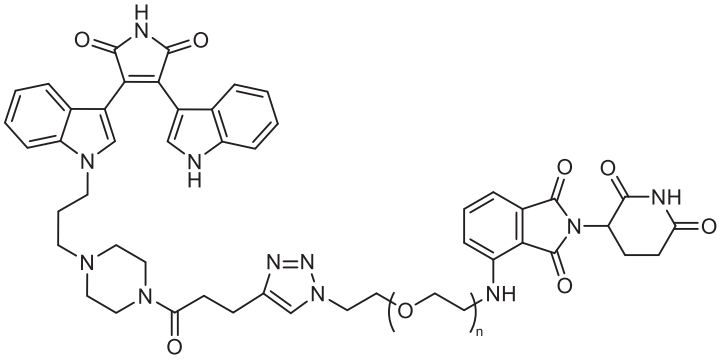

n=1, **4-11a**
n=2, **4-11b**
n=3, **4-11c**
n=4, **4-11d**

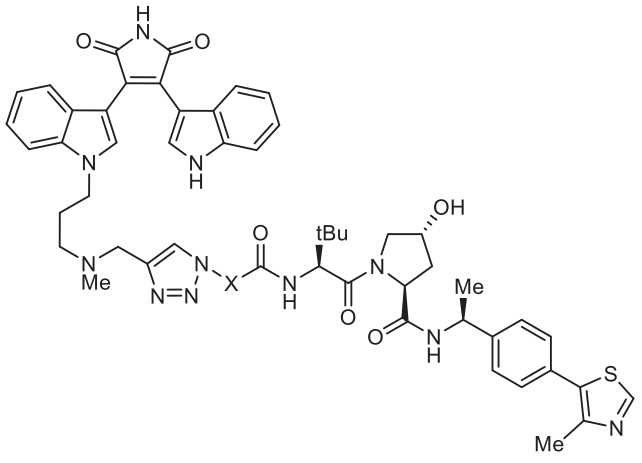

x=

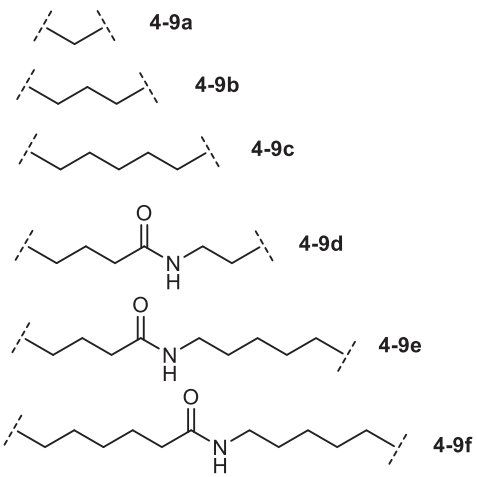

4-9a
4-9b
4-9c
4-9d
4-9e
4-9f

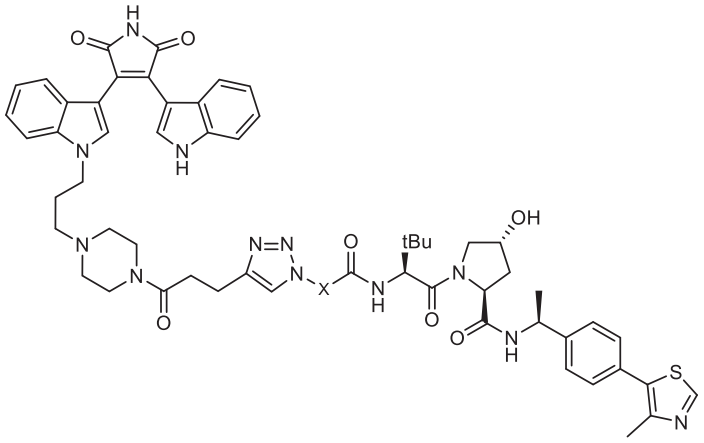

x= **4-12a**

4-12b

4-12c

4-12d

4-12e

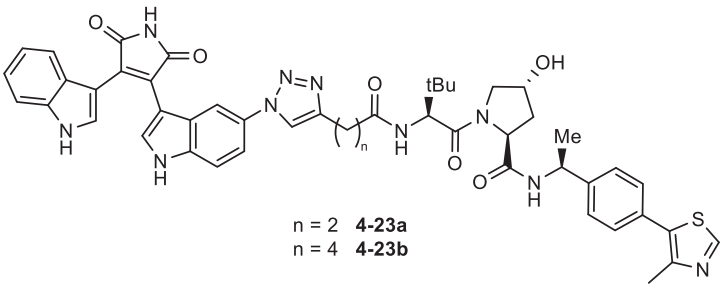

n = 2 **4-23a**
n = 4 **4-23b**

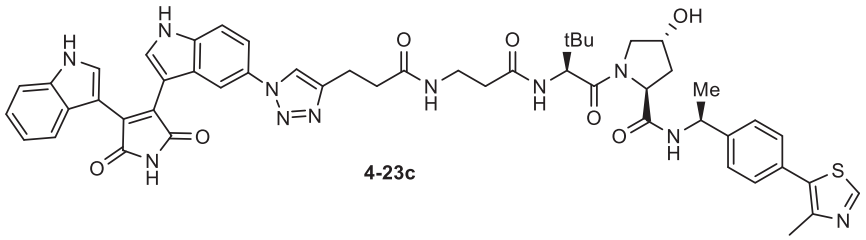

4-23c

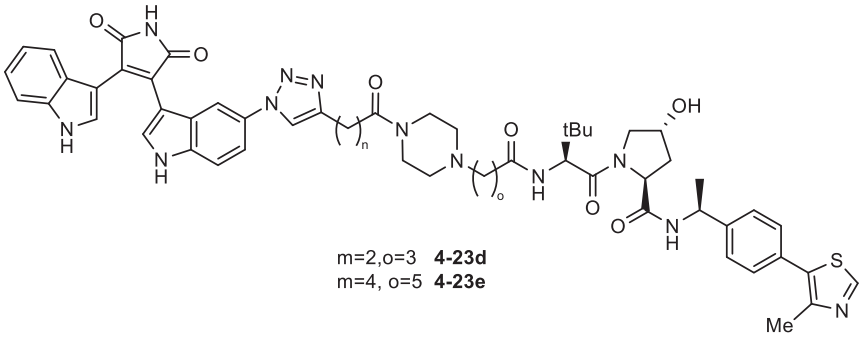

m=2,o=3 **4-23d**
m=4, o=5 **4-23e**

p38 PROTACs

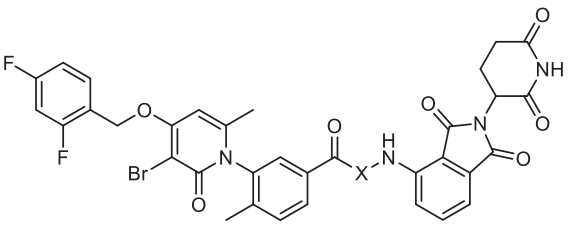

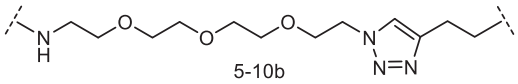

5-10b

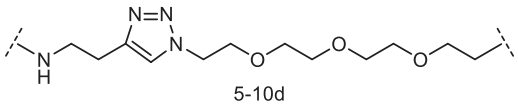

5-10d

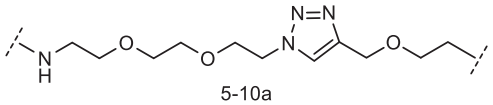

5-10a

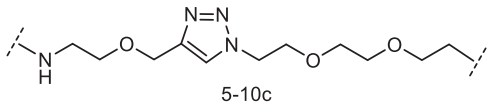

5-10c

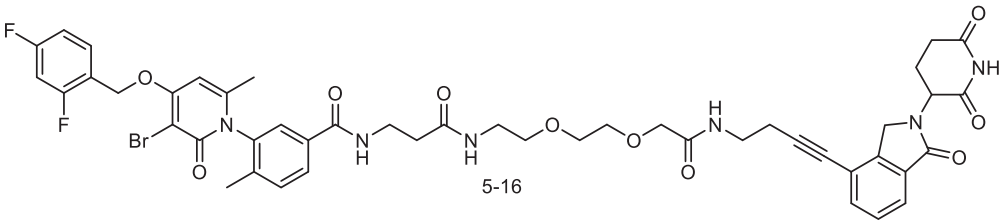

5-16

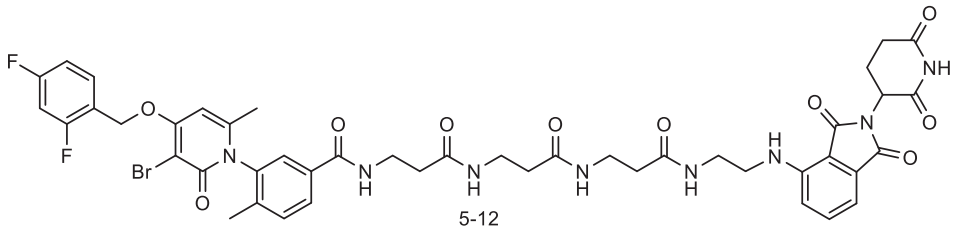

5-12

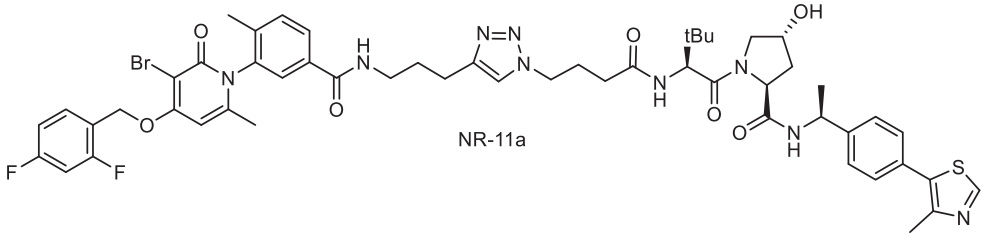

NR-11a

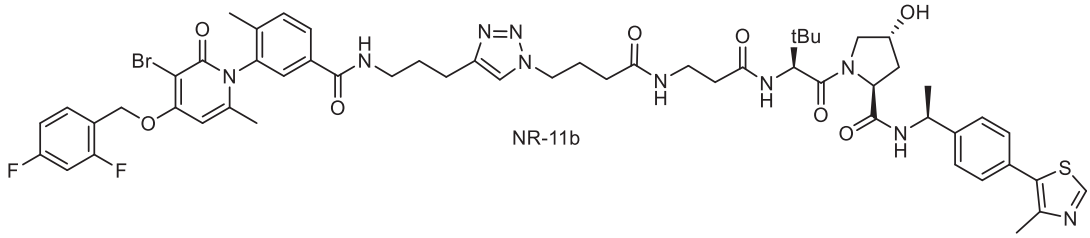

NR-11b

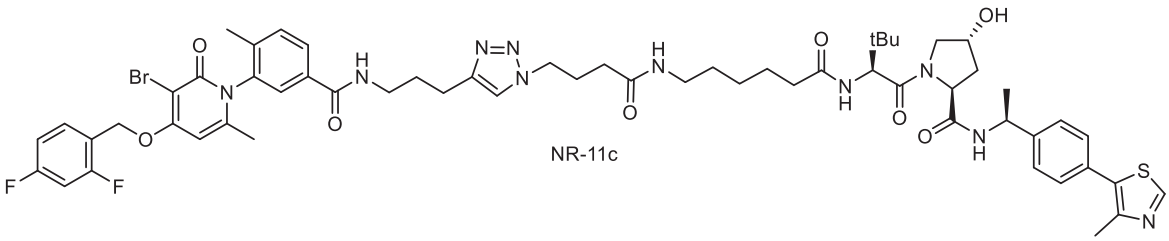

NR-11c

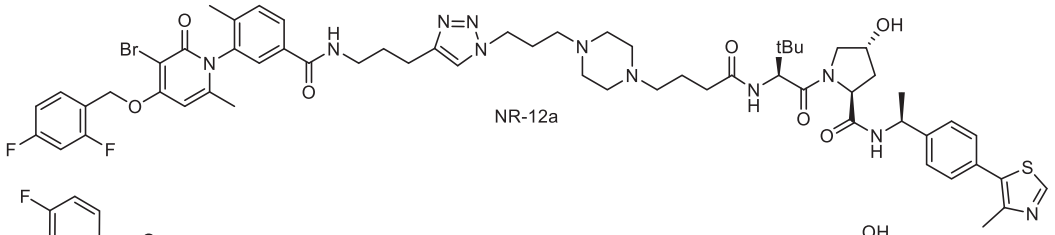

NR-12a

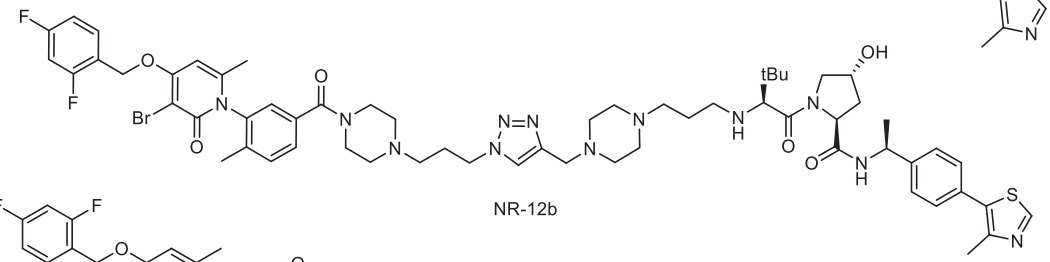

NR-12b

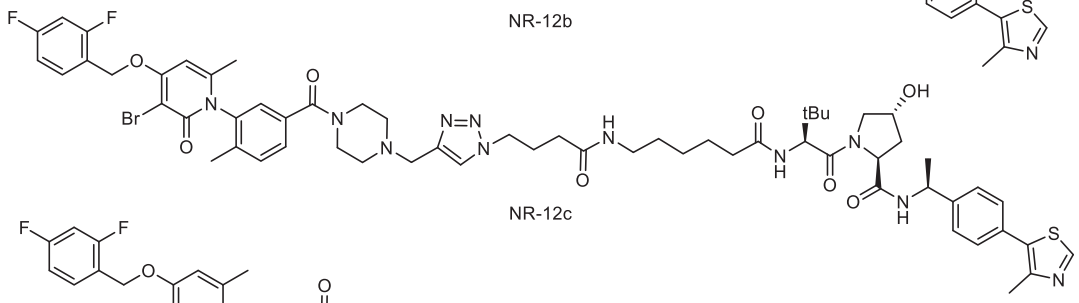

NR-12c

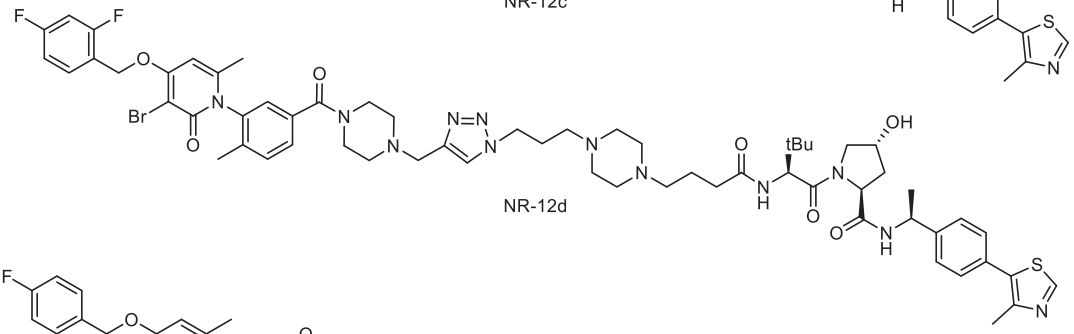

NR-12d

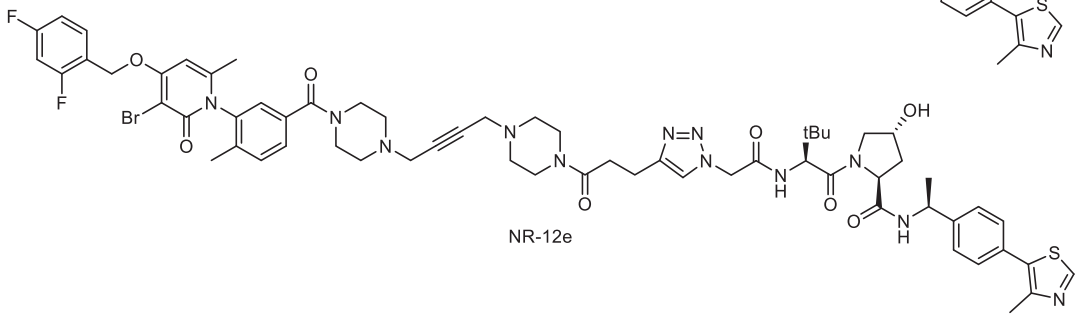

NR-12e

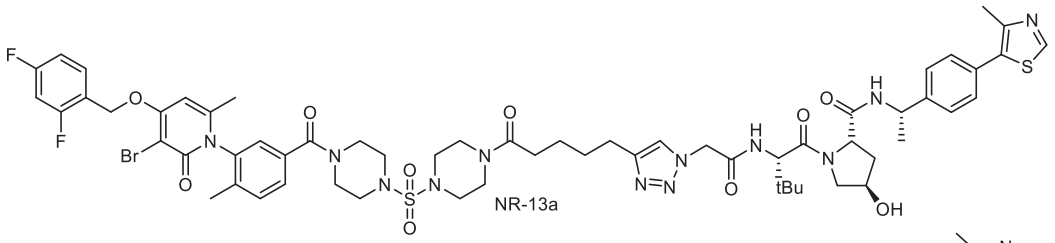

NR-13a

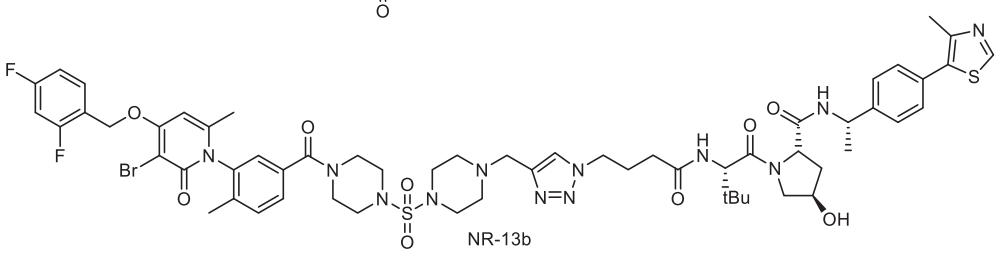

NR-13b

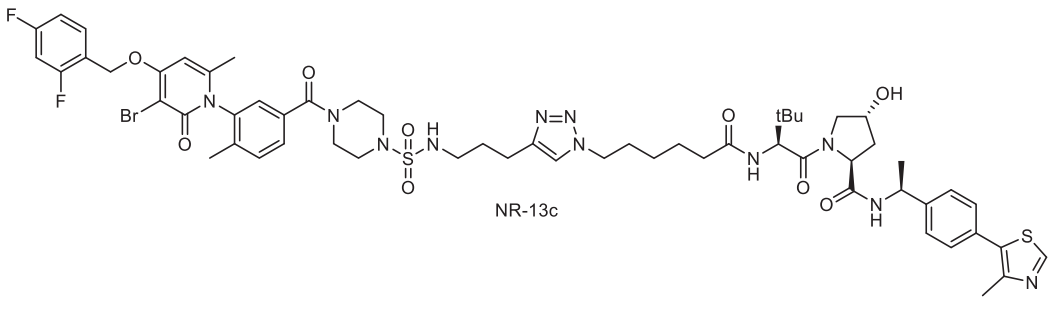

NR-13c

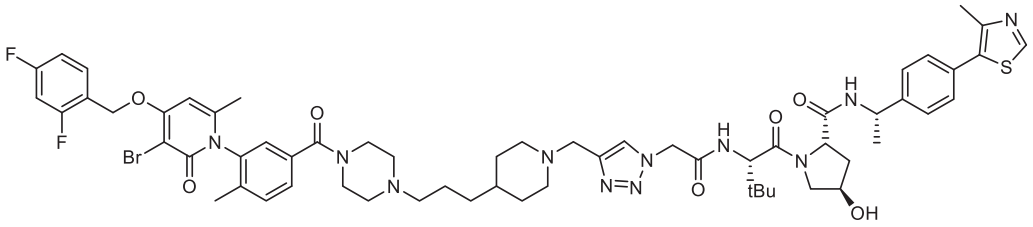

NR-14a

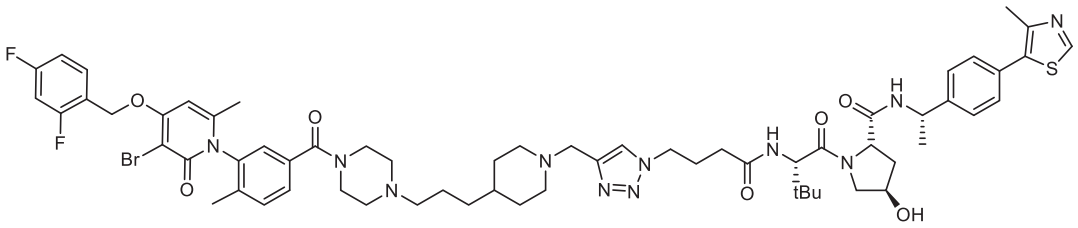

NR-14b

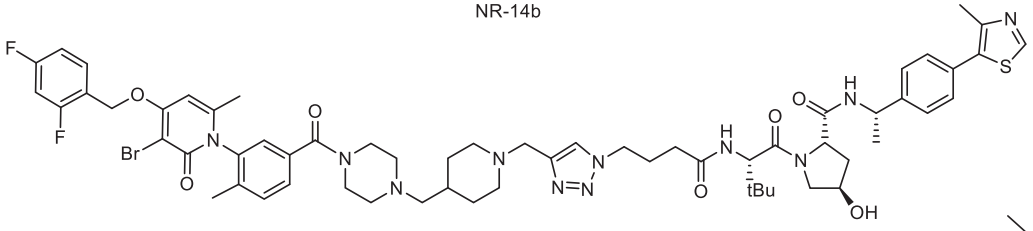

NR-14c

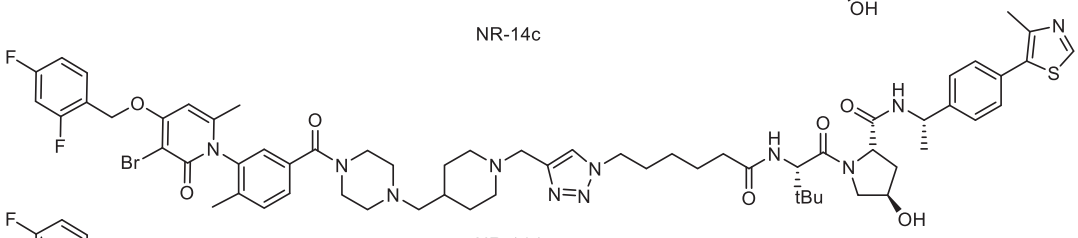

NR-14d

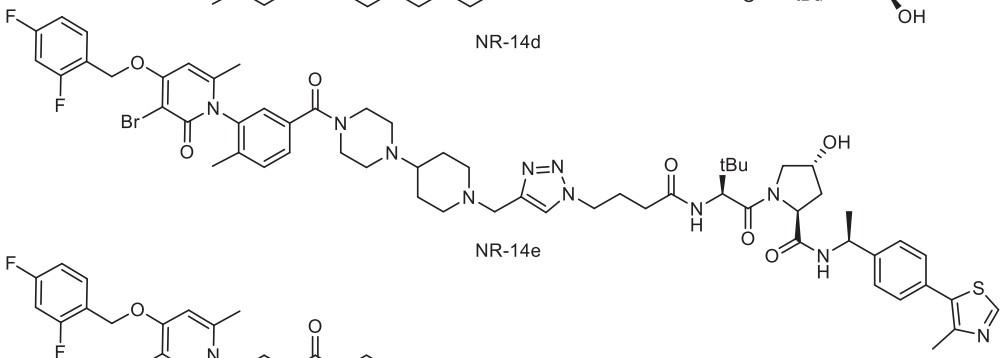

NR-14e

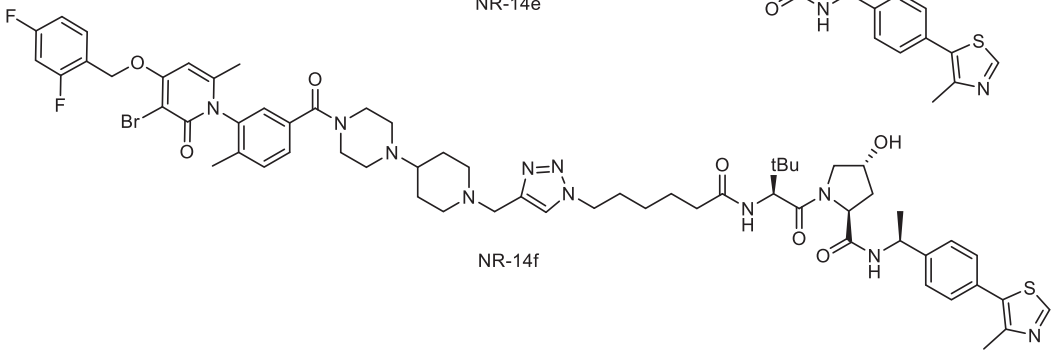

NR-14f

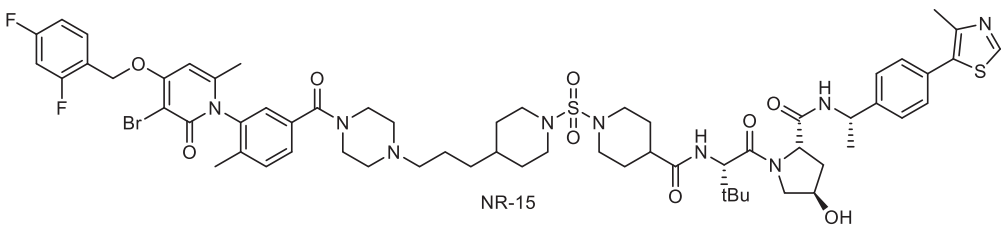

NR-15

Phosphorylation Inducers

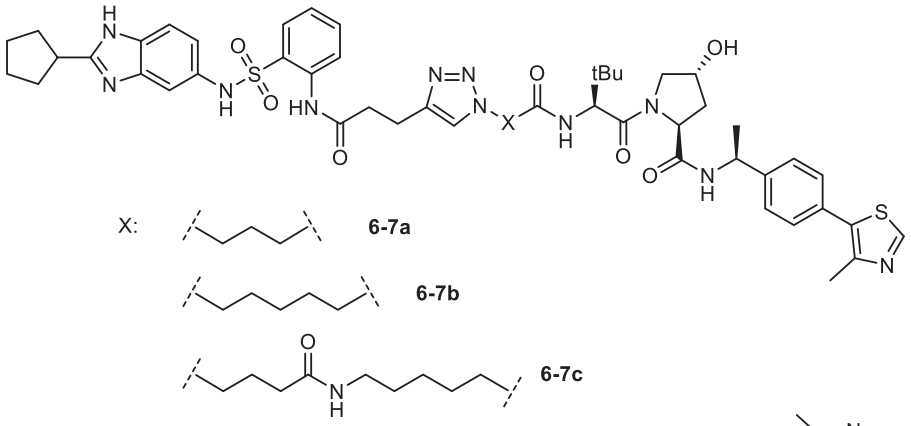

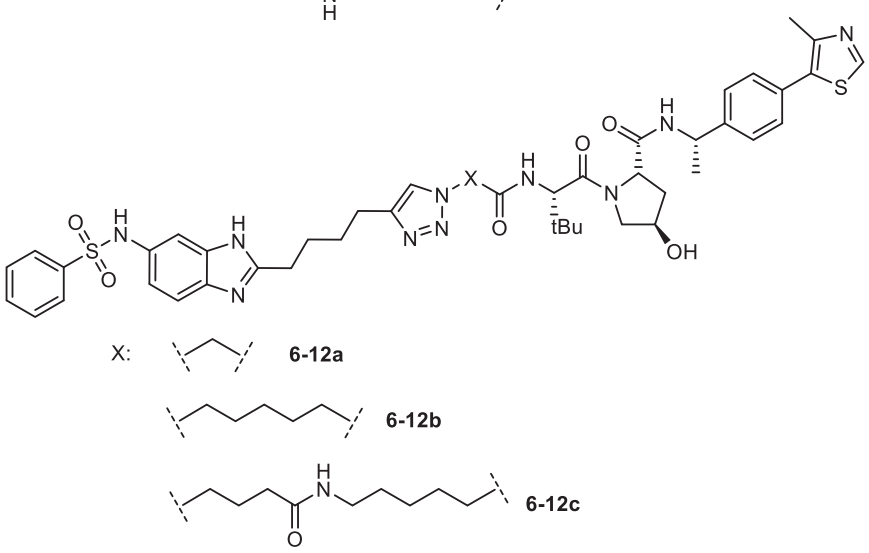

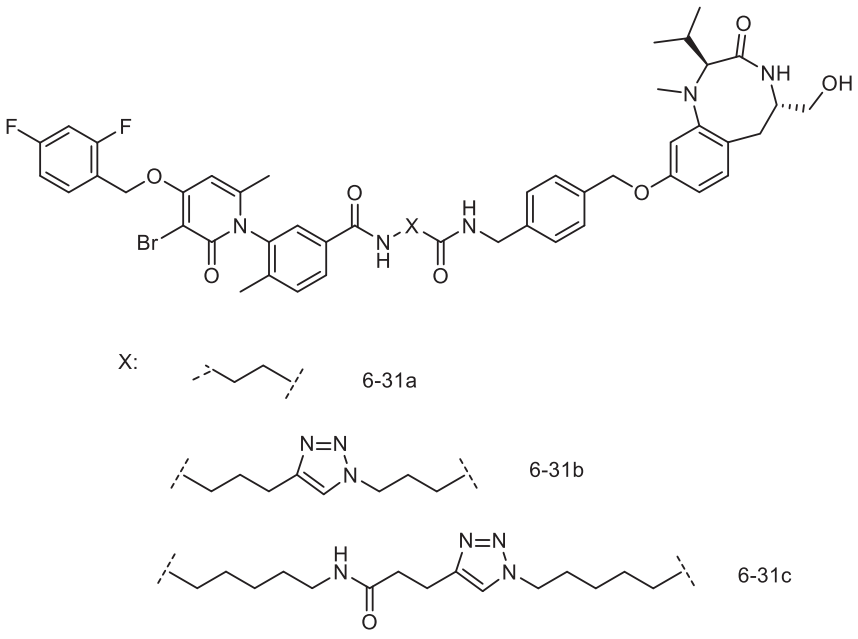

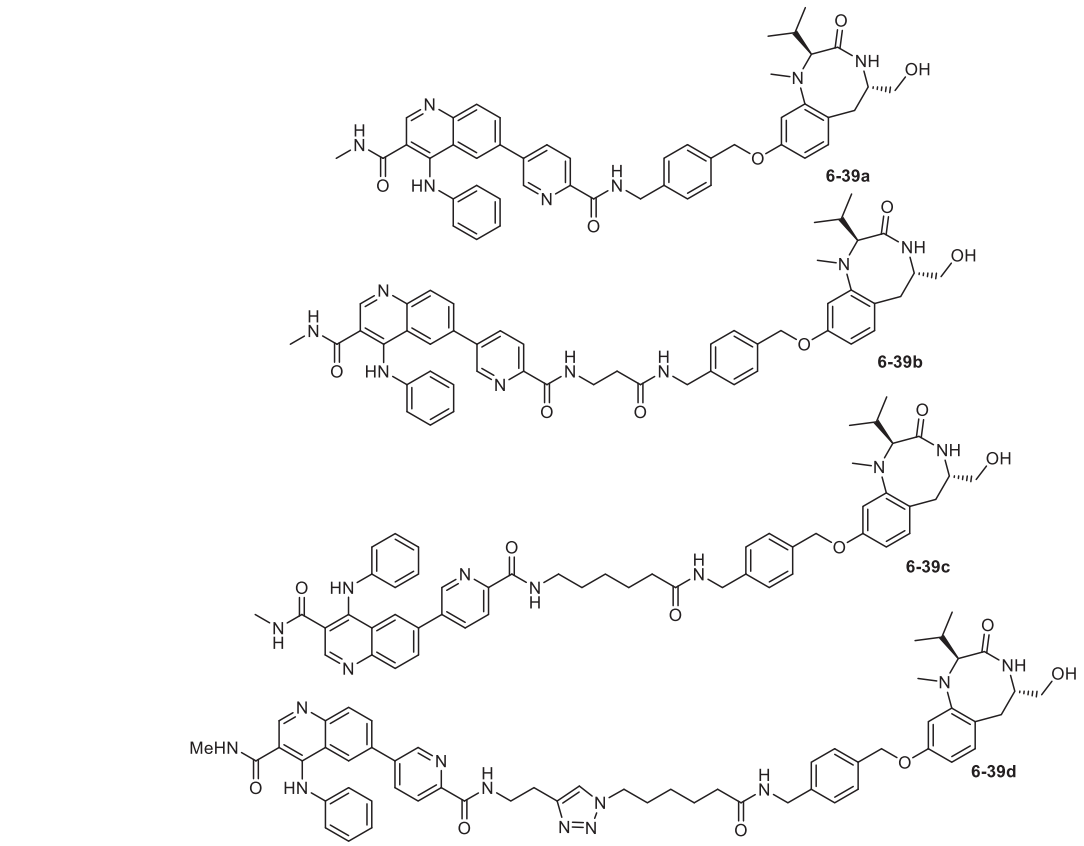
6-39a
6-39b
6-39c
6-39d

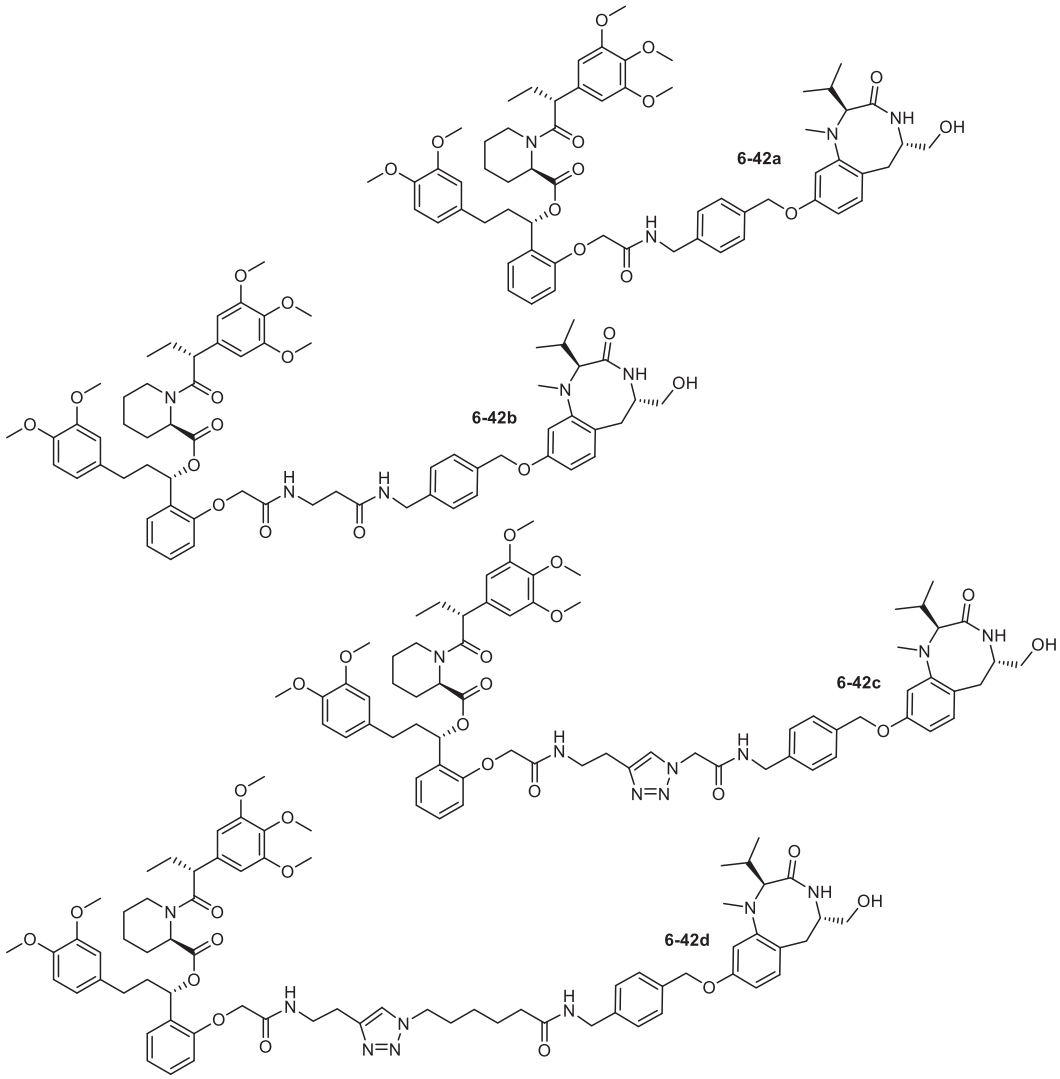
6-42a
6-42b
6-42c
6-42d

Appendix 2: Selected Spectra

Fluorothalidomide (3-10)

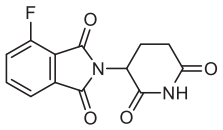

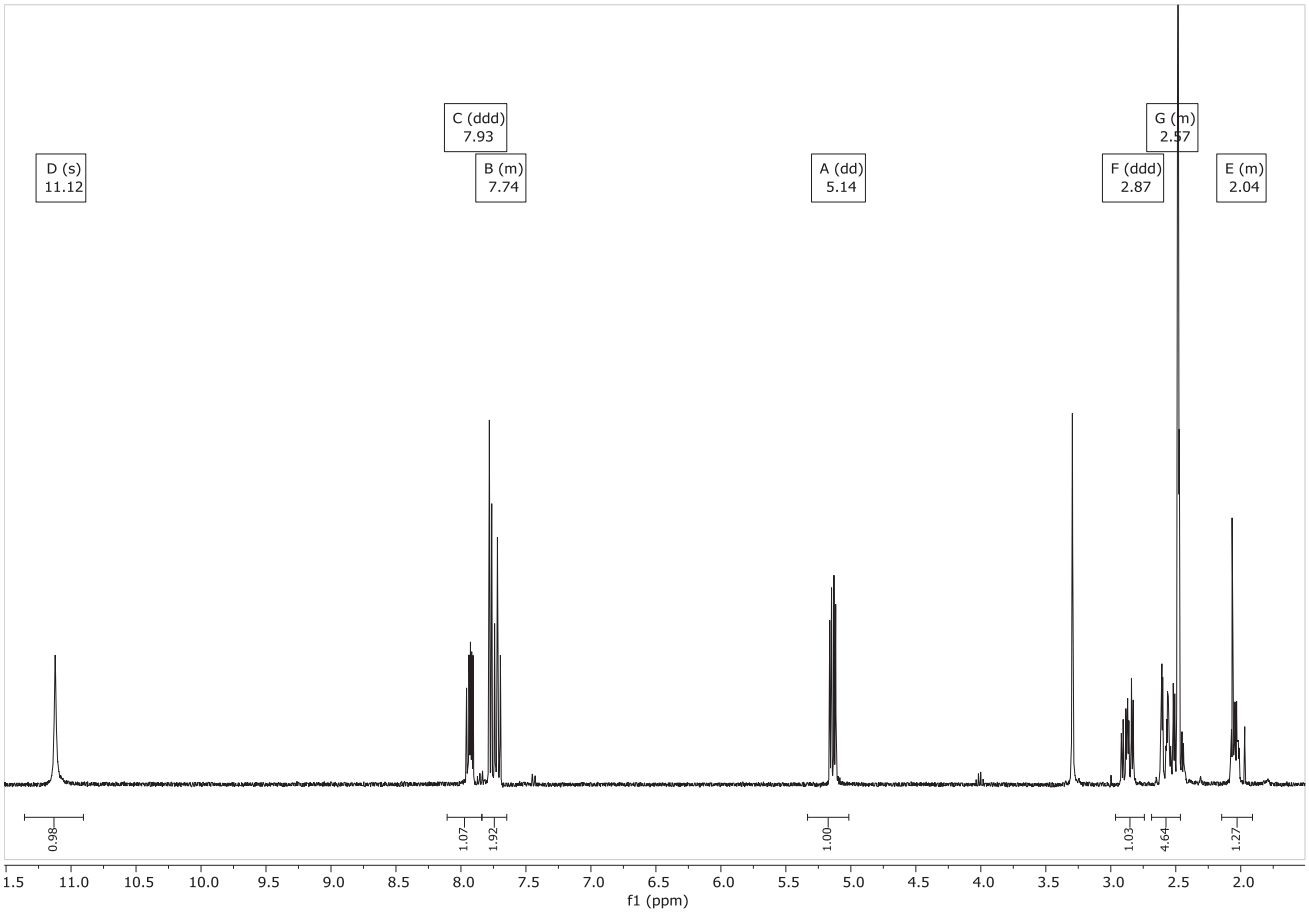

VHL Ligand (3-29)

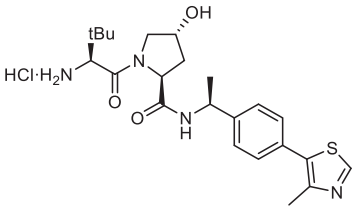

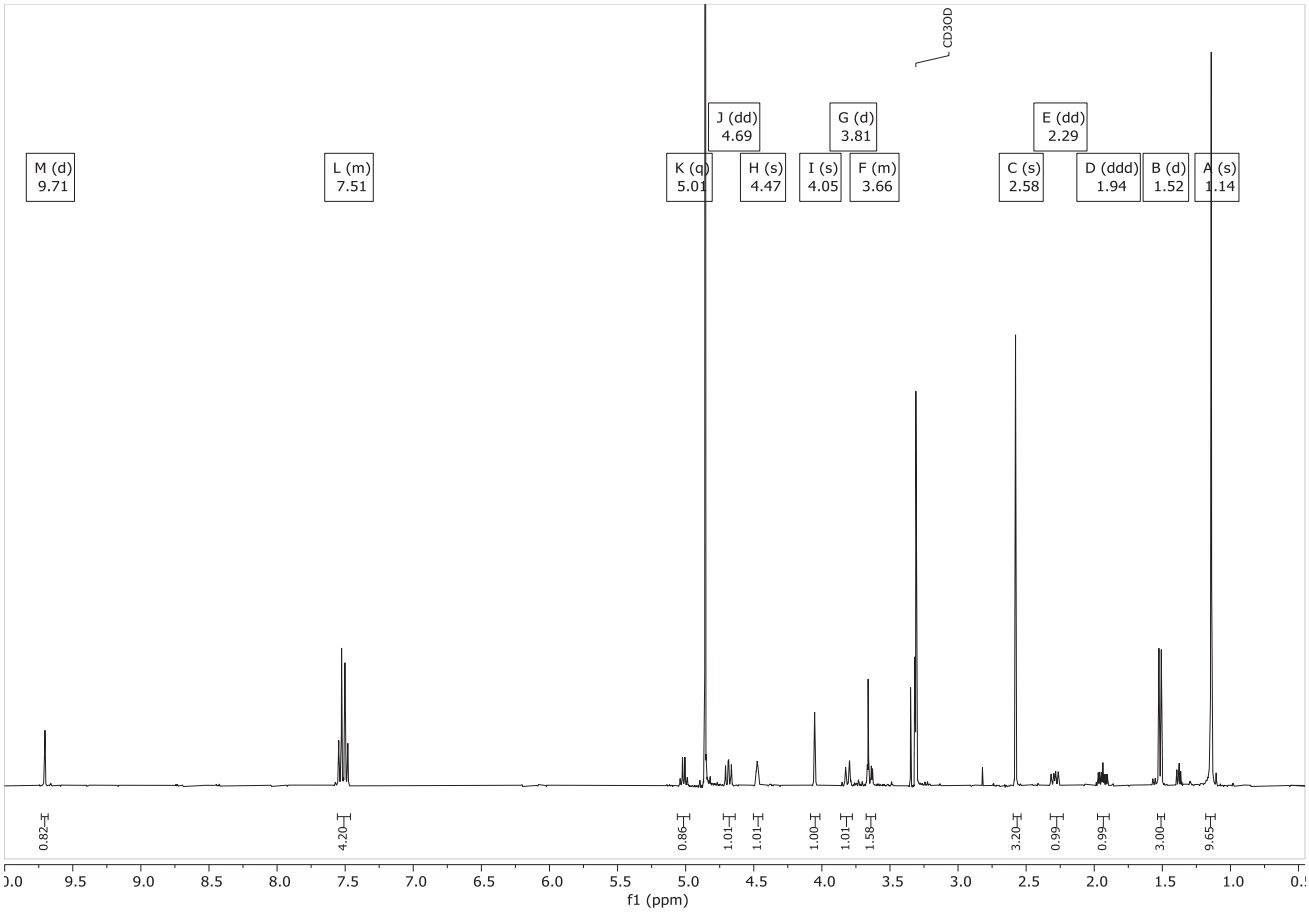

Tamoxifen-based warhead (3-2)

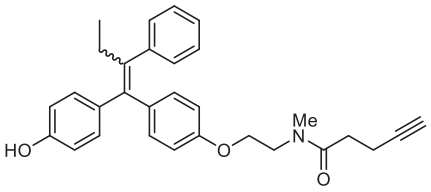

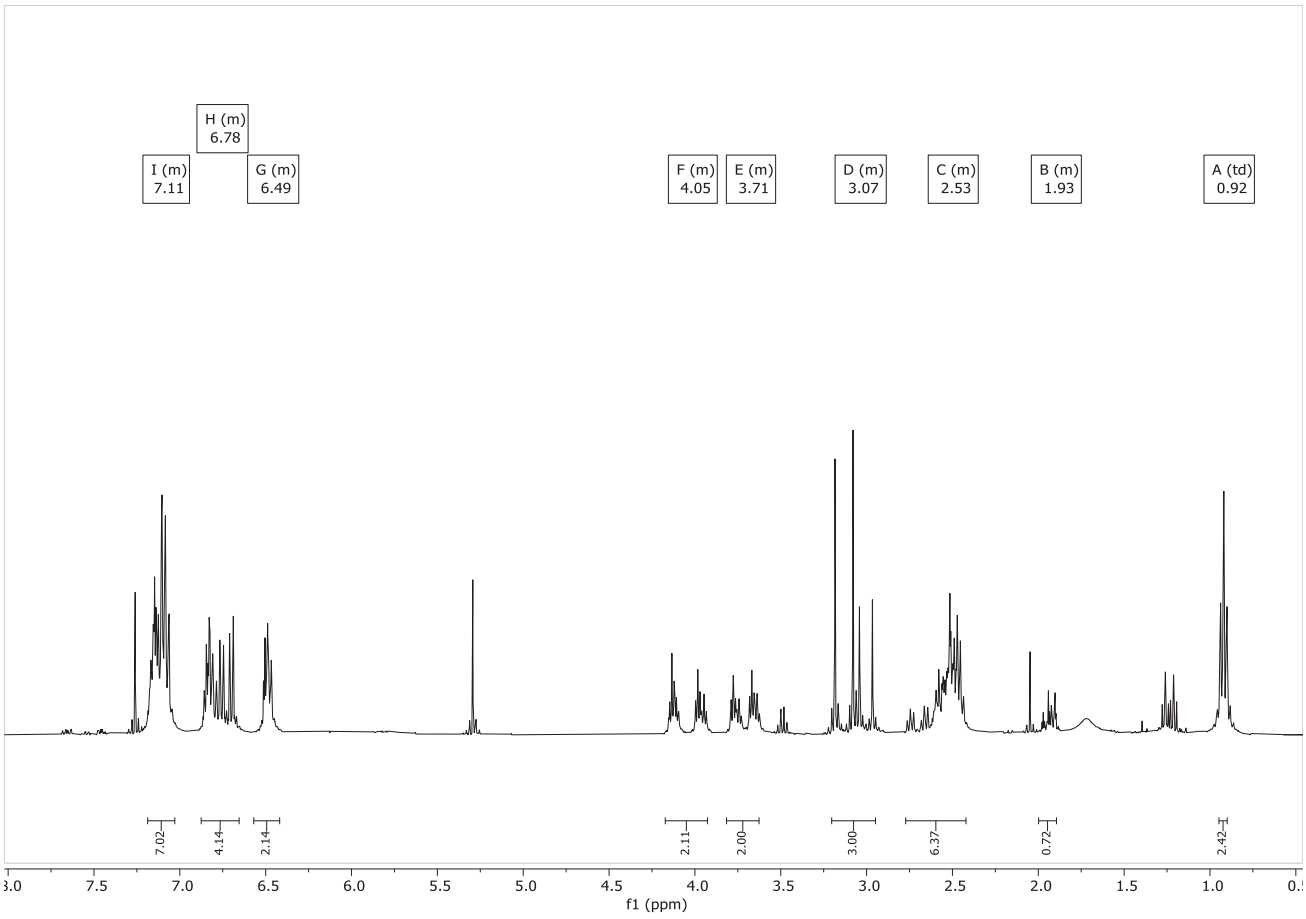

TAM-PO-3

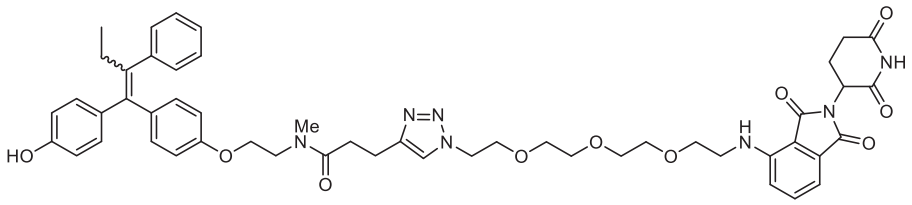
HO
O
Me
N
O
N=N
N
O
O
O
O
H
N
O
N
O
NH
O
O

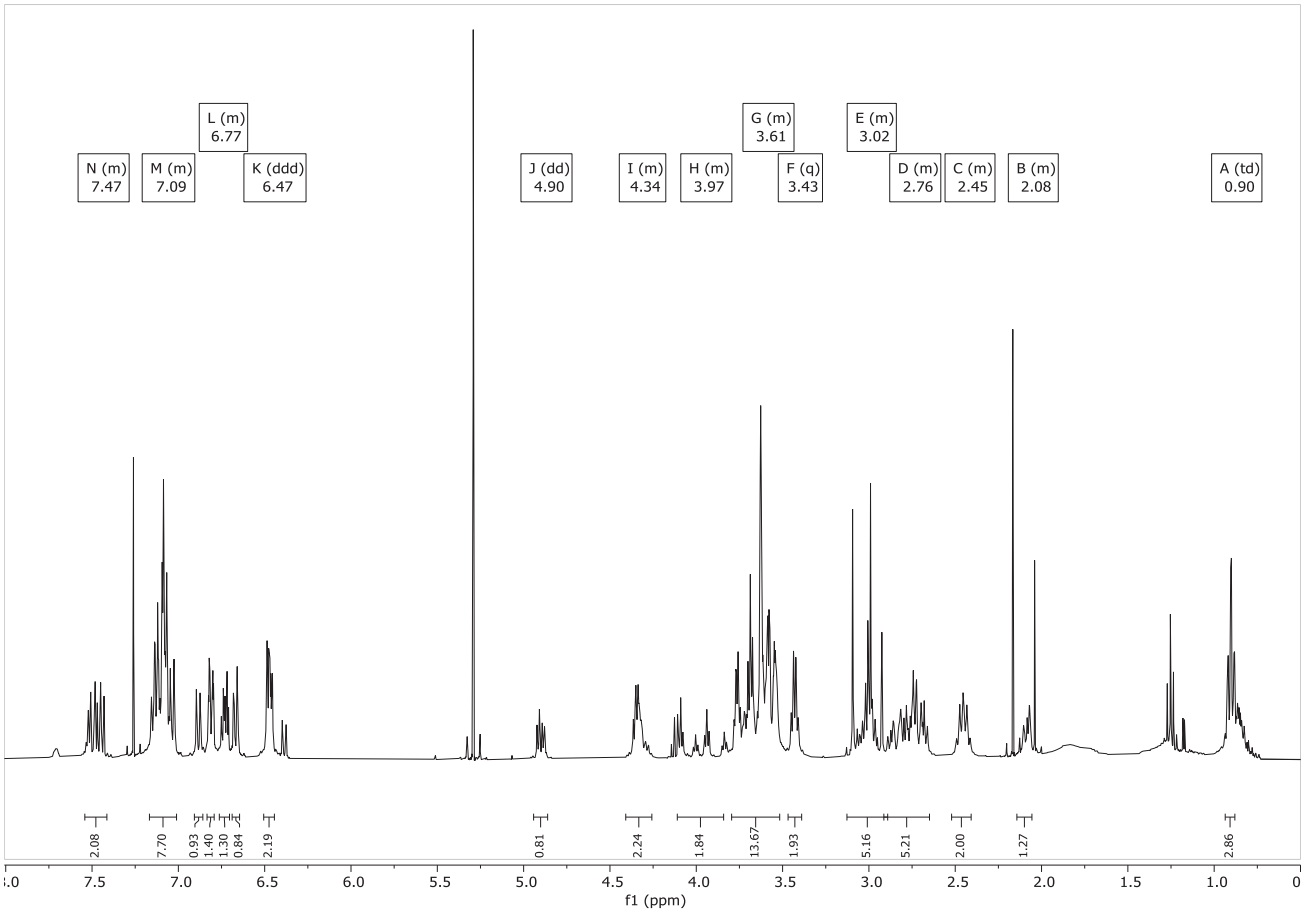
N (m) 7.47
M (m) 7.09
L (m) 6.77
K (ddd) 6.47
J (dd) 4.90
I (m) 4.34
H (m) 3.97
G (m) 3.61
F (q) 3.43
E (m) 3.02
D (m) 2.76
C (m) 2.45
B (m) 2.08
A (td) 0.90
2.08
7.70
0.93
1.40
1.30
0.84
2.19
0.81
2.24
1.84
13.67
1.93
5.16
5.21
2.00
1.27
2.86
7.5
7.0
6.5
6.0
5.5
5.0
4.5
4.0
3.5
3.0
2.5
2.0
1.5
1.0
f1 (ppm)

TAM-VHL-1

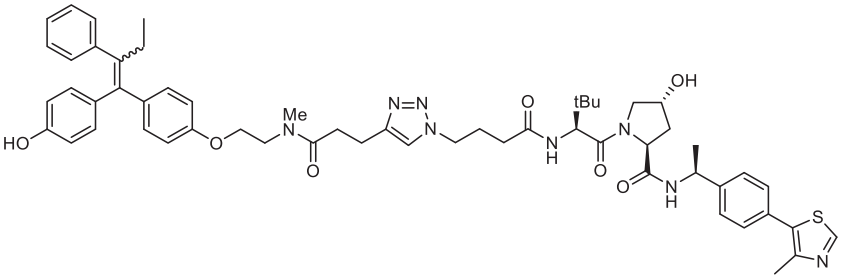
HO
O
Me
N
O
N=N
N
O
N
H
tBu
O
N
OH
O
N
H
S
N

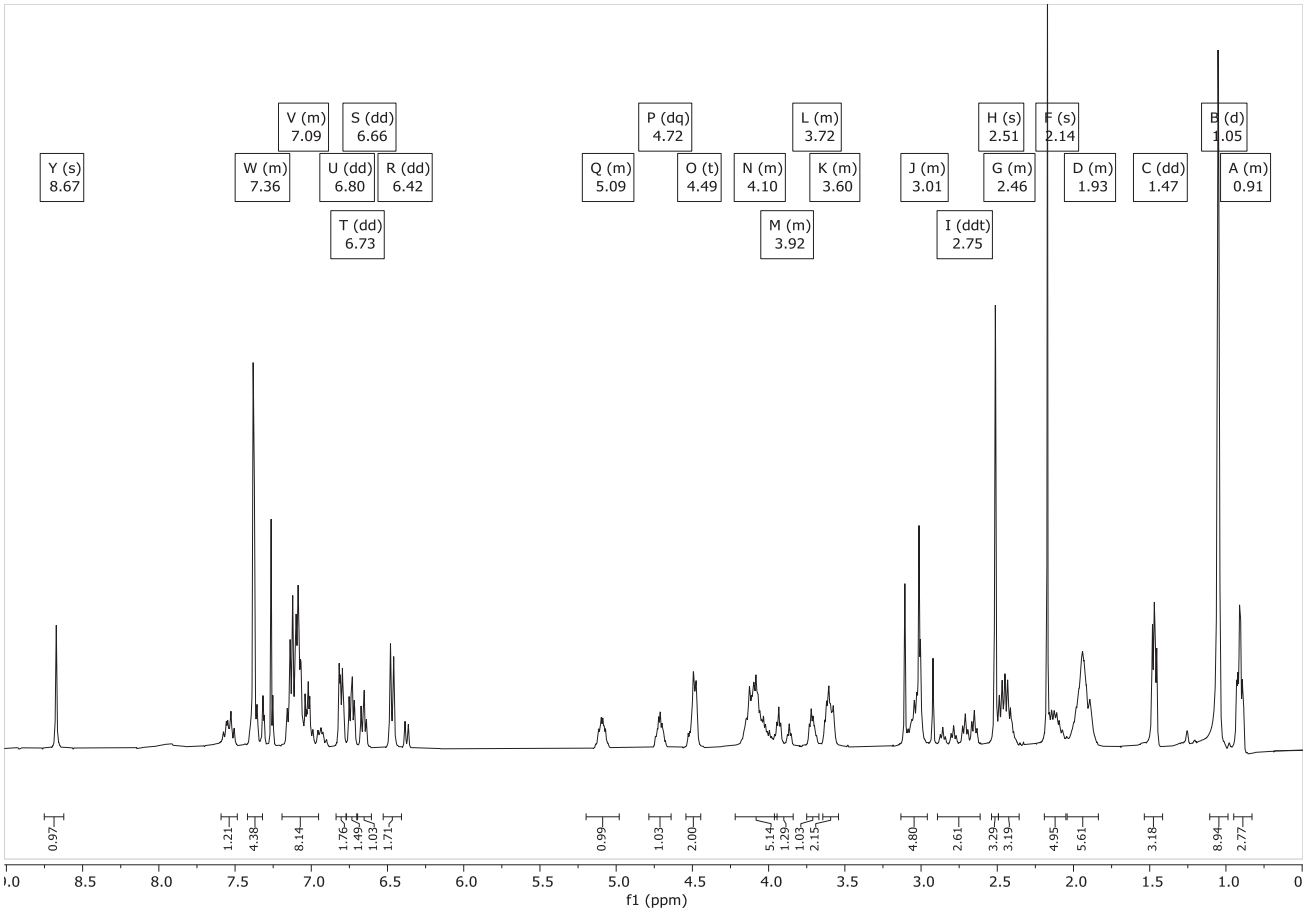
Y (s) 8.67
W (m) 7.36
V (m) 7.09
U (dd) 6.80
S (dd) 6.66
R (dd) 6.42
T (dd) 6.73
Q (m) 5.09
P (dq) 4.72
O (t) 4.49
N (m) 4.10
M (m) 3.92
L (m) 3.72
K (m) 3.60
J (m) 3.01
I (ddt) 2.75
H (s) 2.51
G (m) 2.46
F (s) 2.14
D (m) 1.93
C (dd) 1.47
B (d) 1.05
A (m) 0.91
0.97
1.21
4.38
8.14
1.76
1.49
1.03
1.71
0.99
1.03
2.00
5.14
1.29
1.03
2.15
4.80
2.61
3.29
3.19
4.95
5.61
3.18
8.94
2.77
8.5
8.0
7.5
7.0
6.5
6.0
5.5
5.0
4.5
4.0
3.5
3.0
2.5
2.0
1.5
1.0
f1 (ppm)

p38-targeting warhead (5-7)

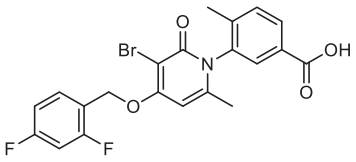

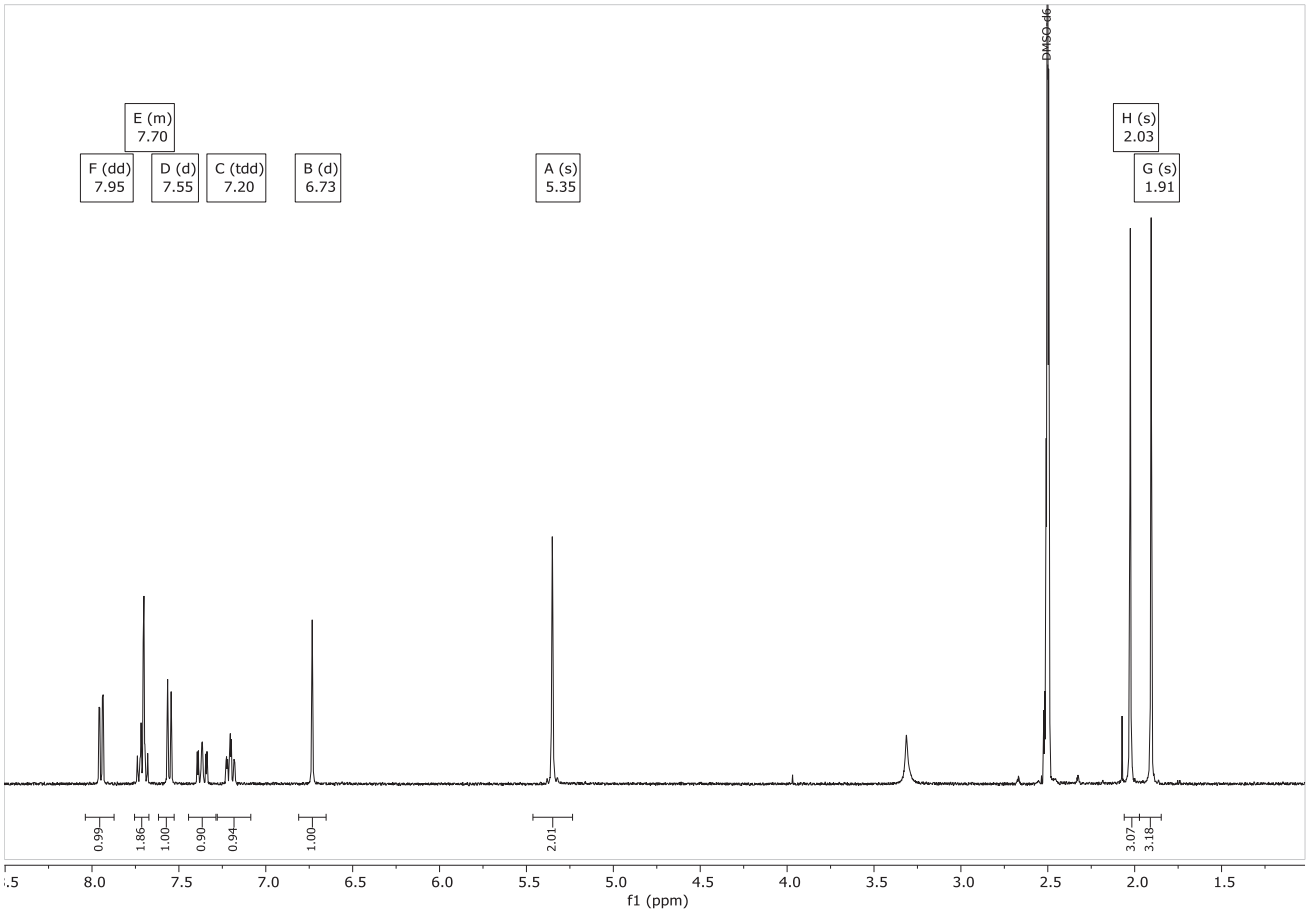

NR-11c

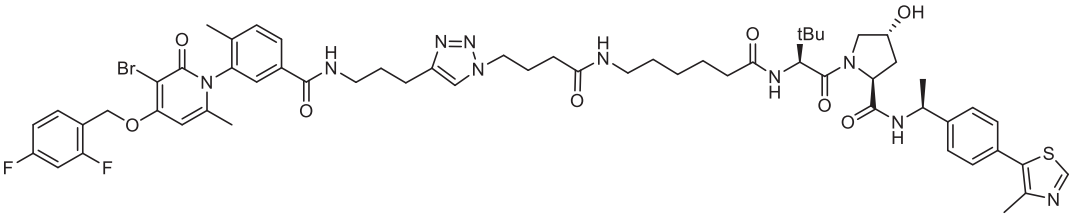
Br
O
N
O
O
F
F
H
N
N=N
N
H
N
O
O
tBu
O
N
H
N
O
OH
N
O
S
N

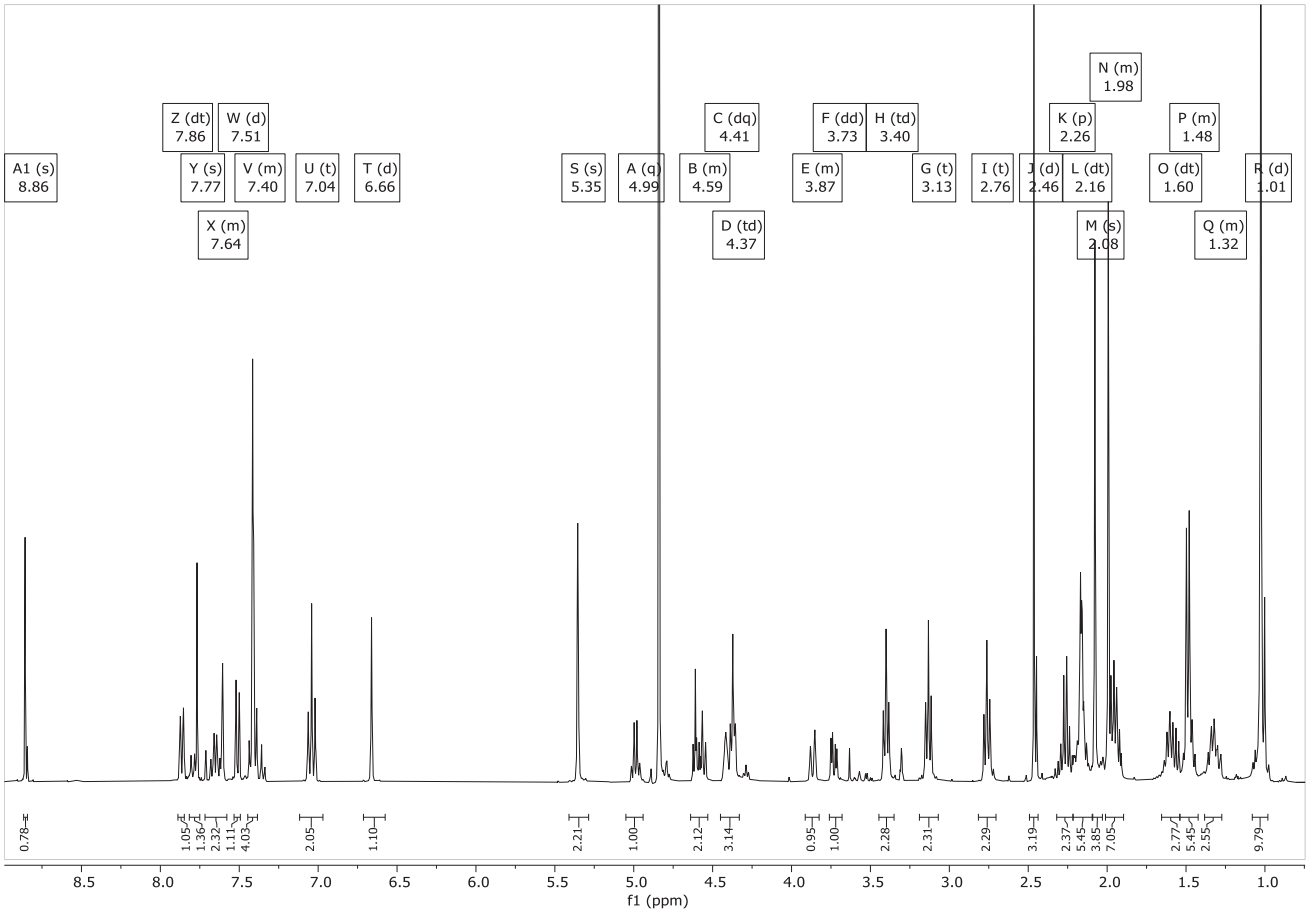
A1 (s) 8.86
Z (dt) 7.86
W (d) 7.51
Y (s) 7.77
V (m) 7.40
U (t) 7.04
T (d) 6.66
X (m) 7.64
S (s) 5.35
A (q) 4.99
C (dq) 4.41
B (m) 4.59
D (td) 4.37
F (dd) 3.73
H (td) 3.40
E (m) 3.87
G (t) 3.13
I (t) 2.76
J (d) 2.46
K (p) 2.26
L (dt) 2.16
N (m) 1.98
M (s) 2.08
P (m) 1.48
O (dt) 1.60
Q (m) 1.32
R (d) 1.01
0.78
1.05
1.36
2.32
1.11
4.03
2.05
1.10
2.21
1.00
2.12
3.14
0.95
1.00
2.28
2.31
2.29
3.19
2.37
5.45
3.85
7.05
2.77
5.45
2.55
9.79
8.5
8.0
7.5
7.0
6.5
6.0
5.5
5.0
4.5
4.0
3.5
3.0
2.5
2.0
1.5
1.0
f1 (ppm)

NR-14c

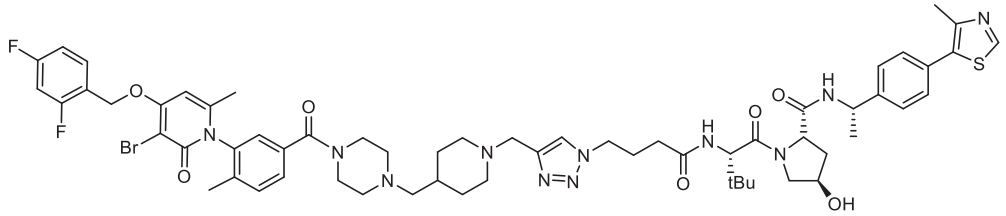
F
F
O
Br
O
N
O
N
N
N
N
N
N
N
H
N
O
O
tBu
O
H
N
O
N
OH
S

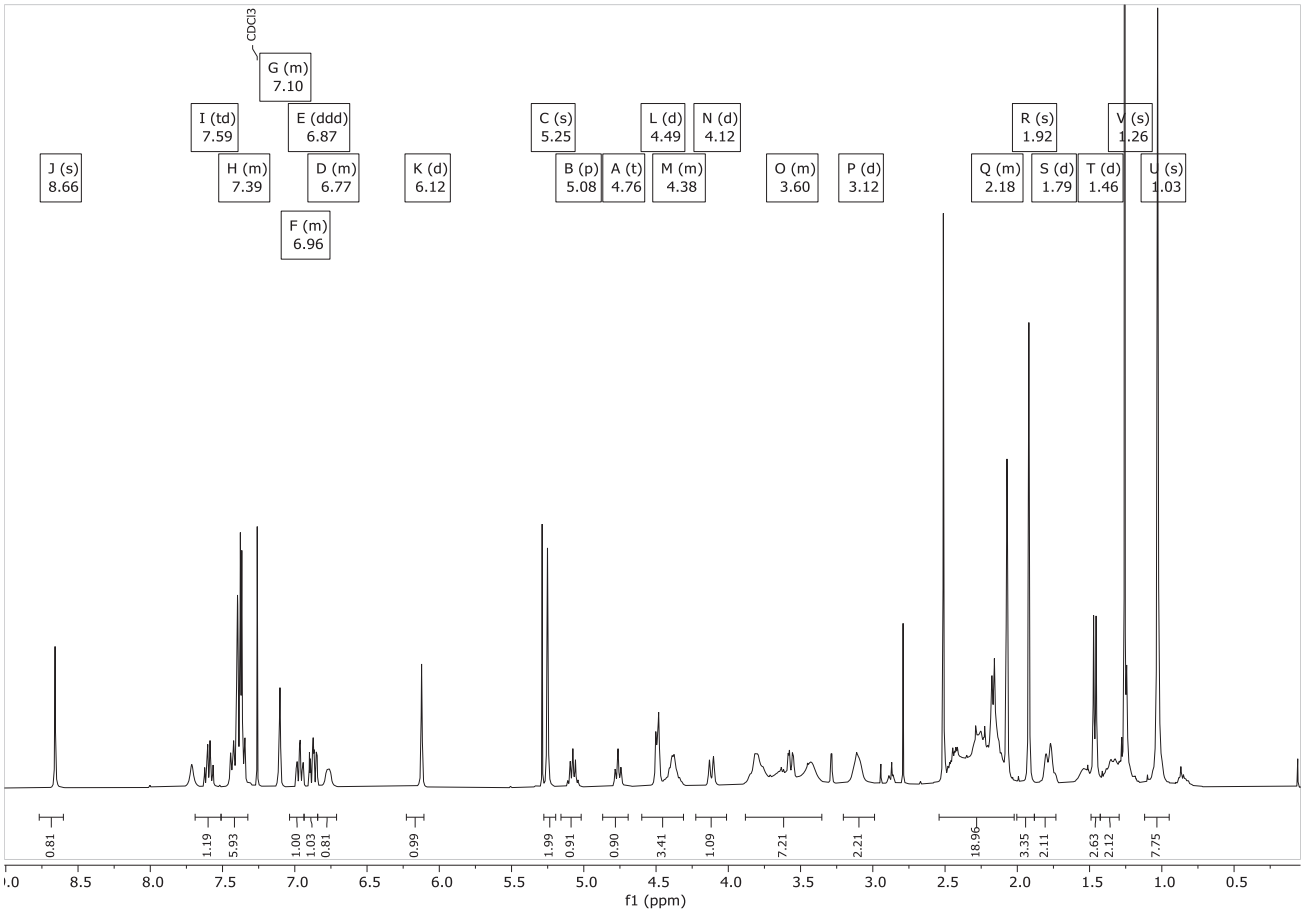
CDCl3
G (m) 7.10
I (td) 7.59
E (ddd) 6.87
C (s) 5.25
L (d) 4.49
N (d) 4.12
R (s) 1.92
V (s) 1.26
J (s) 8.66
H (m) 7.39
D (m) 6.77
K (d) 6.12
B (p) 5.08
A (t) 4.76
M (m) 4.38
O (m) 3.60
P (d) 3.12
Q (m) 2.18
S (d) 1.79
T (d) 1.46
U (s) 1.03
F (m) 6.96
0.81
1.19
5.93
1.00
1.03
0.81
0.99
1.99
0.91
0.90
3.41
1.09
7.21
2.21
18.96
3.35
2.11
2.63
2.12
7.75
8.5
8.0
7.5
7.0
6.5
6.0
5.5
5.0
4.5
4.0
3.5
3.0
2.5
2.0
1.5
1.0
0.5
f1 (ppm)

NR-14f

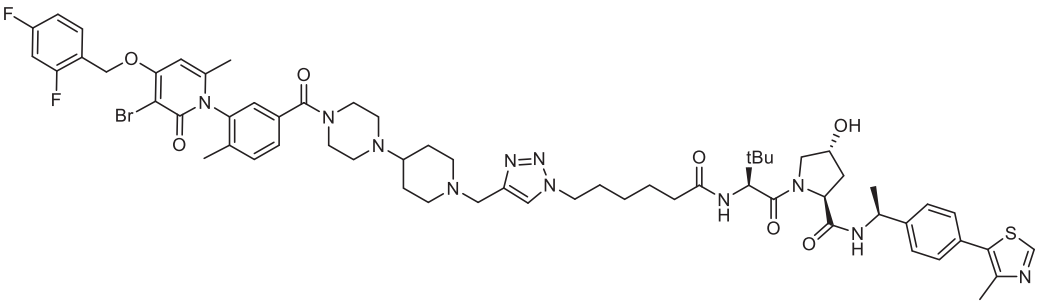
F
F
O
Br
O
N
O
N
N
N
N
N
N
O
N
H
tBu
O
N
OH
O
N
H
S
N

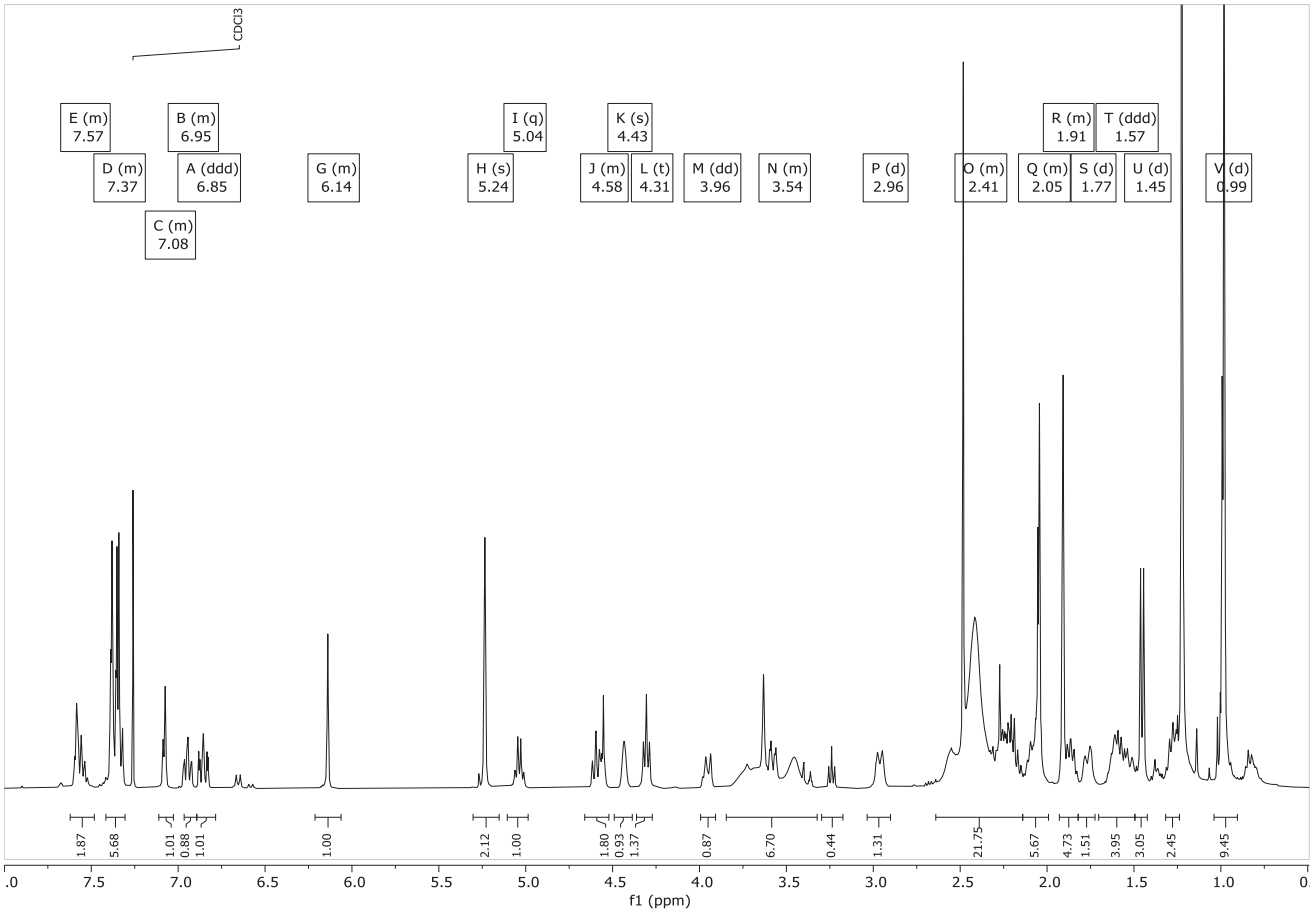
CDCl3
E (m) 7.57
D (m) 7.37
C (m) 7.08
B (m) 6.95
A (ddd) 6.85
G (m) 6.14
I (q) 5.04
H (s) 5.24
K (s) 4.43
J (m) 4.58
L (t) 4.31
M (dd) 3.96
N (m) 3.54
P (d) 2.96
O (m) 2.41
R (m) 1.91
Q (m) 2.05
T (ddd) 1.57
S (d) 1.77
U (d) 1.45
V (d) 0.99
1.87
5.68
1.01
0.88
1.01
1.00
2.12
1.00
1.80
0.93
1.37
0.87
6.70
0.44
1.31
21.75
5.67
4.73
1.51
3.95
3.05
2.45
9.45
7.5
7.0
6.5
6.0
5.5
5.0
4.5
4.0
3.5
3.0
2.5
2.0
1.5
1.0
f1 (ppm)

6-39c

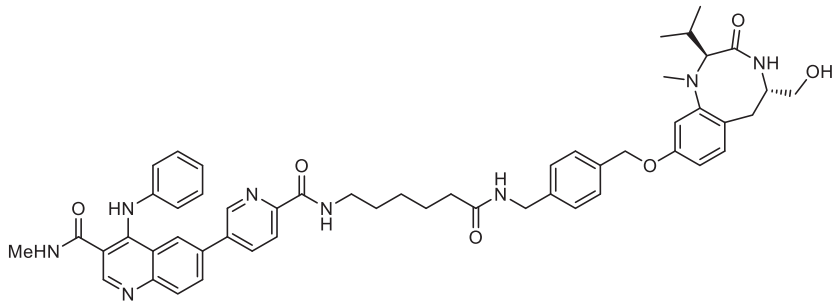
O
NH
N
OH
O
HN
MeHN
N
O
N
H
N
H
O
O
N

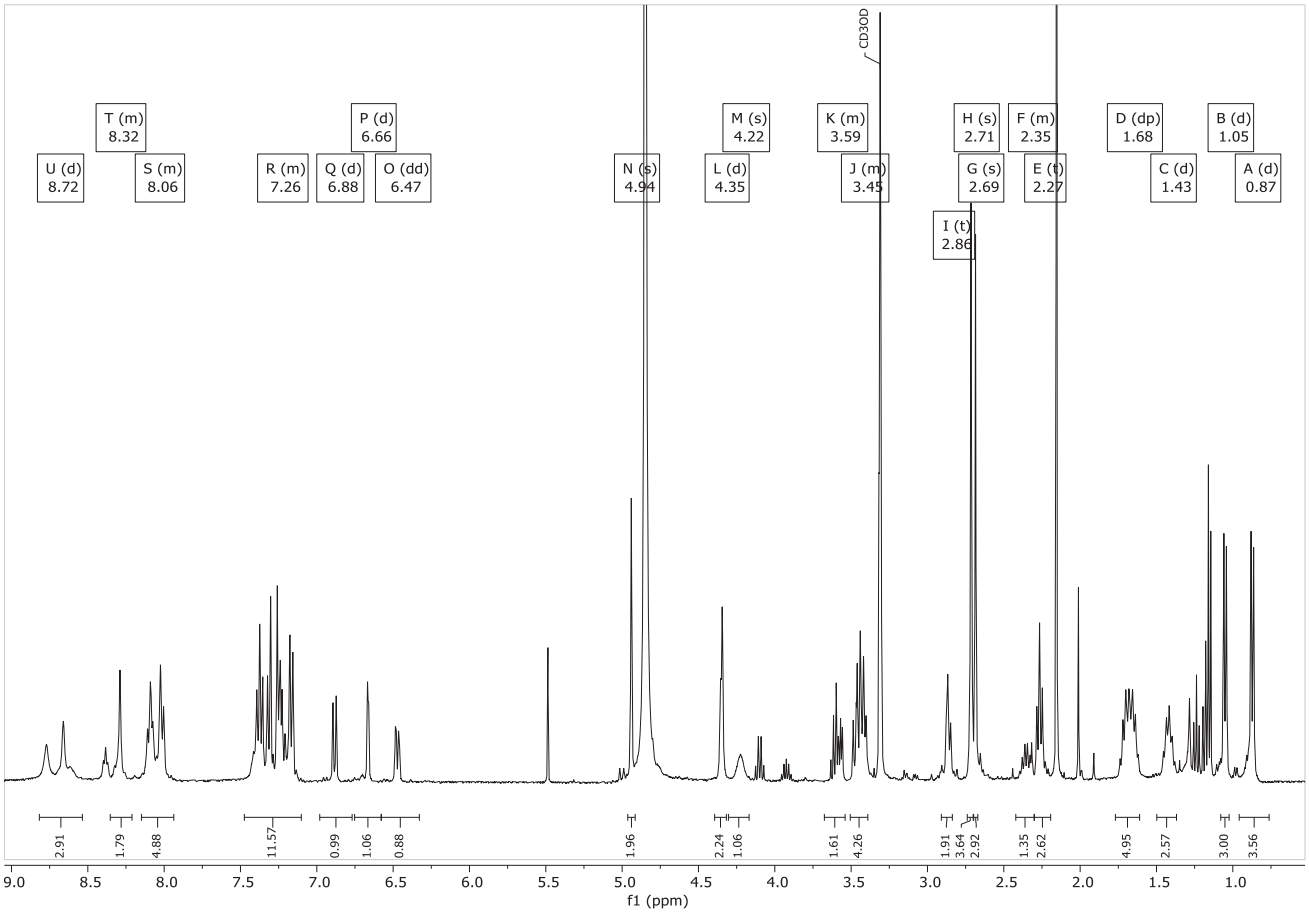
CD3OD
U (d) 8.72
T (m) 8.32
S (m) 8.06
R (m) 7.26
P (d) 6.66
Q (d) 6.88
O (dd) 6.47
N (s) 4.94
M (s) 4.22
L (d) 4.35
K (m) 3.59
J (m) 3.45
H (s) 2.71
I (t) 2.86
G (s) 2.69
F (m) 2.35
E (t) 2.27
D (dp) 1.68
C (d) 1.43
B (d) 1.05
A (d) 0.87
2.91
1.79
4.88
11.57
0.99
1.06
0.88
1.96
2.24
1.06
1.61
4.26
1.91
3.64
2.92
1.35
2.62
4.95
2.57
3.00
3.56
9.0
8.5
8.0
7.5
7.0
6.5
6.0
5.5
5.0
4.5
4.0
3.5
3.0
2.5
2.0
1.5
1.0
f1 (ppm)

6-42b

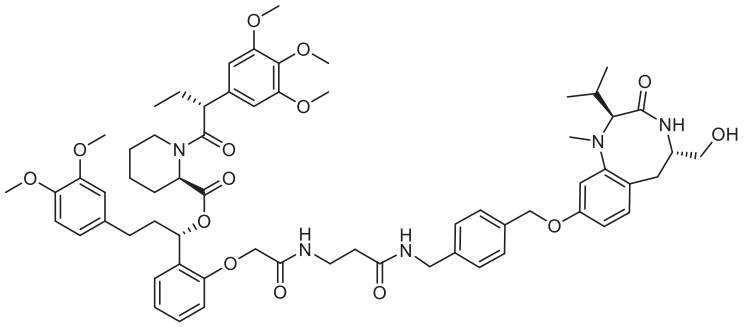

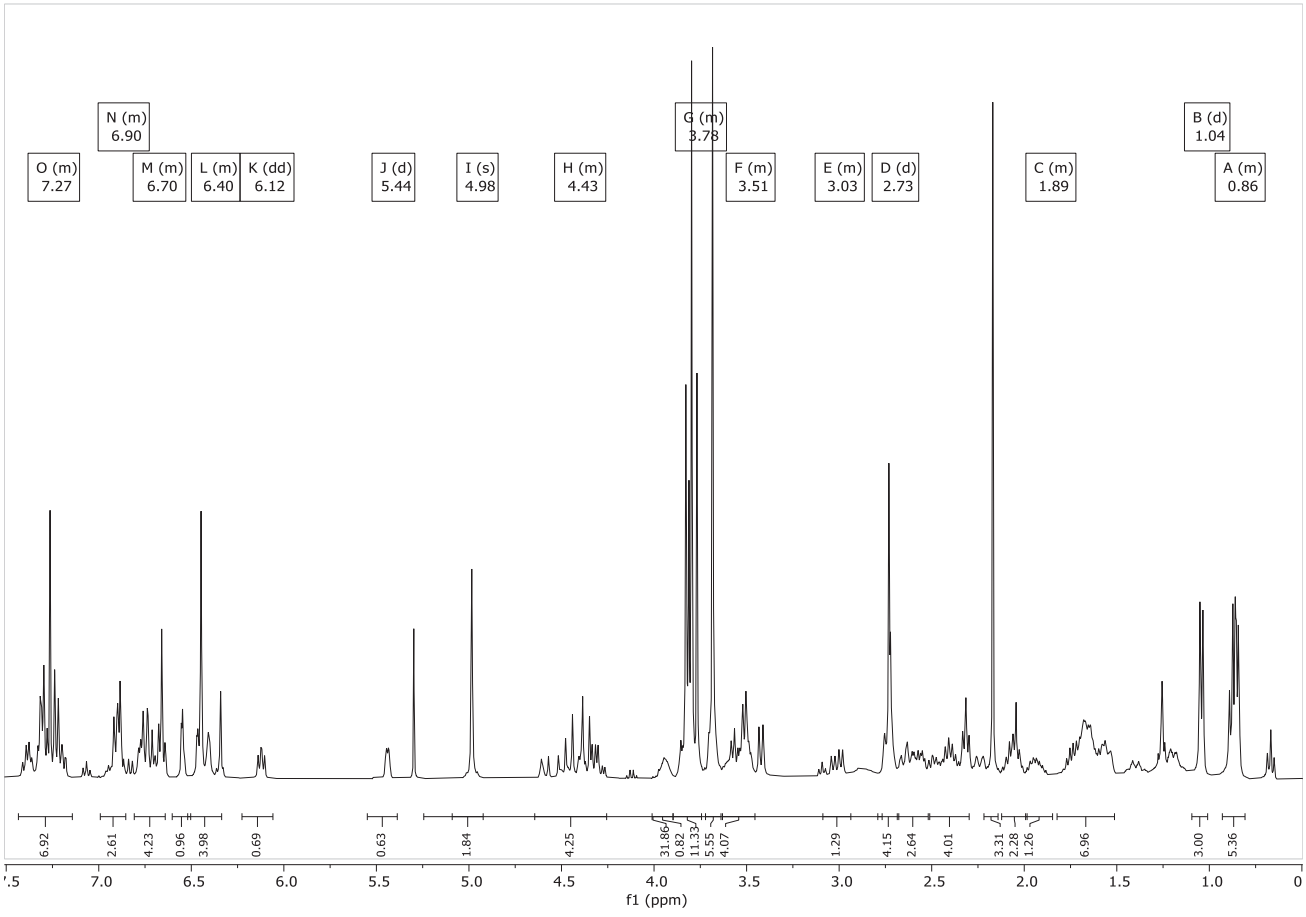
O (m) 7.27
N (m) 6.90
M (m) 6.70
L (m) 6.40
K (dd) 6.12
J (d) 5.44
I (s) 4.98
H (m) 4.43
G (m) 3.78
F (m) 3.51
E (m) 3.03
D (d) 2.73
C (m) 1.89
B (d) 1.04
A (m) 0.86
6.92
2.61
4.23
0.96
3.98
0.69
0.63
1.84
4.25
31.86
0.82
11.33
5.55
4.07
1.29
4.15
2.64
4.01
3.31
2.28
1.26
6.96
3.00
5.36
7.5
7.0
6.5
6.0
5.5
5.0
4.5
4.0
3.5
3.0
2.5
2.0
1.5
1.0
0
f1 (ppm)

6-42d

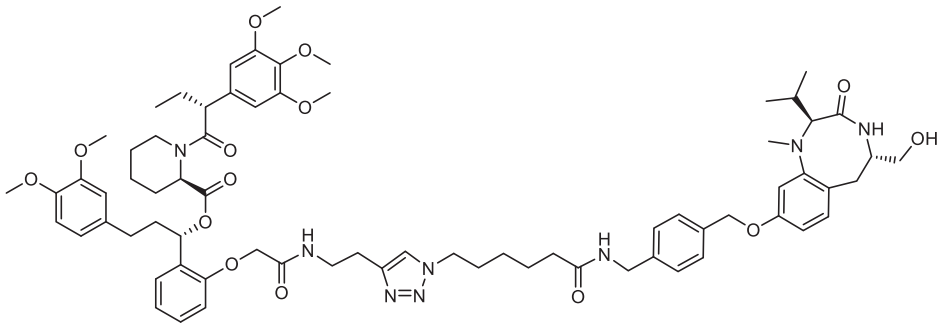

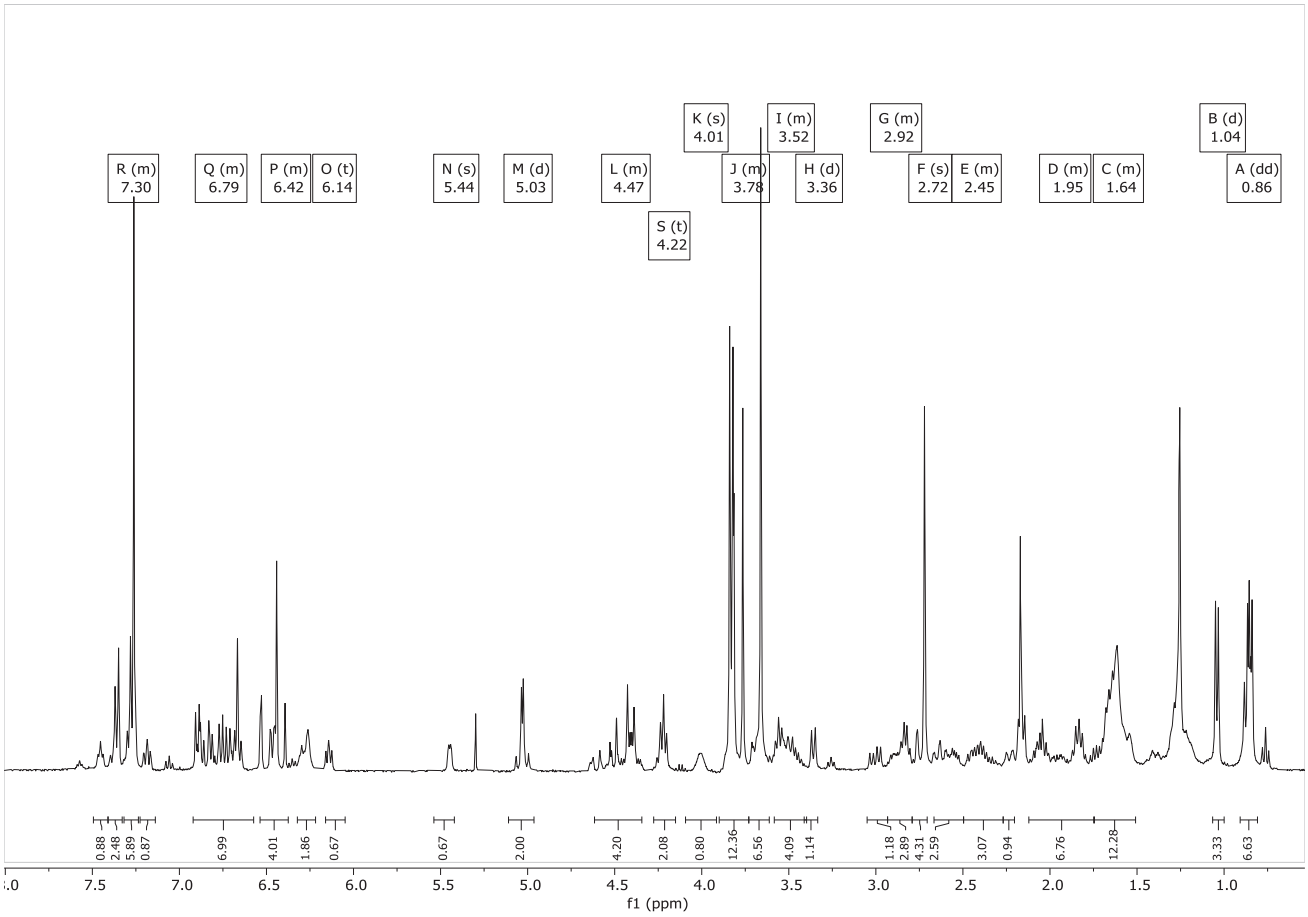
R (m) 7.30
Q (m) 6.79
P (m) 6.42
O (t) 6.14
N (s) 5.44
M (d) 5.03
L (m) 4.47
S (t) 4.22
K (s) 4.01
J (m) 3.78
I (m) 3.52
H (d) 3.36
G (m) 2.92
F (s) 2.72
E (m) 2.45
D (m) 1.95
C (m) 1.64
B (d) 1.04
A (dd) 0.86
0.88
2.48
5.89
0.87
6.99
4.01
1.86
0.67
0.67
2.00
4.20
2.08
0.80
12.36
6.56
4.09
1.14
1.18
2.89
4.31
2.59
3.07
0.94
6.76
12.28
3.33
6.63
7.5
7.0
6.5
6.0
5.5
5.0
4.5
4.0
3.5
3.0
2.5
2.0
1.5
1.0
f1 (ppm)

Appendix 3: List of Abbreviations

4OHT	4-Hydroxytamoxifen
AcOEt	Ethyl Acetate
AcOH	Acetic Acid
AIBN	Azobisisobutyronitrile
AMPK	AMP-activated protein kinase
AR	Androgen Receptor
BESF	1-Bromoethene-1-sulfonyl fluoride
BET	Bromodomain and Extra-terminal domain
BRD4	Bromodomain-containing protein 4
BTZ	Bortezomib
Cat	Catalytic
cIAP1	Cellular Inhibitor of Apoptosis Protein-1
CIP	Chemically Induced Proximity
CRBN	Cereblon
CRL	Cullin Ring Ubiquitin Ligases
CuAAC	Copper-catalyzed Alkyne Azide Cycloaddition
DABCO	1,4-diazabicyclo[2.2. 2]octane
DC_{50}	Half-maximal Degradation Concentration
DCAF15	DDB1 And CUL4 Associated Factor 15
DCAF16	DDB1 And CUL4 Associated Factor 16
DCM	Dichlorometane
DHP	3,4-Dihydropyran
DHT	Dihydrotestosterone
DIC	N,N'-Diisopropylcarbodiimide
DIPEA	N,N-Diisopropiletilamina
D_{max}	Degradation Maximum
DMF	Dimethylformamide
DNA	Deoxyribonucleic Acid
E_2	17β-oestradiol
eq.	Equivalent
ER	Oestrogen Receptor
ER+	Oestrogen Receptor Positive
ERF	ETS2 Repressor Factor
ERK	Extracellular Signal-Regulated Kinases
ESF	Ethane Sulfonyl Fluoride
FKBP12	12-kDa FK506-binding protein
g	Gram
h	Hour
HIF1α	Hypoxia-inducible factor 1-alpha
HIV	Human Inmunodeficency Virus
HPLC	High-performance Liquid Chromatography
HyT	Hydrophobic Tagging
IC_{50}	Half-maximal Inhibition Concentration
IMIDs	Immunomodulatory Drugs
IP	Intraperitoneal
IRB	Institute for Research in Biomedecine
IV	Intraveous

JNK	c-Jun N-terminal Kinases
K_d	Dissociation Constant
LBD	Ligand Binding Domain
LEN	Lenalidomide
M	Molar
MAP2K	MAP Kinase Kinase
MAP3K	MAP Kinase Kinase Kinase
MAPK	Mitogen-activated Protein Kinase
MDM2	Mouse Double Minute 2
MeCN	Acetonitrile
MeOH	Methanol
MG	Molecular Glue
M_p	Melting Point
mRNA	Messenger Ribonucleic Acid
Ms	Mesyl
mTOR	Mamalian Target of Rapamycin
NAEi	NEDD8-activating enzyme inhibitor
NMO	N-Methylmorpholine N-oxide
NMP	N-Methylpyrrolidine
PDB	Protein Database Bank
PEG	Polyethylene glycol
PH	PH-12348314
PHICS	Phosphorylation Inducing Chimaeras or Phosphorylation Inducing Chimeric Small Molecules
PKC	Protein Kinase C
POI	Protein of Interest
POM	Pomalidomide
PP1	Protein Phosphatase 1
PP2A	Protein Phosphatase 2A
PP5	Protein Phosphatase 5
PPI	Protein-Protein Interaction
PROTAC	Proteolysis Targeting Chimaeras
PTM	Post-translational Modification
r.t.	Room Temperature
RING	Really Interesting New Gene
SAR	Structure-Activity Relationship
Ser	Serine
SERD	Selective Oestrogen Receptor Degrader
SERM	Selective Oestrogen Receptor Degrader
siRNA	Silencing Ribonucleic Acid
SNIPER	Specific and non-genetic IAP dependent protein eraser
SPPS	Solid Phase Pepetide Synthesis
***t*-BuOH**	tert-butyl alcohol
TEA	Triethylamine
Tf	Triflate
THF	Tetrahydrofurane
Thr	Threonine
TLK	Tousled-like Kinase
TPD	Targeted Protein Degradation
Tyr	Tyrosine
UPS	Ubiquitin-Proteasome System
Vh	Vehicle
VHL	Von-Hippel Lindau

Acknowledgements/Agraïments

Acabo aquesta memòria amb un breu llistat d'agraïments, a aquelles persones que han contribuït, directa o indirectament, a la realització d'aquest treball, i més generalment a les experiències viscudes durant els quatre anys i mig que ha durat.

Primerament, a l'Antoni Riera, director d'aquesta tesi doctoral, per haver-me brindat l'oportunitat de treballar al laboratori i pel guiatge a través de tots els projectes pels quals he anat treballant.

A en Craig Donoghue, pel mentoratge durant les primeres etapes del doctorat, sens dubte les més dures. Your work undoubtely paved the way for all the PROTACs that came after.

Als membres d'URSA, en especial els qui fèiem el doctorat al laboratori durant els últims dos anys. Per a mi sou l'essència del laboratori, els que estàveu picant pedra a les vitrines dia rere dia, de mentre els veterans es jubilaven i els estudiants venien i marxaven. És durant aquesta etapa que tinc les millors memòries del doctorat, quan la química deixava ja d'angoixar-me tant i començava a gaudir més del temps que passàvem junts. Les boleres i els viatges que vam fer, i algun sopar, em temo que serà el que més recordi d'aquests anys. Sergi, Caro, Pep, Marina, gràcies pel temps compartit!

També a la resta, que no sou tan propers en la memòria, però que també va haver-hi bons temps quan encara hi éreu al laboratori, en especial abans de la pandèmia. A en Craig, l'Enric, l'Albert, l'Anna, l'Ernest. I als que han anat venint després, ja sigui per una temporada curta o per a quedar-se; Carlitos, Martí, Rory, Mireia, Clara, Yisong, Inés, Dom, Medea. L'ambient al laboratori ha sigut excepcional, gràcies pels mems i les bromes.

Als estudiants que han estat treballant amb mi en els projectes que portava, també la seva feina queda reflectida en aquesta tesi. Yusuf, Ana, Lea, bona feina.

A les col·laboracions amb altres laboratoris dins de l'IRB, ja que sense la seva feina aquesta tesi seria incomplerta. Mónica, Irene, Alicia, Ana. Y por supuesto a ti también Maria! Que a pesar de no ser una colaboración científica la nuestra, ha sido esencial para sobrevivir.

Als membres del IRB Chess Club, per les tardes més divertides de la setmana, de birra i *dirty chess*.

I per acabar, també a la família, pel seu suport tan necessari. Una forta abraçada.